Title

Identification and characterization of novel flagellar cAMP signaling systems in the human-infectious parasite Trypanosoma brucei

Author

Saada, Edwin A.

Publication Date

2015

Peer reviewed|Thesis/dissertation

UNIVERSITY OF CALIFORNIA

Los Angeles

Identification and characterization of novel flagellar cAMP signaling systems in the human-infectious parasite *Trypanosoma brucei*

A dissertation submitted in partial satisfaction of the requirements for the degree of Doctor of Philosophy in Microbiology, Immunology and Molecular Genetics

By

Edwin Albert Saada

2015

ABSTRACT OF THE DISSERTATION

Identification and characterization of novel flagellar cAMP signaling systems in the human-infectious parasite *Trypanosoma brucei*

by

Edwin Albert Saada

Doctor of Philosophy in Microbiology, Immunology, and Molecular Genetics

University of California, Los Angeles 2015

Professor Kent L. Hill, Chair

African trypanosomes are devastating human and animal pathogens transmitted by tsetse flies between mammalian hosts. The trypanosome surface forms a critical host interface that is essential for sensing and adapting to diverse host environments. However, trypanosome surface protein composition and diversity remain largely unknown. In the following works, we identify the trypanosome cell and flagellar surface proteomes using surface labelling, affinity purification, and proteomic analyses of both insect-stage and mammalian bloodstream-stage *Trypanosoma brucei.* We identify a substantial number of novel proteins with unknown functionalities, indicating that the surface proteomes are larger and more diverse than previously anticipated. We demonstrate stage-specificity for a number of proteins, suggesting that the parasite surface undergoes fine-tuning in order to adapt to specific, but diverse, host environments.

Similar analyses were performed on the trypanosome flagellum, an essential and multifunctional organelle involved in motility, morphogenesis, and host-parasite interactions. Previous attempts to characterize flagellar composition were limited by the inability to purify intact flagellum. Using a combination of genetic and mechanical approaches in conjunction with surface labeling and affinity purification, we conducted independent analyses of the flagellum surface and matrix fractions. We identified a broad spectrum of proteins with predicted signaling functionalities, indicating that the flagellum is a diverse and dynamic host-parasite interface that is well-suited for host-parasite signaling.

In procyclic, or insect-stage, parasites, we reported identification of several receptor-type adenylate cyclases (ACs) that are specifically upregulated in procyclic

T. brucei. Previously studied ACs were constitutively expressed or confined to bloodstream stage parasites. Using gene-specific tags, we find that ACs are glycosolated surface-exposed proteins that dimerize and possess catalytic activity. Notably, while some ACs were found to be distributed along the flagellum length, others specifically localized to the flagellum tip. Differential localization suggests that the membrane is organized into specific subdomains, suggesting a specific-role for cAMP signaling in procyclic-stage parasites.

Functional analyses of ACs were done in the context of socio-microbiological analyses. There are sophisticated systems for cell-cell communication that enable microbes to act as a group. In their native environment, *T. brucei* lives on host tissue surfaces, and *in vitro* cultivation on surfaces causes the parasites to actively assemble into densely packed communities, from which they coordinately migrate outwards in radial projections across the surface. This behavior is termed social motility (SoMo) due to analogies with bacterial systems. Functional analyses revealed that flagellar ACs cooperate with cAMP-specific phosphodiesterase to regulate trypanosomal social behaviors. This supports the hypothesis that ACs transduce extracellular signals and are involved in stage-specific signaling pathways. Experiments using cAMP analogues suggest that the phenotype is specific to cAMP, and not due to downstream metabolic byproducts. Notably, knockdown of only some ACs impacts social motility, indicating segregation of AC functions.

There are several possibilities for why only some ACs are involved in social motility. One of the most intriguing explanations has to do with the differential localization. Some ACs localize along the flagellum length, while others are specific to

the tip. Such localization is novel, and this protein family is the first known example of transmembrane proteins in *T. brucei,* and one of the first in any system, to localize exclusively to the flagellar tip. Despite the importance of flagellar protein trafficking, flagellar targeting signals are virtually unknown. In these works, we investigate whether flagellar subdomain localization impacts AC functionality. Using protein truncations, chimeras, and point mutants, we identify an intracellular segment and specific residues required for flagellum and flagellum subdomain targeting. Strikingly, the social motility defect of a flagellum-tip AC mutant can be rescued by redirection of another AC from along the length to the flagellum tip. These results demonstrate the importance of protein targeting to specific subdomains within the flagellum, and implicates cAMP signaling at the flagellum tip as a key regulator of cell-cell communication required for social behavior.

These combined works identify and define the cell surface and flagellar proteomes, with in depth characterization and analysis of a group of novel cAMP signaling proteins. Through usage of the social motility assay, these works identify the first known regulators of trypanosomal social behavior, and the first direct evidence of cAMP functionalities in procyclic-stage parasites. Furthermore, signaling functionality is tied to differential localization of ACs to specific flagellar subdomains. Our works thus advance understanding of principles that govern protein targeting to flagellum subdomains and provides insight into *T. brucei* signaling mechanisms, both of which are poorly understood but fundamentally important features of flagellar and trypanosomal biology.

The dissertation of Edwin Albert Saada is approved:

David Campbell

Wenyuan Shi

James Wohlschlegel

Kent L. Hill, Committee Chair

University of California, Los Angeles

2015

DEDICATION

Many people have provided support and assistance along this journey, for which I will be eternally grateful. I've made many friends along the way, and I thank you all.

This dissertation is dedicated to my family. To my parents, Jack & Ninva, who always encouraged my interests in the sciences and to this day still push me to challenge myself. To my brother, Andrew, who has provided endless support, encouragement, and entertainment throughout the years. Most of all, this dissertation is dedicated to my wife, Angela. She has been with me every single day of this journey, and provided a constant source of love, happiness, and support. Without her, this would not have been possible.

TABLE OF CONTENTS

VITA

Education

University of California at Davis, 2006.
B.S. in Biotechnology, specialized in Fermentation & Microbiology.
Minor in Economics.
Awarded with High Honors.

Honors and Awards

- 2009-2011 Funded by NIH: Genetic Mechanisms Training Program
- 2013-2014 Dept. of MIMG, UCLA: Graduate Student Award
- 2013 Certificate of Entrepreneurship, UCLA Business of Science Center
- 2006 UC Davis, Citation for Outstanding Performance in the Department of Biotechnology
- 2006 UC Davis, High Honors in the College of Agricultural and Environmental Sciences
- 2002 Golden State Scholar

Mentoring and Teaching Experience

- 2013-Current Mentor, the Sheldon Biotechnology Academy's High-School eMentorship Program
- 2012- 2014 Research Mentor for MARC Undergraduate Research Fellow
- 2012 Research Mentor for AMGEN Scholars Research Fellow
- 2011-2012 Research Mentor for HHMI Undergraduate Research Fellow
- 2010 Course Teaching Assistant, LS 4: "Genetics." Dept. of Life Sciences
- 2009 Course Teaching Assistant, MIMG101: "Introductory Microbiology." Dept. of MIMG

National Conference Presentations

- Talk: Kinetoplastid Molecular Cell Biology Meeting, Marine Biological Laboratory in Woods Hole, MA (April 2015) *Identification and characterization of novel cAMP signaling systems within the flagellum of the sleeping sickness parasite Trypanosoma brucei*
- Talk: Southern California Eukaryotic Pathogen Symposium, UC Riverside (Nov. 2013) *Targeting and function of receptor-type adenylate cyclases in flagellum membrane sub-domains in T. brucei.*
- Poster: FASEB: Biology of Cilia and Flagella Conference, Niagara Falls, New York (June 2013) *Targeting and function of receptor-type adenylate cyclases in flagellum membrane sub-domains in procyclic T. brucei.*
- Poster: Southern California Eukaryotic Pathogen Symposium, UC Riverside (Nov. 2012) *Targeting of receptor-type adenylate cyclases to flagellum membrane sub-domains in procyclic T. brucei.*
- Poster: Kinetoplastid Molecular Cell Biology Meeting, Marine Biological Laboratory in Woods Hole, MA. (April 2011) *Targeting of receptor-type adenylate cyclases to flagellum membrane sub-domains in procyclic T. brucei.*

Intramural Presentations

- Talk: Parasitology Affinity Group Meeting, UCLA (Dec. 2012) *Targeting of receptor-type adenylate cyclases to flagellum membrane sub-domains in T. brucei.*
- Talk: Parasitology Affinity Group Meeting, UCLA (Nov. 2010) *Differential localization of receptor adenylate-cyclases in procyclic-form T. brucei.*
- Poster: Department of Microbiology Annual Conference, UCLA (Dec. 2012) *Targeting of receptor-type adenylate cyclases to flagellum membrane sub-domains in procyclic T. brucei.*

Publications

- **Saada EA**, Kabututu ZP, Lopez M, Shimogawa MM, Langousis G, Oberholzer M, Riestra A, Jonsson ZO, Wohlschlegel JA, Hill KL. 2014. Insect Stage-Specific Receptor Adenylate Cyclases Are Localized to Distinct Subdomains of the *Trypanosoma brucei* Flagellar Membrane. Eukaryotic Cell 13:1064-1076
  - This publication was "Spotlight Featured" by the Editors as an article of significant interest (13:949; doi:10.1128/EC.00156-14)
- **Saada EA**, Shimogawa MM, DeMarco, ST, Hill KL. 2014. Modulation of *Trypanosoma brucei* social behaviors requires flagellar sub-domain localization of receptor adenylate cyclases [Manuscript in preparation].
- **Saada EA,** DeMarco ST, Hill KL.. 2015. Social behaviors of *Trypanosoma brucei* [PLOS Pathogens Pearls: manuscript submitted]
- Oberholzer M, **Saada EA**, Hill KL. 2015. Cyclic AMP regulates social behavior in African trypanosomes. mBio 6(3):e01954-14. doi:10.1128/mBio.01954-14.
- Shimogawa MM, **Saada EA**, Vashisht AA, Barshop, WD, Wohlschlegel JA, Hill KL. 2015. Cell surface proteomics provides insight into stage-specific remodeling of the host parasite interface in *Trypanosoma brucei*. Molecular & Cellular Proteomics doi:10.1074/mcp.M114.045146
- Lopez MA, **Saada EA**, Hill KL. 2015. Insect stage-specific adenylate cyclases regulate social motility in African trypanosomes. Eukaryotic Cell. 14:104-112. Doi:10.1128/EC.00217-14
- Oberholzer M*, Langousis G**, Nguyen HT**, **Saada EA****, Shimogawa MM***, Jonsson ZO, Nguyen SM, Wohlschlegel JA, Hill KL. 2011. Independent analysis of the flagellum surface and matrix proteomes provides insight into flagellum signaling in mammalian-infectious *Trypanosoma brucei*. Mol Cell Proteomics 10:M111 010538.M
  - **equally credited as co-secondary authors
- Freire ER, Vashisht AA, Malvezzi AM, Zuberek J, Langousis G, **Saada EA**, Nascimento Jde F, Stepinski J, Darzynkiewicz E, Hill K, De Melo Neto OP, Wohlschlegel JA, Sturm NR, Campbell DA. 2014. eIF4F-like complexes formed by cap-binding homolog TbEIF4E5 with TbEIF4G1 or TbEIF4G2 are implicated in post-transcriptional regulation in *Trypanosoma brucei*. RNA 20:1272-1286.
- Freire ER, Malvezzi AM, Vashisht AA, Zuberek J, **Saada EA**, Langousis G, Nascimento JD, Moura D, Darzynkiewicz E, Hill K, de Melo Neto OP, Wohlschlegel JA, Sturm NR, Campbell DA. 2014. *Trypanosoma brucei* translation initiation factor homolog EIF4E6 forms a tripartite cytosolic complex with EIF4G5 and a capping enzyme homolog. Eukaryotic Cell 13:896-908.
  - This publication was "Spotlight Featured" by the Editors as an article of significant interest (13:549; doi:10.1128/EC.00078-14)

Chapter I:

Introduction

African trypanosomes and the Kinetoplasta

The Kinetoplastida are a class of flagellated protists, and are distinguished by the presence of a kinetoplast, which is a DNA-containing structure within the single mitochondrion. The order Trypanosomatida is comprised of kinetoplastid protozoans with only a single flagellum, the name being derived from the Greek words for "borer" (trypano) and "body" (soma), due to their cork-screw like movements (1).

The trypanosomatids are exclusively parasitic, living in a wide range of hosts, with several genera living in more than one host (2). Of these, there are several human-infectious species. These trypanosomatids are the etiological agents of three major diseases, which constitute a global public health problem (Figure 1-01) (3-7). *Leishmania spp.* are the causative agents of leishmaniasis. Depending on the species, this may present as a cutaneous, mucocutaenous, or visceral form of leishmanias. They are spread by various sandflies, which are the common name for various groups of bloodfeeding flies from the order Diptera. South American Trypanosomes, such as *Trypanosoma cruzi,* cause American Trypanosomiasis, colloquially known as Chagas disease. They're spread by bloodfeeding triatomine insects. African trypanosomes, such as *Trypanosoma brucei*, are the focus of this dissertation. They cause Human African Trypanosomiasis, colloquially known as sleeping sickness. They're transmitted by the bite of their bloodfeeding tsetse-fly vector.

Epidemiology and global impact

Collectively, these parasites are considered neglected diseases, and massively impact the developing world. They can be found throughout over 100 countries, mostly in tropical regions of the world. African trypanosomes are endemic to sub-Saharan Africa, as will be discussed later, while American trypanosomes are endemic to South and Central America. Leishmania can be divided into old and new-world species, and as such are found spanning several continents. These broad geographic ranges put nearly 500 million people at risk, with over 20 million people a year infected. This results in tens of thousands of human deaths annually, with incredibly large medical and economic impacts (Figure 1-01).

Many of these parasites were once considered under control, particularly in the 1960's and 70's, due to disease surveillance efforts and active prevention/eradication policies. However, negligence and abandonment of these policies resulted in resurgence of these parasitic diseases. Various reasons such as political turmoil and instability/war, lack of funding, and even the environmental movement of the 1960's, where public support over indiscriminate insecticide usage waned, have allowed many of these diseases to rise again to greater prominence.

Due to the nature of insect vectors, re-emergence often occurs in epidemic outbreaks. A classic example of this has been seen in Uganda, where Human African Trypanosomiasis was considered to be nearly eliminated thanks to proficient control

practices, with very few documented cases in the late 60's and early 70's (8). This changed in the early 1970's. A military coup put Dictator Idi Amin in charge of Uganda, leading to a decade of political unrest and civil warfare. It's estimated that 100,000 to 500,000 people died during his regime (9). Civil warfare sidelined anti-trypanosomal efforts, and coupled with rapidly crumbling infrastructure and decreasing availability of healthcare, conditions were ripe for a new epidemic. Uganda went an entire decade with less than 1,000 deaths attributed to sleeping sickness, to over 50,000 deaths spanning just a few years. It wasn't until the early 80's, after Amin's downfall, where new government and public health programs were re-established and control measures were re-taken, drastically reducing infectious rates (8). Unfortunately, the damage was already done: insects do not recognize or respect geopolitical boundaries. As such, there are two major consequences to outbreaks: first, trypanosomes were introduced into new districts and regions that were previously unaffected. Secondly, infection rates in neighboring countries raise, as the large influx of infectious insect vectors overwhelms existing infrastructure and control efforts (10). Similar events have been observed in several countries, causing outbreaks for all three trypanosomatid-derived diseases. These diseases reflect that decades of work can be undone by the breakage of a single, weak link. Therefore, it's essential to have a coordinated global effort, with unilateral support, dedicated to prevention, treatment, and control.

History of African trypanosomiasis

Human African Trypanosomiasis (HAT) is colloquially known as African sleeping sickness, and in humans is caused by two subspecies of *Trypanosoma brucei (11). T. b. rhodesiense* is found in eastern and southern Africa, and causes an acute form of the disease. *T. b. gambiense* is found through most of central and western Africa, and causes a long-term chronic infection. The clinical manifestations of the disease are virtually identical and described below, with the major difference between these two subspecies being the time frame (12-14). Acute trypanosomiasis progresses rapidly, leading to patient death within weeks to months and is thought to reflect a more recently evolved pathogen. In contrast, the chronic disease progresses slowly, leading to patient death within one to two years.

Sleeping sickness and Nagana, an animal wasting disease, were long known to be serious threats to the people of sub-Saharan Africa. Arabian geographers and traders would relay tales of their African travels to historians, leaving the oldest written accounts of these diseases. Descriptions around 1200AD described villages whose inhabitants had animal and livestock which were always “skin and bones and asleep” (15). The first recorded mention of sleeping sickness in humans is traced to noted historian, Ibn Khaldun, considered the founding father of sociology and historiography (16, 17). Ibn Khaldun wrote in his records the passing of a Sultan King: “He told me that Jata had been smitten by the sleeping illness, a disease which frequently afflicts the inhabitants of that climate, especially the chieftains who are

habitually affected by sleep. Those afflicted are virtually never awake or alert. The sickness harms the patient and continues until he perishes. He said that the illness persisted in Jata's humour for a duration of two years after which he died in the year [1373AD] (18)." Nearly 700 years later this remains a simple, yet accurate, description of the disease.

As with most infectious diseases, the causative agents remained unknown for a very long time. Trypanosomes were first identified in European fish and frogs in 1841/1842, but were not at the time suspected of being pathogens (19). It was not until the later part of the 1800's that scientists began to comprehend the true nature and impact of trypanosomes (11, 18, 20-22). In 1880, Griffith Evans, a veterinarian in India found trypanosomes in the blood of animals suffering from Surra, a wasting disease, providing the first evidence of pathogenesis by what became known as *Trypanosoma evansi* (23). Towards the end of the 1800's, medical scientists flocked to investigate debilitating illnesses in what is now South Africa. In 1895, David Bruce was the first to show that trypanosomes (*Trypanosoma brucei)* were the causative agent of Nagana in cattle. Several years later, in Gambia, Michael Forde examined the blood of a patient suffering from recurrent fevers, and noticed the presence of trypanosomes. This was the first link between the human disease and the similar animal diseases. The parasites were named *Trypanosoma gambiense,* later reclassified as *Trypanosoma brucei gambiense.* Over the following few years, dedicated medical and field research positively identified the insect vectors responsible for parasite transmission. Additionally, studies on patients with brain

abnormalities discovered the presence of trypanosomes within the cerebrospinal fluid. The discovery that trypanosomes can cross the blood-brain barrier began to answer the mysteries of the neural and cognitive dysfunction during trypanosomiasis.

Disease and treatment

Human African Trypanosomiasis can be divided into two distinct stages. Infection begins when parasites are transmitted into a mammalian host via the bite of a tsetse fly. Fly feeding behavior typically punctures several blood vessels, forming a subdermal pool of blood, and allowing trypanosomes an entry point from the subcutaneous tissue into the bloodstream. In a stage one infection, parasites survive and replicate extracellularly within the host's bloodstream. *T. brucei* is able to indefinitely evade the host immune response due to antigenic variation, as well as active recycling of the coat surface, reducing immunoglobulin effectiveness (24-26). Clinical manifestations of a stage-one infection include moderate to severe flu-like symptoms, with cyclical waves of fever. One distinctive feature is excessive swelling of the lymph nodes near the neck, known as Winterbottom's sign. It's important to note that despite being the first stage of infection, the disease is now already lethal if left untreated. Even in the first stage, many patients succumb to the septicemia, or blood infection, and additional clinical symptoms include immunosuppression, anemia, and related complications, and progression to a second-stage infection is inevitable (12, 27, 28).

Trypanosomiasis is considered to have reached a stage-two infection when parasites traverse across blood vessels in the brain, and now infect the central nervous system (29-32). This may happen within weeks for an acute infection strain, or several months for the chronic strains. In late stage infections, *T. brucei* will have additionally penetrated into several tissues or organs, although it remains extracellular at all times. Within the central nervous system, the parasite is now responsible for various neurologic disruptions. Patients have altered sleep-wake cycles, headaches, and eventually fall into a coma, from which they'll never recover. Due to the constant attack and overwhelming of the immune system, many patients succumb to secondary infections of other commensal or pathogenic microbes.

As a neglected disease, little focus has been put into developing pharmaceutical therapeutics against trypanosomiasis. Most of the front-line drugs are antiquated, difficult to administer, toxic, and increasingly ineffective as resistance mounts (33-36). It's critical to diagnose and treat patients before a secondary-stage infection could occur, as very few remaining therapeutic options are available. Several treatments are only effective against one subspecies, and due to difficulties in crossing the blood-brain barrier, are only useful for stage-one diseases. In fact, misdiagnosis and treatment with a stage-one therapeutic can be quite dangerous. Cerebral-spinal fluid acts as a safe haven, from which parasites can cross-back into the bloodstream, effectively causing a relapse of the disease. This highlights the need for both rapid, and accurate, clinical diagnosis.

Current front line drugs include pentamidine, which has been in use since the 1930's. This compound is administered by 10 deep muscle injections, and is only effective against stage-one *T. b. gambiense.* For *T. b. rhodesiense,* suramin has been used since 1922 for stage-one infections. Since the 1940's, the major front-line drug has been melarsoprol, that until 1990, was the only second-stage drug effective against both subspecies. Tragically, this compound is incredibly toxic, being an arsenic-based compound. 10 to 15% of patients undergo reactive encephalophies from treatment, and half of those suffer through a pulmonary edema and then death within 72 hours (37). Additionally, melarsoprol is administered intravenously, which is difficult to administer given the nature of the afflicted regions. Disturbingly, it's only soluble in propylene glycol, which makes intravenous administration extremely painful, where it also destroys the veins at site of injections, resulting in tissue damage.

The first beacon of hope in a long time was both a great success and a near tragedy (38-41). DFMO, known as eflornithine, was developed in the 1970's as an anti-cancer drug, but was ineffective and shelved. In the 1980's, the Gillette company discovered that DFMO had an interesting side effect: it's a potent inhibitor of hair growth. This resulted in the development and patenting of several chemical variants. By 1990, it was serendipitously discovered to be effective at treating trypanosomiasis, and remained effective even against pentamidine-resistant strains. In fact, it was hailed as the "resurrection drug" by the WHO, for its ability to save late-stage

patients. DFMO was produced for treatment of trypanosomiasis only for a few short years before being shelved, due to the exorbitant cost of production, and the utter lack of profitability from economically repressed sub-Saharan Africa. International ire was raised when production was re-initiated, not for anti-trypanosomal therapeutics but for Vaniqa, a new product targeted to prevent female facial-hair (42). Efforts by the WHO, Doctors without Borders, and humanitarian groups pushed for a partnership to allow for DFMO to be used for treatment of trypanosomiasis. In just five years, spanning 2001 to 2006, over 110,000 patients were treated. Unfortunately, resistance to DFMO has been growing, resulting in the need to continue administration of other more toxic compounds, such as melarsoprol (43). Therefore, there is a pressing need to better understand the biology of the parasite and develop new therapeutics.

Impact of trypanosomiasis on agriculture and development

In discussions of African trypanosomes, it is important that one consider them not as a symptom of poverty, but as a continuing cause of poverty (44-46). In addition to their massive impact on human health and productivity, agricultural development is seriously strained in endemic areas. Several strains of African trypanosomes, including the non-human infectious *T. congolense, T. vivax* and *T. b. brucei,* are able to infect various mammalian animals resulting in Nagana, a severe wasting disease. Many native African animals have some inherent resistance to trypanosomes, lessening the impact of Nagana, and are considered trypanotolerant (47-49). Although this has

prompted intense interest in the genetic basis of trypanotolerance, modern agricultural practices rarely use native livestock, preferring animals bred for specific characteristics. Therefore, agricultural expansion contributes to difficulties in controlling trypanosomiasis, as millions of livestock are raised in endemic areas. Non-native livestock serve as an extremely convenient food source for bloodfeeding tsetse flies, as well as an animal reservoir for trypanosomes.

Nagana-stricken animals are a major economic burden. These animals breed less often, produce less milk, offer less meat, and similar difficulties, yet consume plenty of resources. Coinciding with the epidemic outbreak of human trypanosomiasis above was a massive outbreak in Ugandan agriculture, in which millions of livestock died and millions more were culled (10, 50) . In recent decades, trypanosomal control methods have focused effort on misleading tsetse flies. Zimbabwe, for example, utilizes over 60,000 artificial cows. Pumped full of insecticides, but coated with bovine-odorants, these fake cows can trap bloodfeeding insects without the need for discriminate usage of environmental insecticides (51).

It is not surprising that numerous impact analyses have declared trypanosomes to be a very serious medical, and economic, burden on the developing world (44-46) . In 2006, the World Health Organization has declared that the control of these neglected zoonotic diseases is a route towards alleviating poverty in sub-Saharan Africa that must be taken, echoing the need for a concerted, global effort towards control and eradication (22).

There are many additional impacts of African trypanosomiasis that are lesser known. One facet is the major difficulty and risk posed to animal conservation programs. Africa has long been a destination for trophy hunting, and plagued with illegal poaching of animals, for products such as ivory horns or meat. In modern times, many African countries have dedicated animal reserves and game parks as safe havens for the protection and guardianship of rare and endangered wildlife. Rescue efforts involving relocation of animals, either to or from trypanosome endemic areas, must therefore be done with great caution.

One of the most unfortunate examples of conservation attempts gone awry due to trypanosomiasis involves the Northern White Rhinoceros (52). Over the last few decades, there were many attempts to conserve and breed this critically endangered species, either by captive-zoo breeding programs, or by protecting them from poachers in patrolled game reserves. In the early 80's, one such program involved relocation of a breeding group composed of five white rhinos, from a tsetse-free region to a game reserve endemic to tsetse flies and trypanosomes. Within several years, four of the five white rhinos succumbed to a mystery disease, diagnosed post-mortem as trypanosomiasis (53). Their chronic, trypanosomal-related health problems included several miscarriages, dealing a devastating setback to the effort to save the rhinoceros. Due to failure of captive zoo-breeding programs, ongoing illegal poaching, and trypanosomiasis, the northern white rhinoceros is anticipated to go extinct. As of June, 2015, there is only a single male and a handful of females left of their species

(54). At 42 years old, he has already surpassed the life-span of most wild rhinoceroses. "Sudan," the last of his species, is kept under armed guard day and night, to live out his remaining days in peace.

Life cycle of *Trypanosoma brucei*

African trypanosomes have a very complicated life cycle (Figure 1-02). As discussed earlier, trypanosomes are heteroxenous, requiring both an insect vector and a mammalian host to complete the life cycle. Parasites are injected into a mammalian host during the feeding of an infected tsetse fly, where parasites enter the bloodstream and replicate indefinitely. Although trypanosomes will eventually penetrate the blood brain barrier, only parasites in the bloodstream are accessible to tsetse flies, and eligible to able to continue the life cycle. In an established infection, a small percentage of bloodstream-form parasites differentiate into stumpy-form parasites, likely due to a quorum sensing mechanism (55-58). This is a growth-arrested stage, and it's suggested that stumpy parasites are preadapted for uptake into new, uninfected tsetse vectors during their inaugural bloodmeal.

Trypanosoma brucei ultimately colonizes two main regions of the fly, the midgut and salivary gland tissues, in a long and lengthy process (59-61). The tsetse fly bloodmeal, laden with stumpy-form parasites, is taken into the posterior end of the fly midgut. Here, the fly begins digestion of blood proteins, while the trypanosomes

differentiate into procyclic, or insect-midgut stage, forms. These parasites then proliferate within the gut, ultimately traversing the peritrophic membrane and establishing an infection within the ectoperitrophic space surrounding the midgut. *T. brucei* then performs a directed series of tissue tropisms, migrating through different organs and tissues until they ultimately reach the salivary gland. These migrations are accompanied by additional differentiation events, with different cellular morphology and protein expression. The salivary gland is the critical destination, where parasites form a tight attachment with the gland epithelial cells, triggering parasite differentiation into mammalian-infectious metacyclic forms. Metacyclic parasites freely move within the saliva into the next unassuming target of a tsetse bloodmeal, continuing the life cycle. Every step in this developmental pathway needs to be met, as failure to reach the salivary glands leads to a literal dead-end for *T. brucei.*

Sensory needs of *Trypanosoma brucei*

Trypanosomes, being heteroxenous, live a very complicated life cycle. In the mammalian host, trypanosomes are under constant threat and attack by the immune system. In the tsetse fly, the parasites must proliferate and migrate from the midgut, where the bloodmeal is stored, up to the salivary gland, as described earlier. The parasites must be able to interact with the external environment in both hosts, as each presents unique challenges and obstacles that must be accommodated for the parasite to be transmitted and cause pathogenesis (60, 62).

A critical, but poorly understood, aspect of host-parasite interactions is the parasite's cell surface, which is the direct interface with the host environment (Figure 1-03). Surface proteins must be responsible for nutrient uptake, sensing navigational and developmental cues, as well as impact pathogenesis, immune evasion, and resistance to therapeutics (63-65). Despite their importance, the proteins comprising the host-parasite interface remain mostly unknown and uncharacterized. It's long been known that bloodstream form parasites are dominated by a dense coat of variant surface glycoprotein (VSG) (66). VSG effectively shields other surface proteins from the host immune system, by blocking macromolecular access and is therefore thought to be one of the primary roadblocks preventing vaccine development. *T. brucei* VSG undergoes antigenic variation, by switching expression to alternate VSG genes, allowing the parasite to indefinitely evade the immune system (67). Antigenic variation of VSG is why a stage-one bloodstream infection is inevitably lethal without treatment, as VSG variants account for over 10% of the genome (68). Other life-stages are also known to be dominated by a singular surface coat, for example, the insect-stage parasites utilize procyclin. These major surface proteins are thought to be responsible for immune evasion, and are unlikely to contribute to the other essential parasite needs, such as nutrient uptake, navigation, and similar sensory inputs.

In their different environments, trypanosomes undergo extreme morphological changes (57). Presumably, these changes include remodeling of the parasite surface,

beyond the known exchanges of the major protein coats. Such remodeling would be required in order for the surface proteome to function as the dynamic host-parasite interface that is optimized for such different, hostile environments. In order to better understand the biology of the parasite and find candidate targets for therapeutic intervention, there's a pressing need to identify the *T. brucei* surface proteome. These works, and further discussion thereof, are the focus of Chapter II.

The flagellum: a multifunctional organelle

The trypanosome flagellum is one of the most prominent features of the parasite. First noted in 1841 as an "undulating membrane" (19), the single flagellum is attached along the length of the cell body, emerging from the posterior end of the cell. Trypanosomes have long been a model organism for structure and function analyses of the eukaryotic cilium (synonymous with flagellum), a highly conserved organelle (69-73). In trypanosomes, the flagellum is critical in parasite development, morphology, transmission, and pathogenesis. It's long been anticipated that, as a subset of the cell surface, the flagellum plays roles in signaling and sensing of the external environment.

In the last decade, extensive characterization of the eukaryotic cilium (synonymous with flagellum) has determined that they are multifunctional. In addition to well-defined roles in motility, they function as a signaling center acting

figuratively, and sometimes literally, as cellular antennae (Figure 1-04, (74-78). Flagella are a ubiquitous organelle, found in nearly every tissue type in mammals performing key mechano- and chemo-sensory functionalities. For example, our perception of light is due to photoreceptors in our eyes, which are really just modified flagella. Similarly, our sense of smell can be attributed to flagellated olfactory neurons. Specific signaling functions can be seen in the kidney, for example. Here, flagella function as mechanosensors, bending in the kidney ducts bend under fluid flow pressure, triggering polycystin-activation (79). These mechanosensitive ion-channels activate calcium-mediated signaling pathways via release of intracellular calcium. Flagella also function in many chemosensory pathways, such as in the hedgehog signaling pathway, which is well-defined for vertebrate development (80-83). The receptor protein Patched localizes to the flagellum, where it inhibits Smoothened. Upon binding of hedgehog-ligand, this inhibition is ceased, which allows for Smoothened to accumulate in the flagellar membrane. Smoothened is then able to activate the GLI transcription factors, reservoirs of which are near the flagellar tip in an inactive-state. Activated GLI is then trafficked out of the flagellum, and to the nucleus, where it activates transcription of the hedgehog target genes. The flagellum thereby acts as an antenna, and as such hedgehog signaling requires a complicated interplay between activation and trafficking of several flagellar proteins.

Any defects in structure of functional properties of the flagellum thereby can have massive effects on the cell or organism. In humans, there a wide range of heritable diseases, collectively termed ciliopathies (74, 84-86) Clinical manifestations

may include infertility, respiratory malfunction, polycystic kidney disease, retinopathies, polydactyl and assorted developmental defects, et cetera. Many known genetic abnormalities can be more easily studied in a model organism, such as *Trypanosoma brucei*, as will be discussed shortly.

Despite a rapidly increasing understanding of ciliopathies, the sensory role of the flagellum is not well established in eukaryotic pathogens. Many parasitic protozoa are flagellated, and in addition to the kinetoplastids this group includes parasites causing several serious infectious diseases, including malaria, trichimoniasis, and giardiasis (87-89). In *T. brucei*, the flagellum has long been suspected of playing important sensory roles (69-73). Attachment of the parasite to the tsetse salivary gland epithelium, which is required for differentiation into mammalian-infectious forms, is mediated by outgrowths of the flagellar membrane. In bloodstream-stage parasites, very few virulence factors have been positively identified, but all are flagellum associated. Recent efforts have attempted to define and characterize the composition of the trypanosome flagellum, in an effort to elucidate signaling and sensory pathways. Such works are the focus of Chapters III and IV.

Cyclic-nucleotide signaling systems

One of the best characterized signaling systems in flagellated organisms utilizes cyclic-AMP (cAMP), an important secondary messenger involved in many different

biological processes (90-92). cAMP binds to and regulates the function of many ion-channels, including those used in phototransduction and olfactory sensation signaling pathways. Production of cAMP is typically triggered by G-Protein Coupled Receptors (GPCRS), which bind various ligands and hormones and activate adenylate cyclases, which catalyze cAMP from ATP. cAMP can then activate PKA (protein kinase A), which will allow for phosphorylation of target substrates.

Perhaps owing to their early, eukaryotic lineage (93), trypanosomal cAMP signaling systems are very incredibly divergent from mammalian systems (94, 95). The trypanosomal homolog of PKA appears to be repressed, not activated, by cAMP. Furthermore, the trypanosome genome is devoid of any GPCRs and heterotrimeric G proteins, indicating that they must utilize other sensory inputs (68). Instead, trypanosomal ACs utilize a different protein domain structure than the canonical architecture of mammalian adenylate cyclases (65). Canonical ACs are multi-transmembrane-pass proteins that have two catalytic domains on a single polypeptide and lack direct receptor activity, relying instead on upstream GPCR signaling pathways. Trypanosomal ACs, on the other hand, have a singular catalytic domain connected by a transmembrane segment to a large, extracellular, putative ligand binding domain. The trypanosomal AC extracellular domain exhibits homology to bacterial periplasm binding proteins, which bind small ligands to direct chemotaxis and other cellular responses (95-97). Interestingly, ACs have been localized to the flagellum (98), which as discussed earlier, is a signaling organelle. Such an

arrangement therefore offers the ability to directly couple ligand-binding with direct signaling output, utilizing a single protein.

What makes adenylate cyclases a fascinating gene family is that they are vastly expanded specifically in *T. brucei* (Figure 1-05). Such an expansion has been postulated to accommodate various sensory needs in different, and species specific, host environments (99). To date, very few adenylate cyclases have been characterized, making this gene family an intriguing biological mystery. How does cAMP signaling function in *T. brucei*, and are ACs a major component of the host-parasite interface? Identification and functional characterization of adenylate cyclases and cAMP signaling systems comprise a major focus of this dissertation, and are discussed in depth in Chapters IV, V, and VI and Appendix I.

Social behaviors of *T. brucei*

Trypanosomes typically live most of their lifecycle on or near tissue surfaces, particularly in the tsetse-fly insect vector. As discussed, parasites must first colonize the tsetse-fly midgut before migrating to the salivary gland across several tissues. Within the salivary gland, attachment to the epithelium is required to trigger differentiation into mammalian-infectious forms. Despite the ubiquity of parasite-surface interactions during *T. brucei* transmission, studies of these organisms are almost exclusively conducted using axenic, *in vitro* suspension cultures (69). In many

microbes, it's known that exposure to surfaces induces developmental and behavioral changes (100). This paradigm, however, had not been explored in parasitic protozoa.

When cultured on surfaces, *Trypanosoma brucei* also engages in a collective, social behavior (Figure 1-06). Parasites initially assemble into small aggregates, which grow by clonal expansion and active recruitment of neighboring communities. Eventually, a large densely-packed colony is formed, from which groups of parasites migrate radially outwards, away from the center. This behavior was termed "social motility" due to analogies with bacterial systems (101, 102).

Studies of surface-exposure in other microbes have unveiled a broad range of responses, including quorum-sensing systems, biofilm formation, various types of swarming motility, and even differentiation events (103-108). In comparison to a strictly unicellular life cycle, social behaviors offer many advantages, including a competitive edge in nutrient acquisition, pathogenesis, and enhanced ability to colonize, penetrate, or migrate across surfaces. All of these processes may be similarly beneficial and relevant to the *T. brucei* life cycle, and are reviewed in Chapter VII.

Notably, mechanistic studies have uncovered a broad range of signaling systems, and considerable ingenuity has gone into the ability to co-opt these systems for the general public good. The most common example would be the development of antibiotics, which are generally a feature of microbial competition (109, 110). Many

bacteria secrete various polysaccharides or adhesion proteins to generate biofilms, and many of these are being considered for industrial usage (111, 112).

In all systems, collective social behaviors require the ability to sense and respond to external signals, allowing the community to coordinate their collective action (112-115). Studies of microbes demonstrate that there are many ways to achieve a common goal. For example, the social swarming bacteria *Paenibacillus spp.* utilizes a protease (116). *Myxococcus spp.* uses cell-cell contact, as well as extracellular signaling mechanisms (117-120).*Pseudomonas spp.* utilize rhamnolipids, which is distinct to their genera (121). Interestingly, detailed functional analyses of pseudomonads have revealed that cyclic-nucleotide signaling plays a regulatory role in control of biofilm and swarming motility (122, 123).

Trypanosomal social motility is therefore anticipated to be a rich source of novel biological function, and serves as an excellent system with which to assess the signaling capacity of insect-stage parasites. Such works comprise a large focus of this dissertation, and are discussed in depth in Chapters V, VI, VII, and Appendix I and II.

Trypanosoma brucei is an excellent experimental system and model organism

Trypanosomes are single-celled, protozoan pathogens. As the etiological agent of African trypanosomiasis, there is a pressing need to better understand the biology

of the parasite and develop new therapeutics. Due to dedicated efforts by many research groups over the last half century, trypanosomes have transitioned from field studies to controlled laboratory studies (Figure 1-07).

Two stages of the parasite, the bloodstream-stage and the procyclic-insect midgut stage, can be cultured axenically *in vitro.* This allows for convenient biochemical and physiological assessment, without the need for culturing mammalian or insect tissues, or maintaining animals. However, defined animal models are available, allowing for pathogenesis studies in rodents using both chronic and acute infectious strains. Tsetse-fly colonies can also be maintained within a laboratory setting, allowing for fly colonization and transmission studies.

Trypanosomes are amenable to most molecular genetic approaches, offering researchers a broad array of tools. As *Trypanosoma brucei* is amenable to transfection, as well as endogenously capable of homologous recombination, gene-targeting studies are routine. Using selectable drug-markers, one can generate strains containing gene knock-outs, knock-ins, gene replacements, or epitope-tagging proteins endogenously (69, 124, 125). *T. brucei* has homologues to the RISC complex, allowing for usage of targeted RNAi. Many laboratory strains have been modified to express a T7 polymerase and tetracycline-repressor, allowing the usage of stably-integrated, inducible systems (126-129).

In addition to their roles as pathogens, trypanosomes are also utilized as a model organism to study the eukaryotic flagellum, as discussed above. Several sub-species have been sequenced, and fully annotated genomes are available, allowing for rapid application of the above tools (68, 130). Annotated genomes opened the gates for trypanosomal researchers to use modern, cutting-edge systems level analyses. This includes RNA-sequencing and transcriptomics, quantitative proteomics, and can be used in conjunction with existing RNAi libraries, allowing for unbiased screens (131-134).

T. brucei serves as an excellent experimental system with a powerful suite of tools for molecular genetics and systems biology. These tools are used throughout all of the following works and chapters to further our understanding of the host-parasite interface and characterize signaling systems of *Trypanosoma brucei.*

FIGURES

Figure 1-01. Kinetoplastid parasites are a global public health problem

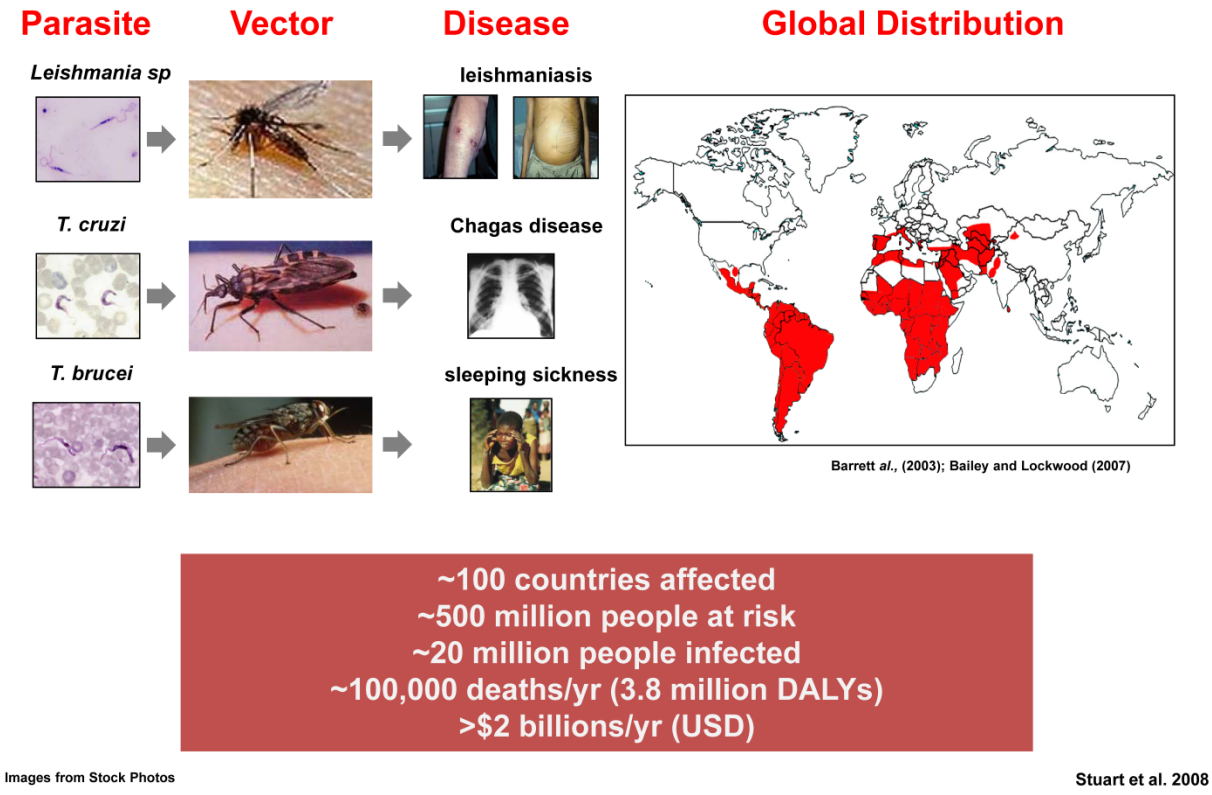

(Top-left) Three major diseases caused by kinetoplastid parasites and their insect vectors.

(Top-right) Global distribution of kinetoplastid parasites.

(Bottom) Summary table of the global impact of kinetoplastid parasites.

Figure 1-02. *Trypanosoma brucei* **life cycle**

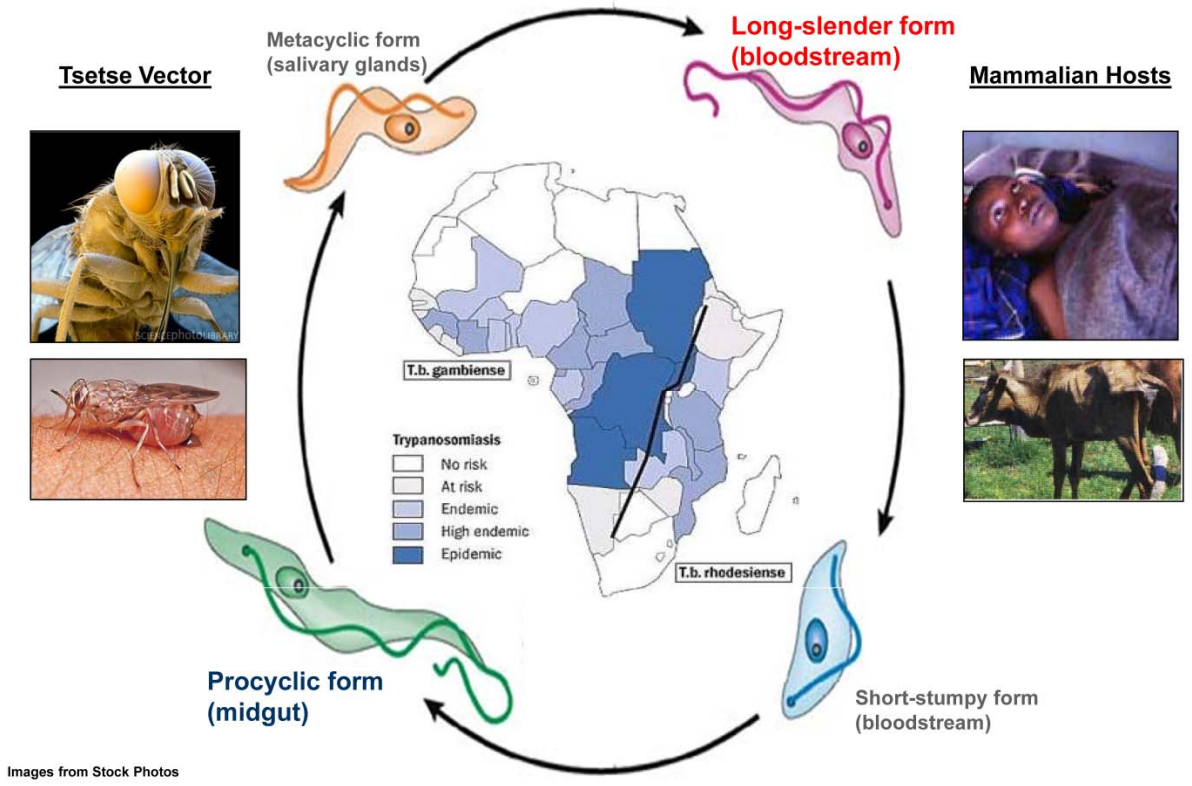

Trypanosoma brucei has a complicated life cycle, requiring both mammalian hosts (right), and tsetse-fly insect vectors (left). There are two subspecies which infect humans (center). *T. b. gambiense* causes a chronic infection and is found in central and western Africa, while *T. b. rhodesiense* causes an acute infection and is found in south-eastern Africa. The life-cycle image is modified from Lee *et al (135).* The map of Africa is courtesy of the WHO (22).

Figure 1-03. Parasite surface proteins are critical

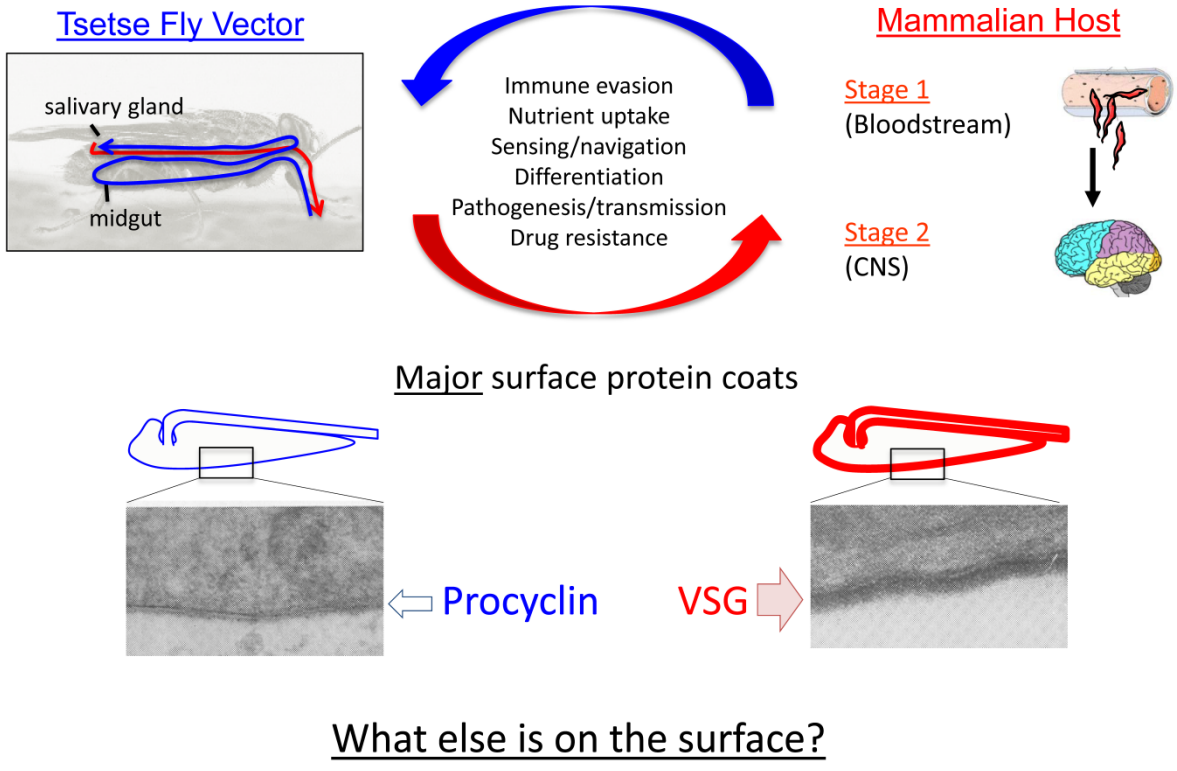

(Top) *T. brucei* lives in varied, host environments. Within the fly, it must migrate through several tissues, while in the mammalian host they eventually cross the blood-brain barrier. Parasite surface proteins are therefore critical for many functionalities, including nutrient uptake, immune evasion, and sensing/navigation (top-center). The *T. brucei* surface is mostly unknown, except for the major surface protein coats (bottom). Insect-stage parasites utilize procyclin, while bloodstream-stage parasites utilize variable surface glycoproteins, which form a thick layer blocking macromolecular access to the cell surface, as seen by electron microscopy cross-sections.

Figure 1-04. The eukaryotic flagellum is a sensory organelle

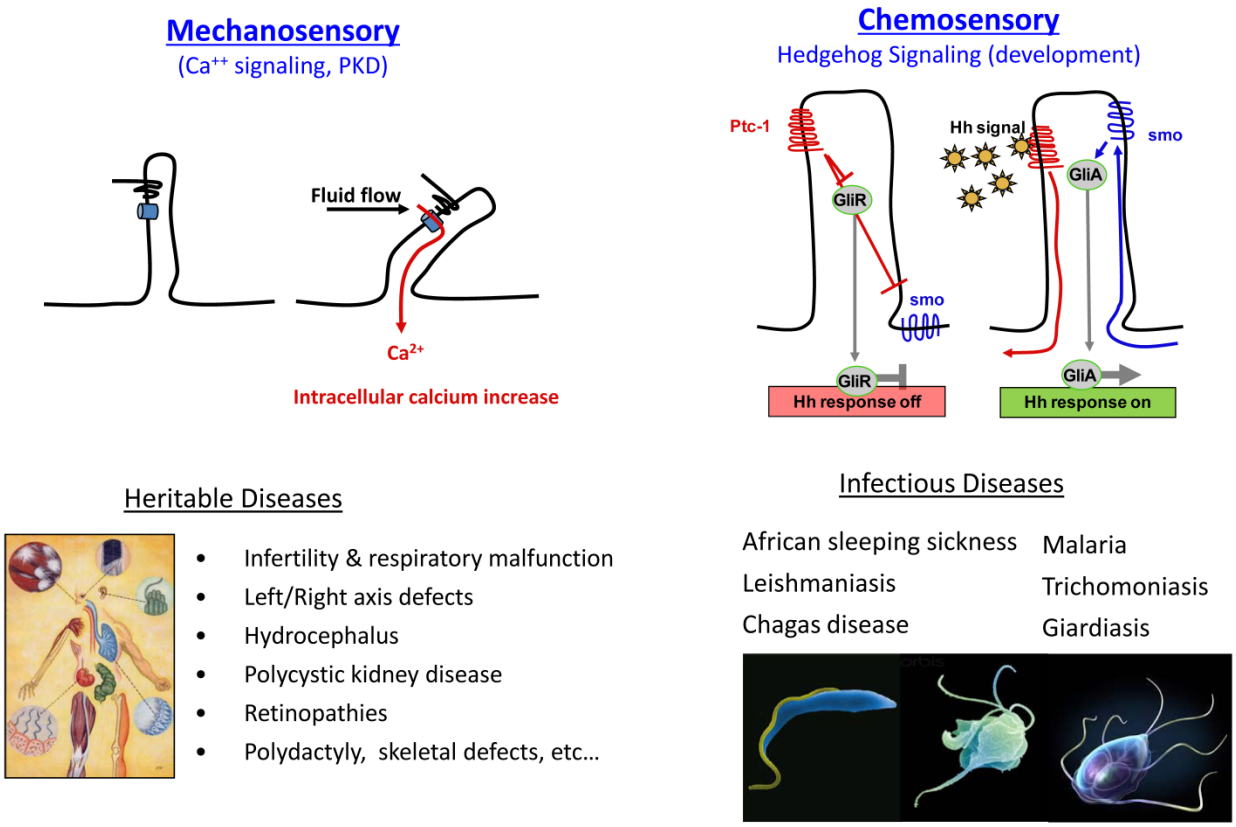

(Top) Schematics representing two major sensory inputs attributed to flagellum. Mechanosensory ion-channels, such as polycystin in kidney epithelial cells, trigger an influx of calcium when the flagellum bends under fluid flow. There are many chemosensory pathways, including hedgehog signaling, in which hedgehog-ligand binding induces trafficking of proteins into and out of the flagellum in order to direct a cellular response.

(Bottom left) Virtually all tissues in the human body have or can make a cilium (synonymous with flagellum). Defects in structure or functional capabilities result in a wide range of heritable diseases, collectively known as ciliopathies.

(Bottom right) Examples of infectious diseases that are the result of infection by flagellated, eukaryotic pathogens. Images are pseudo-colored scanning electron micrographs, or artistic representations of the parasites (from left to right) *Trypanosoma brucei, Trichomonas vaginalis,* and *Giardia lamblia.*

Figure 1-05.

The adenylate cyclase family size correlates with complexity of the parasite life cycle

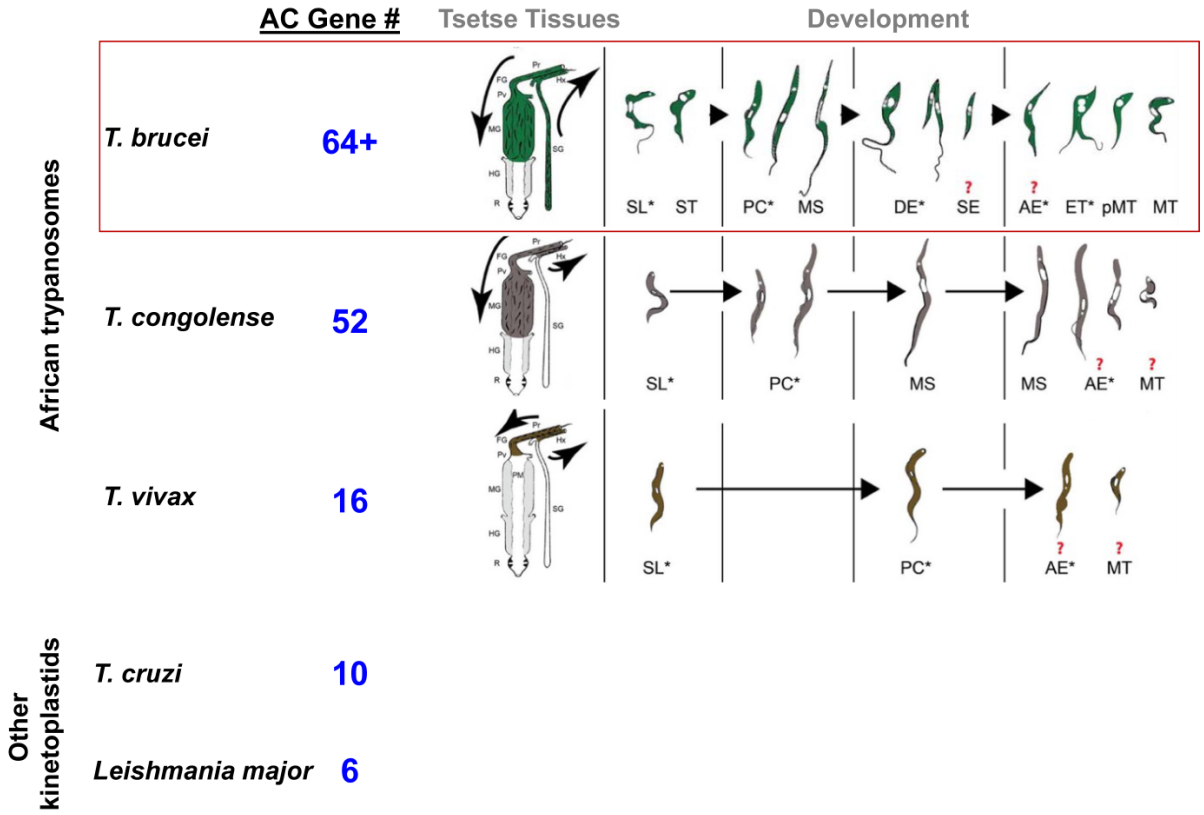

Expansion of the adenylate cyclase gene family is lineage-specific. Parasites with greater penetrance and colonization of tsetse tissues, and additional developmental forms, have greater number of adenylate cyclase paralogs. Taken together, this correlation suggests that ACs play stage-specific roles, particularly within the tsetse-fly vector. The tissue and development schematic (right) is adapted from Rotureau *et al*, 2013 (136).

Figure 1-06. Social motility requires sensing and cell-cell communication

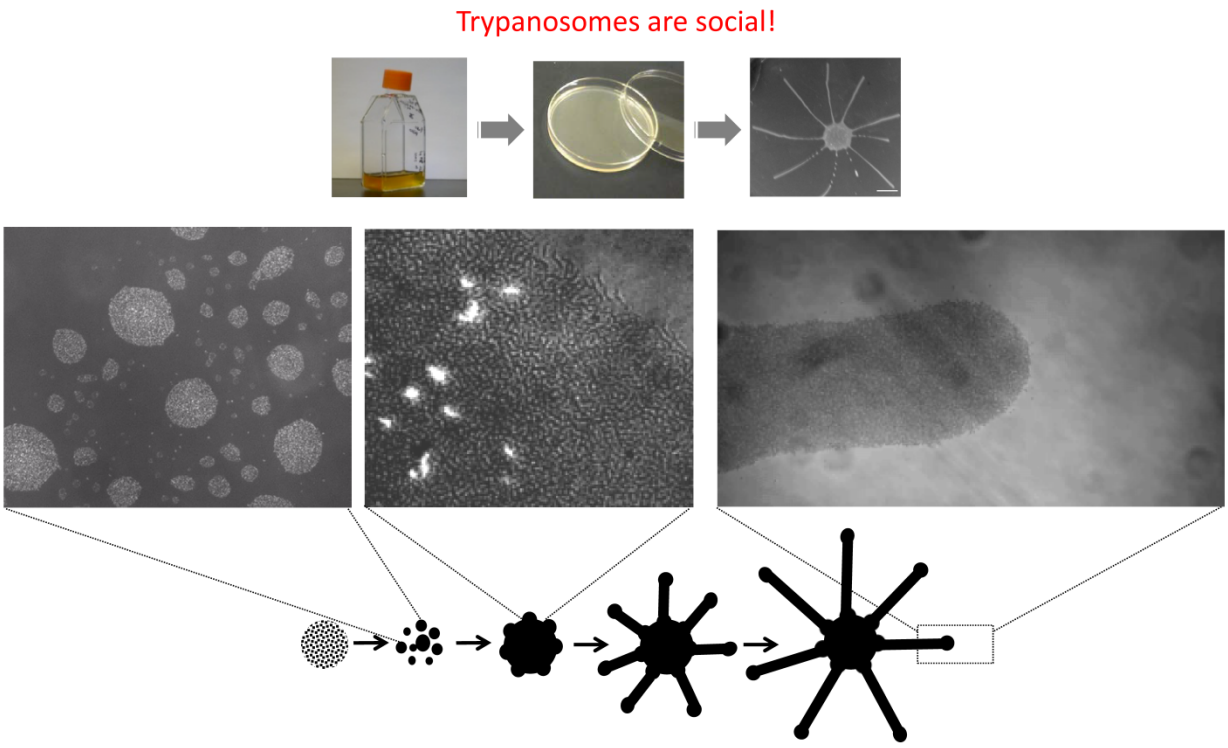

Although trypanosomes are typically grown in suspension culture, when inoculated on an agar surface, they perform social motility (top row). This social behavior is a several day process, and requires sensing and active response in order to fulfill. Parasites expand clonally, and actively aggregate into larger communities (left). Eventually, the parasites reach a densely packed colony. Using fluorescent reporter cells, parasites are free to move in all directions within the constraints of the colony (center). Eventually, nodes of highly concentrated cells emerge from the periphery, and parasites migrate *en masse* outwards across the surface (right).

Figure 1-07. *Trypanosoma brucei:* **an excellent experimental system**

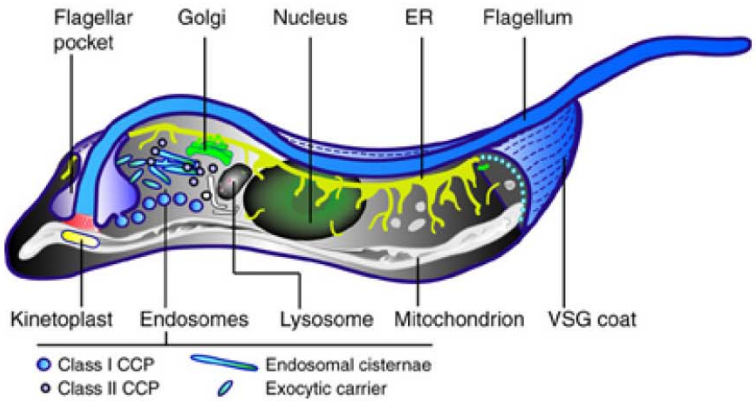

Powerful suite of tools for molecular genetics and systems biology

Cell Culture	Molecular Genetics	Systems Biology
• Fly stage	• Selectable markers	• Sequenced & Annotated
• Mammal stage	• Gene replacement	• Multiple species
• Axenic in defined medium	• Knockout/Knockin	• RNAi libraries
• Animal infection models	• Epitope-tagging	• Screens
	• Inducible expression	• RNA Seq
	• Inducible RNAi	• Quantitative Proteomics

(Top) A schematic of the eukaryotic pathogen, *Trypanosoma brucei*, highlighting several features and organelles. Of particular note is the kinetoplast, a DNA containing organelle that anchors the flagellum at the posterior end of the cell to the single mitochondrion. Schematic used courtesy of the Engstler laboratory webpage.

(Bottom) Table summarizing the available molecular tools and advantages of using *T. brucei* as an experimental system.

References

1. Gruby M. 1843. Recherches et observations sur une nouvelle espèce d'hématozoaire, Trypanosoma sanguinis. Comptes rendus hebdomadaire des séances de l'Académie des Sciences, Paris 17:1134-1136.
2. Simpson AG, Stevens JR, Lukes J. 2006. The evolution and diversity of kinetoplastid flagellates. Trends Parasitol 22:168-174.
3. Stuart K, Brun R, Croft S, Fairlamb A, Gurtler RE, McKerrow J, Reed S, Tarleton R. 2008. Kinetoplastids: related protozoan pathogens, different diseases. J Clin Invest 118:1301-1310.
4. Sileghem M, Flynn JN, Darji A, De Baetselier P, Naessens J. 1994. African Trypanosomiasis., p. 1-51. *In* Kierszenbaum F (ed.), Parasite infections and the immune system. Academic Press, Inc., San Diego, CA.
5. Bailey MS, Lockwood DN. 2007. Cutaneous leishmaniasis. Clin Dermatol 25:203-211.
6. Kirchhoff LV. 1999. American Trypanosomiasis (Chagas' Disease). *In* Guerrant R, Walker DH, Weller PF (ed.), Tropical Infectious Diseases: Principles, Pathogens and Practice., 1st ed, vol. 1. Churchill Livingstone, Philadelphia, PA.
7. Nussbaum K, Honek J, Cadmus CM, Efferth T. 2010. Trypanosomatid parasites causing neglected diseases. Curr Med Chem 17:1594-1617.
8. Berrang-Ford L, Odiit M, Maiso F, Waltner-Toews D, McDermott J. 2006. Sleeping sickness in Uganda: revisiting current and historical distributions. Afr Health Sci 6:223-231.

9. Ilman RH. 1978. Human Rights and Economic Power: The United States versus Idi Amin. Foreign Affairs 56:529-543.

10. Rutto JJ, Osano O, Thuranira EG, Kurgat RK, Odenyo VA. 2013. Socio-economic and cultural determinants of human african trypanosomiasis at the Kenya - Uganda transboundary. PLoS Negl Trop Dis 7:e2186.

11. Maudlin I. 2006. African trypanosomiasis. Ann Trop Med Parasitol 100:679-701.

12. Blum J, Schmid C, Burri C. 2006. Clinical aspects of 2541 patients with second stage human African trypanosomiasis. Acta Trop 97:55-64.

13. Welburn SC, Coleman PG, Maudlin I, Fevre EM, Odiit M, Eisler MC. 2006. Crisis, what crisis? Control of Rhodesian sleeping sickness. Trends Parasitol 22:123-128.

14. Welburn SC, Fevre EM, Coleman PG, Odiit M, Maudlin I. 2001. Sleeping sickness: a tale of two diseases. Trends Parasitol 17:19-24.

15. Kea RA. 2004. Expansions and contractions: World-Historical Change and the Western Sudan World-System (1200/1000 B.C. - 1200/1250A.D.). Journal of World-Systems Research 10:723-816.

16. Gates WE. 1967. The Spread of Ibn Khaldun's ideas on Climate and Culture. Journal of the History of Ideas 28:415-442.

17. Dhaouadi M. 1990. Ibn Khaldun: the Founding Father of Eastern Sociology. International Sociology 5:319-335.

18. Williams BI. 1996. African trypanosomiasis. The Wellcome Trust Illustrated History of Tropical Diseases:178-191.

19. Valentin GG. 1841. Uebr ein Entozoon im Blute von Salmo fario. Arch. Anat. Phys:435-436.

20. Steverding D. 2008. The history of African trypanosomiasis. Parasit Vectors 1:3.

21. Seed JR. 2001. African trypanosomiasis research: 100 years of progress, but questions and problems still remain. Int J Parasitol 31:434-442.

22. WHO. The World Health Organization. http://www.WHO.int.

23. Evans G. 1880. Report on "surra" disease in the Dera Ismail Khan District. Military Dept of Medicine.

24. Borst P. 2002. Antigenic variation and allelic exclusion. Cell 109:5-8.

25. Pays E. 2005. Regulation of antigen gene expression in Trypanosoma brucei. Trends Parasitol 21:517-520.

26. Baral TN. 2010. Immunobiology of African trypanosomes: need of alternative interventions. J Biomed Biotechnol 2010:389153.

27. Pepin J, Donelson JE. 1999. African trypanosomiasis (Sleeping Sickness), p. 774 - 784. *In* Guerrant R, Walker DH, Weller PF (ed.), Tropical Infectious Diseases: Principles, Pathogens and Practice., 1st ed, vol. 1. Churchill Livingstone, Philadelphia, PA.

28. Kennedy PG. 2007. Animal models of human African trypanosomiasis--very useful or too far removed? Trans R Soc Trop Med Hyg 101:1061-1062.

29. Tuomanen E. 1996. Entry of pathogens into the central nervous system. FEMS Microbiol Rev 18:289-299.

30. Enanga B, Burchmore RJ, Stewart ML, Barrett MP. 2002. Sleeping sickness and the brain. Cell Mol Life Sci 59:845-858.

31. Barragan A, Sibley LD. 2002. Transepithelial migration of Toxoplasma gondii is linked to parasite motility and virulence. J Exp Med 195:1625-1633.

32. Mulenga C, Mhlanga JD, Kristensson K, Robertson B. 2001. Trypanosoma brucei brucei crosses the blood-brain barrier while tight junction proteins are preserved in a rat chronic disease model. Neuropathol Appl Neurobiol 27:77-85.

33. Bacchi CJ. 2009. Chemotherapy of human african trypanosomiasis. Interdiscip Perspect Infect Dis 2009:195040.

34. Burchmore RJ, Ogbunude PO, Enanga B, Barrett MP. 2002. Chemotherapy of human African trypanosomiasis. Curr Pharm Des 8:256-267.

35. Fairlamb AH. 2003. Chemotherapy of human African trypanosomiasis: current and future prospects. Trends Parasitol 19:488-494.

36. Keiser J, Burri C, Stich A. 2001. New drugs for the treatment of human African trypanosomiasis: research and development. Parasitol Today 17:42-49.

37. Chappuis F. 2007. Melarsoprol-free drug combinations for second-stage Gambian sleeping sickness: the way to go. Clin Infect Dis 45:1443-1445.

38. Karbe E, Bottger M, McCann PP, Sjoerdsma A, Freitas EK. 1982. Curative effect of alpha-difluoromethylornithine on fatal Trypanosoma congolense infection in mice. Tropenmed Parasitol 33:161-162.

39. Pepin J, Milord F, Guern C, Schechter PJ. 1987. Difluoromethylornithine for arseno-resistant Trypanosoma brucei gambiense sleeping sickness. Lancet 2:1431-1433.

40. De Groof D, Bruneel H, Musumari TS, Ruppol JF. 1992. [Treatment of sleeping disease caused by trypanosoma brucei gambiense with alpha-

difluoromethylornithine (DFMO) in a rural hospital in Zaire]. Med Trop (Mars) 52:369-375.

41. Pepin J, Guern C, Milord F, Ethier L, Bokelo M, Schechter PJ. 1989. [The use of difluoromethylornithine in congenital trypanosomiasis due to Trypanosoma brucei-gambiense]. Med Trop (Mars) 49:83-85.

42. Hickman JG, Huber F, Palmisano M. 2001. Human dermal safety studies with eflornithine HCl 13.9% cream (Vaniqa), a novel treatment for excessive facial hair. Curr Med Res Opin 16:235-244.

43. Vincent IM, Creek D, Watson DG, Kamleh MA, Woods DJ, Wong PE, Burchmore RJ, Barrett MP. 2010. A molecular mechanism for eflornithine resistance in African trypanosomes. PLoS Pathog 6:e1001204.

44. Yamey G, Torreele E. 2002. The world's most neglected diseases. Bmj 325:176-177.

45. Jannin J, Simarro PP, Louis FJ. 2003. [The concept of neglected disease]. Med Trop (Mars) 63:219-221.

46. Fevre EM, Wissmann BV, Welburn SC, Lutumba P. 2008. The burden of human African trypanosomiasis. PLoS Negl Trop Dis 2:e333.

47. Trail JC, D'Ieteren GD, Teale AJ. 1989. Trypanotolerance and the value of conserving livestock genetic resources. Genome 31:805-812.

48. Murray M, Morrison WI, Whitelaw DD. 1982. Host susceptibility to African trypanosomiasis: trypanotolerance. Adv Parasitol 21:1-68.

49. Mattioli RC, Wilson RT. 1996. Trypanosomes, tsetse and trypanotolerance: coevolution in tropical Africa. Parassitologia 38:531-535.

50. Swallow BM. 2000. Impacts of trypanosomiasis on African agriculture. Afr Health Sci.

51. Ferriman A. 2001. Fake cows help to reduce sleeping sickness and use of insecticides. Bmj 323:711.

52. Groves CP, Fernando P, Robovsky J. 2010. The sixth rhino: a taxonomic re-assessment of the critically endangered northern white rhinoceros. PLoS One 5:e9703.

53. Penzhorn BL, Krecek, R.C., Horak, I.G., Verster, A.J.M., Walker, J.B., Boomker, J.D.F., Knapp, S.E., Quandt, S.K.F. 1994. Parasites of African Rhinos: a documentation. Proceedings of South Africa Symposium on Game Animals:1-242.

54. Jones J. 2015. "A picture of loneliness: youa re looking at the last male northern white rhino" The Guardian http://www.theguardian.com/commentisfree/2015/may/12/last-male-northern-white-rhino.

55. Reuner B, Vassella E, Yutzy B, Boshart M. 1997. Cell density triggers slender to stumpy differentiation of Trypanosoma brucei bloodstream forms in culture. Mol Biochem Parasitol 90:269-280.

56. Macgregor P, Matthews KR. 2010. New discoveries in the transmission biology of sleeping sickness parasites: applying the basics. J Mol Med (Berl).

57. Fenn K, Matthews KR. 2007. The cell biology of Trypanosoma brucei differentiation. Curr Opin Microbiol 10:539-546.

58. Vassella E, Reuner B, Yutzy B, Boshart M. 1997. Differentiation of African trypanosomes is controlled by a density sensing mechanism which signals cell cycle arrest via the cAMP pathway. J Cell Sci 110 (Pt 21):2661-2671.

59. Vickerman K, Tetley L, Hendry KA, Turner CM. 1988. Biology of African trypanosomes in the tsetse fly. Biol Cell 64:109-119.

60. Vickerman K. 1985. Developmental cycles and biology of pathogenic trypanosomes. Br Med Bull 41:105-114.

61. Welburn SC, Maudlin I. 1999. Tsetse-trypanosome interactions: rites of passage. Parasitol Today 15:399-403.

62. Muller N, Mansfield JM, Seebeck T. 1996. Trypanosome variant surface glycoproteins are recognized by self- reactive antibodies in uninfected hosts. Infect Immun 64:4593-4597.

63. Shimogawa MM, Saada EA, Vashisht AA, Barshop WD, Wohlschlegel JA, Hill KL. 2015. Cell surface proteomics provides insight into stage-specific remodeling of the host-parasite interface in Trypanosoma brucei. Mol Cell Proteomics.

64. Oberholzer M, Langousis G, Nguyen HT, Saada EA, Shimogawa MM, Jonsson ZO, Nguyen SM, Wohlschlegel JA, Hill KL. 2011. Independent analysis of the flagellum surface and matrix proteomes provides insight into flagellum signaling in mammalian-infectious Trypanosoma brucei. Mol Cell Proteomics 10:M111 010538.

65. Pays E, Nolan DP. 1998. Expression and function of surface proteins in Trypanosoma brucei. Mol Biochem Parasitol 91:3-36.

66. Cross GA, Holder AA, Allen G, Boothroyd JC. 1980. An introduction to antigenic variation in trypanosomes. Am J Trop Med Hyg 29:1027-1032.

67. Berriman M, Hall N, Sheader K, Bringaud F, Tiwari B, Isobe T, Bowman S, Corton C, Clark L, Cross GA, Hoek M, Zanders T, Berberof M, Borst P, Rudenko G. 2002. The architecture of variant surface glycoprotein gene expression sites in Trypanosoma brucei. Mol Biochem Parasitol 122:131-140.

68. Berriman M, Ghedin E, Hertz-Fowler C, Blandin G, Renauld H, Bartholomeu DC, Lennard NJ, Caler E, Hamlin NE, Haas B, Bohme U, Hannick L, Aslett MA, Shallom J, Marcello L, Hou L, Wickstead B, Alsmark UC, Arrowsmith C, Atkin RJ, Barron AJ, Bringaud F, Brooks K, Carrington M, Cherevach I, Chillingworth TJ, Churcher C, Clark LN, Corton CH, Cronin A, Davies RM, Doggett J, Djikeng A, Feldblyum T, Field MC, Fraser A, Goodhead I, Hance Z, Harper D, Harris BR, Hauser H, Hostetler J, Ivens A, Jagels K, Johnson D, Johnson J, Jones K, Kerhornou AX, Koo H, Larke N, Landfear S, Larkin C, Leech V, Line A, Lord A, Macleod A, Mooney PJ, Moule S, Martin DM, Morgan GW, Mungall K, Norbertczak H, Ormond D, Pai G, Peacock CS, Peterson J, Quail MA, Rabbinowitsch E, Rajandream MA, Reitter C, Salzberg SL, Sanders M, Schobel S, Sharp S, Simmonds M, Simpson AJ, Tallon L, Turner CM, Tait A, Tivey AR, Van Aken S, Walker D, Wanless D, Wang S, White B, White O, Whitehead S, Woodward J, Wortman J, Adams MD, Embley TM, Gull K, Ullu E, Barry JD, Fairlamb AH, Opperdoes F, Barrell BG, Donelson JE, Hall N, Fraser CM, Melville SE, El-Sayed NM. 2005. The genome of the African trypanosome Trypanosoma brucei. Science 309:416-422.

69. Oberholzer M, Lopez MA, Ralston KS, Hill KL. 2009. Approaches for functional analysis of flagellar proteins in African trypanosomes. Methods in Cell Biology 93:21-57.

70. Branche C, Kohl L, Toutirais G, Buisson J, Cosson J, Bastin P. 2006. Conserved and specific functions of axoneme components in trypanosome motility. J Cell Sci 119:3443-3455.

71. Gadelha C, Wickstead B, Gull K. 2007. Flagellar and ciliary beating in trypanosome motility. Cell Motil Cytoskeleton 64:629-643.

72. Ralston KS, Hill KL. 2008. The flagellum of Trypanosoma brucei: new tricks from an old dog. Int J Parasitol 38:869-884.

73. Kohl L, Bastin P. 2005. The flagellum of trypanosomes. Int Rev Cytol 244:227-285.

74. Calvet JP. 2003. Ciliary signaling goes down the tubes. Nat Genet 33:113-114.

75. Pan J, Wang Q, Snell WJ. 2005. Cilium-generated signaling and cilia-related disorders. Lab Invest 85:452-463.

76. Satir P, Christensen ST. 2007. Overview of structure and function of mammalian cilia. Annu Rev Physiol 69:377-400.

77. Berbari NF, O'Connor AK, Haycraft CJ, Yoder BK. 2009. The primary cilium as a complex signaling center. Current Biology 19:R526-535.

78. Singla V, Reiter JF. 2006. The primary cilium as the cell's antenna: signaling at a sensory organelle. Science 313:629-633.

79. Nauli SM, Alenghat FJ, Luo Y, Williams E, Vassilev P, Li X, Elia AE, Lu W, Brown EM, Quinn SJ, Ingber DE, Zhou J. 2003. Polycystins 1 and 2 mediate mechanosensation in the primary cilium of kidney cells. Nat Genet 33:129-137.

80. Huangfu D, Liu A, Rakeman AS, Murcia NS, Niswander L, Anderson KV. 2003. Hedgehog signalling in the mouse requires intraflagellar transport proteins. Nature 426:83-87.

81. Goetz SC, Anderson KV. 2010. The primary cilium: a signalling centre during vertebrate development. Nat Rev Genet 11:331-344.

82. Kim J, Kato M, Beachy PA. 2009. Gli2 trafficking links Hedgehog-dependent activation of Smoothened in the primary cilium to transcriptional activation in the nucleus. Proc Natl Acad Sci U S A 106:21666-21671.

83. Huangfu D, Anderson KV. 2006. Signaling from Smo to Ci/Gli: conservation and divergence of Hedgehog pathways from Drosophila to vertebrates. Development 133:3-14.

84. Sharma N, Berbari NF, Yoder BK. 2008. Ciliary dysfunction in developmental abnormalities and diseases. Curr Top Dev Biol 85:371-427.

85. Yuan S, Sun Z. 2013. Expanding Horizons: Ciliary Proteins Reach Beyond Cilia. Annu Rev Genet.

86. Tobin JL, Beales PL. 2009. The nonmotile ciliopathies. Genet Med 11:386-402.

87. Ghosh S, Frisardi M, Rogers R, Samuelson J. 2001. How Giardia swim and divide. Infect Immun 69:7866-7872.

88. de Miguel N, Riestra A, Johnson PJ. 2012. Reversible association of tetraspanin with Trichomonas vaginalis flagella upon adherence to host cells. Cell Microbiol 14:1797-1807.

89. Sinden RE, Talman A, Marques SR, Wass MN, Sternberg MJ. 2010. The flagellum in malarial parasites. Curr Opin Microbiol 13:491-500.

90. Conti M, Mika D, Richter W. 2014. Cyclic AMP compartments and signaling specificity: role of cyclic nucleotide phosphodiesterases. J Gen Physiol 143:29-38.

91. Green J, Stapleton MR, Smith LJ, Artymiuk PJ, Kahramanoglou C, Hunt DM, Buxton RS. 2014. Cyclic-AMP and bacterial cyclic-AMP receptor proteins revisited: adaptation for different ecological niches. Curr Opin Microbiol 18:1-7.

92. Fajardo AM, Piazza GA, Tinsley HN. 2014. The role of cyclic nucleotide signaling pathways in cancer: targets for prevention and treatment. Cancers (Basel) 6:436-458.

93. He D, Fiz-Palacios O, Fu CJ, Fehling J, Tsai CC, Baldauf SL. 2014. An alternative root for the eukaryote tree of life. Curr Biol 24:465-470.

94. Seebeck T, Schaub R, Johner A. 2004. cAMP signalling in the kinetoplastid protozoa. Curr Mol Med 4:585-599.

95. Seebeck T, Gong K, Kunz S, Schaub R, Shalaby T, Zoraghi R. 2001. cAMP signalling in Trypanosoma brucei. Int J Parasitol 31:491-498.

96. Alexandre S, Paindavoine P, Tebabi P, Pays A, Halleux S, Steinert M, Pays E. 1990. Differential expression of a family of putative adenylate/guanylate cyclase genes in Trypanosoma brucei. Mol Biochem Parasitol 43:279-288.

97. Felder CB, Graul RC, Lee AY, Merkle HP, Sadee W. 1999. The Venus flytrap of periplasmic binding proteins: an ancient protein module present in multiple drug receptors. AAPS PharmSci 1:E2.

98. Paindavoine P, Rolin S, Van Assel S, Geuskens M, Jauniaux JC, Dinsart C, Huet G, Pays E. 1992. A gene from the variant surface glycoprotein expression site encodes one of several transmembrane adenylate cyclases located on the flagellum of Trypanosoma brucei. Mol Cell Biol 12:1218-1225.

99. Saada EA, Kabututu ZP, Lopez M, Shimogawa MM, Langousis G, Oberholzer M, Riestra A, Jonsson ZO, Wohlschlegel JA, Hill KL. 2014. Insect stage-specific receptor adenylate cyclases are localized to distinct subdomains of the Trypanosoma brucei Flagellar membrane. Eukaryot Cell 13:1064-1076.

100. Irie Y, Parsek MR. 2008. Quorum sensing and microbial biofilms. Curr Top Microbiol Immunol 322:67-84.

101. Oberholzer M, Lopez MA, McLelland BT, Hill KL. 2010. Social motility in african trypanosomes. PLoS Pathog 6:e1000739.

102. Lopez MA, Nguyen HT, Oberholzer M, Hill KL. 2011. Social parasites. Curr Opin Microbiol 14:642-648.

103. Fraser GM, Hughes C. 1999. Swarming motility. Curr Opin Microbiol 2:630-635.

104. Ingham CJ, Ben Jacob E. 2008. Swarming and complex pattern formation in Paenibacillus vortex studied by imaging and tracking cells. BMC Microbiol 8:36.

105. Kaiser D. 2007. Bacterial swarming: a re-examination of cell-movement patterns. Curr Biol 17:R561-570.

106. Rauprich O, Matsushita M, Weijer CJ, Siegert F, Esipov SE, Shapiro JA. 1996. Periodic phenomena in Proteus mirabilis swarm colony development. Journal of Bacteriology 178:6525-6538.

107. Shapiro JA. 1998. Thinking about bacterial populations as multicellular organisms. Annu Rev Microbiol 52:81-104.

108. Velicer GJ, Yu YT. 2003. Evolution of novel cooperative swarming in the bacterium Myxococcus xanthus. Nature 425:75-78.

109. Whiteley M, Bangera MG, Bumgarner RE, Parsek MR, Teitzel GM, Lory S, Greenberg EP. 2001. Gene expression in Pseudomonas aeruginosa biofilms. Nature 413:860-864.

110. Duerkop BA, Varga J, Chandler JR, Peterson SB, Herman JP, Churchill ME, Parsek MR, Nierman WC, Greenberg EP. 2009. Quorum-sensing control of antibiotic synthesis in Burkholderia thailandensis. Journal of bacteriology 191:3909-3918.

111. Rainey PB, Rainey K. 2003. Evolution of cooperation and conflict in experimental bacterial populations. Nature 425:72-74.

112. West S.A. DSP, Buckling A., Gardner A., Griffin A.S. 2007. The Social Lives of Microbes. Annual Review of Ecology, Evolution, and Systematics 38:53-77.

113. Shrout JD, Tolker-Nielsen T, Givskov M, Parsek MR. 2011. The contribution of cell-cell signaling and motility to bacterial biofilm formation. MRS Bull 36:367-373.

114. Parsek MR, Greenberg EP. 2005. Sociomicrobiology: the connections between quorum sensing and biofilms. Trends Microbiol 13:27-33.

115. Kaiser D. 2003. Coupling cell movement to multicellular development in myxobacteria. Nat Rev Microbiol 1:45-54.

116. Be'er A, Ariel G, Kalisman O, Helman Y, Sirota-Madi A, Zhang HP, Florin EL, Payne SM, Ben-Jacob E, Swinney HL. 2010. Lethal protein produced in response to competition between sibling bacterial colonies. Proc Natl Acad Sci U S A 107:6258-6263.

117. Zusman DR, Scott AE, Yang Z, Kirby JR. 2007. Chemosensory pathways, motility and development in Myxococcus xanthus. Nat Rev Microbiol 5:862-872.

118. Welch R, Kaiser D. 2001. Cell behavior in traveling wave patterns of myxobacteria. Proc Natl Acad Sci U S A 98:14907-14912.

119. Ward MJ, Zusman DR. 1997. Regulation of directed motility in Myxococcus xanthus. Mol Microbiol 24:885-893.

120. Nudleman E, Wall D, Kaiser D. 2005. Cell-to-cell transfer of bacterial outer membrane lipoproteins. Science 309:125-127.

121. Caiazza NC, Shanks RM, O'Toole GA. 2005. Rhamnolipids modulate swarming motility patterns of Pseudomonas aeruginosa. Journal of bacteriology 187:7351-7361.

122. Merritt JH, Brothers KM, Kuchma SL, O'Toole GA. 2007. SadC reciprocally influences biofilm formation and swarming motility via modulation of exopolysaccharide production and flagellar function. J Bacteriol 189:8154-8164.

123. Kuchma SL, Brothers KM, Merritt JH, Liberati NT, Ausubel FM, O'Toole GA. 2007. BifA, a cyclic-Di-GMP phosphodiesterase, inversely regulates biofilm formation and swarming motility by Pseudomonas aeruginosa PA14. J Bacteriol 189:8165-8178.

124. Oberholzer M, Morand S, Kunz S, Seebeck T. 2006. A vector series for rapid PCR-mediated C-terminal in situ tagging of Trypanosoma brucei genes. Mol Biochem Parasitol 145:117-120.

125. Biebinger S, Wirtz LE, Lorenz P, Clayton C. 1997. Vectors for inducible expression of toxic gene products in bloodstream and procyclic *Trypanosoma brucei.* Molecular & Biochemical Parasitology 85:99-112.

126. Shi H, Djikeng A, Mark T, Wirtz E, Tschudi C, Ullu E. 2000. Genetic interference in Trypanosoma brucei by heritable and inducible double-stranded RNA. Rna 6:1069-1076.

127. Wirtz E, Clayton C. 1995. Inducible gene expression in trypanosomes mediated by a prokaryotic repressor. Science 268:1179-1183.

128. Wirtz E, Leal S, Ochatt C, Cross GA. 1999. A tightly regulated inducible expression system for conditional gene knock-outs and dominant-negative genetics in *Trypanosoma brucei*. Mol. Biochem. Parasitol. 99:89-101.

129. Morris JC, Wang Z, Drew ME, Paul KS, Englund PT. 2001. Inhibition of bloodstream form Trypanosoma brucei gene expression by RNA interference using the pZJM dual T7 vector. Mol Biochem Parasitol 117:111-113.

130. Aslett M, Aurrecoechea C, Berriman M, Brestelli J, Brunk BP, Carrington M, Depledge DP, Fischer S, Gajria B, Gao X, Gardner MJ, Gingle A, Grant G, Harb

OS, Heiges M, Hertz-Fowler C, Houston R, Innamorato F, Iodice J, Kissinger JC, Kraemer E, Li W, Logan FJ, Miller JA, Mitra S, Myler PJ, Nayak V, Pennington C, Phan I, Pinney DF, Ramasamy G, Rogers MB, Roos DS, Ross C, Sivam D, Smith DF, Srinivasamoorthy G, Stoeckert CJ, Jr., Subramanian S, Thibodeau R, Tivey A, Treatman C, Velarde G, Wang H. 2009. TriTrypDB: a functional genomic resource for the Trypanosomatidae. Nucleic Acids Res 38:D457-462.

131. Morris JC, Wang Z, Drew ME, Englund PT. 2002. Glycolysis modulates trypanosome glycoprotein expression as revealed by an RNAi library. Embo J 21:4429-4438.

132. Baker N, Alsford S, Horn D. 2011. Genome-wide RNAi screens in African trypanosomes identify the nifurtimox activator NTR and the eflornithine transporter AAT6. Mol Biochem Parasitol 176:55-57.

133. Drew ME, Morris JC, Wang Z, Wells L, Sanchez M, Landfear SM, Englund PT. 2003. The adenosine analog tubercidin inhibits glycolysis in Trypanosoma brucei as revealed by an RNA interference library. J Biol Chem 278:46596-46600.

134. Schumann Burkard G, Jutzi P, Roditi I. 2011. Genome-wide RNAi screens in bloodstream form trypanosomes identify drug transporters. Mol Biochem Parasitol 175:91-94.

135. Lee SH, Stephens JL, Englund PT. 2007. A fatty-acid synthesis mechanism specialized for parasitism. Nat Rev Microbiol 5:287-297.

136. Rotureau B, Van Den Abbeele J. 2013. Through the dark continent: African trypanosome development in the tsetse fly. Front Cell Infect Microbiol 3:53.

Chapter II:

Cell surface proteomics provides insight into stage-specific remodeling of the host-parasite interface in *Trypanosoma brucei*

PREFACE

The following chapter is a modified version of "Cell surface proteomics provides insight into stage-specific remodeling of the host-parasite interface in *Trypanosoma brucei,"* by Shimogawa *et* al, originally accepted for publication in Molecular and Cellular Proteomics in 2015, doi:10.1074/mcp.M114.045146, and reprinted with permission.

In this work, we utilized surface protein labeling, combined with affinity purification and shotgun proteomics, to describe the surface proteomes of trypanosomes from the mammalian bloodstream and tsetse fly midgut stages. Results uncover proteins important for host-parasite interactions and reveal extensive remodeling between the parasite life-cycle stages. As second author, I contributed significantly to this manuscript. I was involved in discussions and planning of experiments, and contributed to writing of the manuscript. Specific experimental contributions include various bioinformatics analyses of the large datasets (phylogeny, cross-comparison to existing transcriptomic data sets, etc), performing the qRT-PCR analyses, and general technical assistance.

SUMMARY

African trypanosomes are devastating human and animal pathogens transmitted by tsetse flies between mammalian hosts. The trypanosome surface forms a critical host interface that is essential for sensing and adapting to diverse host environments. However, trypanosome surface protein composition and diversity remain largely unknown. Here, we use surface labeling, affinity purification and proteomic analyses to describe cell surface proteomes from insect-stage and mammalian bloodstream-stage *Trypanosoma brucei*. The cell surface proteomes contain most previously characterized surface proteins. We additionally identify a substantial number of novel proteins, whose functions are unknown, indicating the parasite surface proteome is larger and more diverse than generally appreciated. We also demonstrate stage-specific expression for individual paralogues within several protein families, suggesting that fine-tuned remodeling of the parasite surface allows adaptation to diverse host environments, while still fulfilling universally essential cellular needs. Our surface proteome analyses complement existing transcriptomic, proteomic and *in silico* analyses by highlighting proteins that are surface-exposed and thereby provide a major step forward in defining the host-parasite interface.

INTRODUCTION

Parasitic protozoa afflict nearly one billion people worldwide and constitute a substantial global public health burden. Owing to infection of livestock and crop plants, protozoa also cause economic hardship and limit development in some of the most impoverished regions of the world. A critical but poorly understood aspect of parasite-host interactions is the parasite cell surface, which is the direct interface with the host environment. Parasite surface proteins function in attachment and invasion of host tissues, defense against host attack and uptake of essential nutrients (1). For many parasites, transmission between human hosts occurs through invertebrate vectors and intermediate hosts, requiring that the surface proteome be sufficiently flexible to accommodate diverse extracellular environments.

The protozoan parasite *Trypanosoma brucei* causes lethal sleeping sickness in humans and nagana in cattle, which together impose a tremendous medical and economic burden across sub-Saharan Africa. There is no vaccine for sleeping sickness and current treatments are antiquated, toxic and increasingly ineffective (2). Transmission between mammalian hosts occurs through the bite of a tsetse fly vector and *T. brucei* is extracellular throughout all stages of its life cycle. Therefore, a dynamic and multifunctional surface proteome is paramount for *T. brucei* survival, transmission and pathogenesis (3-5).

In the mammalian host, *T. brucei* replicates indefinitely in the bloodstream, where surface proteins must continuously protect against attacks from the host immune system and simultaneously compete with host cells for uptake of essential nutrients (6). The surface of bloodstream-form parasites is dominated by a dense coat of variant surface glycoprotein (VSG), which shields other parasite surface proteins from host antibodies and allows evasion of the immune system through antigenic variation (7-9). Upon uptake during a tsetse fly bloodmeal, the parasites undergo a dramatic differentiation, marked by pronounced changes in cell morphology and metabolism and replacement of VSG with a surface coat of procyclin (10). The resulting procyclic-form parasites establish an infection in the fly midgut. Parasites then migrate from the midgut to the salivary glands and undergo several further differentiations, including modification of procyclin isoforms and acquisition of a surface coat of "*brucei* alanine-rich proteins" (BARPs) (11-14). Upon establishing a salivary gland infection, parasites undergo a final differentiation into mammalian-infectious forms that reacquire a VSG coat in preparation for transmission to a new host. Remodeling of major surface proteins between life cycle stages reflects the parasite's need to adapt to varied and generally hostile host environments (4, 15). In addition to the major surface proteins discussed above, less abundant surface proteins are responsible for sensation of signals that direct tissue-specific differentiation events crucial for infection chronicity and transmission (16-20).

Beyond their role in host-parasite interaction, *T. brucei* surface proteins are directly relevant for therapeutic intervention, impacting nearly all currently available

drug treatments. For example, cell surface transporters mediate uptake of pentamidine and melarsoprol, two of the frontline drugs used to treat bloodstream and central nervous system infections, respectively (21-23). Mutations in these surface transporters cause naturally occurring drug resistance in field isolates (24-26), underscoring the clinical relevance of parasite surface proteome composition and function.

Despite its importance to transmission and pathogenesis, the *T. brucei* surface protein repertoire remains largely unknown, presenting a major gap in our understanding of parasite biology and host-parasite interactions. Here, we utilize surface biotinylation, coupled with affinity purification and shotgun proteomics (27, 28), to obtain cell surface proteomes from procyclic (insect midgut) and bloodstream-form *T. brucei*. We identify many proteins not previously known to be surface exposed, indicating great diversity of proteins that function at the host-parasite interface. Comparison of surface proteomes from procyclic and bloodstream forms reveals extensive stage-specific surface protein remodeling that includes individual paralogues within protein families. As such, our studies suggest that the surface proteome is larger and more diverse than generally appreciated and that fine-tuned remodeling enables adaptation to different host environments, while still accommodating universally essential cellular needs.

EXPERIMENTAL PROCEDURES

Cell lines

427-derived bloodstream form trypanosomes, 221 single marker cell line, and procyclic form, 2913 cell line were cultivated as described (29).

Purification of biotinylated proteins and VSG depletion

Surface biotinylation with sulfo-NHS-SS-biotin (Pierce) and purification of biotinylated proteins was done as described (27, 28), with the exception that flagella were not removed. 1-5x10^8 cells were washed twice in phosphate buffered saline (PBS) and resuspended in PBS + 0.5 mg/ml Sulfo-NHS-SS-biotin (Pierce) for 10 min on ice. Unreacted biotin was blocked by addition of 100 mM Tris for 10 min on ice, followed by two washes in PBS + 100 mM Tris. Purification of biotinylated proteins was performed as described (28). Briefly, cells were lysed in PBS + 0.5% NP-40 + SigmaFAST EDTA-free protease inhibitors (Sigma) for 10 min on ice. Soluble and insoluble proteins were separated by centrifugation at 13,000 rpm for 10 min at 4 °C. The supernatant containing soluble proteins was incubated with Streptavidin Sepharose High Performance beads (GE Healthcare) for 30 min at 4 °C. Beads were collected by centrifugation and washed as described (28).

VSG depletion

VSG was removed by activation of GPI-PLC (30). Surface-biotinylated cells were hypotonically lysed at 8e8 cells/ml in ice-cold H2O + SigmaFAST EDTA-free protease

inhibitors (Sigma) for 5 min on ice. Membranes were pelleted at 3,000 x g for 10 min at 4 °C and resuspended in 10 mM sodium phosphate, pH 8 + protease inhibitors at 37 °C for 5 min. After chilling briefly on ice, VSG-depleted membranes were pelleted at 12,000 x g for 10 min at 4 °C. Purification of surface-biotinylated proteins from VSG-depleted membranes was performed as described above.

Western blotting

Aliquots from each purification step were analyzed by SDS-PAGE using standard protocols. Non-reducing sample buffer was used to prevent cleavage of the Sulfo-NHS-SS-biotin. Primary antibodies were 1:8,000 mouse anti-biotin (Jackson ImmunoResearch), 1:100,000 rabbit anti-VSG 221 (Jay Bangs), 1:10,000 rabbit anti-EP9 procyclin (Jay Bangs), 1:50,000 rabbit anti-BiP (Jay Bangs) and 1:5,000 rabbit anti-EIF4AI (Osvaldo Pompilio de Melo-Neto). Horseradish peroxidase-coupled goat anti-mouse and goat anti-rabbit secondaries (Bio-Rad) were used at 1:5,000.

Shotgun proteomic analysis of surface proteomes

Proteomic analyses were performed essentially as described (28). TCA precipitates and on bead samples were mixed with digestion buffer (100 mM Tris-HCl, pH 8.5, 8M urea). The samples were reduced and alkylated by sequential treatment with 5 mM tris(2-carboxyethyl) phosphine (TCEP) and 10mM iodoacetamide as described earlier (31, 32). Afterward, samples were sequentially digested with Lys-C and trypsin proteases as previously described (32). The digestion was stopped by addition of 5% formic acid and peptide digests were analyzed by mass spectrometry. An initial set of

surface proteome samples were prepared from both BSF (n=3) and PCF (n=5) stage cultures and analyzed by 2D-LC-MS/MS on a Thermofisher LTQ-Orbitrap XL as described in (27, 28). Additional surface proteome samples were subsequently prepared in order to either (1) assess the relative abundance of putative surface proteins in the Input versus streptavidin-bound fractions or (2) perform label-free MS1-based quantitation of surface proteins that were differentially identified in the initial BSF or PCF samples. These subsequent surface proteome preparations were desalted and analyzed by LC-MS/MS on a Thermofisher Q-Exactive. For Q-Exactive experiments, desalted peptide digests were separated online using reversed-phase chromatography on a 75 μM inner diameter fritted fused silica capillary column with a 5 μM pulled electrospray tip that was packed in-house with 15 cm of Luna C18(2) 3 μM reversed phase particles. An EASY-nLC 1000 ultra high pressure liquid chromatography (UHPLC) system (Thermo Scientific) was used to deliver a linear acetonitrile gradient from 3% to 30% solvent B (Buffer A: 0.1% formic acid, Buffer B: Acetonitrile / 0.1% formic acid) was delivered by at a flow rate of 200-300nl/min. MS/MS spectra were collected on a Q-Exactive mass spectrometer (Thermo Scientific) as described in (33, 34).

Raw data files were converted to MS2 files using RawExtractor v.1.8 and v.1.9.9.2 for LTQ-Orbitrap XL and Q-Exactive data, respectively. Data analysis was performed using ProLuCID for database searching and DTASelect2 for probabilistic filtering as implemented in the Integrated Proteomics Pipeline v. 2 - IP2 (Integrated Proteomics Applications, Inc., San Diego, CA) (35-37). MS/MS spectra were searched against a

protein FASTA database obtained from TriTrypDB (downloaded from tritrypdb.org on February 9, 2012) appended with sequences for ESAGs from the 221 VSG expression site (GI numbers 189094616-189094632) and concatenated to a decoy database in which the amino acid sequence of each entry was reversed (19686 total entries). The search parameters (31) for LTQ-Orbitrap XL data were as follows: (1) precursor ion mass tolerance of +/- 20 ppm, (2) fragment ion mass tolerance of +/-400 ppm, (3) only peptides with fully tryptic ends and unlimited missed cleavages were considered as candidates, and (4) a static modification of +57.02156 Da on cysteine residues resulting from carbamidomethylation. The search parameters for analysis of Q-Exactive data were identical except precursor ion mass tolerance and fragment ion mass tolerance were each set +/- 10 ppm.

Protein and peptide identifications were filtered using DTASelect and required at least two unique peptides per protein and a spectra-level false positive rate of less than 5% as estimated by a decoy database strategy (38). When protein-level false positive rates are estimated using a decoy database approach, these filtering criteria give a protein-level FDR of <1% for all datasets included in the manuscript. Normalized spectral abundance factor (NSAF) values including shared peptides was calculated as described and multiplied by 10^5 to improve readability (39). Proteins that could not be distinguished by available peptides in any given replicate were considered as a group. The numbers in the text refer to the number of protein groups, corresponding to the minimum number of proteins present. See Tables S8-S13. Proteomic mass spectrometry data have been deposited to the ProteomeXchange

Consortium via the MassIVE partner repository with the dataset identifier PXD001946 (40).

MS1 analysis

To validate the PCF- and BSF-specific classifications made based on the initial qualitative datasets, additional surface proteomic analyses were performed for both BSF and PCF samples. These additional datasets were acquired on the Q-Exactive instrument and subjected to MS1-based, label-free quantitative analysis. Data were acquired as two technical replicates from single biological preparations for both BSF and PCF stages. Proteins were identified and filtered as above, and the identifications were used to generate spectral libraries within the Skyline v2.6 proteomic mass spectrometry software suite (41). Identifications were filtered within Skyline to only include fully tryptic, uniquely mapping peptides with no missed proteolytic cleavage sites. Peaks were picked in an automated fashion using the default Skyline peak picking model. Integrated peak areas were generated from extracted ion chromatograms for each peptide's [M], [M+1] and [M+2] isotopic precursor masses. The calculated peak-areas were exported for statistical analysis using the linear mixed-effects model provided within the R package MSstats v2.3.4 (42). Settings for the group-comparison within MSstats are as follows: (1) peak intensities were log2 transformed, (2) intensity normalization between runs was accomplished by means of quantile normalization, (3) the scope of conclusions for biological and technical replication was set to restricted and expanded respectively, (4) settings for inclusion of interference transitions and assumption of equal feature variance were both set to

"TRUE." P-values were corrected within MSstats via Benjamini-Hochberg correction. See Table S13.

Volcano plots of Log_2(PCF/BSF) ratios and significance were plotted using Microsoft Excel. Plots showing distributions of Log_2(PCF/BSF) ratios in cell surface and whole-cell proteomes were plotted using GraphPad Prism. Proteins were binned by Log_2(PCF/BSF) ratio, using a bin width of 0.7 and proteins with Log_2(PCF/BSF) ratios $\leq$ 5.25 or $\geq$ 5.25 were consolidated into the first and last bins, respectively.

Enrichment in the Bound versus Input or Unbound fractions

For bound versus input or unbound analyses, surface biotinylation was performed as described above. Half of the soluble NP-40 extracted supernatant was reserved for shotgun proteomic analysis (Input) and the other half was incubated with streptavidin beads to obtain the Bound and Unbound fractions. Bound fractions were analyzed by on-bead digestion as described above. Input and Unbound fractions were TCA precipitated and analyzed using shotgun proteomics as described above. See Table S12. IP2 software (Integrated Proteomics) was used to compare protein identification between samples (Table S4). The relative abundance of proteins within each fraction was determined by dividing the number of spectra for each protein over the total number of spectra for all proteins in that fraction. The Bound/Input and Bound/Unbound ratios for each protein were then determined based on relative abundance in the corresponding fractions.

Bioinformatics Analyses

Prediction of membrane-targeting domains, reciprocal best BLAST analysis, and DAVID/GO classification are described in Supplemental Experimental Procedures.

Comparison to whole-cell SILAC proteomes

Three stage-specific whole-cell proteomes have been published (43-45). A detailed comparison to the Urbaniak *et al.* (44) and Butter *et al.* (43) studies is shown in Figure 2-05. The third study utilized a different trypanosome strain and analyzed parasites extracted from mice instead of culture (45) (Table S6), so was excluded from the comparison. The distribution of Log_2(PCF/BSF) protein ratios from MS1 quantification of proteins in the cell surface proteome or SILAC quantification of proteins in the whole cell proteomes are plotted (Figure 2-05B). For Butter *et al*. (43), replicate protein ratios from SupTable3 were converted to Log_2(PCF/BSF) and averaged. Urbaniak *et al*. (44) reported 10.6% of their whole cell proteome to be 5-fold differentially expressed between the BSF and PCF life cycle stages. Our analysis of SupTable3 from Butter *et al*. (43) indicates that 8.6% of the proteome was 5-fold differentially regulated in both replicates. Proteins 5-fold differentially regulated were considered stage-specific and proteins less than 5-fold differentially regulated were considered constitutively expressed for analyses in Figure 2-05C.

Mass spectrometry analysis of stage-enriched cell surface family members

The list of proteins comprising the *T. brucei* cell surface phylome (46) was kindly provided by Dr. Andrew Jackson. Families represented in the cell surface proteomes

were analyzed with respect to stage-specificity of individual members. Categorization as BSF-specific or PCF-specific was strictly defined as exclusive expression in one or the other life cycle stage (Figure 2-03). Owing to challenges presented by proteins with closely related sequences, we additionally examined the distribution of unambiguous peptides mapping to individual proteins (Table S5). Proteins detected by at least two unambiguous peptides in two different samples were categorized as putatively BSF-enriched, PCF-enriched, or constitutive. Phylogenetic trees (FigTree, http://tree.bio.ed.ac.uk/software/figtree/) display MUSCLE alignments of the protein sequences in each family. In the case of Fam51, four additional family members were added: two ESAG4s from the 221 VSG expression site (GI# 189094619, 1890946250), ACP4 (Tb927.10.13040) (47), and ACP2 (Tb927.10.16190) (48). For Fam57, the 221 expression site does not contain an ESAG10, so an ESAG10 from an alternate expression site was included (Tb427.BES15.1; GI 189094656) to show the approximate relationship between PCF-specific and BSF-specific isoforms. Peptide data are included in Tables S10-S11.

Quantitative real-time PCR (qRT-PCR)

Total RNA was extracted using Qiagen's RNAeasy kit. DNAse treatment was followed by reverse transcription using oligodT primers for first-strand cDNA synthesis. qRT-PCR was performed as described (49) using iQ SYBR Green Supermix (Bio-Rad) on a DNA Engine Opticon 2 (Bio-Rad). All analyses were performed in duplicate on two independent RNA preparations and values were normalized to PFR2 and TERT2 (50) using the $2^{-\Delta\Delta C}{}_{T}$ method (51). Gene-specific primers were designed using NCBI Primer-

BLAST to amplify a region of 150-200 base pairs (see Supplemental Experimental Procedures).

RESULTS AND DISCUSSION

Purification of cell surface proteins from *T. brucei*

We used a combination of cell surface biotinylation, affinity purification, and shotgun proteomic mass spectrometry (Figure 2-01A) to determine the protein composition of the parasite surface from insect stage procyclic culture-form (PCF) and mammalian bloodstream form (BSF) *T. brucei*. Live cells were incubated with a cell-impermeant biotin conjugate to label surface-exposed proteins. Immunofluorescence against intracellular and cell surface markers confirmed that cells remained intact during surface biotinylation (Figure S1A). Labeled cells were lysed with non-ionic detergent and the detergent-soluble fraction was incubated with streptavidin beads to purify biotinylated proteins. The vast majority of proteins fractionated with unbound material, while biotinylated proteins were quantitatively purified with the streptavidin-bound fraction (Figure 2-01B). Known surface proteins VSG and procyclin co-purified with the biotinylated fraction, while known intracellular proteins such as BiP were almost exclusively in the unbound fraction (Figure 2-01C). As a control, streptavidin purification was also performed on unbiotinylated samples from each life cycle stage. No biotinylated proteins were detected by anti-biotin staining (Figure S1B) and in the absence of surface biotinylation, VSG and procyclin were restricted to

the unbound fraction. Thus, surface biotinylation and streptavidin purification enabled effective enrichment of *T. brucei* surface proteins.

VSG depletion improves detection of other surface proteins

Abundance of the major surface proteins (5-10 million copies/cell), procyclin on PCF cells and VSG on BSF cells, poses a potential barrier to a comprehensive analysis of the parasite surface proteome. Shotgun proteomic analysis of the streptavidin-bound fraction from PCF cells revealed very few spectra for procyclin (Figure 2-02A), presumably due to its lack of tryptic cleavage sites. In contrast, the overwhelming majority of mass spectra (nearly 80%) from BSF samples mapped to VSG, presenting a potential dynamic range challenge for reliable detection of low abundance proteins. To overcome this, we took advantage of endogenous GPI-specific phospholipase C (GPI-PLC) activity to release VSG from the cell surface (30) prior to streptavidin purification of surface proteins (Figure 2-02B). Using this strategy we obtained a streptavidin-bound fraction that was relatively free of VSG and intracellular marker proteins EIF4AI and BiP based on Western blotting (Figure 2-02C). To determine whether VSG depletion improved detection of non-VSG proteins, we compared proteomic analyses of VSG-depleted and non-depleted samples. VSG depletion increased the total number of proteins identified by >50% and reduced the proportion of mass spectra corresponding to VSG from approximately 80% to 15% of total spectra (Figure 2-02A). Spectra from another GPI-anchored surface protein, transferrin receptor, were also reduced, though not absent (Figure 2-02D). In contrast, spectra derived from other surface proteins increased markedly, while

spectra from known intracellular contaminants remained relatively constant. Therefore, VSG depletion dramatically increased sensitivity of detection for non-VSG surface proteins.

Surface proteomes provide high-confidence datasets of surface protein candidates.

Having established a method for effective enrichment of *T. brucei* surface proteins, we performed surface biotinylation, purification and proteomic analysis on multiple biological replicates for each life cycle stage. To minimize the effects of sample variation, only proteins reproducibly identified in 3 of 3 VSG-depleted BSF samples or at least 4 of 5 PCF samples were considered high-confidence surface protein candidates (Figure 2-03). This yielded datasets of 239 BSF proteins and 198 PCF proteins, referred to as BSF and PCF surface proteomes, respectively (Table S1), for a combined surface proteome of 372 non-redundant proteins. As expected, the surface proteomes contain most currently known and suspected classes of surface proteins (Table S2) and are enriched for proteins with predicted membrane-association domains (Figure S2A). Notably, despite use of GPI-PLC to deplete VSG, proteins with predicted GPI anchors were still identified. Endogenously biotinylated proteins were not a significant confounding factor, as proteomic analyses of two unbiotinylated samples from each life cycle stage identified very few proteins (Table S3).

Rigorous assessment of surface location demands a great deal of effort for any single protein, let alone a large set of randomly selected proteins, which would be necessary to use localization as a means of evaluating the surface proteome dataset. We therefore evaluated the dataset as a whole by determining the relative abundance of known surface and intracellular proteins in streptavidin-bound versus unbound and input fractions. In BSF cells, most surface protein controls (19 of 24) were enriched in the bound fraction (Bound/Input > 1), while most intracellular controls (78 of 87) were depleted (Bound/Input <1) (Figure 2-04, Table S4). Strikingly, amongst the controls examined, an enrichment ≥2.0 was observed almost exclusively for *bona fide* surface proteins. Likewise, in PCF cells, a fold-enrichment of ≥2.5 was observed for 15 of 20 known surface proteins, but only 3 of 96 intracellular controls (Figure 2-04, Table S4). Notably, 46 proteins meeting this enrichment threshold among BSF or PCF proteomes are annotated as hypothetical (Table S1), with no clear conserved domains, indicating novel functionalities for trypanosome surface proteins.

As with any biochemical purification or analysis of the scale presented here, we expect to miss some surface proteins and to identify some false positives. Nonetheless, several independent lines of evidence demonstrate that the surface proteomes reported here represent high-confidence datasets of candidate surface proteins. These include high quality of the purified samples, multiple independent biological replicates to minimize the impact of prep-to-prep variability, excellent coverage of known surface proteins, and label-free quantitation of intracellular and surface protein controls in the Bound vs. Input fractions.

The parasite surface proteome is enriched for life cycle stage-specific proteins, including stage-specific paralogues within protein families.

As different hosts present varied environments and challenges, stage-specific surface proteins are primary contributors to host-parasite interactions. We therefore examined cell surface proteomes for proteins that were exclusively identified in only one life cycle stage. We identified 72 BSF-specific proteins and 74 PCF-specific proteins, (Figure 2-03, Table S1). Note that proteins present in both life cycle stages, but up-regulated or down-regulated between life cycle stages would be missed by this approach. However, the stage-specific proteins identified constitute the most prominent and robust changes between the surface proteomes during the parasite's transmission between hosts. To test the robustness of these stage-specific assignments, we completed additional independent surface proteome analyses using MS1 label-free quantitation, with two technical replicates for each life cycle stage. Nearly all proteins assigned as stage-specific could be quantitated in MS1 analyses (Table S1), and of these, the majority showed significant ($p < 0.01$) upregulation in the assigned life cycle stage (Figure 2-05A). Therefore, these analyses provided strong statistical support for stage-specific assignments based on exclusive detection in one or the other life cycle stage. In addition, MS1 analyses revealed stage-specific enrichment of several proteins in the surface proteome that were not exclusive to one stage (Figure S3, Table S1).

The cell surface is the direct interface with the host. We therefore asked whether the cell surface proteome is enriched for stage-specific proteins compared to

the whole-cell proteome. The distribution of relative protein abundance in BSF and PCF surface proteomes was plotted against the distributions in published BSF and PCF whole cell proteomes (43, 44). The data demonstrate that the cell surface proteome is enriched for proteins that are differentially regulated between BSF and PCF stages (Figure 2-05B). Likewise, among proteins identified in whole-cell proteome analyses (43, 44), roughly 25% of the stage-specific proteins are present in the cell surface proteome, as compared to only 5% of constitutive proteins (Figure 2-05C). Therefore, a substantial fraction of developmentally regulated gene expression changes in *T. brucei* are devoted to remodeling the host-parasite interface.

We noticed that paralogues from large protein families (46) were well-represented among stage-specific surface proteins (Figures 6 and S4, Table S5). While stage-specificity has been described for some families, e.g. adenylate cyclases (47), glucose transporters (52) and nucleoside transporters (53), stage-specific regulation was not previously known for others, e.g. hypothetical proteins (Fam72 and Fam79) (Figure 2-06, Tables S1 and S5). We therefore used qRT-PCR to independently assess stage-specific expression for several of these protein families (Figures 6 and S4). The qRT-PCR results fully supported the stage-specificity determined by mass spectrometry, validating the mass spectrometry analysis and suggesting that dedicated use of distinct paralogues in different environments is a common feature of *T. brucei* host adaptation.

Implications for expanded gene families and host adaptation

One of the largest protein families encoded by the *T. brucei* genome is a family of approximately 75 receptor-type adenylate cyclases (ACs) (Fam51, (46), Figure 2-06). The canonical AC is the BSF-specific ESAG4 (54, 55), which contributes to parasite virulence by modulating the immune response of the mammalian host (48). Recent work described five ACs that are specifically upregulated in PCF cells (47), one of which regulates social behavior (56), demonstrating that both BSF-specific and PCF-specific ACs mediate parasite interaction with the environment. In addition to these previously identified ACs, we identify two additional PCF-specific and BSF-specific ACs (Tables S1 and S5, Figure 2-06), further supporting an important role for ACs in host-specific adaptation. We speculate that individual ACs not identified in our studies are optimized for host environments that are not recapitulated in cultured PCF and BSF forms.

Gene expansion is a well-known phenomenon in *T. brucei* and other kinetoplastid parasites (57). The reasons for gene expansion are not clear, though it has been suggested to reflect redundant gene duplication. Based on the size of the *T. brucei* AC family and the identification of PCF-specific ACs, we have previously proposed that the greatly expanded repertoire of *T. brucei* ACs reflects the relative complexity of the life cycle within the insect vector, as compared to other kinetoplastids (47, 56). Our discovery in the present work that stage-specific expression of distinct paralogues is common across multiple families argues against simple redundancy as the explanation for gene expansion. Moreover, some families

are described to have undergone faster diversification since the divergence of African trypanosomes from other trypanosomatids (46), indicating that gene expansion confers a selective advantage. Thus, rather than redundancy, our results suggest surface protein families have expanded in response to the need for alternately-expressed isoforms that are each tuned to a specific host environment, as has been suggested for the nucleoside transporter family (53). This would allow the parasite to continually meet essential cellular needs that are common in all environments, such as uptake of an essential nutrient, while still responding to unique pressures imposed by hostile and markedly different environments in each host. Given that adapting to a multitude of different extracellular environments is intrinsic to a parasitic lifestyle, we speculate this is a paradigm that applies broadly to surface proteome remodeling in other parasites.

Cell surface proteomes represent the first direct analysis of stage-specific surface protein remodeling

Aside from major surface proteins, the parasite surface proteome has remained largely uncharacterized. Previous efforts to define life cycle stage-specific proteomes have almost exclusively focused on the whole-cell proteome (43-45) (Table S6). The flagellum surface proteome has been examined (28, 58). However, efforts to define the *T. brucei* whole-cell surface proteome have been limited to *in silico* prediction (46) and a subtractive proteomic analysis of crude fractions containing plasma membranes and cytoskeletons from bloodstream form parasites (59) (Table S6). *In silico* predictions are powerful, but they do not distinguish between cell surface and

intracellular membranes. Likewise, while subtractive proteomics can be a useful approach, no attempt was made to directly separate surface-exposed proteins from intracellular contaminants and no comparable analysis was done in procyclic-stage parasites. Therefore, the cell surface proteomes described here present the first analyses to directly isolate and define the cell surface proteome and to do so from both the insect and mammalian life cycle stages of *T. brucei* (Table S6).

Functional implications of the cell surface proteomes

Proteomic analyses identify a large and diverse surface proteome important for host-parasite interaction and therapeutics

An important finding to come from our studies is that the *T. brucei* cell surface proteome is larger and more diverse than generally appreciated. Surface proteins identified encompass a broad range of molecular functionalities (Table S7), including activities anticipated for cell surface function, such as receptors, transporters and proteases, as well as numerous proteins of completely unknown function.

Approximately 10-20% of the BSF and PCF surface proteomes are restricted to kinetoplastids, with nearly half of those being exclusive to *T. brucei* (Figure S2). Only a handful of *T. brucei* surface proteins have been studied in depth and virtually all perform critical functions, particularly in the context of host-parasite interaction and therapeutics. Examples include VSG and transferrin receptor in BSF cells (60-62), as well as surface proteins modulating resistance to human serum (63, 64) and recent

studies showing virulence functions for ESAG4 and calflagin (48, 65). In procyclic forms, procyclin is required for robust infection and transmission through the tsetse fly (66). From a clinical perspective, parasite genes impacting the efficacy of all five currently available drugs have been identified and the majority of these encode surface-exposed proteins (67-71). Importantly, nearly all of these proteins were identified in the cell surface proteome, emphasizing the functional relevance of the surface proteome. Thus, our studies define a cohort of proteins important for host-parasite interaction with potential to impact success of therapeutic interventions.

The surface proteome prioritizes proteins important for fitness and host-parasite interaction

Our surface proteome analyses advance systems-level studies of protein function in *T. brucei*. For example, unbiased high-throughput RNAi target sequencing (RIT-seq) analysis has identified nearly 4,500 genes that impact parasite fitness or differentiation from bloodstream to procyclic forms in culture (72). While these 4,500 genes are interesting for their potential as drug targets, there are far too many candidates for effective prioritization. We conducted a meta-analysis of the surface proteome versus the RNAi target dataset. Our analyses substantially pare down the number of proteins required for parasite fitness from 4,500 (72) to approximately 65 that are surface-exposed based on enrichment in Bound vs. Input fractions (Table S1) and thus accessible to small molecules added to live cells. These genes can therefore be prioritized for investigation as therapeutic targets that may circumvent the need for cell-permeant drugs. Moreover, nearly half of these proteins are of unknown

function, emphasizing novel features of the cell surface proteome and suggesting host-interaction functions for approximately 30 of the ~5,000 *T. brucei* genes annotated as hypothetical (73). Relevance to host-parasite interaction also comes from considering stage-specific expression, as our analyses distinguish surface proteins, which would directly interface with the host, from intracellular proteins, such as those uncovered in whole proteome stage-specific analyses (43-45), that may simply reflect downstream metabolic or structural consequences of differentiation.

Cell surface proteome analyses distinguish between cell surface and intracellular membranes

Our data provide a valuable resource for resolving outstanding questions regarding individual proteins. As an example, conflicting evidence for surface exposure of GPI-PLC has been reported (74, 75). We observe a Bound/Input ratio <1 for this protein (Table S1), supporting intracellular localization. Similarly, a Bound/Input ratio of <1 for the virulence factor metacaspase 4 (Table S1) supports previous data suggesting it is predominantly intracellular (76). In contrast, we see strong surface enrichment for flagellar calflagins (65) and a flagellum tip-localized calpain-like protease (65, 77) (Table S1), suggesting these proteins function at the flagellum surface. Our bound/input analyses also provide insight into the large family of *T. brucei* ABC transporters. Out of ~20 annotated ABC transporters in the genome, only four have B/I ratios of $\geq$ 2.3, indicating they function in substrate exchange with the host environment, while the remainder function intracellularly (Table S1). Another interesting discovery is a group of three phospholipid-transporting ATPases

that are enriched ≥12-fold in the bound fraction compared to input (Table S1). A role for phospholipid transporters at the cell surface has not been demonstrated, but could be important for host-parasite interactions by maintaining distinct lipid compositions of the cell surface membrane and critical subdomains, such as the flagellum and flagellar pocket membranes (78). These proteins will be interesting targets for further functional studies.

SUMMARY AND PERSPECTIVE

The surface of parasitic protozoa remains vastly understudied relative to its importance for parasite biology, pathogenesis, transmission and clinical influence. Here we find that the *T. brucei* surface proteome is larger and more diverse than generally recognized and includes proteins known or predicted to be important for host-parasite interaction and drug action. Additionally, our studies reveal extensive remodeling of the surface proteome, indicating the parasite strives to accommodate specific requirements of hostile host environments while continuing to maintain fundamental processes essential for viability.

FIGURES

Figure 2-01. Purification of cell surface proteins from procyclic and bloodstream form *T. brucei*

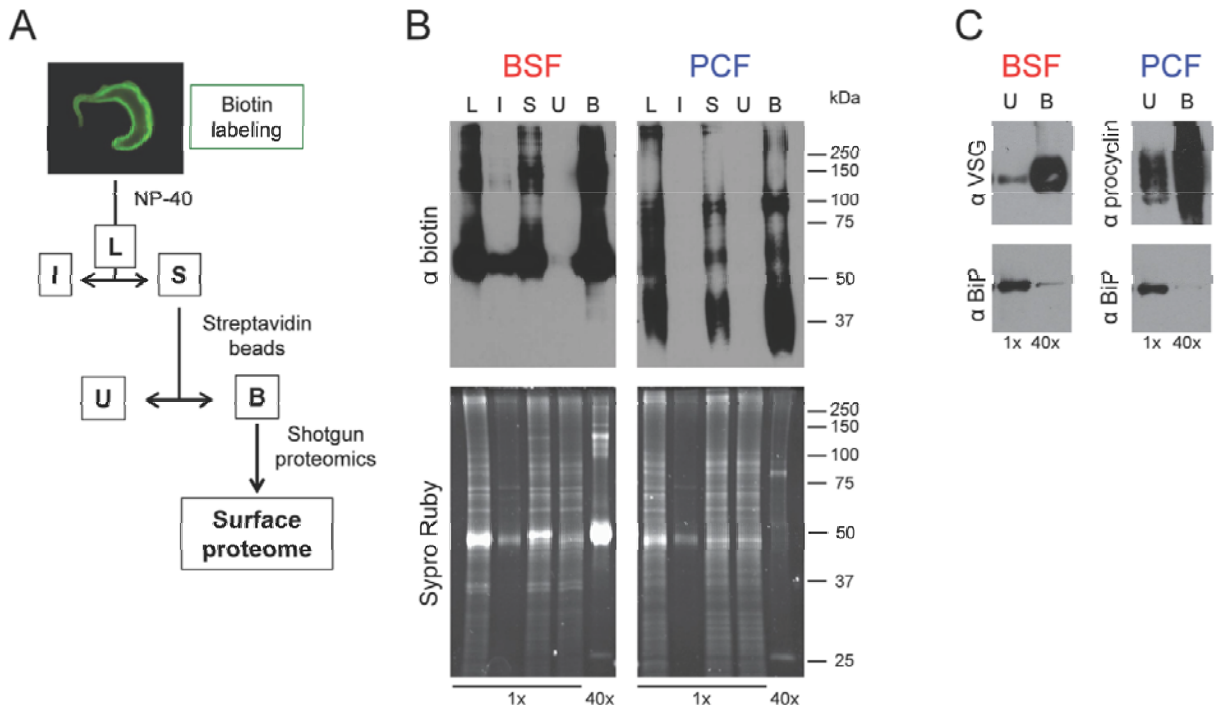

(A) Strategy for biotinylation and streptavidin purification of surface proteins. Surface-biotinylated cells were fractionated into Lysate (L), Insoluble (I), Soluble (S), Unbound (U), and Bound (B) fractions. (B) Fractions labeled in panel A were analyzed by anti-biotin Western blotting (top) and Sypro Ruby staining of total protein (bottom). Numbers below the blots indicate relative number of cell equivalents loaded. (C) Western blotting shows enrichment for major surface proteins VSG and procyclin in the bound fraction, while the intracellular protein BiP remains in the unbound fraction.

Figure 2-02. VSG depletion improves detection of low abundance surface proteins.

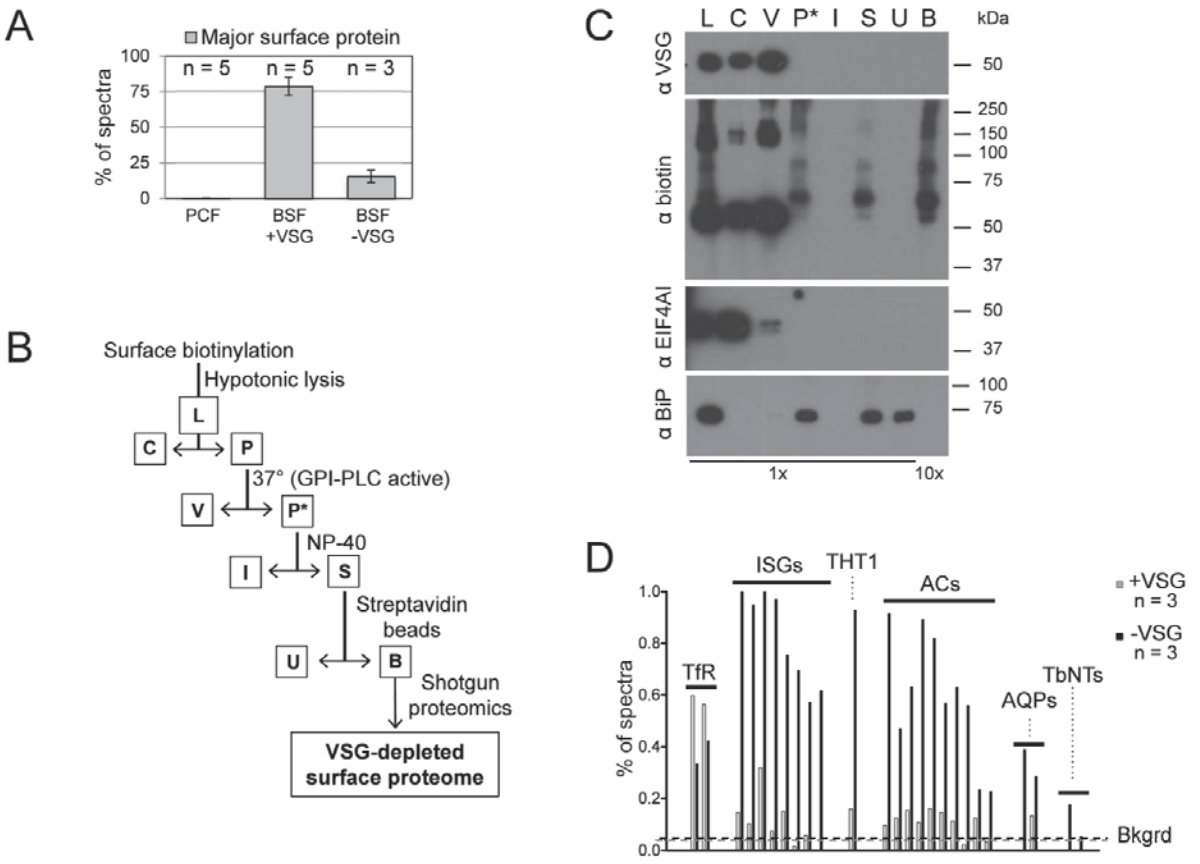

(A) Abundance of mass spectra corresponding to the major surface proteins procyclin and VSG, calculated as a fraction of total mass spectra in PCF and BSF samples, respectively. Data are the mean +/- SD. Procyclin spectra were less than 0.5% of the total. (B) Strategy for proteomics of VSG-depleted surface fractions. Fractions are Lysate (L), Cytosol (C), Pellet (P), soluble VSG (V), VSG-depleted pellet (P*), Insoluble (I), Soluble (S), Unbound (U), and Bound (B). (C) Western blotting of fractions, as labeled in panel B, probed with the indicated antisera. The majority of VSG is removed in the soluble VSG fraction (V), leaving no detectable VSG in the VSG-

depleted pellet fraction (P*). Intracellular markers EIF4AI (cytoplasmic) and BiP (ER lumen) are removed in the cytosolic (C) or unbound (U) fractions. Numbers below the blots indicate relative number of cell equivalents loaded. (D) Relative abundance of individual known surface proteins is shown as a fraction of total mass spectra. Black bars represent the mean from VSG-depleted samples, while white bars represent the mean from samples without VSG depletion (n=3 for each). Known surface proteins are transferrin receptor (TfR), invariant surface glycoproteins (ISGs), glucose transporter (THT1), adenylate cyclases (ACs), aquaporins (AQPs), and nucleoside transporters (TbNTs). The dashed lines (Bkgrd) indicate the average relative abundance of known intracellular proteins (e.g. proteins annotated as ribosomal proteins and histones) from VSG-depleted (black line) and non-depleted (gray line) samples.

Figure 2-03. Defining cell surface and stage-specific cell surface proteomes.

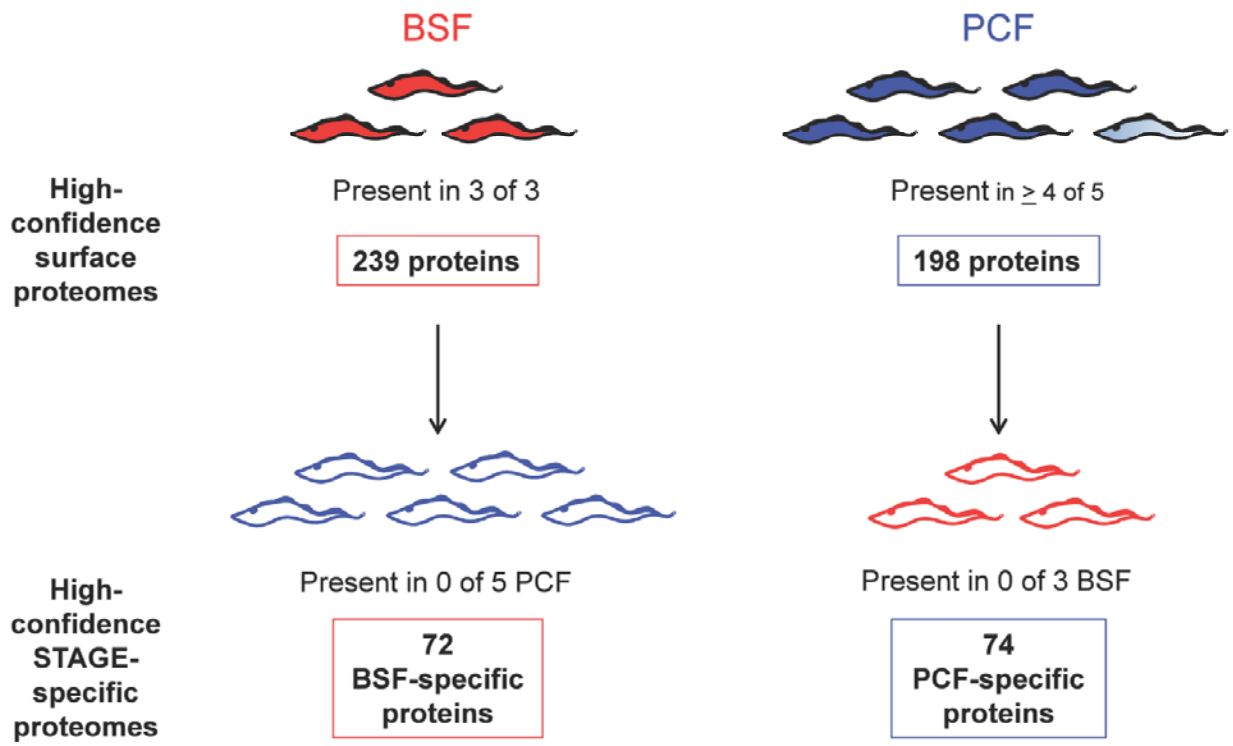

Schematic illustrating criteria for inclusion in the cell surface and stage-specific cell surface proteomes. Surface biotinylation, purification and shotgun proteomic analysis were performed on multiple biological replicates for each life cycle stage. The BSF and PCF cell surface proteomes were defined as proteins reproducibly identified in 3 of 3 VSG-depleted BSF or ≥4 of 5 PCF replicates, respectively. Proteins that could not be distinguished by available peptides in any given replicate were considered as a group (see Tables S1 and S8-S11). The numbers listed are the number of protein groups identified, corresponding to the minimum number of proteins present. The number of non-redundant protein groups identified in the combined surface proteome

from either life cycle stage was 372. Stage-specific proteomes were defined as proteins or protein groups that were exclusive to one life cycle stage (Table S1).

Figure 2-04. Surface proteome datasets show enrichment for known surface proteins.

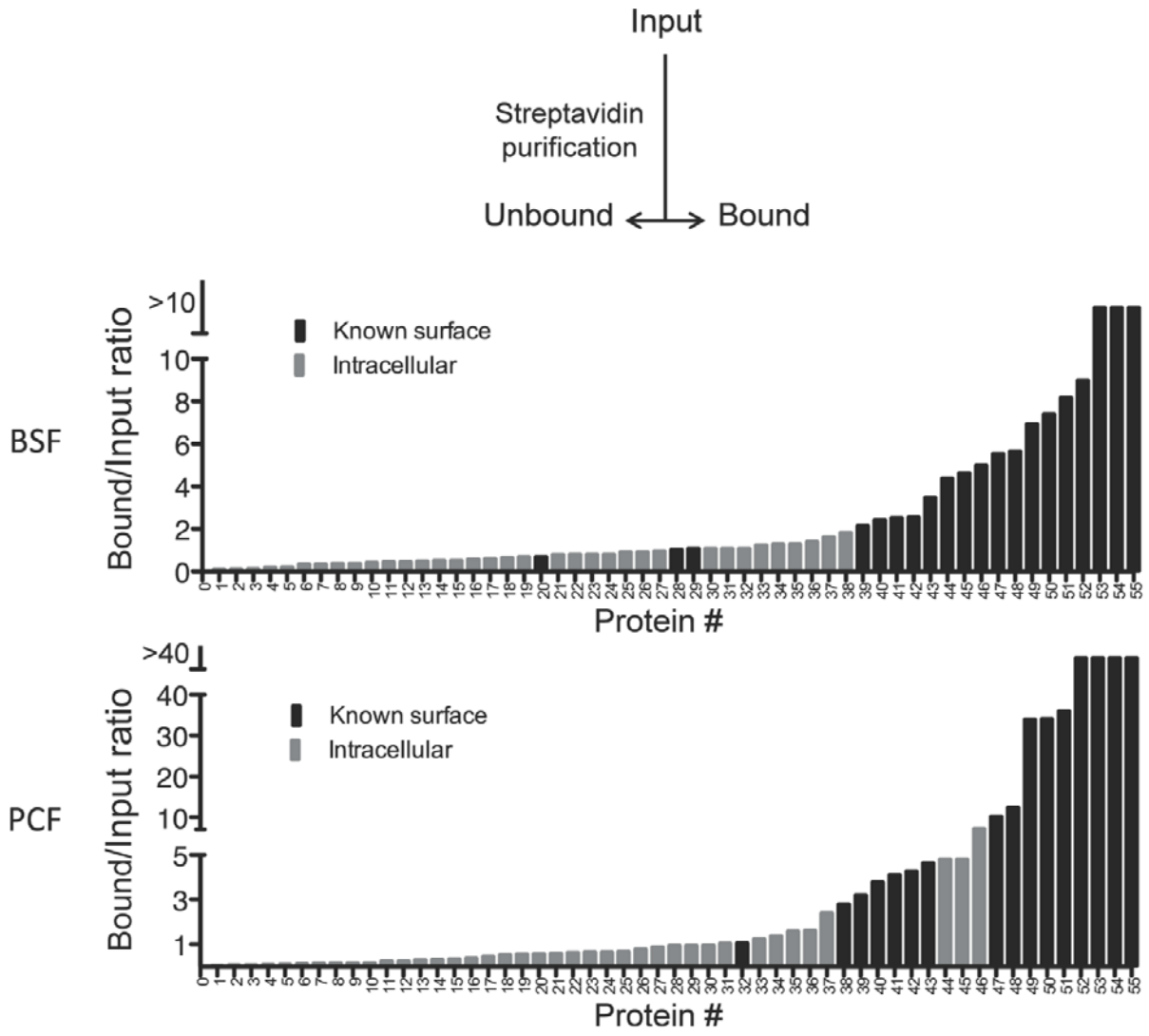

Unbound and Bound fractions from a single independent PCF or VSG-depleted BSF surface purification were analyzed by shotgun proteomics. The relative abundance of individual proteins was determined as a percentage of the total mass spectra in each fraction, and the ratio of relative abundance in the Bound vs. Input fractions is plotted for several known surface proteins (black) and intracellular proteins (grey) in ascending order (see columns in Table S4). Intracellular controls included alpha and

beta tubulin, two dynein heavy chains, BiP, and proteins annotated as ribosomal proteins or histones. A ratio >1 indicates enrichment, while a ratio <1 indicates depletion. Proteins identified in the Bound but not Input fraction were plotted as >10 (BSF) or >40 (PCF) in the figure. Note that the graph does not include proteins not identified in the Bound fraction.

Figure 2-05. Cell surface proteomes are enriched for stage-specific proteins.

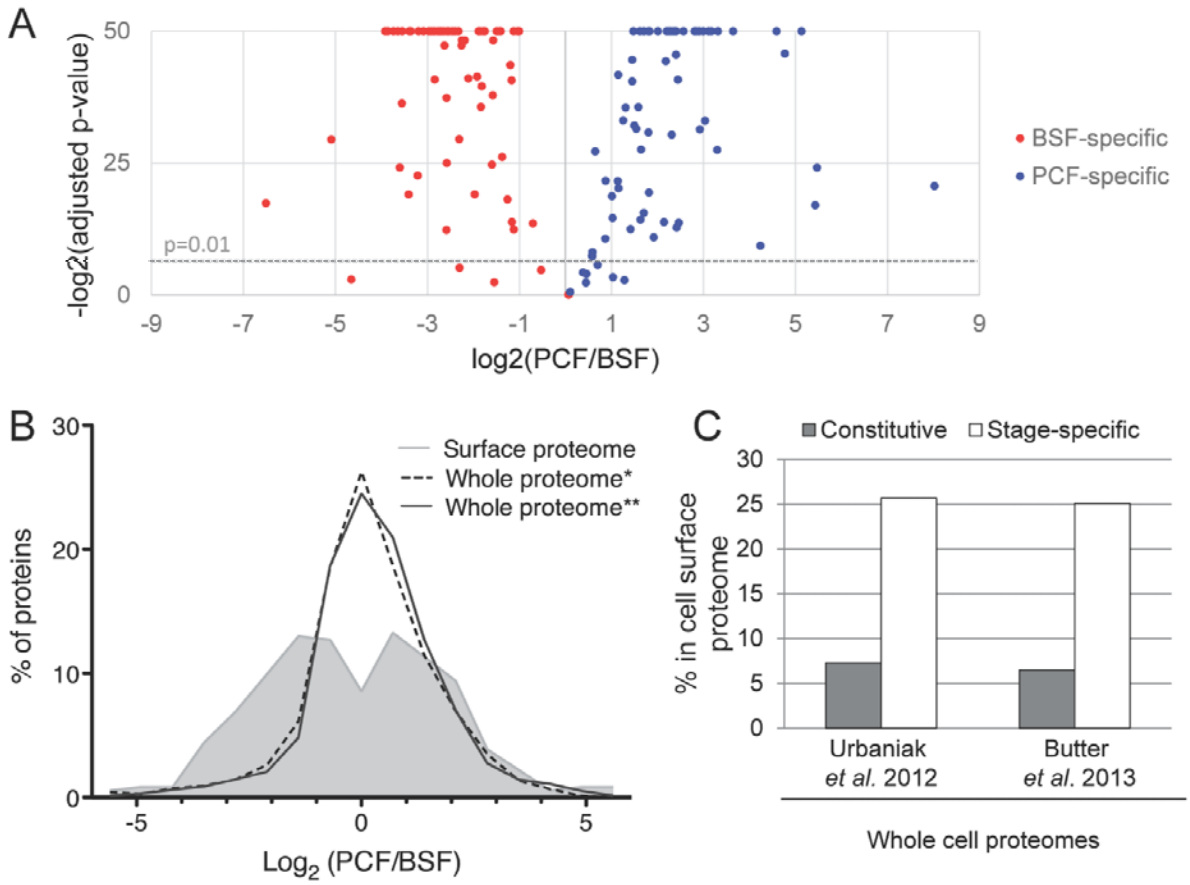

(A) Stage-specific proteins exclusively identified in either the cell surface proteome from BSF cells (red circles) or PCF cells (blue circles) were analyzed by MS1 label-free quantitation in two technical replicates each. The Log_2(PCF/BSF) fold change measured for each protein is plotted on the x-axis. Statistical significance is plotted on the y-axis, with $p < 0.01$ above the dashed line. (B) Graph shows the distribution of Log_2(PCF/BSF) protein ratios from MS1 analysis of the cell surface proteome (shaded area), relative to whole-cell proteomes determined by SILAC analyses (*Urbaniak *et al.*, 2012 (44), black dashes; **Butter *et al.*, 2013 (43), black line). (C) Chart shows

the relative fraction of constitutive and stage-specific proteins identified in published whole-cell proteome SILAC analyses (43, 44) that were also identified in the cell surface proteome. Proteins at least 5-fold differentially regulated between PCF and BSF in published SILAC studies were defined as stage-specific (43, 44).

Figure 2-06. Life cycle stage-specific paralogues of surface protein families.

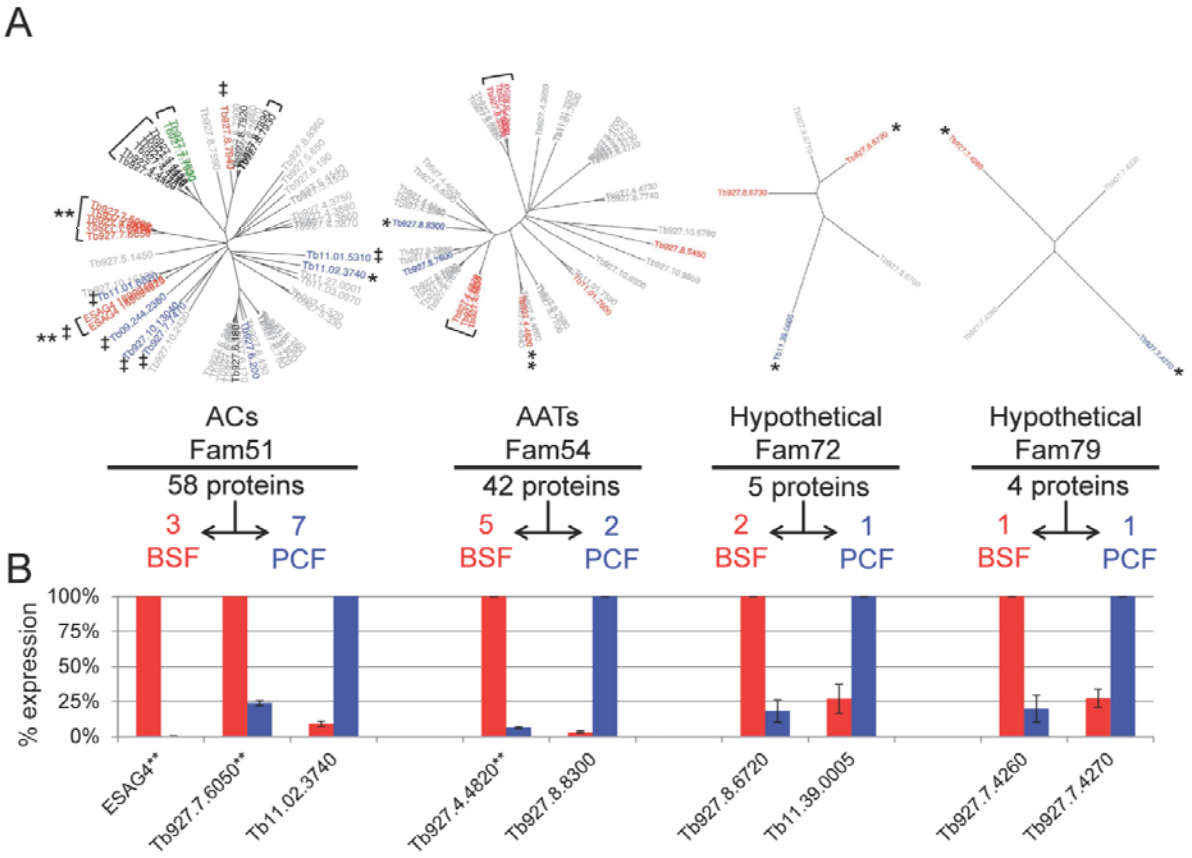

(A) Phylogenetic trees illustrate relationships within protein families predicted in the cell surface phylome (46) for which we identified life cycle stage-specific paralogues. Families are adenylate cyclases (ACs), amino acid transporters (AATs), and two families annotated as hypothetical proteins. Proteins are colored according to the predicted expression profile inferred from mass spectrometry data (Table S5). (Red = BSF-enriched; Blue = PCF-enriched; Green = Constitutive, Grey = Not identified, Black = identified but expression profile could not be reliably predicted). The total number of proteins in each family is shown along with the number of BSF-enriched and PCF-

enriched proteins identified in the cell surface proteomes. If two or more proteins could not be distinguished based on peptides identified they are counted as a single entry, and the group is indicated by a bracket in the phylogenetic tree. ‡Proteins for which stage-specific expression has been previously described (see Table S5 for references). *Proteins whose stage-specific expression was examined by qRT-PCR in panel B. (B) Expression levels for the indicated genes were determined by qRT-PCR analysis using RNA from BSF (red) and PCF (blue) cells. Data are the mean +/- SD of two independent biological replicates and expression is normalized to the stage having higher expression. **Groups of closely related genes detected by the primer pair used for qRT-PCR analysis (189094619/189094625; Tb927.7.6050/Tb927.7.6060/Tb927.7.6070; Tb927.4.4820/Tb927.4.4840/Tb927.4.4860).

REFERENCES

1. Borst, P., and Fairlamb, A. H. (1998) Surface receptors and transporters of Trypanosoma brucei. *Annu Rev Microbiol* 52, 745-778

2. Kennedy, P. G. (2013) Clinical features, diagnosis, and treatment of human African trypanosomiasis (sleeping sickness). *Lancet Neurol* 12, 186-194

3. Pays, E., and Nolan, D. P. (1998) Expression and function of surface proteins in Trypanosoma brucei. *Mol Biochem Parasitol* 91, 3-36

4. Borst, P., and Fairlamb, A. H. (1998) Surface receptors and transporters of Trypanosoma brucei. *Annu Rev Microbiol* 52, 745-778

5. Field, M. C., and Carrington, M. (2009) The trypanosome flagellar pocket. *Nat Rev Microbiol* 7, 775-786

6. Gadelha, C., Holden, J. M., Allison, H. C., and Field, M. C. (2011) Specializations in a successful parasite: what makes the bloodstream-form African trypanosome so deadly? *Mol Biochem Parasitol* 179, 51-58

7. Schwede, A., Jones, N., Engstler, M., and Carrington, M. (2011) The VSG C-terminal domain is inaccessible to antibodies on live trypanosomes. *Mol Biochem Parasitol* 175, 201-204

8. Hall, J. P., Wang, H., and Barry, J. D. (2013) Mosaic VSGs and the scale of Trypanosoma brucei antigenic variation. *PLoS Pathog* 9, e1003502

9. Morrison, L. J., Marcello, L., and McCulloch, R. (2009) Antigenic variation in the African trypanosome: molecular mechanisms and phenotypic complexity. *Cell Microbiol* 11, 1724-1734

10. Roditi, I., Schwarz, H., Pearson, T. W., Beecroft, R. P., Liu, M. K., Richardson, J. P., Buhring, H. J., Pleiss, J., Bulow, R., and Williams, R. O. (1989) Procyclin gene expression and loss of the variant surface glycoprotein during differentiation of Trypanosoma brucei. *Journal of Cell Biology* 108, 737-746

11. Roditi, I., and Lehane, M. J. (2008) Interactions between trypanosomes and tsetse flies. *Curr Opin Microbiol* 11, 345-351

12. Acosta-Serrano, A., Vassella, E., Liniger, M., Kunz Renggli, C., Brun, R., Roditi, I., and Englund, P. T. (2001) The surface coat of procyclic Trypanosoma brucei: programmed expression and proteolytic cleavage of procyclin in the tsetse fly. *Proceedings of the National Academy of Sciences of the United States of America* 98, 1513-1518

13. Vassella, E., Den Abbeele, J. V., Butikofer, P., Renggli, C. K., Furger, A., Brun, R., and Roditi, I. (2000) A major surface glycoprotein of trypanosoma brucei is expressed transiently during development and can be regulated post-transcriptionally by glycerol or hypoxia. *Genes & development* 14, 615-626

14. Urwyler, S., Studer, E., Renggli, C. K., and Roditi, I. (2007) A family of stage-specific alanine-rich proteins on the surface of epimastigote forms of Trypanosoma brucei. *Molecular microbiology* 63, 218-228

15. Dyer, N. A., Rose, C., Ejeh, N. O., and Acosta-Serrano, A. (2013) Flying tryps: survival and maturation of trypanosomes in tsetse flies. *Trends Parasitol* 29, 188-196

16. MacGregor, P., Szoor, B., Savill, N. J., and Matthews, K. R. (2012) Trypanosomal immune evasion, chronicity and transmission: an elegant balancing act. *Nat Rev Microbiol* 10, 431-438

17. Ooi, C. P., and Bastin, P. (2013) More than meets the eye: understanding *Trypanosoma brucei* morphology in the tsetse. *Frontiers in cellular and infection microbiology* 3, 71

18. Dean, S., Marchetti, R., Kirk, K., and Matthews, K. R. (2009) A surface transporter family conveys the trypanosome differentiation signal. *Nature* 459, 213-217

19. Maric, D., Epting, C. L., and Engman, D. M. (2010) Composition and sensory function of the trypanosome flagellar membrane. *Curr Opin Microbiol* 13, 466-472

20. Rotureau, B., Morales, M. A., Bastin, P., and Späth, G. F. (2009) The flagellum-mitogen-activated protein kinase connection in Trypanosomatids: a key sensory role in parasite signalling and development? *Cell Microbiol* 11, 710-718

21. Baker, N., Glover, L., Munday, J. C., Aguinaga Andres, D., Barrett, M. P., de Koning, H. P., and Horn, D. (2012) Aquaglyceroporin 2 controls susceptibility to melarsoprol and pentamidine in African trypanosomes. *Proc Natl Acad Sci U S A* 109, 10996-11001

22. Maser, P., Sutterlin, C., Kralli, A., and Kaminsky, R. (1999) A nucleoside transporter from *Trypanosoma brucei* involved in drug resistance. *Science* 285, 242-244

23. Carter, N. S., and Fairlamb, A. H. (1993) Arsenical-resistant trypanosomes lack an unusual adenosine transporter. *Nature* 361, 173-176

24. Matovu, E., Seebeck, T., Enyaru, J. C., and Kaminsky, R. (2001) Drug resistance in *Trypanosoma brucei* spp., the causative agents of sleeping sickness in man and nagana in cattle. *Microbes Infect* 3, 763-770

25. Stewart, M. L., Krishna, S., Burchmore, R. J., Brun, R., de Koning, H. P., Boykin, D. W., Tidwell, R. R., Hall, J. E., and Barrett, M. P. (2005) Detection of arsenical drug resistance in *Trypanosoma brucei* with a simple fluorescence test. *Lancet* 366, 486-487

26. Graf, F. E., Ludin, P., Wenzler, T., Kaiser, M., Brun, R., Pyana, P. P., Buscher, P., de Koning, H. P., Horn, D., and Maser, P. (2013) Aquaporin 2 mutations in *Trypanosoma brucei* gambiense field isolates correlate with decreased susceptibility to pentamidine and melarsoprol. *PLoS Negl Trop Dis* 7, e2475

27. de Miguel, N., Lustig, G., Twu, O., Chattopadhyay, A., Wohlschlegel, J. A., and Johnson, P. J. (2010) Proteome analysis of the surface of Trichomonas vaginalis reveals novel proteins and strain-dependent differential expression. *Mol Cell Proteomics* 9, 1554-1566

28. Oberholzer, M., Langousis, G., Nguyen, H. T., Saada, E. A., Shimogawa, M. M., Jonsson, Z. O., Nguyen, S. M., Wohlschlegel, J. A., and Hill, K. L. (2011) Independent Analysis of the Flagellum Surface and Matrix Proteomes Provides Insight into Flagellum Signaling in Mammalian-infectious *Trypanosoma brucei*. *Mol Cell Proteomics* 10, M111 010538

29. Oberholzer, M., Lopez, M. A., Ralston, K. S., and Hill, K. L. (2009) Approaches for functional analysis of flagellar proteins in African trypanosomes. *Methods in Cell Biology* 93, 21-57

30. Cross, G. A. (1984) Release and purification of *Trypanosoma brucei* variant surface glycoprotein. *J Cell Biochem* 24, 79-90

31. Kaiser, P., and Wohlschlegel, J. (2005) Identification of ubiquitination sites and determination of ubiquitin-chain architectures by mass spectrometry. *Methods Enzymol* 399, 266-277

32. Wohlschlegel, J. A. (2009) Identification of SUMO-conjugated proteins and their SUMO attachment sites using proteomic mass spectrometry. *Methods Mol Biol* 497, 33-49

33. Michalski, A., Damoc, E., Hauschild, J. P., Lange, O., Wieghaus, A., Makarov, A., Nagaraj, N., Cox, J., Mann, M., and Horning, S. (2011) Mass spectrometry-based proteomics using Q Exactive, a high-performance benchtop quadrupole Orbitrap mass spectrometer. *Mol Cell Proteomics* 10, M111 011015

34. Kelstrup, C. D., Young, C., Lavallee, R., Nielsen, M. L., and Olsen, J. V. (2012) Optimized fast and sensitive acquisition methods for shotgun proteomics on a quadrupole orbitrap mass spectrometer. *J Proteome Res* 11, 3487-3497

35. Tabb, D. L., McDonald, W. H., and Yates, J. R., 3rd (2002) DTASelect and Contrast: tools for assembling and comparing protein identifications from shotgun proteomics. *J Proteome Res* 1, 21-26

36. Cociorva, D., D, L. T., and Yates, J. R. (2007) Validation of tandem mass spectrometry database search results using DTASelect. *Current protocols in bioinformatics / editoral board, Andreas D. Baxevanis ... [et al.]* Chapter 13, Unit 13 14

37. Xu, T., Venable, J.D., Kyu Park, S., Cociorva, C., Lu, B., Liao, L., Wohlschlegel, J., Hewel, J., and Yates III, J.R. (2006) ProLuCID, a Fast and Sensitive Tandem Mass Spectra-based Protein Identification Program. *Mol Cell Proteomics* 5, S174

38. Elias, J. E., and Gygi, S. P. (2007) Target-decoy search strategy for increased confidence in large-scale protein identifications by mass spectrometry. *Nat Methods* 4, 207-214

39. Florens, L., Carozza, M. J., Swanson, S. K., Fournier, M., Coleman, M. K., Workman, J. L., and Washburn, M. P. (2006) Analyzing chromatin remodeling complexes using shotgun proteomics and normalized spectral abundance factors. *Methods* 40, 303-311

40. Vizcaino, J. A., Deutsch, E. W., Wang, R., Csordas, A., Reisinger, F., Rios, D., Dianes, J. A., Sun, Z., Farrah, T., Bandeira, N., Binz, P. A., Xenarios, I., Eisenacher, M., Mayer, G., Gatto, L., Campos, A., Chalkley, R. J., Kraus, H. J., Albar, J. P., Martinez-Bartolome, S., Apweiler, R., Omenn, G. S., Martens, L., Jones, A. R., and Hermjakob, H. (2014) ProteomeXchange provides globally coordinated proteomics data submission and dissemination. *Nat Biotechnol* 32, 223-226

41. MacLean, B., Tomazela, D. M., Shulman, N., Chambers, M., Finney, G. L., Frewen, B., Kern, R., Tabb, D. L., Liebler, D. C., and MacCoss, M. J. (2010) Skyline: an open source document editor for creating and analyzing targeted proteomics experiments. *Bioinformatics* 26, 966-968

42. Clough, T., Thaminy, S., Ragg, S., Aebersold, R., and Vitek, O. (2012) Statistical protein quantification and significance analysis in label-free LC-MS experiments with complex designs. *BMC bioinformatics* 13 Suppl 16, S6

43. Butter, F., Bucerius, F., Michel, M., Cicova, Z., Mann, M., and Janzen, C. J. (2013) Comparative proteomics of two life cycle stages of stable isotope-labeled

Trypanosoma brucei reveals novel components of the parasite's host adaptation machinery. *Mol Cell Proteomics* 12, 172-179

44. Urbaniak, M. D., Guther, M. L., and Ferguson, M. A. (2012) Comparative SILAC proteomic analysis of *Trypanosoma brucei* bloodstream and procyclic lifecycle stages. *PLoS One* 7, e36619

45. Gunasekera, K., Wuthrich, D., Braga-Lagache, S., Heller, M., and Ochsenreiter, T. (2012) Proteome remodelling during development from blood to insect-form *Trypanosoma brucei* quantified by SILAC and mass spectrometry. *BMC Genomics* 13, 556

46. Jackson, A. P., Allison, H. C., Barry, J. D., Field, M. C., Hertz-Fowler, C., and Berriman, M. (2013) A cell-surface phylome for African trypanosomes. *PLoS Negl Trop Dis* 7, e2121

47. Saada, E. A., Kabututu, Z. P., Lopez, M., Shimogawa, M. M., Langousis, G., Oberholzer, M., Riestra, A., Jonsson, Z. O., Wohlschlegel, J. A., and Hill, K. L. (2014) Insect Stage-Specific Receptor Adenylate Cyclases Are Localized to Distinct Subdomains of the *Trypanosoma brucei* Flagellar Membrane. *Eukaryot Cell* 13, 1064-1076

48. Salmon, D., Vanwalleghem, G., Morias, Y., Denoeud, J., Krumbholz, C., Lhomme, F., Bachmaier, S., Kador, M., Gossmann, J., Dias, F. B., De Muylder, G., Uzureau, P., Magez, S., Moser, M., De Baetselier, P., Van Den Abbeele, J., Beschin, A., Boshart, M., and Pays, E. (2012) Adenylate cyclases of *Trypanosoma brucei* inhibit the innate immune response of the host. *Science* 337, 463-466

49. Kabututu, Z. P., Thayer, M., Melehani, J. H., and Hill, K. L. (2010) CMF70 is a subunit of the dynein regulatory complex. *Journal of Cell Science* 123, 3587-3595

50. Brenndorfer, M., and Boshart, M. (2010) Selection of reference genes for mRNA quantification in *Trypanosoma brucei*. *Molecular and biochemical parasitology* 172, 52-55

51. Livak, K. J., and Schmittgen, T. D. (2001) Analysis of relative gene expression data using real-time quantitative PCR and the 2(-Delta Delta C(T)) Method. *Methods* 25, 402-408

52. Barrett, M. P., Tetaud, E., Seyfang, A., Bringaud, F., and Baltz, T. (1998) Trypanosome glucose transporters. *Mol Biochem Parasitol* 91, 195-205

53. Sanchez, M. A., Tryon, R., Green, J., Boor, I., and Landfear, S. M. (2002) Six related nucleoside/nucleobase transporters from *Trypanosoma brucei* exhibit distinct biochemical functions. *J Biol Chem* 277, 21499-21504

54. Paindavoine, P., Rolin, S., Van Assel, S., Geuskens, M., Jauniaux, J. C., Dinsart, C., Huet, G., and Pays, E. (1992) A gene from the variant surface glycoprotein expression site encodes one of several transmembrane adenylate cyclases located on the flagellum of *Trypanosoma brucei*. *Mol Cell Biol* 12, 1218-1225

55. Alexandre, S., Paindavoine, P., Tebabi, P., Pays, A., Halleux, S., Steinert, M., and Pays, E. (1990) Differential expression of a family of putative adenylate/guanylate cyclase genes in *Trypanosoma brucei*. *Mol Biochem Parasitol* 43, 279-288

56. Lopez, M. A., Saada, E. A., and Hill, K. L. (2015) Insect stage-specific adenylate cyclases regulate social motility in african trypanosomes. *Eukaryot Cell* 14, 104-112

57. Jackson, A. P. (2007) Tandem gene arrays in *Trypanosoma brucei*: comparative phylogenomic analysis of duplicate sequence variation. *BMC Evol Biol* 7, 54

58. Subota, I., Julkowska, D., Vincensini, L., Reeg, N., Buisson, J., Blisnick, T., Huet, D., Perrot, S., Santi-Rocca, J., Duchateau, M., Hourdel, V., Rousselle, J. C., Cayet, N., Namane, A., Chamot-Rooke, J., and Bastin, P. (2014) Proteomic analysis of intact flagella of procyclic *Trypanosoma brucei* cells identifies novel flagellar proteins with unique sub-localization and dynamics. *Mol Cell Proteomics* 13, 1769-1786

59. Bridges, D. J., Pitt, A. R., Hanrahan, O., Brennan, K., Voorheis, H. P., Herzyk, P., de Koning, H. P., and Burchmore, R. J. (2008) Characterisation of the plasma membrane subproteome of bloodstream form *Trypanosoma brucei*. *Proteomics* 8, 83-99

60. Borst, P., and Cross, G. A. (1982) Molecular basis for trypanosome antigenic variation. *Cell* 29, 291-303

61. Gerrits, H., Mussmann, R., Bitter, W., Kieft, R., and Borst, P. (2002) The physiological significance of transferrin receptor variations in *Trypanosoma brucei*. *Mol Biochem Parasitol* 119, 237-247

62. Bitter, W., Gerrits, H., Kieft, R., and Borst, P. (1998) The role of transferrin-receptor variation in the host range of *Trypanosoma brucei*. *Nature* 391, 499-502

63. Oli, M. W., Cotlin, L. F., Shiflett, A. M., and Hajduk, S. L. (2006) Serum resistance-associated protein blocks lysosomal targeting of trypanosome lytic factor in *Trypanosoma brucei*. *Eukaryot Cell* 5, 132-139

64. Vanhollebeke, B., De Muylder, G., Nielsen, M. J., Pays, A., Tebabi, P., Dieu, M., Raes, M., Moestrup, S. K., and Pays, E. (2008) A haptoglobin-hemoglobin receptor conveys innate immunity to *Trypanosoma brucei* in humans. *Science* 320, 677-681

65. Emmer, B. T., Daniels, M. D., Taylor, J. M., Epting, C. L., and Engman, D. M. (2010) Calflagin inhibition prolongs host survival and suppresses parasitemia in *Trypanosoma brucei* infection. *Eukaryot Cell* 9, 934-942

66. Ruepp, S., Furger, A., Kurath, U., Renggli, C. K., Hemphill, A., Brun, R., and Roditi, I. (1997) Survival of *Trypanosoma brucei* in the tsetse fly is enhanced by the expression of specific forms of procyclin. *The Journal of cell biology* 137, 1369-1379

67. Alsford, S., Eckert, S., Baker, N., Glover, L., Sanchez-Flores, A., Leung, K. F., Turner, D. J., Field, M. C., Berriman, M., and Horn, D. (2012) High-throughput decoding of antitrypanosomal drug efficacy and resistance. *Nature* 482, 232-236

68. Shahi, S. K., Krauth-Siegel, R. L., and Clayton, C. E. (2002) Overexpression of the putative thiol conjugate transporter TbMRPA causes melarsoprol resistance in *Trypanosoma brucei*. *Mol Microbiol* 43, 1129-1138

69. Vincent, I. M., Creek, D., Watson, D. G., Kamleh, M. A., Woods, D. J., Wong, P. E., Burchmore, R. J., and Barrett, M. P. (2010) A molecular mechanism for eflornithine resistance in African trypanosomes. *PLoS Pathog* 6, e1001204

70. Schumann Burkard, G., Jutzi, P., and Roditi, I. (2011) Genome-wide RNAi screens in bloodstream form trypanosomes identify drug transporters. *Mol Biochem Parasitol* 175, 91-94

71. Baker, N., Alsford, S., and Horn, D. (2011) Genome-wide RNAi screens in African trypanosomes identify the nifurtimox activator NTR and the eflornithine transporter AAT6. *Molecular and biochemical parasitology* 176, 55-57

72. Alsford, S., Turner, D., Obado, S., Sanchez-Flores, A., Glover, L., Berriman, M., Hertz-Fowler, C., and Horn, D. (2011) High throughput phenotyping using parallel sequencing of RNA interference targets in the African trypanosome. *Genome Res*

73. Berriman, M., Ghedin, E., Hertz-Fowler, C., Blandin, G., Renauld, H., Bartholomeu, D. C., Lennard, N. J., Caler, E., Hamlin, N. E., Haas, B., Bohme, U., Hannick, L., Aslett, M. A., Shallom, J., Marcello, L., Hou, L., Wickstead, B., Alsmark, U. C., Arrowsmith, C., Atkin, R. J., Barron, A. J., Bringaud, F., Brooks, K., Carrington, M., Cherevach, I., Chillingworth, T. J., Churcher, C., Clark, L. N., Corton, C. H., Cronin, A., Davies, R. M., Doggett, J., Djikeng, A., Feldblyum, T., Field, M. C., Fraser, A., Goodhead, I., Hance, Z., Harper, D., Harris, B. R., Hauser, H., Hostetler, J., Ivens, A., Jagels, K., Johnson, D., Johnson, J., Jones, K., Kerhornou, A. X., Koo, H., Larke, N., Landfear, S., Larkin, C., Leech, V., Line, A., Lord, A., Macleod, A., Mooney, P. J., Moule, S., Martin, D. M., Morgan, G. W., Mungall, K., Norbertczak, H., Ormond, D., Pai, G., Peacock, C. S., Peterson, J., Quail, M. A., Rabbinowitsch, E., Rajandream, M. A., Reitter, C., Salzberg, S. L., Sanders, M., Schobel, S., Sharp, S., Simmonds, M., Simpson, A. J., Tallon, L., Turner, C. M., Tait, A., Tivey, A. R., Van Aken, S., Walker, D., Wanless, D., Wang, S., White, B., White, O., Whitehead, S., Woodward, J., Wortman, J., Adams, M. D., Embley, T. M., Gull, K., Ullu, E., Barry, J. D., Fairlamb, A. H., Opperdoes, F., Barrell, B. G., Donelson, J. E., Hall, N., Fraser, C.

M., and et al. (2005) The genome of the African trypanosome *Trypanosoma brucei*. *Science* 309, 416-422

74. Hanrahan, O., Webb, H., O'Byrne, R., Brabazon, E., Treumann, A., Sunter, J. D., Carrington, M., and Voorheis, H. P. (2009) The glycosylphosphatidylinositol-PLC in *Trypanosoma brucei* forms a linear array on the exterior of the flagellar membrane before and after activation. *PLoS Pathog* 5, e1000468

75. Sunter, J., Webb, H., and Carrington, M. (2013) Determinants of GPI-PLC localisation to the flagellum and access to GPI-anchored substrates in trypanosomes. *PLoS Pathog* 9, e1003566

76. Proto, W. R., Castanys-Munoz, E., Black, A., Tetley, L., Moss, C. X., Juliano, L., Coombs, G. H., and Mottram, J. C. (2011) *Trypanosoma brucei* metacaspase 4 is a pseudopeptidase and a virulence factor. *J Biol Chem* 286, 39914-39925

77. Liu, W., Apagyi, K., McLeavy, L., and Ersfeld, K. (2010) Expression and cellular localisation of calpain-like proteins in *Trypanosoma brucei*. *Molecular and biochemical parasitology* 169, 20-26

78. Demmel, L., Schmidt, K., Lucast, L., Havlicek, K., Zankel, A., Koestler, T., Reithofer, V., de Camilli, P., and Warren, G. (2014) The endocytic activity of the flagellar pocket in *Trypanosoma brucei* is regulated by an adjacent phosphatidylinositol phosphate kinase. *J Cell Sci* 127, 2351-2364

Chapter III:

Independent analysis of the flagellum surface and matrix proteomes provides insight into flagellum signaling in mammalian-infectious *Trypanosoma brucei*

PREFACE

The following chapter is a modified version "Independent analysis of the flagellum surface and matrix proteomes provides insight into flagellum signaling in mammalian-infectious *Trypanosoma brucei,"* by Oberholzer *et al,* originally published in Molecular and Cellular Proteomics, 2011: 10(10):M111.010538 and reprinted with permission.

In this work, we utilized a mutant cell line that results in readily-detached flagella, allowing us to mechanically separate and isolate the flagellum of bloodstream form *t. brucei* in order to do surface protein proteomic analyses, similar as described in Chapter II. We additionally used the non-biotinylated soluble proteins to establish the flagellar matrix proteome. As a co-second author, I contributed significantly to this manuscript. Experimental contributions included assisting in validation of the flagellar surface proteome by epitope tagging candidate flagellar membrane proteins (FS21, FS31, and FS105) as well as the sole person validating candidate matrix proteins by epitope tagging (FAP174, FAP265) and RNAi (FAP174). Additionally, I assisted in optimization of immunofluorescence and analysis of extracted flagella (ie, Figure 03-2). Furthermore, I was responsible for most of the technical bioinformatics-based analyses on both surface and matrix proteomes. This included cross-referencing against existing RNAseq and proteomic data, analyzing and categorizing our proteins by putative function (DAVID analysis) or presence of surface-association features (such as signal peptides and transmembrane domains, GPI anchors, dual-acylation motifs, et cetera). The full manuscript (and all supplemental files) are available on the journal website.

SUMMARY

The flagellum of African trypanosomes is an essential and multifunctional organelle that functions in motility, cell morphogenesis and host-parasite interaction. Previous studies of the trypanosome flagellum have been limited by the inability to purify flagella without first removing the flagellar membrane. This limitation is particularly relevant in the context of studying flagellum signaling, as signaling requires surface-exposed proteins in the flagellar membrane and soluble signaling proteins in the flagellar matrix. Here we employ a combination of genetic and mechanical approaches to purify intact flagella from the African trypanosome, *Trypanosoma brucei*, in its mammalian-infectious stage. We combined flagellum purification with affinity-purification of surface-exposed proteins to conduct independent proteomic analyses of the flagellum surface and matrix fractions. The proteins identified encompass a broad range of molecular functionalities, including many predicted to function in signaling. Immunofluorescence and RNA interference (RNAi) studies demonstrate flagellum localization and function for proteins identified and provide insight into mechanisms of flagellum attachment and motility. The flagellum surface proteome includes many *T. brucei*-specific proteins and is enriched for proteins upregulated in the mammalian-infectious stage of the parasite life-cycle. The combined results indicate that the flagellum surface presents a diverse and dynamic host-parasite interface that is well-suited for host-parasite signaling.

INTRODUCTION

The eukaryotic flagellum is recognized as a major signaling center that acts as a cellular antenna to sense and transduce extracellular signals [1-4]. A sensory function for the flagellum is broadly conserved across diverse taxa [5]. In metazoans, receptor-guanylate cyclases, ion channels and G protein-coupled receptors (GPCRs) in the flagellar membrane perceive chemical and mechanical cues that are necessary for normal development, physiology and reproduction [6-9]. Important examples include wingless (Wnt) and hedgehog signaling responses in vertebrates [3,10]. In protists, flagellum-localized ion channels, agglutinins and receptor-kinases control motility, mating and response to extracellular growth factors [11-13]. Flagella are prominent among pathogenic protozoa, which cause tremendous human suffering worldwide and present a barrier to economic development in some of the poorest regions of the world [14-17]. These include the etiological agents of African sleeping sickness, leishmaniasis, malaria, epidemic diarrhea and trichomoniasis [14-16,18]. In most cases these pathogens are obligate parasitic organisms whose survival depends upon their ability to sense and respond to extracellular cues in diverse host environments. The flagellum's motility function in protozoan parasites is self-evident, but its capacity for sensing and responding to external signals is largely unexplored.

African trypanosomes, e.g. *Trypanosoma brucei*, are uniflagellated protozoan parasites that cause African sleeping sickness in humans and related diseases in wild and domestic animals [19]. *T. brucei* is transmitted to the bloodstream of a mammalian host through the bite of a tsetse fly vector. To be successful, *T. brucei* must integrate environmental signals that direct parasite movements and

developmental transformations within specific host compartments [20-22]. For example, entry into the mammalian bloodstream promotes cellular adaptations that define the bloodstream-form life cycle stage, including changes in metabolism, morphology and surface protein composition [23]. Prominent among these is differentiation of proliferative, 'long-slender' forms into cell cycle-arrested, 'short-stumpy' forms that are adapted for survival in the tsetse [23,24]. Parasite-host signaling is also reported to contribute to invasion of the central nervous system [25]. In the tsetse, bloodstream-forms differentiate into procyclic-forms, which reenter the cell cycle and establish an infection in the fly midgut. Procyclic-form parasites undergo a defined series of directional migrations and tissue-specific developmental transformations, culminating in flagellum attachment to epithelial cells in the tsetse salivary gland and differentiation into human-infectious forms [26,27]. Except for surface-exposed carboxylate transporters that participate in stumpy-to-procyclic differentiation [24], proteins that perceive signals for directing parasite navigation and tissue-specific development are mostly unknown.

The paradigm of the flagellum as a sensory organelle in other eukaryotes, together with the observation that the trypanosome flagellum interacts directly with host tissues [26,28], has fueled the hypothesis that the parasite flagellum functions as a signaling organelle for integrating host-derived and parasite-derived signals [20,22]. In *T. brucei*, this idea is supported by the finding that specific proteins from cyclic nucleotide and Ca^{2+} signaling pathways are present in the flagellum [29-34]. The *T. brucei* flagellum (Fig. 3-01) is built around a microtubule-based axoneme plus an extra-axonemal filament, termed the paraflagellar rod (PFR), which runs alongside

and is attached to the axoneme [15,35]. The axoneme and PFR are ensheathed by a flagellar membrane whose protein and lipid composition are distinct from the cell surface membrane [36,37]. The lumen of the flagellum, termed the flagellar matrix, is contiguous with the cytoplasm, but selective filters at the base of the flagellum restrict access to the matrix, such that protein composition of the matrix is distinct from that of the cytoplasm [38]. The flagellum emerges from the cytoplasm at the cell posterior and is laterally connected to the cell body by cytoskeletal filaments that connect the axoneme and PFR to subpellicular microtubules in the cell body and maintain tight apposition of the flagellar and cell surface membranes [39,40]. These connections form a "flagellum attachment zone" (FAZ) that runs along most of the length of the flagellum, with a small distal portion of the flagellum extending free of the cell body. A specialized membrane domain, termed the flagellar pocket, surrounds the flagellum at the site where it emerges from the cytoplasm at the cell posterior [39,41,42]. As the sole site of surface protein turnover and macromolecular uptake in trypanosomes, the flagellar pocket is a key portal for host-parasite interaction [41,42], yet little is known about its protein and lipid compositions.

Lateral attachment of the flagellum to the cell body poses significant challenges for isolating intact flagella from *T. brucei*. Existing procedures employ detergent-extraction and salt-extraction to isolate the insoluble flagellum skeleton, which contains the axoneme and PFR, but lacks the membrane and matrix [43-45]. Thus, although several hundred axonemal and PFR proteins have been identified [31,43,46], the protein compositions of the flagellar membrane and matrix in *T. brucei* are largely unknown. This poses a particular limitation for studying flagellum

signaling, because signaling capacity is dictated by surface-exposed membrane proteins coupled to soluble components of signaling cascades in the matrix [2].

Here we employ a combined genetic and mechanical approach to isolate intact, membrane-enclosed flagella from *T. brucei* in its mammalian-infectious stage. We used flagellum purification, combined with affinity purification of surface-exposed proteins and multidimensional protein identification technology (MudPIT) to define the flagellum surface and flagellum matrix proteomes. Immunofluorescence and RNAi demonstrate flagellum localization and function for proteins identified and provide insight into mechanisms of flagellum attachment and motility. Our combined studies indicate that the trypanosome flagellum presents a diverse and dynamic signaling platform adapted for host-pathogen interaction.

EXPERIMENTAL PROCEDURES

Cell lines

Bloodstream-form trypanosomes, 221 single marker cell line [47], were used for all experiments and were cultivated in HMI-9 medium supplemented with 10-15% fetal bovine serum (Gibco) as described previously [48]. The *fla1* cell line was generated by transfection with the p2T7-Fla1 plasmid [49] using standard procedures [48]. Selection for transformants was done using 5µg/ml Phleomycin (InvivoGen).

Surface biotinylation

Cells were washed twice in ice-cold PBS and resuspended in ice-cold PBS + 0.5 mg/ml sulfosuccinimidyl-2-[biotinamido]ethyl-1,3-dithiopropionate (Sulfo-NHS-SS-biotin; Thermo Scientific). After incubation on ice for 10-30 min with gentle agitation, unreacted Sulfo-NHS-SS-biotin was blocked by addition of Tris to 100 mM final concentration. Biotinylated cells were washed three times in ice-cold PBS + 100 mM Tris.

Purification of flagella and flagellar surface proteins

Cells harboring the *fla1* tet-inducible RNAi cassette (density $5x10^5$ cells/ml) were induced for 18 h with 1 µg/ml tetracycline. From this step onward all procedures were performed at 4°C unless otherwise stated and all solutions were cooled on ice. Induced cells were surface biotinylated as described above. Flagella were removed

from the cell bodies by repeated passage (five times) through a 28G needle. Some (<1%) of isolated flagella remained motile. The resulting flagella plus cell body mixture was loaded on a 30% sucrose bed and centrifuged for 10 min at 770g. The supernatant and interface containing isolated flagella were collected and sucrose sedimentation was repeated. Purified flagella were collected by a high-speed spin (15,000g, 1h) and resuspended in 200 µl PBS, containing 2.5 µg/ml Leupeptin and 0.5 µg/ml Pepstatin. Purified, biotinylated flagella were lysed by addition of NP40 to 0.5% final concentration and incubation on ice for 10 min. Soluble proteins (flagellum matrix and membrane) were separated from insoluble proteins (flagellum skeleton) by centrifugation (15,000g, 30min). The resulting soluble flagellar proteins (200 µl) were incubated with 50µl streptavidin beads (Streptavidin Sepharose High Performance, GE Healthcare) for 30 min with agitation. Proteins bound to streptavidin beads were separated from the unbound fraction by centrifugation and washed at room temperature once in buffer A (8M Urea, 200 mM NaCl, 2% SDS, 100 mM Tris, pH 8), once in buffer B (8M Urea, 1.2 M NaCl, 0.2% SDS, 100 mM Tris, 10% Ethanol, 10% Isopropanol, pH 8), once in buffer C (8M Urea, 200 mM NaCl, 0.2% SDS, 100 mM Tris, 10% Ethanol, 10% Isopropanol, pH 8) and twice in buffer D (8M Urea, 100 mM Tris, pH 8). All fractions were analyzed by Western blotting using standard protocols (Fig. 3-03). Antibodies used were anti-BiP 1:10,000 [50], anti-PFR 1:1,000 [45], anti-VSG221 1:10,000 [51], anti-biotin 1:2,000 (Jackson Immunoresearch). Secondary antibodies were HRP-coupled donkey anti-mouse or donkey anti-rabbit 1:2,500 (Bio-Rad).

MudPIT analysis

Streptavidin-bound proteins were digested directly on beads by the sequential addition of lys-C and trypsin proteases [52,53]. Peptide samples were fractionated online using multidimensional chromatography followed by tandem mass spectrometric analysis on a LTQ-Orbitrap mass spectrometer (ThermoFisher) as previously described [53,54]. RawXtract (ver. 1.8) was used to extract peaklist information from Xcalibur-generated RAW files. Database searching of the MS/MS spectra was performed using the ProLuCID algorithm (ver 1.0) and a user assembled database consisting of all protein entries from the TriTrypDB for *T. brucei* strain 927 (version 2.3, 10533 entries) and seven sequences from *T. brucei* strain 427: 453391 (Tb-1.7g), 458439 (Tb-24), 18413545 (ESAG4.a from 221 expression site), 18413551 (ESAG4.b from 221 expression site), 189094632 (VSG-221), 18413541 (ESAG7 from 221 expression site), 18413542 (ESAG6 from 221 expression site) [55]. Other database search parameters included: (1) precursor ion mass tolerance of +/- 20 ppm, (2) fragment ion mass tolerance of +/- 400 ppm, (3) only peptides with fully tryptic ends were considered candidate peptides in the search with no consideration for missed cleavages, and (4) static modification of +57.02156 on cysteine residues. Peptide identifications were organized and filtered using the DTASelect algorithm which uses a linear discriminant analysis to identify peptide scoring thresholds that yield a peptide-level false discovery rate of less than 5% as estimated using a decoy database approach. Proteins were considered present in the analysis if they were identified by two or more peptides using the 5% peptide-level false discovery rate [56-58].

Immunofluorescence microscopy

Cells or isolated flagella were washed once in PBS and fixed by addition of paraformaldehyde to 0.01% for 5 min on ice. Fixed cells were washed once in PBS and air-dried onto coverslips. The coverslips were incubated for 10 min in -20°C methanol and 10 min in -20°C acetone. After a re-hydration step (10-30 min in PBS) the slides were blocked for 1.5 h in blocking solution (PBS + 5% BSA + 5% Normal donkey serum (Gibco)). Coverslips were incubated with primary antibodies diluted in blocking solution for 1.5 h. Antibodies used were anti-biotin 1:2000 (Jackson ImmunoResearch), anti-BiP 1:10,000 [50], anti-HA.11 1:200-1:1,000 (Covance), anti-PFR 1:500 [45], anti-tyrosinated tubulin YL1/2 1:500 (Chemicon International). After 3 washes in PBS + 0.05% Tween-20 for 10 min each, samples were stained with secondary antibodies diluted in blocking solution for 1.5 h (donkey anti-mouse Alexa Fluor 488, donkey anti-rabbit Alexa Fluor 594, goat anti-rat Alexa Fluor 594 1:500 (Molecular Probes)). Cells were washed three times in PBS + 0.05% Tween-20, once in PBS and mounted with Vectashield containing DAPI (Vector Laboratories). Flagellar pocket staining with biotinylated tomato lectin was performed as described [59]. Biotinylated tomato lectin was visualized using streptavidin Alexa Fluor 594 (Molecular Probes). Images were taken using a 100x objective on a Zeiss Axioskop II compound microscope and processed using Axiovision (Zeiss, Inc.) and Adobe Photoshop (Adobe Systems, Inc.).

NP40 fractionation of whole cells

Cells were washed once in PBS and lysed in ice-cold PBS + 0.5% NP40 + protease inhibitors (complete mini, Roche) for 10 min on ice. Lysates were centrifuged for 30 min at 15,000g at 4°C and supernatant and pellet fractions were analyzed by western blotting using standard procedures. Primary antibodies used were anti-HA.11, anti-BiP (as described above) and anti-trypanin 1:1,000 [60]. Secondary antibodies were HRP-coupled donkey anti-mouse or donkey anti-rabbit 1:2,500 (Bio-Rad).

In situ tagging

In situ tagging was carried out as previously described [61] to introduce epitope-tagged copies of each gene analyzed into the corresponding endogenous chromosomal locus. In brief, 500-800 bp DNA fragments homologous to the target gene open reading frame or 3' UTR were PCR-amplified from genomic DNA and cloned upstream of the 3xHA or downstream of the puromycin resistance marker in pMOTag2H. pMOTag2H is an *in situ* tagging plasmid containing a 3xHA epitope tag and a puromycin resistance marker, adapted from [61]. All sequences were verified by DNA sequencing at the UCLA Sequencing and Genotyping Core center. The tagging cassettes were excised from the pMOTag2H vector backbone by restriction digestion, then purified and transfected into 221 bloodstream-form *T. brucei* using standard methods [48]. Stable transformants were selected using 0.1µg/ml puromycin.

RNAi

The targets for RNAi against FS179 and RSU (FM458) were identified by the Trypanofan RNAit algorithm [62], then PCR-amplified from genomic DNA using primers listed below: (restriction enzyme cleavage sites are underlined):

FS179-RNAi-f: 5' CATAAGCTTTCATTGCGTCATTTTGCCTA 3'

FS179-RNAi-r: 5' CATCTAGAAAGGCTGACGAGATCTTGGA 3'

RSU-RNAi-f: 5' TGTGAAGCAACCCAACACAT 3'

RSU-RNAi-r: 5' GTAATGCGAGAGCGGAGTTC 3'

The resulting DNA fragments for RNAi were ligated into the p2T7-Ti/B-RNAi vector, which is a tetracycline-controlled expression vector with opposing T7 promoters [49]. Inserts were verified by sequencing at the UCLA genomics center. The p2T7-Ti/B-RNAi vector containing the FS179 or RSU target sequence was linearized with NotI, ethanol precipitated and transfected into 221 bloodstream form *T. brucei* as described above. Transformants were selected using 5 μg/ml phleomycin.

Imaging and motility traces

FS179 RNAi imaging (Fig.7 a-c): Cells were induced for 48 h with 1 μg/ml tetracycline, fixed using 4% PFA and mounted with Vectashield containing DAPI (Vector Laboratories). Images were taken and processed as described above. FM458 RNAi motility traces (Fig.7 d,e): Cells were induced for 48h with 1 μg/ml tetracycline and motility traces were obtained for induced and uninduced control cells as described previously [48]. The movie of the isolated flagellum was recorded and played at 30 frames per second as described previously [48].

Bioinformatic and protein comparisons

Protein domains were assessed using the SMART database [63]. For homology searches, we employed eight ciliated (*L. major, T. cruzi, P. falciparum, C. reinhardtii, M. brevicollis, C. elegans, D. melanogaster, H. sapiens*) and 4 non-ciliated (*D. discoideum, S. cerevisiae, C. merolae, A. thaliana*) eukaryotic species, including both unicellular and multicellular representatives. Homology searches were performed using NCBI BLAST with default parameters. Proteins with an expect-value of $\leq 1 \times 10^{-10}$ were considered as homologues and identical criteria were applied across all datasets and comparisons. For *T. brucei* flagellum skeleton proteomes, we used the combined, non-overlapping set of proteins identified in three proteomic analyses of extracted flagellum skeletons from procyclic-form parasites [31,43,46]. Comparison to the *C. reinhardtii* flagellum proteome was done locally with proteins downloaded from [64]. For analysis of molecular function (Table 1), the DAVID Bioinformatics Resource, v6.7 [65,66] was used for functional annotation of proteins in TbFSP and TbFMP. Proteins were categorized using annotated GO terms for molecular function [67], using the GOTERM_MF_2 category with a threshold count of 2 and an EASE of 0.1. Expression analysis (Fig.3-10) was done using RNA sequencing data from [68].

RESULTS

Purification of intact, membrane-enclosed flagella from *T. brucei* in its mammalian-infectious form

The *T. brucei* flagellum is laterally connected to the cell body along most of its length by filamentous connectors and tightly apposed membrane-membrane contacts (40). These connections present significant challenges for isolating intact flagella. Current approaches employ detergents to remove membranes, together with salt-extraction to disrupt filamentous connectors, followed by centrifugation to isolate flagellum skeletons from solubilized material (43-45). Resultant preparations contain the axoneme and PFR, but are stripped of flagellar membrane and soluble matrix proteins. To obviate the need for detergent and salt-extraction, and thus retain the flagellar membrane, we employed tetracycline-inducible RNA interference (RNAi) against *fla1* to disrupt lateral flagellum attachment to the cell body (49). This allowed intact flagella to be separated from cell bodies by shearing, without using detergent (Fig. 3-02). Importantly, some isolated flagella remained motile without addition of exogenous ATP (Fig. 3-02b), indicating that they retained an intact flagellum membrane, as well as internal proteins and small molecules necessary for motility. Flagella were purified from cell bodies by sucrose density sedimentation (Fig. 3-02). To enable purification of surface-exposed proteins, cells were surface biotinylated prior to flagellum purification (Fig. 3-02d). Surface-biotinylation was retained in purified flagella (Fig. 3-02e). The bulbous enlargement at one end of purified flagella

contains material from the basal body, kinetoplast and flagellar pocket (Fig. 3-02e). Thus, purified flagella retain an intact membrane that includes flagellar pocket membrane.

Purified, surface-biotinylated flagella were lysed with non-ionic detergent (NP40) and lysates were centrifuged to separate the insoluble fraction, containing flagellum skeleton proteins, from the soluble fraction, containing matrix plus membrane proteins. Biotinylated proteins in the soluble fraction were purified by adsorption to streptavidin beads and fractions from the purification were analyzed for total protein, biotin and specific marker proteins (Fig. 3-03). Purified flagella were enriched for flagellum markers (PFR) relative to intracellular markers (BiP). Streptavidin-binding quantitatively purified biotinylated proteins and SYPRO-Ruby staining revealed unique protein profiles for the streptavidin-bound and unbound fractions. The bound fraction contained surface proteins (variable surface glycoprotein, VSG (68)), but not abundant intracellular proteins (Binding Protein, BiP (50)), or intraflagellar proteins (paraflagellar rod protein, PFR (45)) (Fig. 3-03). These results support immunofluorescence data (Fig. 3-02d and e) indicating that biotinylation was specific for surface proteins.

Identification of flagellum surface and matrix proteins by mass spectrometry

Proteins in the streptavidin-bound and unbound fractions were identified by MudPIT proteomic analysis. In some cases peptide coverage allowed unambiguous identification of proteins. In other cases, peptides did not distinguish between proteins with very similar sequences. As such, each proteomic dataset represents a

maximum number and minimum number of total proteins, with the minimum number reflecting groups of proteins whose sequences could not be unambiguously distinguished. From here on, we refer to the minimum number of proteins identified in each fraction. This analysis identified 158 proteins in the bound fraction, termed the *T. brucei* flagellum surface proteome ("TbFSP", Supplemental Table ST3-01) and 666 proteins in the unbound fraction, termed the *T. brucei* flagellum matrix proteome ("TbFMP", Supplemental Table ST3-03). Proteins in the two datasets encompassed a broad range of predicted functionalities and both datasets included a large number of proteins with no annotated molecular function (Table T1). We next employed several independent analyses to validate the proteomic datasets. Each dataset included suspected contaminants, e.g. ribosomal proteins. However, to avoid user bias, no subjective filters were applied to remove these suspected contaminants and analyses were performed on the unfiltered datasets, i.e. 158 proteins in TbFSP and 666 proteins in TbFMP. We focused on the flagellum surface proteome because the primary interest was surface-exposed proteins.

Validation of the flagellum surface proteome.

As a first step in assessing the quality of the proteomic datasets, we probed each dataset for proteins known to localize to specific flagellum compartments (Fig. 3-04). The flagellum surface proteome contained most known flagellum membrane proteins and was generally devoid of intraflagellar proteins, i.e. flagellum matrix and

skeleton proteins (Fig. 3-04a, supplemental table ST5 and ST8, ST2). By comparison, the flagellum matrix proteome contained 7 of 21 known matrix proteins, 9 of 10 known membrane proteins and 62 of 532 flagellum skeleton proteins (Fig. 3-04b, supplemental table ST8, ST4). We also examined each dataset for predicted transmembrane (TM) domains, as these are expected to be enriched in the surface proteome. As expected, proteins with predicted TM domains were enriched in the surface proteome (51%) compared to the genome as a whole (19%) [70,71], the flagellum matrix (20%) or the flagellum skeleton (2%) (Fig. 3-05). Proteins with a predicted signal peptide were also enriched in the flagellum surface proteome (38%) versus the genome (24%) and the matrix (20%) (ST2 and ST4). By using the minimal number of proteins identified, our analysis is suspected to underestimate the enrichment of TM domains and signal peptides in the flagellum surface proteome, because the genome numbers include redundant and closely related sequences.

We next used epitope-tagging and immunofluorescence microscopy to determine the subcellular location of ten proteins from the flagellum surface proteome. All tagged proteins were detergent-soluble (Supplemental Fig. S2 and not shown), consistent with membrane association. Eight of ten tagged proteins localized to one or more sub-domains of the flagellum membrane, e.g. along the entire length of the flagellum, the flagellar pocket or the flagellum attachment zone (Fig.6, Supplemental Fig. S3 and data not shown). Four of these eight proteins were exclusively located in the flagellum and/or flagellar pocket, one was distributed throughout the whole cell surface and three were also observed in intracellular compartments (summarized in Supplemental Table ST6). In sum, the flagellum surface

proteome includes most experimentally characterized flagellum membrane proteins, is largely devoid of intraflagellar proteins and immunolocalization demonstrates flagellar location for several proteins identified. Thus, the results indicate that the flagellum surface proteome is enriched for flagellum membrane proteins.

RNAi knockdown reveals flagellar functions for proteins identified

We used tetracycline-inducible RNAi to determine whether loss of a particular protein impacted flagellum function. In most cases, RNAi directed against proteins in the flagellum surface proteome did not reveal an obvious phenotype in culture (not shown). One notable exception was FS179, which encodes a putative calcium channel. Immunofluorescence showed that FS179 was localized to the flagellum attachment zone (Fig. 3-06b), suggesting a potential role in flagellum attachment. RNAi knockdown of FS179 caused the flagellum to become detached from the cell body and the daughter flagellum was preferentially affected (Fig. 3-07 a-c). This result supports FS179 localization to the flagellum attachment zone and is consistent with previous studies suggesting a requirement for Ca^{2+} in flagellum attachment [40]. The flagellar matrix protein FM458 corresponds to the protein kinase A regulatory subunit (RSU) [72] and was of interest based on the importance of protein kinase A and cyclic nucleotide signaling to flagellum function in other organisms [13,73,74]. RNAi knockdown of FM458 inhibited forward motility, consistent with a role in flagellum function (Fig. 3-07 d,e). Interestingly, despite motility defects, bloodstream-form FM458 knockdowns were viable, which contrasts to the lethal phenotype caused by knockdown of flagellum skeleton proteins [29,43,60].

Host-parasite signaling capacity of the flagellum surface

Prominent within the flagellum surface proteome were proteins known or suspected to function in host-parasite interaction and/or signaling (Fig. 3-08). For example, VSG, MSP-A and GPI-PLC, are characterized surface proteins that function in antigenic variation and VSG clearance [69,75,76]. Likewise, transferrin receptor and glucose transporter function in host nutrient uptake [77,78], while adenylate cyclases and calflagins are predicted to function in host-parasite signaling [30,33,34,79]. In addition, many uncharacterized flagellum surface ("FS") proteins have domain architectures that indicate receptor function, with a large extracellular domain suitable for binding host ligands connected to an intracellular signaling module, e.g. kinase domains in FS164, FS190 and FS201. In some cases, extracellular domains exhibit homology to characterized ligand-binding motifs, such as the periplasmic binding protein superfamily (receptor-type adenylate cyclases) or EGF-like domain superfamily involved in protein-protein interaction (FS133) [80,81]. Also well-represented among uncharacterized proteins are several classes of ion and metabolite transporters, including ABC-transporters (FS166), P-type ATPase pumps (FS60, FS80, FS163, FS188, FS193, FS198), ion channels (FS179), amino acid transporters (FS group 108 and 121), glucose transporters (FS192) and a group of major facilitator proteins (FS group 126) related to the PAD surface receptors that perceive extracellular signals for bloodstream-form to procyclic-form differentiation [24]. In sum, the data indicate a diverse flagellar surface protein repertoire that is suitable for mediating a broad range of host-parasite interactions.

The flagellum surface is enriched for *T. brucei*-specific proteins

The flagellum surface is postulated to function in detection of extracellular signals and is therefore anticipated to include cell-specific proteins that accommodate environments uniquely encountered by *T. brucei*. The availability of an independent flagellum surface proteome allowed us to test this idea directly by examining the phylogenetic distribution of proteins in the flagellum surface and matrix proteomes (Fig. 3-09, ST1, ST3). As reference organisms, we chose 8 ciliated (*L. major, T. cruzi, P. falciparum, C. reinhardtii, M. brevicollis, C. elegans, D. melanogaster, H. sapiens*) and 4 non-ciliated (*D. discoideum, S. cerevisiae, C. merolae, A. thaliana*) eukaryotic species, including both unicellular and multicellular representatives. Among the 158 flagellum surface proteins, 16% were specific to *T. brucei*. By comparison, 5% of matrix proteins and 1% of flagellum skeleton proteins were *T. brucei*-specific.

Conserved flagellum surface proteins are not biased toward flagellated organisms

Proteins required for flagellum structure and motility are broadly conserved among organisms with flagella, but are generally absent in organisms that lack flagella [82-84]. To determine if the same bias applied to flagellum surface and matrix proteins, we examined the phylogenetic distribution of 'conserved' proteins in each dataset, i.e. proteins that were encoded in the genome of at least one non-kinetoplastid organism (Fig. 3-09). As expected [82-84], a large fraction (42%) of conserved flagellum skeleton proteins were restricted to organisms with flagella. In

contrast, only 3% of conserved flagellum surface proteins and 7% of conserved flagellum matrix proteins were restricted to organisms with flagella.

DISCUSSION

Flagellum purification

The *T. brucei* flagellum is an essential and multifunctional organelle that is required for cell motility and cell morphogenesis and is postulated to function in immune evasion and host-parasite signaling [15,20,35,85-87]. Previous studies of the *T. brucei* flagellum have been limited by the inability to purify intact, membrane-enclosed flagella. Here we combine genetic manipulation and mechanical force to isolate intact flagella from mammalian-infectious *T. brucei*. The quality of the preparation is evidenced by motility of flagella separated from cell bodies, combined with biochemical and microscopic analysis of purified flagella. The flagellum preparation is further validated by independent analyses showing flagellum localization and/or function for several proteins identified in the purified sample. The availability of intact flagellum preparations opens new opportunities for studying unique and conserved features of *T. brucei* flagella. In other organisms, the ability to purify intact flagella has been critical for advancing studies of flagellum biology, including the recent resurgence in awareness of the important roles played by flagella in human health and disease [7,64,88]. Development of a method for flagellum isolation from *T. brucei* is anticipated to advance efforts to understand flagellum biology in these pathogens and will expand the utility of trypanosomes as an experimental system for studying flagellum biology.

Identification of flagellum surface and flagellum matrix proteins

We took advantage of our flagellum purification to conduct a proteomic analysis of surface-exposed flagellum membrane proteins and soluble flagellum matrix proteins. We identified 158 and 666 proteins in the flagellum surface and matrix fractions, respectively, with 87 proteins common between the two datasets. The combined surface and matrix proteomes include 165 proteins for which homologs were identified in a proteomic analysis of intact flagella from *C. reinhardtii* [64] (supplemental table ST7). Gene ontology annotation indicates that proteins identified in the *T. brucei* surface and matrix fractions encompass a wide range of functionalities (Table 1). A notable feature of each dataset was the large number of proteins, 52% of the surface and 52% of the matrix proteome, for which gene ontology analyses did not reveal predicted functionality.. Previously, pioneering proteomic studies of detergent-extracted flagellum skeletons from procyclic *T. brucei* provided important insights into flagellum biology [31,43,46]. Novelty of the membrane and matrix proteomes identified in the current study is illustrated by comparison with these previous analyses. There is minimal overlap among the proteomes, with 91% of proteins identified in the surface and matrix proteomes being unique to the current analysis. The combined studies make *T. brucei* one of few organisms for which analysis of the entire flagellum, i.e. membrane, matrix and skeleton, is available and, to our knowledge, provides the first example where an independent analysis of surface-exposed flagellar proteins is available.

Analysis of the surface dataset is particularly interesting, as it shows enrichment for transmembrane proteins, including several predicted transporters and

proteins predicted to initiate host-parasite signaling (see below). The number and predicted functionalities of proteins identified in the flagellum surface fraction indicate that *T. brucei* surface protein diversity is greater than might be inferred from the relatively few previously characterized surface proteins [89]. The surface dataset has relevance from a therapeutic standpoint because the identified proteins are accessible to small molecules added to live, mammalian-infectious parasites.

Signaling capacity of the trypanosome flagellum

The trypanosome flagellum has been hypothesized to participate in host-parasite signaling, but proteins responsible for detection and transduction of extracellular signals are mostly unknown. Previously, only a handful of flagellar membrane (including the flagellar pocket) and matrix proteins have been identified in *T. brucei* [24,30,33,34,75,90-97]. In other organisms, flagellum-dependent signaling is dominated by three signal transduction pathways: cyclic nucleotide signaling, Ca^{2+} signaling and phosphorylation cascades initiated by receptor-kinases on the flagellar membrane [2,8]. The *T. brucei* flagellum surface proteome is replete with proteins capable of initiating signal transduction in each of these signaling pathways (Fig. 3-08), including receptor kinases, receptor adenylate cyclases [30] and proteins predicted to function in Ca^{2+} signaling [33,36]. The surface proteome also includes many proteins predicted to function in transport of solutes across the cell membrane (Table 1). The combined data indicate a diverse flagellar surface protein repertoire suitable for mediating a broad range of signaling functions, thus providing molecular

support for the hypothesis that the flagellum membrane is an important host-parasite signaling interface.

A role for the *T. brucei* flagellum as a signaling platform is supported by previous work that identified downstream targets of cyclic nucleotide, Ca^{2+} and phospho-signaling pathways anchored to the *T. brucei* flagellum skeleton (Fig. 3-08) [29,31,32,43]. The flagellar matrix fraction included many of these effectors, as well as several other candidate signaling proteins (Supplemental Table ST3) (Fig. 3-08). A major effector of cyclic nucleotide signaling that was not identified in previous studies of the *T. brucei* flagellum is the protein kinase A regulatory subunit ("RSU"), which binds cyclic nucleotide [72]. RSU mediates cyclic nucleotide signaling in diverse organisms [98,99], although a function has not been defined for this protein in *T. brucei*. We identified RSU in the flagellum matrix fraction (Supplemental Table S3). Absence of RSU from detergent-extracted flagellum preparations [31,43,46] indicates it is not stably associated with the axoneme or PFR. To test for a requirement of RSU in flagellum function, we used RNAi. RSU knockdown inhibited motility of bloodstream-form cells (Fig. 3-07 d,e). The motility defect caused by RSU knockdown supports the identification of RSU in the flagellum matrix and provides experimental evidence for cyclic nucleotide-dependent signaling in regulating flagellum function.

Functional analysis of flagellum surface proteins provides insight into mechanisms of flagellum attachment.

One of the most distinctive features of the *T. brucei* flagellum is lateral attachment to the cell body, via regularly-spaced, desmosome-like adhesions between

the flagellar and cell surface membranes [40]. Immunofluorescence revealed that some proteins in the flagellum surface fraction, e.g. FS179 (Fig. 3-06b) and FS105 (Supplemental Fig. S3), are restricted to the flagellum-cell body interface and do not extend to the flagellum tip, suggesting a potential role in flagellum attachment. RNAi knockdown of FS179, which encodes a putative Ca^{2+} channel, caused the flagellum to become detached from the cell body, with the daughter flagellum being preferentially affected (Fig. 3-07a-c). The phenotype was ultimately lethal (Supplemental Fig. S4). FS179 knockdown phenocopies flagellum detachment caused by treatment of bloodstream trypanosomes with Ca^{2+} chelators, as reported by Vickerman forty years ago [40]. These results indicate a requirement for Ca^{2+} in establishment of flagellum-cell body adhesion in *T. brucei* [40] and suggest that FS179 is critical for maintaining Ca^{2+} homeostasis at the flagellum-cell body interface. In other organisms Ca^{2+} is required for homophilic cell-cell adhesion, including fibrous linkages between the connecting cilium and the periciliary inner segment collar of mammalian photoreceptors [100]. Defects in these periciliary attachments cause Usher syndrome in humans [101]. Previous analogies have been drawn between mammalian Ca^{2+}-dependent cell-cell adhesions and trypanosome flagellum-cell body adhesions [40]. Our findings support this view at the molecular level. Flagellum attachment is essential in *T. brucei,* suggesting that Ca^{2+} channels might be exploited as targets for therapeutic intervention in trypanosomiases. Indeed, Ca^{2+} channels are major targets of the pharmaceutical industry for treating of a variety of human diseases [102] and Ca^{2+} channel blockers have anti-protozoal activity *in vitro* [103].

Matrix-specific proteins include IFT proteins and components of the ubiquitin conjugating system

Many proteins identified in the flagellum surface fraction were also identified in the flagellum matrix fraction. This result is expected because biotinylation and avidin purification are not 100% efficient. On the other hand, the vast majority (87%) of proteins in the flagellum matrix were exclusive to this fraction. Matrix-specific proteins include components of the intraflagellar transport (IFT) system that are required for flagellum assembly and signaling [104,105]. We identified five IFT complex B proteins, one complex A protein, and the IFT anterograde kinesin motor, KIF3A (Supplemental Table ST8). Notably, none of the IFT proteins were identified in the surface fraction, or in previous proteomic analyses of the flagellum skeleton [31,43,46].

Another interesting group of proteins specifically identified in the matrix fraction includes components of the ubiquitin conjugating system (Supplemental Table ST9). Ubiquitination is a post-translational protein modification that has essential roles in many cellular processes, including cell-cycle control, protein quality control and signaling [106-108]. A recent study identified a functional ubiquitination system in the flagellum of *C. reinhardtii,* where it is postulated to control flagellar resorption and cAMP-dependent signaling in the flagellum during mating [109]. Several ubiquitinated proteins were identified, including the polycystin 2 cation channel (CrPKD2) and a cyclic GMP-dependent protein kinase (CrPKG) that both participate in flagellum signaling during mating [109]. Polyubiquitin was identified in all three *T. brucei* flagellum fractions (Supplemental Tables ST9 [31,43,46]),

indicating ubiquitination of *T. brucei* flagellar proteins. The identification of an ubiquitin-activating enzyme and three ubiquitin conjugating enzymes in the flagellum matrix fraction suggests that ubiquitination might be carried out within the flagellum itself. While the function of ubiquitination in the *T. brucei* flagellum remains to be determined, we postulate that this pathway participates in regulation of flagellum function as described for *C. reinhardtii* [109].

The flagellum surface presents a dynamic and cell-specific host-parasite interface

Phylogenetic analysis revealed that 16% of flagellar surface proteins are *T. brucei*-specific. By comparison, only 5% of proteins in the flagellar matrix and 1% in the flagellum skeleton are *T. brucei*-specific. These results suggest that flagellum surface proteins must accommodate cell-specific functions, such as perception of signals specific to the parasite's extracellular environment. In contrast, composition of the flagellar matrix and skeleton fractions reflect more broadly conserved functions, e.g. downstream signal transduction and motility capacity of the organelle. Trypanosomes infect a broad range of organisms and survival in diverse host environments necessitates specialized surface proteins for signaling, nutrient acquisition and protection against host defenses. A cell-specific flagellum surface proteome would provide an interface that is tailored to meet the demands specifically imposed on *T. brucei* in each host. In support of this idea, we found that 21% of flagellum surface proteins are upregulated by 2-fold or more in the bloodstream life cycle stage (Fig. 3-10) [68,71]. This is higher than seen for matrix proteins (10%), flagellum skeleton proteins (3%) or for the genome as a whole (3%) (Fig. 3-10) [68,71].

Thus, the flagellum surface proteome is a dynamic host-parasite interface that is particularly subject to life cycle stage-specific regulation.

Conserved flagellum surface proteins are not biased toward flagellated organisms

Comparing the phylogenetic distribution of conserved proteins, i.e. those that are not kinetoplastid-specific, in each flagellum sub-fraction revealed an interesting feature of surface and matrix proteins. Namely, conservation of surface and matrix proteins is not biased toward flagellated organisms. This result contrasts markedly from what is observed for conserved flagellum skeleton proteins, which are generally more restricted to flagellated organisms (Fig. 3-09). The bias toward flagellated organisms reflects the requirement of flagellum skeleton proteins for axoneme structure and motility, which are unique to organisms with flagella [82-84]. Flagellum surface and matrix proteins on the other hand, are predicted to be involved in perception and transduction of extracellular signals, i.e. processes that are not unique to flagellated organisms. An exception is the group of IFT proteins in the matrix, which are involved in flagellum assembly but represent a small fraction of matrix proteins. The combined phylogenetic analyses indicate that protein composition of the eukaryotic flagellum surface is shaped by selective forces that are a combination of cell-specific demands, imposed by unique extracellular environments, and more broadly conserved signaling needs. This finding has practical implications, as it means comparative genomic approaches, which are useful for identifying flagellum assembly and motility genes [82-84], are not well-suited for identification of genes involved in flagellum signaling.

FIGURES

Fig. 3-01. Flagellum architecture of *T. brucei*.

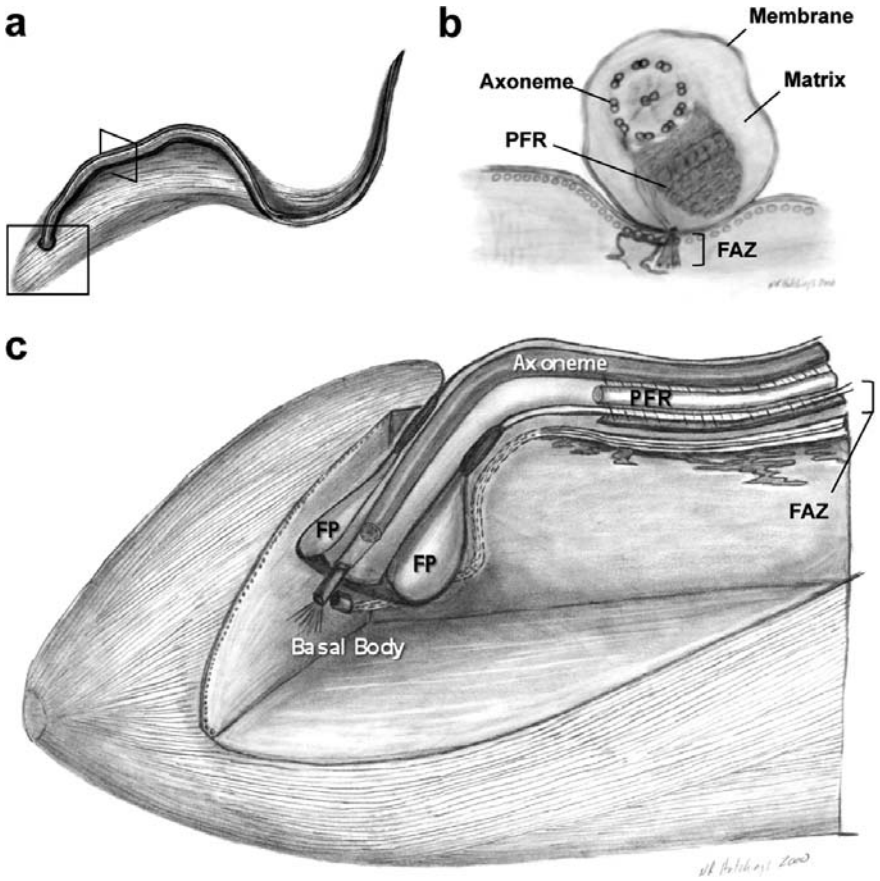

Schematic diagrams showing the *T. brucei* cell and flagellum (a), together with cross sectional (b) and cut-away (c) views corresponding to the regions indicated by boxes in panel a. Relevant structural features are labeled, including the flagellum membrane, matrix, axoneme and paraflagellar rod (PFR), as well as the flagellum attachment zone (FAZ), flagellar pocket (FP) and basal body. See text for details. Figure adapted from reference (104), with permission.

Fig. 3-02. Purification of flagellum surface and matrix proteins from bloodstream-form *T. brucei*.

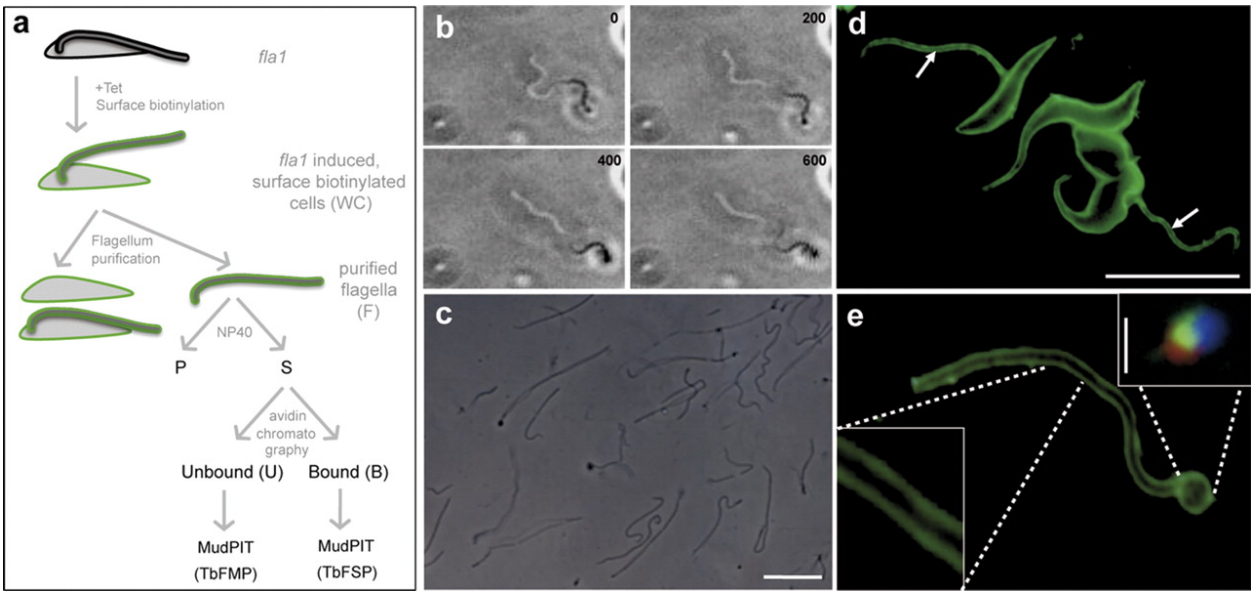

(a) Schematic diagram illustrating the strategy for flagellum purification and separation of flagellum surface and matrix proteins. Lateral connections between the flagellum and cell body were removed by tetracycline-induced (+Tet) RNAi against Fla1 (49). Induced *fla1* cells were surface biotinylated (*fla1*-induced, surface biotinylated cells) and flagella were removed from the cell body by mechanical shearing, then purified by sucrose sedimentation (purified flagella). Purified, surface-biotinylated flagella were lysed with non-ionic detergent (NP40) and soluble proteins (S) were separated from insoluble flagellar skeletons (P) by centrifugation. Soluble proteins were applied to streptavidin beads (avidin chromatography). Proteins in the streptavidin-bound (B) and streptavidin-unbound (U) fractions were identified using multidimensional protein identification technology (MudPIT). (b) Time-lapsed image sequence (from supplemental movie 1, recorded and played at 30 fps), showing that some flagella continued to beat after detachment from cell bodies (timestamps are

given in ms). (c) Phase contrast image of purified flagella (Scale bar 5 μm). (d) Anti-biotin immunofluorescence (green) of surface-biotinylated RNAi-induced *fla1* cells showing detached flagella (arrows, scale bar 25 μm). (e) Anti-biotin immunofluorescence (green) of purified flagella shows surface labeling (inset, bottom left). The bulbous structure at one end of the flagellum (inset, upper right) includes material from the flagellar pocket (tomato lectin staining, red), the basal body (tyrosinated tubulin staining, green) and kinetoplast DNA (DAPI staining, blue).

Fig. 3-03. Analysis of flagellum purification fractions.

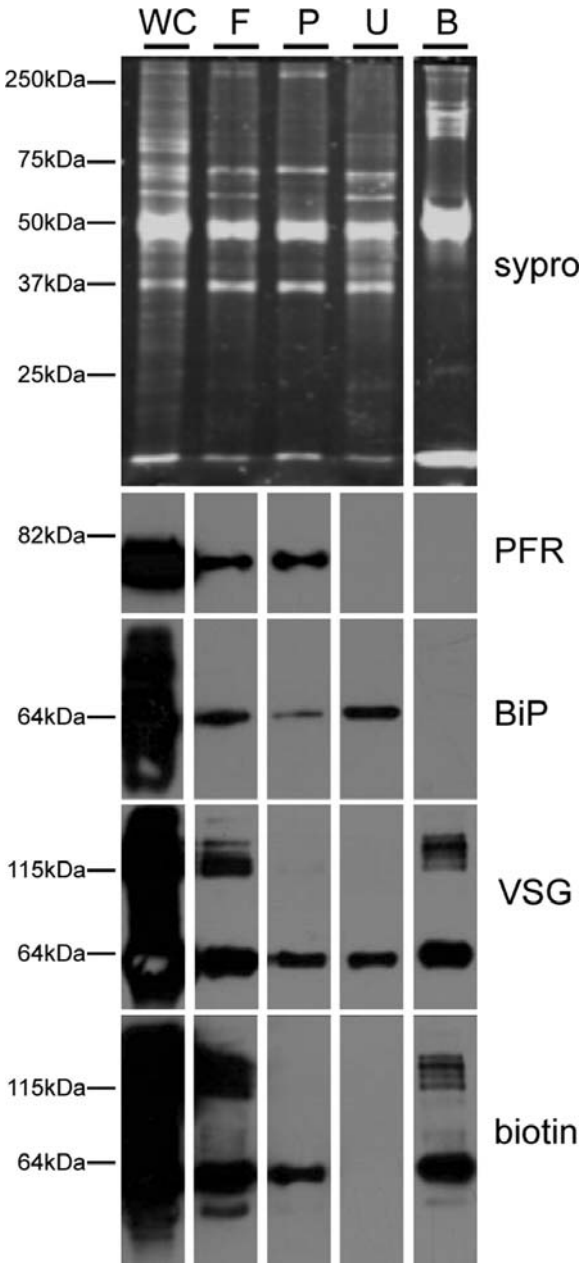

Proteins from the indicated fractions of the purification were analyzed by SDS-PAGE and SYPRO-Ruby staining (top) or Western blotting (bottom) with antibodies against intracellular (BiP), flagellar skeleton (PFR) and cell surface (VSG) markers. Biotinylated proteins were detected with anti-biotin antibody. Whole cells (WC), purified flagella (F), detergent-insoluble flagellum pellets (P) and the streptavidin-unbound (U) and bound (B) fractions are as indicated in Fig. 3-02A. Flagellum enrichment is indicated by the increased ratio of the flagellar marker PFR to the intracellular marker BiP in the purified flagellum fraction (F) versus whole cells (WC). Both PFR and BiP are largely absent from the streptavidin bound fraction (B).

Fig. 3-04. The flagellum surface proteome contains known flagellum surface proteins but is generally devoid of intraflagellar proteins.

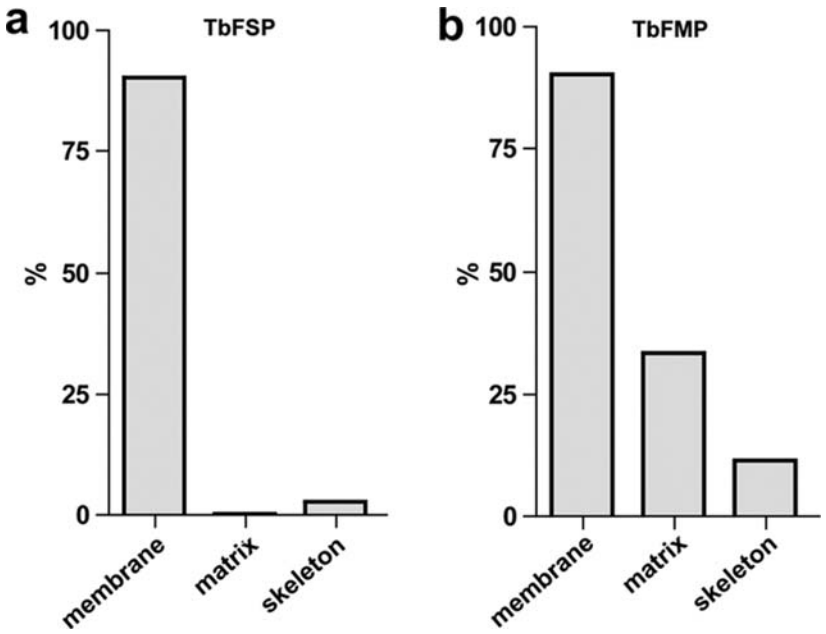

Chart shows the percentage of known flagellum membrane, matrix and skeleton proteins that were (a) identified in the flagellum surface proteome (TbFSP) and (b) flagellum matrix proteome (TbFMP). Flagellum skeleton proteins are from (31, 43, 46). Known flagellum membrane and matrix proteins are given in supplemental table ST5 and table ST8, respectively. TbFSP included 9 of 10 (90%) membrane, none of 21 (0%) matrix and 14 of 532 (2.6%) skeleton proteins. TbFMP included 9 of 10 (90%) membrane, 7 of 21 (33%) matrix and 62 of 532 (11.6%) skeleton proteins.

Fig. 3-05. The flagellum surface proteome is enriched for transmembrane proteins.

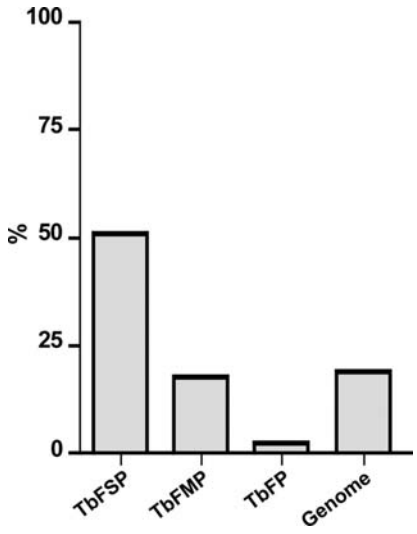

Chart shows the percentage of proteins in the flagellum surface (TbFSP), matrix (TbFMP) and skeleton (TbFP) (31, 43, 46) proteomes that are predicted to contain transmembrane domains. For comparison, the relative number of predicted transmembrane-containing proteins in the *T. brucei* genome (70) is shown. Numbers are 80/158, 118/666, 12/532 and 2133/11425 for TbFSP, TbFMP, TbFP and genome, respectively.

Fig. 3-06. Immunofluorescence shows flagellum localization for proteins identified in the flagellum surface proteome.

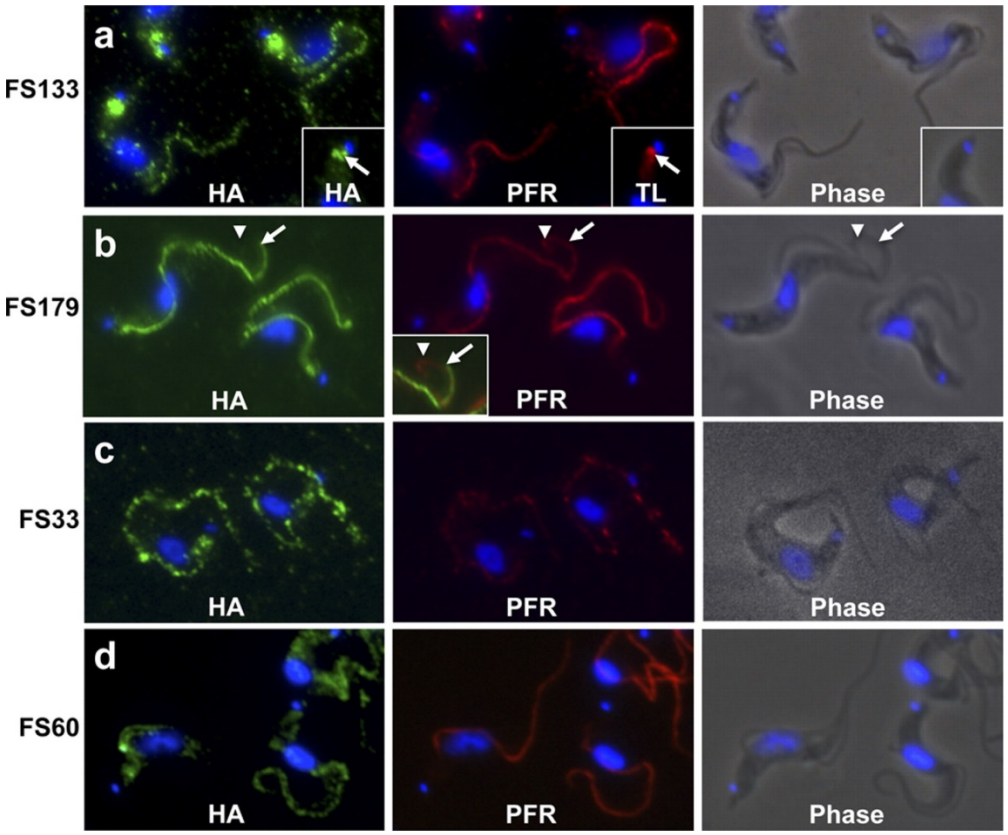

Immunofluorescence analysis of bloodstream-form trypanosomes expressing the indicated HA-tagged flagellum surface proteins (FS133, FS179, FS33 or FS60). Cells were co-stained for the HA epitope (green), the paraflagellar rod (PFR, red) or the flagellar pocket marker tomato lectin (TL, red) as indicated. DNA was visualized with DAPI. (a) FS133 localizes along the flagellum and in the flagellar pocket (inset, arrows). (b) FS179 localizes along the flagellum, but does not extend to the flagellum distal tip, as evidenced by the extension of PFR staining (arrowhead) beyond the end of FS179 staining (arrow). See inset for merged images. (c, d) FS33 and FS60 localize along the entire length of the flagellum. FS60 was also observed in cytoplasmic puncta (not shown).

Fig. 03-7. RNAi knockdown indicates flagellum function for FS179 and FM458.

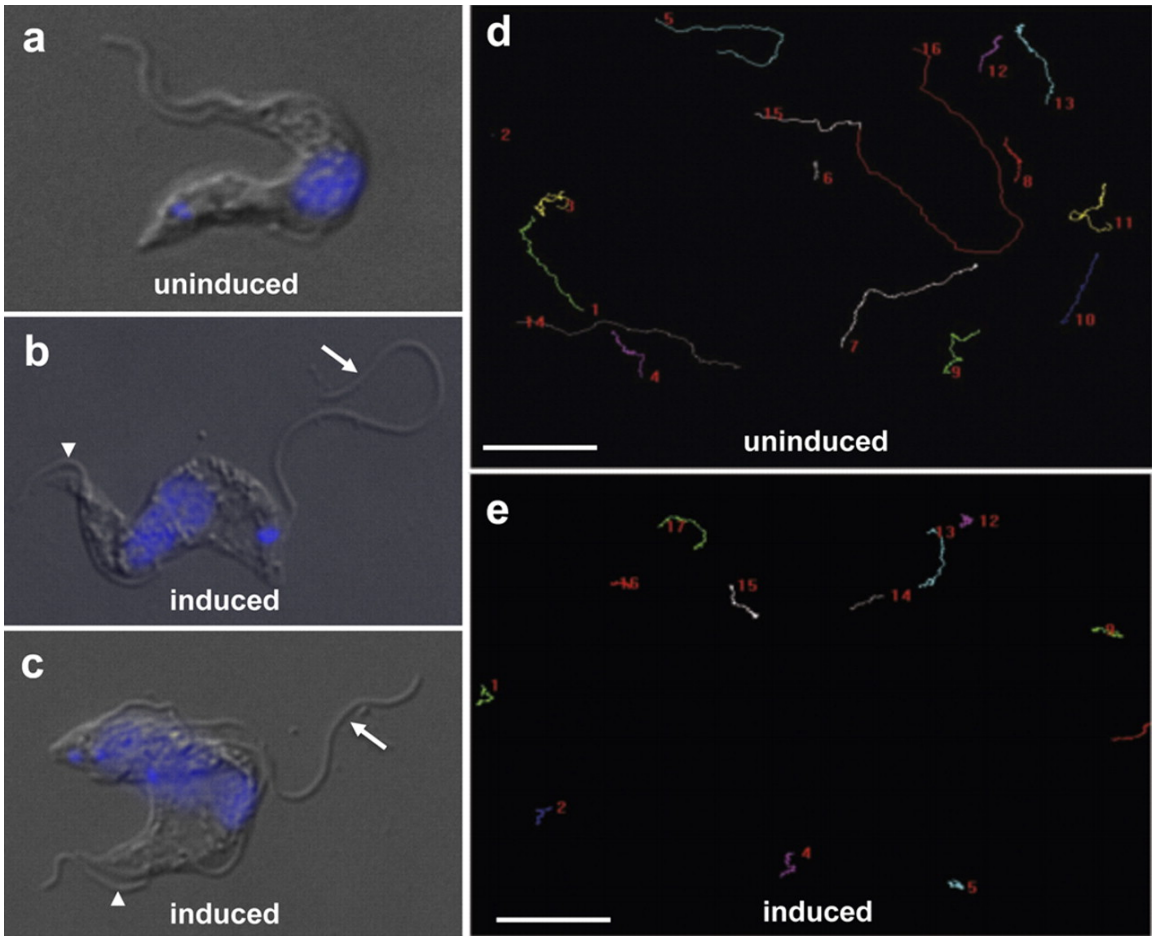

(a-c) Phase contrast images of tetracycline-inducible FS179 RNAi cells grown in the absence (a) or presence (b and c) of tetracycline to induce RNAi. FS179 knockdown causes the daughter flagellum to become detached (arrows in b and c), while the parental flagellum remains connected to the cell body (arrowheads in b and c). DNA is visualized with DAPI. (d and e) Motility trace analysis of FM458 RNAi cells grown in the absence (d) or presence (e) of tetracycline to induce RNAi. Each line traces the path of a single cell for 2 minutes (Scale bar 50 μm).

Fig. 03-8. The trypanosome flagellum provides a diverse signaling platform.

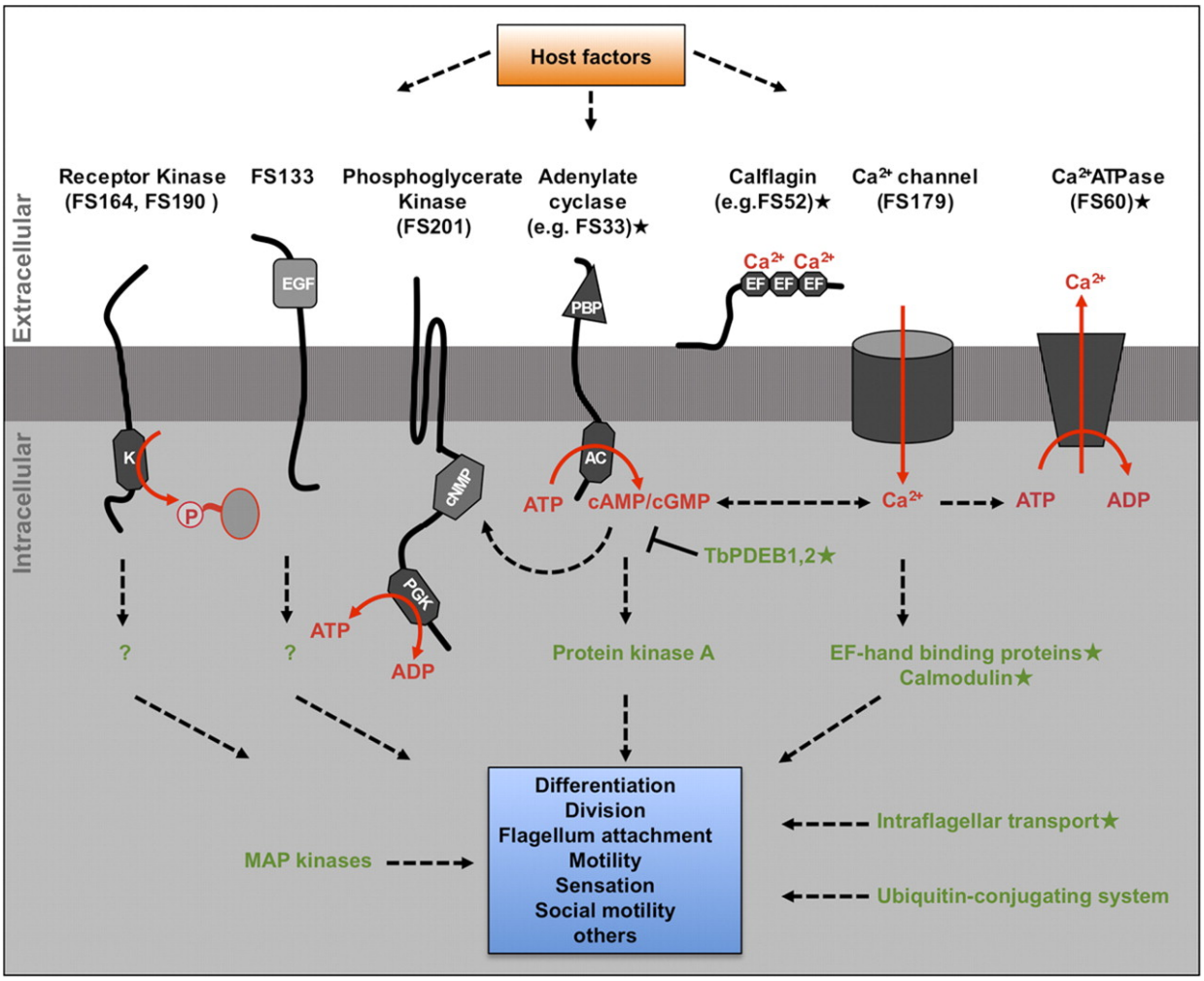

Diagram shows representative components of signalig pathways identified in the flagellum surface proteome (black text) and flagellum matrix proteome (green text). These include receptors and transporters for initiating signal transduction (black text) and downstream signaling proteins (green text). Predicted domain structures are indicated for flagellum surface proteins (K: kinase; EGF: epidermal growth factor domain superfamily; cNMP: cyclic nucleotide binding domain; PGK: phosphoglycerate kinase domain; PBP: periplasmic binding protein domain; AC: adenylate cyclase

domain; EF: EF hand calcium-binding domain). Predicted interactions are indicated with dashed lines. Unknown host factors (orange box) are predicted to engage signaling pathways, which mediate downstream trypanosome processes (blue box). ★ Indicates proteins that have been demonstrated to be flagellar by independent studies (29-33, 89, 92-94)

Fig. 3-09. The flagellum surface proteome contains many *T. brucei*-specific proteins.

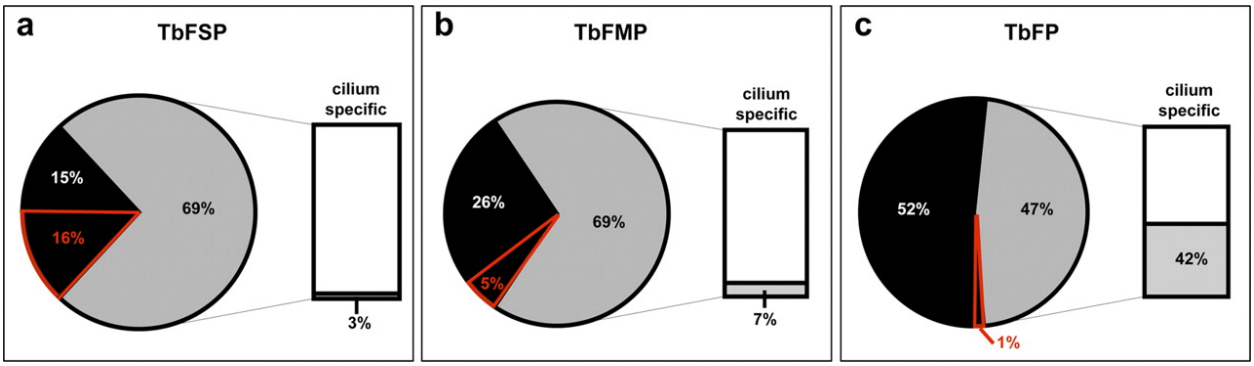

Pie charts show phylogenetic distribution of proteins in the flagellum surface (TbFSP), flagellum matrix (TbFPM) or flagellum skeleton (TbFP) proteomes. Percentages are shown for proteins that are conserved in at least one non-kinetoplastid organism (gray), or are kinetoplastid-specific (black), or *T. brucei*-specific (red outline). Bar charts show the percentage of conserved proteins, i.e. not kinetoplastid-specific, that are restricted to ciliated organisms.

Fig. 3-10. Flagellum surface proteins are upregulated in bloodstream-form cells.

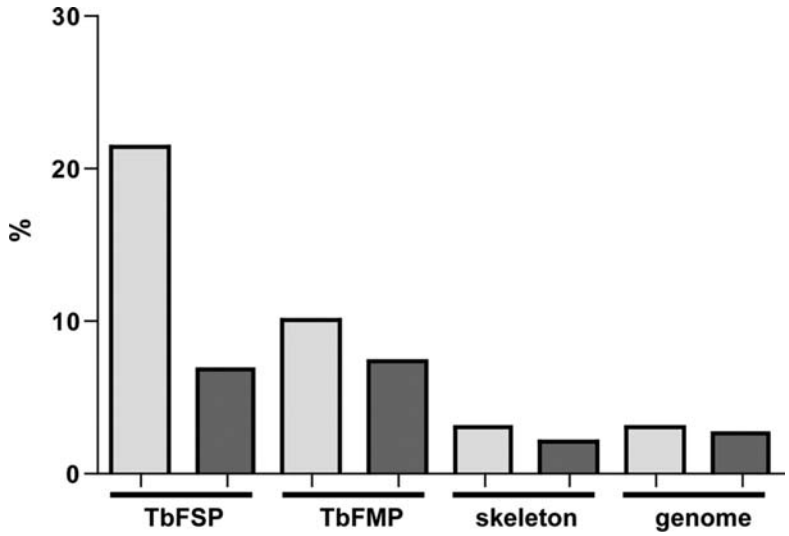

Chart shows the percentage of proteins in each proteomic dataset that are up-regulated in bloodstream-form cells (light gray bars) or procyclic-form cells (dark gray bars) by two-fold or more based on RNA sequencing analysis (67). Proteomic datasets are for the flagellum surface (TbFSP), the flagellum matrix (TbFMP) and the flagellum skeleton (TbFP) proteomes (31, 43, 46).

Table 3-01: Predicted molecular function of proteins identified in TbFSP and TbFMP. Proteins in the flagellum surface proteome (TbFSP) and flagellum matrix proteome (TbFMP) were analyzed for predicted molecular function using the DAVID database for gene ontology and protein domain analysis

Predicted molecular function	TbFSP (158)	TbFMP (666)
Cyclase activity	17	0
Lyase activity	18	0
Substrate-specific transporter activity	12	0
Transmembrane transporter activity	15	0
Nucleotide binding	31	117
Hydrolase activity	0	117
Protein binding	0	54
Oxidoreductase activity	0	52
Cofactor binding	0	20
Translation factor activity, nucleic acid binding	0	12
Carboxylic acid binding	0	5
Peroxidase activity	0	4
Carbohydrate binding	0	4
No Annotated Function	83	350
Not in DAVID	22	46

REFERENCES

1. Berbari NF, O'Connor AK, Haycraft CJ,Yoder BK (2009) The primary cilium as a complex signaling center. Curr Biol 19: R526-535.
2. Christensen ST,Ott CM (2007) Cell signaling. A ciliary signaling switch. Science 317: 330-331.
3. Corbit KC, Aanstad P, Singla V, Norman AR, Stainier DY,Reiter JF (2005) Vertebrate Smoothened functions at the primary cilium. Nature 437: 1018-1021.
4. Bloodgood RA Sensory reception is an attribute of both primary cilia and motile cilia. J Cell Sci 123: 505-509.
5. Satir P, Mitchell DR,Jekely G (2008) How did the cilium evolve? Curr Top Dev Biol 85: 63-82.
6. Badano JL, Mitsuma N, Beales PL,Katsanis N (2006) The ciliopathies: an emerging class of human genetic disorders. Annu Rev Genomics Hum Genet 7: 125-148.
7. Fliegauf M, Benzing T,Omran H (2007) When cilia go bad: cilia defects and ciliopathies. Nat Rev Mol Cell Biol 8: 880-893.
8. Kaupp UB, Kashikar ND,Weyand I (2008) Mechanisms of sperm chemotaxis. Annu Rev Physiol 70: 93-117.
9. Pan J, Wang Q,Snell WJ (2005) Cilium-generated signaling and cilia-related disorders. Lab Invest 85: 452-463.
10. Rohatgi R, Milenkovic L,Scott MP (2007) Patched1 regulates hedgehog signaling at the primary cilium. Science 317: 372-376.

11. Christensen ST, Guerra CF, Awan A, Wheatley DN,Satir P (2003) Insulin receptor-like proteins in Tetrahymena thermophila ciliary membranes. Curr Biol 13: R50-52.

12. Ogura A,Takahashi K (1976) Artificial deciliation causes loss of calcium-dependent responses in Paramecium. Nature 264: 170-172.

13. Pan J,Snell WJ (2000) Signal transduction during fertilization in the unicellular green alga, Chlamydomonas. Curr Opin Microbiol 3: 596-602.

14. Dawson SC,House SA (2010) Life with eight flagella: flagellar assembly and division in Giardia. Curr Opin Microbiol 13: 480-490.

15. Ralston KS, Kabututu ZP, Melehani JH, Oberholzer M,Hill KL (2009) The Trypanosoma brucei flagellum: moving parasites in new directions. Annu Rev Microbiol 63: 335-362.

16. Sinden RE, Talman A, Marques SR, Wass MN,Sternberg MJ (2010) The flagellum in malarial parasites. Curr Opin Microbiol 13: 491-500.

17. WHO (2004) Available at http://www.who.int/evidence/bod.

18. Bastin P The peculiarities of flagella in parasitic protozoa. Curr Opin Microbiol 13: 450-452.

19. Brun R, Blum J, Chappuis F,Burri C (2010) Human African trypanosomiasis. Lancet 375: 148-159.

20. Maric D, Epting CL,Engman DM (2010) Composition and sensory function of the trypanosome flagellar membrane. Curr Opin Microbiol 13: 466-472.

21. Parsons M,Ruben L (2000) Pathways involved in environmental sensing in trypanosomatids. Parasitol Today 16: 56-62.

22. Rotureau B, Morales MA, Bastin P,Spath GF (2009) The flagellum-MAP kinase connection in Trypanosomatids: a key sensory role in parasite signaling and development? Cell Microbiol.

23. Fenn K,Matthews KR (2007) The cell biology of Trypanosoma brucei differentiation. Curr Opin Microbiol 10: 539-546.

24. Dean S, Marchetti R, Kirk K,Matthews KR (2009) A surface transporter family conveys the trypanosome differentiation signal. Nature 459: 213-217.

25. Nikolskaia OV, de ALAP, Kim YV, Lonsdale-Eccles JD, Fukuma T, Scharfstein J,Grab DJ (2006) Blood-brain barrier traversal by African trypanosomes requires calcium signaling induced by parasite cysteine protease. J Clin Invest 116: 2739-2747.

26. Tetley L,Vickerman K (1985) Differentiation in Trypanosoma brucei: host-parasite cell junctions and their persistence during acquisition of the variable antigen coat. J Cell Sci 74: 1-19.

27. Van Den Abbeele J, Claes Y, van Bockstaele D, Le Ray D,Coosemans M (1999) Trypanosoma brucei spp. development in the tsetse fly: characterization of the post-mesocyclic stages in the foregut and proboscis. Parasitology 118 (Pt 5): 469-478.

28. Gluenz E, Hoog JL, Smith AE, Dawe HR, Shaw MK,Gull K (2010) Beyond 9+0: noncanonical axoneme structures characterize sensory cilia from protists to humans. Faseb J 24: 3117-3121.

29. Oberholzer M, Marti G, Baresic M, Kunz S, Hemphill A,Seebeck T (2007) The Trypanosoma brucei cAMP phosphodiesterases TbrPDEB1 and TbrPDEB2: flagellar enzymes that are essential for parasite virulence. Faseb J 21: 720-731.

30. Paindavoine P, Rolin S, Van Assel S, Geuskens M, Jauniaux JC, Dinsart C, Huet G,Pays E (1992) A gene from the variant surface glycoprotein expression site encodes one of several transmembrane adenylate cyclases located on the flagellum of Trypanosoma brucei. Mol Cell Biol 12: 1218-1225.

31. Portman N, Lacomble S, Thomas B, McKean PG,Gull K (2009) Combining RNA interference mutants and comparative proteomics to identify protein components and dependences in a eukaryotic flagellum. J Biol Chem 284: 5610-5619.

32. Ridgley E, Webster P, Patton C,Ruben L (2000) Calmodulin-binding properties of the paraflagellar rod complex from Trypanosoma brucei. Mol Biochem Parasitol 109: 195-201.

33. Wu Y, Deford J, Benjamin R, Lee MG,Ruben L (1994) The gene family of EF-hand calcium-binding proteins from the flagellum of Trypanosoma brucei. Biochem J 304 (Pt 3): 833-841.

34. Wu Y, Haghighat NG,Ruben L (1992) The predominant calcimedins from Trypanosoma brucei comprise a family of flagellar EF-hand calcium-binding proteins. Biochem J 287 (Pt 1): 187-193.

35. Kohl L,Bastin P (2005) The flagellum of trypanosomes. Int Rev Cytol 244: 227-285.

36. Balber AE (1990) The pellicle and the membrane of the flagellum, flagellar adhesion zone, and flagellar pocket: functionally discrete surface domains of the bloodstream form of African trypanosomes. Crit Rev Immunol 10: 177-201.

37. Tyler KM, Fridberg A, Toriello KM, Olson CL, Cieslak JA, Hazlett TL,Engman DM (2009) Flagellar membrane localization via association with lipid rafts. J Cell Sci 122: 859-866.

38. Hu Q, Milenkovic L, Jin H, Scott MP, Nachury MV, Spiliotis ET,Nelson WJ A septin diffusion barrier at the base of the primary cilium maintains ciliary membrane protein distribution. Science 329: 436-439.

39. Lacomble S, Vaughan S, Gadelha C, Morphew MK, Shaw MK, McIntosh JR,Gull K (2009) Three-dimensional cellular architecture of the flagellar pocket and associated cytoskeleton in trypanosomes revealed by electron microscope tomography. J Cell Sci 122: 1081-1090.

40. Vickerman K (1969) On the surface coat and flagellar adhesion in trypanosomes. J Cell Sci 5: 163-193.

41. Field MC,Carrington M (2009) The trypanosome flagellar pocket. Nat Rev Microbiol 7: 775-786.

42. Webster P,Russell DG (1993) The flagellar pocket of trypanosomatids. Parasitol Today 9: 201-206.

43. Broadhead R, et al. (2006) Flagellar motility is required for the viability of the bloodstream trypanosome. Nature 440: 224-227.

44. Robinson DR,Gull K (1991) Basal body movements as a mechanism for mitochondrial genome segregation in the trypanosome cell cycle. Nature 352: 731-733.

45. Schlaeppi K, Deflorin J,Seebeck T (1989) The major component of the paraflagellar rod of Trypanosoma brucei is a helical protein that is encoded by two identical, tandemly linked genes. J Cell Biol 109: 1695-1709.

46. Hart SR, et al. (2009) Analysis of the trypanosome flagellar proteome using a combined electron transfer/collisionally activated dissociation strategy. J Am Soc Mass Spectrom 20: 167-175.

47. Wirtz E, Leal S, Ochatt C,Cross GA (1999) A tightly regulated inducible expression system for conditional gene knock-outs and dominant-negative genetics in Trypanosoma brucei. Mol Biochem Parasitol 99: 89-101.

48. Oberholzer M, Lopez MA, Ralston KS,Hill KL (2009) Approaches for functional analysis of flagellar proteins in African trypanosomes. Methods Cell Biol 93: 21-57.

49. LaCount DJ, Barrett B,Donelson JE (2002) Trypanosoma brucei FLA1 is required for flagellum attachment and cytokinesis. J Biol Chem 277: 17580-17588.

50. Bangs JD, Uyetake L, Brickman MJ, Balber AE,Boothroyd JC (1993) Molecular cloning and cellular localization of a BiP homologue in Trypanosoma brucei. Divergent ER retention signals in a lower eukaryote. J Cell Sci 105 (Pt 4): 1101-1113.

51. McDowell MA, Ransom DM,Bangs JD (1998) Glycosylphosphatidylinositol-dependent secretory transport in Trypanosoma brucei. Biochem J 335 (Pt 3): 681-689.

52. Tagwerker C, Flick K, Cui M, Guerrero C, Dou Y, Auer B, Baldi P, Huang L,Kaiser P (2006) A tandem affinity tag for two-step purification under fully denaturing conditions: application in ubiquitin profiling and protein complex identification combined with in vivocross-linking. Mol Cell Proteomics 5: 737-748.

53. Wohlschlegel JA (2009) Identification of SUMO-conjugated proteins and their SUMO attachment sites using proteomic mass spectrometry. Methods Mol Biol 497: 33-49.

54. Florens L, Carozza MJ, Swanson SK, Fournier M, Coleman MK, Workman JL,Washburn MP (2006) Analyzing chromatin remodeling complexes using shotgun proteomics and normalized spectral abundance factors. Methods 40: 303-311.

55. Xu TV, Venable, J. D., Cociorva, D., Lu, B., Liao, L., Wohlschlegel, J.,Hewel J, and Yates, J. R., 3rd (2006) ProLuCID, a fast and sensitive
tandem mass spectra-based protein identification program. Molecular & Cellular Proteomics 5.

56. Eng JK,McCormack AL YJI (1994) An approach to correlate tandem mass spectral data of peptides with amino acid sequences in a protein database. *Journal of the American Society for Mass Spectrometry* 5: 976-989.

57. Tabb DL, McDonald WH,Yates JR, 3rd (2002) DTASelect and Contrast: tools for assembling and comparing protein identifications from shotgun proteomics. J Proteome Res 1: 21-26.

58. Cociorva D LTD, Yates JR (2007) Validation of tandem mass spectrometry database search results using DTASelect. Curr Protoc Bioinformatics 13.

59. Tazeh NN, Silverman JS, Schwartz KJ, Sevova ES, Sutterwala SS,Bangs JD (2009) Role of AP-1 in developmentally regulated lysosomal trafficking in Trypanosoma brucei. Eukaryot Cell 8: 1352-1361.

60. Ralston KS,Hill KL (2006) Trypanin, a component of the flagellar Dynein regulatory complex, is essential in bloodstream form African trypanosomes. PLoS Pathog 2: e101.

61. Oberholzer M, Morand S, Kunz S,Seebeck T (2006) A vector series for rapid PCR-mediated C-terminal in situ tagging of Trypanosoma brucei genes. Mol Biochem Parasitol 145: 117-120.

62. Redmond S, Vadivelu J,Field MC (2003) RNAit: an automated web-based tool for the selection of RNAi targets in Trypanosoma brucei. Mol Biochem Parasitol 128: 115-118.

63. Schultz J, Milpetz F, Bork P,Ponting CP (1998) SMART, a simple modular architecture research tool: identification of signaling domains. Proc Natl Acad Sci U S A 95: 5857-5864.

64. Pazour GJ, Agrin N, Leszyk J,Witman GB (2005) Proteomic analysis of a eukaryotic cilium. J Cell Biol 170: 103-113.

65. Huang da W, Sherman BT,Lempicki RA (2009) Systematic and integrative analysis of large gene lists using DAVID bioinformatics resources. Nat Protoc 4: 44-57.

66. Huang da W, Sherman BT,Lempicki RA (2009) Bioinformatics enrichment tools: paths toward the comprehensive functional analysis of large gene lists. Nucleic Acids Res 37: 1-13.

67. Ashburner M, et al. (2000) Gene ontology: tool for the unification of biology. The Gene Ontology Consortium. Nat Genet 25: 25-29.

68. Siegel TN, Hekstra DR, Wang X, Dewell S,Cross GA Genome-wide analysis of mRNA abundance in two life-cycle stages of Trypanosoma brucei and identification of splicing and polyadenylation sites. Nucleic Acids Res 38: 4946-4957.

69. Vanhamme L, Pays E, McCulloch R,Barry JD (2001) An update on antigenic variation in African trypanosomes. Trends Parasitol 17: 338-343.

70. Berriman M, et al. (2005) The genome of the African trypanosome Trypanosoma brucei. Science 309: 416-422.

71. Aslett M, et al. TriTrypDB: a functional genomic resource for the Trypanosomatidae. Nucleic Acids Res 38: D457-462.

72. Shalaby T, Liniger M,Seebeck T (2001) The regulatory subunit of a cGMP-regulated protein kinase A of Trypanosoma brucei. Eur J Biochem 268: 6197-6206.

73. Gaillard AR, Diener DR, Rosenbaum JL,Sale WS (2001) Flagellar radial spoke protein 3 is an A-kinase anchoring protein (AKAP). J Cell Biol 153: 443-448.

74. Eisenbach M,Giojalas LC (2006) Sperm guidance in mammals - an unpaved road to the egg. Nat Rev Mol Cell Biol 7: 276-285.

75. Hanrahan O, Webb H, O'Byrne R, Brabazon E, Treumann A, Sunter JD, Carrington M,Voorheis HP (2009) The glycosylphosphatidylinositol-PLC in Trypanosoma brucei forms a linear array on the exterior of the flagellar membrane before and after activation. PLoS Pathog 5: e1000468.

76. LaCount DJ, Gruszynski AE, Grandgenett PM, Bangs JD,Donelson JE (2003) Expression and function of the Trypanosoma brucei major surface protease (GP63) genes. J Biol Chem 278: 24658-24664.

77. Salmon D, Geuskens M, Hanocq F, Hanocq-Quertier J, Nolan D, Ruben L,Pays E (1994) A novel heterodimeric transferrin receptor encoded by a pair of VSG expression site-associated genes in T. brucei. Cell 78: 75-86.

78. Tetaud E, Barrett MP, Bringaud F,Baltz T (1997) Kinetoplastid glucose transporters. Biochem J 325 (Pt 3): 569-580.

79. Emmer BT, Daniels MD, Taylor JM, Epting CL,Engman DM (2010) Calflagin inhibition prolongs host survival and suppresses parasitemia in Trypanosoma brucei infection. Eukaryot Cell 9: 934-942.

80. Felder CB, Graul RC, Lee AY, Merkle HP,Sadee W (1999) The Venus flytrap of periplasmic binding proteins: an ancient protein module present in multiple drug receptors. AAPS PharmSci 1: E2.

81. Campbell ID, Baron M, Cooke RM, Dudgeon TJ, Fallon A, Harvey TS,Tappin MJ (1990) Structure-function relationships in epidermal growth factor (EGF) and transforming growth factor-alpha (TGF-alpha). Biochem Pharmacol 40: 35-40.

82. Li JB, et al. (2004) Comparative genomics identifies a flagellar and basal body proteome that includes the BBS5 human disease gene. Cell 117: 541-552.

83. Avidor-Reiss T, Maer AM, Koundakjian E, Polyanovsky A, Keil T, Subramaniam S,Zuker CS (2004) Decoding cilia function: defining specialized genes required for compartmentalized cilia biogenesis. Cell 117: 527-539.

84. Baron DM, Ralston KS, Kabututu ZP,Hill KL (2007) Functional genomics in Trypanosoma brucei identifies evolutionarily conserved components of motile flagella. J Cell Sci 120: 478-491.

85. Bastin P (2010) The peculiarities of flagella in parasitic protozoa. Curr Opin Microbiol 13: 450-452.

86. Rodriguez JA, et al. (2009) Propulsion of African trypanosomes is driven by bihelical waves with alternating chirality separated by kinks. Proc Natl Acad Sci U S A 106: 19322-19327.

87. Engstler M, Pfohl T, Herminghaus S, Boshart M, Wiegertjes G, Heddergott N,Overath P (2007) Hydrodynamic flow-mediated protein sorting on the cell surface of trypanosomes. Cell 131: 505-515.

88. Smith JC, Northey JG, Garg J, Pearlman RE,Siu KW (2005) Robust method for proteome analysis by MS/MS using an entire translated genome: demonstration on the ciliome of Tetrahymena thermophila. J Proteome Res 4: 909-919.

89. Borst P,Fairlamb AH (1998) Surface receptors and transporters of Trypanosoma brucei. Annu Rev Microbiol 52: 745-778.

90. Mussmann R, Engstler M, Gerrits H, Kieft R, Toaldo CB, Onderwater J, Koerten H, van Luenen HG,Borst P (2004) Factors affecting the level and localization of the transferrin receptor in Trypanosoma brucei. J Biol Chem 279: 40690-40698.

91. Vanhollebeke B, De Muylder G, Nielsen MJ, Pays A, Tebabi P, Dieu M, Raes M, Moestrup SK,Pays E (2008) A haptoglobin-hemoglobin receptor conveys innate immunity to Trypanosoma brucei in humans. Science 320: 677-681.

92. Engstler M, Weise F, Bopp K, Grunfelder CG, Gunzel M, Heddergott N,Overath P (2005) The membrane-bound histidine acid phosphatase TbMBAP1 is essential for endocytosis and membrane recycling in Trypanosoma brucei. J Cell Sci 118: 2105-2118.

93. Luo S, Rohloff P, Cox J, Uyemura SA,Docampo R (2004) Trypanosoma brucei plasma membrane-type Ca(2+)-ATPase 1 (TbPMC1) and 2 (TbPMC2) genes encode functional Ca(2+)-ATPases localized to the acidocalcisomes and plasma membrane, and essential for Ca(2+) homeostasis and growth. J Biol Chem 279: 14427-14439.

94. Ziegelbauer K, Multhaup G,Overath P (1992) Molecular characterization of two invariant surface glycoproteins specific for the bloodstream stage of Trypanosoma brucei. J Biol Chem 267: 10797-10803.

95. Vanhamme L, et al. (2003) Apolipoprotein L-I is the trypanosome lytic factor of human serum. Nature 422: 83-87.

96. Absalon S, Blisnick T, Kohl L, Toutirais G, Dore G, Julkowska D, Tavenet A,Bastin P (2008) Intraflagellar transport and functional analysis of genes required for flagellum formation in trypanosomes. Mol Biol Cell 19: 929-944.

97. Franklin JB,Ullu E Biochemical analysis of PIFTC3, the Trypanosoma brucei orthologue of nematode DYF-13, reveals interactions with established and putative intraflagellar transport components. Mol Microbiol 78: 173-186.

98. Howard DR, Habermacher G, Glass DB, Smith EF,Sale WS (1994) Regulation of Chlamydomonas flagellar dynein by an axonemal protein kinase. J Cell Biol 127: 1683-1692.

99. Francis SH,Corbin JD (1999) Cyclic nucleotide-dependent protein kinases: intracellular receptors for cAMP and cGMP action. Crit Rev Clin Lab Sci 36: 275-328.

100. Maerker T, et al. (2008) A novel Usher protein network at the periciliary reloading point between molecular transport machineries in vertebrate photoreceptor cells. Hum Mol Genet 17: 71-86.

101. Williams DS (2008) Usher syndrome: animal models, retinal function of Usher proteins, and prospects for gene therapy. Vision Res 48: 433-441.

102. Abernethy DR,Schwartz JB (1999) Calcium-antagonist drugs. N Engl J Med 341: 1447-1457.

103. Reimao JQ, Scotti MT,Tempone AG Anti-leishmanial and anti-trypanosomal activities of 1,4-dihydropyridines: In vitro evaluation and structure-activity relationship study. Bioorg Med Chem 18: 8044-8053.

104. Cole DG (2003) The intraflagellar transport machinery of Chlamydomonas reinhardtii. Traffic 4: 435-442.

105. Rosenbaum JL,Witman GB (2002) Intraflagellar transport. Nat Rev Mol Cell Biol 3: 813-825.

106. Okiyoneda T, Barriere H, Bagdany M, Rabeh WM, Du K, Hohfeld J, Young JC,Lukacs GL Peripheral protein quality control removes unfolded CFTR from the plasma membrane. Science 329: 805-810.

107. Hershko A (2005) The ubiquitin system for protein degradation and some of its roles in the control of the cell division cycle. Cell Death Differ 12: 1191-1197.

108. Wilkinson KD (1999) Ubiquitin-dependent signaling: the role of ubiquitination in the response of cells to their environment. J Nutr 129: 1933-1936.

109. Huang K, Diener DR,Rosenbaum JL (2009) The ubiquitin conjugation system is involved in the disassembly of cilia and flagella. J Cell Biol 186: 601-613.

110. Hill KL, Hutchings NR, Grandgenett PM,Donelson JE (2000) T lymphocyte-triggering factor of african trypanosomes is associated with the flagellar fraction of the cytoskeleton and represents a new family of proteins that are present in several divergent eukaryotes. J Biol Chem 275: 39369-39378.

111. Buchanan KT, Ames JB, Asfaw SH, Wingard JN, Olson CL, Campana PT, Araujo AP,Engman DM (2005) A flagellum-specific calcium sensor. J Biol Chem 280: 40104-40111.

112. Bangs JD (1998) Surface coats and secretory trafficking in African trypanosomes. Curr Opin Microbiol 1: 448-454.

Chapter IV:

Insect stage-specific receptor adenylate cyclases are localized to distinct subdomains of the *Trypanosoma brucei* flagellar membrane

PREFACE

The following chapter is a reprint with minor modifications of "Insect stage-specific receptor adenylate cyclases are localized to distinct subdomains of the *Trypanosoma brucei* flagellar membrane" by Saada *et al*, with permission from Eukaryotic Cell, 2014: (13)1064-1076. Additionally, this publication was spotlight featured by the editors of the journal as an article of significant interest (doi: 10.1128/EC.00156-14), due to the identification and initial characterization of procyclic-specific receptor cyclases. Some of these putative signaling proteins localize to the flagellum tip, and the results indicate that compartmentalization of cAMP signaling in the ciliary membrane suggest stage-specific roles, as well as specific subdomain targeting, which will be explored in Chapters V and VI.

ABSTRACT

Increasing evidence indicates that the *Trypanosoma brucei* flagellum (synonymous with cilium) plays important roles in host-parasite interactions. Several studies have identified virulence factors and signaling proteins in the flagellar membrane of bloodstream stage *T. brucei*, but less is known about flagellar membrane proteins in procyclic, insect-stage, parasites. Here we report identification of several receptor-type flagellar adenylate cyclases (ACs) that are specifically upregulated in procyclic *T. brucei*. Identification of insect stage-specific ACs is novel, as previously studied ACs were constitutively expressed or confined to bloodstream stage parasites. We show that procyclic-specific ACs are glycosylated, surface-exposed proteins that dimerize and possess catalytic activity. We used gene-specific tags to examine the distribution of individual AC isoforms. All ACs examined localized to the flagellum. Notably however, while some ACs were distributed along the length of the flagellum, others specifically localized to the flagellum tip. These are the first transmembrane domain proteins to be localized specifically at the flagellum tip in *T. brucei*, emphasizing that the flagellum membrane is organized into specific subdomains. Deletion analysis reveals that C-terminal sequences are critical for targeting ACs to the flagellum and sequence comparisons suggest that differential sub-flagellar localization might be specified by isoform-specific C-termini. Our combined results suggest insect stage-specific roles for a subset of flagellar adenylate cyclases and support a microdomain model for flagellar cAMP signaling in *T. brucei*. In this model cAMP production is compartmentalized through differential localization of individual

ACs, thereby allowing diverse cellular responses to be controlled by a common signaling molecule.

INTRODUCTION

African trypanosomes, including *Trypanosoma brucei* and related species, are the causative agents of African trypanosomiasis, also known as sleeping sickness in humans and nagana in animals. Sleeping sickness is recognized as one of the world's most neglected diseases and poses a threat to 60 million people living in sub-Saharan Africa (1). The disease is fatal if left untreated and therapeutic treatments are antiquated, difficult to administer and increasingly ineffective (2, 3). Due to its ability to infect livestock, *T. brucei* also hinders economic growth and agricultural development and as such represents a significant contributor to poverty in some of the most impoverished regions of the world (4).

T. brucei is heteroxenous, requiring a tsetse-fly vector and a mammalian host in order to complete its life-cycle. In both hosts the parasite must sense and respond to extracellular signals, but very little is known about how trypanosomes accomplish this. In other eukaryotes, the flagellum (synonymous with cilium) harbors membrane proteins and signal transduction pathways that mediate cellular responses to changing extracellular signals (5). In mammals for example, ciliary receptor-guanylate cyclases, ion channels and G-protein coupled receptors (GPCRs) control development in response to external signals (5-7). The *T. brucei* flagellar membrane is a direct interface with the host and accumulating evidence indicates that flagellar proteins of these parasites play important roles in mediating interaction with the host environment (8-15). For example, proteomic analysis of the flagellum in bloodstream-form *T. brucei* identified receptor and transporter proteins predicted to

function in signaling, as well as corresponding effector proteins (9). In addition, recent forward genetic screens for downstream effectors in quorum sensing and cAMP signaling pathways in bloodstream-stage *T. brucei* identified putative flagellar proteins (16, 17).

Perhaps the best-characterized flagellar protein involved in host-parasite interaction is "expression site associated gene 4" (ESAG4), a bloodstream-form specific adenylate cyclase (AC) that is localized along the length of the flagellar membrane (18). ESAG4 contributes to virulence in mice and upon encountering host cells is postulated to be activated to drive cAMP production, which in turn inhibits host TNF□ production, thereby resisting the host's early innate immunity attack (15). Several other virulence factors are also localized to the *T. brucei* flagellum, including GPI-PLC (11) , calflagin (13), and metacaspase 4 (14). The precise role of these proteins in host interaction is not known, but each is required for full virulence, as mice infected with corresponding knockout or knockdown parasites show prolonged survival compared to mice infected with control parasites.

The flagellum is also important for parasite interaction within the tsetse fly vector. For example, flagellum-dependent motility is required for transmission through the tsetse fly (19), and parasite attachment to the fly salivary gland epithelium is mediated by outgrowths of the flagellar membrane (10). Flagellum attachment is a critical step in the transmission cycle, as it enables the parasite to establish a permanent infection in the salivary gland and marks the onset of differentiation into mammalian-infectious forms (20, 21). Little is known about flagellar membrane and matrix proteins in insect-stage *T. brucei (22)*, but one

interesting family of proteins is a set of adenylate cyclases encoded by "genes related to ESAG4" (GRESAG4) (23). *T. brucei* encodes approximately 65 GRESAG4 proteins (15), some of which cross-react with anti-ESAG4 antibodies and are localized along the flagellum in both bloodstream and procyclic (fly midgut stage) cells (18). Trypanosomal ACs (ESAG4 and GRESAG4s) have a domain structure that differs from the canonical architecture of mammalian adenylate cyclases. Canonical ACs are multi-transmembrane pass proteins that have two catalytic domains on a single polypeptide and lack direct receptor activity, relying instead on upstream G-protein coupled receptor (GPCR) signaling pathways. Trypanosomal ACs on the other hand resemble mammalian receptor-guanylate cyclases, having an intracellular catalytic domain connected by a single transmembrane segment to a large, extracellular, putative ligand binding domain (23, 24). The trypanosome AC extracellular domain exhibits homology to bacterial periplasmic binding proteins, which bind small ligands to direct chemotaxis and other cellular responses in bacteria (25-27). Trypanosomes have no known GPCRs, and it's been suggested that trypanosomal ACs function directly as receptors, similar to the mammalian receptor-guanylate cyclases they resemble (24, 28).

In vitro differentiation of bloodstream form cells into procyclic cells and subsequent proliferation is associated with bursts of cAMP production, which suggests procyclic-specific cAMP-dependent processes are important for parasite differentiation (29-31). Trypanosomal adenylate cyclases exhibit sequence diversity in their extracellular domains, suggesting a mechanism for ligand-specific regulation of AC activity (24, 32), making these proteins well-suited for directing cAMP signaling

in response to host-specific signals. To date, however, all GRESAG4 genes studied have been found to be expressed in both bloodstream-stage and insect-stage cells (18, 23, 29, 33, 34), raising questions about whether they are responsible for procyclic-specific regulation of cAMP production. Here we report the identification of a group of *T. brucei* adenylate cyclases whose expression is upregulated in procyclic cells. We show that procyclic-specific ACs are glycosylated, assemble into multimeric complexes, exhibit catalytic activity, and are localized to the flagellum where they are surface-exposed. Interestingly, individual ACs are located in distinct subdomains of the flagellum, indicating specialized functions and trafficking mechanisms. Our studies provide the first analysis of individual trypanosome adenylate cyclases within insect-stage cells and support a model for microdomain organization of cAMP signaling in the *T. brucei* flagellum.

MATERIALS AND METHODS

Cell culture and RNAi knockdown.

Procyclic-form cells were used for all experiments and cultured in Cunningham's SM medium as previously described (35). Transfections and selection of clonal lines by limiting dilution were done as described (35). The Fla1 knockdown cell line was generated by transfection of 2913 cells (36) with the p2T7-Fla1 plasmid, as described previously (37). For ACP1 knockdown, the RNAi target region, corresponding to 311 bp of the 3'UTR, was PCR-amplified using the following primers with restriction sites in italics: ACP1-RNAi-F: AT*AAGCTT*TCCTTCTGGCTTCGTCACTT, ACP1-RNAi-R:

at*tctaga*ttcatcccggaacaaaactc. Resulting DNA was ligated into the p2T7-Ti-B RNAi vector (37). Insertion was verified by sequencing by Genewiz, Inc. The p2T7-ACP1-RNAi vector was linearized with Not1, transfected into 29-13 cells and stable transfectants were selected wit 10μg/ml phleomycin. Transfected cells were maintained in selective medium and clonal lines were generated by limiting dilution.

Proteomic identification of flagellar adenylate cyclases.

Procyclic *T. brucei* Fla1 knockdown cells (37) were induced for 25 hours with 1μg/ml tetracycline. After addition of 0.2M sucrose to cells at a density of 4 x10^6 cells/ml, cells were sonicated for 6 min and spun at 2,000xg for 5 min to pellet cell bodies (P1), leaving flagella in the supernatant (S1). The S1 fraction was spun again at 2,000xg for 5 min to remove debris and then subjected to a high-speed centrifugation at 20,000xg for 35 min. The pellet (P2) was resuspended in PBS, layered on top of a 13 ml step gradient of sucrose (10/20/30/40/55/68%), and then centrifuged at 245,000xg for 4 hours at 4°C in a Beckman Optima L-90K ultracentrifuge using a SW 41 rotor. 14 fractions of approximately 1 ml each were collected from the top of the gradient and spun at 14,000xg for 1 hour at 4°C to concentrate the samples for examination by phase-contrast microscopy. Flagella were found primarily in fractions 8 and 9, corresponding to the interface between the 40% and 55% sucrose layers. To solubilize membranes, this flagellum fraction was incubated for 10 min at RT with 0.1% NP40 in PBS and then centrifuged at 10,000xg for 10 min to separate the axoneme-containing pellet (P3) from the supernatant (S3) harboring flagellar membranes and matrix proteins. Since NP40 can degrade the quality of MS spectra, proteins were

precipitated from the flagellum (S3) fraction by trichloroacetic acid (TCA) precipitation, followed by two washes with acetone. Cell bodies (P1) were disrupted by hypotonic lysis (38), sonicated for 2 min, and incubated for 10 min at RT with 0.1% NP40 in PBS. Solubilized proteins were precipitated by TCA and washed with acetone. TCA-precipitated proteins from solubilized flagellum and cell body fractions were digested by the sequential addition of lys-C and trypsin proteases (39, 40) and subjected to MudPIT analysis as described previously (9). Proteins were considered present in the analysis if they were identified by two or more peptides using a 5% peptide-level false discovery rate (41-43).

The majority of proteins were uniquely identified by specific peptides (unique, "U"). Proteins identified only by peptides shared with other proteins were assigned to groups. The set of proteins identified in the cell body fraction was subtracted from the combined flagellum fractions, yielding a subtracted dataset of 175 proteins arranged in 157 groups (Supplemental Table 4-01). *In situ* tagging and immunofluorescence localization analyses (44) were done for four proteins of the subtracted dataset. All of these localized to the cytoplasm or cell body surface, but not the flagellum (not shown), indicating the subtracted dataset contained substantial cell body contamination and precluding analysis of the dataset as a stand-alone flagellar proteome. Interestingly however, the subtracted dataset included a group of six receptor-type adenylate cyclases that were not found in previous analysis of bloodstream-form flagellar membranes (9) (Table 4-01, Supplemental Table 4-01). These proteins were selected for further study. Sequence comparisons were done by

pairwise alignments using VectorNTI's AlignX module (Invitrogen) with sequences obtained from the TriTrypDB database [91].

Quantitative real-time PCR.

Cells were harvested at a density of approximately $5x10^6$ cells/ml (PCF) and $1x10^6$ cells/ml (BSF) . For ACP1-knockdowns, cells were grown with or without tetracycline at 1 μg/ml for 72 hours prior to harvesting. Total RNA was extracted using Qiagen's RNAeasy kit, and quantitative reverse transcriptase –real time PCR (qRT-RTPCR) was performed as described (45). Gene-specific primer sets were designed using the Trypanofan RNAit algorithim (46) and NCBI Primer-Blast (47). Primers used were: ACP1-F: CGTTGACTTCACGGCTTACA, ACP1-R: acatttcgttctcccactgc, ACP2-F: GCCATGTCGTTGATTTCACA, ACP2-R: ccaaccagaccacagacctt, ACP4-F: AGCTTACGAGGGCTGTGAAA, ACP4-R: aaatacactgccccttgtcg, ACP5-F: TCTGCTTATGCAGGACGATG, ACP5-R: cctcaaaagtctcgaggtgc, FS33-F: GCGCTAGCATAAGACGTGGT, FS33-R: gaaccgttctcacaccaaca, ISG65-F: CATGACAGAGGAGTGGCAGA, ISG65-R: catgctcggttgaagcacta. qRT-PCR was conducted on a DNA Engine Opticon 2 (MJ Research, Bio-Rad) using iQ SYBR Green Supermix (Bio-Rad) according to the manufacturer's instructions. All analyses were performed in technical duplicates on at least two independent RNA preparations and values were normalized against two stage-independent control genes, TERT and PFR2 (48), using the 2(-ΔΔC(T)) method (45, 49).

In situ **epitope tagging.**

In situ tagging was done by amplifying short (300 to 600bp) fragments of DNA homologous to the target gene's open reading frame or 3'UTR and cloning these upstream of the 3xHA tag, or downstream of the puromycin resistance gene of the pMOTag2H vector, or the 3xMYC tag and phleomycin resistance gene of pMOTag53M (44). The primers used, with restriction sites italicized, were: ACP1orfF: AT*GGTACC*ACATGGCTGCCCGCACAGAG, ACP1orfR: at*ctcgag*gttttcctcctttggggttga, ACP1utrF: AT*GGATCC*GGGTCGTAGGCATGCGCCAT, ACP1utrR: at*tctaga*gggggagcaggcgcctcaat, ACP2orfF: AT*GGTACC*TTGTGAATTGGGTCAGTCGCA, ACP2orfR: at*ctcgagttctcgttcgctgcttgt*, ACP2utrF:AT*GGATCC*CATCAAGAAGGAAACCGAGTA, ACP2utrR: at*tctaga*tgaactaaattgcagtctccca, ACP4orfF: GAT*GGTACC*TGCGCGGACGGAAAATGTGACGAAC, ACP4orfR: gat*ctcgag*aaacttatcaaaatccgtggtccgattgggga, ACP4utrF: GAT*GGATCC*GGGTTTTGGGGGGTTAATGGCACAA, ACP4utrR: gat*tctaga*atttcaccgccggagacgttgttga ACP5orfF: AT*GGTACC*ATGGCTGCGGGACGGAGAG, ACP5orfR: at*ctcgagccgctgcgcttcgggtttc,* ACP5utrF:AT*GGATCC*AAACCACTCCACGAACTAATGAC, ACP5utrR: at*tctaga*gaaggagtgttccctgcgataa. For ACP1 and ACP2 truncations, the following primers for amplification of the ORF were designed to eliminate the final 45 codons: ACP1ΔC45F: ATAT*GGTACC*AGGGTTACGACTACTATGGTCA, ACP1ΔC45R atat*ctcga*aacgacgtgtcccacttttg, ACP2ΔC46F: AT*GGTACC*CCGTCAATGAGCTTCAGAGACCCTAGCGAAGGAAAACTC, ACP2ΔC46R: at*ctcgagcatatg*aacgacatggcccacttttgttgctatacgccgcataac. All sequences were verified

by direct sequencing at the UCLA Sequencing and Genotyping Core Center. Tagging cassettes were excised by restriction digestion, purified, and transfected into 2913 cells. Transfected cells were maintained in selective medium and clonal lines were generated by limiting dilution.

Southern Blots.

Genomic DNA was isolated using a PureLink Genomic DNA kit (Invitrogen) according to manufacturer's instructions. Restriction enzyme digestions (New England Biolabs) were done for eight hours, and samples were then separated on a 0.8% agarose gel. Gels were treated for fifteen minutes each in depurination buffer (0.25M HCl), denaturation buffer (0.5M NaOH, 1.0M NaCL), and neutralization buffer (1 M Tris-HCL [pH 7.5], 3M NaCl), and rinsed in distilled water. DNA was transferred to Hybond-XL membrane (GE Healthcare) using capillary transfer overnight in SSC buffer (3M NaCl, 300 mM $Na_3C_6H_5O_7$). The membrane was cross-linked using 1500J on a UV Stratalinker (Stratagene). Digoxigenin-probes were PCR-generated using the following primers: PuroProbe_F: CACCGAGCTGCAAGAACT, PuroProbe_R: ctcgtagaaggggaggttg, ACP1_probeF: ATTCTAGAGGGGGAGCAGGCGCCTCAAT, ACP1_probeR: atggatccggtcgtaggcatgcgccat. Hybridization, washes and detection were done according to manufacturer's instructions using Roche's DIG EasyHyb buffer, CDP-Star substrate, and PCR DIG-probe synthesis kit (Roche, Inc.).

Cell fractionation and immunoblotting.

To assay for association with detergent-resistant membranes (Figure 4-03A), cells were washed once in PBS and lysed at either 4°C or 37°C in PBS with 1% Triton-X100 and protease inhibitors (SigmaFAST cocktail, Sigma Aldrich) as described (50)). Lysates were centrifuged for 20 min at 15,000g at either 4 °C or room temperature to separate solubilized proteins (S) from the insoluble pellet (P) fraction. Immunoblotting was done as previously described (45).

Blue Native analysis and de-glycosylation.

Cells were harvested and washed in PBS, then resuspended into PEME buffer (100mM PIPES, 1mM MgSO4, 0.1mM EDTA, 2mM EGTA, pH 6.9) with 1% NP40 and protease inhibitors (SigmaFAST cocktail, Sigma Aldrich). Following a 10-minute incubation at room temperature, lysates were spun for 15 minutes at 13K rpm at 4 °C. Supernatants were transferred to new tubes and spun again for 10 minutes to clear debris, and the resultant soluble fractions were used. For Blue-Native analysis, NativePAGE sample buffer and 5% G-250 sample additive (Invitrogen) were added, and samples were run on a NativeMARK 4-16% Bis-Tris native gel and transferred to a polyvinylidene difluoride (PVDF) membrane per manufacturer's suggested protocols (Invitrogen), followed by immunoblotting. For deglycosylation, the soluble fraction was denatured and treated with PNGaseF (New England Biolabs) for one hour at 37°C using the manufacturer's suggested protocols, followed by SDS-PAGE and immunoblotting.

Immunoprecipitation.

Cells were harvested and washed in PBS, then lysed in IP buffer (150 mM NaCl, 50mM HEPES, 5mM EDTA, 5mM EGTA, 1% NP40, 10% glycerol, and 1xSigmaFAST protease inhibitors). After 10 minutes on ice, lysates were centrifuged at 4°C for 30mins to remove insoluble material. A fraction of the soluble fraction was retained, and the rest was added to EZview red anti-HA affinity matrix (Sigma Aldrich) and incubated for approximately 3.5 hours at 4°C on a nutator. Beads were collected by centrifugation and washed several times in IP buffer. Input, unbound and bead fractions were boiled in sample buffer and analyzed by SDS-PAGE and immunoblotting.

Surface biotinylation and streptavidin purification.

Surface biotinylation was done as described previously (9). Cells were harvested and washed in ice-cold PBS then resuspended in 3mls of cold 0.5mg/ml biotin (Pierce 21331) solution, and incubated for 10 minutes on ice. 2M Tris pH 6.8 was added to a final concentration of 100mM to block unreacted biotin, and incubated on ice for 10 minutes. Cells were pelleted, washed with cold PBS + 100mM Tris and extracted with 1% NP40 in PBS with 100mM Tris and SigmaFast Protease Inhibitors. After a 10-minute incubation on ice, samples were centrifuged at 14,000 rpm for 10 minutes at 4°C to pellet insoluble material. A fraction of supernatant was retained ("input") and the remainder was transferred to a new tube with 50ul of GE Healthcare Streptavidin Sepharose High Performance Beads and incubated for one hour at 4°C on a nutator to allow biotin-strepatavidin binding. Beads were pelleted and washed as described (9),

then resuspended and boiled in native sample buffer ("bound" samples) for analysis by immunoblotting.

Yeast Complementation.

For yeast complementation, adenylate cyclase open reading frames were subcloned into a modified version of the pRS315 *Saccharomyces cerevisiae* expression vector (51), pRS315-GPDp-CYCt, which contains a glyceraldehyde 3-phosphte dehydrogenase (GPD) promoter to allow constitutive high expression, with a cytochrome C isoform 1 (CYC1) terminator. The pRS315-GPDp-CYCt plasmid was kindly provided by Drs. Giancarlo Costaguta and Gregory Payne (UCLA). The *S. cerevisiae* wild type adenylate cyclase (CYR1) coding sequence was amplified from the YCp50-CYR1 plasmid (52) and full length *T. brucei* adenylate cyclase coding sequences were amplified from genomic DNA using the following forward (F) and reverse (R) primers, with restriction sites italicized: CYR1F: ATAT*GGATCC*ATGTCATCAAAACCTGATACTGGTTCG, CYR1R: atat*gtcgac*tcaagttgataaatcctttgcgttc, ACP1F: ATAT*ACTAGT*ACTGCGATGAATATGCTTCACTTG, ACP1R: atat*ctcgaggtcgac*acgaccctcagttttcctcc, ACP2F: ATAT*AAGCTTACTAGT*ATGAATATGCTTCACTTGGACGAC, ACP2R: atat*ctcgaggtcgac*ttattctcgttcgctgcttgtg, ACP4F: ATAT*ACTAGT*ATGAAAGCACCAGCCTTGC, ACP4R: atat*ctcgag*ttaaaacttatcaaaatccgtggtc, ACP5F: ATAT*ACTAGT*ATGACCACCACGAAGGCTTCGTGTC, ACP5R: atat*aagctt*tcaccgctgcgcttcggggtttc. Amplified coding sequences were cloned into the pRS315-GPDp-CYCt using the corresponding restriction sites (italicized in primers) and

the resulting plasmids transformed into the *S. cerevisiae* cyr1-2 mutant (53) using standard methods (54). Transformants were selected and maintained on "SD -Leu" selective media as described (54). Clonal strains were resuspended in PBS at an OD_{600} of 1.0 and five-fold serial dilutions were spotted onto YPD-rich media agar plates, which were incubated at permissive (22ºC) or restrictive (35ºC) temperatures.

Antibody production.

Anti-ACP1 antibody was generated by Pacific Immunology, Inc. against a synthetic peptide corresponding to the C-terminal 15 amino acids of ACP1, CAVGERNVSTPKEEN, which is unique and distinguishes ACP1 from ACP2. Antibodies were raised in New Zealand white rabbits and ACP1-specific antibodies were affinity-purified by the vendor using peptide coupled to agarose beads. Antibody specificity was determined by immunoblotting with total protein extracts from ACP1 RNAi knockdown cells grown with or without tetracycline. For PFR antibodies, a fragment encoding the N-terminal 328 amino acids of PFR2 (NCBI#XP_847327.1) was amplified from genomic DNA and expressed using the pETDuet-1 system (Novagen). Recombinant protein was purified using the manufacturer's suggested protocols, and used to raise polyclonal antibodies in rabbits by Pacific Immunology, Inc.

Immunofluorescence microscopy.

Immunofluorescence on whole cells was done as described previously (9). Monoclonal anti-HA antibody HA.11 (Covance) was used at a 1:250 dilution and detected using donkey anti-mouse secondary coupled to AlexaFluor488 (Molecular Probes) at 1:750.

Polyclonal PFR anti-sera was used at a 1:1250 dilution, polyclonal affinity-purified anti-ACP1 antibodies were used at 1:500, and both were detected using donkey anti-rabbit antibody coupled to either AlexaFluor 488 or 597 (Molecular Probes) at 1:750. Coverslips were mounted in VectaShield mounting medium with DAPI. Samples were imaged on a Zeiss Axioskop II (Zeiss, Inc.).

RESULTS

Identification of procyclic stage-specific adenylate cyclases.

We previously reported isolation of intact flagella and proteomic analysis of flagellar membrane and matrix proteins from bloodstream form (BSF) *T. brucei* (9). We attempted a similar analysis using procyclic culture form (PCF) *T. brucei*, corresponding to insect midgut stage parasites, but our analyses indicated a high level of contamination by cellular proteins, likely owing to the use of sonication to remove flagella from cell bodies (methods). Among the proteins identified, however, were a group of receptor-type adenylate cyclases that were not detected in BSF flagellum preparations (Table 4-01). These adenylate cyclases are part of a previously described family of "genes related to ESAG-4" (GRESAG4), based on their sequence similarity to the expression site associated gene 4 (ESAG4) (23). ESAG4 is expressed only in BSF parasites, while previously examined GRESAG4 genes were found to be constitutively expressed in both BSF and PCF parasites (18, 23, 29, 33, 34). We were therefore surprised to uncover a group of GRESAG4s that were detected only in procyclic flagella and we investigated these further. We termed these proteins ACP1 through 6, to reflect the fact that they were found in procyclic, but not bloodstream, proteomic analyses.

The *T. brucei* genome includes approximately 65 GRESAG4 genes, each having a large extracellular domain at the N-terminus, followed by a single transmembrane region and a cytoplasmic catalytic domain (15). The catalytic domain is followed by a short C-terminal region of approximately 150-175 amino acids. Sequence

relationships among trypanosomal ACs, including ACP1-6, have been described previously (15, 55). Amino acid sequence diversity among ACP1 - 6 is highest within the N-terminal and C-terminal regions (Figure 4-01B). Pairwise alignments revealed that ACP1 and 2 are approximately 90% identical in amino acid sequence throughout their length, with differences lying primarily within the C-terminus. The other ACs identified exhibit considerable sequence differences between one another (Figure 4-01B).

Peptides specific to ACP1 – 6 were not detected in a proteomic analysis of flagella from bloodstream form cells (9), suggesting these proteins are expressed only in the procyclic life cycle stage. However, sequence similarities among the AC protein family make it difficult to unambiguously identify specific isoforms using proteomics alone. For example, while one or more peptides uniquely mapped to each of ACP1 and 3 - 6 in the current study (Table 4-01), the five peptides that mapped to ACP2 also mapped to ACP1. We therefore used quantitative reverse-transcriptase, real-time PCR (qRT-PCR) with gene-specific primers to directly determine the developmental expression profile for ACP1 through 6. We found that ACP1 and 3 - 6 were each expressed primarily in procyclic-form parasites (Figure 4-01C), while ACP2 expression was similar in both life cycle stages. Notably, qRT-PCR also demonstrated that expression of FS33, an AC identified in BSF flagella (9) but not PCF flagella, was indeed upregulated in BSF cells (Figure 4-01C). Thus ACP1 and 3-6 show developmentally-regulated expression distinct from that reported for all other GRESAG4 genes studied to date.

In situ epitope tagging enables analysis of individual ACs.

The large size of the AC gene family, together with extensive sequence homology among individual genes, has complicated efforts to analyze any single AC gene or protein. Our proteomic analyses identified a small subset of ACs as being expressed in procyclic cells, thereby allowing prioritization of individual genes for direct analysis. We focused our studies here on ACP1, 2, 4 and 5, while ACP3 and 6 are the focus of separate work. To study each protein individually, *in situ* tagging (44) was used to incorporate an HA epitope tag at the 3' end of each gene. Western blot analysis of cell lysates demonstrated a single HA-tagged protein of the expected size was expressed in each tagged cell line, and Southern blotting demonstrated integration of the HA epitope tag at the expected locus in each case (Figure 4-02). Having established gene-specific tags for each AC, we set out to characterize the individual proteins.

Biochemical analysis reveals that *T. brucei* ACs are surface-exposed glycoprotein multimers.

The cellular distribution of adenylate cyclases in procyclic *T. brucei* has previously been examined only in conglomerate (18). The availability of gene-specific epitope tags provided a unique opportunity to monitor the fractionation and distribution of individual AC proteins. The ACs studied here were identified in detergent-solubilized cell fractions. To determine whether this represented the entire cellular pool for each protein, we performed Western blot analysis of

detergent-soluble and detergent-insoluble fractions. Each AC fractionated exclusively in detergent-soluble supernatants, consistent with what would be anticipated for membrane-associated proteins (Figure 4-03A). Some flagellar membrane proteins are associated with detergent resistant membranes (56). To determine whether this is the case for ACs, we asked whether solubilization with TritonX-100 at 4°C shifts ACs to the pellet fraction, as seen for proteins in detergent-resistant membranes, such as calflagin (56). The AC fractionation patter was unchanged at 4°C and 37°C indicating they are not associated with detergent-resistant membranes. *T. brucei* ACs are predicted to be surface exposed and this has been demonstrated for ESAG4 and FS33 in BSF parasites, as well as for a group of AC proteins in conglomerate in procyclic cells (9, 18). We asked whether ACP4 and 5 were surface-exposed using surface biotinylation, followed by affinity purification with streptavidin. Western blot analysis of bound and unbound fractions demonstrated that each AC eluted with the bound, i.e. surface-biotinylated, fraction, while the intracellular marker BiP eluted in the unbound fraction (Fig 4-03B). Therefore, ACP4 and 5 are exposed on the cell-surface of procyclic-form *T. brucei*.

The calculated molecular weights of ACP1 and 2 are nearly identical, 137.5 and 137.9 kDa, respectively (Table 4-01). However, Western blots revealed significant size differences between these proteins (Figure 4-02), suggesting differential post-translational modifications. Trypanosomal ACs have a receptor-type structure and are predicted to function in recognition of extracellular ligands. Glycosylation is a common feature of surface proteins and can be critically important for receptor-ligand interactions (57). Moreover, there are several putative glycosylation sites

present in both proteins, and all are predicted to be within the extracellular N-terminal domains (data not shown). We therefore asked whether glycosylation accounted for the size difference between ACP1 and 2. To test for glycosylation, we used digestion with peptide N-glycosidase F (PNGase F), which cleaves N-linked carbohydrate groups. PNGase F treatment caused a significant reduction in size for each AC as seen by SDS-PAGE (Figure 4-03C). As a control, the cytoplasmic protein E1F4AI (58) showed no change in protein size with PNGase F treatment. Therefore, individual ACs are differentially glycosylated, although some difference in size remains, suggesting additional modifications may be present.

All characterized nucleotide cyclase catalytic domains operate as dimers, with catalysis occurring at the dimer interface (59, 60). Unlike conventional adenylate cyclases, which have two cyclase domains on a single polypeptide, trypanosomal cyclases have only a single catalytic domain per protein (Figure 4-01A). *In vitro* studies with recombinant catalytic domains previously demonstrated that *T. brucei* AC catalytic domains require dimerization for catalytic activity (34, 59) but whether the full-length proteins form dimers *in vivo* is not known. We therefore asked whether native *T. brucei* ACs formed multimeric complexes by examining cell lysates using Blue Native gels in non-reducing conditions. Western blots of Blue Native gels showed that each of the ACs examined migrated as multiple species, ranging in size from approximately 160 kDa to 500 kDa, with the major species in each case being the larger MW (>300kDa) bands (Figure 4-03D). The size of the smaller species in each case agrees with the predicted size of the monomeric protein, ~150kDa. Therefore, AC proteins form multimeric complexes under native conditions.

Multimeric complexes observed by BlueNative gels suggested dimerization, but could be due to interaction with proteins other than ACs themselves. To test for dimerization directly, we generated doubly-tagged lines, in which one ACP1 allele is HA-tagged and the other is MYC-tagged. We also did this for ACP2. Immunoprecipitation with anti-HA in each case demonstrated that the Myc-tagged protein co-precipitated with the HA-tagged protein (Figure 4-03E), while singly-tagged ACP1-Myc was not precipitated with anti-HA antibody (4-03G). Notably, co-immunoprecipitation was only observed if the HA-tagged and Myc-tagged proteins were expressed in the same cells. Using a mixture of cells, in which one half expressed HA-tagged protein and the other half expressed Myc-tagged protein, co-immunoprecipitation was not observed (Figure 4-03F). Although dimerization is anticipated, this is the first direct evidence that ACs dimerize *in vivo*.

To test whether the ACs identified here are catalytically active, we tested their ability to rescue growth of *Saccharomyces cerevisiae* mutants that lack a functional adenylate cyclase. The yeast *cyr1-2* strain harbors a temperature-sensitive mutation that disrupts function of the endogenous adenylate cyclase, CYR1, rendering c*yr1-2* yeast non-viable at the restrictive temperature due to a cAMP deficiency (53). Expression of *T. brucei* ACP1, 2, 4 or 5 restored viability of the *cyr1-2* mutant at restrictive temperatures (Figure 4-04). Thus, each of these proteins individually possesses adenylate cyclase catalytic activity *in vivo.*

Individual adenylate cyclases are localized to different domains of the flagellar membrane.

Subcellular distribution has not been determined for most adenylate cyclases in *T. brucei*. Two individual ACs, ESAG4 (18)and FS33 (9) have been shown to localize along the length of the flagellum in bloodstream form parasites. Immunofluorescence using pan-specific antibodies showed localization along the length of the flagellum for a group of GRESAG4 proteins in procyclic form parasites, but individual proteins were not examined in this life cycle stage and it is not known to which specific GRESAG4 genes the labeling (18). The availability of clonal lines, each having a single, uniquely epitope-tagged AC protein made it possible to examine the location of each AC individually by immunofluorescence microscopy. Using immunofluorescence with anti-HA antibody, we found ACP1, 2, 4 and 5 to be localized exclusively to the flagellum (Figure 4-05). Notably, the specific distribution within the flagellum was different for individual ACs. ACP1 and 4 were localized primarily to the distal tip of the flagellum, whereas ACP2 was evenly distributed along the entire length of the flagellum. ACP5 was concentrated at the flagellum tip with weaker signal seen along the flagellum. The tip-specific localization of ACP1 and 4 distinguishes them from trypanosomal ACs studied previously and is to our knowledge a novel finding for a transmembrane protein in *T. brucei.*

Localization of individual trypanosomal ACs to distinct regions indicates that different structural features must be present to distinguish the tip of the flagellum from the length of the flagellum in order to enable tip-specific targeting. To assess when such features are established, we examined AC protein localization as a function of the cell cycle. Trypanosome cultures grow asynchronously and morphogenetic markers are available to easily define cell cycle stage for any given

cell in the population (61). Cells that have completed kinetoplast division but not mitosis contain two kinetoplasts and a single nucleus (2K1N). These cells possess one fully formed flagellum and one newly forming flagellum, whose tip connects to the side of the old flagellum (61). Anti-HA immunofluorescence showed that 2K1N cells have two spots of fluorescence in cells expressing ACP1-HA or ACP4-HA, one corresponding to the tip of the old flagellum and one corresponding to the tip of the newly forming flagellum (Figure 4-06B). Therefore any cellular features required for flagellum tip-specific localization are established prior to completion of mitosis, while the nascent flagellum is still growing.

To assess whether the HA epitope tag influenced protein localization, we raised ACP1-specific antibodies and used these antibodies to determine the location of the endogenous protein. To test specificity of anti-ACP1 antibody, we generated a gene-specific RNAi knockdown of ACP1. qRT-PCR demonstrated specific and efficient knockdown of ACP1 without affecting expression of ACP2 (Figure 4-06A) , which is the protein most closely related to ACP1. Knockdown of ACP1 did not affect parasite growth or motility (not shown). Western blots with anti-ACP1 antibodies detected a single band of the expected size that was lost following induction of RNAi (Figure 4-06B). Anti-ACP1 antibody failed to detect any signal in lysates from bloodstream-form parasites, corroborating the qRT-PCR results demonstrating that ACP1 is a procyclic-specific protein. These results further demonstrate that the antibody distinguishes ACP1 from ACP2, as ACP2 expression is unaffected by ACP1 knockdown. Immunofluorescence with ACP1-specific antibody showed that endogenous ACP1 is located at the distal tip of the flagellum (Figure 4-06C), as seen for the HA-tagged

protein, and the tip-signal is lost upon RNAi induction against ACP1. Therefore the HA-tagged protein (Figure 4-05) correctly reports localization of the endogenous protein.

Protein targeting to specific subcellular locations requires cis-acting targeting sequences within the protein. ACP1 and 2 are almost identical in sequence, except for their C-termini, suggesting that this region is important for specifying flagellar and/or sub-flagellar localization. We therefore generated epitope-tagged deletion mutants lacking the C-terminal 45 or 46 amino acids of ACP1 and 2, respectively, to assess the influence of these amino acids on flagellar localization. In both cases, expression was reduced and the deletion mutants exhibited a punctate distribution throughout the cell, but were completely absent from the flagellum (Figure 4-07), demonstrating that these residues are critical for targeting to the flagellum.

DISCUSSION

Insect stage-specific adenylate cyclases.

Our studies reveal a new paradigm for trypanosomal ACs through identification of a group of AC genes upregulated in the procyclic life cycle stage, indicating a specific role within the tsetse fly. There are approximately 65 chromosome-internal adenylate cyclase genes in the *T. brucei* genome (55) but only a few of these have been studied directly. Among the ACs identified here, ACP4 corresponds to previously studied GRESAG 4.2/4.3 (33, 55). ACP1 and 2 correspond to two "ESAG4-like" genes identified as being upregulated in BSF parasites following knockout of ESAG4 (55), though they were not examined in PCF parasites. ACP3, 5 and 6 do not correspond to previously studied GRESAG4 genes. Procyclic-specific expression is a novel finding, as all ACs examined previously have been found to be either BSF-specific, ESAG4 (23, 29) and FS33 (Figure 4-01) (9), or constitutively expressed, GRESAG4.1, 4.2/4.3 and 4.4 (18, 23, 33, 34). Prior analysis of GRESAG 4.2/4.3, corresponding to ACP4, reported equal expression in BSF and PCF parasites by Northern blot (23) , while our qRT-PCR analysis shows six-fold up-regulation of ACP4 in PCF versus BSF parasites. We suspect that the discrepancy may lie in greater capacity for gene-specific analysis in qRT-PCR. Additionally, earlier studies may have underestimated potential for cross-reactivity in Northern blots, because the size and extent of sequence similarity among the AC/GRESAG gene family was not known.

ESAG4 functions in manipulation of host immune responses to trypanosome infection (15) and potentially in cytokinesis in bloodstream form parasites (55).

However, the functions of chromosomal-internal GRESAG4 ACs and the reasons for expansion of the AC gene family remain unknown. ACP1 and 2 are upregulated in bloodstream cells following knockout of ESAG4, compensating for loss of ESAG4 (55). Thus, some ACs may substitute for others under selective pressure. Nonetheless, our data argue against a strictly redundant role for *T. brucei* ACs, because we see developmentally-regulated expression profiles that differ from expression profiles described for ESAG4 and all other GRESAG4 genes studied to date. Distinct functions for individual ACs is also supported by sequence diversity among different isoforms (28) and our finding here that individual isoforms show distinct distributions along the flagellum

Non-redundant functions for individual ACs in parasite-tsetse interactions are also consistent with the observation that expansion of the AC gene family varies among different tsetse-transmitted trypanosomes. *T. vivax* for example, which develops only in the fly mouthparts and foregut (62), has 14 AC genes (15). By comparison, development of *T. congolense* and *T. brucei* occurs not only in the mouthparts and foregut but also the midgut, with *T. brucei* additionally advancing through the salivary glands (62). Correspondingly, *T. congolense* and *T. brucei* have a larger cohort of AC genes, with approximately 45 and 65 chromosome-internal AC genes, respectively (15). Therefore, size of the AC gene family in different African trypanosomes directly correlates with complexity of the parasite's developmental cycle and tissue distribution in the tsetse, consistent with the idea that ACs function in tsetse-parasite interactions. *In vitro* differentiation of bloodstream parasites into

procyclic forms and subsequent proliferation is accompanied by spikes in cellular cAMP (18, 29) and procyclic-specific ACs provide a potential source for this cAMP.

Functional consequences of tip-localized adenylate cyclases.

Previous studies showed flagellum localization for ACs in procyclic parasites, but the antibodies could not distinguish between isoforms (18). By using gene-specific epitope tagging, we were able to determine the unique distribution of individual AC proteins. Surprisingly, we discovered distinct patterns of localization for different isoforms. Most notably, ACP1 and 4 were localized to the flagellum tip, which has not been reported for any previously studied *T. brucei* AC. Hundreds of *T. brucei* flagellar proteins have been described (9, 22, 63). However, aside from ACs reported here, only three flagellar tip proteins have been identified. These are two axonemal proteins, kinesin KIF13.2 (64) and FLAM8 (22), and one membrane protein, calpain1.3, which associates with the membrane via acylation (65). KIF13.2 functions in flagellum length control, while the functions of calpain1.3 and FLAM8 are not known. Flagellum tip proteins in other organisms play important functions in cell signaling. Examples include vertebrate polycystins and Gli proteins that function in Ca^{++} and hedgehog signaling, respectively (66-68). Examples in other protists include flagellar tip agglutinins in *Chlamydomonas* that mediate cell adhesion events associated with cAMP signaling and mating (69, 70). Thus, identification of tip-localized ACs that could modulate cAMP signaling in *T. brucei* is of great interest.

Unlike mammalian ACs, trypanosomal ACs are postulated to function as receptors modulating signaling, with specificity conferred by divergent N-terminal

ligand binding domains (24, 28). Consistent with this idea, the AC N-terminal domain shares homology with bacterial periplasmic binding proteins (PBPs) that function in chemotaxis and signaling through recognition of diverse ligands (Figure 4-01) (25, 71). A receptor function for trypanosome ACs remains speculative at present, but demonstration that procyclic-specific ACs dimerize and are catalytically active supports their function in cAMP production. Differential localization would provide a mechanism to spatially restrict cAMP output from different AC isoforms, allowing them to interface with distinct effector proteins. Thus, segregating individual isoforms to distinct flagellum sub-compartments would allow two different ACs to initiate specific responses despite using a common output. Such an arrangement provides support for a micro-domain model for cAMP signaling postulated for *T. brucei* and observed in other eukaryotic cells, where close proximity of ACs, phosphodiesterases and effectors confines cAMP signaling to distinct foci (72-74). Importantly, the *T. brucei* cAMP-specific phosphodiesterase PDEB1 is distributed along the length of the flagellum (75) and is thus positioned to act as a diffusion barrier, limiting cAMP to the site of production by differentially localized adenylate cyclases (74).

Protein localization to the flagellum tip is also interesting in the context of parasite development because the tip initiates attachment to the fly salivary gland prior to differentiation into mammalian-infectious metacyclics (20). Reorganization of cytoskeletal filaments and the flagellum membrane at the site of attachment (76), as well as subsequent cellular and molecular changes that accompany differentiation into metacyclics (20, 21), presumably involves signaling events triggered by flagellum

contact. Consistent with this idea, metacyclogenesis in *T. congolense* can be triggered *in vitro* via flagellum contact with plastic surfaces (77). There is also a precedent for flagellum-tip attachment triggering cellular differentiation in the protist *Chlamydomonas reinhardtii*, whereby, flagellum tip adhesion between two gametes triggers a cAMP signaling cascade resulting in gamete fusion (69, 70, 78). Recent ex-vivo reconstruction of the *T. brucei* mating cycle identified gamete-like cells that interact via their flagella prior to fusion (79), raising the intriguing possibility that flagellum-dependent interactions may be part of the *T. brucei* mating cycle. The flagellum functions in mechanosensation in other protists (80, 81), and may therefore function in contact-mediated signaling in *T. brucei*. Surface-exposed adenylate cyclases at the tip of the flagellar membrane are ideally positioned to perceive and transduce responses to flagellum attachment. Tests of this hypothesis will require tsetse infection experiments using trypanosomes lacking specific ACs. The insect stage-specific ACs identified here present excellent candidates for testing this idea and the lack of any growth defect following RNAi knockdown of ACP1 demonstrates that such experiments are now feasible. Apart from host-parasite interaction, the flagellum tip is also distinguished structurally from the rest of the flagellum and is the site of flagellar structures important to cell division (82, 83). Thus, tip-specific ACs are located in a unique region of the cell that plays several important functions in parasite biology.

Flagellum tip-targeting signals

The C-terminal 45 and 46 amino acids are required for flagellar targeting of ACP1 and 2, respectively. Previous work showed that a 21-amino acid fragment near the C-terminus of calpain 1.3 is required for flagellar targeting (65). We did not observe any obvious sequence similarities between the C-terminal sequences of ACs and Calpain 1.3, nor did we identify similarities to published targeting sequences in flagellar membrane proteins of other organisms (84). Protein localization within specific flagellum sub-domains is emerging as an important aspect of flagellum biology (22, 85-87) , but sequences responsible for directing sub-flagellar targeting are unknown (88, 89). In this regard, ACP1 and 2 in *T. brucei* offer potential insights, because they are ~90% identical in amino acid sequence and differences are primarily restricted to the C-terminal region that is required for flagellum localization. This region is expected to be intracellular and thus accessible to targeting machinery. Alignment of the C-terminal 42 amino acids of ACP1 and 2 revealed differences at 31 positions (Figure 4-07). Of these 31 positions, only 5 are conserved between ACP1 and the other tip-localized AC, ACP4. Therefore, these 5 residues are likely to be important for specifying sub-compartment localization within the flagellum. Notably, 3 of these 5 residues are conserved in ACP5, consistent with the intermediate, i.e. "tip-enriched + length", localization observed for ACP5. The localization of ACP3 and 6 were not determined, but based on sequence conservation within the putative tip-targeting domain (Figure 4-07), these proteins are likely to be tip-localized, or tip-enriched.

The flagellum and cAMP signaling in trypanosomes

Cyclic AMP is important in *T. brucei* development and pathogenesis (15, 29, 32). ACs are the source of cAMP production and are therefore critical for cAMP signaling. All of the adenylate cyclases so far studied in *T. brucei* are concentrated in the flagellum, which also contains cAMP-specific phosphodiesterases (75)and cAMP effectors (16). Together, this indicates an important role for the flagellum in *T. brucei* cAMP signaling. Future studies aimed at understanding AC function as well as mechanisms of targeting to the flagellum and specific flagellum sub-compartments offer opportunities for understanding key aspects of trypanosome biology and host-parasite interaction.

FIGURES

Table 4-01. *T. brucei* adenylate cyclases identified in the present study.

Protein	GeneID	A.A.	Predicted kDa	Peptides Identified	Relatedness*
AC-P1	Tb927.11.17040	1253	137.5	R.YETLPEDFIK.E, R.ADPAAETLALIR.Y, R.YVINDIVIGDYGGTCEGEAAK.H, R.TESAANGGQILLTR.A, K.EQLELETDQNK.I, R.ALISQYECYEVK.T	ESAG4-Like
AC-P2	Tb927.10.16190	1254	137.9	R.ADPAAETLALIR.Y, R.YVINDIVIGDYGGTCEGEAAK.H, R.TESAANGGQILLTR.A, K.EQLELETDQNK.I, R.ALISQYECYEVK.T	ESAG4-Like
AC-P3	Tb927.7.7470	1205	132.9	R.NYLTEYK.E, R.SLIENYDCYEVK.T, R.GVSEPVEVYQLNAVPGR.S, K.SASAWDDSYCEEVVR.R, K.EALEEANAPFVPR.R, R.SLIENYDCYEVK.T	GRESAG 4.2/4.3
AC-P4	Tb927.10.13040	1208	133.3	R.TAFMESLYEQR.R, K.GYDYYGQVPNLAAR.T, R.EEFDVTPLGEVPLR.G, R.VIDVLEEGGDGTGTSGSDR.A, K.EIAEGYR.L, K.IGTSAVSADGEDDDVDR.L, R.VIDVLEEGGDGTGTSGSDR.A	GRESAG 4.2/4.3
AC-P5	Tb927.11.13740	1214	133.8	K.SFEFVEK.L, R.TGQVIFSGTNPLACDTEYK.A, R.YVVDDLVIGDYGNECGEEAIR.Q, R.VDNLNSVVPDR.S, R.EYNPPTAYLDSEVYSR.L, R.TESVANGGQVLMTR.G, R.GVPEPVEMYQLDAVAGR.V	
AC-P6	Tb927.9.15660	1242	137.5	K.DGTVGLAALR.C, R.TESIANGGQVLLTR.A, R.GVPEPVEIYQLDAVPGR.T	

* based on GeneID assignments in Salmon *et al* (15)

Figure 4-01. Procyclic-specific receptor adenylate cyclases.

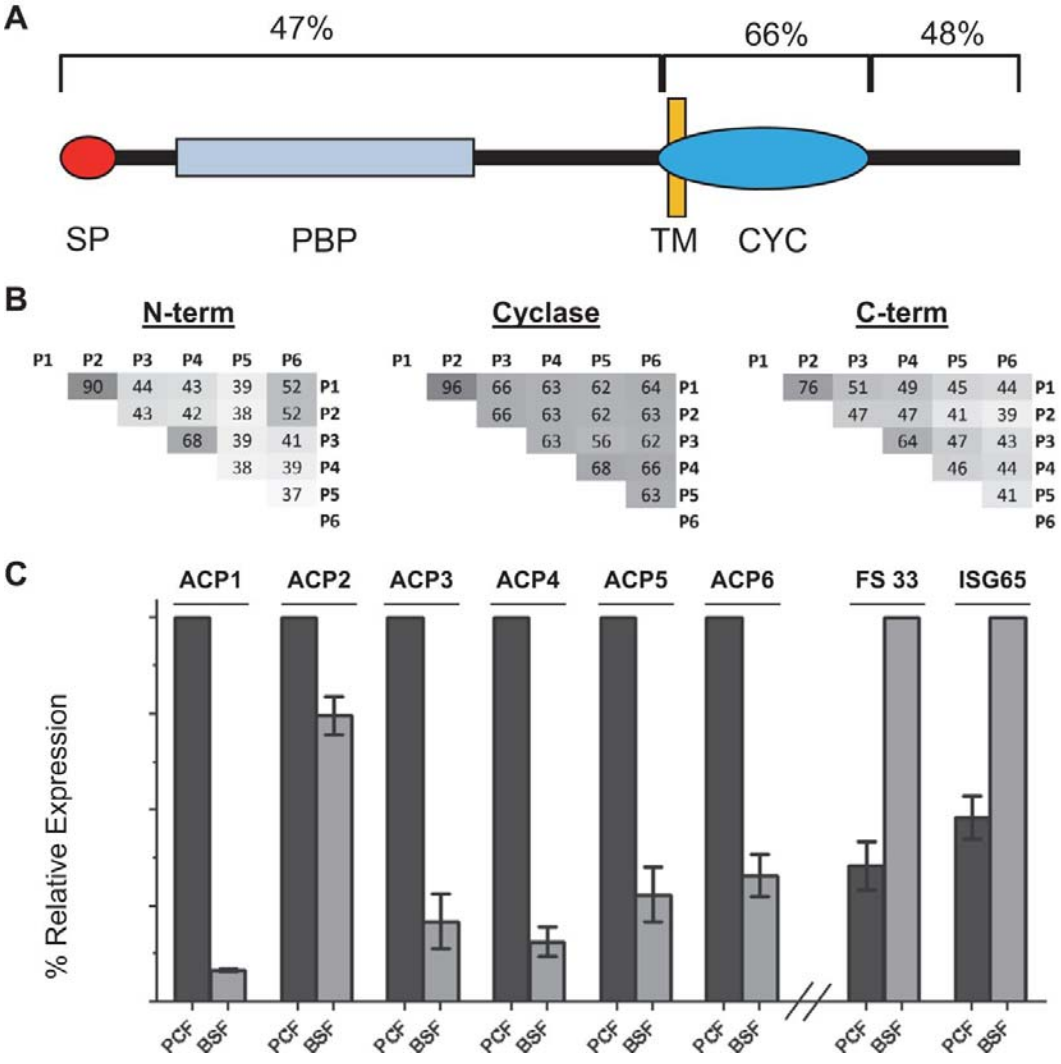

(A) Schematic shows the general architecture of *T. brucei* adenylate cyclases, including a signal peptide (SP), a single pass transmembrane domain (TM) and cyclase catalytic domain (CYC), followed by a short intracellular C-terminal region. Within the N-terminal region are one to two domains homologous to periplasmic binding proteins (PBP) of bacteria. The average sequence identity among ACP1-6 (P1-P6) is shown above each section. (B) Pairwise amino acid sequence identities within the N-

terminal, catalytic and C-terminal domains of ACP1-6. (C) Chart shows relative mRNA abundance in procyclic form (PCF) and bloodstream form (BSF) cells for adenylate cyclase genes ACP1-6 (and FS33, as determined by qRT-PCR. ISG65 is a bloodstream form-enriched gene (90) used as a control. Expression levels for each gene are normalized to the higher expressing life-cycle stage.

Figure 4-02. Isoform-specific epitope tagging of trypanosomal adenylate cyclases.

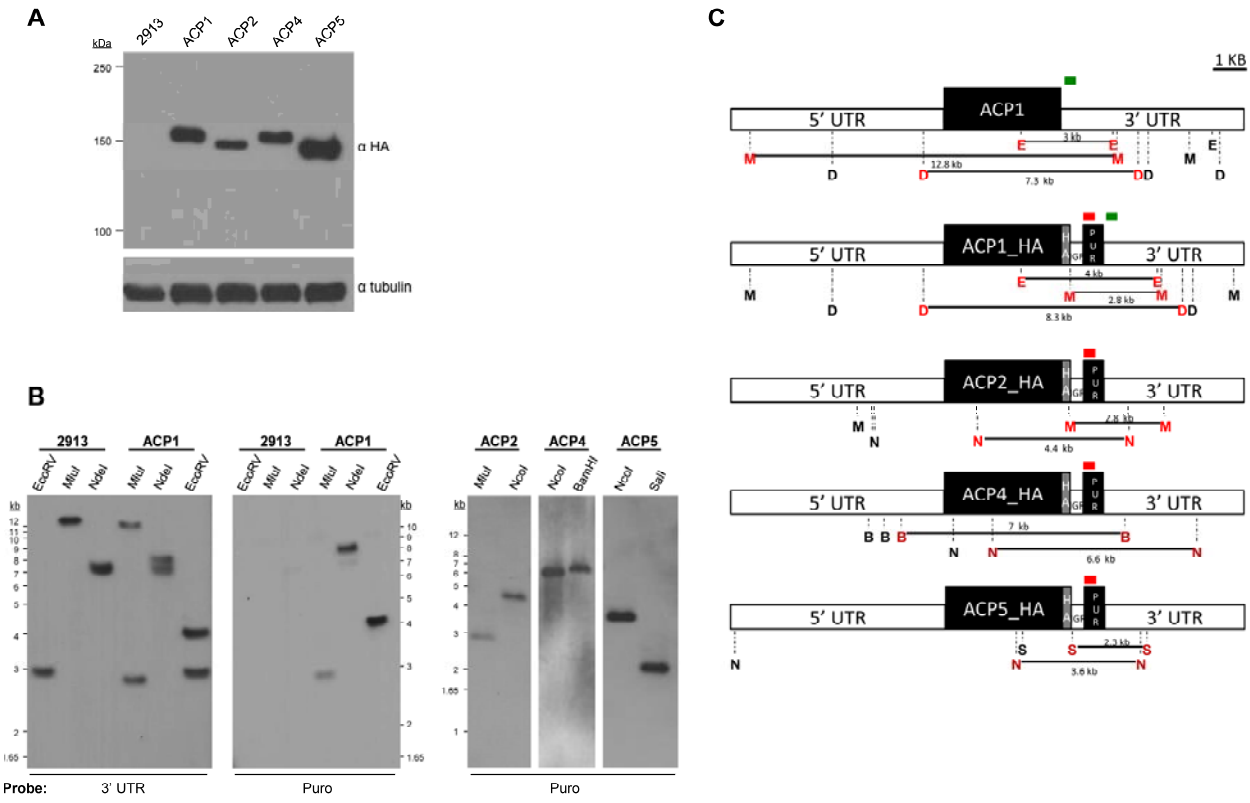

(A) Western blot analysis of whole cell lysates from 2913 control cells and 2913 cells in which an HA epitope tag was integrated into the genomic locus of ACP1, 2, 4 or 5. Blots were probed with anti-HA (top) or anti-tubulin (bottom) antibodies. (B) Southern blots using genomic DNA prepared from 2913 control cells, or cells with an HA epitope integrated into the indicated ACP1, 2, 4 or 5 genomic locus. DNA was digested with the indicated restriction enzymes and blots were probed with probes specific to the ACP1 3' UTR (3' UTR) or the coding sequence of the puromycin resistance gene (Puro). The ACP1 UTR probe hybridizes to two bands in the tagged line, one corresponding to the untagged allele, which is also observed in 2913 cells,

and one corresponding to the tagged allele, which is specific to the tagged line. The puroR probe does not hybridize to control (2913) DNA and hybridizes to a single band in each tagged line that corresponds to the size expected for integration at the corresponding locus. (C) Diagrams show restriction maps for the ACP1 locus and the indicated HA-tagged genes, as determined based on the *T. brucei* 427 genomic sequence in the TriTryp genome database (91). Restriction enzymes correspond to those used for the Southern blots in panel B, and are EcoRV (E), Nde1 (D), Mlu1 (M), Nco1 (N), Sal1 (S), and BamH1 (B). The green and red bars indicate the position of probes corresponding to the ACP1 3'UTR (green) and PuroR coding sequence (red), and the size of restriction fragments recognized by these probes are shown below the restriction map.

Figure 4-03. Trypanosomal adenylate cyclases are glycosylated surface proteins that dimerize.

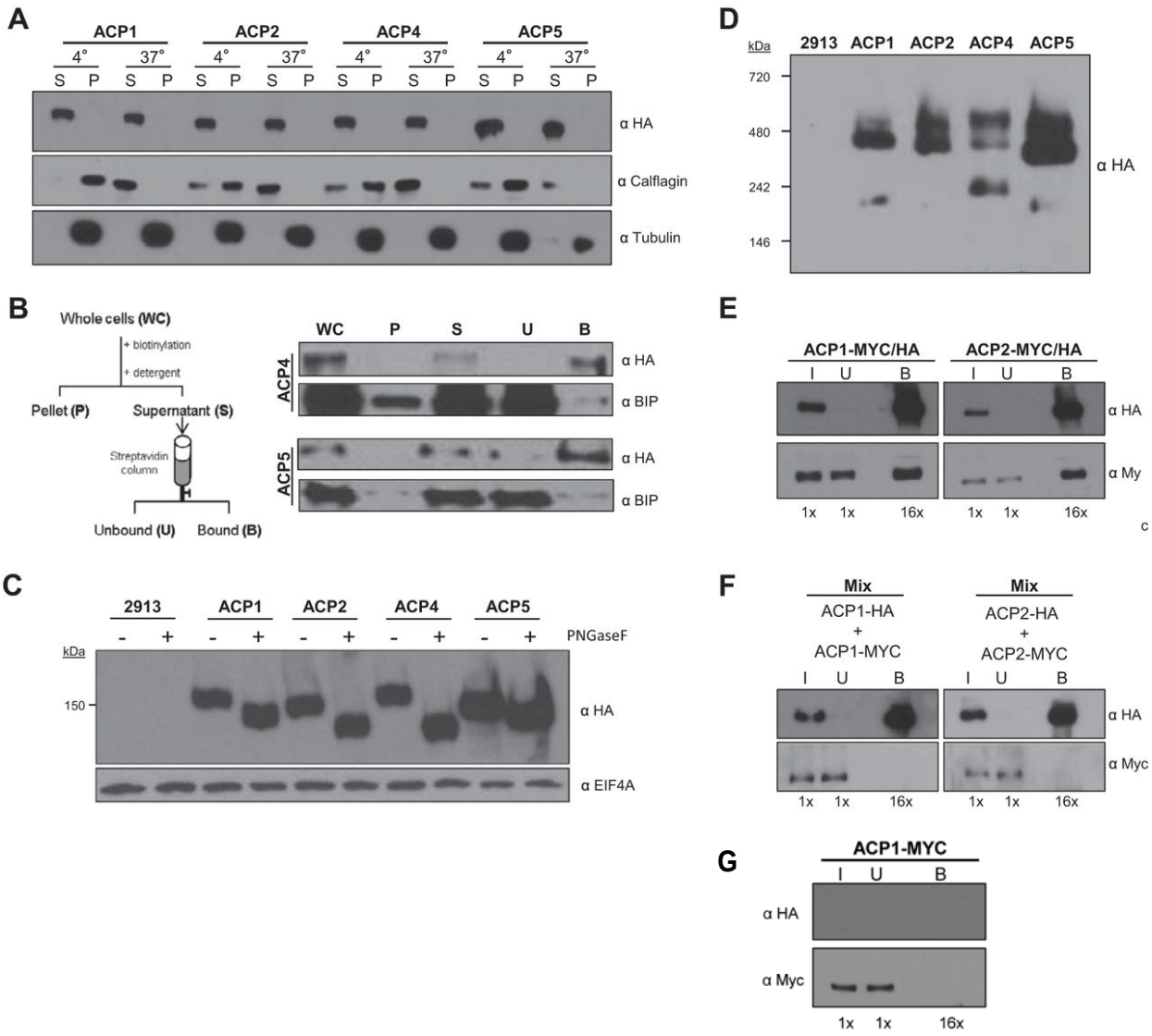

(A) Western blot analysis of soluble (S) and insoluble (P) proteins from cells extracted withTritonX-100 at the indicated temperature (4° or 37°C). Protein samples from cells expressing the indicated HA-tagged ACP (1, 2, 4 or 5) were probed with antibodies against HA , calflagin, and tubulin. (B) Cells expressing HA-tagged ACP4 or

5 were surface-biotinylated and protein extracts harvested as indicated in the schematic were subjected to Western blot analysis with antibodies against HA or BiP. (C) Whole cell lysates were prepared from 2913 control cells or cells expressing HA-tagged ACP1, 2, 4 or 5. Samples were untreated (-) or treated (+) with PNGaseF, then subjected to Western blot analysis with antibodies against HA or EIF4AI. (D) Whole cell lysates prepared from 2913 control cells or cells expressing HA-tagged ACP1, 2, 4 or 5 were separated by Blue Native gel electrophoresis then transferred to a PVDF membrane and probed with anti-HA antibodies. (E) Cells with two tagged alleles of ACP1 (ACP1-Myc/HA) or two tagged alleles of ACP2 (ACP2-Myc/HA) were used for co-immunoprecipitation to test for homodimerization. In test samples, one allele of the indicated AC gene contains an HA-tag and the other allele has a Myc-tag. Samples were immunoprecipitated with anti-HA antibody and input (I), unbound (U) and bound (B) fractions were probed in Western blots with anti-HA or anti-Myc antibody. As a negative control, ACP1-Myc lacks any HA tag and is not precipitated by anti-HA antibody (panel G). Numbers below each lane indicate the relative number of cell equivalents analyzed. (F) Cells expressing ACP1-HA were mixed with cells expressing ACP1-Myc, cells in the mixture were lysed and immunopreciptated using anti-HA antibody. Input, unbound and bound fractions were probed in Western blots with anti-HA or anti-Myc antibody. (G) Myc-tagged ACP1 is not precipitated by anti-HA antibody. Cells expressing Myc-tagged ACP1 were subjected to immunoprecipitation and analyzed by Western blot as above with anti-HA or anti-Myc antibodies.

Figure 4-04. Trypanosomal adenylate cyclases are catalytically active.

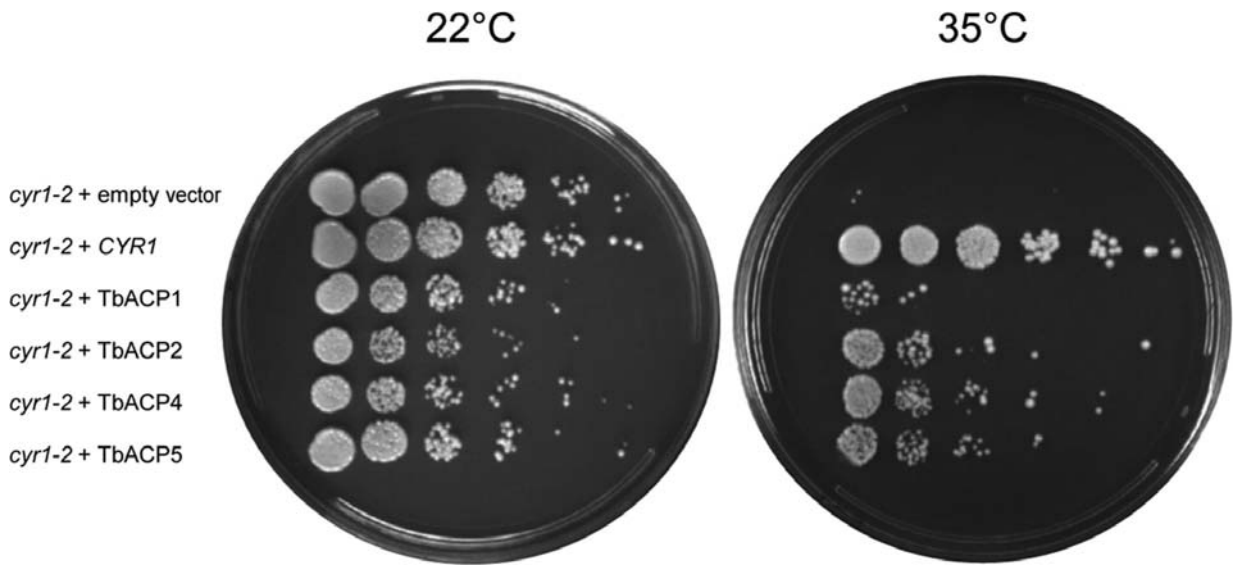

The temperature-sensitive *Saccharomyces cerevisiae* adenylate cyclase mutant (*cyr1-2*) was transformed with a yeast expression vector containing either the *S. cerevisiae* wild-type adenylate cyclase (*CYR1*) or the *T. brucei* adenylate cyclase genes (TbACP1, 2, 4 or 5). An empty vector was transformed as a control, and yeast viability was assessed at the permissive (22ºC) and restrictive (35ºC) temperatures.

Figure 4-05. Trypanosomal adenylate cyclases localize to flagellum subdomains.

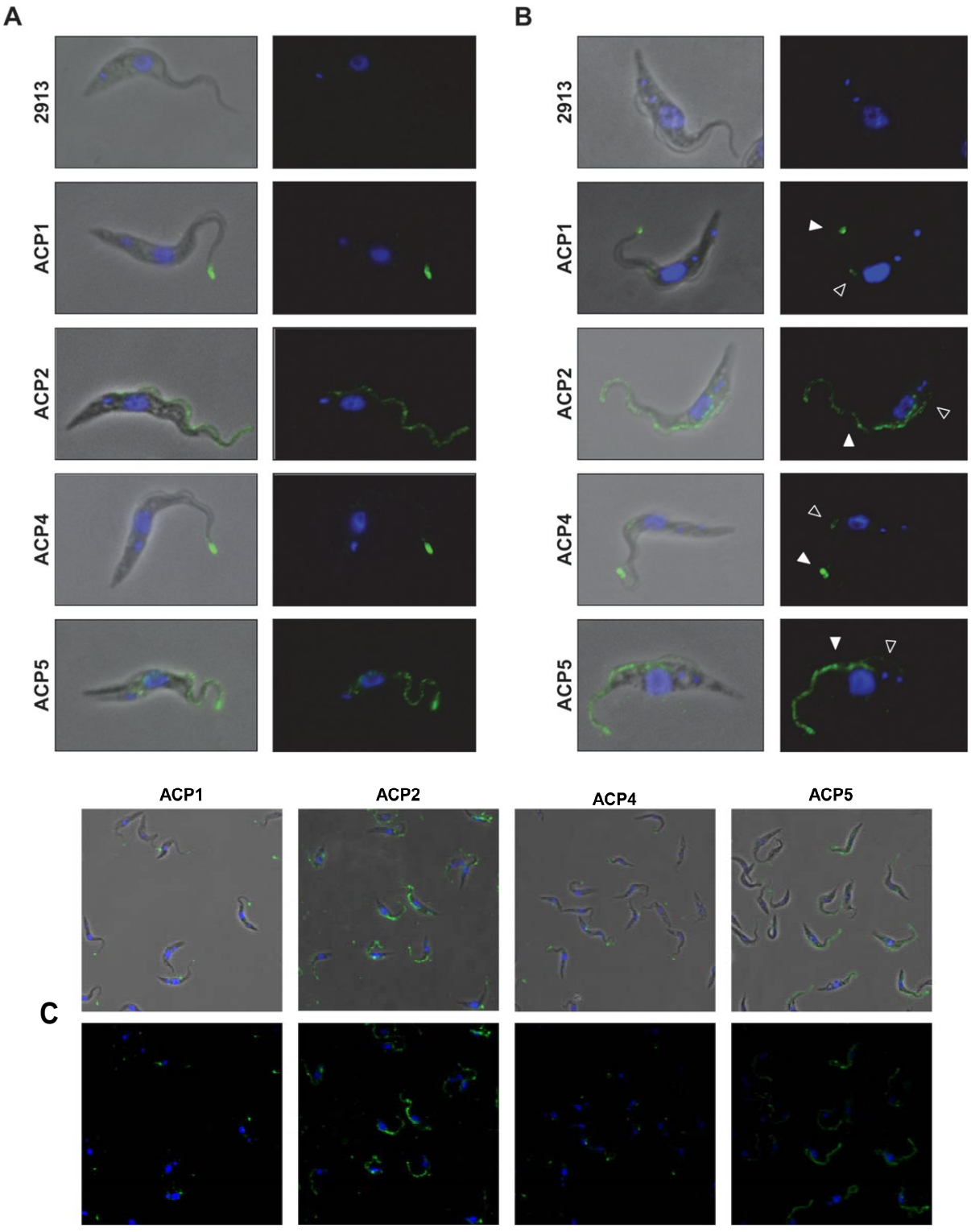

(A) Trypanosomes expressing the indicated HA-tagged adenylate cyclase were subjected to immunofluorescence. Cells were stained with anti-HA antibodies (green), and nuclear and kinetoplast DNA were visualized with DAPI (blue). (B) Immunofluorescence analysis as in panel A, showing dividing cells. Cells have a single nucleus and two kinetoplasts, indicating they have not completed mitosis, and possess a mature flagellum (filled arrowhead) as well as a newly forming daughter flagellum (unfilled arrowhead). (C) Images show additional examples of immunofluorescence on trypanosomes expressing the indicated HA-tagged adenylate cyclases.

Figure 4-06. Endogenous ACP1 localizes to the flagellum tip.

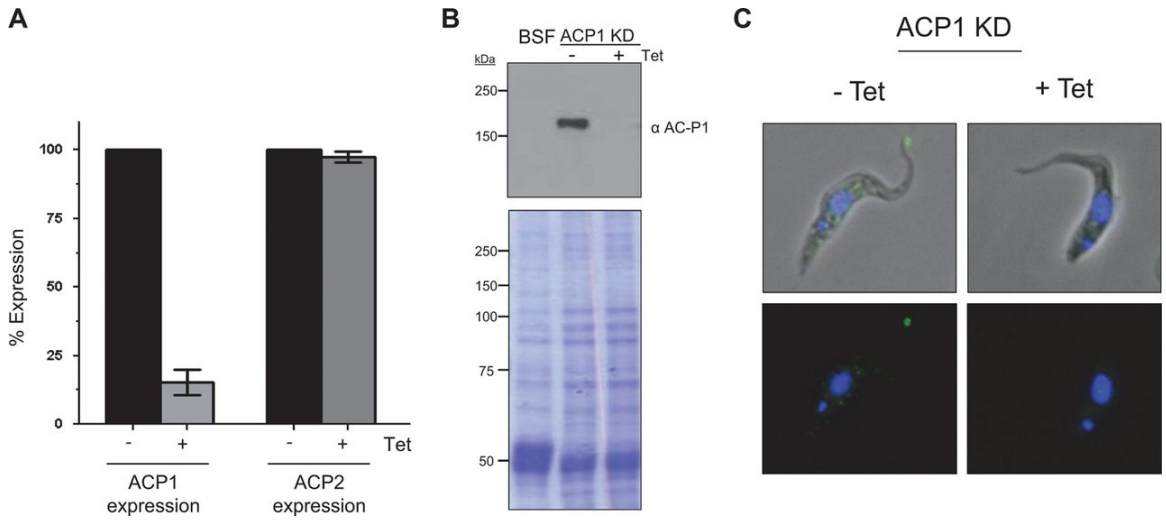

(A) mRNA levels for ACP1 and 2 were determined by qRT-PCR in ACP1-knockdown cells grown in the absence (-) or presence (+) of tetracycline (Tet). (B) Total protein extracts were prepared from bloodstream form cells (BSF) and from procyclic ACP1-knockdown cells (ACP1-KD) grown without (-) or with (+) Tet, then subjected to Western blot analysis (Top) using affinity-purified anti-ACP1 antibodies. The bottom panel shows total protein in the same samples visualized by Coommassie staining of SDS-PAGE gels. (C) Immunofluorescence of ACP1-knockdown cells grown without or with tetracycline and probed with affinity-purified anti-ACP1 antibodies. Nuclear and kinetoplast DNA are stained with DAPI (blue).

Figure 4-07. C-terminal sequences are required for targeting to the flagellum.

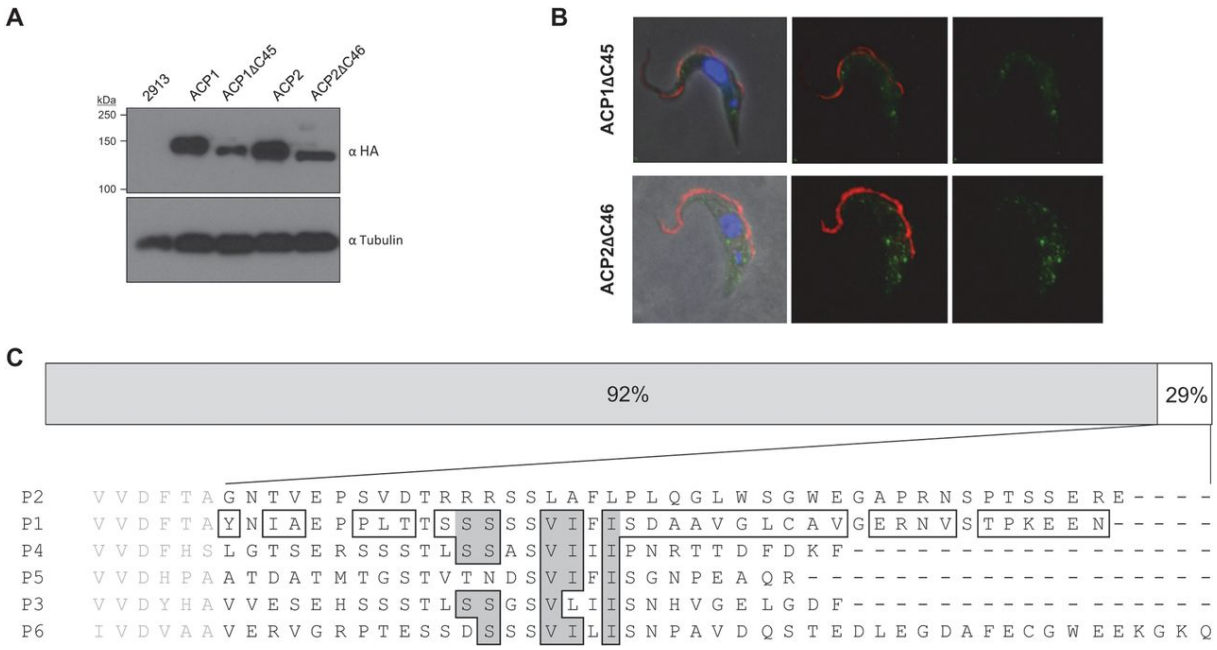

(A) Western blot analysis of whole cell lysates from cells expressing the indicated HA-tagged protein. Blots were probed with anti-HA or anti-tubulin antibodies. (B) Trypanosomes expressing the indicated HA-tagged deletion mutants were subjected to immunofluorescence. Cells were stained with anti-HA antibodies (green), anti-PFR antibodies (red). Nuclear and kinetoplast DNA were visualized with DAPI (blue). (C) (Top) Schematic diagram illustrating amino acid sequence identities between ACP1 and 2, which are nearly identical except for a short region at the C-terminus. (Bottom) Alignment of the C-termini of ACP1-6. ACP1 residues that differ from ACP2 are boxed and among these, those residues that are conserved between ACP1 and 4 are highlighted in gray.

References

1. Yamey G, Torreele E. 2002. The world's most neglected diseases. Bmj 325:176-177.
2. Yamey G. 2002. Public sector must develop drugs for neglected diseases. BMJ 324:698b-.
3. Baral TN. 2010. Immunobiology of African trypanosomes: need of alternative interventions. J Biomed Biotechnol 2010:389153.
4. Nussbaum K, Honek J, Cadmus CM, Efferth T. 2010. Trypanosomatid parasites causing neglected diseases. Curr Med Chem 17:1594-1617.
5. Christensen ST, Pedersen LB, Schneider L, Satir P. 2007. Sensory cilia and integration of signal transduction in human health and disease. Traffic 8:97-109.
6. Berberi N, LEwis, JS., Bishop, GA., Askwith, CC., Mykytyn, K. . 2008. Bardet-Biedl syndrome proteins are required for the localization of G protein-coupled receptors to primary cilia. Proc Natl Acad Sci:424204246.
7. Kaupp UB, Kashikar ND, Weyand I. 2008. Mechanisms of sperm chemotaxis. Annu Rev Physiol 70:93-117.
8. Maric D, Epting CL, Engman DM. 2010. Composition and sensory function of the trypanosome flagellar membrane. Curr Opin Microbiol 13:466-472.
9. Oberholzer M, Langousis G, Nguyen HT, Saada EA, Shimogawa MM, Jonsson ZO, Nguyen SM, Wohlschlegel JA, Hill KL. 2011. Independent analysis of the flagellum surface and matrix proteomes provides insight into flagellum

signaling in mammalian-infectious Trypanosoma brucei. Mol Cell Proteomics 10:M111 010538.

10. Tetley L, Vickerman K. 1985. Differentiation in Trypanosoma brucei: host-parasite cell junctions and their persistence during acquisition of the variable antigen coat. J Cell Sci 74:1-19.

11. Webb H, Carnall N, Vanhamme L, Rolin S, Van Den Abbeele J, Welburn S, Pays E, Carrington M. 1997. The GPI-phospholipase C of Trypanosoma brucei is nonessential but influences parasitemia in mice. J Cell Biol 139:103-114.

12. Rotureau B, Morales MA, Bastin P, Spath GF. 2009. The flagellum-MAP kinase connection in Trypanosomatids: a key sensory role in parasite signaling and development? Cell Microbiol.

13. Emmer BT, Daniels MD, Taylor JM, Epting CL, Engman DM. 2010. Calflagin inhibition prolongs host survival and suppresses parasitemia in Trypanosoma brucei infection. Eukaryot Cell 9:934-942.

14. Proto WR, Castanys-Munoz E, Black A, Tetley L, Moss CX, Juliano L, Coombs GH, Mottram JC. 2011. Trypanosoma brucei metacaspase 4 is a pseudopeptidase and a virulence factor. J Biol Chem 286:39914-39925.

15. Salmon D, Vanwalleghem G, Morias Y, Denoeud J, Krumbholz C, Lhomme F, Bachmaier S, Kador M, Gossmann J, Dias FB, De Muylder G, Uzureau P, Magez S, Moser M, De Baetselier P, Van Den Abbeele J, Beschin A, Boshart M, Pays E. 2012. Adenylate cyclases of Trypanosoma brucei inhibit the innate immune response of the host. Science 337:463-466.

16. Gould MK, Bachmaier S, Ali JA, Alsford S, Tagoe DN, Munday JC, Schnaufer AC, Horn D, Boshart M, de Koning HP. 2013. Cyclic AMP Effectors in African Trypanosomes Revealed by Genome-Scale RNA Interference Library Screening for Resistance to the Phosphodiesterase Inhibitor CpdA. Antimicrob Agents Chemother 57:4882-4893.

17. Mony BM, Macgregor P, Ivens A, Rojas F, Cowton A, Young J, Horn D, Matthews K. 2013. Genome-wide dissection of the quorum sensing signalling pathway in Trypanosoma brucei. Nature.

18. Paindavoine P, Rolin S, Van Assel S, Geuskens M, Jauniaux JC, Dinsart C, Huet G, Pays E. 1992. A gene from the variant surface glycoprotein expression site encodes one of several transmembrane adenylate cyclases located on the flagellum of Trypanosoma brucei. Mol Cell Biol 12:1218-1225.

19. Rotureau B, Ooi CP, Huet D, Perrot S, Bastin P. 2014. Forward motility is essential for trypanosome infection in the tsetse fly. Cell Microbiol 16:425-433.

20. Vickerman K, Tetley L, Hendry KA, Turner CM. 1988. Biology of African trypanosomes in the tsetse fly. Biol Cell 64:109-119.

21. Rotureau B, Subota I, Buisson J, Bastin P. 2012. A new asymmetric division contributes to the continuous production of infective trypanosomes in the tsetse fly. Development 139:1842-1850.

22. Subota I, Julkowska D, Vincensini L, Reeg N, Buisson J, Blisnick T, Huet D, Perrot S, Santi-Rocca J, Duchateau M, Hourdel V, Rousselle JC, Cayet N, Namane A, Chamot-Rooke J, Bastin P. 2014. Proteomic analysis of intact

flagella of procyclic Trypanosoma brucei cells identifies novel flagellar proteins with unique sub-localisation and dynamics. Mol Cell Proteomics.

23. Alexandre S, Paindavoine P, Tebabi P, Pays A, Halleux S, Steinert M, Pays E. 1990. Differential expression of a family of putative adenylate/guanylate cyclase genes in Trypanosoma brucei. Mol. Biochem. Parasitol. 43:279-288.

24. Seebeck T, Gong K, Kunz S, Schaub R, Shalaby T, Zoraghi R. 2001. cAMP signalling in Trypanosoma brucei. Int J Parasitol 31:491-498.

25. Felder CB, Graul RC, Lee AY, Merkle HP, Sadee W. 1999. The Venus flytrap of periplasmic binding proteins: an ancient protein module present in multiple drug receptors. AAPS PharmSci 1:E2.

26. Emes RD, Yang Z. 2008. Duplicated paralogous genes subject to positive selection in the genome of Trypanosoma brucei. PLoS One 3:e2295.

27. Anantharaman V, Iyer LM, Aravind L. 2007. Comparative genomics of protists: new insights into the evolution of eukaryotic signal transduction and gene regulation. Annu Rev Microbiol 61:453-475.

28. Pays E, Nolan DP. 1998. Expression and function of surface proteins in Trypanosoma brucei. Mol Biochem Parasitol 91:3-36.

29. Rolin S, Paindavoine P, Hanocq-Quertier J, Hanocq F, Claes Y, Le Ray D, Overath P, Pays E. 1993. Transient adenylate cyclase activation accompanies differentiation of Trypanosoma brucei from bloodstream to procyclic forms. Mol Biochem Parasitol 61:115-125.

30. Rolin S, Hanocq-Quertier J, Paturiaux-Hanocq F, Nolan D, Salmon D, Webb H, Carrington M, Voorheis P, Pays E. 1996. Simultaneous but independent

activation of adenylate cyclase and glycosylphosphatidylinositol-phospholipase C under stress conditions in Trypanosoma brucei. J Biol Chem 271:10844-10852.

31. Vassella E, Reuner B, Yutzy B, Boshart M. 1997. Differentiation of African trypanosomes is controlled by a density sensing mechanism which signals cell cycle arrest via the cAMP pathway. J Cell Sci 110 (Pt 21):2661-2671.

32. Gould MK, de Koning HP. 2011. Cyclic-nucleotide signalling in protozoa. FEMS Microbiol Rev 35:515-541.

33. Alexandre S, Paindavoine P, Hanocq-Quertier J, Paturiaux-Hanocq F, Tebabi P, Pays E. 1996. Families of adenylate cyclase genes in Trypanosoma brucei. Mol Biochem Parasitol 77:173-182.

34. Naula C, Schaub R, Leech V, Melville S, Seebeck T. 2001. Spontaneous dimerization and leucine-zipper induced activation of the recombinant catalytic domain of a new adenylyl cyclase of Trypanosoma brucei, GRESAG4.4B. Mol Biochem Parasitol 112:19-28.

35. Oberholzer M, Lopez MA, Ralston KS, Hill KL. 2009. Approaches for functional analysis of flagellar proteins in African trypanosomes. Methods in Cell Biology 93:21-57.

36. Wirtz E, Leal S, Ochatt C, Cross GA. 1999. A tightly regulated inducible expression system for conditional gene knock-outs and dominant-negative genetics in *Trypanosoma brucei*. Mol. Biochem. Parasitol. 99:89-101.

37. LaCount DJ, Barrett B, Donelson JE. 2002. Trypanosoma brucei FLA1 is required for flagellum attachment and cytokinesis. J Biol Chem 277:17580-17588.

38. Kubata BK, Duszenko M, Kabututu Z, Rawer M, Szallies A, Fujimori K, Inui T, Nozaki T, Yamashita K, Horii T, Urade Y, Hayaishi O. 2000. Identification of a novel prostaglandin f(2alpha) synthase in Trypanosoma brucei. J Exp Med 192:1327-1338.

39. Tagwerker C, Flick K, Cui M, Guerrero C, Dou Y, Auer B, Baldi P, Huang L, Kaiser P. 2006. A tandem affinity tag for two-step purification under fully denaturing conditions: application in ubiquitin profiling and protein complex identification combined with in vivocross-linking. Mol Cell Proteomics 5:737-748.

40. Wohlschlegel JA. 2009. Identification of SUMO-conjugated proteins and their SUMO attachment sites using proteomic mass spectrometry. Methods Mol Biol 497:33-49.

41. Tabb DL, McDonald WH, Yates JR, 3rd. 2002. DTASelect and Contrast: tools for assembling and comparing protein identifications from shotgun proteomics. J Proteome Res 1:21-26.

42. Yates JR, 3rd, Eng JK, McCormack AL, Schieltz D. 1995. Method to correlate tandem mass spectra of modified peptides to amino acid sequences in the protein database. Anal Chem 67:1426-1436.

43. Cociorva D, D LT, Yates JR. 2007. Validation of tandem mass spectrometry database search results using DTASelect. Curr Protoc Bioinformatics Chapter 13:Unit 13 14.

44. Oberholzer M, Morand S, Kunz S, Seebeck T. 2006. A vector series for rapid PCR-mediated C-terminal in situ tagging of Trypanosoma brucei genes. Mol Biochem Parasitol 145:117-120.

45. Kabututu ZP, Thayer M, Melehani JH, Hill KL. 2010. CMF70 is a subunit of the dynein regulatory complex. J Cell Sci 123:3587-3595.

46. Redmond S, Vadivelu J, Field MC. 2003. RNAit: an automated web-based tool for the selection of RNAi targets in Trypanosoma brucei. Mol Biochem Parasitol 128:115-118.

47. Ye J, Coulouris G, Zaretskaya I, Cutcutache I, Rozen S, Madden TL. 2012. Primer-BLAST: a tool to design target-specific primers for polymerase chain reaction. BMC Bioinformatics 13:134.

48. Brenndorfer M, Boshart M. 2010. Selection of reference genes for mRNA quantification in Trypanosoma brucei. Mol Biochem Parasitol 172:52-55.

49. Livak KJ, Schmittgen TD. 2001. Analysis of relative gene expression data using real-time quantitative PCR and the 2(-Delta Delta C(T)) Method. Methods 25:402-408.

50. Tyler KM, Fridberg A, Toriello KM, Olson CL, Cieslak JA, Hazlett TL, Engman DM. 2009. Flagellar membrane localization via association with lipid rafts. J Cell Sci 122:859-866.

51. Sikorski RS, Hieter P. 1989. A system of shuttle vectors and yeast host strains designed for efficient manipulation of DNA in Saccharomyces cerevisiae. Genetics 122:19-27.

52. Dubacq C, Guerois R, Courbeyrette R, Kitagawa K, Mann C. 2002. Sgt1p contributes to cyclic AMP pathway activity and physically interacts with the adenylyl cyclase Cyr1p/Cdc35p in budding yeast. Eukaryot Cell 1:568-582.

53. Morishita T, Matsuura A, Uno I. 1993. Characterization of the cyr1-2 UGA mutation in Saccharomyces cerevisiae. Mol Gen Genet 237:463-466.

54. Gietz D, St Jean A, Woods RA, Schiestl RH. 1992. Improved method for high efficiency transformation of intact yeast cells. Nucleic Acids Res 20:1425.

55. Salmon D, Bachmaier S, Krumbholz C, Kador M, Gossmann JA, Uzureau P, Pays E, Boshart M. 2012. Cytokinesis of Trypanosoma brucei bloodstream forms depends on expression of adenylyl cyclases of the ESAG4 or ESAG4-like subfamily. Mol Microbiol 84:225-242.

56. Emmer BT, Maric D, Engman DM. 2010. Molecular mechanisms of protein and lipid targeting to ciliary membranes. J Cell Sci 123:529-536.

57. Walsh CT. 2006. Posttranslational modification of proteins: expanding nature's inventory. Roberts and Co. Publishers, Englewood, Colorado.

58. Dhalia R, Reis CR, Freire ER, Rocha PO, Katz R, Muniz JR, Standart N, de Melo Neto OP. 2005. Translation initiation in Leishmania major: characterisation of multiple eIF4F subunit homologues. Mol Biochem Parasitol 140:23-41.

59. Bieger B, Essen LO. 2001. Structural analysis of adenylate cyclases from Trypanosoma brucei in their monomeric state. EMBO Journal 20:433-445.

60. Linder JU. 2006. Class III adenylyl cyclases: molecular mechanisms of catalysis and regulation. Cell Mol Life Sci 63:1736-1751.

61. Vaughan S. 2010. Assembly of the flagellum and its role in cell morphogenesis in Trypanosoma brucei. Curr Opin Microbiol 13:453-458.

62. Rotureau B, Van Den Abbeele J. 2013. Through the dark continent: African trypanosome development in the tsetse fly. Front Cell Infect Microbiol 3:53.

63. Broadhead R, Dawe HR, Farr H, Griffiths S, Hart SR, Portman N, Shaw MK, Ginger ML, Gaskell SJ, McKean PG, Gull K. 2006. Flagellar motility is required for the viability of the bloodstream trypanosome. Nature 440:224-227.

64. Chan KY, Matthews KR, Ersfeld K. 2010. Functional characterisation and drug target validation of a mitotic kinesin-13 in Trypanosoma brucei. PLoS Pathog 6.

65. Liu W, Apagyi K, McLeavy L, Ersfeld K. 2010. Expression and cellular localisation of calpain-like proteins in Trypanosoma brucei. Mol Biochem Parasitol 169:20-26.

66. Bloodgood RA. 2012. The future of ciliary and flagellar membrane research. Mol Biol Cell 23:2407-2411.

67. Kottgen M, Walz G. 2005. Subcellular localization and trafficking of polycystins. Pflugers Arch 451:286-293.

68. Kim J, Kato M, Beachy PA. 2009. Gli2 trafficking links Hedgehog-dependent activation of Smoothened in the primary cilium to transcriptional activation in the nucleus. Proc Natl Acad Sci U S A 106:21666-21671.

69. Goodenough UW, Adair WS, Caligor E, Forest CL, Hoffman JL, Mesland DA, Spath S. 1980. Membrane-membrane and membrane-ligand interactions in Chlamydomonas mating. Soc Gen Physiol Ser 34:131-152.

70. Pan J, Snell WJ. 2000. Signal transduction during fertilization in the unicellular green alga, Chlamydomonas. Curr Opin Microbiol 3:596-602.

71. Dwyer MA, Hellinga HW. 2004. Periplasmic binding proteins: a versatile superfamily for protein engineering. Current Opinion in Structural Biology 14:495-504.

72. Buxton IL, Brunton LL. 1983. Compartments of cyclic AMP and protein kinase in mammalian cardiomyocytes. J Biol Chem 258:10233-10239.

73. Rich TC, Fagan KA, Nakata H, Schaack J, Cooper DM, Karpen JW. 2000. Cyclic nucleotide-gated channels colocalize with adenylyl cyclase in regions of restricted cAMP diffusion. J Gen Physiol 116:147-161.

74. Oberholzer M, Bregy P, Marti G, Minca M, Peier M, Seebeck T. 2007. Trypanosomes and mammalian sperm: one of a kind? Trends Parasitol 23:71-77.

75. Oberholzer M, Marti G, Baresic M, Kunz S, Hemphill A, Seebeck T. 2007. The Trypanosoma brucei cAMP phosphodiesterases TbrPDEB1 and TbrPDEB2: flagellar enzymes that are essential for parasite virulence. Faseb J 21:720-731.

76. Fenn K, Matthews KR. 2007. The cell biology of Trypanosoma brucei differentiation. Curr Opin Microbiol 10:539-546.

77. Gray MA, Cunningham I, Gardiner PR, Taylor AM, Luckins AG. 1981. Cultivation of infective forms of Trypanosoma congolense from trypanosomes in the proboscis of Glossina morsitans. Parasitology 82:81-95.

78. Mesland DA, Hoffman JL, Caligor E, Goodenough UW. 1980. Flagellar tip activation stimulated by membrane adhesions in Chlamydomonas gametes. J Cell Biol 84:599-617.

79. Peacock L, Bailey M, Carrington M, Gibson W. 2013. Meiosis and Haploid Gametes in the Pathogen Trypanosoma brucei. Curr. Biol.

80. Bloodgood RA. 2010. Sensory reception is an attribute of both primary cilia and motile cilia. J Cell Sci 123:505-509.

81. de Miguel N, Riestra A, Johnson PJ. 2012. Reversible association of tetraspanin with Trichomonas vaginalis flagella upon adherence to host cells. Cell Microbiol 14:1797-1807.

82. Moreira-Leite FF, Sherwin T, Kohl L, Gull K. 2001. A trypanosome structure involved in transmitting cytoplasmic information during cell division. Science 294:610-621.

83. Hughes L, Towers K, Starborg T, Gull K, Vaughan S. 2013. A cell-body groove housing the new flagellum tip suggests an adaptation of cellular morphogenesis for parasitism in the bloodstream form of Trypanosoma brucei. J Cell Sci 126:5748-5757.

84. Pazour G, Bloodgood R. 2008. Chapter 5 Targeting Proteins to the Ciliary Membrane. 85:115-149.

85. Dorn KV, Hughes CE, Rohatgi R. 2012. A Smoothened-Evc2 complex transduces the Hedgehog signal at primary cilia. Dev Cell 23:823-835.

86. Blacque OE, Sanders AA. 2014. Compartments within a compartment: What can tell us about ciliary subdomain composition, biogenesis, function, and disease. Organogenesis 10.

87. Cevik S, Sanders AA, Van Wijk E, Boldt K, Clarke L, van Reeuwijk J, Hori Y, Horn N, Hetterschijt L, Wdowicz A, Mullins A, Kida K, Kaplan OI, van Beersum

SE, Man Wu K, Letteboer SJ, Mans DA, Katada T, Kontani K, Ueffing M, Roepman R, Kremer H, Blacque OE. 2013. Active transport and diffusion barriers restrict Joubert Syndrome-associated ARL13B/ARL-13 to an Inv-like ciliary membrane subdomain. PLoS Genet 9:e1003977.

88. Pazour GJ, Bloodgood RA. 2008. Targeting proteins to the ciliary membrane. Curr Top Dev Biol 85:115-149.

89. Nachury MV, Seeley ES, Jin H. 2010. Trafficking to the ciliary membrane: how to get across the periciliary diffusion barrier? Annu Rev Cell Dev Biol 26:59-87.

90. Chung WL, Carrington M, Field MC. 2004. Cytoplasmic targeting signals in transmembrane invariant surface glycoproteins of trypanosomes. J Biol Chem 279:54887-54895.

91. Aslett M, Aurrecoechea C, Berriman M, Brestelli J, Brunk BP, Carrington M, Depledge DP, Fischer S, Gajria B, Gao X, Gardner MJ, Gingle A, Grant G, Harb OS, Heiges M, Hertz-Fowler C, Houston R, Innamorato F, Iodice J, Kissinger JC, Kraemer E, Li W, Logan FJ, Miller JA, Mitra S, Myler PJ, Nayak V, Pennington C, Phan I, Pinney DF, Ramasamy G, Rogers MB, Roos DS, Ross C, Sivam D, Smith DF, Srinivasamoorthy G, Stoeckert CJ, Jr., Subramanian S, Thibodeau R, Tivey A, Treatman C, Velarde G, Wang H. 2009. TriTrypDB: a functional genomic resource for the Trypanosomatidae. Nucleic Acids Res 38:D457-462.

Chapter V:

Insect stage-specific adenylate cyclases

regulate social motility in African trypanosomes

PREFACE

The following chapter is a modified version of "Insect stage-specific adenylate cyclases regulate social motility in African trypanosomes," by Lopez, Saada, and Hill, originally published January, 2015 in Eukaryotic Cell (doi:10.1128/EC.00217-14) and reprinted with permission.

In this work, we utilized a reverse genetic approach to interrogate functions of the adenylate cyclases identified in Chapter IV, discovering that a subset are involved in the regulation of social motility through generation of cAMP. As second author, I contributed significantly to this work. In addition to assisting in planning and writing the manuscript, specific experimental contributions included: assisting with the qRTR analyses, designing the primers and constructs for the point-mutations, isolating RNA and performing Northern Blots to assess knockdown levels, and planning, designing, and co-performing the ELISA analysis.

This work is complemented by functional studies focusing on cAMP-specific phosphodiesterase B1, (Appendix I).

SUMMARY

Sophisticated systems for cell-cell communication enable unicellular microbes to act as multicellular entities, capable of group-level behaviors that are not evident in individuals. These group behaviors influence microbe physiology and the underlying signaling pathways are considered potential drug targets in microbial pathogens. *Trypanosoma brucei* is a protozoan parasite that causes substantial human suffering and economic hardship in some of the most impoverished regions of the world. *T. brucei* lives on host tissue surfaces during transmission through its tsetse fly vector, and cultivation on surfaces causes the parasites to assemble into multicellular communities in which individual cells coordinate their movements in response to external signals. This behavior is termed "social motility", based on similarities with surface-induced social motility in bacteria, and demonstrates that trypanosomes are capable of group-level behavior. Mechanisms governing *T. brucei* social motility are unknown. Here we report that a subset of receptor-type adenylate cyclases (ACs) in the trypanosome flagellum regulate social motility. RNAi-mediated knockdown of adenylate cyclase 6 (AC6), or dual knockdown of AC1 and AC2, causes a hypersocial phenotype but has no discernable effect on individual cells in suspension culture. Mutation of the AC6 catalytic domain phenocopies AC6 knockdown, demonstrating loss of adenylate cyclase activity is responsible for the phenotype. Notably, knockdown of other ACs did not affect social motility, indicating segregation of AC functions. These studies reveal interesting parallels in systems that control social behavior in trypanosomes and bacteria, and provide insight into a feature of parasite biology that may be exploited for novel intervention strategies.

INTRODUCTION

Trypanosoma brucei and other African trypanosomes are protozoan parasites that cause sleeping sickness in humans and related wasting diseases in wild and domestic animals. Sleeping sickness is recognized as one of the world's most neglected diseases with approximately 60 million people living at risk of infection, while livestock infections account for significant economic hardship in some of the most impoverished regions of the planet (18, 26). Dedicated efforts over the last decade have reduced the human health burden, but these parasites remain a continuing threat for re-emergence owing to their capacity for explosive outbreaks and their historical ability to resist eradication (8, 11). Sleeping sickness is fatal if untreated, no vaccine exists and current treatment options are toxic, antiquated and increasingly ineffective (1, 52). Therefore, new perspectives on trypanosome biology, transmission and pathogenesis are urgently needed to facilitate novel intervention strategies.

T. brucei is transmitted between mammalian hosts by blood feeding tsetse flies. Transmission through the fly requires extensive interaction with host tissue surfaces as parasites move across and through tissues en route from the fly midgut, through the alimentary tract and mouthparts and then into the salivary gland (56). Once in the salivary gland, parasites colonize the gland epithelial surface and complete the final stages of development into mammalian-infectious forms (58). Thus, as is the case for many microbes (17), *T. brucei* in its natural habitat lives in intimate and continuous contact with surfaces.

Despite the ubiquity of parasite-surface interactions during *T. brucei* transmission, studies of these organisms are almost exclusively conducted using suspension cultures. While such studies have yielded many important insights, they overlook an important and ubiquitous feature of trypanosome biology. To overcome this gap in knowledge, we utilized semisolid agarose matrices to assess the influence of surface cultivation on parasite behavior (38). This led to the surprising discovery that rather than acting as individuals, surface cultivated procyclic (insect-stage) trypanosomes assemble into multicellular groups that coordinate their movements across the surface (38). Initially, parasites collect into small groups and these grow larger through recruitment of other cells. At the periphery of the inoculation site, parasites assemble in nodes of high cell density and from there they advance outward. Movement is polarized such that cells move outward but not laterally, leading to the formation of thin projections radiating away from the center. When cells in radial projections encounter a separate group of parasites they halt or divert their movement to avoid contact, implicating cell-cell signaling in the control of trypanosome group behavior. We termed this behavior "social motility" (SoMo) based on features shared with surface-induced social motility in bacteria (17, 20).

As is the case in bacteria (3, 13, 55), social motility in *T. brucei* requires cell motility and some ability of cells to sense and respond to external cues (38). Surface-induced group behaviors such as social motility and biofilm formation have been extensively studied in bacteria (20, 55), but molecular mechanisms that govern surface-induced group behavior in trypanosomes are completely unknown. In other microbes, collective activities of groups of cells are commonly controlled by cyclic

nucleotides, which function as second messengers and as secreted signaling molecules. In *Dictyostelium discoideum* for example, cAMP acts as a chemoattractant and signaling molecule to direct surface motility of individual cells, enabling them to assemble into multicellular fruiting bodies (10). In several species of bacteria, cyclic-di-GMP (c-di-GMP) governs the transition between surface-induced swarming motility and biofilm formation (32) (5, 22, 30, 51). In this case, decreased intracellular c-di-GMP promotes swarming, while elevated c-di-GMP inhibits swarming and promotes biofilm formation (23, 31, 50, 55). In the yeast *Candida albicans*, cyclic nucleotides regulate dimorphic transitions connected to surface penetration and pathogenesis (21).

Cyclic nucleotide synthesis in *T. brucei* depends on a large family of receptor-type adenylate cyclases (ACs) that are localized to the flagellum membrane (14, 33, 42, 46). Trypanosomal ACs are distinguished from mammalian ACs in that the intracellular catalytic domain is directly connected to an extracellular, putative ligand binding domain on a single polypeptide (42). As such, trypanosome ACs may be regulated by extracellular ligands directly rather than via upstream GPCRs as observed for mammalian ACs (42). The canonical *T. brucei* AC is "expression site-associated gene 4" (ESAG4), a bloodstream stage-specific AC that modulates the host immune response to promote parasite survival during infection (49). Aside from ESAG4, functions for *T. brucei* ACs are unknown. Notably, several flagellar ACs were recently identified that are specifically upregulated in procyclic *T. brucei* (46), the parasite life cycle stage that undergoes social motility (42). Given the widespread use of cyclic nucleotides in control of microbial social behavior and the emerging role of

the eukaryotic flagellum in coordinating cellular responses to external signals (12, 25), we asked whether *T. brucei* flagellar ACs function in social motility. Here we report that AC6, a procyclic stage-specific AC (46), is localized to the tip of the flagellum and regulates social motility. RNAi-mediated knockdown of AC6 causes a hypersocial phenotype, while knockdown of several other flagellar ACs does not affect social motility. Importantly, point mutations in the AC6 catalytic domain phenocopy the knockdown, demonstrating that loss of activity, rather than loss of the protein is responsible for the phenotype. These studies are, to our knowledge, the first to demonstrate function for trypanosomal ACs in the insect life cycle stage and extend the paradigm of cyclic nucleotide control of microbial social behavior to parasitic protozoa.

MATERIALS AND METHODS

Cell culture and motility assays

Procyclic cells derived from the 2913 cell line (59) were used for all experiments. Suspension cultures were maintained using Cunningham's semi-defined medium (SM) as described previously (39). For RNAi lines, 2.5mg/ml Phleomycin, was included in the medium for selection of stable transfectants and RNAi was induced by adding 1mg/ml tetracycline. Lines carrying pMOT vector-based sequences for rescue and HA-tagging were cultured with 1 µg/ml of puromycin. Motility in suspension culture was assayed as previously described (39). Social motility assays were done as

previously described (38). For quantitation, several independent assays were done and the numbers of projections formed per plate were quantitated.

RNAi and QRT-PCR

RNAi target regions for the ACs were chosen by the Trypanofan RNAit algorithm (45) and were PCR-amplified using the following primers: AC1&2KD_F: TTGATGATGATGGTAGCGGA, AC1&2KD_R: ACATACACCGCCTTACTGCC. AC3KD_F: GACGGTTCTGTCCCTGTTGT, AC3KD_R: TGGCTCTGAACAGTGAATGC.

AC4KD_F: AGCTTACGAGGGCTGTGAAA, AC4KD_R: AAATACACTGCCCCTTGTCG. AC5KD_F: TCTGCTTATGCAGGACGATG, AC5_R: CCTCAAAAGTCTCGAGGTGC. AC6KD_F: TGGAGCAGCAAATCTACGTG, AC6_R: TTTTCTCGGCTCTCCACTGT

AC6uKD_F: AT*AAGCTT*ACGGGGTTCCCTCATTTAAC, AC6uKD_R: AT*TCTAGA*ACAACAACAACCCCCAAAAA, with restriction sites italicized.

Fragments were amplified using genomic DNA from 2913 cells and ligated into the p2T7Ti-B RNAi plasmid (24). All sequences were verified by direct DNA sequencing. RNAi vectors were linearized, transfected and selected with antibiotic as previously described (39). Clonal lines were generated by limiting dilution. Efficacy of knockdown was assessed via Quantitative reverse-transcriptase real-time PCR (qRT-PCR) as described (34) at 72 hr post induction. qRT-PCR results are reported as arithmetic means (+/- standard deviation) from at least two independent RNA preparations, each analyzed in duplicate and normalized against the housekeeping

genes glyceraldehyde-3-phosphate dehydrogenase (GAPDH; Tb927.6.4280/ Tb927.6.4300) and RPS23 (Tb10.70.7020/Tb10.70.7030). Relative gene expression was determined using the $2^{-\Delta\Delta CT}$method as previously described (19, 27). Primers used for qRT-PCR::

AC1_F: F- CGTTGACTTCACGGCTTACA, AC1_R: ACATTTCGTTCTCCCACTGC, AC2_F: GCCATGTCGTTGATTTCACA, AC2_R: CCAACCAGACCACAGACCTT, AC3_F: ACTGATGGGCGTCTTCACACAA, AC3_R: GGATGCACTTTTCTTGGGCAAC, AC4_F: CTGCGAGTGCGAGTTGGTGT, AC4_R: ACGTTCTGCGGTGCTGAGTG, AC5_F: CACATCTCAGCGCCAAAAACTG, AC5_R: TAGACCGCATAATCGCCTCACA, AC6_F: TGCAGTTAAGGTGGGTCACA, AC6_R: GATCCACCGCAGGATTAGAA, GAPDH_F: GGCTGATGTCTCTGTGGTGGA, GAPDH_R: GGCTGTCGCTGATGAAGTCG. RPS_F: AGATTGGCGTTGGAGCGAAA, RPS_R: GACCGAAACCAGAGACCAGCA

Western blots and immunofluorescence

Protein extracts were prepared and analyzed by Western blotting as described (44). $1x10^6$ cell equivalents per lane were used. Monoclonal mouse anti-HA antibody from Covance (used at 1:5000) and monoclonal anti-ß-tubulin E7 hybridoma supernatant (used at 1:7000 dilution) were used at as primary antibodies, and detected by horseradish peroxidase-coupled goat anti-mouse antibodies (BioRad) at a 1:5000 dilution. Immunofluorescence was carried out on whole cells as described previously (47), with the monoclonal anti-HA antibody HA.11 (Covance) used at 1:250 dilution, and donkey anti-mouse secondary coupled to AlexaFluor488 (Molecular Probes) used at 1:2,500.

Generation of AC6-Ri and AC6-Ri mutant cell lines**

AC6-Ri and AC6**-Ri were generated as described (43). To generate the AC6-Ri line, a 426-bp fragment corresponding to the 3' terminus of the AC6 open reading frame was cloned immediately upstream of the α/ß tubulin intergenic region in the pMOTag plasmid (41) . A fragment of the AC6 3'UTR was then cloned downstream of the puromycin resistance gene in this plasmid to generate plasmid "pMOT-AC6WT426'. Primers used were AC6_ORF_F: ATGGTACCGAGGCATATGTGGCGGATG, AC6_ORF_R: ATGTCGACCTACTGCTTCCCCTTTTCCT, AC6_UTR_F: ATGGATCCTAACAGCAGTAGTGAATTGAAG, AC6_UTR_R: ATTCTAGAACGTGGACTTCACCTTCATC.

Plasmid DNA sequences were confirmed by plasmid sequencing (Genewiz, Inc.) Tagging cassettes were excised by restriction digest, purified, and transfected into AC6uKD cells. Stable transfectants were selected and clonal lines were generated by limiting dilution.

To generate AC6**-Ri, the 426-bp AC6 fragment in pMOT-AC6WT426 was replaced with a fragment the terminal 3' 1332bp of the AC6 ORF, encompassing the catalytic domain, to generate pMOT-AC6WT1332. The Stratagene Quickchange mutagenesis Kit (Stratagene, Inc.) was used to mutate coding sequences for conserved active site residues NMAART (amino acids 1031-1036), that are essential for AC catalytic activity (4). The NMART sequence was mutated to AAAAAA to generate plasmid pMOT-AC6**1332. Primers used to amplify the 1332 bp fragment were: AC6_1332_F: ATGGTACCACGCGCATTAGTGTGTGGTC, AC6_1332_R:

ATGTCGACCTACTGCTTCCCCTTTTCCT. Site-directed mutagenesis was done using the Stratagene Quickchange Kit (Agilent), using primers MUT_F: ggatatgactattacggtcaaacggcagccgcggctgccgccgcggagagcattgcgaa, MUT_R: ttcgcaatgctctccgcggcggcagccgcggctgccgtttgaccgtaatagtcatatcc. Plasmid sequence verification and generation of stably-transfected clonal lines were done as described above.

Epitope tagging

Cell lines carrying HA-tagged versions of AC6 and AC6** were generated by *in situ* tagging with the pMOTag-HA plasmid, as described (39). The 3' end of the wild type AC6 ORF was amplified genomic DNA of 2913 cells using primers:

F- ATGGTACCGAGGCATATTGTGGCGGATG

R- ATCTCGAGCTGCTTCCCCTTTTCCTCC

The AC** catalytic domain mutant fragment was PCR-amplified from the pMOT-AC6**1332 plasmid using primers:

F- ATGGTACCACGCGCATTAGTGTGTGGTC

R- ATCTCGAGCTGCTTCCCCTTTTCCTCC

Amplified fragments were cloned upstream of the HA tag in pMOTag-HA. All sequences were confirmed by direct DNA sequencing (GeneWiz, Inc.), tagging cassettes were excised and used to generate stably-transfected clonal lines as describe above.

cAMP ELISA

Total cellular cyclic AMP levels were measured using the cyclic-AMP Direct ELISA Kit (EnzoLife Sciences) essentially as described previously (60). $4x10^7$ cells were harvested, washed in PBS, re-suspended into a hypotonic lysis buffer (1 mM Hepes, 1 mM EDTA, 1x SigmaFAST Protease Inhibitors) and left on ice for 10 minutes. Samples were then passed through a 25+3/8G needle ten times, before the addition of 1M HCL to give a final concentration of 0.1M HCL. Cells were spun at 14,000xg at 4^0C for 10 minutes, and supernatant fractions were saved for analysis. 100ul of supernatant corresponding to $2.5x10^7$ cells was used per well. The ELISA was done following the manufacturer's suggested protocols, and output was read at 405nM and analyzed using MasterPlex2010 (MiraiBio Group of Hitachi America). A best-fit curve using 5PL logistics was utilized. All values are averages of independent biological replicates that were assayed in technical duplicates.

Northern blot

Northern blots were done similar to previously described (29), except that digoxygenin was used for detection rather than 32P-labeling. A probe unique to the AC 6 ORF was generated with primers F-TGTGCTTTTGTTTGGTGCTC and R-AGTAGTTCGGGTCCGTGATG and suspended into DIG-EasyHyb Buffer (Roche). This corresponds to a 305-bp region that is AC 6 specific according to RNAit (45) and NCBI-BLAST. Blots were visualized using the DIG Nucleic-Acid Detection Kit (Roche). As a loading control, total RNA was visualized by UV shadowing (54).

RESULTS

A subset of insect-stage specific ACs regulate social motility without impacting individual cell motility in suspension culture

Cyclic AMP production in *T. brucei* is catalyzed by a large family of receptor-type adenylate cyclases (ACs) whose biological functions are mostly unknown (15). We recently identified a group of 6 ACs in the flagellum of procyclic *T. brucei* and found that five of these are specifically upregulated in procyclic stage cells (46). To test whether any of these ACs function in social motility, we generated gene-specific, tetracycline-inducible RNAi knockdowns by targeting unique regions of each gene's open reading frame. The open reading frames of AC1 and AC2 are 89% identical, with a single region of high divergence near the 3' end that distinguishes between the two genes. We therefore generated a single RNAi construct for simultaneous knockdown of both AC1 and AC2, allowing us to reserve unique regions for assessing expression of each gene individually. Quantitative reverse transcription-PCR (qRT-PCR) demonstrated that the targeted mRNA was significantly reduced following tetraycycline induction of RNAi. Parasite growth rates in suspension culture were not affected in any of the AC knockdowns. This differs from bloodstream-form *T. brucei*, where knockdown of ESAG4 causes morphological defects and is lethal (49). Knockdown of AC3, 5 or 6, and dual knockdown of AC1&2, did not impact motility of individual cells in suspension culture, while AC4 knockdown parasites showed reduced motility.

We next examined social motility in each of the AC knockdowns. *T. brucei* social motility is characterized by the formation of multicellular communities that grow through recruitment of nearby cells (35). Collective motility of parasites outward produces radial projections that radiate away from the site of inoculation (28, 38). There were no apparent differences in social motility of AC3, 4 or 5 knockdowns compared to wild type (Figure 5-01). However, social motility in the AC1&2 dual knockdown and the AC6 knockdown differed from that of wild type cells (Figure 5-01). The general pattern was the same, with projections extending outward and tending to spiral in a clockwise direction, but the number of projections formed was greater in the knockdowns and projections were more closely spaced. We termed this behavior "hypersocial," by analogy to hyper-swarming observed in bacterial diguanylate cyclase mutants (31, 32, 55). The hypersocial phenotype of AC1&2 dual knockdown and AC6 knockdown cell lines was dependent on tetracycline-induced RNAi (Figure 5-01).

Restoring AC6 expression in AC6 uKD cells rescues the hypersocial phenotype

Our results implicate a subset of *T. brucei* ACs in trypanosome social motility. As AC1 and 2 are 89% identical at the nucleotide level, distinguishing their specific contributions poses challenges and we therefore focused our analyses on AC6. To assess the specific role of AC6, we asked whether the hypersocial phenotype could be rescued by restoring expression of the wild type protein in the knockdown cell line. To achieve this, we generated a knockdown line targeting the AC6 3' UTR, "AC6-

uKD", because this enables one to test for rescue under RNAi-inducing conditions by expressing an AC6 transgene with an alternate 3' UTR that is immune to RNAi (34, 43). Tetracycline induction of AC6-uKD cells effectively reduced AC6 expression, without affecting growth or individual cell motility in suspension culture. Expression of other ACs was unaffected. Importantly, the AC6-uKD phenocopied the open reading frame knockdown, exhibiting an RNAi-dependent hypersocial phenotype that was qualitatively and quantitatively indistinguishable from that observed for the open reading frame knockdown. These results establish a background in which an AC6 transgene can be expressed while the endogenous gene is knocked down.

We next replaced the 3' UTR of one AC6 allele with the alpha tubulin 3' UTR. We refer to this cell line as "AC6-RNAi-immune" (AC6-Ri). Northern blots demonstrated that AC6 mRNA is upregulated in procyclic cells (Figure 5-02), consistent with qRT-PCR results (46). A single AC6 mRNA was observed in control and AC6-uKD cells while AC6-Ri cells expressed two mRNAs, corresponding to endogenous and RNAi-immune transcripts (Figure 5-02). Abundance of the endogenous transcript was substantially reduced upon RNAi induction, while the RNAi-immune transcript was unaffected (Figure 5-02). Thus, AC6-Ri cells maintain AC6 expression following knockdown of the endogenous gene. Growth and individual cell motility in suspension culture were unaffected in AC6-Ri cells with or without RNAi induction. Maintenance of AC6 expression under RNAi induced conditions rescued the hyper social phenotype (Figure 5-0 2), demonstrating that the hyper-social phenotype is a consequence of AC6-specific knockdown.

RNAi alone does not distinguish between phenotypes caused by loss of protein activity, versus indirect consequences arising from loss of` the target protein (43). For example, while the AC6 knockdown phenotype might be a direct result of impaired cAMP output, it might alternatively be due to changes in potential interaction partners of AC6 caused by loss of the protein. To distinguish between these possibilities, we asked if blocking AC catalytic function without altering protein levels alters social motility. The *T. brucei* AC active site contains a highly conserved NMAART domain that is required for catalytic activity (4). We therefore mutated the NMAART domain to all alanines to generate a catalytically inactive version, termed "AC6**" and introduced an RNAi-immune copy of AC6** into the AC6 uKD line. This cell line is referred to as AC6**-Ri. Following tetracycline induction, endogenous AC6 mRNA levels were substantially reduced while AC6**-Ri mRNA levels were unaffected. Growth and motility in suspension culture were unaffected in AC6**-Ri cells, but expression of the AC6** catalytic mutant failed to compensate for loss of endogenous AC6 (Figure 5-02).

It is possibile that the phenotype of AC6**-Ri mutants might be due to altered expression levels and/or localization of the mutant protein. To test this, we compared expression and localization of wild type AC6 to that of AC6**. For this, we used *in situ* tagging (41) to place an HA epitope at the C-terminus of the wild type and mutant proteins. Western blot analysis showed a single band of approximately equal abundance in AC6-HA and AC6**-HA cells (Figure 5-03). Immunofluorescence revealed that wild type AC6-HA localized to the flagellum, but interestingly, was restricted to the flagellar tip (Figure 5-03). Interestingly, tip localization for AC6 was

predicted previously based on sequences within a C-terminal domain that is required for flagellum targeting (46). Importantly, the AC6** catalytic mutant gave a flagellum-tip distribution that was indistinguishable from wild type (Figure 5-03), indicating that the hyper social phenotype of AC6**-Ri cells is a consequence of lost activity and is not caused by altered expression or mislocalization.

We next asked whether knockdown of AC6, or expression of AC6** affected total cellular cAMP levels (Figure 5-04). Although there was a trend toward reduced total cellular cAMP following RNAi-induction in AC6uKD and AC6**-Ri cells, the changes were not statistically significant. Given the discrete localization of AC6 to a tiny subdomain of the parasite surface, and the fact that this is just one of several ACs expressed in this life cycle stage, it is not surprising that RNAi did not cause gross perturbation of total cellular cAMP.

DISCUSSION

Recognition of social behavior and cell–cell communication as ubiquitous properties of bacteria (3, 17) transformed our view of microbiology and microbial pathogenesis, but protozoan parasites have not generally been considered in this context. Recently, we showed that the paradigm of microbial social behavior applies to the protozoan parasite *T. brucei* when cultivated on surfaces to mimic their natural environment (38). Here we provide the first molecular dissection of mechanisms underlying social motility in trypanosomes and our results suggest that cAMP signaling systems in the flagellum control *T. brucei* social behavior. As discussed below, our

studies reveal intriguing parallels in systems used by trypanosomes and bacteria for controlling surface-induced social behavior. Moreover, by discovering an accessible readout for receptor-type adenylate cyclase function in *T. brucei*, our findings provide a foundation for dissecting structure-function of these enigmatic proteins and by extension cAMP signaling in trypanosomes.

Several independent analyses point to a specific role for cAMP produced by AC6 in social motility. Firstly, a hypersocial phenotype is observed in two independent AC6 knockdown lines targeting distinct regions of the AC6 mRNA, while expression of other ACs is unaffected. Secondly, the phenotype is rescued by expression of wild type AC6, but not by a catalytic domain mutant. Thus, normal social motility depends on AC6 activity and the mutant phenotype is not due to off target effects of knockdown.

cAMP is implicated in the *T. brucei* transmission cycle as well as pathogenesis, and elevated cAMP is lethal for bloodstream form cells, making cAMP pathways a target of drug discovery efforts (7). Pathways of cAMP signaling in these organisms remain poorly characterized however and lack familiar features found in mammalian cells (14). One outstanding question is why trypanosomes have so many AC genes, ~75 compared to ~10 in mammals for example (16). Some *T. brucei* ACs may substitute for others (48), suggesting some redundancy or overlap in function. However, the presence of ACs that are specific to different life cycle stages and that exhibit distinct subcellular localizations (42, 46) argues against strictly redundant functions for these proteins. The idea of distinct functions for individual ACs is also supported by the fact that expression of AC1-AC5 is unaltered in AC6 knockdowns but do not accommodate for loss of AC6. Likewise, normal expression of AC6 does not

accommodate for loss of AC1&2. At least two possibilities may explain the inability of AC6 to compensate for loss of AC1&2 or vice versa. One possibility is that normal social motility requires interaction between different AC isoforms, such that each isoform must be present to form an active complex. It is also possible that rather than direct interaction, independent signaling through each is required and different isoforms function as coincidence detection modules.

Simultaneous expression of several ACs in a single cell presents a conundrum if each AC controls a different pathway, because cAMP output must be segregated to avoid interference. In mammalian cells this problem is mitigated via a microdomain model, in which spatial separation of cAMP signaling output enables different ACs to control distinct cellular responses (2). Such a model has been suggested for *T. brucei* (36) and is supported by our results. In this model (Figure 5-05) social motility is regulated by local levels of intraflagellar cAMP specifically derived from an AC6-microdomain at the flagellum tip. When levels are high, social motility is attenuated and when levels are low, social motility ensues. In wild type cells (Figure 5-05A) AC6 activity is down-regulated in response to a specific signal, e.g. presence of an inhibitor or loss of an activator, resulting in reduced local cAMP levels and initiation of social motility. Upon constitutive inactivation of AC6, e.g. through knockdown or expression of a catalytic mutant (Figure 5-05B), a signal-independent decrease in local cAMP within the AC6 microdomain results in a precocious, hypersocial phenotype. A key tenet of this model is that cAMP-specific phosphodiesterase localized throughout the flagellum provides a diffusion barrier (36, 40) to shield the AC6 tip domain from cAMP generated by other flagellar ACs (36, 40). As such, the

model predicts that if local cAMP levels are constitutively elevated through loss of the diffusion barrier, social motility would be blocked. In support of this model, in separate work (Oberholzer and Hill, submitted) we show that genetic or pharmacological inhibition of flagellum-localized cAMP-specific phosphodiesterase leads to elevated cAMP and a complete block of social motility (37).

Our findings extend the concept of cyclic nucleotides as regulators of microbial social behaviors to parasitic protozoa and reveal parallels with c-di-GMP regulation of bacterial swarming motility. Two specific examples are the SadC/BifA system in *Pseudomonas aeruginosa* and the ScrABC system in *Vibrio parahaemolyticus* (31, 55). *Pseudomonas* and *Vibrio* species undergo surface-dependent swarming motility. In *P. aeruginosa* swarming is regulated by the combined activities of SadC , a diguanylate cyclase (DC) that synthesizes c-di-GMP, and BifA, a phosphodiesterase (PDE) that specifically degrades c-di-GMP (31). Knockout of the cyclase reduces intracellular c-di-GMP levels and causes hyper swarming, while knockout of the phosphodiesterases results in elevated c-di-GMP levels and blocks swarming (31). In *V. parahaemolyticus* swarming motility is regulated by the ScrABC system. Here, the ScrC protein is a c-di-GMP cyclase and phosphodiesterase that is regulated by the periplasmic binding protein, ScrB (55). The ligand for ScrB is an extracellular “S-signal” that accumulates in a cell density-dependent fashion and binds ScrB. Once bound to it’s ligand, ScrB neutralizes the c-di-GMP cyclase activity of ScrC and simultaneously activates its phosphodiesterase activity. This causes intracellular c-di-GMP levels to drop and stimulates swarming. At low density, in the absence of S-signal, the cyclase activity of ScrC predominates, resulting in elevated c-di-GMP and inhibition of swarming. Thus,

in both bacteria and trypanosomes, the extent of social motility on surfaces is inversely proportional to levels of intracellular cyclic nucleotide, as controlled by reciprocal regulation of cyclase and phosphodiesterase activities. In bacteria, an expanded repertoire of DC genes is common and makes it possible to use c-di-GMP signaling for responding to a wide variety of signals (46).

In addition to pathway architecture, the domain structure of ScrC in Vibrio is similar to that of trypanosome ACs, having a surface exposed ligand binding domain coupled via a transmembrane segment to a cytoplasmic nucleotide cyclase domain (42, 55). Ligand binding to trypanosome ACs has not been demonstrated, but the AC extracellular domain bears homology to bacterial periplasmic binding proteins (9), such as ScrB. Bacterial periplasmic binding proteins bind a variety of small molecule ligands and control chemotaxis and swarming motility (53, 55), raising the intriguing possibility that small molecule ligands might control social motility through AC6 in *T. brucei*. In bacteria where social motility has been well-studied, this behavior facilitates rapid colonization of surfaces, antibiotic resistance and efficient use of nutrients (6, 17, 57). Although the *in vivo* correlates of social motility in *T. brucei* are not yet known, similar activities would be beneficial to parasites in the tsetse fly (38). More broadly, studies of bacterial surface-associated group behaviors have provided tremendous insight into signaling mechanisms used by these organisms (3, 55). Likewise, our findings present an important advance by providing the first demonstrated requirement for ACs in procyclic form parasites and establishing a foundation for dissecting cAMP signaling systems in these organisms using a readily accessible *in vitro* assay.

FIGURES

Figure 5-01. Social motility is regulated by a subset of procyclic stage-specific adenylate cyclases.

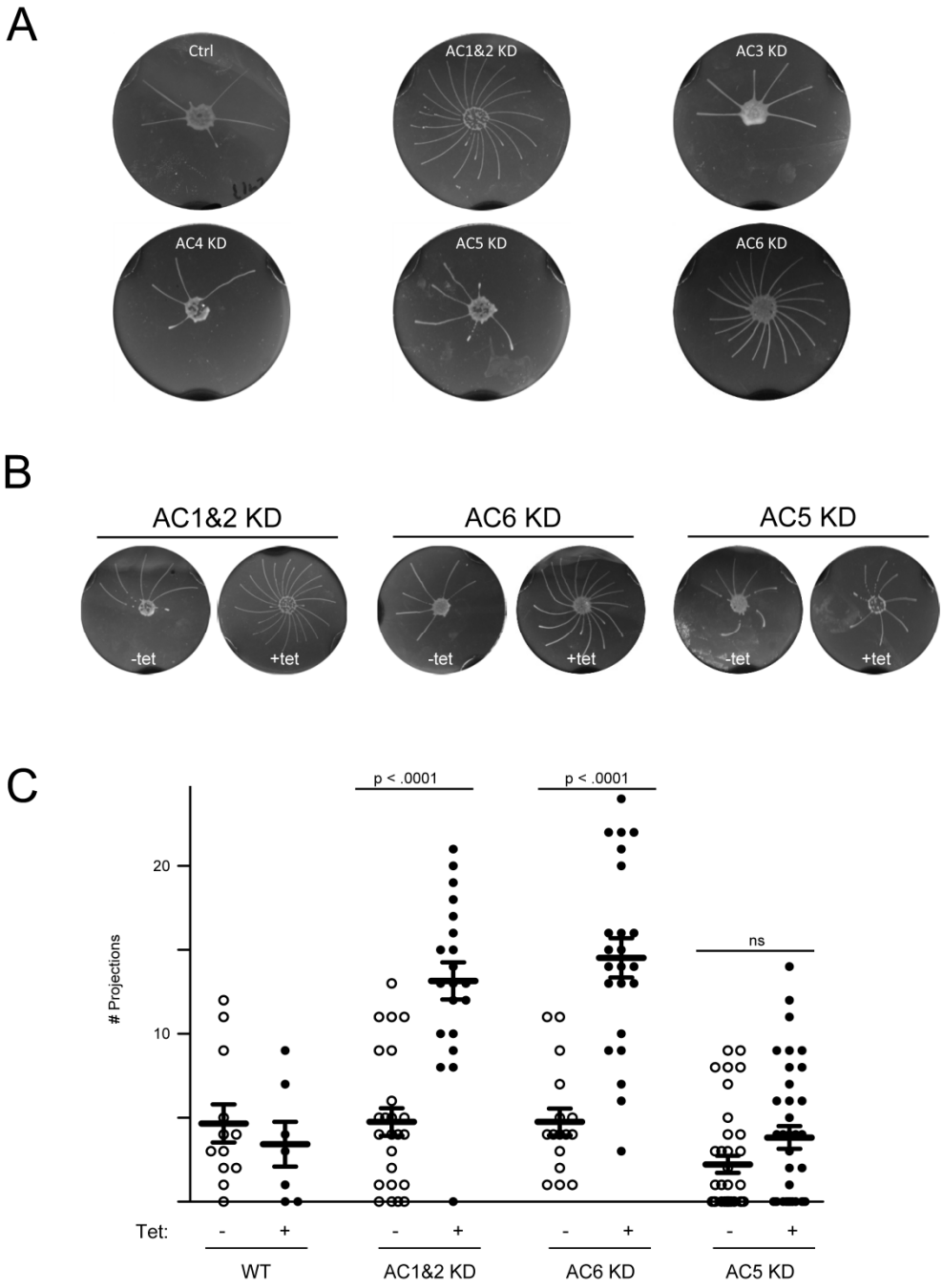

Figure 5-01 (A) Gene specific knockdowns targeting the indicated ACs were assayed for social motility compared to 2913 control cells (ctrl) on plates containing tetracycline to induce RNAi. (B) Social motility assays are shown for the indicated knockdowns maintained in the absence or presence of tetracycline (Tet) to induce RNAi. (C) Quantitation of the number of projections formed for wild type cells (WT) or the indicated knockdown lines maintained in the absence or presence of tetracycline. Mean values and standard error are shown. P values for unpaired t-test are shown. WT –Tet: n=12, +Tet n=7; AC1&2KD –Tet n=24, +Tet n=20; AC6KD –Tet n=16, +Tet n=23; AC5KD –Tet n=36, +Tet n=36.

Figure 5-02. Social motility is modulated by AC6 catalytic activity.

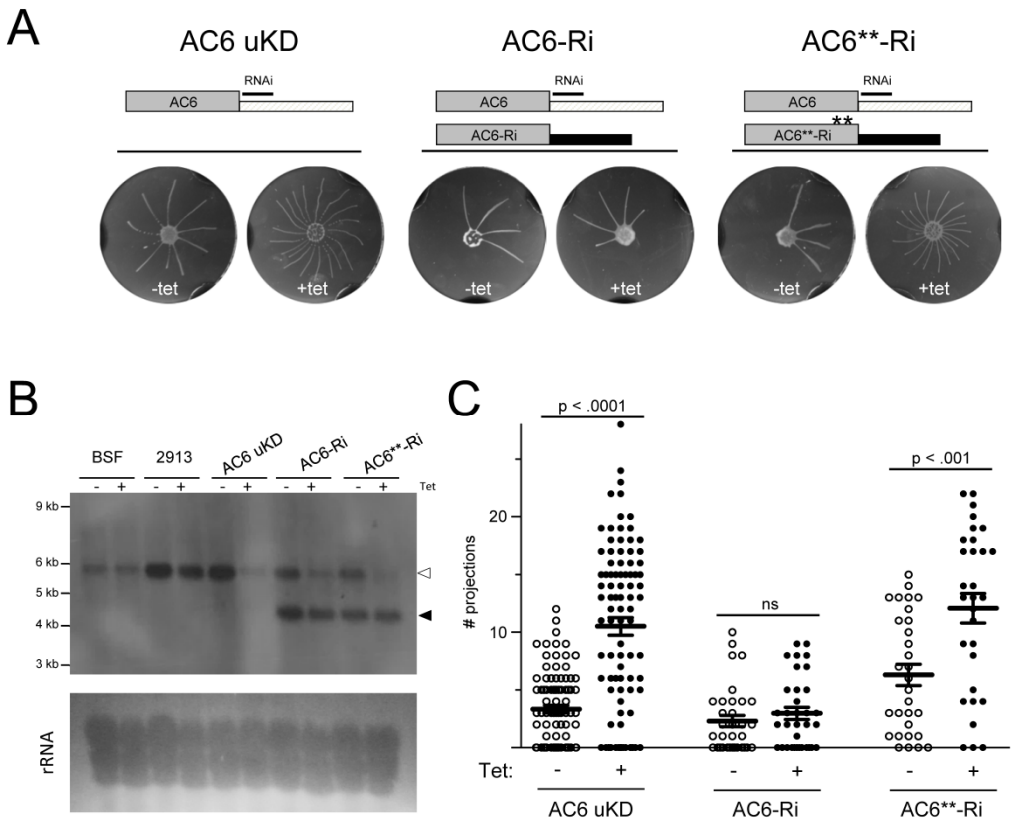

(A) Social motility assays on AC6-UTR-knockdown (AC6 uKD), AC6-RNAi-immune (AC6-Ri) or the RNAi-immune catalytic domain mutant (AC6**-Ri). Cells were maintained in the absence or presence of tetracycline (Tet) to induce RNAi. Schematics at the top of the panel illustrate the region targeted for RNAi. RNAi targets the 3'UTR of the endogenous AC6 gene, while transgenes are immune to RNAi owing to presence of an alternate UTR. (B) Northern blot probed with an AC6-specific probe (top). RNA was prepared from bloodstream cells (BSF), procyclic 2913 control cells (PCF), AC6-uKD cells, AC6-Ri cells or AC6**-Ri cells maintained with or without tet as indicated.

Position of the endogenous AC6 mRNA (open arrowhead) and transgene mRNA (closed arrowhead) are indicated. Total RNA was visualized by UV illumination of the blot (bottom). (C) Quantitation of the number of projections formed for the indicated cell lines maintained in the absence or presence of tet. Mean values and standard error are shown. P values for unpaired t-test are shown. AC6uKD –Tet n=90, +Tet n=90; AC6-Ri –Tet n=34, +Tet n=34; AC6**-Ri –Tet n=30, +Tet n=30.

Figure 5-03. AC6 is localized to the tip of the trypanosome flagellum.

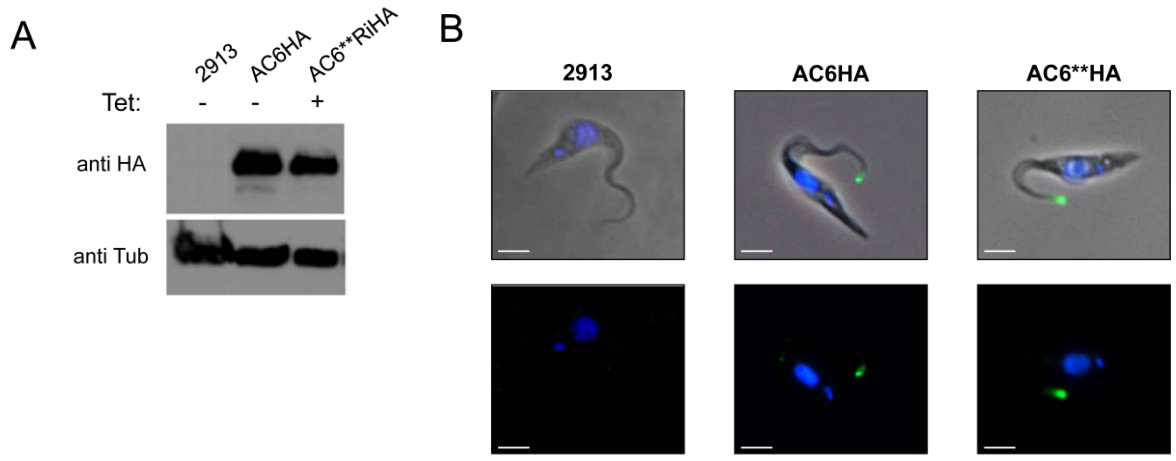

(A) Western blot of protein extracts from 2913 cells and from cells expressing wild type HA-tagged AC6 (AC6HA) or catalytically inactive AC6 (AC6**HA). Blots were probed with anti-HA antibody, or anti-tubulin antibody as a loading control. (B) Control cells (2913) or cells expressing HA-tagged wild type (AC6HA) or the catalytic domain mutant (AC6**HA) were subjected to immunofluorescence with anti-HA antibody (green) and DAPI (blue). Scale bar is 2 um.

Figure 5-04. ELISA analysis of total cellular cAMP

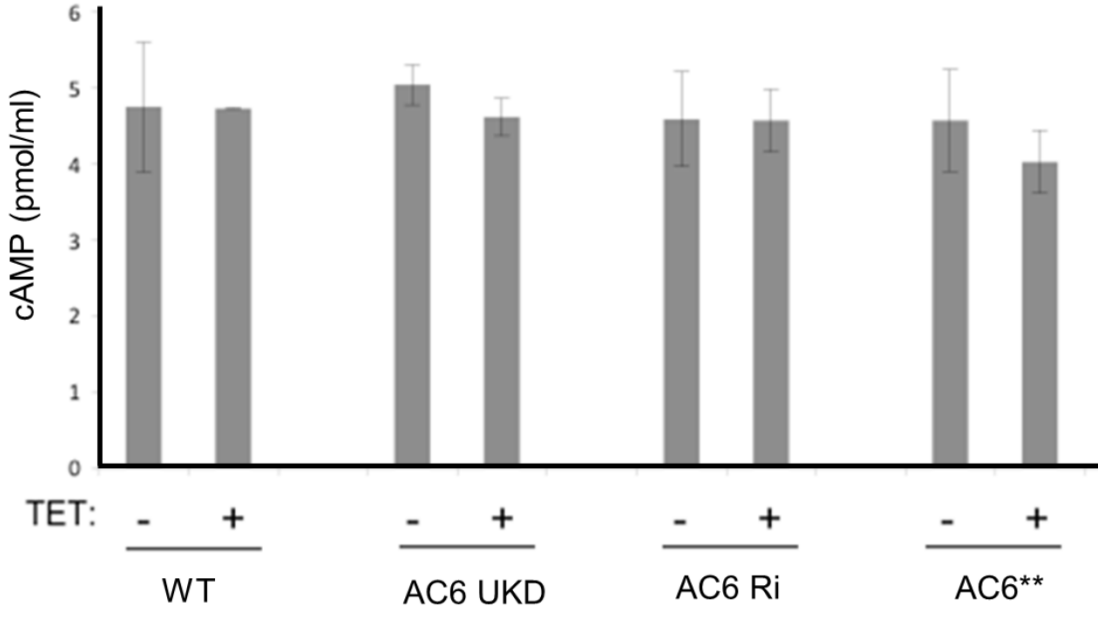

Total cellular cAMP levels were determined for the indicated lines grown in the absence or presence of tetracycline to induce RNAi as indicated. Error bars indicate standard deviation.

Figure 5-05. Model for cAMP microdomain regulation of social motility.

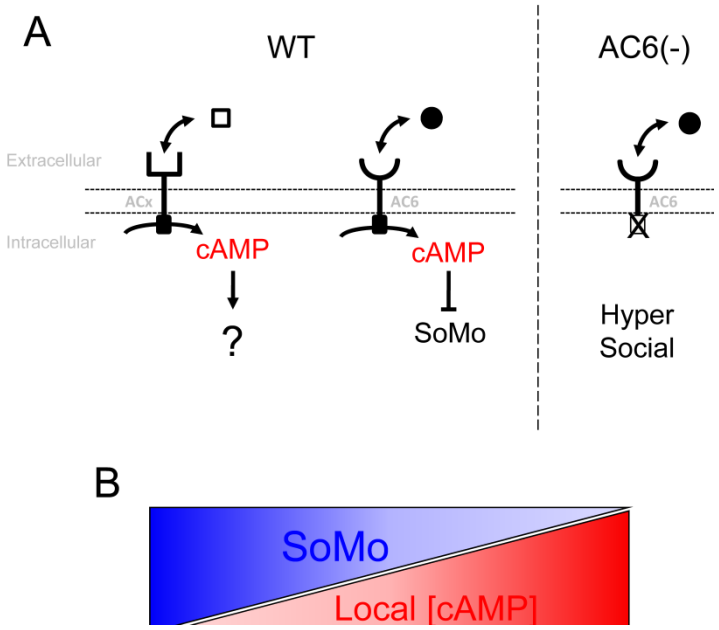

(A) Schematic model for AC6-dependent control of social motility in wild type cells (WT) and AC6 knockdown or catalytic mutant cells (AC6(-)). AC6 is one of several ACs in the trypanosome flagellum. The model posits that ACs recognize different ligands depending on their divergent extracellular domains and that ligand binding regulates AC activity. cAMP produced specifically by AC6 acts to inhibit social motility and when AC6 activity is reduced through ligand-mediated regulation (WT), this results in reduced cAMP and activation of social motility. Constitutive inactivation of AC6, e.g. through knockdown or expression of a catalytic mutant (AC6(-)), causes a signal-independent decrease in local cAMP, resulting in a precocious, hypersocial phenotype. (B) Reciprocal relationship between social motility (SoMo) and cAMP concentrations.

References

1. Alsford, S., S. Eckert, N. Baker, L. Glover, A. Sanchez-Flores, K. F. Leung, D. J. Turner, M. C. Field, M. Berriman, and D. Horn. 2012. High-throughput decoding of antitrypanosomal drug efficacy and resistance. Nature 482:232-236.

2. Baillie, G. S., and M. D. Houslay. 2005. Arrestin times for compartmentalised cAMP signalling and phosphodiesterase-4 enzymes. Curr. Opin. Cell Biol. 17:129-134.

3. Bassler, B. L., and R. Losick. 2006. Bacterially speaking. Cell 125:237-246.

4. Bieger, B., and L. O. Essen. 2001. Structural analysis of adenylate cyclases from Trypanosoma brucei in their monomeric state. EMBO J. 20:433-445.

5. Boyd, C. D., and G. A. O'Toole. Second messenger regulation of biofilm formation: breakthroughs in understanding c-di-GMP effector systems. Annu Rev Cell Dev Biol 28:439-462.

6. Butler, M. T., Q. Wang, and R. M. Harshey. 2010. Cell density and mobility protect swarming bacteria against antibiotics. Proc. Natl. Acad. Sci. USA 107:3776-3781.

7. de Koning, H. P., M. K. Gould, G. J. Sterk, H. Tenor, S. Kunz, E. Luginbuehl, and T. Seebeck. 2012. Pharmacological validation of Trypanosoma brucei phosphodiesterases as novel drug targets. J. Infect. Dis. 206:229-237.

8. Ekwanzala, M., J. Pepin, N. Khonde, S. Molisho, H. Bruneel, and P. De Wals. 1996. In the heart of darkness: sleeping sickness in Zaire. Lancet 348:1427-1430.

9. Emes, R. D., and Z. Yang. 2008. Duplicated paralogous genes subject to positive selection in the genome of Trypanosoma brucei. PLoS One 3:e2295.

10. Firtel, R. A., and R. Meili. 2000. Dictyostelium: a model for regulated cell movement during morphogenesis. Curr. Opin. Genet. Dev. 10:421-427.

11. Franco, J. R., P. P. Simarro, A. Diarra, and J. G. Jannin. 2014. Epidemiology of human African trypanosomiasis. Clinical epidemiology 6:257-275.

12. Gerdes, J. M., E. E. Davis, and N. Katsanis. 2009. The vertebrate primary cilium in development, homeostasis, and disease. Cell 137:32-45.

13. Gibiansky, M. L., J. C. Conrad, F. Jin, V. D. Gordon, D. A. Motto, M. A. Mathewson, W. G. Stopka, D. C. Zelasko, J. D. Shrout, and G. C. Wong. 2010. Bacteria use type IV pili to walk upright and detach from surfaces. Science 330:197.

14. Gould, M. K., S. Bachmaier, J. A. Ali, S. Alsford, D. N. Tagoe, J. C. Munday, A. C. Schnaufer, D. Horn, M. Boshart, and H. P. de Koning. 2013. Cyclic AMP effectors in African trypanosomes revealed by genome-scale RNA interference library screening for resistance to the phosphodiesterase inhibitor CpdA. Antimicrob. Agents Chemother. 57:4882-4893.

15. Gould, M. K., and H. P. de Koning. 2011. Cyclic-nucleotide signalling in protozoa. FEMS Microbiol. Rev. 35:515-541.

16. Hanoune, J., and N. Defer. 2001. Regulation and role of adenylyl cyclase isoforms. Annu. Rev. Pharmacol. Toxicol. 41:145-174.

17. Harshey, R. M. 2003. Bacterial motility on a surface: many ways to a common goal. Annu. Rev. Microbiol. 57:249-273.

18. Hill, K. L. 2003. Mechanism and biology of trypanosome cell motility. Euk Cell 2:200-208.

19. Kabututu, Z. P., M. Thayer, J. H. Melehani, and K. L. Hill. 2010. CMF70 is a subunit of the dynein regulatory complex. J. Cell Sci. 123:3587-3595.

20. Kaiser, D. 2003. Coupling cell movement to multicellular development in myxobacteria. Nat Rev Microbiol 1:45-54.

21. Klengel, T., W. J. Liang, J. Chaloupka, C. Ruoff, K. Schroppel, J. R. Naglik, S. E. Eckert, E. G. Mogensen, K. Haynes, M. F. Tuite, L. R. Levin, J. Buck, and F. A. Muhlschlegel. 2005. Fungal adenylyl cyclase integrates CO2 sensing with cAMP signaling and virulence. Curr. Biol. 15:2021-2026.

22. Kuchma, S. L., K. M. Brothers, J. H. Merritt, N. T. Liberati, F. M. Ausubel, and G. A. O'Toole. 2007. BifA, a cyclic-Di-GMP phosphodiesterase, inversely regulates biofilm formation and swarming motility by Pseudomonas aeruginosa PA14. J Bacteriol 189:8165-8178.

23. Kuchma, S. L., K. M. Brothers, J. H. Merritt, N. T. Liberati, F. M. Ausubel, and G. A. O'Toole. 2007. BifA, a cyclic-Di-GMP phosphodiesterase, inversely regulates biofilm formation and swarming motility by Pseudomonas aeruginosa PA14. J. Bacteriol. 189:8165-8178.

24. LaCount, D. J., B. Barrett, and J. E. Donelson. 2002. Trypanosoma brucei FLA1 is required for flagellum attachment and cytokinesis. J. Biol. Chem. 277:17580-17588.

25. Langousis, G., and K. L. Hill. 2014. Motility and more: the flagellum of Trypanosoma brucei. Nat Rev Microbiol 12:505-518.

26. Legros, D., G. Ollivier, M. Gastellu-Etchegorry, C. Paquet, C. Burri, J. Jannin, and P. Buscher. 2002. Treatment of human African trypanosomiasis--present situation and needs for research and development. Lancet Infect Dis 2:437-440.

27. Livak, K. J., and T. D. Schmittgen. 2001. Analysis of relative gene expression data using real-time quantitative PCR and the 2(-Delta Delta C(T)) Method. Methods 25:402-408.

28. Lopez, M. A., H. T. Nguyen, M. Oberholzer, and K. L. Hill. 2011. Social parasites. Curr Opin Microbiol 14:642-648.

29. Merchant, S., K. Hill, and G. Howe. 1991. Dynamic interplay between two copper-titrating components in the transcriptional regulation of cyt c6 [published erratum appears in EMBO J 1991 Aug;10(8):2320]. EMBO J. 10:1383-1389.

30. Merritt, J. H., K. M. Brothers, S. L. Kuchma, and G. A. O'Toole. 2007. SadC reciprocally influences biofilm formation and swarming motility via modulation of exopolysaccharide production and flagellar function. J Bacteriol 189:8154-8164.

31. Merritt, J. H., K. M. Brothers, S. L. Kuchma, and G. A. O'Toole. 2007. SadC reciprocally influences biofilm formation and swarming motility via modulation of exopolysaccharide production and flagellar function. J. Bacteriol. 189:8154-8164.

32. Merritt, J. H., D. G. Ha, K. N. Cowles, W. Lu, D. K. Morales, J. Rabinowitz, Z. Gitai, and G. A. O'Toole. 2010. Specific control of Pseudomonas aeruginosa surface-associated behaviors by two c-di-GMP diguanylate cyclases. mBio 1.

33. Naula, C., R. Schaub, V. Leech, S. Melville, and T. Seebeck. 2001. Spontaneous dimerization and leucine-zipper induced activation of the recombinant catalytic domain of a new adenylyl cyclase of Trypanosoma brucei, GRESAG4.4B. Mol. Biochem. Parasitol. 112:19-28.

34. Nguyen, H. T., J. Sandhu, G. Langousis, and K. L. Hill. 2013. CMF22 Is a Broadly Conserved Axonemal Protein and Is Required for Propulsive Motility in Trypanosoma brucei. Euk Cell 12:1202-1213.

35. Oberholzer, M., M. A. AND Lopez, B. T. McLelland, and K. L. Hill. 2010. Social motility in african trypanosomes. PLoS Pathog 6:e1000739.

36. Oberholzer, M., P. Bregy, G. Marti, M. Minca, M. Peier, and T. Seebeck. 2007. Trypanosomes and mammalian sperm: one of a kind? Trends Parasitol 23:71-77.

37. Oberholzer, M., and K. L. Hill. Submitted. cAMP regulates social behavior in African trypanosomes.

38. Oberholzer, M., M. A. Lopez, B. T. McLelland, and K. L. Hill. 2010. Social motility in african trypanosomes. PLoS Pathog 6:e1000739.

39. Oberholzer, M., M. A. Lopez, K. S. Ralston, and K. L. Hill. 2009. Approaches for functional analysis of flagellar proteins in African trypanosomes. Methods Cell Biol. 93:21-57.

40. Oberholzer, M., G. Marti, M. Baresic, S. Kunz, A. Hemphill, and T. Seebeck. 2007. The Trypanosoma brucei cAMP phosphodiesterases TbrPDEB1 and TbrPDEB2: flagellar enzymes that are essential for parasite virulence. FASEB J. 21:720-731.

41. Oberholzer, M., S. Morand, S. Kunz, and T. Seebeck. 2006. A vector series for rapid PCR-mediated C-terminal in situ tagging of Trypanosoma brucei genes. Mol. Biochem. Parasitol. 145:117-120.

42. Paindavoine, P., S. Rolin, S. Van Assel, M. Geuskens, J. C. Jauniaux, C. Dinsart, G. Huet, and E. Pays. 1992. A gene from the variant surface glycoprotein expression site encodes one of several transmembrane adenylate cyclases located on the flagellum of Trypanosoma brucei. Mol. Cell. Biol. 12:1218-1225.

43. Ralston, K. S., N. K. Kisalu, and K. L. Hill. 2011. Structure-function analysis of dynein light chain 1 identifies viable motility mutants in bloodstream-form Trypanosoma brucei. Euk Cell 10:884-894.

44. Ralston, K. S., A. G. Lerner, D. R. Diener, and K. L. Hill. 2006. Flagellar Motility Contributes to Cytokinesis in Trypanosoma brucei and Is Modulated by an Evolutionarily Conserved Dynein Regulatory System. Euk Cell 5:696-711.

45. Redmond, S., J. Vadivelu, and M. C. Field. 2003. RNAit: an automated web-based tool for the selection of RNAi targets in Trypanosoma brucei. Mol. Biochem. Parasitol. 128:115-118.

46. Saada, E. A., Z. P. Kabututu, M. Lopez, M. M. Shimogawa, G. Langousis, M. Oberholzer, A. Riestra, Z. Jonsson, J. A. Wohlschlegel, and K. L. Hill. 2014. Insect

stage-specific receptor adenylate cyclases are localized to distinct subdomains of the Trypanosoma brucei flagellar membrane. Euk Cell.

47. Saada, E. A., Z. P. Kabututu, M. Lopez, M. M. Shimogawa, G. Langousis, M. Oberholzer, A. Riestra, Z. O. Jonsson, J. A. Wohlschlegel, and K. L. Hill. 2014. Insect stage-specific receptor adenylate cyclases are localized to distinct subdomains of the Trypanosoma brucei Flagellar membrane. Eukaryot Cell 13:1064-1076.

48. Salmon, D., S. Bachmaier, C. Krumbholz, M. Kador, J. A. Gossmann, P. Uzureau, E. Pays, and M. Boshart. 2012. Cytokinesis of Trypanosoma brucei bloodstream forms depends on expression of adenylyl cyclases of the ESAG4 or ESAG4-like subfamily. Mol. Microbiol. 84:225-242.

49. Salmon, D., G. Vanwalleghem, Y. Morias, J. Denoeud, C. Krumbholz, F. Lhomme, S. Bachmaier, M. Kador, J. Gossmann, F. B. Dias, G. De Muylder, P. Uzureau, S. Magez, M. Moser, P. De Baetselier, J. Van Den Abbeele, A. Beschin, M. Boshart, and E. Pays. 2012. Adenylate cyclases of Trypanosoma brucei inhibit the innate immune response of the host. Science 337:463-466.

50. Simm, R., M. Morr, A. Kader, M. Nimtz, and U. Romling. 2004. GGDEF and EAL domains inversely regulate cyclic di-GMP levels and transition from sessility to motility. Mol. Microbiol. 53:1123-1134.

51. Srivastava, D., and C. M. Waters. A tangled web: regulatory connections between quorum sensing and cyclic Di-GMP. J Bacteriol 194:4485-4493.

52. Stuart, K., R. Brun, S. Croft, A. Fairlamb, R. E. Gurtler, J. McKerrow, S. Reed, and R. Tarleton. 2008. Kinetoplastids: related protozoan pathogens, different diseases. J. Clin. Invest. 118:1301-1310.

53. Tam, R., and M. H. Saier, Jr. 1993. Structural, functional, and evolutionary relationships among extracellular solute-binding receptors of bacteria. Microbiol. Rev. 57:320-346.

54. Thurston, S. J., and J. D. Saffer. 1989. Ultraviolet shadowing nucleic acids on nylon membranes. Anal Biochem 178:41-42.

55. Trimble, M. J., and L. L. McCarter. 2011. Bis-(3'-5')-cyclic dimeric GMP-linked quorum sensing controls swarming in Vibrio parahaemolyticus. Proc. Natl. Acad. Sci. USA 108:18079-18084.

56. Van Den Abbeele, J., Y. Claes, D. van Bockstaele, D. Le Ray, and M. Coosemans. 1999. *Trypanosoma brucei* spp. development in the tsetse fly: characterization of the post-mesocyclic stages in the foregut and proboscis. Parasitology 118:469-478.

57. Velicer, G. J., and M. Vos. 2009. Sociobiology of the myxobacteria. Annu. Rev. Microbiol. 63:599-623.

58. Vickerman, K., L. Tetley, K. A. Hendry, and C. M. Turner. 1988. Biology of African trypanosomes in the tsetse fly. Biol. Cell 64:109-119.

59. Wirtz, E., S. Leal, C. Ochatt, and G. A. Cross. 1999. A tightly regulated inducible expression system for conditional gene knock-outs and dominant-negative genetics in *Trypanosoma brucei*. Mol. Biochem. Parasitol. 99:89-101.

60. Zoraghi, R., S. Kunz, K. Gong, and T. Seebeck. 2001. Characterization of TbPDE2A, a novel cyclic nucleotide-specific phosphodiesterase from the protozoan parasite Trypanosoma brucei. J. Biol. Chem. 276:11559-11566.

Chapter VI:

Modulation of *Trypanosoma brucei* social behaviors requires flagellar sub-domain localization of receptor adenylate cyclases

PREFACE

The following chapter describes efforts to understand whether the differential flagellum localizations of ACs, as characterized in Chapter IV, are functionally relevant to their regulatory roles in social motility, as described in Chapter V. The following chapter represents work that, at time of dissertation submission, is a manuscript in preparation for submission to a journal for peer review and publication. I am lead author and contributor of the manuscript, and responsible for most experimental design, generation of all vector constructs and cell lines, and performed all of the social motility, immunofluorescence, and immunoblot assays, with one exception. Michelle Shimogawa, the second author, performed the surface biotinylation assay, as well as provided general technical assistance throughout the project, and contributed to writing of this manuscript.

ABSTRACT

Trypanosomes are devastating human and animal pathogens. These protozoan parasites are known to engage in complex social behaviors, although the underlying molecular mechanisms are mostly unknown. We recently reported on functional analyses of cAMP signaling systems within *Trypanosoma brucei,* revealing that receptor adenylate cyclases (ACs) cooperate with cAMP-specific phosphodiesterases to regulate trypanosomal social behaviors. Interestingly, we previously localized several procyclic-specific ACs to either the flagellum length or flagellum-tip, suggesting specialization of flagellum membrane subdomains. RNAi studies implicate at least one flagellar-tip AC as a regulator of *T. brucei* social motility, indicating flagellum subdomain-specific cAMP signaling. Despite the importance of flagellar protein trafficking, flagellar and subflagellar targeting signals are virtually unknown in any organism. Here, we investigate whether flagellar subdomain localization impacts AC function, utilizing protein truncations, chimeras, and point mutants to define flagellar and flagellar-tip targeting sequences. We identify a 45 amino acid segment within the AC intracellular domain that is necessary for flagellum membrane targeting and further define a nine amino acid sequence within this domain that directs targeting to the flagellar tip. Strikingly, the social motility defect of a flagellum-tip AC mutant can be rescued by redirecting another AC from its native localization along the flagellum length to the flagellum tip. This result demonstrates the importance of protein targeting to specific subdomains within the flagellum, and implicates cAMP signaling at the flagellum tip as a key regulator of cell-cell communication required for social

behavior. Our work thus advances understanding of principles that govern protein targeting to flagellum subdomains and provides insight into *T. brucei* signaling mechanisms, both of which are poorly understood but fundamentally important features of flagellar and trypanosomal biology.

INTRODUCTION

Trypanosoma brucei is a flagellated protozoan parasite that afflicts humans and other mammals throughout sub-Saharan Africa. The human disease, African sleeping sickness, is fatal if untreated, and infection of animals imposes a severe agricultural burden, making *T. brucei* a vector-borne parasite of incredible medical and economic importance. *T. brucei* alternates between tsetse flies and mammalian hosts, and therefore must sense and respond to external signals in both organisms. Within the tsetse, the parasite must undergo an ordered series of directional migrations from the midgut through the mouthparts and into the salivary glands to complete development into mammalian-infectious forms (1). Little is known about the signaling and sensory pathways by which these complicated developmental programs are accomplished.

The eukaryotic flagellum (also known as cilium) is a major site for perception of external signals, and serves as a diverse signaling platform. The flagellar membrane contains transmembrane receptors that function as chemo- and mechano-sensors (2-4). In mammals, the cilium membrane controls hedgehog and Wnt signaling and ciliary defects cause a long list of human diseases, including polycystic kidney disease, obesity and cancer (5-8). *T. brucei*'s single flagellum is a major feature of trypanosomal biology, and is a critical host-pathogen interface. In the mammalian host, *T. brucei* flagellar membrane proteins modulate infection and virulence (3, 9, 10). In the tsetse fly, the trypanosome flagellar membrane attaches to salivary gland epithelial cells, enabling the parasite to establish permanent infection and marking

the onset of parasite differentiation into human-infectious forms (5). Key to the sensory and signaling roles of the eukaryotic flagellum is the specialized and regulated targeting of transmembrane receptors to the flagellar membrane, such that its protein composition is distinct from the rest of the cell surface (11, 12). Despite advances in identifying flagellar proteins, little is known about targeting signals and mechanisms for flagellar membrane proteins in any organism. Efforts to study the sensory role of the *T. brucei* flagellum have further been hampered by a lack of specific assays for signaling function.

T. brucei spends most of its life cycle in direct contact with host-tissue surfaces. This is particularly evident in the tsetse fly, where flagellum interactions with the salivary gland epithelium are required for parasite development (1, 13). A recently discovered, and largely unexplored, aspect of trypanosome biology is the capacity for individual parasites to engage in collective behaviors. As observed in many other microbes (14), surface exposure induces profound changes in trypanosome behavior. Individual trypanosomes actively assemble into densely packed communities, from which millions of cells coordinately emerge and migrate across the surface in the form of radial projections (15). This process has been termed social motility (SoMo) due to analogies with similar bacterial behaviors. Parasites must collectively be able to sense, respond, and communicate to accomplish these processes. Thus, surface-induced social motility likely reflects distinct features of parasite behavior occurring *in vivo* (15, 16), as trypanosomes must colonize and migrate through several fly tissues. Recent findings support this hypothesis. Work from the Roditi group has posited that procyclic (insect midgut-stage) parasites can

be further classified into early and late forms, such that only the early procylics are SoMo-competent, and represent early stage fly infections (17). Furthermore, the RFT1-/- mutant line is incapable of engaging in social motility, and shows impaired colonization of the tsetse fly (18), providing the first link between *in vitro* social motility and parasite success *in vivo.*

We recently reported on the first known signaling pathways regulating social motility in trypanosomes. Adenylate cyclases (ACs) catalyze cAMP production, and inhibition of some procyclic-specific ACs by RNAi or mutagenesis results in a hyper-social phenotype, characterized by a significant increase in the number of outwardly migrating radial projections (19). Conversely, RNAi or pharmaceutical inhibition of phosphodiesterase B1 (PDEB1), which degrades cAMP, prevents social motility, resulting in parasites being unable to form radial projections (20). Utilization of FRET-based cAMP sensors as well as cAMP analogues indicates that the loss of social motility is correlated with increases in intracellular cAMP, while *in vitro* viability, morphology, and standard propulsive motility are unaffected (20). The discovery that *T. brucei* social motility is controlled by cAMP signaling provides a concrete link to social behaviors in other systems, such as *Pseudomonas spp.*, which have also been shown to be regulated by cyclic nucleotide levels (21, 22).

Trypanosomal ACs are of particular interest for two major reasons: firstly, they are the sole source of cAMP production, which has been linked to viability and virulence defects in bloodstream forms (10, 23), and now social motility in procyclic parasites. Secondly, ACs are a vastly expanded gene family in *T. brucei,* with variable extracellular N-terminal domains and putative roles as receptors. Many are life-stage

specific (24, 25). We previously characterized several procyclic-specific ACs, demonstrating them to be surface-exposed glycoproteins that homo-dimerize and possess catalytic activity (24). Notably, immunofluorescence analysis revealed that some ACs were distributed along the flagellum length, while others were restricted to the flagellum tip, indicating specialization of flagellum membrane subdomains (24). The recent discovery that only some of the ACs regulate social motility, notably AC6 which localizes to the flagellar tip (19), has generated interest in whether flagellar subdomain compartmentalization impacts cAMP signaling and output. Therefore, trypanosomal adenylate cyclases provide an excellent system for uncovering flagellar and subflagellar targeting signals, as well as determining the impact of flagellar subdomain localization on cAMP signaling.

Here, we demonstrate that AC flagellar localization impacts social motility in *Trypanosoma brucei*, utilizing protein truncations, chimeras, and point mutants. We report that AC flagellar and flagellar-tip targeting sequences are contained with the intracellular C-terminal region, and that these regions are necessary for AC flagellar trafficking but not sufficient to drive heterologous reporters. Strikingly, the social motility defect of a flagellum-tip AC mutant can be rescued when a flagellum-length AC is redirected to the flagellar tip. Thus, our studies provide insight into targeting of flagellar membrane proteins, as well as evidence for flagellar subdomain-specific cAMP signaling in *Trypanosoma brucei.*

MATERIALS & METHODS

Cell culture and RNAi

The 2913 procyclic cell line was used for all experiments (26). Suspension cultures were maintained using SM media as described previously (27). For RNAi lines, 2.5 mg/ml phleomycin was included in the medium to maintain stable transfectants, and RNAi was induced by addition of 1μg/ml tetracycline. Cell lines expressing epitope-tagged proteins were cultured in 1 μg/ml puromycin.

Generation of epitope-tagged proteins

In situ epitope tagging was done by amplifying fragments of DNA homologous to the target gene's open reading frame (ORF) or 3' untranslated region (UTR) and cloning these into the pMOTag vector series (28). For ectopic expression of the synthetic and 'minimal construct' genes, the full ORF was cloned into the pKR10 inducible expression vector (27). The full set of primers and cloning sequences used are available in Supplemental Table 1. Mutagenesis primers were designed using Stratagene's QuikChangeII mutagenesis kit and website tool, and generated following the manufacturer's suggested protocols within the above epitope-tagging plasmids. Transfections and selection of clonal lines by limiting dilution were done as described previously (27). Integration of epitope tags was verified by Western Blot analysis and mutations were confirmed by sequencing of genomic DNA (data not shown) using allele-specific primers (Supplemental Table 1). Genes used to test sufficiency of

flagellum targeting sequences, e.g., FS179, were previously epitope-tagged and localized (29).

Immunoblotting

Protein samples were analyzed by immunoblotting as previously described (30, 31). Anti-HA monoclonal antibody HA.11 (Covance, Emeryville, CA) was used at 1:2500. ß-tubulin was used as a loading control and was detected by the monoclonal antibody E7 (32) obtained from the Developmental Studies Hybridoma Bank maintained by University of Iowa Department of Biological Sciences. Anti-BiP antibodies were provided by Jay Bangs (33).

Blue native PAGE

Cells were harvested and washed in PBS and then resuspended in PEME buffer (100 mM PIPES [piperazine-*N*,*N*′-bis(2-ethanesulfonic acid)], 1 mM $MgSO_4$, 0.1 mM EDTA, 2 mM EGTA, pH 6.9) with 1% NP-40 and protease inhibitors (SigmaFAST cocktail; Sigma-Aldrich). Following a 10 min incubation at room temperature, lysates were spun for 15 min at 13,000 rpm and 4°C. Supernatants were transferred to new tubes and spun again for 10 min to clear debris, and the resultant soluble fractions were used. For Blue Native PAGE, NativePAGE sample buffer and 5% G-250 sample additive (Invitrogen) were added, and samples were run on a NativePAGE Novex 4-16% Bis-Tris protein gel and transferred to a polyvinylidene difluoride (PVDF) membrane per the manufacturer's suggested protocols (Invitrogen), followed by immunoblotting.

Surface biotinylation and streptavidin purification

Surface biotinylation was done as described previously (29). Cells were harvested and washed in ice-cold PBS and then resuspended at 1e8 cells/ml in PBS + 0.5 mg/ml sulfo-NHS-SS-biotin (catalog no. 21331; Pierce) and incubated for 10 min on ice. Tris (2 M, pH 6.8) was added to a final concentration of 100 mM for 10 min on ice to block unreacted biotin. Cells were pelleted, washed with cold PBS+100 mM Tris, and extracted with IP buffer (150 mM NaCl, 50 mM HEPES, 5 mM EDTA, 5 mM EGTA, 1% NP-40, 10% glycerol, 1× SigmaFAST protease inhibitors). After a 10 min incubation on ice, samples were centrifuged at 14,000 rpm for 10 min at 4°C to pellet insoluble material. A fraction of the supernatant (the input) was retained, and the remainder was transferred to a new tube with 50 µl of streptavidin Sepharose high performance beads (GE Healthcare) and incubated for 2 h at 4°C on a nutator mixer to allow biotin-streptavidin binding. The beads were pelleted and a fraction of the supernatant (the unbound) was retained. Beads were washed in IP buffer and then resuspended and boiled in Laemmli sample buffer for analysis by immunoblotting.

Northern blotting

Total RNA was extracted from the indicated cell lines using an RNeasy mini kit (Qiagen). Northern blot assays were done using total RNA essentially as previously described (34, 35). Digoxigenin (DIG)-labeled probes were generated using AC1-specific primers (Supplemental Table 1), and were visualized by the DIG nucleic acid detection kit (Roche). Total RNA was visualized by UV shadowing of the nylon

membrane (Amersham Hybond-XL).

Immunofluorescence microscopy

Immunofluorescence microscopy on whole cells was done as previously described (36), using mouse anti-HA antibody (Covance) at a 1:250 dilution and detected using donkey anti-mouse secondary antibody coupled to AlexaFluor 488 (Molecular Probes) at 1:1500. Polyclonal PFR antiserum was used at a 1:1250 dilution and detected using donkey anti-rabbit antibodies coupled to AlexaFluor 594 (Molecular Probes) at 1:1500. Coverslips were mounted in mounting medium containing DAPI and imaged on a Zeiss Axioskop II microscope (Zeiss, Inc).

Social motility assays

Social motility assays were done with some variations to the original protocol (15). Suspension cultures were grown to mid-log density, then centrifuged and resuspended to allow for inoculation of 6e4 cells in 4.25ul. The indicated cell lines were inoculated onto agar plates supplemented with 1µg/ml tetracycline to allow for RNAi induction. Plates were incubated at 28°C with 3.5% CO_2 for approximately 72 to 96 hours, and then imaged using a digital camera. The number of projections per plate was quantified and results were plotted using GraphPad Prism.

RESULTS

The C-terminus is required for flagellar targeting of adenylate cyclases (ACs) AC1 and AC2

We previously reported the first identification and characterization of procyclic-specific receptor adenylate cyclases (ACs) (35, 36). The discovery that a flagellar tip-localized AC is involved in regulation of social motility supports the proposed microdomain signaling model, in which cAMP production and signaling are confined to distinct foci by differential localization of ACs.

We therefore sought to test whether social motility is regulated by the precise flagellar and sub-flagellar localization of AC proteins, rather than total cellular cAMP levels. To do this, we took advantage of two closely related PCF-specific ACs that localize to different flagellar subdomains (Figure 1A). AC1 and 2 are the most closely related procyclic-specific ACs identified (36), and dual-knockdown of these proteins results in a hyper-social phenotype (35). Interestingly, despite being nearly identical throughout most of their sequence (Figure 1B), AC1 is restricted to the flagellum tip while AC2 is along the length of the flagellum (Figure 1A).

Sequences responsible for protein targeting to flagellar subdomains are completely unknown, and flagellar targeting signals have only been characterized for a few proteins in any system. In all known cases, these signals are contained within an intracellular loop of multipass transmembrane proteins, or near the C-terminal end of single-pass transmembrane proteins (2). Consistent with this, divergence between AC1

and 2 is primarily concentrated within the intracellular C-terminal region (Figure 1B), which was previously shown to be important for AC trafficking to the flagellum (36).

We therefore asked whether flagellar targeting sequences are present in the C-terminal regions of AC1 and 2. We generated truncation mutants of AC1 and AC2, lacking the entire C-terminal 145 or 146aa, respectively. Immunoblot analysis shows the truncated proteins were expressed at the expected sizes and at levels similar to the wild-type protein (Figure 1C). As anticipated, truncation of the C-terminal region resulted in loss of flagellar localization and dispersal throughout the cell body (Figure 1D), consistent with previously published experiments, in which only the C-terminal 45aa were truncated (36).

The C-terminal domain of AC1 is sufficient to redirect AC2 from the flagellum to the flagellum tip

We also generated chimeric fusion proteins, to ask whether the C-terminal region contains signals that control targeting to flagellar subdomains. Unexpectedly, the chimeric fusions had interesting, non-reciprocal effects. Fusing the C-terminal of AC1 onto AC2 redirected the protein from the entire length of the flagellum to just the flagellar tip, clearly demonstrating that the C-terminal sequences are important for flagellar localization. In contrast, however, fusing the C-terminal of AC2 onto AC1 did not redirect the protein away from its normal location at the flagellar tip.

Trypanosomes are diploid, containing two alleles for every gene. In considering possibilities for why localization of the AC1 chimera was not altered, we sought to test whether interactions with the wildtype AC1 protein influence retention at the

flagellar tip. Therefore, we expressed the AC1 chimera in the previously described AC1-UTR-RNAI line, allowing us to inhibit expression of the wildtype allele (36). Interestingly, knockdown of endogenous AC1 actually appeared to enhance tip-localization (Supplemental Figure 1), suggesting there may be other mechanisms or interaction partners that contribute to AC1 flagellum tip localization. To minimize confounding factors, we therefore focused efforts on the C-terminal 145aa of AC1, which was sufficient to redirect the AC2-chimera to the flagellar tip.

The C-terminal domain of AC1 is not sufficient to direct flagellar targeting of other proteins

To test whether this sequence was sufficient to direct flagellar tip localization of a synthetic reporter, we generated a series of synthetic, single-pass transmembrane reporter constructs designed to represent a "minimalized AC" (Supplemental Figure 2A). Initial designs incorporated short N-terminal regions, the transmembrane domain, and fragments of AC1 C-terminal sequence fused to an HA epitope tag, but were not expressed (Supplemental Table 1, data not shown). Instead, a larger synthetic reporter was designed by expressing the first 100 N-terminal amino acids of AC2, a 60 amino acid region containing the AC2 transmembrane domain, and the entire C-terminal sequence of AC1. This protein was expressed, but failed to localize to the flagellum (Supplemental Figure 2B). The transmembrane domain of adenylate cyclases falls in the beginning of the catalytic cyclase domain, and flanking sequence may include additional secondary structure. We therefore substituted this fragment with the transmembrane domain and flanking sequence from two other

surface-localized proteins, ISG65D and PSSA2 (37, 38). In both cases, expression of the synthetic reporter increased, but the reporter still failed to localize to the flagellum, displaying a concentrated localization at the flagellar pocket and endosomal region (Supplemental Figure 2B).

We therefore proceeded to test whether the AC sequence was sufficient to redirect other native surface and flagellar proteins. In a few cases, fusion of the AC1 sequence resulted in lowered expression levels, presumably due to protein instability, and assessment of protein localization was not possible (data not shown). One protein examined was PSSA2, a membrane-spanning phosphoprotein that localizes to the cell surface. Chimeric fusion of AC1-sequence to the C-terminal end of PSSA2 resulted in reduced protein expression, and disruption of surface localization (Supplemental Figure 2C). The PSSA2 C-terminal region is comprised of degenerate repeats, and our result mirrors observations that disruption of the repeat sequences reduces PSSA2 expression and results in protein accumulation in the flagellar pocket and endosomal pathway (38). We additionally examined FS179, an ion channel that localizes to the flagellum attachment zone (29). Chimeric fusion to the AC1-sequence did not alter localization, as the protein still localizes along the length of the flagellum attachment zone, ending at the anterior end of the cell body (Supplemental Figure 1D). Cumulatively, these results indicate that although this sequence is necessary for flagellar targeting in the context of trypanosomal adenylate cyclases, it is not sufficient for heterologous or synthetic reporters, as has been observed for most characterized flagellar targeting sequences (2, 39, 40).

AC2 can be redirected to the flagellum tip by mutation of six residues in the C-terminal domain

The sufficiency of the AC1 sequence for redirection of AC2 to the flagellar tip was a striking result. We therefore went forward with studies to dissect flagellar targeting of AC2. We previously demonstrated that truncating the terminal 45aa of ACs was enough to disrupt flagellar localization (36), so we asked whether chimeric complementation of that region could restore flagellar localization, and be sufficient for redirection to the flagellar tip. We find that AC2, with the C-terminal 45aa of AC1, localizes to the flagellum tip (Figure 2A), indicating that targeting signals are present within the C-terminal 45aa.

In a preliminary sequence analysis of the procyclic-specific ACs, we had predicted a region within the C-terminus that may correlate with flagellar subdomain localization, but not all of the ACs had been localized (36). We have since found that AC6 is also localized to the flagellar tip (35), as is AC3 (Supplemental Figure 3), consistent with the earlier prediction. Therefore, we focused our attention on this stretch of predictive residues within the C-terminal tail of the adenylate cyclases (Figure 2B). Knowing that AC2 can be redirected to the flagellar tip when complemented with AC1 sequences, we opted to use point mutagenesis to target specific residues and minimize changes to the protein sequence (Figure 2C, Supplemental Figure 4). Most notably, AC2 has three arginines whereas AC1 has three serines. Considering the potential for post-translational modifications, we first opted to mutate all three residues from arginine to serine. There was no apparent effect on localization (Figure 2C), so we mutated three additional residues to match AC1

sequence, changing a leucine to valine, alanine to isoleucine, and a leucine to isoleucine. Combined, these six mutations were sufficient to redirect AC2 to the flagellar tip (Figure 2C).

These residues therefore clearly impact flagellar localization, and the results suggest two distinct models for how flagellar targeting may be regulated: the first is that we provided AC2 with a "tip-targeting" signal from AC1. The second is that the flagellum tip is the default localization for ACs, and that AC2 has a "flagellum length" targeting signal that we have disrupted. To distinguish between these models, we mutated these same residues to alanines, finding no discernable impact on the flagellar localization of AC2 (Figure 2D), and ruling out the latter model. To further test the impact of these six specific residues, we performed mutagenesis within the AC2 chimeric protein. AC2, with the C-terminal 45aa of AC1, localizes to the flagellar tip. Yet, when the corresponding six residues within the chimeric AC1 region are mutated back to AC2 sequence, the protein is completely excluded from the flagellum (Figure 2E, Supplemental Figure 4). These results therefore suggest that these residues contribute to flagellar and flagellar-tip targeting in the context of a larger signal or sequence requirement.

AC1 truncation mutants do not rescue the social motility defect of an AC1 RNAi line

Having identified determinants that affect flagellar localization of ACs, we now have the opportunity to assess whether flagellar AC localization impacts regulation of trypanosomal social behaviors. AC1 and 2 were previously implicated in control of

social behavior in a dual-knockdown line (35), however the individual contributions were not examined. We recently generated an AC1-specific RNAi line, but were unable to generate specific knockdown of AC2 (36). Therefore, we sought to determine whether AC1 alone is able to exert regulatory effects on social motility. RNAi inhibition of AC1 results in a hyper-social phenotype, which is characterized by a dramatic increase in the number of projections formed in comparison to a control line (Figure 3A). This hyper-social phenotype resembles the phenotype seen when AC1 and AC2 are dually-targeted. Furthermore, we show that normal social motility can be restored by introducing an RNAi-immune allele of AC1-HA, suggesting AC1-specific functionality in control of social motility.

Having generated AC1-truncation mutants that fail to localize to the flagellum, we next asked whether flagellar localization of AC1 is required for rescue of this phenotype. RNAi-immune alleles of AC1 lacking either the last 145 (AC1ΔC) or 45 (AC1 ΔC_{45}) amino acids were introduced into the AC1 RNAi line and expression verified by Northern blot analysis (Supplemental Figure 5A). Neither truncation rescued the hyper-social phenotype, indicating that flagellar localization of AC1 may be required for proper social motility. A potential caveat of this result is that ACs are surface-exposed, putative receptors that require dimerization for catalytic activity (41). We therefore assessed whether the mislocalized AC1-truncation mutants were still surface-exposed and able to dimerize. Blue native PAGE analysis indicates that the truncation mutant AC1 ΔC_{45} is smaller in size, but, like the full-length protein, is still primarily in a dimer or multimer (Supplemental Figure 5B), and presumably catalytically active. As expected, full-length AC1 can be immunoprecipitated by a

combination of cell surface-biotinylation followed by streptavidin affinity purification, consistent with surface exposure. However, both of the truncation mutants remained in the unbound fractions, indicating they were inaccessible to extracellular biotin and unlikely to be surface-exposed (Supplemental Figure 5C).

Redirection of AC2 to the flagellum tip rescues the social motility defect caused by AC1 knockdown

To avoid confounding variables from the truncation mutants, we instead took advantage of our ability to redirect AC2 from the flagellum length to the flagellum tip. This allows us to ask whether tip-specific production of cAMP is required for normal social motility. AC2 expression and localization along the length of the flagellum are unaffected in the AC1-RNAi line (36). We generated an epitope-tagged AC2-HA allele in the AC1-RNAi line, and as anticipated, AC2-HA had no impact on the hyper-social phenotype. However, expression of the tip-localized AC2 chimera rescues the hyper-social phenotype, dramatically reducing the number of projections observed to near control levels (Figure 3B). Normal social motility is observed in this line, despite efficient RNAi inhibition of AC1 as confirmed by Northern blot analysis (Supplemental Figure 5D). Thus, it is the relocalization of AC2 to the flagellum tip that rescues the social motility defect caused by loss of AC1.

DISCUSSION

Flagellum and flagellum-tip protein trafficking

The eukaryotic cilium (synonymous with flagellum) is a critical signaling center and ubiquitous organelle, found in nearly every tissue type in mammals. Signaling systems within the flagellum involve various mechano- and chemo-sensory pathways, which often require coordinated trafficking of proteins into and out of the flagellum (42-47). Despite the importance of flagellar localization for many proteins and receptors, targeting systems to this organelle are poorly understood. The flagellum contains no ribosomes, and is cordoned off from the rest of the cell by a barrier at the base, preventing free diffusion of membrane and matrix proteins (48). Therefore, proteins are thought to either be actively trafficked into and out of the flagellum or contain a targeting signal allowing free access through the diffusion barrier. Efforts to identify flagellar targeting signals (FTS) have been largely unsuccessful; fewer than two dozen FTS have been identified that are sufficient to grant flagellar localization to heterologous reporters.

One major obstacle is the apparent lack of common consensus sequences, such as those identified for nuclear localization signals. Instead, it appears that FTS are contextual to a specific group of proteins, and lack any definitive patterns across different organisms or protein families. For example, the phototransduction protein rhodopsin localizes to ciliary membrane stacks using a single VxPx motif (49), while the flagellar somatostatin3 receptor uses a motif that must contain AxSxQxxxAxAxQ

(50). The one feature common to all proteins with known FTS is that the motifs are contained within an intracellular region of the protein. For multipass transmembrane proteins, such as rhodopsin, the FTS is typically in the largest intracellular loop (49, 51). As seen here for the adenylate cyclases, the FTS for single-pass transmembrane proteins is typically near the C-terminal end. The inability of the C-terminal AC sequence to redirect a heterologous reporter to the flagellum is also a common finding. In fact, dozens of sequences found to be necessary for flagellar localization of a specific protein or protein family are insufficient to drive other proteins or reporters to the flagellum.

Very little is known about trafficking of proteins to flagellum subdomains. In mammalian systems, an "inversin" compartment has been described to be next to the transition zone (52-54), though very little is known about the distal, flagellar tip. Despite the obvious potential for functional specialization at the tip, very few transmembrane proteins have been localized there, with trypanosomal ACs being among the most prominent examples. We identified six residues within the C-terminal region that were sufficient to redirect a flagellum length AC to the tip, uncovering a major component of the AC FTS. Attempts to find a more minimal motif were not successful, as mutations to the first three amino acids did not alter localization, and mutations to the latter three amino acids were essentially already tested in AC5 (Figure 2B), which is not tip-specific (36). Additional factors regulating flagellar and subflagellar targeting are yet to be identified.

The trypanosome flagellum emerges from the posterior end of the cell, and is attached along the length of the cell body, except for a short, unattached region at

the anterior end that encompasses the flagellar tip. It's unclear whether the localization of some ACs specifically to the flagellum tip is actually restricted to the free region of the flagellum. Super-resolution microscopy may be better able to resolve the precise localization and offer mechanistic insight into how differential localizations are achieved. Our work on flagellar tip-targeting signals supports a couple of models that are not mutually exclusive. The first is that localization to the flagellum tip is actually a result of flagellar/cell-body exclusion. Such a model may require an inhibitory effect from proteins that localize specifically to the flagellar attachment zone (FAZ), and could explain why experiments using chimeric proteins were only able to redirect proteins towards, and not away from, the tip. A modification of this model may involve differing membrane composition, such that lipid composition at the free-flagellar tip differs than that among the flagellum length. However, earlier results indicate that ACs are not preferentially associated with lipid rafts (36). Alternatively, there may be interacting proteins at the flagellar tip. Such a model would be consistent with our observations that tip localization of the AC1-chimeric proteins appears enhanced by knockdown of the endogenous AC1 allele (Supplemental Figure 1), and that the AC2 chimera redirected to the tip displays a small shift in size by Blue native PAGE (Supplemental Figure 5E). Alternatively, this latter result may simply reflect conformational changes or differences between the native and chimeric C-terminal amino acid compositions. Ongoing studies will focus on identifying interaction partners of AC1 and AC2 to address these possibilities.

cAMP signaling pathways in *Trypanosoma brucei*

Adenylate cyclases comprise one of the largest gene families in *T. brucei*, and have been postulated to provide life-cycle specific functionalities. The bloodstream-specific ESAG4 is known to be a virulence factor (10, 55), while some procyclic-specific ACs cooperate with a cAMP-specific phosphodiesterase (PDE) to regulate trypanosome social behaviors (20, 35). Despite these important roles, little is known about cAMP signaling pathways in *T. brucei.*

Differential localization of individual ACs (36) suggests that the microdomain signaling model applies to *T. brucei.* In this model, cAMP production is compartmentalized through localization of individual ACs to different flagellar subdomains, allowing for diverse cellular responses to be controlled by a common signaling molecule without crosstalk. A key tenet of this model would be the requirement of corresponding effector proteins. The first known cAMP effectors in *T. brucei* (CARP1-4) were only recently described (56), and have not yet been characterized or localized in procyclic form parasites. A key prediction of the microdomain signaling model would suggest that at least one CARP effector protein localizes to the flagellum tip, allowing for specific responses to catalytic output from the subset of ACs at the flagellum tip that contribute to regulation of social motility. This regulation may be mediated in several ways. In mammalian systems, effector proteins have been implicated in feedback loops controlling cyclase activity, activation of downstream signaling functions such as phosphorylation or

opening/closing ion channels, or even activation of different transcriptional pathways (57). The usage of social motility as a signaling assay and further mechanistic studies in procyclic-parasites can help elucidate these potential cAMP signaling pathways.

Regulation of SoMo by cAMP signaling at the flagellum tip

The flagellum tip is at the parasite's anterior end, and adenylate cyclases are therefore ideally positioned to perceive and transduce responses to flagellar interactions within the environment. Trypanosomal adenylate cyclases primarily vary in their extracellular, ligand binding domains. The lineage-specific gene family expansion correlates with the complexity of the life cycle within the tsetse fly, with *Trypanosoma brucei* having far more ACs than *T. congolense* or *T. vivax,* suggesting life-stage specific roles. Such interactions may be particularly relevant in the tsetse fly, where *T. brucei* development into infectious metacyclic forms is triggered by attachment to the salivary gland epithelium (1). Functional analyses of ACs involved in regulation of social motility thereby offer interesting perspectives on cAMP signaling specific to the flagellum tip.

Currently, one simple model is that total cAMP levels at the flagellar tip are critical to maintain normal social motility. In this model, inhibition of a tip-cyclase, such as AC1 or AC6, results in a hyper-social phenotype, as insufficient cAMP levels are available at the flagellum tip. In such a model, redirection of AC2 to the flagellum tip restores the normal phenotype by either raising cAMP levels at the tip or reducing cAMP levels along the flagellum length. An alternative model relies on the different

ligand-binding domains, as described above. With the exception of AC1 and AC2, the other procyclic-specific cyclases are divergent in their extracellular region, and presumably react to different ligands. In this scenario, cAMP levels at the flagellum tip are critical at specific time points and/or in response to specific environmental cues. AC1/2 and AC6 may respond to different environmental cues, such that inhibition of either would result in a hyper-SoMo phenotype. We favor this model, which is supported by experimental data on AC3 and AC4, which both localize to the flagellum tip, yet have no observable impact on social motility when inhibited (35).

The apparent paradox that knockdown of all tip-localized ACs does not result in the same SoMo phenotype could be explained by ligand-mediated regulation of ACs. For example, if ACs are inhibited by ligand, then RNAi inhibition would only affect cAMP output when the ligand remains absent. In this example, AC4 may already be inhibited by a ligand present in the SoMo *in vitro* assay conditions, rendering RNAi ineffective, whereas AC1 and AC6 would be catalytically active, allowing RNAi to effectively lower flagellar-tip cAMP levels. The inverse of this model, whereby the presence of ligand activates AC activity, is equally applicable. As SoMo is an *in vitro* assay, it lacks the presence of normal tsetse fly environmental signals, therefore additional resolving power and insight is expected to come from complementary in vivo analyses of AC function in vivo.

Connection between cAMP signaling and differentiation within the fly

cAMP signaling has been often hypothesized to link critical differentiation events in the trypanosome life cycle, but this has never been directly demonstrated. Early studies found that *in vitro* differentiation from bloodstream to procyclic form parasites causes a large spike of cAMP levels approximately 6 to 10 hours after induction (58). This timing coincided with the shedding of the VSG coat, and it was hypothesized that AC activity triggers this differentiation event. Later work using a mutant was able to inhibit shedding of the VSG, but still observe a cAMP spike, indicating that these are independently-regulated events (59). Around the same time, studies in bloodstream parasites implicated cAMP in the long-slender bloodstream to stumpy-form differentiation event (60). It was later discovered that it was likely cAMP metabolic byproducts that had a much more potent effect, rather than direct action due to cAMP (61). Despite the presumed importance of cAMP, direct links to the life-cycle have not been elucidated.

Interestingly, it's recently been proposed that the insect-stage parasite can further be classified into early or late procyclics, reflecting newly defined developmental stages within the fly (62). Proteomic analysis indicated that several proteins, including a few uncharacterized adenylate cyclases, are differentially regulated between these two procyclic forms. A connection between this developmental transition and AC regulation is interesting, as it suggests priming for new environmental conditions in line with our proposed model of stage-specific functionality of ACs, and fits earlier hypotheses that cAMP signaling is linked to differentiation events. Remarkably, late-procyclics are SoMo incompetent, suggesting that only early-procyclic forms need to engage in social behaviors. The biomarker for

this early to late transition is the GPEET-procyclin surface protein, which is expressed in early procyclics but down-regulated in late procyclic forms. Here, we see that inhibition of flagellum-tip ACs results in a hyper-social phenotype, with no change in GPEET expression (data not shown). Our previous analysis of the SoMo-incompetent PDEB1 mutant, which has elevated intracellular cAMP levels, also expresses GPEET-procyclin (20). Expression of GPEET in the PDEB mutant indicates that an increase in cAMP levels can inhibit SoMo without triggering a clear differentiation from early to late, GPEET-negative procyclics, though further studies are needed to determine whether these pathways are directly linked.

Additional work from the Roditi group demonstrated that the RFT1-/- mutant line, which is incapable of engaging in social motility, shows impaired colonization of the tsetse fly (63). Studies of AC mutant and knockout lines in a tsetse fly model therefore have the capability to offer additional insights into signaling and sensing systems of *T. brucei.* It would be interesting to note whether the hyper-SoMo phenotype observed *in vitro* would manifest or be observable in an *in vivo* model. For example, if social motility corresponds to the intra-tsetse migratory routes and subsequent tissue colonizations, one might predict that the hyper-SoMo mutant would display an increased tsetse-infection rate. Of particular interest might be assessment of AC mutants, such as AC4, that do not display any apparent SoMo phenotype *in vitro.* Any phenotype gleaned from *in vivo* studies would likely indicate the presence of fly-specific ligands or signals as a regulator of cAMP signaling, and provide insight into the evolution and expansion of the AC gene family.

Summary and perspective

Microbes in their natural environments do not survive axenically, but in rich, complex environments. *Trypanosoma brucei,* which infects many mammals and uses a tsetse-fly vector, offers a prime example of the varied environments a microorganism may face in its lifecycle. cAMP signaling has been demonstrated to be important in all cultivable stages of the parasite life cycle, as evidenced by expansion of the trypanosomal adenylate cyclase family of receptor proteins. Despite their importance, most are still uncharacterized, and thus little is known about cAMP signaling pathways. Our analyses indicate that flagellar and flagellar-tip targeting sequences are contained within the C-terminal region of ACs and are necessary for flagellar localization. Gene-specific RNAi implicates cAMP signaling at the flagellum tip as a key regulator of social motility, and provides direct evidence for the microdomain organization model of cAMP signaling in the *T. brucei* flagellum. Our studies therefore offer important insights into many important aspects of trypanosomal and flagellar biology.

FIGURES

Figure 1. The C-terminus is required for flagellar targeting of adenylate cyclases (ACs) AC1 and AC2.

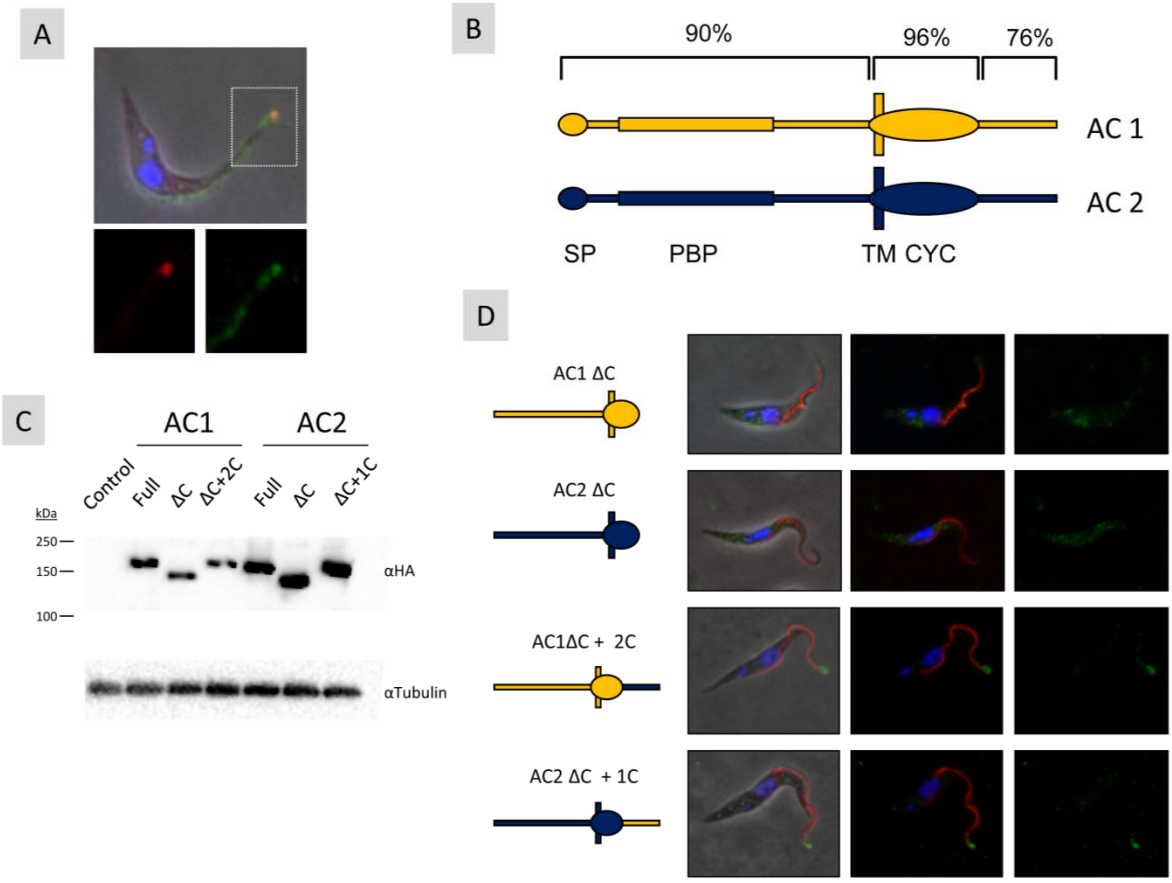

A) AC1 (red) localizes to the flagellum tip, while AC2 (green) localizes along the entire length of the flagellum. B) Schematic illustrating the % identity between AC1 and AC2. C) Western blots of whole cell lysates from cell lines expressing HA-tagged full-length or C-terminally truncated AC1 and AC2 constructs. Control is an untagged line. As indicated, blots were probed with anti-HA or anti-tubulin antibody (as loading

control). D) Immunofluorescence microscopy of AC1 and 2 C-terminal truncation mutants and chimeric proteins with the AC1 and 2 C-terminal domains swapped. Schematics on the left depict the HA-tagged AC constructs, with AC1 sequence in yellow and AC2 sequence in blue. Panels show localization of the indicated AC constructs (green) relative to PFR (red) and DAPI-stained DNA (blue).

Figure 2. Residues within the C-terminal domain are sufficient to redirect AC2 from the flagellum to the flagellum tip.

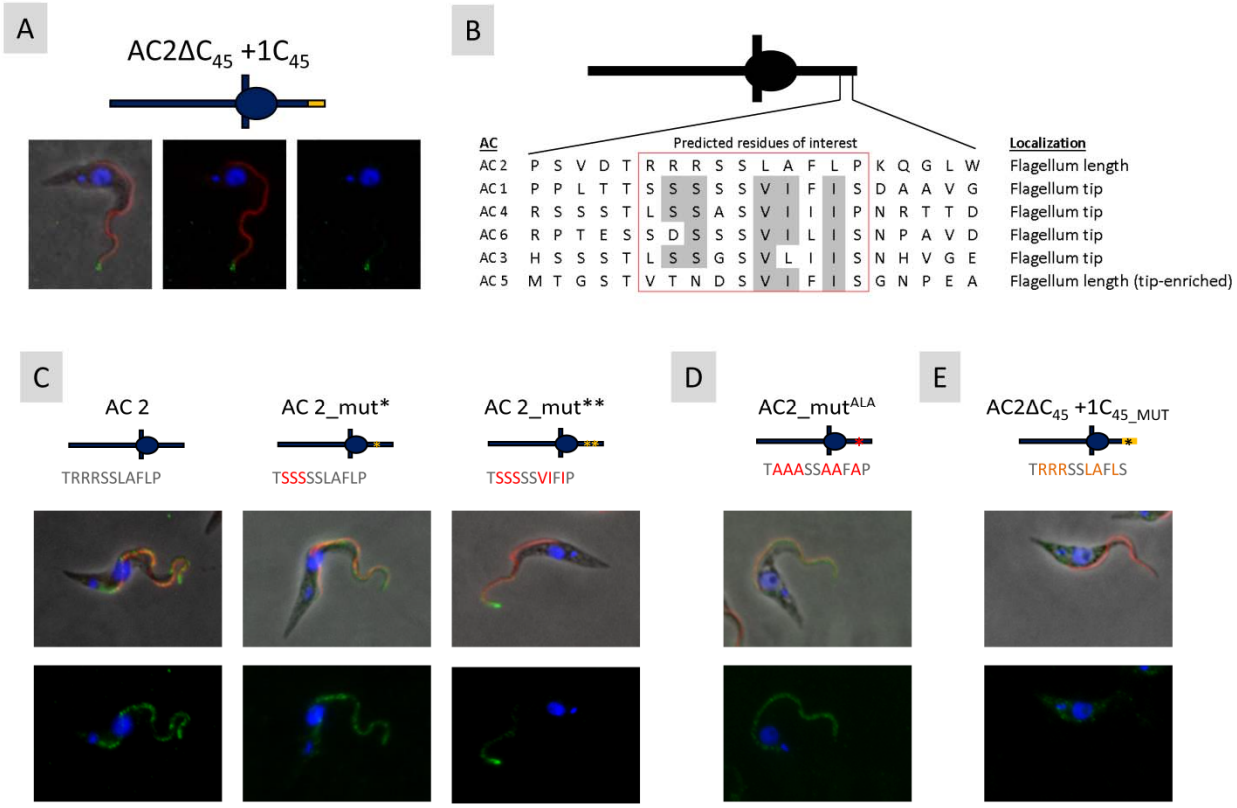

A) Localization of a chimeric AC2 protein containing the last 45 amino acids of AC1. Schematic depicts the HA-tagged construct, with AC1 sequence in yellow and AC2 sequence in blue. Immunofluorescence shows localization of the AC construct (green) relative to PFR (red) and DAPI-stained DNA (blue). B) Amino acid alignment of C-terminal domains from AC1 and 2 relative to other previously identified procyclic-specific ACs {Saada}. Localization of each protein to the flagellum or flagellum subdomains is indicated. Conserved amino acids are highlighted in grey. C-E) Immunofluorescence microscopy of HA-tagged AC2 point mutants. Schematics show the residues (red) that have been mutated. Panels show localization of the indicated AC constructs (green) relative to PFR (red) and DAPI-stained DNA (blue).

Figure 3. Redirection of AC2 to the flagellum tip rescues the social motility defect caused by AC1 knockdown.

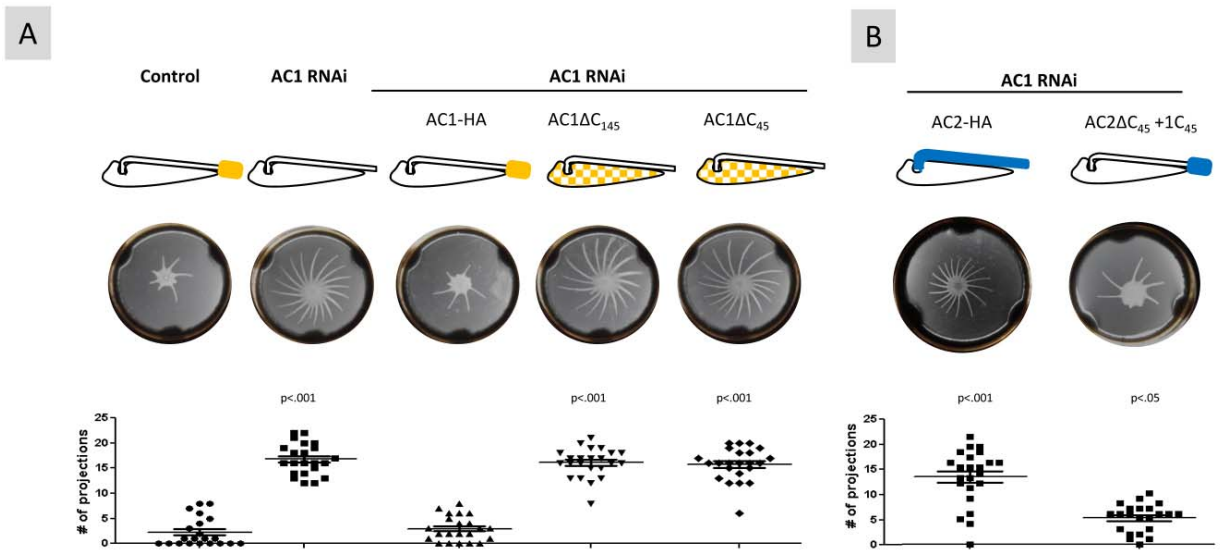

A-B) AC1 RNAi cell lines expressing the indicated RNAi-immune AC constructs were tested for their ability to perform social motility (SoMo). All cell lines were inoculated on plates containing 1 µg/ml tetracycline to induce AC1 knockdown. Control is a wild-type strain. The schematics indicate the localization of AC1 (yellow) or AC2 (blue) in each cell line. Images show a representative example of colony morphology approximately 3.5 days after inoculation. Graphs show the number of radial projections quantified from each plate, with the median number of colonies indicated by a line. Statistically significant p-values are indicated relative to control.

Supplemental Figure 1. AC1 knockdown enhances tip localization of an AC1 chimera containing the C-terminal domain of AC2.

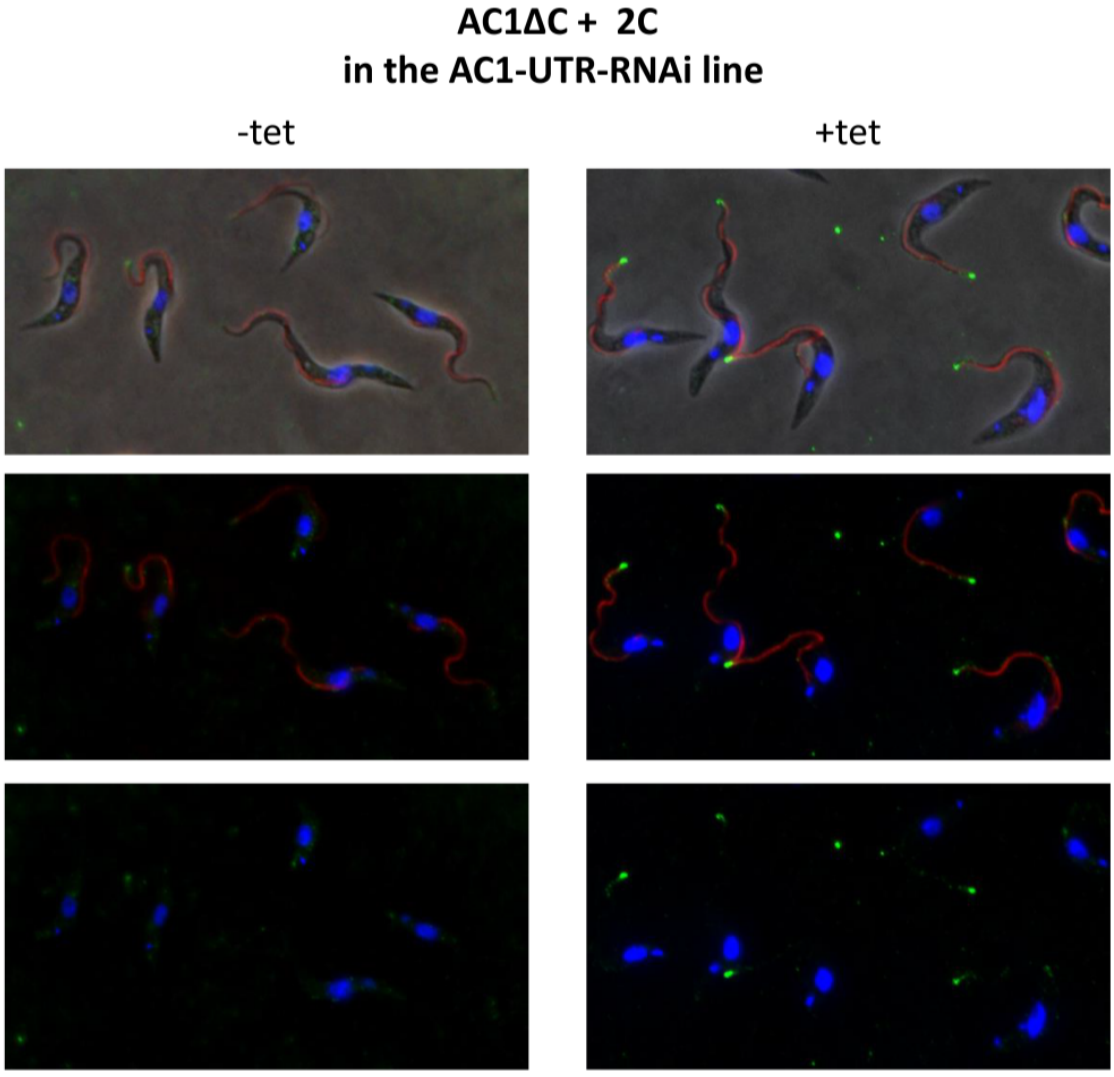

Immunofluorescence microscopy depicting localization of the chimeric protein (green) relative to PFR (red) and DAPI-stained DNA (blue). Left panels show uninduced (-Tet) conditions. Right panels show localization 48 hours after induction of AC1 RNAi (+Tet).

Supplemental Figure 2. AC1 sequences are not sufficient to drive synthetic or heterologous reporters to the flagellum.

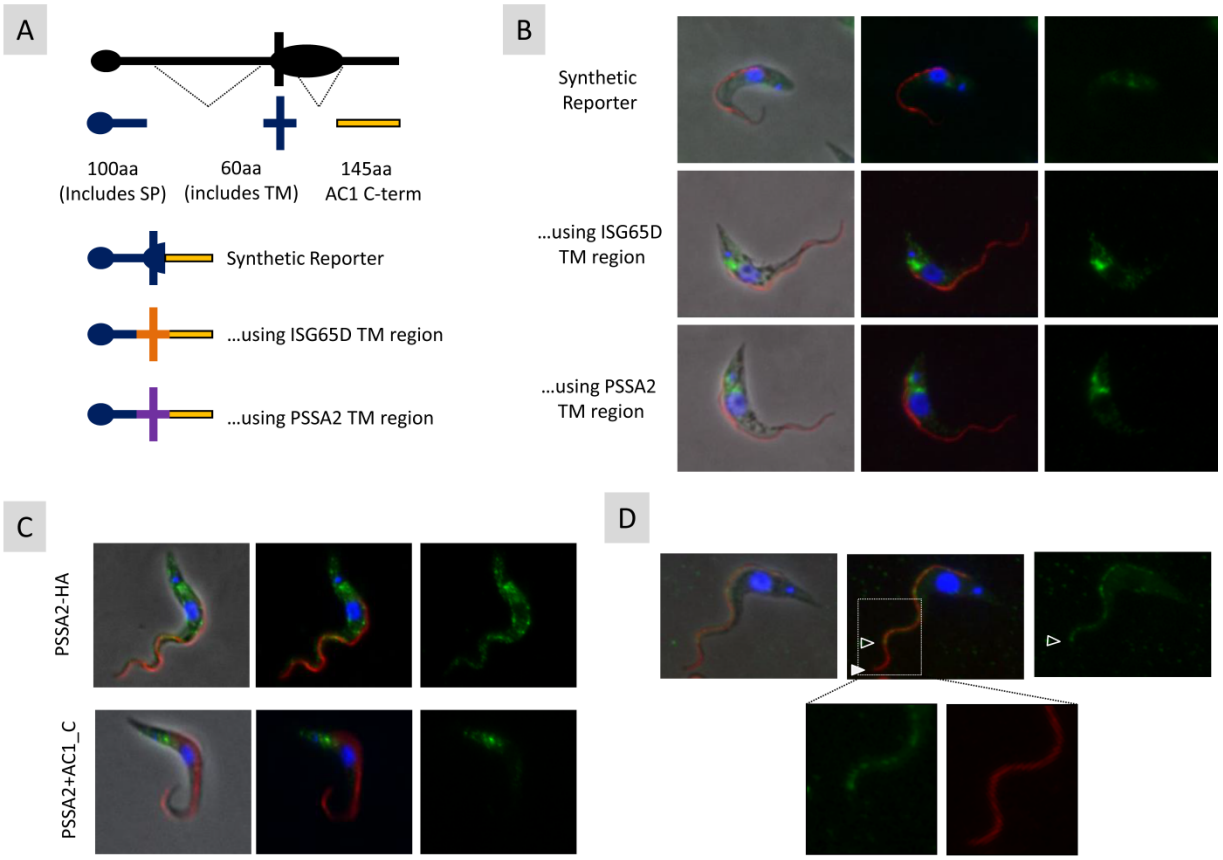

A-B) Schematic and localization of synthetically designed reporter constructs. C) Immunofluorescence microscopy of control PSSA2 compared to the PSSA2-chimeric protein expressing the AC1 C-terminal sequence. D) Immunofluorescence microscopy of FS179-chimeric protein expressing the AC1 C-terminal sequence. **All** panels show localization of the indicated AC constructs (green) relative to PFR (red) and DAPI-stained DNA (blue).

Supplemental Figure 3. AC3-HA localizes to the flagellum tip. Immunofluorescence microscopy of HA-tagged AC3.

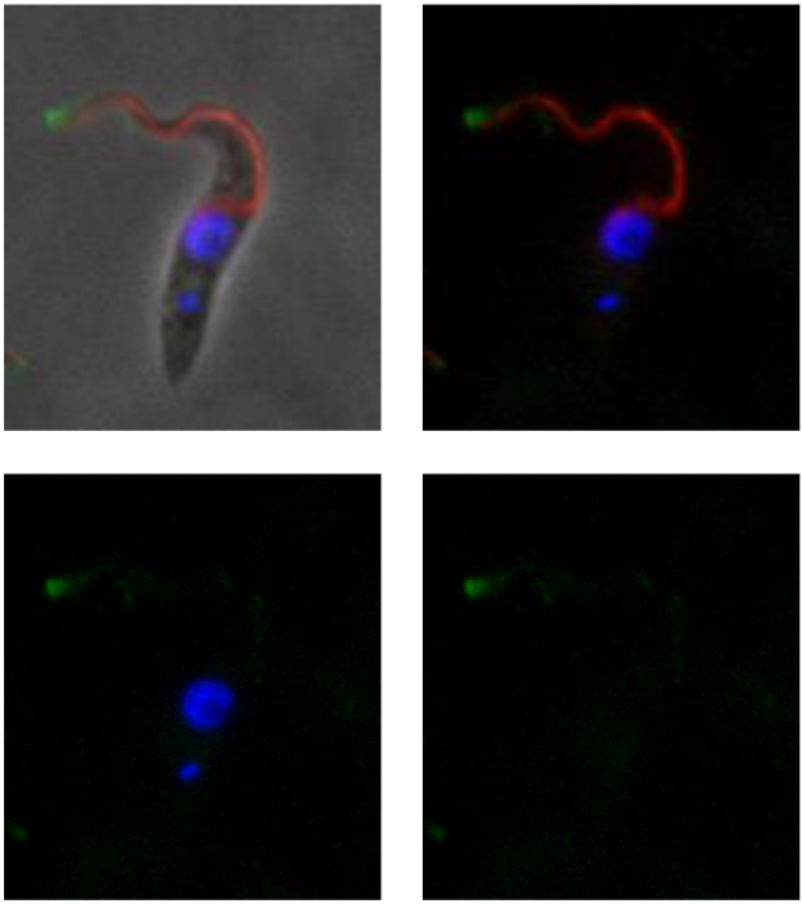

Panels show AC3-HA localization (green) relative to PFR (red) and DAPI-stained DNA (blue).

Supplemental Figure 4. AC2 chimeric and point mutants are expressed at comparable levels.

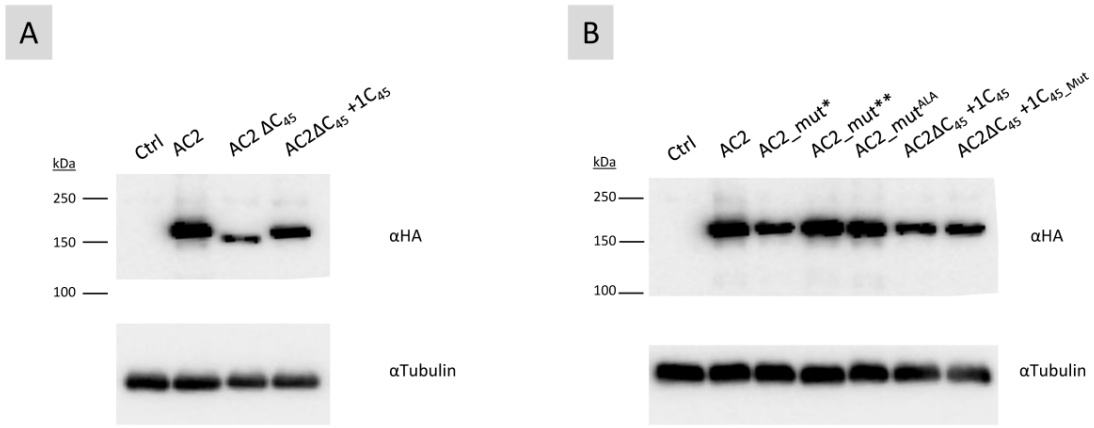

A-B) Western blots of whole cell lysates from cell lines expressing the HA-tagged AC2 constructs from Figure 2. Control is an untagged line. As indicated, blots were probed with anti-HA or anti-tubulin antibody (as loading control).

Supplemental Figure 5. Characterization of the cell lines used for the social motility assays in Figure 3.

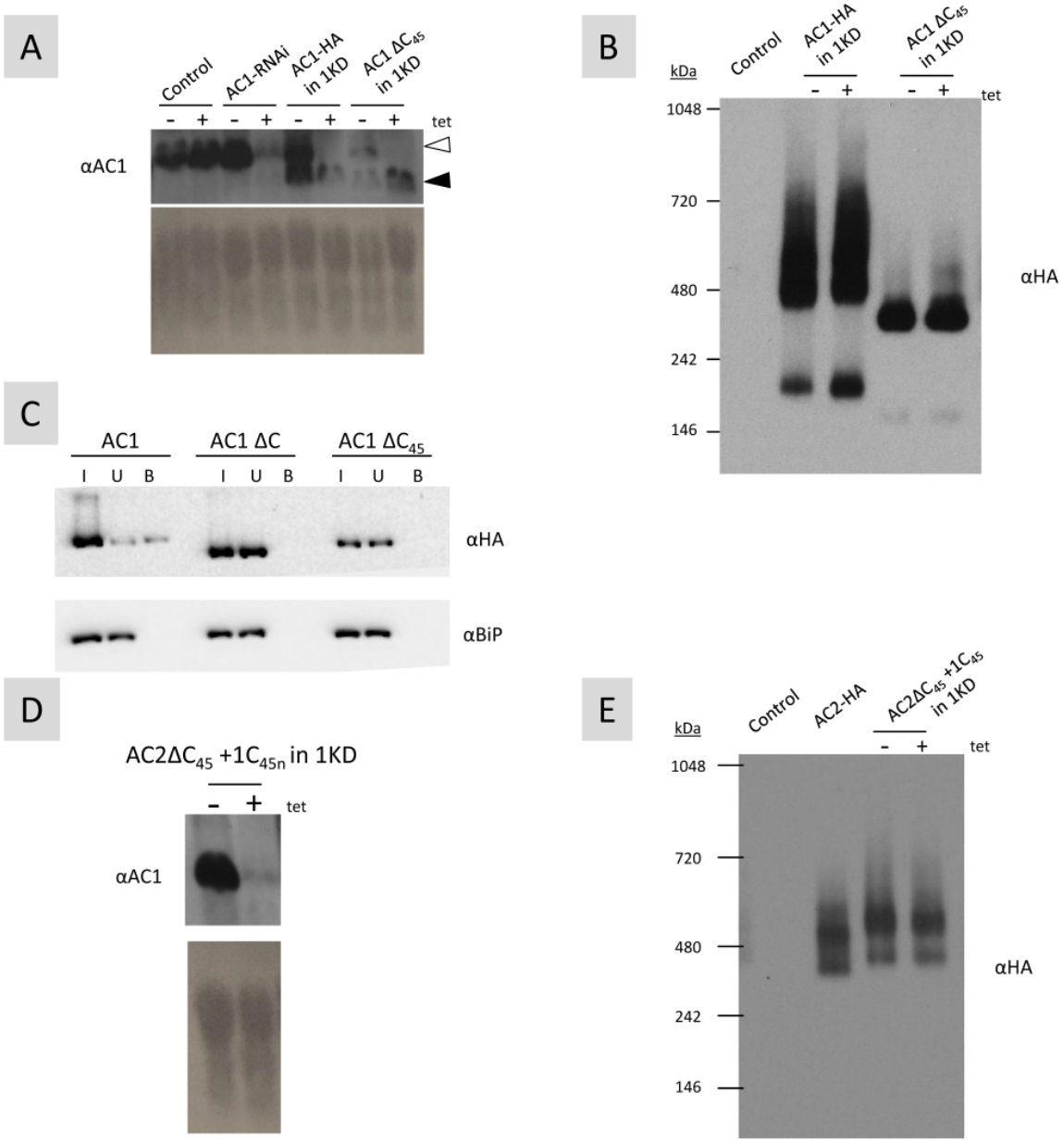

A) Northern blot probed with an AC1-specific probe. RNA was prepared from the indicated cell lines. The position of the endogenous AC1 mRNA (open arrowhead) and

transgene mRNA (closed arrowhead) are indicated. Total RNA was visualized by UC shadowing of the membrane (bottom). B) Whole cell lysates prepared from the indicated cell lines were separated by Blue Native gel electrophoresis, and transferred to a PVDF membrane and probed with anti-HA antibodies. C) The indicated cell lines were surface biotinylated then fractionated and subjected to affinity purification. Lysates were subjected to Western Blot analysis using antibodies against HA or BiP, as indicated. D) Northern blot probed with an AC1-specific probe. RNA was prepared from the indicated cell lines. Total RNA was visualized by UC shadowing of the membrane (bottom). E) Whole cell lysates prepared from the indicated cell lines were separated by Blue Native gel electrophoresis, and transferred to a PVDF membrane and probed with anti-HA antibodies.

Supplemental Table 1

Plasmids used derived from

pMOTag2H, in situ epitope tagging
pKR10, inducible expression
Modifications onto previously generated constructs

Primers used, with restriction sites underlined

Plasmid sequencing and verification of genomic integration	
AC_catalytic_F	acacgtgcaacatacctttcg
Puromycin_R	aggccttccatctgttgctg
IGR_R	gtgcctcctacacaaagggtgag
M13_F	tgtaaaacgacggccagt
M13_R	caggaaacagctatgac
pKR10seq_F	cgtcccgggctgcacgcgccttcg
pKR10seq_R	cccttcctaaccaacctgcaggcgcacctc
Northern Blot (AC1-specific probe)	
AC1_NorthernProbe_F	agtttatccagagcggtacga
AC1_NorthernProbe_R	accgccgcacctccc
Site-Directed Mutagenesis	
AC2_mut1_F	gcaataccgttgagccctccgtggacacatcaagcagctcatccctagcattcttacctt
AC2_mut1_R	aaggtaagaatgctagggatgagctgcttgatgtgtccacggagggctcaacggtattgc
AC2_mut2_F	tggacacatcaagcagctcatccgtcatattcattcctttgcaaggtctgtggcctgg
AC2_mut2_R	ccaggccacagaccttgcaaaggaatgaatatgacggatgagctgcttgatgtgtcca
AC2_mut_ala_F	ccgttgagccctccgtggacacagcggcagcgtcatccgcagcattcgcacctttgcaaggtctg
AC2_mut_ala_R	cagaccttgcaaaggtgcgaatgctgcggatgacgctgccgctgtgtccacggagggctcaacgg
AC1_mut2_F	cgaggcgacggtcgtccctagcattcttatccgacgccgccgtggg
AC1_mut2_R	cccacggcggcgtcggataagaatgctagggacgaccgtcgcctcg
AC1 Related	
AC1_ΔC_Gibson_F	actaaagggaacaaaagctgggtaccgtgtggtctatggcccgtg
AC1_ΔC_Gibson_R	cgaggcgctcgagcagtgcagcgaaggaccg
AC1_145_F	atatctcgaggcacatatgcgcctcgacagggaggtc
AC1_145_R	tatctcgaggcacttaaggttttcctcctttggggttgag
AC1_45aa_F	atggtacccatatggacttcacggcttacaacatcgctgag
AC1_45aa_R	tatctcgaggcacttaaggttttcctcctttggggttgag
AC2 Related	
AC2_ΔC_F	atggtacccgtcaatgagcttcagagaccctagcgaaggaaaactc
AC2_ΔC_R	atctcgagcatatgcagtgcagcgaaggaccgaccgaccacagc
AC2_Cterm_Gibson_F	cttcgctgcactgctcgagcgcctcgacggggaag
AC2_Cterm_Gibson_R	gtaatcaggcacatcgtaagggtactcgagttctcgttcgctgcttgtggg
Synthetic and Heterologous Reporter Testing	
PSSA2-HA_F	atataagcttatgtgcatcgaacagctcg
PSSA2-HA_R	atatcttaaggcacatatgcactgtaggatttggttgggg
AC2_N_100aa_F	atataagcttgaattcatgaatatgcttcacttggacgac
AC2_N_100aa_R	atatgggcccgacagtccagtttcgtgactct
ISG65D_TMregion_F	atatgggcccgaattcaccgaggctgcagaagtaaa
ISG65D_TMregion_R	atatgaattc tccagtgtccacatcctggg
PSSA2_TMregion_F	atatgggcccgaattcgagcgtgaaacgatgggc
PSSA2_TMregion_R	atatgaattcaggtgtatcaggatcactcgtat

Initial synthetic reporter construct generated by Genewiz, Inc.	ggtaccgaattcatgaatatgcttcacttggacgaccgcaatgcctcacccgcaccg agtggcggggaacattcccttccgacgggaggagctgtgtgtcgtgtcgccatggac acagggcccggaaaactctccggggcgtcgctggtgggcgtcatcatcggtgctac ctttgctttgtttcttatggtggctctgggcgtggttccatactttgtcctgcgcagcacc cgtgataacaacagcgcgccacatatgctcgagcccctcacaacgtcaagcagctc gtccgtcatattcatttccgacgccgccgtgcttaagtacccttacgatgtgcctgatt acgcgtacccatacgacgtgccagactacgcatacccgtacgatgtgcccgattac gcatagcaattggtcgac

References

1. Rotureau B, Van Den Abbeele J. 2013. Through the dark continent: African trypanosome development in the tsetse fly. Front Cell Infect Microbiol 3:53.
2. Pazour GJ, Bloodgood RA. 2008. Targeting proteins to the ciliary membrane. Curr Top Dev Biol 85:115-149.
3. Emmer BT, Daniels MD, Taylor JM, Epting CL, Engman DM. 2010. Calflagin inhibition prolongs host survival and suppresses parasitemia in Trypanosoma brucei infection. Eukaryot Cell 9:934-942.
4. Pazour GJ, Witman GB. 2003. The vertebrate primary cilium is a sensory organelle. Curr Opin Cell Biol 15:105-110.
5. Goetz SC, Anderson KV. 2010. The primary cilium: a signalling centre during vertebrate development. Nat Rev Genet 11:331-344.
6. Kim J, Kato M, Beachy PA. 2009. Gli2 trafficking links Hedgehog-dependent activation of Smoothened in the primary cilium to transcriptional activation in the nucleus. Proc Natl Acad Sci U S A 106:21666-21671.
7. Tobin JL, Beales PL. 2007. Bardet-Biedl syndrome: beyond the cilium. Pediatr Nephrol 22:926-936.
8. Bisgrove BW, Yost HJ. 2006. The roles of cilia in developmental disorders and disease. Development 133:4131-4143.
9. Proto WR, Castanys-Munoz E, Black A, Tetley L, Moss CX, Juliano L, Coombs GH, Mottram JC. 2011. Trypanosoma brucei metacaspase 4 is a pseudopeptidase and a virulence factor. J Biol Chem 286:39914-39925.

10. Salmon D, Vanwalleghem G, Morias Y, Denoeud J, Krumbholz C, Lhomme F, Bachmaier S, Kador M, Gossmann J, Dias FB, De Muylder G, Uzureau P, Magez S, Moser M, De Baetselier P, Van Den Abbeele J, Beschin A, Boshart M, Pays E. 2012. Adenylate cyclases of Trypanosoma brucei inhibit the innate immune response of the host. Science 337:463-466.
11. Maric D, Epting CL, Engman DM. 2010. Composition and sensory function of the trypanosome flagellar membrane. Curr Opin Microbiol 13:466-472.
12. Rohatgi R, Snell WJ. 2010. The ciliary membrane. Curr Opin Cell Biol 22:1-6.
13. Vickerman K, Tetley L, Hendry KA, Turner CM. 1988. Biology of African trypanosomes in the tsetse fly. Biol Cell 64:109-119.
14. West S.A. DSP, Buckling A., Gardner A., Griffin A.S. 2007. The Social Lives of Microbes. Annual Review of Ecology, Evolution, and Systematics 38:53-77.
15. Oberholzer M, Lopez MA, McLelland BT, Hill KL. 2010. Social motility in african trypanosomes. PLoS Pathog 6:e1000739.
16. Bastin P, Rotureau B. 2015. Social motility in African trypanosomes: fact or model? Trends Parasitol 31:37-38.
17. Imhof S, Knusel S, Gunasekera K, Vu XL, Roditi I. 2014. Social motility of African trypanosomes is a property of a distinct life-cycle stage that occurs early in tsetse fly transmission. PLoS Pathog 10:e1004493.
18. Imhof S, Vu XL, Butikofer P, Roditi I. 2015. A glycosylation mutant of Trypanosoma brucei links social motility defects in vitro to impaired colonisation of tsetse in vivo. Eukaryot Cell.

19. Lopez MA, Saada EA, Hill KL. 2015. Insect stage-specific adenylate cyclases regulate social motility in African trypanosomes. Eukaryot Cell 14:104-112.

20. Oberholzer M, Saada EA, Hill KL. 2015. Cyclic AMP Regulates Social Behavior in African Trypanosomes. MBio 6.

21. Kuchma SL, Brothers KM, Merritt JH, Liberati NT, Ausubel FM, O'Toole GA. 2007. BifA, a cyclic-Di-GMP phosphodiesterase, inversely regulates biofilm formation and swarming motility by Pseudomonas aeruginosa PA14. J Bacteriol 189:8165-8178.

22. Merritt JH, Brothers KM, Kuchma SL, O'Toole GA. 2007. SadC reciprocally influences biofilm formation and swarming motility via modulation of exopolysaccharide production and flagellar function. J Bacteriol 189:8154-8164.

23. Salmon D, Bachmaier S, Krumbholz C, Kador M, Gossmann JA, Uzureau P, Pays E, Boshart M. 2012. Cytokinesis of Trypanosoma brucei bloodstream forms depends on expression of adenylyl cyclases of the ESAG4 or ESAG4-like subfamily. Mol Microbiol 84:225-242.

24. Saada EA, Kabututu ZP, Lopez M, Shimogawa MM, Langousis G, Oberholzer M, Riestra A, Jonsson ZO, Wohlschlegel JA, Hill KL. 2014. Insect stage-specific receptor adenylate cyclases are localized to distinct subdomains of the Trypanosoma brucei Flagellar membrane. Eukaryot Cell 13:1064-1076.

25. Shimogawa MM, Saada EA, Vashisht AA, Barshop WD, Wohlschlegel JA, Hill KL. 2015. Cell surface proteomics provides insight into stage-specific remodeling of the host-parasite interface in Trypanosoma brucei. Mol Cell Proteomics.

26. Wirtz E, Leal S, Ochatt C, Cross GA. 1999. A tightly regulated inducible expression system for conditional gene knock-outs and dominant-negative genetics in *Trypanosoma brucei*. Mol. Biochem. Parasitol. 99:89-101.

27. Oberholzer M, Lopez MA, Ralston KS, Hill KL. 2009. Approaches for functional analysis of flagellar proteins in African trypanosomes. Methods in Cell Biology 93:21-57.

28. Oberholzer M, Morand S, Kunz S, Seebeck T. 2006. A vector series for rapid PCR-mediated C-terminal in situ tagging of Trypanosoma brucei genes. Mol Biochem Parasitol 145:117-120.

29. Oberholzer M, Langousis G, Nguyen HT, Saada EA, Shimogawa MM, Jonsson ZO, Nguyen SM, Wohlschlegel JA, Hill KL. 2011. Independent analysis of the flagellum surface and matrix proteomes provides insight into flagellum signaling in mammalian-infectious Trypanosoma brucei. Mol Cell Proteomics 10:M111 010538.

30. Ralston KS, Hill KL. 2006. Trypanin, a Component of the Flagellar Dynein Regulatory Complex, Is Essential in Bloodstream Form African Trypanosomes. PLoS Pathog 2:873-882, e101 doi:810.1371/journal.ppat.0020101.

31. Hill KL, Hutchings NR, Russell DG, Donelson JE. 1999. A novel protein targeting domain directs proteins to the anterior cytoplasmic face of the flagellar pocket in African trypanosomes. J. Cell Sci. 112:3091-3101.

32. Chu DT, Klymkowsky MW. 1989. The appearance of acetylated alpha-tubulin during early development and cellular differentiation in Xenopus. Dev Biol 136:104-117.

33. Bangs JD, Uyetake L, Brickman MJ, Balber AE, Boothroyd JC. 1993. Molecular cloning and cellular localization of a BiP homologue in Trypanosoma brucei. Divergent ER retention signals in a lower eukaryote. J Cell Sci 105:1101-1113.

34. Merchant S, Hill K, Howe G. 1991. Dynamic interplay between two copper-titrating components in the transcriptional regulation of cyt c6. Embo J 10:1383-1389.

35. Lopez MA, Saada EA, Hill KL. 2015. Insect stage-specific adenylate cyclases regulate social motility in African trypanosomes. Eukaryot Cell 14:104-112.

36. Saada EA, Kabututu ZP, Lopez M, Shimogawa MM, Langousis G, Oberholzer M, Riestra A, Jonsson ZO, Wohlschlegel JA, Hill KL. 2014. Insect stage-specific receptor adenylate cyclases are localized to distinct subdomains of the Trypanosoma brucei Flagellar membrane. Eukaryot Cell 13:1064-1076.

37. Chung WL, Carrington M, Field MC. 2004. Cytoplasmic targeting signals in transmembrane invariant surface glycoproteins of trypanosomes. J Biol Chem 279:54887-54895.

38. Fragoso CM, Schumann Burkard G, Oberle M, Renggli CK, Hilzinger K, Roditi I. 2009. PSSA-2, a membrane-spanning phosphoprotein of Trypanosoma brucei, is required for efficient maturation of infection. PLoS One 4:e7074.

39. Nachury MV, Seeley ES, Jin H. 2010. Trafficking to the ciliary membrane: how to get across the periciliary diffusion barrier? Annu Rev Cell Dev Biol 26:59-87.

40. Follit JA, Li L, Vucica Y, Pazour GJ. 2010. The cytoplasmic tail of fibrocystin contains a ciliary targeting sequence. Journal of Cell Biology 188:21-28.

41. Bieger B, Essen LO. 2001. Structural analysis of adenylate cyclases from Trypanosoma brucei in their monomeric state. EMBO Journal 20:433-445.

42. Bloodgood RA. 2012. The future of ciliary and flagellar membrane research. Mol Biol Cell 23:2407-2411.

43. Calvet JP. 2003. Ciliary signaling goes down the tubes. Nat Genet 33:113-114.

44. Huangfu D, Anderson KV. 2005. Cilia and Hedgehog responsiveness in the mouse. Proc Natl Acad Sci U S A 102:11325-11330.

45. Scholey JM. 2008. Intraflagellar transport motors in cilia: moving along the cell's antenna. J Cell Biol 180:23-29.

46. Singla V, Reiter JF. 2006. The primary cilium as the cell's antenna: signaling at a sensory organelle. Science 313:629-633.

47. Sloboda RD. 2005. Intraflagellar transport and the flagellar tip complex. J Cell Biochem 94:266-272.

48. Hu Q, Milenkovic L, Jin H, Scott MP, Nachury MV, Spiliotis ET, Nelson WJ. 2010. A septin diffusion barrier at the base of the primary cilium maintains ciliary membrane protein distribution. Science 329:436-439.

49. Tam BM, Moritz OL, Hurd LB, Papermaster DS. 2000. Identification of an outer segment targeting signal in the COOH terminus of rhodopsin using transgenic Xenopus laevis. J Cell Biol 151:1369-1380.

50. Ammon C, Schafer J, Kreuzer OJ, Meyerhof W. 2002. Presence of a plasma membrane targeting sequence in the amino-terminal region of the rat somatostatin receptor 3. Arch Physiol Biochem 110:137-145.

51. Pazour GJ, Baker SA, Deane JA, Cole DG, Dickert BL, Rosenbaum JL, Witman GB, Besharse JC. 2002. The intraflagellar transport protein, IFT88, is essential for vertebrate photoreceptor assembly and maintenance. J Cell Biol 157:103-113.

52. Blacque OE, Sanders AA. 2014. Compartments within a compartment: what C. elegans can tell us about ciliary subdomain composition, biogenesis, function, and disease. Organogenesis 10:126-137.

53. Czarnecki PG, Shah JV. 2012. The ciliary transition zone: from morphology and molecules to medicine. Trends Cell Biol 22:201-210.

54. Reiter JF, Blacque OE, Leroux MR. 2012. The base of the cilium: roles for transition fibres and the transition zone in ciliary formation, maintenance and compartmentalization. EMBO Rep 13:608-618.

55. Salmon D, Bachmaier S, Krumbholz C, Kador M, Gossmann JA, Uzureau P, Pays E, Boshart M. 2012. Cytokinesis of Trypanosoma brucei bloodstream forms depends on expression of adenylyl cyclases of the ESAG4 or ESAG4-like subfamily. Mol Microbiol 84:225-242.

56. Gould MK, Bachmaier S, Ali JA, Alsford S, Tagoe DN, Munday JC, Schnaufer AC, Horn D, Boshart M, de Koning HP. 2013. Cyclic AMP Effectors in African Trypanosomes Revealed by Genome-Scale RNA Interference Library Screening for Resistance to the Phosphodiesterase Inhibitor CpdA. Antimicrob Agents Chemother 57:4882-4893.

57. Johnson JL, Leroux MR. 2010. cAMP and cGMP signaling: sensory systems with prokaryotic roots adopted by eukaryotic cilia. Trends Cell Biol 20:435-444.

58. Rolin S, Paindavoine P, Hanocq-Quertier J, Hanocq F, Claes Y, Le Ray D, Overath P, Pays E. 1993. Transient adenylate cyclase activation accompanies differentiation of Trypanosoma brucei from bloodstream to procyclic forms. Mol Biochem Parasitol 61:115-125.

59. Rolin S, Hanocq-Quertier J, Paturiaux-Hanocq F, Nolan D, Salmon D, Webb H, Carrington M, Voorheis P, Pays E. 1996. Simultaneous but independent activation of adenylate cyclase and glycosylphosphatidylinositol-phospholipase C under stress conditions in Trypanosoma brucei. J Biol Chem 271:10844-10852.

60. Reuner B, Vassella E, Yutzy B, Boshart M. 1997. Cell density triggers slender to stumpy differentiation of Trypanosoma brucei bloodstream forms in culture. Mol Biochem Parasitol 90:269-280.

61. Laxman S, Riechers A, Sadilek M, Schwede F, Beavo JA. 2006. Hydrolysis products of cAMP analogs cause transformation of Trypanosoma brucei from slender to stumpy-like forms. Proc Natl Acad Sci U S A 103:19194-19199.

62. Imhof S, Knusel S, Gunasekera K, Vu XL, Roditi I. 2014. Social motility of African trypanosomes is a property of a distinct life-cycle stage that occurs early in tsetse fly transmission. PLoS Pathog 10:e1004493.

63. Imhof S, Vu XL, Butikofer P, Roditi I. 2015. A glycosylation mutant of Trypanosoma brucei links social motility defects in vitro to impaired colonisation of tsetse in vivo. Eukaryot Cell.

Chapter VII:

Social behaviors of *Trypanosoma brucei*

PREFACE

The following chapter, at time of dissertation submission, is a manuscript draft in preparation. We were invited by the journal PLOS Pathogens to contribute to their Pearls series and discuss recent works and applications of trypanosomal social motility. These mini-reviews are meant to be shaped as short, educational articles tailored for graduate students and post-doctoral researchers. The following manuscript is authored by Edwin A. Saada, Stephanie DeMarco, and Kent Hill.

Microbial social behavior: "The whole is greater than the sum of the parts"

In their natural environments, microbes are not found in isolation, but live in groups, where the ability to communicate and cooperate with friends, while thwarting activities of enemies is of paramount importance (1). The capacity for interaction among cells in a group makes possible social behaviors that present as emergent properties of the group and are not evident in individuals. Examples of microbial social behaviors include quorum sensing (QS) as a means to assess population density, allowing coordinated gene expression across a community and limiting premature expenditure of resources. Other social behaviors include those occurring in the context of surfaces, such as biofilm formation and various forms of swarming motility across surfaces as seen in bacteria and slime molds. Microbial social activities provide a number of advantages for free-living and pathogenic species and recognizing social behavior as a ubiquitous property of bacteria has transformed our view of microbiology and microbial pathogenesis (1, 2).

However, this paradigm has not been applied to protozoan parasites, which are responsible for tremendous human suffering worldwide and are also capable of social interactions, although they are not generally considered in this context. This is exemplified by the discovery that the malaria causing parasites, *Plasmodium spp*, adjust their gamete sex-ratio in response to the diversity of the parasite population (3), and the long known QS-dependent differentiation of long slender to short stumpy bloodstream forms of *Trypanosoma brucei (4).* More recently, the discovery of social motility (SoMo) in *T. brucei* revealed a previously unrecognized aspect of trypanosome biology and highlights the capacity of these organisms for group-level behavior (5).

Several recent studies of SoMo emphasize the potential for social behavior concepts to provide insight into parasite biology, which is the focus of this review.

Social motility in *Trypanosoma brucei*

African trypanosomes are protozoan parasites that cause sleeping sickness in humans and nagana in livestock. These parasites, e.g. *T. brucei* and related species, constitute a substantial medical and economic burden across a 9-million km^2 region of sub-Saharan Africa, where 60 million people live at risk of infection (6). They are transmitted between mammalian hosts by blood-feeding tsetse flies. Most *T. brucei* studies consider the parasites as individual cells in suspension cultures, yet in both the mammalian host and insect vector, the organism lives on tissue surfaces. This is most evident in the tsetse fly, where the parasite undergoes extensive movement across fly tissue surfaces, culminating in the colonization of the salivary gland epithelium (7).

In bacteria, surface cultivation influences microbe physiology and pathogenesis. To understand influence of surfaces on trypanosome biology, Oberholzer and colleagues cultivated procyclic form (insect midgut stage) *T. brucei* on semisolid agarose plates. This led to the surprising observation that individual parasites collected into groups, forming a densely-packed colony. Ultimately, parasites collectively form projections migrating radially outward from the center, synchronously moving across the agar surface. Although individual parasites can move laterally the group only moves at the leading edge and can alter their direction to

avoid other groups of parasites, indicating that the parasites sense and respond to diffusible signals. This process was termed "social motility" because of analogies to social motility in bacteria (5).

….but why would a parasite need to be social? What does social motility do?

In bacteria social behaviors are ubiquitous, and provide numerous advantages, including increased protection from host defenses, greater accessibility to nutrients, opportunities for genetic exchange, and an enhanced ability to penetrate and move across surfaces (1, 8-10). Although the *in vivo* ramifications of *T. brucei* social motility are not yet known, it's likely that *the parasite* benefits from the same advantages as other microbes.

In the insect vector, *T. brucei* is faced with immense challenges. In order for parasites to complete their life cycle and ensure transmission, they must reach and colonize the fly's salivary gland epithelium, where they differentiate into mammalian-infective forms (7). This journey begins within the midgut and is fraught with hazards as they cross through and across several tissues. They must overcome the fly immune system consisting of antimicrobial peptides and lectins, harsh alkaline conditions in the midgut, and competition for resources (7, 11). Therefore, the ability of the parasites to sense, communicate, and cooperate in collective group behaviors *in vitro* is thought to reflect distinct parasite features required to overcome obstacles and establish *in vivo* infections.

Recent work from the Roditi group supports these hypotheses. They propose that procyclic-form parasites are divided into two classes: early-procyclics, representing initial fly-infection stages, and late-procyclics, representing later fly-infection stages. They see that only early-procyclics are SoMo competent, suggesting that social motility is a characteristic of this specific procyclic lifecycle stage (12). Additionally, an Rft1-mutant line, which fails to generate N-linked glycans, was found to be SoMo incompetent and significantly defective in establishing an *in vivo* fly infection (13). This work provides the first correlation between *in vitro* social motility defects to impaired *in vivo* colonization of the tsetse fly. Future work will be needed to test Rft1 directly for its role in SoMo. In addition, social motility mutants isolated *in vitro* will need to be studied for their role *in vivo* in fly infection.

How does it work? What are the known signaling pathways that impact SoMo?

A universal requirement of microbial social behaviors is the ability to sense respond to environmental signals. Unfortunately, signal transduction pathways in *T. brucei* are virtually uncharacterized (14). In other systems, the eukaryotic flagellum has been characterized as a multifunctional, signaling organelle, and much work the last few years has focused on the trypanosome flagellum as a signaling platform (15-17). It's long been known that the trypanosome flagellum plays a critical role in insect-stage parasites, as it integrates into the tsetse's salivary gland epithelium as part of the differentiation process.

In other systems, the eukaryotic flagellum is known to be a multifunctional, signaling organelle. In 2014, Saada *et al* identified a subset of procyclic-specific, receptor-type adenylate cylases (18). Adenylate cyclases (ACs) catalyze cyclic-AMP, while phosphodiesterases (PDEs) degrade it. Cyclic-nucleotide signaling systems have been well characterized in other flagellated organisms, and are involved in photo-transduction, olfactory sensation, and many other signaling pathways (19). ACs comprise one of the largest gene families in *T. brucei,* and although components of cAMP signaling have long been known to be in the parasite flagellum, they have not been well characterized (20). Notably, Saada *et al* localized some ACs along the flagellar length, while others specifically localized to the flagellum tip, indicating a specialization of flagellum subdomains. Trypanosomal ACs are novel in structure, with a single catalytic domain and large, extracellular ligand binding domain, prompting the hypothesis that some must perform procyclic-specific functionalities.

A procyclic-specific functionality was a stark contrast to the prevailing model. ESAG4 is a bloodstream-specific AC, and has been linked to viability and virulence defects (21, 22). It'd long been thought that the other ACs were *constitutively* expressed and redundant in function. Social motility therefore offered the first opportunity to assess the putative sensory roles of these proteins in procyclic parasites. Lopez *et al* utilized gene-specific RNAi against these procyclic-ACs, finding no significant difference in cell viability, morphology, or motility in suspension culture (23). However, when subjected to SoMo assays a new phenotype was discovered: the trypanosomes regularly formed far more projections, in what was dubbed hyper-SoMo. Utilization of specific point mutations within the catalytic domain implicated cAMP-

specific functionality, rather than just loss of the protein. This study was the first to identify genes regulating an aspect of trypanosomal social behavior, as well as the first procyclic-specific functionality of cAMP signaling.

In complementary studies, Oberholzer *et al* interrogated the role of phosphodiesterases, which degrade cAMP (24). Using genetic and pharmaceutical inhibition of PDEB1, progression of social motility progression was blocked, such that the parasites never formed radial projections. Generation of a cAMP-specific FRET sensor allowed for *in vivo* imaging of cAMP levels, noting a massive increase in intracellular cAMP during PDEB inhibition, suggesting that increases in cAMP block social motility. To test this, they utilized membrane-permeable compounds, showing that non-hydrolysable and hydrolysable cAMP analogues have strong SoMo inhibitory effects, whereas downstream metabolic products such as AMP and adenosine show little response. Oberholzer *et al* conducted trans-complementation assays, utilizing strains of control and mutant parasites that constitutively express either GFP or RFP. Motility mutants, which are incapable of SoMo, are restricted to growth by clonal expansion. When co-inoculated with control cells, the motility mutants are found restricted to the center of the colony, and are never found in the radial projections. In contrast, PDEB1 mutants are capable of moving freely within the community. Both PDEB1 mutants and control cells are found at equal ratios at the center of the colony, at the base of the radial projections, and even at the distal tip. This indicates that the PDEB1 mutants are socially-defective, and need a helping hand. The mechanisms or signaling factors have not yet been identified.

What do these works tell us about signaling in *T. brucei*?

These studies have uncovered new cAMP-signaling pathways in *T. brucei* that are life-stage specific. In bloodstream-stage parasites, cAMP and metabolic byproducts are potent anti-proliferatives, and PDE inhibition is lethal. In contrast, procyclic-stage parasites show virtually no ill effect in similar assays. However, cAMP levels critically impact the ability of the procyclic-stage parasites to perform social motility. These complementary works suggest a cAMP-gradient model for regulation of social motility. When cAMP is decreased (by AC inhibition or inactivation), social motility is enhanced. When cAMP is increased (by inhibition of PDEB, or usage of permeable cAMP analogues), social motility is blocked.

This model is analogous to what's been described in *Pseudomonas spp. (25, 26).* With context to the environmental conditions, pseudomonads can decide to create a biofilm, or to engage in swarming motility. However, loss of the c-di-GMP specific phosphodiesterase results in them only generating biofilms when grown on a surface. Conversely, loss of a c-di-GMP producing cyclase results in a constitutive, hyper-swarming state, indicating that Pseudomonas also uses cyclic-nucleotide signaling to control its social behavior.

Research into quorum sensing and social behaviors of microbes have unveiled a vast array of diverse signaling systems (1). Pseudomonas, for example, additionally uses rhamnolipids. *Paenibacillus dendritiformis* utilizes a specific protease (substilin) to inhibit rival communities during swarming motility (27). Other microbes use production of extracellular polysaccharides, peptides or hormones such as homoserine

lactones, or even cell-cell contact depending signaling to regulate their behaviors (1, 28, 29). These findings expand what is known about biological mechanisms, demonstrating that there are multiple ways to achieve a common goal, and are often targets for species-specific clinical intervention.

How might studies on social behaviors impact the average person?

The interplay between different microbes has long been a field of interest, particularly when it comes to reaping the benefits. In order to gain a competitive advantage some competing microbes, in what's known as microbial warfare, can produce inhibitory or lethal compounds, many of which have been developed into modern antibiotics for clinical usage, or products for industrial and biomedical applications, as discussed earlier. Modern humanity has massively benefited from co-opting microbial systems.

There are often quite unexpected uses as well. *Physarum polycephalum* is a slime mold that is being used as a 'living computer' to help generate more efficient, adaptable networks (30). When given irregularly spaced food sources, this mold is able to generate the shortest path between multiple points, can solve labyrinth mazes, and when the food is spaced to represent metropolitan cities, can generate a network map similar considered superior to existing railroad infrastructure (31). Social behaviors therefore offer a surprising amount of innovative capability. Next time you're stuck in traffic, ask yourself whether a slime mold could have done a better job designing the freeway on and off ramps.

What's the future of social motility in trypanosomes?

SoMo has proven to be a great sensory assay for procyclic-stage parasites. Previously, the only available assays were physical assessments of parasites (growth, morphology, standard motility), or comparing *in vivo* infection rates in tsetse fly studies. The corroboration that a SoMo incompetent mutant line is ineffective at establishing normal fly infections makes SoMo a very promising *in vitro* performance assay. For example, in conjunction with existing RNAi libraries, one could rapidly screen through hundreds of mutant lines in a controlled, experimental setting. Such studies are impractical or very challenging to do within an *in vivo* model, allowing SoMo to be used in conjunctions with modern systems biology approaches. It's known that SoMo requires propulsive motility, and thus SoMo is an effective way of finding motility mutants (33). Through the studies described earlier, we know that cAMP signaling systems are involved in regulation of SoMo.

Analyses of trypanosome cell and flagellar surface proteomes find a wide array of putative signaling pathways, with ligand-binding proteins, kinases, calcium channels, ATPases, etc. (16, 32). Functional analyses using SoMo as a proxy assay may uncover new roles for signaling and sensation. Additionally, SoMo can be used in conjunction with modern systems biology approaches, such as RNA-seq, proteomics, and metabolomics, which will offer massive resolving power and the technical capability to ask critical and intriguing scientific questions.

References

1. West S.A. DSP, Buckling A., Gardner A., Griffin A.S. 2007. The Social Lives of Microbes. Annual Review of Ecology, Evolution, and Systematics 38:53-77.
2. Connell JL, Wessel AK, Parsek MR, Ellington AD, Whiteley M, Shear JB. 2010. Probing prokaryotic social behaviors with bacterial "lobster traps". MBio 1.
3. Reece SE, Drew DR, Gardner A. 2008. Sex ratio adjustment and kin discrimination in malaria parasites. Nature 453:609-614.
4. Reuner B, Vassella E, Yutzy B, Boshart M. 1997. Cell density triggers slender to stumpy differentiation of Trypanosoma brucei bloodstream forms in culture. Mol Biochem Parasitol 90:269-280.
5. Oberholzer M, Lopez MA, McLelland BT, Hill KL. 2010. Social motility in african trypanosomes. PLoS Pathog 6:e1000739.
6. Yamey G, Torreele E. 2002. The world's most neglected diseases. Bmj 325:176-177.
7. Rotureau B, Van Den Abbeele J. 2013. Through the dark continent: African trypanosome development in the tsetse fly. Front Cell Infect Microbiol 3:53.
8. Shapiro JA. 1998. Thinking about bacterial populations as multicellular organisms. Annu Rev Microbiol 52:81-104.
9. Fraser GM, Hughes C. 1999. Swarming motility. Curr Opin Microbiol 2:630-635.
10. Harshey RM. 2003. Bacterial motility on a surface: many ways to a common goal. Annu Rev Microbiol 57:249-273.

11. Dyer NA, Rose C, Ejeh NO, Acosta-Serrano A. 2013. Flying tryps: survival and maturation of trypanosomes in tsetse flies. Trends Parasitol 29:188-196.
12. Imhof S, Knusel S, Gunasekera K, Vu XL, Roditi I. 2014. Social motility of African trypanosomes is a property of a distinct life-cycle stage that occurs early in tsetse fly transmission. PLoS Pathog 10:e1004493.
13. Imhof S, Vu XL, Butikofer P, Roditi I. 2015. A glycosylation mutant of Trypanosoma brucei links social motility defects in vitro to impaired colonisation of tsetse in vivo. Eukaryot Cell.
14. Pays E, Nolan DP. 1998. Expression and function of surface proteins in Trypanosoma brucei. Mol Biochem Parasitol 91:3-36.
15. Maric D, Epting CL, Engman DM. 2010. Composition and sensory function of the trypanosome flagellar membrane. Curr Opin Microbiol 13:466-472.
16. Oberholzer M, Langousis G, Nguyen HT, Saada EA, Shimogawa MM, Jonsson ZO, Nguyen SM, Wohlschlegel JA, Hill KL. 2011. Independent analysis of the flagellum surface and matrix proteomes provides insight into flagellum signaling in mammalian-infectious Trypanosoma brucei. Mol Cell Proteomics 10:M111 010538.
17. Singla V, Reiter JF. 2006. The primary cilium as the cell's antenna: signaling at a sensory organelle. Science 313:629-633.
18. Saada EA, Kabututu ZP, Lopez M, Shimogawa MM, Langousis G, Oberholzer M, Riestra A, Jonsson ZO, Wohlschlegel JA, Hill KL. 2014. Insect stage-specific receptor adenylate cyclases are localized to distinct subdomains of the Trypanosoma brucei Flagellar membrane. Eukaryot Cell 13:1064-1076.

19. Johnson JL, Leroux MR. 2010. cAMP and cGMP signaling: sensory systems with prokaryotic roots adopted by eukaryotic cilia. Trends Cell Biol 20:435-444.

20. Seebeck T, Gong K, Kunz S, Schaub R, Shalaby T, Zoraghi R. 2001. cAMP signalling in Trypanosoma brucei. Int J Parasitol 31:491-498.

21. Salmon D, Vanwalleghem G, Morias Y, Denoeud J, Krumbholz C, Lhomme F, Bachmaier S, Kador M, Gossmann J, Dias FB, De Muylder G, Uzureau P, Magez S, Moser M, De Baetselier P, Van Den Abbeele J, Beschin A, Boshart M, Pays E. 2012. Adenylate cyclases of Trypanosoma brucei inhibit the innate immune response of the host. Science 337:463-466.

22. Salmon D, Bachmaier S, Krumbholz C, Kador M, Gossmann JA, Uzureau P, Pays E, Boshart M. 2012. Cytokinesis of Trypanosoma brucei bloodstream forms depends on expression of adenylyl cyclases of the ESAG4 or ESAG4-like subfamily. Mol Microbiol 84:225-242.

23. Lopez MA, Saada EA, Hill KL. 2015. Insect stage-specific adenylate cyclases regulate social motility in African trypanosomes. Eukaryot Cell 14:104-112.

24. Oberholzer M, Saada EA, Hill KL. 2015. Cyclic AMP Regulates Social Behavior in African Trypanosomes. MBio 6.

25. Kuchma SL, Brothers KM, Merritt JH, Liberati NT, Ausubel FM, O'Toole GA. 2007. BifA, a cyclic-Di-GMP phosphodiesterase, inversely regulates biofilm formation and swarming motility by Pseudomonas aeruginosa PA14. J Bacteriol 189:8165-8178.

26. Merritt JH, Brothers KM, Kuchma SL, O'Toole GA. 2007. SadC reciprocally influences biofilm formation and swarming motility via modulation of

exopolysaccharide production and flagellar function. J Bacteriol 189:8154-8164.

27. Be'er A, Ariel G, Kalisman O, Helman Y, Sirota-Madi A, Zhang HP, Florin EL, Payne SM, Ben-Jacob E, Swinney HL. 2010. Lethal protein produced in response to competition between sibling bacterial colonies. Proc Natl Acad Sci U S A 107:6258-6263.

28. Blango MG, Mulvey MA. 2009. Bacterial landlines: contact-dependent signaling in bacterial populations. Curr Opin Microbiol 12:177-181.

29. Shrout JD, Tolker-Nielsen T, Givskov M, Parsek MR. 2011. The contribution of cell-cell signaling and motility to bacterial biofilm formation. MRS Bull 36:367-373.

30. Watanabe S, Tero A, Takamatsu A, Nakagaki T. 2011. Traffic optimization in railroad networks using an algorithm mimicking an amoeba-like organism, Physarum plasmodium. Biosystems 105:225-232.

31. Tero A, Takagi S, Saigusa T, Ito K, Bebber DP, Fricker MD, Yumiki K, Kobayashi R, Nakagaki T. 2010. Rules for biologically inspired adaptive network design. Science 327:439-442.

32. Shimogawa MM, Saada EA, Vashisht AA, Barshop WD, Wohlschlegel JA, Hill KL. 2015. Cell surface proteomics provides insight into stage-specific remodeling of the host-parasite interface in Trypanosoma brucei. Mol Cell Proteomics.

33. Nguyen HT, Sandhu J, Langousis G, Hill KL. 2013. CMF22 is a broadly conserved axonemal protein and is required for propulsive motility in Trypanosoma brucei. Eukaryot Cell 12:1202-1213.

Chapter VIII:

Perspectives and Outlook

PREFACE

The previous chapters in this dissertation offer extensive discussion and analyses of experimental results. The focus of this chapter is therefore on broader perspectives gleaned from a meta-analysis of these works. This includes unpublished data, ongoing studies, and future research directions.

The trypanosome surface is a diverse host-parasite interface

As discussed in great detail in Chapters II and III, the function and composition of the trypanosome surface constitutes a major focal point for trypanosomal researchers. The surface and flagellar proteomes offer great insights into host-parasite interactions, signaling and sensory systems, as well as identifying proteins that are essential for viability and/or pathogenesis. Notably, the extracellular biotinylation approach indicates that identified proteins are presumably accessible to small molecule therapeutics, providing candidates for pharmacological intervention of trypanosomiasis. One major advantage to the purification process developed in Chapter II, that was not discussed, is the potential for further direct studies and analysis. The affinity purified proteome is largely devoid of VSG, and therefore, can be further exploited.

For example, the surface proteome may be used to assess the potential for a protective vaccine (1-3). One could immunize mice using a complex mixture of the affinity-purified surface proteome, in advance of trypanosomal challenge. Using bloodstream parasites of a different VSG expression site, one could assess whether mice that received the surface proteome immunization are better able to inhibit or repress trypanosomal infection. VSG is highly immunogenic, and is thought to be one of the primary immune responses in an active infection (4, 5). Pre-exposure to native surface proteins, without an active infection, may allow for priming of the immune system generation of capable, protective antibodies, which would be a major advance with great promise.

A similar approach would utilize immunized mice for generation of hybridomas, allowing for a high-throughput screen of monoclonal antibodies resulting in a surface-staining (6, 7). Such a screen would provide numerous benefits to the trypanosomal research community. New antibodies would be available to serve as markers of the parasite surface, for which there are currently very few. Availability of a monoclonal antibody would assist in characterization efforts of trypanosomal surface proteins. This would allow for immediate localization, immunoprecipitation, and similar studies on the endogenous protein, without the need for time consuming epitope-modification approaches.

Through these combined efforts, surface-protein antibodies that are also specific to *T. brucei* could provide a promising lead for therapeutic intervention. Our surface proteomes identified many proteins already implicated in viability and virulence, and we anticipate discovering more as characterization efforts advance. Hypothetical antibodies against these candidates may show an inability to access the parasite surface in living bloodstream form parasites, but would still have potential for massive impact. In fact, the existence of one such antibody is not a "dead-end," but instead could result in collaborative efforts with research groups experienced in antibody engineering. Modern artificially engineered forms, such as minibodies, diabodies, or even scFV fragments, are only a fraction of their original size and may have improved access to the parasite surface (8, 9). As such, our studies on the surface proteomes hold promise for therapeutic and/or vaccination development efforts beyond the discussions included in Chapter II.

Trypanosomal adenylate cyclases

Trypanosomal adenylate cyclases (ACs) are a major focal point of this dissertation, and extensive experimental analyses and discussion of cAMP signaling pathways are covered in Chapters III, IV, VI, VIII, and Appendix I.

Although ACs have been directly implicated in signaling and sensory functions, the trigger for catalytic activation or inactivation remains unidentified. One of the major questions left unanswered is: "what are the ligands?" We're very interested in identifying ligands for the ACs, but identification of the ligand for an orphan receptor is extremely challenging. Several bioinformatics analyses, using Phyre2 (10, 11)and similar algorithm-based bioinformatics programs have mapped portions of the AC extracellular domains against existing crystal-structures identified in databases (data not shown). The crystal structure of the catalytic domain of two ACs has been established, and has suggested mechanistic insight into catalytic functionalities (12, 13). Interestingly, the extracellular portion of ACs have fragments of structural homology to several different ligand-binding crystal structures, including ones from bacterial and eukaryotic organisms (data not shown). Although *in vitro* screens against recombinant protein may identify regulatory ligands, such screens often have false positives, and are prohibitively expensive. Instead, our group is collaborating with the Andersen Laboratory, at Aarhus University in Denmark (pers. comm). The Andersen lab specializes in recombinant protein expression, as well as the generalization of crystal structures and corresponding analyses (14, 15). A *bona fide* crystal-structure of

trypanosomal AC ligand-binding domains may be incredibly informative, as it may be used to predict putative ligands, the mechanism of regulatory action, and even highlight critical residues. Such residues can then be the focus of targeted mutagenesis studies, allowing for modification of cAMP regulatory output without disruption of the cyclase domain ultrastructure or interfering with native localization, as done in Chapters IV and VI.

It's quite possible, and perhaps likely, that ACs have interactions with other proteins beyond their cyclase-driven homo-dimerization. Although the CARP effector proteins have not yet been characterized, they may exert regulatory effect on the cAMP producing proteins (16). Similarly, the localization studies featured in Chapter VI suggest the potential for interaction partners influencing localization. Preliminary work have optimized AC immunopurification protocols, which were used for the co-immunoprecipitation assays in Chapter IV, but not yet scaled to a volume suitable for mass-spectrometry analysis (data not shown). A caveat of such analyses is that interaction with other proteins may be transient, and as such would not be captured by immunoprecipitation.

An alternative, indirect method may offer the capability to identify transient interactions, as well as shed more light on the composition of the flagellum subdomains. Over the last two years, there's been great interest in the application of BioID, a method to screen for proximate and interacting proteins in living organisms (17). This approach utilizes fusion of a promiscuous biotin-ligase to the N or C terminal of a gene of interest. In the presence of biotin and ATP this protein will indiscriminately biotinylate everything in range. Utilizing streptavidin affinity-

purification and mass-spectrometry, one could then identify interacting proteins and other proteins "in the same neighborhood." The adenylate cyclases are therefore a prime target for such a technique, as they localize to different regions of the flagellum. Comparative analyses, coupled with quantitative proteomics, may allow for numerous flagellum membrane and matrix proteins to be identified. Proteins of key interest include cAMP effector proteins, which may be in the matrix. Of note, comparative analyses may implicate confidence in flagellar subdomain localization, as AC1 is at the flagellar tip and AC2 is along the flagellum length. Currently, studies within the laboratory group are generating BioID-tagged cell lines on several flagellar proteins (data not shown). Such studies are anticipated to identify new proteins, and provide insight into signaling, functional, or structural roles.

Despite our intense focus on cAMP signaling systems in procyclic-parasites, and the long-known lethal side effects of cAMP in bloodstream parasites, mechanisms of action remain unknown (Chapters IV, V, VI, Appendix I). In mammalian systems, cAMP has many numerous roles that are not conserved in *T. brucei.* For example, there are no known cyclic-nucleotide gated ion channels, or EPAC (exchange proteins activated by cAMP) domains in *T. brucei (18, 19).* Similarly, GPCR-mediated cAMP signaling in mammalian systems often acts through protein kinase A (PKA), which phosphorylates a number of targets, including transcription factors (20). Oddly, the trypanosomal PKA homolog is not affected by PKA, and may even be inhibited. In an effort to understand potential signaling output, future laboratory studies may prefer to opt for unbiased, systems level analyses.

As technology progresses, advanced techniques such as RNA-seq lower in price, becoming a feasible option for more routine, transcriptomic analyses. Our laboratory group has initiated transcriptomic studies to look for gene differences between cells grown in suspension culture, versus doing social motility on a surface (data not shown). Initiating RNA-seq analyses of AC or PDE mutants may unveil specific changes in mRNA expression correlating to differences in social behaviors. Other signaling outputs may include phosphorylation, as there are a number of kinases in the *T. brucei* genome, several of which we localized to the parasite flagellum (Chapter III). Along the same vein, phosphoproteomic analyses may be more fruitful in analysis of cAMP signaling systems and social behavior. Such studies may offer mechanistic insight into the regulation and control of coordinated social behaviors of *T. brucei.*

Adenylate cyclases as a tool to dissecting flagellar protein trafficking systems

In earlier chapters, the usage of protein truncations, chimeras, and point mutations allowed for identifying regions and specific residues involved in flagellar and subflagellar localization. Adenylate cyclases, however, serve as excellent flagellar reporter proteins, and can be used to analyze known flagellar trafficking systems.

In unpublished works, the role of two such systems, intraflagellar transport (IFT) and the BBSome-complex, were examined (Figure 8-01). As described in earlier chapters, protein trafficking into the flagellum is thought to rely on either active or

passive transport processes through a diffusion barrier. IFT has been well-defined in its roles for the active transport and assembly of the flagellum cytoskeleton. Inhibition of IFT88 results in cell-lethality, as trypanosomes are unable to build a new flagellum (21, 22). Interestingly, in the absence of IFT systems in dividing cells, the new flagellum forms a hollow membrane sleeve (23). Attempts to determine whether ACs could localize to the membrane sleeves in the absence of IFT systems were initiated by time-course based microscopy. Preliminary analyses were unsuccessful, and the membrane sleeve itself is difficult to identify without greater resolving capability.

The other trafficking system mentioned above involves the BBSome, a protein complex named for its role in the human ciliopathy, Bardet-Biedl Syndrome (24-27). The BBSome is thought to regulate protein traffic into and out of the flagellum, and direct interactions with flagellar proteins have been identified in a few examples (28, 29). Although the laboratory group now studies the BBSome's role in pathogenesis of bloodstream parasites, the initial focus and studies were with regards to AC protein trafficking. RNAi inhibition of BBS4 showed no effect on the flagellar localization of either AC1 or AC2 (Figure 8-01, data not shown). Later, quantitative proteomic analysis of bloodstream BBSome-knockout lines indicated aberrances in normal surface protein homeostasis (manuscript in preparation). Interestingly, preliminary functional analyses of BBS4-double knockout procyclic cells indicated abnormal social motility in comparison to control lines, which may reflect aberrant surface protein homeostasis in both life stages (data not shown).

The BBSome and IFT system are likely not the only way in and out of the flagellum. There's been a lot of focus on the diffusion barrier at the base of the flagellum, and several proteins are implicated in gate-keeping functionalities, though trypanosomal homologs have not yet been characterized (30-32). On unusual protein recently uncovered appears to be kinetoplastid specific. KHARON1 was first identified in *Leishmania mexicana,* and is involved in involved in flagellar trafficking of a glucose transporter (33). RNAi of KHARON1 is lethal, with gross cellular defects. In collaboration with the Landfear laboratory, several of the flagellar proteins from Chapter III were screened for interactions with the *T. brucei* homolog of KHARON1. Most of them, including an adenylate cyclase, had no interaction or trafficking defects (pers. communication). It remains to be seen whether there are other, kinetoplastid-specific proteins that mediate flagellar targeting.

Additionally, the flagellum-tip localization of several ACs is an interesting phenomenon, and being localized to distinct foci within the flagellum allows for some technical challenges to be overcome. In the previous chapters, ACs were immunolocalized, requiring cell fixation, permeabilization, and usage of antibodies. If one were to generate GFP, or similar fluorescent reporter lines, then one could attempt to do *in vivo* imaging. In other systems, cells can be immobilized and imaged, allowing the tracking of IFT trains for example (34, 35). As some ACs localize specifically to the flagellum tip, technical barriers to microscopy are reduced, as there is lesser confounding signal along the flagellum length. By immobilizing a trypanosome in soft agar, one can record high-resolution video microscopy tracking the fluorescent reporters up or down through the flagellum. Such studies have been

used in other systems to measure the speed of transport, thereby distinguishing between passive diffusion along membranes versus active trafficking up microtubules (34, 35). The studies discussed in this section demonstrate the multidisciplinary goals that adenylate cyclases in *Trypanosoma brucei* can be adapted to study.

Social motility: a versatile toolbox

One of the most strongest and interesting tools *T. brucei* offers is one of the newest and least understood. Social motility was first characterized using motility mutants, and has since been used to assess the capability of several mutant cell lines, as discussed in Appendix II. Although the regulation of social behaviors by cAMP signaling systems is the focus of several chapters, much remains unknown, and the field is ripe for exploration. The *in vitro* assay offers many benefits, some of which are reviewed in Chapter VII.

A major question in the field is how social motility manifests in an *in vivo* system. One would anticipate that phosphodiesterase mutants likely fail to colonize the tsetse fly, but it would be interesting to see whether, and how, an AC mutant would manifest. Would one expect enhanced virulence? Is a fly model capable of showing such nuances? Or do they perhaps lose their navigational capacity, and instead go into different tissue regions? It remains to be seen.

Social motility was a fortuitous discovery within the Hill laboratory group, and explorative works during my doctoral research made several more chance discoveries.

One such discovery involves altering the environmental conditions of the assay. *T. brucei* is standardly cultured in 5% CO_2 at approximately 28°C. When SoMo plates are transferred to an incubator at atmospheric CO_2 conditions, a shocking phenotypic change is seen (Figure 8-02). SoMo is enhanced to a similar degree as what we termed hyper-SoMo. It occurs far more often with more projections, but additionally has a shift in the progression timeframe. It occurs much earlier, and this "CO_2 shift" assay was of major interest, as it implied a signaling pathway.

This was explored by utilizing motility mutants, as well as the PDEB1-RNAi line, both of which are SoMo incompetent. Upon a CO_2 shift assay though, the PDEB1-RNAi line was able to perform SoMo while the motility mutant could not (data not shown). This dramatic result was quite exciting. First, it ruled out the notion that a growth or motility phenotype were behind the failure of PDEB1-RNAi to perform social motility. Second, it either introduces a new signaling pathway in regulation of SoMo, or offers a new aspect into the existing cAMP regulation model. In fungal pathogens, CO_2 sensing has been shown to affect morphology and pathogenesis (36). CO_2 has been linked to regulation of cyclic-nucleotide signaling in mammalian systems, typically in the form of bicarbonate-mediated regulation (37-41). CO_2 concentrations in the fly midgut are likely highest within the concentrated bloodmeal where procyclic-forms develop, as bicarbonate in the bloodmeal is the major source of mammalian CO_2. Trypanosomes quickly migrate through the ectoperitrophic space in a midgut infection, to a region which presumably has lower CO_2 concentrations and is devoid of bicarbonate-buffered blood.

The trypanosome genome encodes a single carbonic anhydrase, an enzyme that interconverts CO_2 to bicarbonate (18). Interestingly, this protein was identified in our flagellar matrix proteome (42). We therefore focused studies on carbonic anhydrase, utilizing RNAi lines to assess whether the CO_2 shift phenotype could be replicated under standard assay conditions, wherein carbonic anhydrase is unable to convert CO_2 to bicarbonate. In our model, bicarbonate directly regulates AC activity, resulting in alternation of normal social motility (Figure 8-02). Preliminary studies were promising, and a carbonic anhydrase double-knockout strain was generated, though its functionality has yet to be characterized (data not shown).

An alternate function of bicarbonate is to act as a weak buffer in a solution. *T. brucei* is grown in SM media, which lacks native buffering capability. When subjected to a CO_2-rich environment, such as a cell-culture incubator, the media will undergo acidification (43). Therefore, an alternate explanation of the CO_2 shift assay is that the change in local pH occurs at a different rate, and that the SoMo response is pH mediated. Interestingly, the tsetse-fly gut and tissues are alkaline, meaning insect-stage parasites must be able to tolerate a more basic pH environment than their mammalian-stage counterparts. To explore the notion that pH may influence social motility, SoMo assays were done modified acidic or basic SM media. Preliminary assays were inconclusive, as cell viability was heavily impacted at non-optimal media pH (data not shown).

To directly address the question, we instead focused on modifying the buffering capacity of the media. As bicarbonate may or may not affect AC activity, we opted to use multiple assay conditions to assess whether it is pH or bicarbonate levels

that result in the phenotype. Medias were modified to either include bicarbonate or HEPES as a buffer, with unbuffered media as a control. Preliminary results indicated a change in the morphology and pattern of the social motility, such that the radial projections are wider and more dispersed, though a clear answer was not determined in the limited sample size (data not shown). Additional studies are needed to better understand these phenotypes and ascertain the role of pH and CO_2 in regulation of social motility.

A completely different phenomenon was also discovered using social motility. Keen observation noted that an experimental first thought to have gone awry due to contamination displayed a remarkable behavior. SoMo appeared to be responsive to the presence of bacterial colonies! In their native environments, procyclic-form trypanosomes interact in a variety of tsetse-tissues. It's important to note that they are not alone. The tsetse fly has several bacterial symbionts, and it's long been known that their presence influences not only tsetse biology, but trypanosomal transmission (44-46). Although the details of bacterial symbiont influence are unclear, the ability of the bacteria to affect trypanosome infection points to the importance of inter-kingdom signaling, where trypanosomes and bacteria interact and cross-talk. These interactions are considered ancient, as trypanosomes have even been gifted bacterial genes via horizontal gene transfer (47).

After initial observation of trypanosomal avoidance and interaction, we intentionally began co-culturing parasites with bacteria. We observe that trypanosomes are strongly attracted to stationary-phase bacterial colonies (Figure 8-03). This behavior contrasts that for trypanosome-trypanosome interactions, and

represents the first known example of a putative chemoattractant. It also clearly demonstrates that trypanosomes do sense and interact within their environment, as they can choose to either avoid or converge on other microbial communities. Very little is known about *T. brucei* chemotaxis and navigation studies, and utilization of social motility therefore provides an excellent toolkit to further study these questions.

Finally, cAMP is not the only signaling pathway known in trypanosomes. In many organisms, flagellar calcium signaling is also a major signaling pathway. Our proteomics uncovered numerous ion channels, ligand-binding proteins, receptor kinases, ATPases, calcium and ion-binding proteins, and other interesting, putative signaling proteins. Social motility offers a convenient, high-throughput assay for functional analysis of signaling of these varied protein families. Additionally, as discussed earlier, *T. brucei* is highly amenable to modern molecular biology techniques, and these studies can further incorporate RNA-seq, quantitative proteomics, or even the use of FRET reporters for deeper, mechanistic insights.

Concluding remarks

The works in this dissertation identify and characterize novel cAMP signaling systems within the flagellum of the sleeping sickness parasite, *Trypanosoma brucei.* Our proteomic analyses of the trypanosome cell surface indicate that the surface is a dynamic, host-parasite interface. Stage-specific remodeling allows for fine-tuning of parasite sensory needs for specific host environments. Similarly, the trypanosome

flagellum surface and matrix serve as a complicated scaffold for a wide array of signaling proteins, though most remain uncharacterized. In a similar analysis in procyclics, we identified several new adenylate cylases (ACs). I characterized them, finding them to be catalytically-active, surface-exposed proteins that localize to novel subdomains of the trypanosome flagellum. Functional analyses revealed that flagellar ACs cooperate with cAMP-specific phosphodiesterase to regulate trypanosomal social behaviors, supporting the hypothesis that ACs transduce extracellular signals. These results are the first direct link to flagellum signaling in *T. brucei,* and suggest that differential localization of ACs is a significant feature. Utilizing truncation, chimeric, and point mutants, I defined flagellar and subflagellar targeting signals of ACs, finding that the cAMP regulation of social motility is subdomain dependent. In these works, we have identified that the first known regulators of social motility are novel flagellum-signaling pathways. We discovered the existence of flagellar subdomains and revealed their functional importance, and provided new insights into flagellar and trypanosomal biology, as well as trypanosomal sociobiology.

FIGURES

Figure 8-01. Flagellar proteins require dedicated trafficking machinery

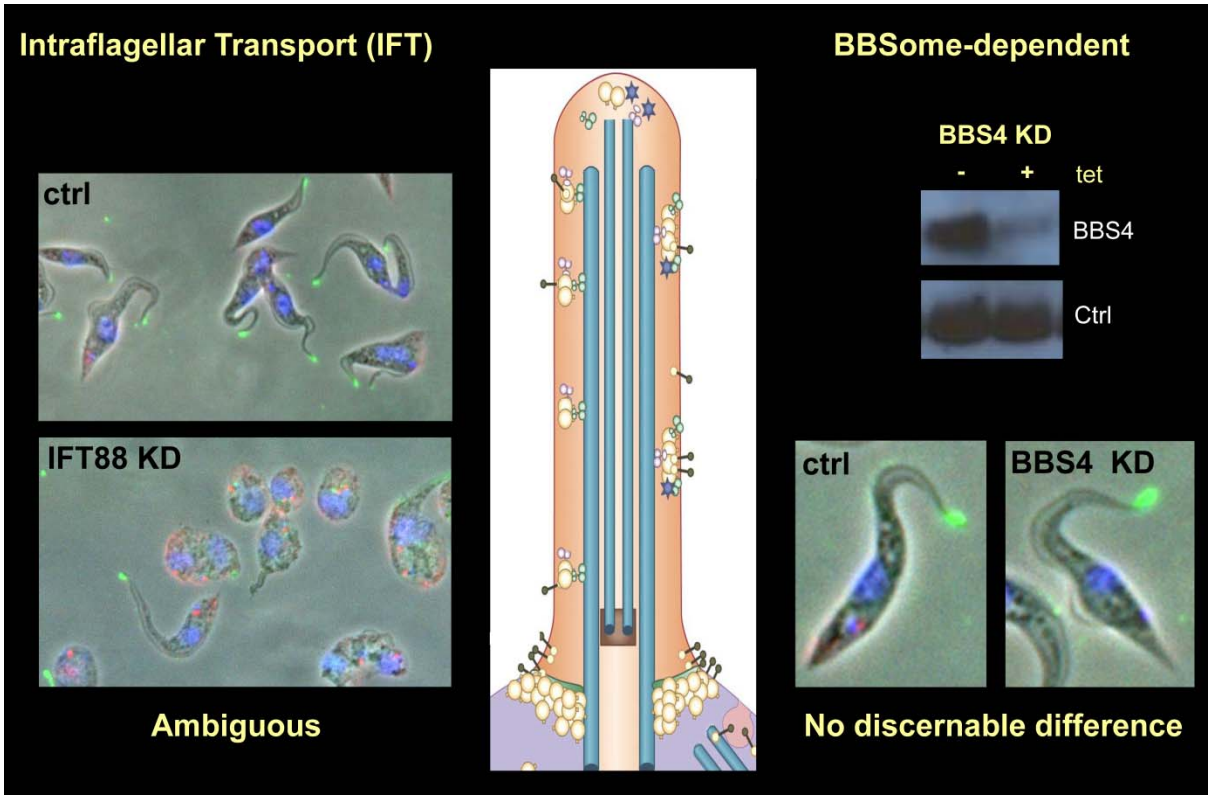

(Center) The eukaryotic flagellum has a diffusion barrier at the base. All flagellar proteins must be actively transported into the flagellum. Intraflagellar transport (IFT) and the BBSome are two traffic control systems.

(Left) Knockdown of IFT88 is lethal in *T. brucei.* Attempts to determine whether ACs could localize to a partially formed flagellum were uninterpretable.

Figure 8-02. Social motility is aberrant during a CO_2-shift assay

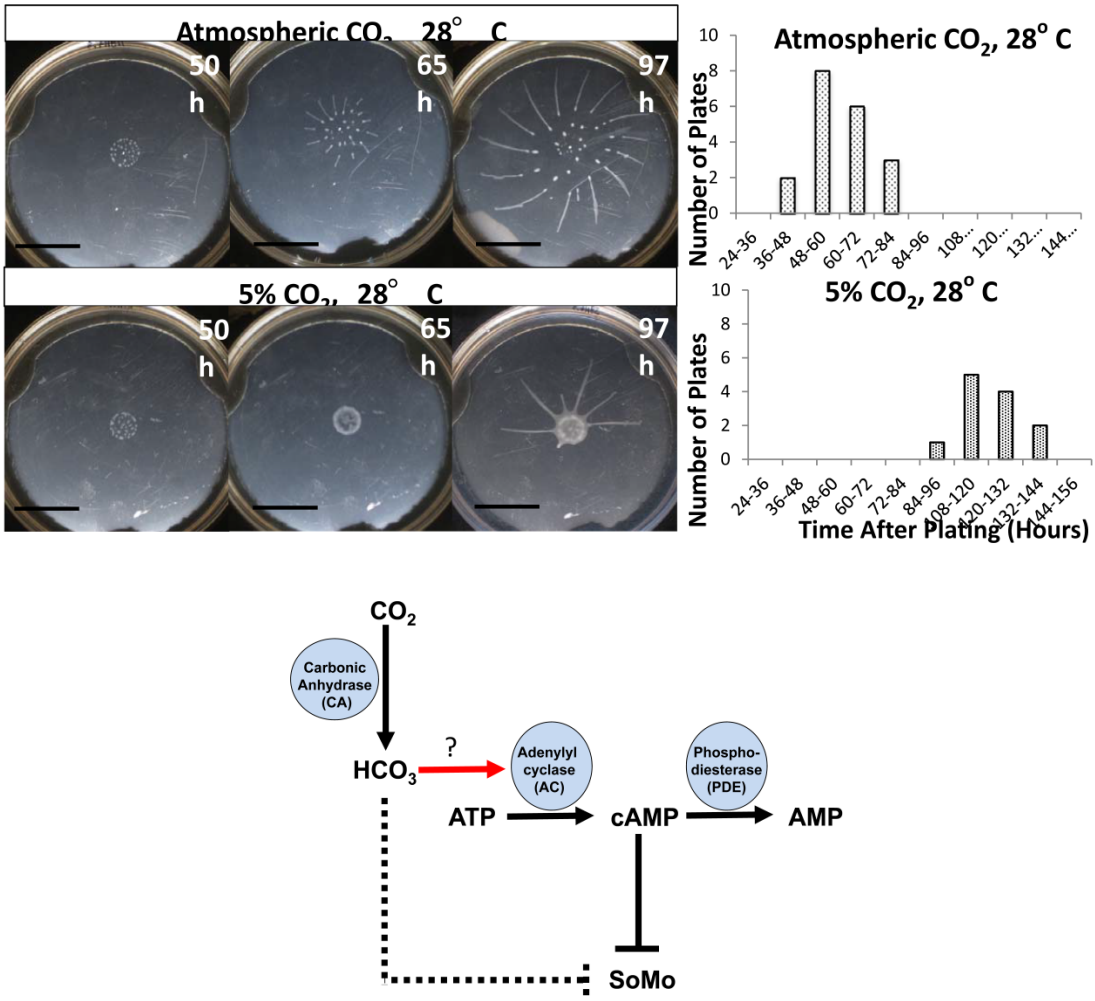

(Top left) Representative plate demonstrating the rapid emergence of radial projections when plates are shifted to atmospheric CO_2 concentrations.

(Top right) A time course quantification of when SoMo initiated radial projections. There is a clear shift in the time course when plates were shifted to atmospheric CO_2 concentrations.

(Bottom) A model for how carbonic anhydrase might regulate SoMo in a CO_2 dependent manner. In this model, bicarbonate may through adenylate cyclases and the known cAMP pathway.

Figure 8-03 Trypanosomes coordinate to sense and respond to external stimuli

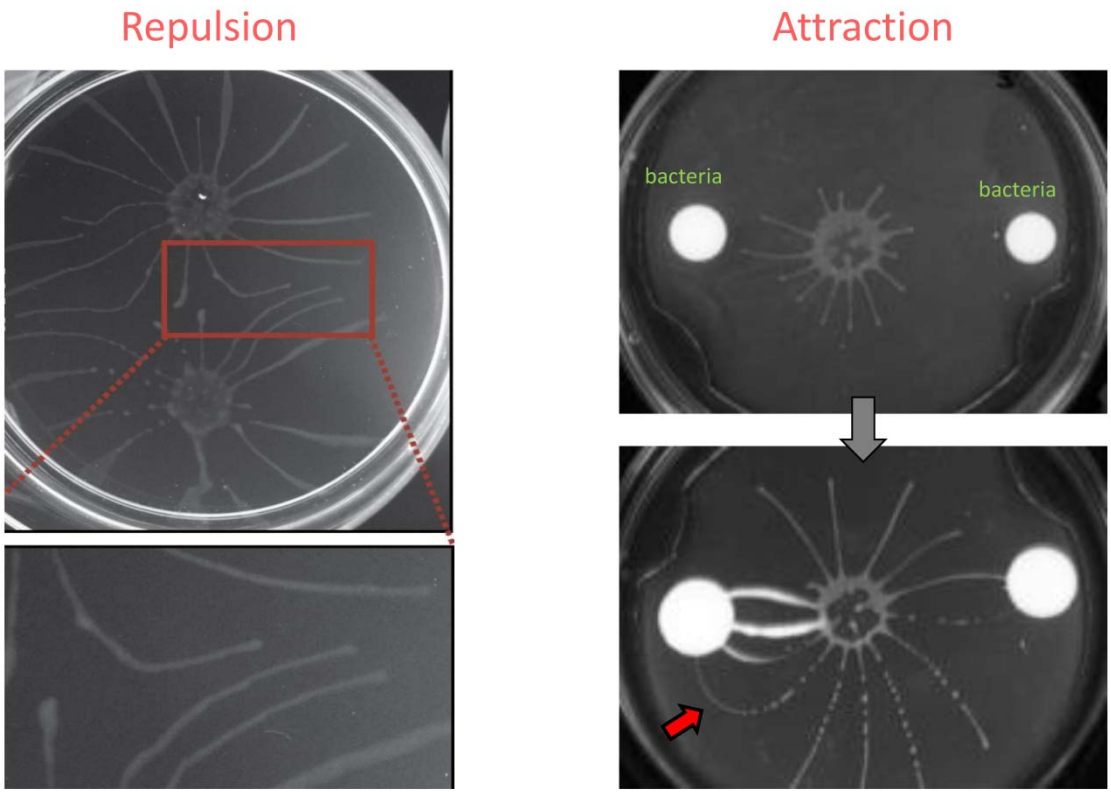

Trypanosoma brucei is capable of different response behaviors in social motility. On the left, trypanosomes actively avoid each other. Sibling colonies never interact. Conversely, trypanosomes show a clear attraction when cultured with bacteria (right). Projections actively alter their course to intentionally migrate towards stationary phase bacteria, demonstrated by the red arrow. This differential response indicates that trypanosomes have different sensory and response capabilities.

References

1. Koff WC, Burton DR, Johnson PR, Walker BD, King CR, Nabel GJ, Ahmed R, Bhan MK, Plotkin SA. 2013. Accelerating next-generation vaccine development for global disease prevention. Science 340:1232910.
2. Pereira VR, Lorena VM, Da Silva AP, Coutinho EM, Silvas ED, Ferreira AG, Miranda P, Krieger MA, Goldenberg S, Soares MB, Correa-Oliveira R, Gomes YM. 2004. Immunization with cytoplasmic repetitive antigen and flagellar repetitive antigen of Trypanosoma cruzi stimulates a cellular immune response in mice. Parasitology 129:563-570.
3. Borst P. 1991. Transferrin receptor, antigenic variation and the prospect of a trypanosome vaccine. Trends Genet 7:307-309.
4. Donelson JE, Hill KL, El-Sayed NM. 1998. Multiple mechanisms of immune evasion by African trypanosomes. Mol Biochem Parasitol 91:51-66.
5. Muller N, Mansfield JM, Seebeck T. 1996. Trypanosome variant surface glycoproteins are recognized by self- reactive antibodies in uninfected hosts. Infect Immun 64:4593-4597.
6. Chronopoulou E, Uribe-Benninghoff A, Corbett CR, Berry JD. 2014. Hybridoma technology for the generation of rodent mAbs via classical fusion. Methods Mol Biol 1131:47-70.

7. Uribe-Benninghoff A, Cabral T, Chronopoulou E, Berry JD, Corbett CR. 2014. Screening hybridomas for cell surface antigens by high-throughput homogeneous assay and flow cytometry. Methods Mol Biol 1131:81-103.
8. Nunez-Prado N, Compte M, Harwood S, Alvarez-Mendez A, Lykkemark S, Sanz L, Alvarez-Vallina L. 2015. The coming of age of engineered multivalent antibodies. Drug Discov Today 20:588-594.
9. Holliger P, Hudson PJ. 2005. Engineered antibody fragments and the rise of single domains. Nat Biotechnol 23:1126-1136.
10. Kelley LA, Sternberg MJ. 2009. Protein structure prediction on the Web: a case study using the Phyre server. Nat Protoc 4:363-371.
11. Bennett-Lovsey RM, Herbert AD, Sternberg MJ, Kelley LA. 2008. Exploring the extremes of sequence/structure space with ensemble fold recognition in the program Phyre. Proteins 70:611-625.
12. Bieger B, Essen LO. 2001. Structural analysis of adenylate cyclases from Trypanosoma brucei in their monomeric state. EMBO Journal 20:433-445.
13. Bieger B, Essen LO. 2000. Crystallization and preliminary X-ray analysis of the catalytic domain of the adenylate cyclase GRESAG4.1 from Trypanosoma brucei. Acta Crystallogr D Biol Crystallogr 56:359-362.
14. Brodersen DE, Andersen GR, Andersen CB. 2013. Mimer: an automated spreadsheet-based crystallization screening system. Acta Crystallogr Sect F Struct Biol Cryst Commun 69:815-820.

15. Stodkilde K, Torvund-Jensen M, Moestrup SK, Andersen CB. 2014. Structural basis for trypanosomal haem acquisition and susceptibility to the host innate immune system. Nat Commun 5:5487.

16. Gould MK, Bachmaier S, Ali JA, Alsford S, Tagoe DN, Munday JC, Schnaufer AC, Horn D, Boshart M, de Koning HP. 2013. Cyclic AMP Effectors in African Trypanosomes Revealed by Genome-Scale RNA Interference Library Screening for Resistance to the Phosphodiesterase Inhibitor CpdA. Antimicrob Agents Chemother 57:4882-4893.

17. Roux KJ, Kim DI, Burke B. 2013. BioID: a screen for protein-protein interactions. Curr Protoc Protein Sci 74:Unit 19 23.

18. Berriman M, Ghedin E, Hertz-Fowler C, Blandin G, Renauld H, Bartholomeu DC, Lennard NJ, Caler E, Hamlin NE, Haas B, Bohme U, Hannick L, Aslett MA, Shallom J, Marcello L, Hou L, Wickstead B, Alsmark UC, Arrowsmith C, Atkin RJ, Barron AJ, Bringaud F, Brooks K, Carrington M, Cherevach I, Chillingworth TJ, Churcher C, Clark LN, Corton CH, Cronin A, Davies RM, Doggett J, Djikeng A, Feldblyum T, Field MC, Fraser A, Goodhead I, Hance Z, Harper D, Harris BR, Hauser H, Hostetler J, Ivens A, Jagels K, Johnson D, Johnson J, Jones K, Kerhornou AX, Koo H, Larke N, Landfear S, Larkin C, Leech V, Line A, Lord A, Macleod A, Mooney PJ, Moule S, Martin DM, Morgan GW, Mungall K, Norbertczak H, Ormond D, Pai G, Peacock CS, Peterson J, Quail MA, Rabbinowitsch E, Rajandream MA, Reitter C, Salzberg SL, Sanders M, Schobel S, Sharp S, Simmonds M, Simpson AJ, Tallon L, Turner CM, Tait A, Tivey AR, Van Aken S, Walker D, Wanless D, Wang S, White B, White O, Whitehead S, Woodward J,

Wortman J, Adams MD, Embley TM, Gull K, Ullu E, Barry JD, Fairlamb AH, Opperdoes F, Barrell BG, Donelson JE, Hall N, Fraser CM, Melville SE, El-Sayed NM. 2005. The genome of the African trypanosome Trypanosoma brucei. Science 309:416-422.

19. Seebeck T, Schaub R, Johner A. 2004. cAMP signalling in the kinetoplastid protozoa. Curr Mol Med 4:585-599.

20. Walsh DA, Van Patten SM. 1994. Multiple pathway signal transduction by the cAMP-dependent protein kinase. Faseb J 8:1227-1236.

21. Follit JA, Xu F, Keady BT, Pazour GJ. 2009. Characterization of mouse IFT complex B. Cell Motil Cytoskeleton 66:457-468.

22. Pazour GJ, Baker SA, Deane JA, Cole DG, Dickert BL, Rosenbaum JL, Witman GB, Besharse JC. 2002. The intraflagellar transport protein, IFT88, is essential for vertebrate photoreceptor assembly and maintenance. J Cell Biol 157:103-113.

23. Davidge JA, Chambers E, Dickinson HA, Towers K, Ginger ML, McKean PG, Gull K. 2006. Trypanosome IFT mutants provide insight into the motor location for mobility of the flagella connector and flagellar membrane formation. J Cell Sci 119:3935-3943.

24. Tobin JL, Beales PL. 2007. Bardet-Biedl syndrome: beyond the cilium. Pediatr Nephrol 22:926-936.

25. Jin H, Nachury MV. 2009. The BBSome. Current Biology 19:R472-473.

26. Loktev AV, Zhang Q, Beck JS, Searby CC, Scheetz TE, Bazan JF, Slusarski DC, Sheffield VC, Jackson PK, Nachury MV. 2008. A BBSome subunit links ciliogenesis, microtubule stability, and acetylation. Dev Cell 15:854-865.

27. Badano JL, Mitsuma N, Beales PL, Katsanis N. 2006. The Ciliopathies: An Emerging Class of Human Genetic Disorders. Annu Rev Genomics Hum Genet 7:125-148.

28. Berbari NF, Lewis JS, Bishop GA, Askwith CC, Mykytyn K. 2008. Bardet-Biedl syndrome proteins are required for the localization of G protein-coupled receptors to primary cilia. Proc Natl Acad Sci U S A 105:4242-4246.

29. Jin H, White SR, Shida T, Schulz S, Aguiar M, Gygi SP, Bazan JF, Nachury MV. 2010. The conserved Bardet-Biedl syndrome proteins assemble a coat that traffics membrane proteins to cilia. Cell 141:1208-1219.

30. Hu Q, Milenkovic L, Jin H, Scott MP, Nachury MV, Spiliotis ET, Nelson WJ. 2010. A septin diffusion barrier at the base of the primary cilium maintains ciliary membrane protein distribution. Science 329:436-439.

31. Nachury MV, Seeley ES, Jin H. 2010. Trafficking to the ciliary membrane: how to get across the periciliary diffusion barrier? Annu Rev Cell Dev Biol 26:59-87.

32. Pazour GJ, Bloodgood RA. 2008. Chapter 5 targeting proteins to the ciliary membrane. Curr Top Dev Biol 85:115-149.

33. Tran KD, Rodriguez-Contreras D, Vieira DP, Yates PA, David L, Beatty W, Elferich J, Landfear SM. 2013. KHARON1 mediates flagellar targeting of a glucose transporter in Leishmania mexicana and is critical for viability of infectious intracellular amastigotes. J Biol Chem 288:22721-22733.

34. Ye F, Breslow DK, Koslover EF, Spakowitz AJ, Nelson WJ, Nachury MV. 2013. Single molecule imaging reveals a major role for diffusion in the exploration of ciliary space by signaling receptors. Elife 2:e00654.

35. Buisson J, Chenouard N, Lagache T, Blisnick T, Olivo-Marin JC, Bastin P. 2013. Intraflagellar transport proteins cycle between the flagellum and its base. J Cell Sci 126:327-338.

36. Klengel T, Liang WJ, Chaloupka J, Ruoff C, Schroppel K, Naglik JR, Eckert SE, Mogensen EG, Haynes K, Tuite MF, Levin LR, Buck J, Muhlschlegel FA. 2005. Fungal adenylyl cyclase integrates CO_2 sensing with cAMP signaling and virulence. Curr Biol 15:2021-2026.

37. Zippin JH, Farrell J, Huron D, Kamenetsky M, Hess KC, Fischman DA, Levin LR, Buck J. 2004. Bicarbonate-responsive "soluble" adenylyl cyclase defines a nuclear cAMP microdomain. J Cell Biol 164:527-534.

38. Visconti PE, Muschietti JP, Flawia MM, Tezon JG. 1990. Bicarbonate dependence of cAMP accumulation induced by phorbol esters in hamster spermatozoa. Biochim Biophys Acta 1054:231-236.

39. Smith JJ, Welsh MJ. 1992. cAMP stimulates bicarbonate secretion across normal, but not cystic fibrosis airway epithelia. J Clin Invest 89:1148-1153.

40. Armstrong WM, Youmans SJ. 1980. The role of bicarbonate ions and of adenosine 3',5'-monophosphate (cAMP) in chloride transport by epithelial cells of bullfrog small intestine. Ann N Y Acad Sci 341:139-155.

41. Visconti PE, Stewart-Savage J, Blasco A, Battaglia L, Miranda P, Kopf GS, Tezon JG. 1999. Roles of bicarbonate, cAMP, and protein tyrosine phosphorylation on

capacitation and the spontaneous acrosome reaction of hamster sperm. Biol Reprod 61:76-84.

42. Oberholzer M, Langousis G, Nguyen HT, Saada EA, Shimogawa MM, Jonsson ZO, Nguyen SM, Wohlschlegel JA, Hill KL. 2011. Independent analysis of the flagellum surface and matrix proteomes provides insight into flagellum signaling in mammalian-infectious Trypanosoma brucei. Mol Cell Proteomics 10:M111 010538.

43. Oberholzer M, Lopez MA, Ralston KS, Hill KL. 2009. Approaches for functional analysis of flagellar proteins in African trypanosomes. Methods in Cell Biology 93:21-57.

44. Hu C, Aksoy S. 2006. Innate immune responses regulate trypanosome parasite infection of the tsetse fly Glossina morsitans morsitans. Mol Microbiol 60:1194-1204.

45. Aksoy S, Rio RV. 2005. Interactions among multiple genomes: tsetse, its symbionts and trypanosomes. Insect Biochem Mol Biol 35:691-698.

46. Rio RV, Wu YN, Filardo G, Aksoy S. 2006. Dynamics of multiple symbiont density regulation during host development: tsetse fly and its microbial flora. Proc Biol Sci 273:805-814.

47. Richmond GS, Smith TK. 2007. A novel phospholipase from Trypanosoma brucei. Mol Microbiol 63:1078-1095.

Appendix I:

Cyclic AMP regulates social behavior in African trypanosomes

PREFACE

This appendix includes a work reprinted in entirety with the publisher's permission. "Cyclic AMP regulates social behavior in African trypanosomes" by Oberholzer, Saada, and Hill. It was originally published in mBio, 2015, 6(3):e01954-14. doi:10.1128/mBio.01954-14.

This work is presented as a complement to the original finding that cAMP activity of adenylate cyclases regulate trypanosomal social behaviors (Chapter V). As second author of this work (as well as the Lopez *et al* work) I contributed to the original experimental concepts, plans, and discussions. In this article, we focused on inhibition of phosphodiesterase B1 through both genetic and pharmacological methods, finding that social motility is completely blocked, which corresponds to an increase in intracellular cAMP as measured by a FRET-sensor. In particular, I performed the social motility assays using membrane-permeable cAMP analogues and downstream metabolic products, demonstrating that this inhibition is cAMP-specific. I additionally assisted and edited the manuscripts at early and late stages.

Cyclic AMP Regulates Social Behavior in African Trypanosomes

Michael Oberholzer,[a] Edwin A. Saada,[a] Kent L. Hill[a,b]

Department of Microbiology, Immunology and Molecular Genetics[a] and Molecular Biology Institute,[b] University of California, Los Angeles, Los Angeles, California, USA

ABSTRACT **The protozoan parasite *Trypanosoma brucei* engages in surface-induced social behavior, termed social motility, characterized by single cells assembling into multicellular groups that coordinate their movements in response to extracellular signals. Social motility requires sensing and responding to extracellular signals, but the underlying mechanisms are unknown. Here we report that *T. brucei* social motility depends on cyclic AMP (cAMP) signaling systems in the parasite's flagellum (synonymous with cilium). Pharmacological inhibition of cAMP-specific phosphodiesterase (PDE) completely blocks social motility without impacting the viability or motility of individual cells. Using a fluorescence resonance energy transfer (FRET)-based sensor to monitor cAMP dynamics in live cells, we demonstrate that this block in social motility correlates with an increase in intracellular cAMP levels. RNA interference (RNAi) knockdown of the flagellar PDEB1 phenocopies pharmacological PDE inhibition, demonstrating that PDEB1 is required for social motility. Using parasites expressing distinct fluorescent proteins to monitor individuals in a genetically heterogeneous community, we found that the social motility defect of PDEB1 knockdowns is complemented by wild-type parasites in *trans*. Therefore, PDEB1 knockdown cells are competent for social motility but appear to lack a necessary factor that can be provided by wild-type cells. The combined data demonstrate that the role of cyclic nucleotides in regulating microbial social behavior extends to African trypanosomes and provide an example of transcomplementation in parasitic protozoa.**

IMPORTANCE **In bacteria, studies of cell-cell communication and social behavior have profoundly influenced our understanding of microbial physiology, signaling, and pathogenesis. In contrast, mechanisms underlying social behavior in protozoan parasites are mostly unknown. Here we show that social behavior in the protozoan parasite *Trypanosoma brucei* is governed by cyclic-AMP signaling systems in the flagellum, with intriguing parallels to signaling systems that control bacterial social behavior. We also generated a *T. brucei* social behavior mutant and found that the mutant phenotype is complemented by wild-type cells grown in the same culture. Our findings open new avenues for dissecting social behavior and signaling in protozoan parasites and illustrate the capacity of these organisms to influence each other's behavior in mixed communities.**

Received 23 September 2014 **Accepted** 2 April 2015 **Published** 28 April 2015

Citation Oberholzer M, Saada EA, Hill KL. 2015. Cyclic AMP regulates social behavior in African trypanosomes. mBio 6(3):e01954-14. doi:10.1128/mBio.01954-14.

Invited Editor Stephen L. Hajduk, University of Georgia **Editor** Thomas E. Wellems, National Institutes of Health

Address correspondence to Kent L. Hill, kenthill@mednet.ucla.edu.

Recognition of social behavior and cell-cell communication as ubiquitous among bacteria transformed our view of microbiology (1, 2). Examples of microbial social behavior are widespread and include assembly of biofilms and fruiting bodies, quorum sensing, and various forms of group motility across surfaces (1–6). Social behaviors enable bacteria to function as multicellular entities exhibiting emergent properties not evident in individual cells (1). Pathogenic bacteria and fungi exploit social behaviors to resist host immune defenses and antibiotics, to promote tissue colonization, and to exclude competing microbes from infection sites (7–9). As such, microbial cell-cell communication and social behavior are important for development and virulence, while the underlying mechanisms are potential targets for therapeutic intervention (10, 11).

Parasitic protozoa present a significant threat to global public health and agriculture and pose an economic burden in some of the world's most impoverished regions (12–16). The paradigm of social behavior can inform questions regarding parasite biology, transmission, and pathogenesis (17–20), but little is known about social behaviors and cell-cell interactions in these organisms. The protozoan parasite *Trypanosoma brucei* is transmitted by blood-sucking tsetse flies, causing sleeping sickness in humans and related diseases in wild and domestic animals throughout sub-Saharan Africa (21). Trypanosomes are typically considered individual cells but are capable of parasite-parasite communication and social behavior. In the mammalian host's bloodstream, for example, quorum sensing directs *T. brucei* development into "short stumpy" forms that are uniquely adapted for transmission through the tsetse fly (22, 23). Here, parasite-derived "stumpy induction factor" (SIF) accumulates in a cell density-dependent fashion and triggers cellular differentiation (22, 23). Procyclic (insect midgut stage) trypanosomes are also capable of social behavior. In this case, surface cultivation causes individual parasites to assemble into multicellular communities that engage in collective motility across the surface and modify their movements in response to signals from nearby parasites (24). This group behavior is termed social motility (SoMo) based on features shared with social motility and swarming motility in bacteria (4, 24).

In bacteria, social motility facilitates rapid surface colonization and promotes survival of bacterial populations in harsh environ-

ments (4, 5, 7). Specific features of transmission or pathogenesis that are reflected in *T. brucei* social motility are not yet known. However, recent work has shown that social motility is a property of a specific life cycle stage that occurs early during colonization of the fly midgut, consistent with the idea that social motility reflects parasite features relevant within the fly transmission stage (25). Moreover, the parasites are in constant contact with tissue surfaces in their natural environment, particularly in the tsetse fly and extravascular spaces in the mammalian host, and would benefit from functions provided by social motility in bacteria. More broadly, social motility presents a complex, group-level behavior that highlights the capacity of trypanosomes for cell-cell communication.

Social behaviors in microbes depend upon cell-cell communication and specific signaling systems in individuals within the population (1, 2, 4, 5). Quorum sensing and cyclic nucleotide signaling via the 2nd messenger cyclic-dimeric-GMP (c-di-GMP) have emerged as important regulators of surface-induced swarming motility in bacteria (26, 27). Quorum sensing and c-di-GMP also regulate biofilm formation, which is another surface-associated group behavior (27, 28). In eukaryotes, cyclic nucleotide signaling via cyclic AMP (cAMP) is critical for the surface motility of the social amoeba *Dictyostelium discoideum* (6).

T. brucei cAMP levels are controlled by receptor-type adenylate cyclases and cAMP-specific phosphodiesterases (PDEs) (29). *T. brucei* encodes five PDEs, PDEA, PDEB1, PDEB2, PDEC, and PDED (30, 31). PDEB1 and PDEB2 are essential for maintaining physiological levels of cAMP in *T. brucei* cells (32). *T. brucei* PDEB1 (TbPDEB1) is localized to the flagellum, while TbPDEB2 is distributed throughout the cell (32). Flagellum localization is of particular significance, because the eukaryotic flagellum is a signaling center that controls communication with the extracellular environment (33–35) and flagellar motility is required for social motility (24). TbPDEB1 and TbPDEB2 are essential in bloodstream trypanosomes *in vitro* and in an *in vivo* mouse infection model (32), making them targets for therapeutic intervention, and drug discovery efforts have led to development of potent and specific *T. brucei* PDE inhibitors (36–38). These inhibitors validate PDEs as drug targets and novel open avenues for dissecting cAMP signaling in trypanosomes with chemical genetics (39).

Given the widespread use of cyclic nucleotides for regulating surface-associated social behaviors in diverse microbes, we hypothesized that cAMP controls social motility in *T. brucei*. To test this hypothesis, we targeted TbPDEB1. We show that pharmacological or genetic inhibition of TbPDEB1 blocks social motility without affecting the viability or motility of individual cells. By employing a fluorescence resonance energy transfer (FRET) sensor for monitoring cAMP in live *T. brucei* cells, we showed that the block in social motility is directly correlated with a rise in intracellular cAMP levels. Finally, using fluorescent markers to monitor genetically distinct individuals in a mixed population, we demonstrated that the social motility defect of TbPDEB1 mutants can be complemented by wild-type (WT) cells in *trans*. Our findings reveal *T. brucei* social motility mechanisms, demonstrate that cyclic nucleotide regulation of microbial surface motility extends to parasitic protozoa, and reveal a novel form of cell-cell interaction in these parasites.

RESULTS

Intracellular cAMP levels regulate *T. brucei* social motility. To test the importance of intracellular cAMP dynamics for social motility, we applied a *T. brucei* PDE inhibitor, cpdA, that inhibits recombinant TbPDEB1 and TbPDEB2 *in vitro* and causes an increase in cellular cAMP concentrations when added to bloodstream-form *T. brucei* in culture (37). We tested cpdA at a range of concentrations, from 25nM to 1μM, for its impact on social motility in procyclic *T. brucei*. When control cells are cultivated on soft agar, parasites assemble at the perimeter of the inoculation site and then move outward as groups, forming projections that radiate away from the center (Fig. 1) (24). cpdA showed dose-dependent inhibition of social motility, and the minimal concentration giving complete inhibition was 100 nM (Fig. 1a and c). Social motility requires active parasite motility (24, 40, 41). We therefore asked if cpdA affects motility of individual cells. We assessed motility using live-video microscopy combined with automated tracking of individual parasites treated with or without 100 nM cpdA in suspension culture. No difference was observed for cpdA-treated versus untreated cells (Fig. 1b). Treatment with 100 nM cpdA did not affect doubling time (Fig. 1d). Therefore, cpdA inhibits social motility in a dose-dependent fashion, with no impact on the proliferation or motility of individual cells.

The inhibitory effect of cpdA on *T. brucei* social motility is anticipated to be due to a rise in intracellular cAMP concentrations. CpdA has been demonstrated to increase intracellular cAMP concentrations in bloodstream-form *T. brucei* (37), but its impact on cAMP in procyclic parasites has not been assessed. We therefore tested this by applying a well-characterized fluorescence resonance energy transfer (FRET)-based sensor for cAMP, Epac1-camps (epac1camps), that has been used to monitor intracellular cAMP dynamics in a variety of cell types, including trypanosomes (38, 42, 43). When excited with a wavelength of 436 nm, epac1camps emits 2 distinct wavelengths, one in the cyan (488-nm) spectrum and one in the yellow (535-nm) spectrum, the latter of which is FRET dependent (see Fig. S2a in the supplemental material) (42). Binding of cAMP to the sensor causes a conformational change that reduces FRET, and the 488-nm/535-nm emission ratio therefore increases as a function of increasing intracellular cAMP concentrations (see Fig. S2a) (42). The dynamic range of epac1camps is 0.2 to 10 μM cAMP (42), consistent with the reported intracellular cAMP concentration for *T. brucei* (30). epac1camps was expressed using a tetracycline (tet)-inducible vector in procyclic *T. brucei*. Fluorescence microscopy analysis of live, immobilized epac1camps-expressing parasites revealed that epac1camps is evenly distributed throughout the cell, including the cytoplasm and flagellum (Fig. 1e, inset). epac1camps reporter parasites were then used in FRET assays (Fig. 1e and f; see also Fig. S2). When excited at 436 nm, epac1camps parasites showed 488-nm and 535-nm emission signals significantly higher than the background observed for WT controls without the reporter (see Fig. S2b and c). Addition of cpdA epac1camps parasites produced a dose-dependent increase in the 488-nm/535-nm emission ratio, which rose rapidly and plateaued within ~400 to 600 s, indicating a rapid and stable rise in cellular cAMP concentrations (Fig. 1e and f). The 488-nm/535-nm ratio did not change in control epac1camps parasites that did not receive cpdA. Therefore, inhibition of social motility by cpdA is directly correlated with a rise in intracellular cAMP concentrations.

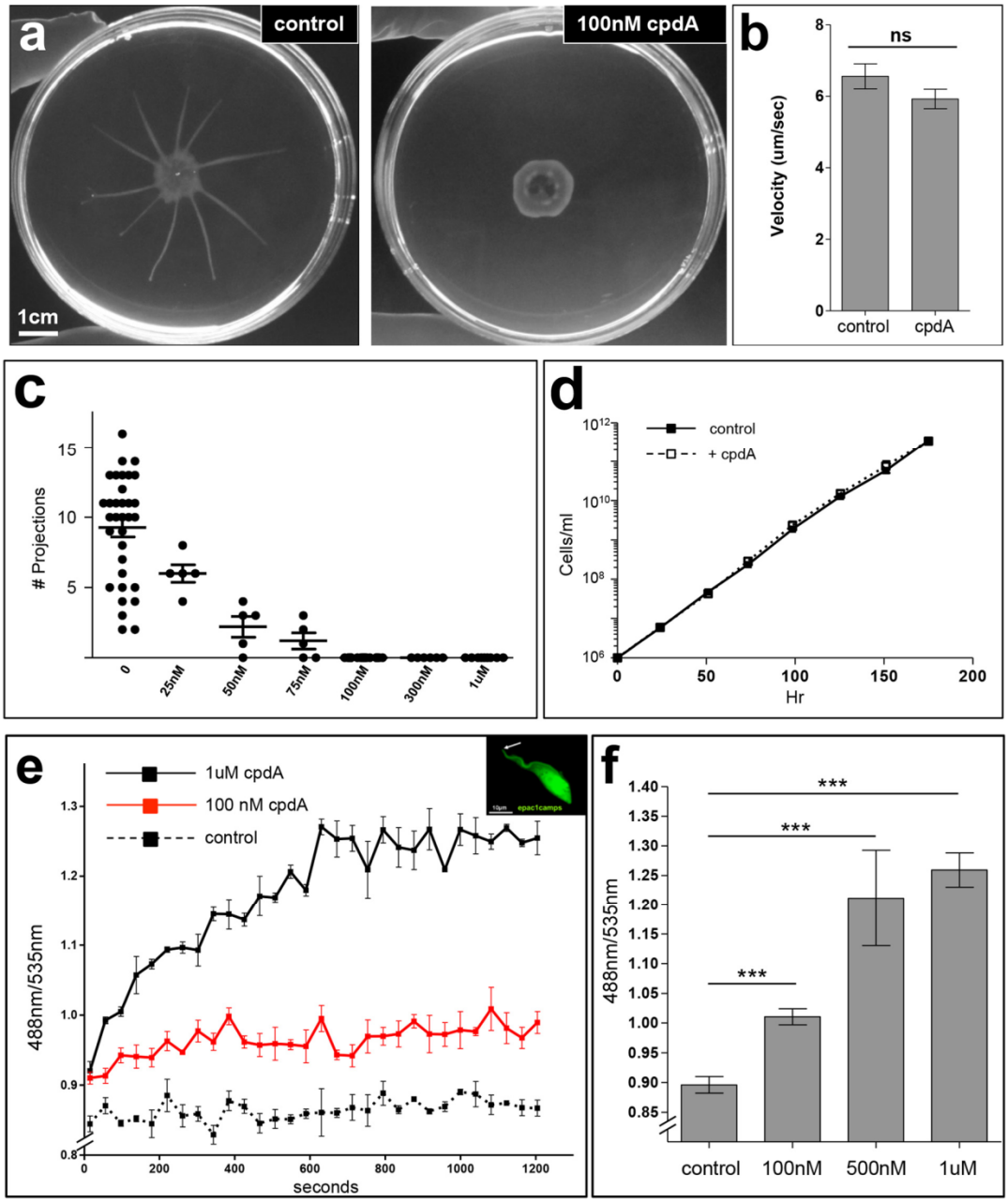

FIG 1 Pharmacological inhibition of *T. brucei* PDE blocks social motility and elevates cellular cAMP levels. (a) Social motility of cells treated with or without 100 nM cpdA as indicated. (b) Motility of individual cells in suspension cultures treated with or without 100 nM cpdA. (c) Chart showing the number of projections produced upon treatment with the indicated concentrations of cpdA (0 nM [$n = 33$]; 25 nM [$n = 5$]; 50 nm [$n = 5$]; 75 nm [$n = 5$]; 100 nM [$n = 27$]; 300 nm [$n = 6$]; 1 μM [$n = 9$]). (d) Growth curve for cells treated with or without 100 nM cpdA. (e) Fluorescence ratio (488 nm/535 nm) of epac1camps-expressing cells as a function of time following addition of cpdA at the indicated concentrations. The inset shows that the cAMP FRET sensor epac1camps is expressed throughout the parasite cell, including the flagellum (arrow). (f) Endpoint analysis of 488-nm/535-nm fluorescence ratio of epac1camps cells following 600 s of treatment with cpdA at the indicated concentration. Error bars show ± standard errors. ***, $P < 0.0001$; ns = not significant.

Previous studies suggested that cAMP mediates stumpy formation in BSF *T. brucei* because addition of cell-permeable cAMP induced stumpy differentiation (23). Subsequent studies showed that differentiation was not induced by hydrolysis-resistant cAMP, even when used at concentrations 20-fold to 200-fold higher than the hydrolyzable cAMP concentrations (44). Moreover, AMP and adenosine metabolic products were 100-fold to 1,000-fold more potent at inducing differentiation than was cAMP, indicating that cAMP downstream products were responsible for stumpy differentiation (44). We tested cAMP analogues for an effect on social motility. In contrast to what was observed for stumpy differentiation, hydrolysis-resistant cAMP inhibited social motility as well as or better than hydrolyzable cAMP, and the effect seen with either compound was equivalent to or more potent than that seen with AMP or adenosine (see Fig. S1 in the supplemental material). Notably, because cAMP added to *T. brucei* cells is unstable (44), the effective cAMP concentration is even lower than what is added. These results support the view that cAMP mediates inhibition of social motility.

Genetic inhibition of TbPDEB1 phenocopies the effect of the PDE inhibitor cpdA. Potent inhibition of TbPDEB1 and TbPDEB2 by cpdA has been demonstrated using recombinant proteins (37). However, there are five PDEs in *T. brucei* and selectivity of cpdA for any given PDE over the others has not been demonstrated. Likewise, as with any pharmacological treatment, there is potential for off-target effects that may produce a phenotype unrelated to inhibition of the drug's expected target. Therefore, to determine if the effect of cpdA on social motility is due to inhibition of a specific PDE, we used RNA interference (RNAi) to test the requirement for PDEB1 in social motility. We chose PDEB1 because of its flagellar localization (Fig. 2a) (45) and our goal of interrogating the role of flagellar cAMP signaling in social motility. Upon tet induction, PDEB1 mRNA levels were reduced to 11% of control parasite levels, while the abundance of PDEB2 mRNA was unaffected (Fig. 2b). Therefore, knockdown was potent and specific. PDEB1 knockdown did not affect the motility of individual cells and had only a modest effect on growth (Fig. 2c and d). When assayed for social motility, PDEB1 knockdown completely blocked social motility (Fig. 2e and f). Therefore, genetic ablation of PDEB1 expression phenocopied cpdA treatment, inhibiting social motility while not affecting the motility of individual cells. Social motility is observed in early procyclic but not late procyclic cells (25). Cells treated with cpdA or PDEB1 RNAi expressed the early procyclic marker GPEET procyclin (see Fig. S5 in the supplemental material), demonstrating that inhibition of social motility is not due to differentiation into late procyclics (25).

The social motility defect of TbPDEB1 knockdown parasites can be complemented by WT cells provided in *trans*. We explored potential mechanisms underlying the role of PDEB1 and cAMP in social motility. We hypothesize at least two alternative models. In model 1, genetic or pharmacological inhibition of PDEB1 leads to misregulation of cAMP signaling, which causes a cell-autonomous inhibition of social motility. In other words, PDEB1-deficient cells are incapable of social motility despite being motile as individuals. In model 2, misregulation of cAMP signaling disrupts an intercellular process that is required for social motility. For example, PDEB1-deficient cells may be competent for social motility but fail to engage in social motility because they lack something that could be provided by other cells. In bacteria, for example, cells with swarming defects can be rescued by wild-type cells in mixed communities, owing to cell-cell transfer of outer membrane proteins important for social behavior (46). To discriminate between these two models, we engineered cell lines with different fluorescent markers to enable monitoring of individual genotypes within a genetically mixed community. We generated WT cells, trypanin knockdowns (47), and PDEB1 knockdowns, with each expressing red fluorescent protein (RFP) or green fluorescent protein (GFP). We then examined these cells in mixed communities. Expression of GFP or RFP did not affect social motility, as WT-RFP and WT-GFP cells are evenly distributed in a mixed social motility community (see Fig. S3d in the supplemental material). Trypanin is a subunit of the flagellar dynein regulatory complex that controls flagellar motility (48). Individual trypanin knockdown cells are incapable of propulsive motility (47) and are consequently defective in social motility (24). We found that the social motility defect of trypanin knockdowns is cell autonomous, as trypanin knockdown-GFP cells were unable to move into radial projections formed by wild-type–RFP cells in a mixed population (Fig. 3a to c and g). The RFP/GFP ratio of the mixed population rose rapidly as a function of the distance from the center, increasing 30-fold within a few millimeters (Fig. 3g). The inability of motility mutants to enter projections formed by wild-type cells demonstrates that parasites are not simply carried into a projection by bulk flow of other cells in the population. Mixing wild-type cells with PDEB1 knockdown cells gave a very different result (Fig. 3d to f and h). In this case, PDEB1 knockdowns, which are incapable of forming projections on their own (Fig. 2), moved into radial projections when cocultured with wild-type cells in a mixed population. Quantitation of relative levels of fluorescence intensity showed that the RFP/GFP ratio remained constant as the population moved outward (Fig. 3h). The result was independent of the status of the cell lines with respect to which harbored GFP versus RFP (see Fig. S4). The ability of the PDEB1 social motility defect to be complemented by wild-type cells in *trans* favors model 2, indicating that wild-type cells provide a critical factor that the PDEB1 mutants can respond to but cannot generate on their own.

DISCUSSION

cAMP regulates *T. brucei* social behavior. The molecular mechanisms underlying trypanosome social motility are unknown. Here we report that flagellar cAMP signaling systems function in regulation of *T. brucei* social motility. Our studies here and in recent work (49) provide the first dissection of the mechanisms underlying social motility in trypanosomes and provide new opportunities for investigating cAMP signaling in these pathogens.

Pharmacological inhibition of *T. brucei* cAMP-specific PDE with cpdA produces a dose-dependent increase in intracellular cAMP concentrations in live trypanosomes that is directly correlated with a dose-dependent block in social motility. These results indicate that PDE activity is required for social motility. Gene-specific knockdown of PDEB1 phenocopies the SoMo(−) defect of cpdA, demonstrating that PDEB1 is specifically required for SoMo. This is in agreement with strong inhibition of recombinant PDEB1 by cpdA at low nanomolar concentrations (50% inhibitory concentration [IC_{50}] = 3.98 nM) (37). *T. brucei* encodes five PDEs, and it is possible that other PDEs may also participate in regulation of social motility, but our data indicate they are not able to substitute for PDEB1.

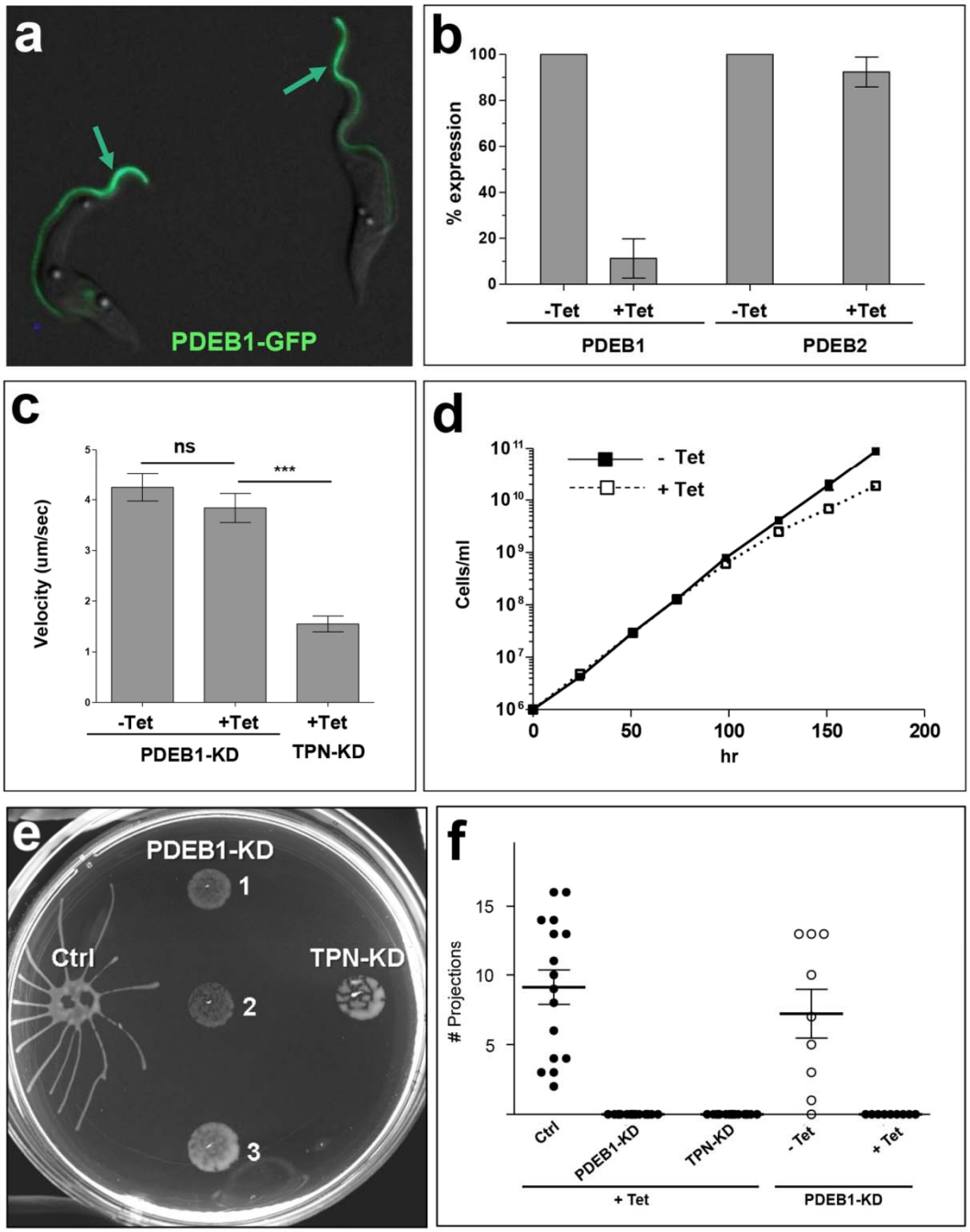

FIG 2 RNAi knockdown of PDEB1 blocks social motility without affecting motility of individual cells. (a) Fluorescence microscopy of procyclic cells expressing a PDEB1-GFP fusion protein, which is localized to the flagellum (arrows). (b) mRNA abundance for PDEB1 and PDEB2, as determined by qRT-PCR, in PDEB1 tetracycline (Tet)-inducible knockdown cells, maintained with or without tetracycline as indicated. Values are normalized to the −Tet expression level. (c) The cell motility of individual cells in suspension culture is shown for Tet-inducible PDEB1 knockdown cells (PDEB-KD), maintained with or without Tet as indicated. Trypanin knockdown (TPN-KD) motility mutants (47) were examined as a control. (d) Growth curve of PDEB1 Tet-inducible knockdown cells grown with or without Tet as indicated. (e) Social motility of 3 independent Tet-inducible PDEB1 knockdown clonal lines (clones 1, 2, and 3), control cells (Ctrl), and trypanin knockdown cells (TPN-KD). PDEB1-KD clone 1 was used for quantitative analysis as shown in panel f. (f) Quantitation of projections formed by control cells (Ctrl), PDEB1 knockdown cells (PDEB1-KD), or trypanin knockdown cells (TPN-KD), grown with or without tet as indicated. Error bars show ± standard errors. ***, $P < 0.0001$; ns = not significant.

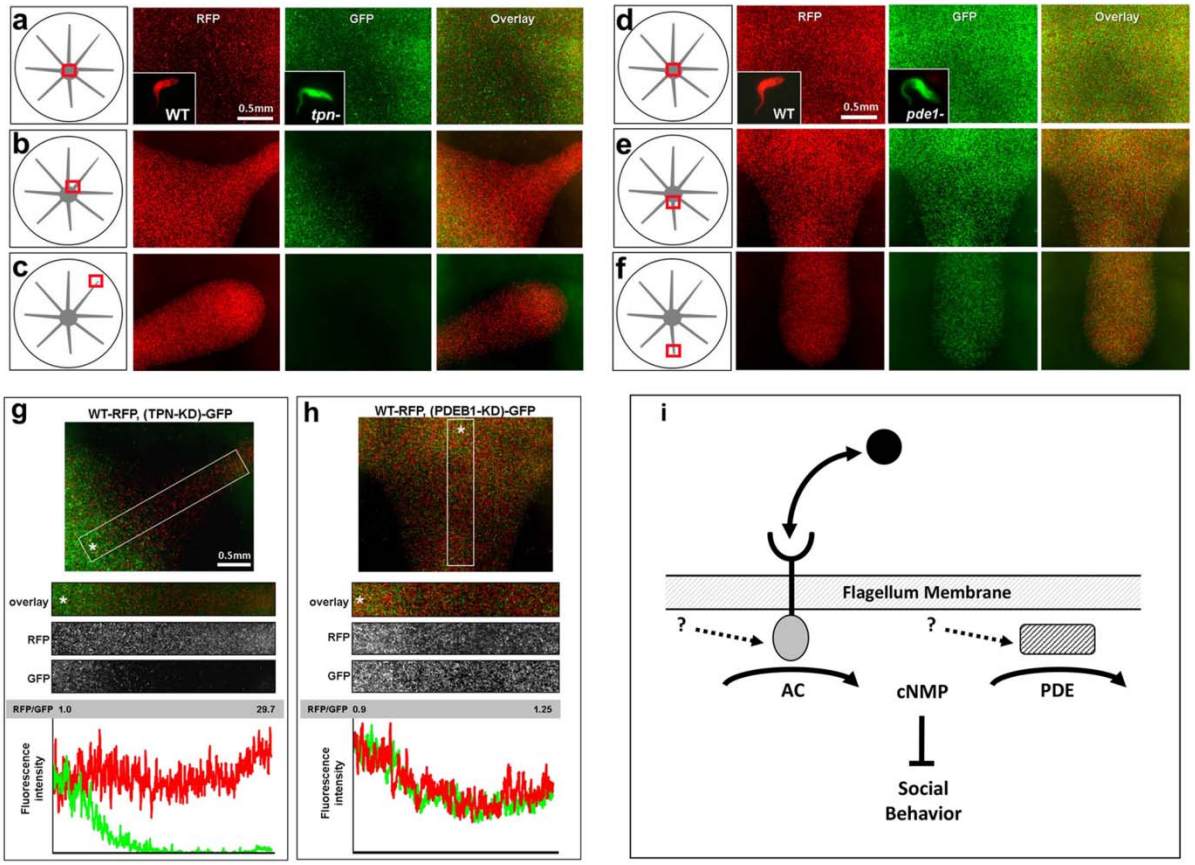

FIG 3 The SoMo(−) defect of PDEB1 knockdowns is complemented by wild-type cells provided in *trans*. (a to c) Social motility assays of mixed communities of wild-type–RFP and trypanin knockdown-GFP cells grown with tetracycline. (d to f) Social motility assays of mixed communities of wild-type–RFP and PDEB1 knockdown-GFP cells grown with tetracycline. Fluorescent images and merged images are shown at the right. The schematic illustrations on the left indicate where the fluorescent images were taken. Insets show representative fluorescent images of individual cells used for the analyses. (g and h) Quantitation of the relative levels of fluorescence of RFP and GFP at the indicated positions of projections formed by communities of wild-type–GFP parasites mixed with either trypanin knockdown-RFP (g) or PDEB1 knockdown-RFP cells (h). Merged and individual fluorescent channels are shown. (i) Generalized model for cyclic nucleotide regulation of social behavior. In *T. brucei*, receptor-type ACs (AC) in the flagellar membrane catalyze formation of cAMP (cNMP) and are responsive to extracellular ligands. cAMP attenuates social motility and is removed by flagellar phosphodiesterase (PDE). Loss of PDE elevates cAMP levels, blocking social motility, while loss of AC activity reduces cAMP levels, stimulating social motility. Dashed arrows indicate potential regulatory inputs. Similar systems operate in bacteria, except that the cyclic nucleotide produced is cyclic-di-GMP (26).

By exploiting a FRET-based cAMP sensor, we were able to directly visualize changes in intracellular cAMP concentrations following cpdA inhibition of PDE activity. Exact measurement of absolute intracellular cAMP levels is challenging. However, the cAMP concentration-dependent response of the epac1camps sensor has been titrated *in vitro*, allowing crude estimates of cAMP levels *in vivo* (42, 43). Based on titration of the epac1camps sensor *in vitro* (42, 43), the FRET ratio of ~0.9 in control *T. brucei* cells corresponds to a cAMP concentration below the 200 nM cAMP detection limit of the sensor. Addition of 100 nM cpdA increases cAMP levels to approximately 200 to 400 nM and completely blocks social motility, while addition of 500 nM or 1 μM cpdA increases cAMP levels to above 2 μM. These values reflect total cellular cAMP concentrations, and the changes within the flagellum are likely smaller. The combined pharmacological, gene knockdown, and FRET data indicate that flux through the cAMP signaling pathway controls *T. brucei* social behavior. In addition, our findings provide the first demonstration, to our knowledge, of a specific function for an individual *T. brucei* phosphodiesterase, an enzyme that is the focus of current drug development efforts (36–38).

Several independent studies have implicated cAMP signaling as critical for *T. brucei* biology, development, and pathogenesis (22, 23, 32, 39, 50, 51), but the individual functions of adenylate cyclases (ACs) and PDEs are mostly unknown. Recent work provided an important advance by demonstrating a requirement for *T. brucei* bloodstream-specific ESAG4 adenylate cyclase function in host-parasite interaction and virulence in mice (51), and elegant genetic studies have identified candidate cAMP downstream effectors (22, 39). Notably, these studies focused exclusively on bloodstream parasites and even less is known regarding cAMP functions in procyclic forms. Recent studies identified procyclic-

specific adenylate cyclases, consistent with the suggestion that cAMP functions in parasite differentiation in the fly (52, 53), and at least two of these procyclic-specific ACs have been shown to regulate social motility (49). A primary contributor to the limited understanding of cAMP signaling in trypanosomes is the lack of convenient assays for cAMP function in live cells. Studies of surface-associated group behaviors have provided insights into cyclic nucleotide signaling in other microbes (26, 27, 54, 55). Thus, in addition to demonstrating a role for cAMP in social motility, our studies provide an important advance by establishing a convenient biological assay for dissecting cAMP signaling in *T. brucei*.

A microdomain model for flagellar cAMP signaling in *T. brucei*. cAMP signaling in eukaryotes is restricted to subcellular microdomains 50 to 100 nm in diameter (56–58). Compartmentalization is important for successful signal transduction, as it limits interference between pathways that use the same signal output, increases sensitivity through higher local cAMP concentrations, and enables transient activation and a rapid response to small changes in cAMP levels (56–58). PDE activity is critical for maintaining cAMP microdomains because it limits diffusion of cAMP to the immediate vicinity of synthesis (56–58). As such, only the proteins that sample these microdomains at the right time can transmit the cAMP-dependent signal. A microdomain model for cAMP operating within the trypanosome flagellum, as proposed by Oberholzer et al. (45), provides a potential explanation for the SoMo(−) phenotype observed upon PDEB1 knockdown or chemical inhibition. PDEB1 is localized throughout the flagellum (32). In separate work, we reported that a specific *T. brucei* adenylate cyclase, AC6, is localized to the tip of the flagellum and that the loss ofAC6 results in hyperactivated social motility, i.e., in an effect opposite that of PDEB1 knockdown (49). The combined data are consistent with a model postulating that social motility is controlled by fluctuations of cAMP concentrations within a specific microdomain at the flagellum tip and that increased cAMP within this microdomain blocks social motility. In this model, PDEB1 is required to insulate the flagellum tip microdomain from cAMP originating elsewhere, for example, from other AC proteins in the flagellum (59). The diffusion coefficient of cAMP in olfactory cilia is estimated to be 2.7×10^{-6} cm^2·s^{-1} (60). Given a length of approximately 20 μm for the *T. brucei* flagellum, cAMP originating at any location would diffuse throughout the flagellum in less than 10 ms under unrestricted conditions. When PDEB1 is inhibited or knocked down, cAMP would be free to diffuse throughout the flagellum, thereby disrupting cAMP homeostasis and inhibiting social motility.

Conserved architecture of pathways that control social behavior in trypanosomes and bacteria. Cyclic nucleotide signaling regulates social behaviors in divergent microbes (6, 27, 61). A classic example is the social amoeba *Dictyostelium* sp., where cAMP functions as an extracellular chemoattractant and an intracellular signaling molecule that promotes development of multicellular fruiting bodies (55). A more directly comparable system is c-di-GMP regulation of bacterial swarming motility (26, 27, 62–64). In bacteria, c-di-GMP levels are controlled through the coordinate activity of diguanylate cyclases (dGCs) that synthesize the molecule and c-di-GMP-specific PDEs that degrade the molecule (54). Perturbation of either the PDE or dGC alters cellular c-di-GMP homeostasis and perturbs swarming motility (26, 27, 62–64). In *Pseudomonas aeruginosa*, knockout of the *bifA* gene, encoding a c-di-GMP-specific PDE, blocks swarming motility, owing to elevated intracellular c-di-GMP concentrations (62). Conversely, knockout of *sadC* or *roeA*, encoding dGCs, reduces cellular c-di-GMP concentrations and generates hyperswarmers (63, 64). The reciprocal effect of PDE and dGC mutants on bacterial swarming motility is analogous to what we observe for PDE and AC (49) mutants in *T. brucei* social motility. As such, our findings indicate a conserved architecture for the signaling pathways that control social behavior in trypanosomes and bacteria (Fig. 3i).

In *Pseudomonas* spp., it is postulated that c-di-GMP derived from specific dGCs, rather than total cellular levels of the molecule, controls swarming (64), and we suspect this may be analogous to the finding that only specific ACs influence *T. brucei* social motility (49). Trypanosomal ACs and PDEs contain known and suspected regulatory input domains, such as the GAF-A domain of PDEB1 and PDEB2 (65) and the periplasmic binding protein (PBP) domain of ACs (29, 65, 66). Thus, *T. brucei* PDE- and AC-mediated control of social motility may be regulated by endogenous molecules, as previously observed for PDEs and dGCs that control swarming motility in bacteria (26, 54).

PDE knockdowns are social motility competent but deficient in an intercellular process that promotes social motility. The genetic tractability of *T. brucei*, combined with the ease with which individual cells can be visualized, makes trypanosomes an excellent system for monitoring the behavior of individuals within a mixed population. Capitalizing on this, we found that the social motility defect of PDEB1 knockdowns can be complemented by WT cells provided in *trans*. To our knowledge, this is the first report of transcomplementation in parasitic protozoa, although such processes are well known in bacteria (46). Notably, individual fluorescent parasites in mixed communities retain either red or green fluorescence, indicating that complementation is not due to exchange of cytoplasmic material. We propose that PDEB1 knockdowns are competent for social motility but fail to produce something extracellularly that is necessary for social motility and that WT cells can provide this factor. The parasite-derived components responsible for transcomplementation of social motility remain unknown. These components might be specific proteins or small molecules, as seen, for example, in rescue of bacterial swarming mutants by outer membrane proteins transferred from wild-type cells in the same community (46, 67). Alternatively, they might be something that alters the physical environment, in analogy to the biosurfactants that promote swarming in bacteria (68). Trypanosomes are known to modify their environment by releasing proteins and uncharacterized low-molecular-weight factors as well as metabolic degradation products (69–71). Regardless of the mechanism, our findings reveal a form of cell-cell communication that was not previously recognized in these organisms.

MATERIALS AND METHODS

Cell culture. 2913 procyclic cells (72) were subjected to two rounds of enrichment by growth on semisolid agarose plates, isolating parasites from the tips of social motility projections (24), cloning by limiting dilution, and repeating. These cells, 2913^{MO2}, were used as controls (WT) for all experiments and were used as the parental line for all transfections. Cell culture, transfections, and isolation of clonal lines by limiting dilution were done as previously described (48).

PDEB1-GFP. The TbPDEB1 (Tb09.160.3590) open reading frame was PCR amplified from plasmid pCR-TbrPDEB1 (gift of T. Seebeck, Bern, Switzerland) using primers B1GAPRONEf and B1GAPRONEr

(primer sequences are provided below). The PCR product was cloned upstream of GFP in pG-eGFP-Blast (gift of Isabel Roditi, University of Bern) (73). The construct was verified by sequencing, linearized with SpeI, and transfected into 2913^{MO2} cells. Expression of the PDEB1-GFP fusion protein was determined by fluorescence microscopy using an Axioskop II microscope (Zeiss, Inc., Germany).

TbPDEB1 RNAi knockdown cells. A 279-bp fragment corresponding to bp 150 to bp 428 of TbPDEB1 (Tb09.160.3590) was subcloned from an RNAi knockdown construct previously published (32) into the p2T7-Ti-B vector (74) using HindIII and BamHI. The construct was verified by sequencing, linearized with NotI, and transfected into 2913^{MO2} cells, and clones were obtained by limiting dilution. Clone B1-1 was used for further analysis. Quantitative reverse transcription-PCR (qRT-PCR) was performed as previously described (75) using mRNA from cells at 72 h postinduction with or without 1 μg/ml tetracycline. Each sample was analyzed in duplicate using three independent RNA preparations. The TbPDEB1-specific primers were qRTPDEB1-f and qRTPDEB1-r. The TbPDEB2-specific primers were qRTPDEB2-f and qRTPDEB2-r (primer sequences are provided below). Values were normalized to GAPDH (glyceraldehyde-3-phosphate dehydrogenase) (Tb927.6.4280) and RPS23 (Tb10.70.7030) as described previously (75).

FRET reporter and RFP and GFP reporter cells. The epac1camps sensor was PCR amplified from plasmid pcDNA3-YFP-epac1-CFP (42) using primers EPACcamp-f and EPACcamp-r1 (primer sequences are provided below). The PCR product was cloned into pCRII Topo (Invitrogen), and the sequences were verified by sequencing. The epac1camps sequence was then subcloned into the HindIII and XbaI sites of pLew100 (72). The construct was linearized with NotI and transfected into 2913^{MO2} cells. epac1camps expression was detected following tet induction by fluorescence microscopy. RFP-expressing and GFP-expressing cells were obtained by transfection with SpeI-linearized pG-RFP-Blast and pG-eGFP-Blast (gift of Isabel Roditi, University of Bern) (73), and stable transfectants were selected using 10 μg/ml blasticidin and cloned by limiting dilution.

Primer sequences. The primers for generating PDEB1-GFP were B1GAPRONEf (5′-ATCTCGAGATGTTCATGAACAAGCCCTTTGG-3′) and B1GAPRONEr (5′-ATACCGGTAAACGAGTACTGCTGTTGTTGCC-3′). The XhoI and AgeI restriction sites are underlined.

The primers for qRT-PCR analysis of PDEB1 RNAi knockdown cells were as follows. The TbPDEB1-specific primers were qRTPDEB1-f (5′-TTCATGAACAAGCCCTTTGG-3′) and qRTPDEB1-r (5′-TGATAGCGAGCGAGGATTG-3′). The TbPDEB2-specific primers were qRTPDEB2-f (5′-CGGTGGTCGTCATCTGCTTG-3′) and qRTPDEB2-r (5′-GGAATCATAAGGGGCGACCA-3′).

The primers for constructing FRET reporter cells were as follows: for the epac1camps sensor, EPACcamp-f (5′-TCACTATAGGGAGACCCAAGCTT-3′) and EPACcamp-r1 (5′-TAACTAGTAGCGGGCGCTTACTTGTAC-3′). The HindIII and SpeI sites are underlined. The reverse primer deletes the internal NotI cloning site at the 3′ end of the cyan fluorescent protein (CFP) moiety.

FRET. epac1camps expression was induced for 24 to 48 h using 1 μg/ml tetracycline. Cells were washed once in culture medium and resuspended to 1.5×10^8 cells/ml in the same medium. A 100-μl volume of cells was added to each well of a 96-well black polystyrene Microplate (Greiner). An additional 100 μl of medium containing cpdA was added to each well to give final concentrations of 100 nM, 500 nM, and 1 μM cpdA. Several controls were performed for normalization of the reading. (i) epac1camps-expressing cells were treated with just dimethyl sulfoxide (DMSO), which is the solvent for cpdA. (ii) 2913^{MO2} parental cells, i.e., without epac1camps, were treated with cpdA. Immediately following addition of cpdA or DMSO, emission ratios were determined using a photospectrometer (FlexStation) and SoftMax Pro 4.8 software. Filter settings were as follows: excitation, 436 nm; emission, 480 nm (cutoff, 475 nm) or 535 nm (cutoff, 530 nm). The experiments at each time point (41-s intervals) were performed in triplicate, and the results are reported ± standard deviations.

Motility traces and social motility assays. Motility trace experiments were done as previously described (76). Movies were exported at a resolution of 1 fps and analyzed using automatic tracking in MetaMorph software (Molecular Devices). For social motility assays, cells were diluted for three consecutive days to 3×10^6 cells/ml in suspension culture. A 4% (wt/vol) solution of SeaPlaque GTG agarose (Lonza) in MilliQ water was sterilized for 20 min at 250°C, evaporated water was replaced with sterile MilliQ water, and the stock solution was cooled to 70°C. Stock was diluted to 0.4% with prewarmed culture medium and then maintained at 37°C and supplemented with cpdA, DMSO, 1 μg/ml tetracycline, or methanol as indicated. Medium (13 ml) was poured into 100-mm-by-15-mm petri dishes (Fisherbrand), and plates were dried open for 1.5 h in a laminar flow hood. A total of 5×10^7 cells at 1.2×10^7 to 1.6×10^7 cell/ml were added to the agarose surface, and plates were sealed with Parafilm and incubated at 27°C and 5% CO_2.

For cAMP analogue experiments, social motility plates were supplemented with 8-Br-cAMP (Sigma) as cell-permeable cAMP; Rp-8-Br-cAMPS (Sigma) as cell-permeable, hydrolysis-resistant cAMP; 8-pCPT-2′-O-Me-Ado (BioLog, Germany) as cell-permeable adenosine; or 8-pCPT-2′-O-Me-5′-AMP (BioLog, Germany) as cell-permeable AMP; and assays were performed as described above, with plates kept in the dark. Concentrations to be used were determined by starting with 8-Br-cAMP at 150 μM, the concentration that induces stumpy formation in *T. brucei* (44), and titrating down to find the minimum concentration that inhibited social motility, which was 1 to 10 μM. The other compounds were then also tested at these concentrations. Inhibition of social motility was not due to inhibition of cell proliferation (not shown). AMP and adenosine gave inhibition when the concentration was raised to 20 μM (not shown), though this was likely due to nonspecific effects, as it is ~200-fold higher than the concentration (84 nM to 125 nM) that blocks proliferation and induces stumpy formation in bloodstream-form cells (44). In contrast, the concentration of externally added cAMP required to inhibit social motility is 10-fold to 100-fold lower than what is required to induce stumpy formation (44). Moreover, because cAMP analogues added to *T. brucei* cells are unstable (44), the effective cAMP concentration is actually much lower than what was added. It is recognized that cAMP analogues have potential off-target effects and may act as agonists or antagonists of cAMP effector proteins (44, 77), and we therefore consider these experiments to be an adjunct to those with the more specific pharmacological *T. brucei* PDE inhibitor cpdA (37) and gene-specific PDEB1 RNAi.

Colony lifts to assess GPEET expression. GPEET expression in cells on plates was assessed by colony lifts. Nitrocellulose membrane was incubated on the surface of social motility plates (day 4 postplating) for 5 min. The membrane was removed, air-dried, and stained with Ponceau S prior to imaging to visualize total protein. The membrane was washed in MilliQ water, blocked in phosphate-buffered saline (PBS) containing 5% powdered milk, and stained with anti-GPEET antibody (1:10,000) overnight at 4°C. The membrane was washed 3 times for 10 min in PBS–0.05% Tween 20 and stained with secondary antibodies coupled to horseradish peroxidase (HRP) (1:2,500) and washed as described above prior to development using an enhanced chemiluminescence (ECL) kit and exposure to film.

Social complementation assay. GFP-expressing cells and RFP-expressing cells were mixed in a 1:1 ratio and plated as described above for social motility assays. Fluorescence imaging of cells on plates was done 96 to 120 h postplating using an Axioskop II microscope (Zeiss, Inc., Jena, Germany) with a 2.56LD Plan NeoFluor objective and a GFP bandpass emission filter (41017; Chroma Technology) or an RFP bandpass emission filter (41007; Chroma Technology) on a Zeiss Axiovert microscope using an AxioCam camera. Pictures were processed using Adobe Photoshop, fluorescence intensities were determined using ImageJ (NIH), and values were plotted using GraphPad PRISM.

SUPPLEMENTAL MATERIAL

Supplemental material for this article may be found at http://mbio.asm.org/lookup/suppl/doi:10.1128/mBio.01954-14/-/DCSupplemental.

Figure S1, PPT file, 0.2 MB.
Figure S2, PPT file, 0.3 MB.
Figure S3, PPT file, 0.7 MB.
Figure S4, PPT file, 1.8 MB.
Figure S5, PPT file, 2.9 MB.

ACKNOWLEDGMENTS

We thank Geert Jan Sterk (Mercachem) for providing cpdA, Isabel Roditi (University of Bern) for GPEET antibody and for providing the pG-eGFP-Blast and pRFP-Blast plasmids prior to publication, Viacheslav O. Nikolaev and Martin J. Lohse (University of Würzburg) for providing the epac1camps construct and advice on its use, and Robert Damoiseaux (Molecular Shared Screening Resource, UCLA) for assistance with the FRET analysis. We thank Thomas Seebeck, Isabel Roditi, and Simon Imhof (University of Bern) for many helpful discussions. We also thank members of the Hill Laboratory, especially Miguel Lopez and Michelle Shimogawa, for helpful discussions and technical assistance.

This work was supported by a Swiss National Science Foundation fellowship to M.O., a Burroughs Wellcome Fund Investigator in Global Infectious Disease award to K.L.H., and an NIH grant (R01AI052348) to K.L.H.

REFERENCES

1. **Bassler BL, Losick R.** 2006. Bacterially speaking. Cell **125:**237–246. http://dx.doi.org/10.1016/j.cell.2006.04.001.
2. **Shapiro JA.** 1998. Thinking about bacterial populations as multicellular organisms. Annu Rev Microbiol **52:**81–104. http://dx.doi.org/10.1146/annurev.micro.52.1.81.
3. **Blankenship JR, Mitchell AP.** 2006. How to build a biofilm: a fungal perspective. Curr Opin Microbiol **9:**588–594. http://dx.doi.org/10.1016/j.mib.2006.10.003.
4. **Harshey RM.** 2003. Bacterial motility on a surface: many ways to a common goal. Annu Rev Microbiol **57:**249–273. http://dx.doi.org/10.1146/annurev.micro.57.030502.091014.
5. **Velicer GJ, Vos M.** 2009. Sociobiology of the myxobacteria. Annu Rev Microbiol **63:**599–623. http://dx.doi.org/10.1146/annurev.micro.091208.073158.
6. **Firtel RA, Meili R.** 2000. *Dictyostelium*: a model for regulated cell movement during morphogenesis. Curr Opin Genet Dev **10:**421–427. http://dx.doi.org/10.1016/S0959-437X(00)00107-6.
7. **Butler MT, Wang Q, Harshey RM.** 2010. Cell density and mobility protect swarming bacteria against antibiotics. Proc Natl Acad Sci U S A **107:**3776–3781. http://dx.doi.org/10.1073/pnas.0910934107.
8. **Høiby N, Bjarnsholt T, Givskov M, Molin S, Ciofu O.** 2010. Antibiotic resistance of bacterial biofilms. Int J Antimicrob Agents **35:**322–332. http://dx.doi.org/10.1016/j.ijantimicag.2009.12.011.
9. **Douglas LJ.** 2003. *Candida biofilms* and their role in infection. Trends Microbiol **11:**30–36. http://dx.doi.org/10.1016/S0966-842X(02)00002-1.
10. **Antunes LC, Ferreira RB, Buckner MM, Finlay BB.** 2010. Quorum sensing in bacterial virulence. Microbiology **156:**2271–2282. http://dx.doi.org/10.1099/mic.0.038794-0.
11. **Landini P, Antoniani D, Burgess JG, Nijland R.** 2010. Molecular mechanisms of compounds affecting bacterial biofilm formation and dispersal. Appl Microbiol Biotechnol **86:**813–823. http://dx.doi.org/10.1007/s00253-010-2468-8.
12. **Stuart K, Brun R, Croft S, Fairlamb A, Gürtler RE, McKerrow J, Reed S, Tarleton R.** 2008. Kinetoplastids: related protozoan pathogens, different diseases. J Clin Invest **118:**1301–1310. http://dx.doi.org/10.1172/JCI33945.
13. **White NJ, Pukrittayakamee S, Hien TT, Faiz MA, Mokuolu OA, Dondorp AM.** 2014. Malaria. Lancet **383:**723–735. http://dx.doi.org/10.1016/S0140-6736(13)60024-0.
14. **Haas BJ, Kamoun S, Zody MC, Jiang RH, Handsaker RE, Cano LM, Grabherr M, Kodira CD, Raffaele S, Torto-Alalibo T, Bozkurt TO, Ah-Fong AM, Alvarado L, Anderson VL, Armstrong MR, Avrova A, Baxter L, Beynon J, Boevink PC, Bollmann SR.** 2009. Genome sequence and analysis of the Irish potato famine pathogen phytophthora infestans. Nature **461:**393–398. http://dx.doi.org/10.1038/nature08358.
15. **Laishram S, Kang G, Ajjampur SS.** 2012. Giardiasis: a review on assemblage distribution and epidemiology in India. Indian J Gastroenterol **31:**3–12. http://dx.doi.org/10.1007/s12664-012-0161-9.
16. **Fletcher SM, Stark D, Harkness J, Ellis J.** 2012. Enteric protozoa in the developed world: a public health perspective. Clin Microbiol Rev **25:**420–449. http://dx.doi.org/10.1128/CMR.05038-11.
17. **MacGregor P, Savill NJ, Hall D, Matthews KR.** 2011. Transmission stages dominate trypanosome within-host dynamics during chronic infections. Cell Host Microbe **9:**310–318. http://dx.doi.org/10.1016/j.chom.2011.03.013.
18. **Lopez MA, Nguyen HT, Oberholzer M, Hill KL.** 2011. Social parasites. Curr Opin Microbiol **14:**642–648. http://dx.doi.org/10.1016/j.mib.2011.09.012.
19. **Reece SE, Drew DR, Gardner A.** 2008. Sex ratio adjustment and kin discrimination in malaria parasites. Nature **453:**609–614. http://dx.doi.org/10.1038/nature06954.
20. **Pollitt LC, MacGregor P, Matthews K, Reece SE.** 2011. Malaria and trypanosome transmission: different parasites, same rules? Trends Parasitol **27:**197–203. http://dx.doi.org/10.1016/j.pt.2011.01.004.
21. **Brun R, Blum J, Chappuis F, Burri C.** 2010. Human African trypanosomiasis. Lancet **375:**148–159. http://dx.doi.org/10.1016/S0140-6736(09)60829-1.
22. **Mony BM, MacGregor P, Ivens A, Rojas F, Cowton A, Young J, Horn D, Matthews K.** 2014. Genome-wide dissection of the quorum sensing signalling pathway in *Trypanosoma brucei*. Nature **505:**681–685. http://dx.doi.org/10.1038/nature12864.
23. **Vassella E, Reuner B, Yutzy B, Boshart M.** 1997. Differentiation of African trypanosomes is controlled by a density sensing mechanism which signals cell cycle arrest via the cAMP pathway. J Cell Sci **110:**2661–2671.
24. **Oberholzer M, Lopez MA, McLelland BT, Hill KL.** 2010. Social motility in African trypanosomes. PLoS Pathog **6:**e1000739. http://dx.doi.org/10.1371/journal.ppat.1000739.
25. **Imhof S, Knüsel S, Gunasekera K, Vu XL, Roditi I.** 2014. Social motility of African trypanosomes is a property of a distinct life-cycle stage that occurs early in tsetse fly transmission. PLoS Pathog **10:**e1004493. http://dx.doi.org/10.1371/journal.ppat.1004493.
26. **Trimble MJ, McCarter LL.** 2011. *Bis*-(3′-5′)-cyclic dimeric GMP-linked quorum sensing controls swarming in *Vibrio parahaemolyticus*. Proc Natl Acad Sci U S A **108:**18079–18084. http://dx.doi.org/10.1073/pnas.1113790108.
27. **Simm R, Morr M, Kader A, Nimtz M, Römling U.** 2004. GGDEF and EAL domains inversely regulate cyclic di-GMP levels and transition from sessility to motility. Mol Microbiol **53:**1123–1134. http://dx.doi.org/10.1111/j.1365-2958.2004.04206.x.
28. **Hickman JW, Tifrea DF, Harwood CS.** 2005. A chemosensory system that regulates biofilm formation through modulation of cyclic diguanylate levels. Proc Natl Acad Sci U S A **102:**14422–14427. http://dx.doi.org/10.1073/pnas.0507170102.
29. **Seebeck T, Schaub R, Johner A.** 2004. cAMP signalling in the kinetoplastid protozoa. Curr Mol Med **4:**585–599. http://dx.doi.org/10.2174/1566524043360113.
30. **Zoraghi R, Seebeck T.** 2002. The cAMP-specific phosphodiesterase TbPDE2C is an essential enzyme in bloodstream form *Trypanosoma brucei*. Proc Natl Acad Sci U S A **99:**4343–4348. http://dx.doi.org/10.1073/pnas.062716599.
31. **Rascón A, Soderling SH, Schaefer JB, Beavo JA.** 2002. Cloning and characterization of a cAMP-specific phosphodiesterase (TbPDE2B) from *Trypanosoma brucei*. Proc Natl Acad Sci U S A **99:**4714–4719. http://dx.doi.org/10.1073/pnas.002031599.
32. **Oberholzer M, Marti G, Baresic M, Kunz S, Hemphill A, Seebeck T.** 2007. The *Trypanosoma brucei* cAMP phosphodiesterases TbrPDEB1 and TbrPDEB2: flagellar enzymes that are essential for parasite virulence. FASEB J **21:**720–731. http://dx.doi.org/10.1096/fj.06-6818com.
33. **Gerdes JM, Davis EE, Katsanis N.** 2009. The vertebrate primary cilium in development, homeostasis, and disease. Cell **137:**32–45. http://dx.doi.org/10.1016/j.cell.2009.03.023.
34. **Rotureau B, Morales MA, Bastin P, Späth GF.** 2009. The flagellum-mitogen-activated protein kinase connection in trypanosomatids: a key sensory role in parasite signalling and development? Cell Microbiol **11:**710–718. http://dx.doi.org/10.1111/j.1462-5822.2009.01295.x.
35. **Maric D, Epting CL, Engman DM.** 2010. Composition and sensory

function of the trypanosome flagellar membrane. Curr Opin Microbiol **13:**466–472. http://dx.doi.org/10.1016/j.mib.2010.06.001.

36. **Seebeck T, Sterk GJ, Ke H.** 2011. Phosphodiesterase inhibitors as a new generation of antiprotozoan drugs: exploiting the benefit of enzymes that are highly conserved between host and parasite. Future Med Chem **3:**1289–1306. http://dx.doi.org/10.4155/fmc.11.77.
37. **De Koning HP, Gould MK, Sterk GJ, Tenor H, Kunz S, Luginbuehl E, Seebeck T.** 2012. Pharmacological validation of *Trypanosoma brucei* phosphodiesterases as novel drug targets. J Infect Dis **206:**229–237. http://dx.doi.org/10.1093/infdis/jir857.
38. **Orrling KM, Jansen C, Vu XL, Balmer V, Bregy P, Shanmugham A, England P, Bailey D, Cos P, Maes L, Adams E, van den Bogaart E, Chatelain E, Ioset JR, van de Stolpe A, Zorg S, Veerman J, Seebeck T, Sterk GJ, de Esch IJ.** 2012. Catechol pyrazolinones as trypanocidals: fragment-based design, synthesis, and pharmacological evaluation of nanomolar inhibitors of trypanosomal phosphodiesterase B1. J Med Chem **55:**8745–8756. http://dx.doi.org/10.1021/jm301059b.
39. **Gould MK, Bachmaier S, Ali JA, Alsford S, Tagoe DN, Munday JC, Schnaufer AC, Horn D, Boshart M, de Koning HP.** 2013. Cyclic AMP effectors in African trypanosomes revealed by genome-scale RNA interference library screening for resistance to the phosphodiesterase inhibitor CpdA. Antimicrob Agents Chemother **57:**4882–4893. http://dx.doi.org/10.1128/AAC.00508-13.
40. **Freire ER, Vashisht AA, Malvezzi AM, Zuberek J, Langousis G, Saada EA, Nascimento Jde F, Stepinski J, Darzynkiewicz E, Hill K, De Melo Neto OP, Wohlschlegel JA, Sturm NR, Campbell DA.** 2014. eIF4F-like complexes formed by cap-binding homolog TbEIF4E5 with TbEIF4G1 or TbEIF4G2 are implicated in post-transcriptional regulation in *Trypanosoma brucei*. RNA **20:**1272–1286. http://dx.doi.org/10.1261/rna.045534.114.
41. **Freire ER, Malvezzi AM, Vashisht AA, Zuberek J, Saada EA, Langousis G, Nascimento JD, Moura D, Darzynkiewicz E, Hill K, de Melo Neto OP, Wohlschlegel JA, Sturm NR, Campbell DA.** 2014. *Trypanosoma brucei* translation initiation factor homolog EIF4E6 forms a tripartite cytosolic complex with EIF4G5 and a capping enzyme homolog. Eukaryot Cell **13:**896–908. http://dx.doi.org/10.1128/EC.00071-14.
42. **Nikolaev VO, Bünemann M, Hein L, Hannawacker A, Lohse MJ.** 2004. Novel single chain cAMP sensors for receptor-induced signal propagation. J Biol Chem **279:**37215–37218. http://dx.doi.org/10.1074/jbc.C400302200.
43. **Börner S, Schwede F, Schlipp A, Berisha F, Calebiro D, Lohse MJ, Nikolaev VO.** 2011. FRET measurements of intracellular cAMP concentrations and cAMP analog permeability in intact cells. Nat Protoc **6:**427–438. http://dx.doi.org/10.1038/nprot.2010.198.
44. **Laxman S, Riechers A, Sadilek M, Schwede F, Beavo JA.** 2006. Hydrolysis products of cAMP analogs cause transformation of *Trypanosoma brucei* from slender to stumpy-like forms. Proc Natl Acad Sci U S A **103:**19194–19199. http://dx.doi.org/10.1073/pnas.0608971103.
45. **Oberholzer M, Bregy P, Marti G, Minca M, Peier M, Seebeck T.** 2007. Trypanosomes and mammalian sperm: one of a kind? Trends Parasitol **23:**71–77. http://dx.doi.org/10.1016/j.pt.2006.12.002.
46. **Nudleman E, Wall D, Kaiser D.** 2005. Cell-to-cell transfer of bacterial outer membrane lipoproteins. Science **309:**125–127. http://dx.doi.org/10.1126/science.1112440.
47. **Hutchings NR, Donelson JE, Hill KL.** 2002. Trypanin is a cytoskeletal linker protein and is required for cell motility in African trypanosomes. J Cell Biol **156:**867–877. http://dx.doi.org/10.1083/jcb.200201036.
48. **Ralston KS, Lerner AG, Diener DR, Hill KL.** 2006. Flagellar motility contributes to cytokinesis in *Trypanosoma brucei* and is modulated by an evolutionarily conserved dynein regulatory system. Eukaryot Cell **5:**696–711. http://dx.doi.org/10.1128/EC.5.4.696-711.2006.
49. **Lopez MA, Saada EA, Hill KL.** 2015. Insect stage-specific adenylate cyclases regulate social motility in African trypanosomes. Eukaryot Cell **14:**104–112. http://dx.doi.org/10.1128/EC.00217-14.
50. **Salmon D, Bachmaier S, Krumbholz C, Kador M, Gossmann JA, Uzureau P, Pays E, Boshart M.** 2012. Cytokinesis of *Trypanosoma brucei* bloodstream forms depends on expression of adenylyl cyclases of the ESAG4 or ESAG4-like subfamily. Mol Microbiol **84:**225–242. http://dx.doi.org/10.1111/j.1365-2958.2012.08013.x.
51. **Salmon D, Vanwalleghem G, Morias Y, Denoeud J, Krumbholz C, Lhommé F, Bachmaier S, Kador M, Gossmann J, Dias FB, De Muylder G, Uzureau P, Magez S, Moser M, De Baetselier P, Van Den Abbeele J, Beschin A, Boshart M, Pays E.** 2012. Adenylate cyclases of *Trypanosoma brucei* inhibit the innate immune response of the host. Science **337:**463–466. http://dx.doi.org/10.1126/science.1222753.
52. **Saada EA, Kabututu ZP, Lopez M, Shimogawa MM, Langousis G, Oberholzer M, Riestra A, Jonsson ZO, Wohlschlegel JA, Hill KL.** 2014. Insect stage-specific receptor adenylate cyclases are localized to distinct subdomains of the *Trypanosoma brucei* flagellar membrane. Eukaryot Cell **13:**1064–1076. http://dx.doi.org/10.1128/EC.00019-14.
53. **Rolin S, Paindavoine P, Hanocq-Quertier J, Hanocq F, Claes Y, Le Ray D, Overath P, Pays E.** 1993. Transient adenylate cyclase activation accompanies differentiation of *Trypanosoma brucei* from bloodstream to procyclic forms. Mol Biochem Parasitol **61:**115–125. http://dx.doi.org/10.1016/0166-6851(93)90164-S.
54. **Boyd CD, O'Toole GA.** 2012. Second messenger regulation of biofilm formation: breakthroughs in understanding c-di-GMP effector systems. Annu Rev Cell Dev Biol **28:**439–462. http://dx.doi.org/10.1146/annurev-cellbio-101011-155705.
55. **Manahan CL, Iglesias PA, Long Y, Devreotes PN.** 2004. Chemoattractant signaling in *Dictyostelium discoideum*. Annu Rev Cell Dev Biol **20:**223–253. http://dx.doi.org/10.1146/annurev.cellbio.20.011303.132633.
56. **Willoughby D, Wong W, Schaack J, Scott JD, Cooper DM.** 2006. An anchored PKA and PDE4 complex regulates subplasmalemmal cAMP dynamics. EMBO J **25:**2051–2061. http://dx.doi.org/10.1038/sj.emboj.7601113.
57. **Baillie GS, Houslay MD.** 2005. Arrestin times for compartmentalised cAMP signalling and phosphodiesterase-4 enzymes. Curr Opin Cell Biol **17:**129–134. http://dx.doi.org/10.1016/j.ceb.2005.01.003.
58. **Karpen JW, Rich TC.** 2005. High-resolution measurements of cyclic adenosine monophosphate signals in 3D microdomains. Methods Mol Biol **307:**15–26. http://dx.doi.org/10.1385/1-59259-839-0:015.
59. **Paindavoine P, Rolin S, Van Assel S, Geuskens M, Jauniaux JC, Dinsart C, Huet G, Pays E.** 1992. A gene from the variant surface glycoprotein expression site encodes one of several transmembrane adenylate cyclases located on the flagellum of *Trypanosoma brucei*. Mol Cell Biol **12:**1218–1225.
60. **Chen C, Nakamura T, Koutalos Y.** 1999. Cyclic AMP diffusion coefficient in frog olfactory cilia. Biophys J **76:**2861–2867. http://dx.doi.org/10.1016/S0006-3495(99)77440-0.
61. **Klengel T, Liang WJ, Chaloupka J, Ruoff C, Schröppel K, Naglik JR, Eckert SE, Mogensen EG, Haynes K, Tuite MF, Levin LR, Buck J, Mühlschlegel FA.** 2005. Fungal adenylyl cyclase integrates CO_2 sensing with cAMP signaling and virulence. Curr Biol **15:**2021–2026. http://dx.doi.org/10.1016/j.cub.2005.10.040.
62. **Kuchma SL, Brothers KM, Merritt JH, Liberati NT, Ausubel FM, O'Toole GA.** 2007. BifA, a cyclic-Di-GMP phosphodiesterase, inversely regulates biofilm formation and swarming motility by *Pseudomonas aeruginosa* PA14. J Bacteriol **189:**8165–8178. http://dx.doi.org/10.1128/JB.00586-07.
63. **Merritt JH, Brothers KM, Kuchma SL, O'Toole GA.** 2007. SadC reciprocally influences biofilm formation and swarming motility via modulation of exopolysaccharide production and flagellar function. J Bacteriol **189:**8154–8164. http://dx.doi.org/10.1128/JB.00585-07.
64. **Merritt JH, Ha DG, Cowles KN, Lu W, Morales DK, Rabinowitz J, Gitai Z, O'Toole GA.** 2010. Specific control of *Pseudomonas aeruginosa* surface-associated behaviors by two c-di-GMP diguanylate cyclases. mBio **1:**00183-10. http://dx.doi.org/10.1128/mBio.00183-10.
65. **Laxman S, Rascón A, Beavo JA.** 2005. Trypanosome cyclic nucleotide phosphodiesterase 2B binds cAMP through its GAF-A domain. J Biol Chem **280:**3771–3779. http://dx.doi.org/10.1074/jbc.M408111200.
66. **Kunz S, Luginbuehl E, Seebeck T.** 2009. Gene conversion transfers the GAF-A domain of phosphodiesterase TbrPDEB1 to one allele of TbrPDEB2 of *Trypanosoma brucei*. PLoS Negl Trop Dis **3:**e455. http://dx.doi.org/10.1371/journal.pntd.0000455.
67. **Pathak DT, Wei X, Bucuvalas A, Haft DH, Gerloff DL, Wall D.** 2012. Cell contact-dependent outer membrane exchange in myxobacteria: genetic determinants and mechanism. PLoS Genet **8:**e1002626. http://dx.doi.org/10.1371/journal.pgen.1002626.
68. **Daniels R, Reynaert S, Hoekstra H, Verreth C, Janssens J, Braeken K, Fauvart M, Beullens S, Heusdens C, Lambrichts I, De Vos DE, Vanderleyden J, Vermant J, Michiels J.** 2006. Quorum signal molecules as biosurfactants affecting swarming in *Rhizobium etli*. Proc Natl Acad Sci U S A **103:**14965–14970. http://dx.doi.org/10.1073/pnas.0511037103.
69. **Proto WR, Castanys-Munoz E, Black A, Tetley L, Moss CX, Juliano L, Coombs GH, Mottram JC.** 2011. *Trypanosoma brucei* metacaspase 4 is a

pseudopeptidase and a virulence factor. J Biol Chem **286:**39914–39925. http://dx.doi.org/10.1074/jbc.M111.292334.

70. **Geiger A, Hirtz C, Bécue T, Bellard E, Centeno D, Gargani D, Rossignol M, Cuny G, Peltier JB.** 2010. Exocytosis and protein secretion in *Trypanosoma*. BMC Microbiol **10:**20. http://dx.doi.org/10.1186/1471-2180-10-20.
71. **Barnwell EM, van Deursen FJ, Jeacock L, Smith KA, Maizels RM, Acosta-Serrano A, Matthews K.** 2010. Developmental regulation and extracellular release of a VSG expression-site-associated gene product from *Trypanosoma brucei* bloodstream forms. J Cell Sci **123:**3401–3411. http://dx.doi.org/10.1242/jcs.068684.
72. **Wirtz E, Leal S, Ochatt C, Cross GA.** 1999. A tightly regulated inducible expression system for conditional gene knockouts and dominant-negative genetics in *Trypanosoma brucei*. Mol Biochem Parasitol **99:**89–101. http://dx.doi.org/10.1016/S0166-6851(99)00002-X.
73. **Urwyler S, Studer E, Renggli CK, Roditi I.** 2007. A family of stage-specific alanine-rich proteins on the surface of epimastigote forms of *Trypanosoma brucei*. Mol Microbiol **63:**218–228. http://dx.doi.org/10.1111/j.1365-2958.2006.05492.x.
74. **LaCount DJ, Barrett B, Donelson JE.** 2002. *Trypanosoma brucei* FLA1 is required for flagellum attachment and cytokinesis. J Biol Chem **277:**17580–17588. http://dx.doi.org/10.1074/jbc.M200873200.
75. **Kabututu ZP, Thayer M, Melehani JH, Hill KL.** 2010. CMF70 is a subunit of the dynein regulatory complex. J Cell Sci **123:**3587–3595. http://dx.doi.org/10.1242/jcs.073817.
76. **Baron DM, Ralston KS, Kabututu ZP, Hill KL.** 2007. Functional genomics in *Trypanosoma brucei* identifies evolutionarily conserved components of motile flagella. J Cell Sci **120:**478–491. http://dx.doi.org/10.1242/jcs.03352.
77. **Poppe H, Rybalkin SD, Rehmann H, Hinds TR, Tang XB, Christensen AE, Schwede F, Genieser HG, Bos JL, Doskeland SO, Beavo JA, Butt E.** 2008. Cyclic nucleotide analogs as probes of signaling pathways. Nat Methods **5:**277–278. http://dx.doi.org/10.1038/nmeth0408-277.

SUPPLEMENTAL MATERIAL LEGENDS

FIGURE S1
Effect of cAMP analogues on social motility. Data represent the social motility of untreated cells (control) or cells treated with cell-permeable cAMP analogues as indicated. 1, hydrolyzable cAMP:8-Br-cAMP; 2, hydrolysis-resistant cAMP (Rp-8-Br-cAMPS); 3, AMP (8-pCPT-2′-O-Me-5′-AMP); 4, adenosine (8-pCPT-2′-O-Me-Ado).The numbers of projections per plate were counted at 72 h postplating. Samples showing statistically significant differences relative to the control are indicated with asterisks. *, $P < 0.0001$; **, $P < 0.01$; ***, $P < 0.03$ (two-tailed, unpaired *t* test). Download **Figure S1, PPT file, 0.2 MB**.

FIGURE S2
FRET assay using epac1camps sensor. (a) Schematic showing the FRET-based cAMP sensor, epac1camps (**42**), and the effect of adding cAMP. (b) Fluorescence emission at 488 and 535 nm for wild-type (WT) cells and cells expressing the epac1camps sensor (epac). (c) Fluorescence ratio (488 nm/535 nm) for epac1camps-expressing cells normalized to the background fluorescence of wild-type cells without the sensor. Download **Figure S2, PPT file, 0.3 MB**.

FIGURE S3
Expression of GFP or RFP does not affect the social motility phenotype. (a to d) Social motility assays with the indicated cell lines expressing RFP or GFP. (a to c) Images of the social motility phenotype. (d) Individual and merged fluorescent channels for mixed communities of wild-type cells expressing RFP or GFP as indicated. Schematic at left shows the region of the projection that was imaged for fluorescence. Download**Figure S3, PPT file, 0.7 MB**.

FIGURE S4
The PDEB1 knockdown social motility defect is rescued by wild-type cells provided in *trans*. Fluorescent and merged images of social motility assays using mixed populations of WT, trypanin knockdown, and PDEB1 knockdown cells as indicated are shown. See the **Fig. 3** legend for details. Here, WT cells express GFP and the knockdown cells express RFP, while in **Fig. 3**, WT cells express RFP and the knockdown cells express GFP. Download **Figure S4, PPT file, 1.8 MB**.

FIGURE S5
GPEET is expressed in PDEB1-RNAi and cpdA-treated cells. Colony lifts were performed on social motility colonies of PDEB1 RNAi cells grown in the absence or presence of tetracycline (tet) as indicated or on control cells grown with or without 0.1 μM cpdA as indicated. Nitrocellulose filters were stained with Ponceau S (top) to visualize total protein and then probed with anti-GPEET antibody to visualize GPEET procyclin (bottom). Download **Figure S5, PPT file, 2.9 MB**.

Oberholzer, Supplemental Figure 1

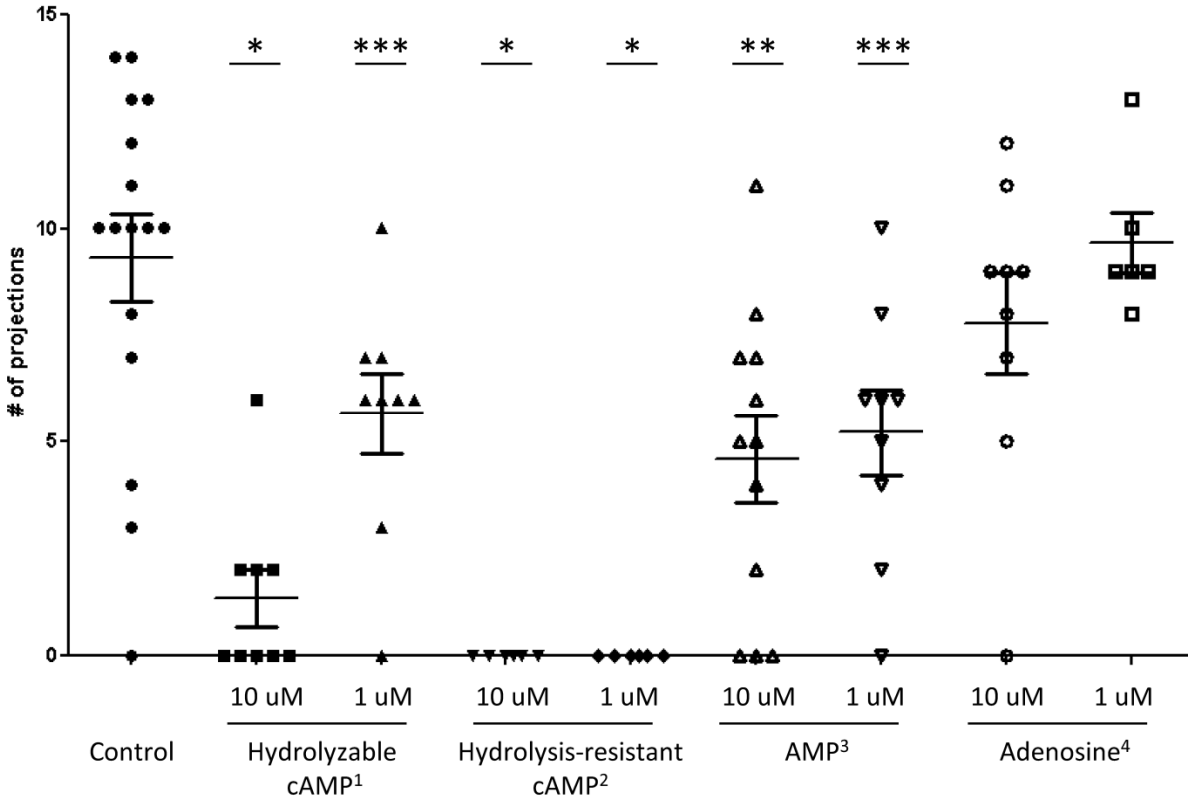

Oberholzer, Supplemental Figure 2

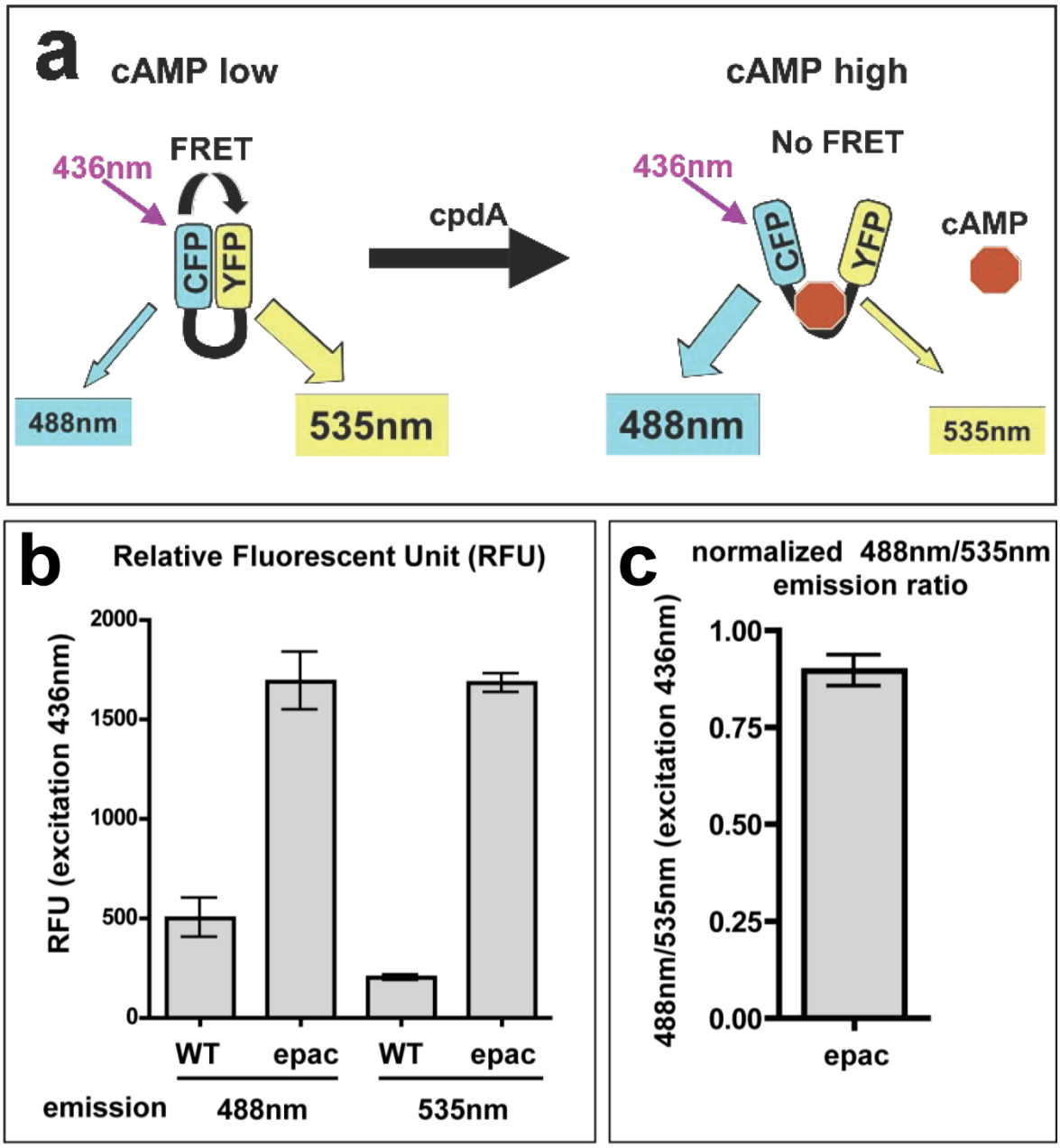

Oberholzer, Supplemental Figure 3

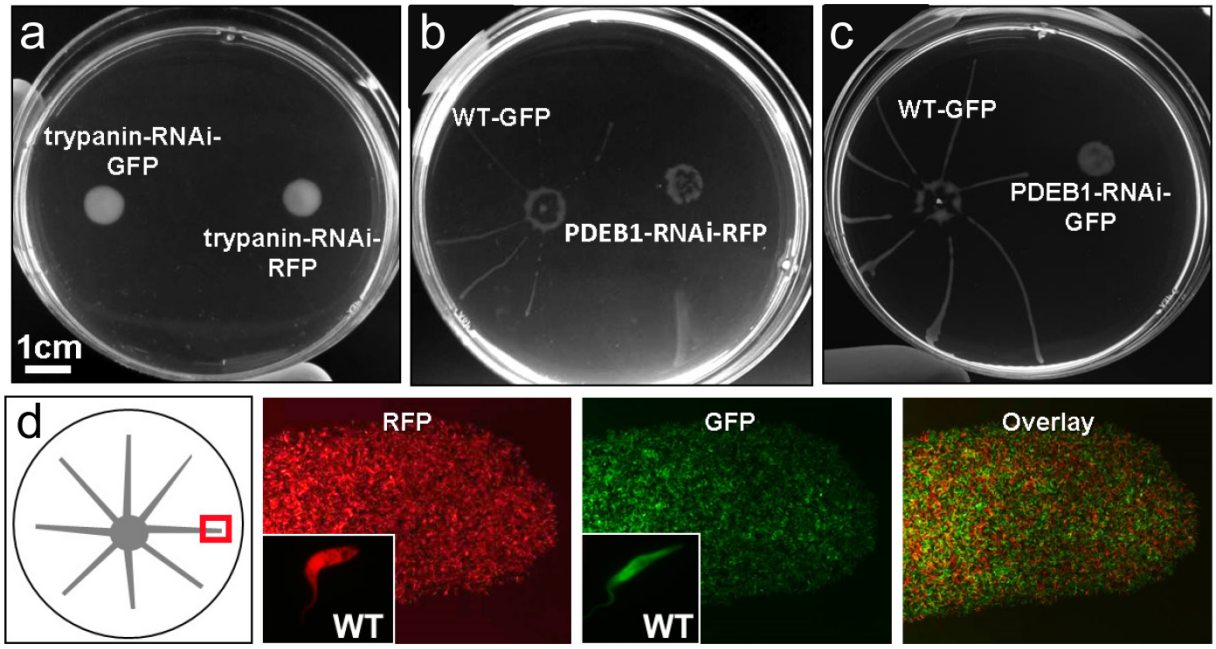

Oberholzer, Supplemental Figure 4

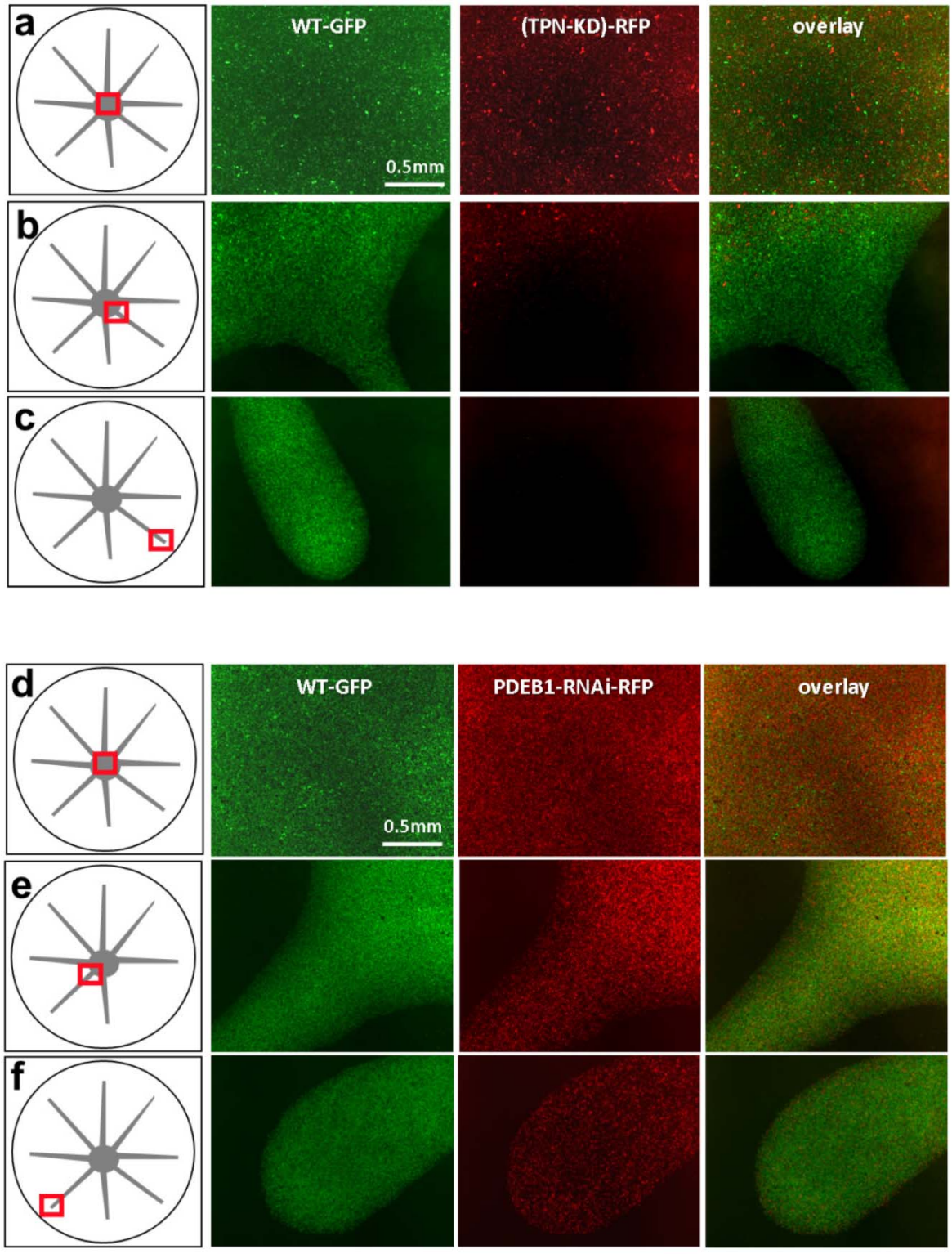

Oberholzer, Supplemental Figure 5

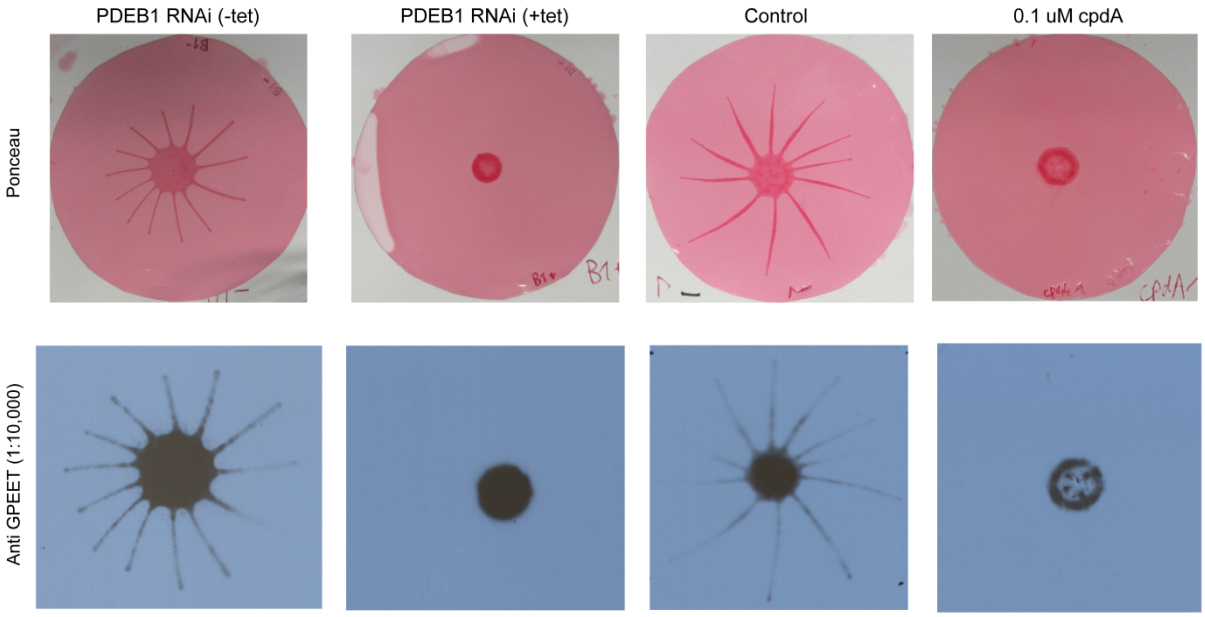

Appendix II:

Social motility analyses of two cytosolic

Trypanosoma brucei eIF4E translation initiation factor-like proteins

that are associated with homologues of mRNA capping enzymes

PREFACE

This appendix includes two works reprinted in entirety with their respective publisher's permission. The first is "*Trypanosoma brucei* translation initiation factor homolog EIF4E6 forms a tripartite cytosolic complex with EIF4G5 and a capping enzyme homolog" by Freire *et al*, and was originally published in Eukaryotic Cell, 2014, 13:896-908. The second is "eIF4F-like complexes formed by cap-binding homolog TbEIF4E5 with TbEIF4G1 or TbEIF4G2 are implicated in post-transcriptional regulation in *Trypanosoma brucei"* by Freire *et* al, and was originally published in RNA, 2014, 20: 1272-1286.

The works characterize two eIF4E translation initiation factor-like proteins. My contribution to both works centered around the usage of social motility analyses. As discussed in Chapters IV and IX, social motility is a powerful tool to analyze trypanosome mutants of both sensory and motility defects. Knockdown or inhibition of EIF4E5 inhibits normal motility of the cells, leading them to sediment more quickly in suspension culture, and fail to perform social motility. Knockdown of EIF4E6 leads to a different phenotype, such that many cells possess a more weakly attached flagellum, and have some motility impairments. Correspondingly, social motility appears to be decreased, but not fully inhibited, in this cell line. Interestingly, when the social motility assay is done in conjugation with CO2 shift experiments (Chapter VIII), EIF4E6 depleted cells are capable of social motility at comparable level to control cells (unpublished, data not shown). This indicates that the social motility

defect can not be completely attributed to a flagellar-motility defect, as initially surmised. This phenotypic difference may be examined in future studies, in conjunction with RNAseq data (Freire, unpublished). This unanticipated finding demonstrates the utility of the social motility assay, and experimental variations, as a powerful tool to better understand and characterize mutants.

Trypanosoma brucei Translation Initiation Factor Homolog EIF4E6 Forms a Tripartite Cytosolic Complex with EIF4G5 and a Capping Enzyme Homolog

Eden R. Freire,[a] Amaranta M. Malvezzi,[a,d] Ajay A. Vashisht,[b] Joanna Zuberek,[c] Edwin A. Saada,[a] Gerasimos Langousis,[a] Janaína D. F. Nascimento,[d] Danielle Moura,[d] Edward Darzynkiewicz,[c,e] Kent Hill,[a] Osvaldo P. de Melo Neto,[d] James A. Wohlschlegel,[b] Nancy R. Sturm,[a] David A. Campbell[a]

Department of Microbiology, Immunology & Molecular Genetics, David Geffen School of Medicine, University of California at Los Angeles, Los Angeles, California, USA[a]; Department of Biological Chemistry, David Geffen School of Medicine, University of California at Los Angeles, Los Angeles, California, USA[b]; Division of Biophysics, Institute of Experimental Physics, Faculty of Physics, University of Warsaw, Warsaw, Poland[c]; Department of Microbiology, Centro de Pesquisas Aggeu Magalhães, Fundaçao Oswaldo Cruz, Recife, PE, Brazil[d]; Centre of New Technologies, University of Warsaw, Warsaw, Poland[e]

Trypanosomes lack the transcriptional control characteristic of the majority of eukaryotes that is mediated by gene-specific promoters in a one-gene–one-promoter arrangement. Rather, their genomes are transcribed in large polycistrons with no obvious functional linkage. Posttranscriptional regulation of gene expression must thus play a larger role in these organisms. The eIF4E homolog TbEIF4E6 binds mRNA cap analogs *in vitro* and is part of a complex *in vivo* that may fulfill such a role. Knockdown of TbEIF4E6 tagged with protein A-tobacco etch virus protease cleavage site-protein C to approximately 15% of the normal expression level resulted in viable cells that displayed a set of phenotypes linked to detachment of the flagellum from the length of the cell body, if not outright flagellum loss. While these cells appeared and behaved as normal under stationary liquid culture conditions, standard centrifugation resulted in a marked increase in flagellar detachment. Furthermore, the ability of TbEIF4E6-depleted cells to engage in social motility was reduced. The TbEIF4E6 protein forms a cytosolic complex containing a triad of proteins, including the eIF4G homolog TbEIF4G5 and a hypothetical protein of 70.3 kDa, referred to as TbG5-IP. The TbG5-IP analysis revealed two domains with predicted secondary structures conserved in mRNA capping enzymes: nucleoside triphosphate hydrolase and guanylyltransferase. These complex members have the potential for RNA interaction, either via the 5′ cap structure for TbEIF4E6 and TbG5-IP or through RNA-binding domains in TbEIF4G5. The associated proteins provide a signpost for future studies to determine how this complex affects capped RNA molecules.

The operon arrangement used by prokaryotes is an elegant solution to the question of regulated gene expression, with coordinated transcription of genes encoding enzymes within a given metabolic pathway under the control of a single promoter. In contrast, the majority of eukaryotes evolved independent promoters to control the expression of individual genes, and promoter types fall into classes that are activated or repressed in synchrony with functionally linked genes. Kinetoplastids employ an unusual blend of these two strategies, the constitutive transcription of polycistronic gene clusters that, apart from tandem gene arrays, typically show no discernible biochemical linkage within arrays (1, 2). The result is the virtual absence of genetic control at the level of gene transcription for mRNAs transcribed by RNA polymerase II (3, 4). *Trypanosoma brucei* has circumvented this limitation for the expression of a set of virulence factors associated with the variant surface glycoproteins. This family provides the coat on the cell surface and cycles a single member over time to allow this parasite to evade the host immune system. RNA polymerase I promoters provide temporal control to this gene set (5, 6). This unusual choice of polymerase is available to trypanosomes because of the mechanism that also provides a complex mRNA cap structure to all nuclear transcripts, namely, *trans* splicing of the spliced leader (SL) RNA (7).

The SL RNA is a small, independently transcribed molecule that is the source of the hypermethylated cap 4 structure that defines nucleus-derived mRNA in kinetoplastids (8). The cap 4 structure consists of cap 0 followed by 2′-*O*-methylation of the first four transcribed nucleotides and an additional three methylations on the first and fourth bases (9). The first 39 nucleotides are transferred by *trans* splicing to each gene transcript in a polycistronic array, which, coupled with 3′ polyadenylation (10), results in a monocistronic mRNA population looking very much like that from any other eukaryote with a few extra 5′ methylations. Other eukaryotes widely separated from each other in evolutionary terms use this combination of polycistronic transcription and *trans* splicing of their own flavor of SL (11–13).

RNA cap formation requires a minimum of three enzymatic activities, a triphosphatase to remove the gamma phosphate of the primary transcript, a guanylyltransferase to attach an inverted GTP cap via a triphosphate bridge, and a methyltransferase to complete the m^7G modification that defines cap 0 (14). This trio of activities is found in various combinations in different systems, including three separate proteins in yeast, a pairing of the first and second activities in metazoa and plants or the second and third

Received 17 March 2014 **Accepted** 12 May 2014
Published ahead of print 16 May 2014
Address correspondence to David A. Campbell, dc@ucla.edu.
Supplemental material for this article may be found at http://dx.doi.org/10.1128/EC.00071-14.

doi:10.1128/EC.00071-14

activities in kinetoplastids, and a single trifunctional enzyme in several viruses (14). In kinetoplastids the proteins adding cap 0 cotranscriptionally to the SL RNA are identified as TbCET1, a triphosphatase, and bifunctional TbCGM1, a guanylyltransferase and methyltransferase (15–17). Subsequent methylation of downstream nucleotides, referred to as cap 1, cap 2, and cap 4, can enhance translation levels (18).

The process of translation is more uniform in eukaryotes, requiring the recognition of a 5′ mRNA cap structure by an RNA cap-binding protein, eIF4E, a component of the eIF4F translation initiation complex. Entrance into the translation pathway could represent a key control point for polycistronically transcribing eukaryotes (19). In organisms with sophisticated mechanisms of transcriptional control such as humans, *Drosophila*, and yeast, the translation initiation machinery provides another level of control (20). The first step of translation initiation involves recognition of the mRNA cap by the eIF4F complex, which consists of eIF4E and the helicase eIF4A bound separately to a scaffold protein, eIF4G. Extended families of eIF4E and eIF4G proteins may result in an array of combinatorial possibilities for the modulation of translation (21). A minimal repertoire is found in the two model yeasts; *Saccharomyces cerevisiae* possesses one eIF4E and two eIF4Gs that have a functional overlap (22); *Schizosaccharomyces pombe* has two eIF4Es and one eIF4G that are distinguished during the stress response (23). Of the *trans*-splicing organisms, *Caenorhabditis elegans* has an extended family of five eIF4Es (24) and two eIF4G isoforms derived from alternative splicing (25). Four eIF4E homologs and five eIF4G homologs have been reported in *Leishmania* and *T. brucei* (26, 27), and the kinetoplastid-specific eIF4G binding partners have been identified for homologs eIF4E3 and eIF4E4 (28), with the eIF4E4 and eIF4G3 combination as the best candidates for the general translation initiation complex (28, 29). Ribosome profiling, the genome-wide analysis of mRNAs protected by the translation machinery, has demonstrated that translational regulation is an important component of regulated protein expression in *T. brucei* (30). The function of the other family members is unknown.

We have identified two further eIF4E family members in kinetoplastids, TbEIF4E5 and TbEIF4E6, focusing here on the molecular and cellular characterization of TbEIF4E6. Knockdown of TbEIF4E6 by RNA interference (RNAi) is linked with a phenotypic abnormality in flagellar attachment along the cell body of *T. brucei* and a notable reduction in social motility (SoMo) behavior. We have confirmed mRNA cap-binding activity for the protein, determined its TbEIF4G binding partner, and identified an intriguing copurifying hypothetical protein with domains predicted to function in mRNA cap 0 formation.

MATERIALS AND METHODS

Bioinformatics. The *T. brucei* eIF4E homolog TbE6 was identified by BLAST searches of the GeneDB database (31) by using the TbEIF4E5 sequence (Tb927.10.5020). Orthologs from *Leishmania tarentolae* and *Bodo saltans* were retrieved by BLAST searches of the TriTrypDB (32) and Wellcome Trust Sanger Institute (33) databases, respectively. Multiple-sequence alignments were performed with Clustal Omega (http://www.ebi.ac.uk/Tools/msa/clustalo/).

Plasmid construction. For the oligonucleotide primers used for amplification, see Table S1 in the supplemental material. Recombinant TbE6 was expressed from the p2171 plasmid. For interaction assays, the open reading frames of all eIF4E and eIF4G homologs were amplified by PCR and cloned into the yeast two-hybrid vectors pGAD and pGBK (Clontech Laboratories, Inc.). For conditional knockdown by RNAi, the TbE6 gene-internal fragments were amplified and cloned into the p2T7-177 vector (34). The 3′-terminal TbE6 gene fragments for carboxy-terminal epitope tagging of genes were PCR amplified, and the resulting fragments were cloned into the pC-PTP-Neo plasmid (35).

***In vitro* cap-binding assay.** Recombinant TbE6 protein tagged with His_6 was expressed in *Escherichia coli* Rosetta 2(DE3) cells. Expression was induced with 0.5 mM isopropyl-β-D-thiogalactopyranoside (IPTG) for 3 h at 37°C. Cells were harvested, disrupted by sonication, and centrifuged. The pellet was washed two times (20 mM HEPES-KOH [pH 7.2] 1 M guanidine hydrochloride, 2 mM dithiothreitol [DTT], 10% glycerol), and the inclusion bodies were dissolved in 50 mM HEPES-KOH (pH 7.2)–6 M guanidine hydrochloride–10% glycerol–2 mM DTT. Cell debris was removed by centrifugation (43,000 × *g* for 30 min). The protein (diluted to <0.1 mg/ml) was refolded by one-step dialysis against 50 mM HEPES-KOH (pH 7.2)–100 mM KCl–0.5 mM EDTA–2 mM DTT and purified by ion-exchange chromatography through a HiTrap SP column.

Time-synchronized fluorescence titrations were carried out on a PerkinElmer LS 55 Fluorescence Spectrometer at 20 ± 0.3°C (36) in 50 mM HEPES-KOH (pH 7.2)–100 mM KCl–0.5 mM EDTA–2 mM DTT. During the time course titration, 1-μl aliquots of cap analogue solutions were added to 1,400 μl of protein solution (0.1, 0.2, or 0.3 μM protein concentration). Changes in fluorescence intensity were measured at 325 or 340 nm with excitation at 280 nm and corrected for sample dilution and for inner-filter effects. Equilibrium association constants (K_{as}) were determined by fitting the theoretical curve of fluorescence intensity for the total cap analogue concentration to the experimental data points (36). The final K_{as} was calculated as a weighted average of three to five independent titrations. The fitting procedure used nonlinear least-squares regression analysis and was performed with Origin 6.0 (MicroCal Software).

***T. brucei* cell culture and RNAi.** YTAT procyclic *T. brucei* was grown at 27°C in SM medium (37) supplemented with 10% fetal bovine serum. Procyclic forms of *T. brucei* Lister 427 strain 29-13 were used for RNAi. Transfection was performed as described previously (38). Selection was performed with G418 (15 μg/ml), puromycin (10 μg/ml), or phleomycin (2.5 μg/ml), and clonal lines of selected cultures were obtained by limiting dilution in 96-well plates. To induce RNAi, 1 μg/ml tetracycline (Tet) was added to mid-log-phase cultures and growth was measured daily. Single-knockout, protein A-tobacco etch virus protease cleavage site-protein C (PTP)-tagged lines were constructed as described previously (35). To generate the $TbE6^{+/PTP}$ cell line, the 29-13 cell line was transfected with the plasmid cPTP-puro-TbE6, selected with puromycin, checked for PTP-tagged protein expression, transfected with the RNAi plasmid p2T7-177-TbE6, and then selected with phleomycin, generating the $TbE6^{+/PTP}$ RNAi cell line. PTP tagging of TbE6 to monitor knockdown in the 29-13 RNAi cell line affected one allele, leaving the second as the wild type (WT). For the genetic structure and validation of the cell lines, see Fig. S1 in the supplemental material.

Fluorescence microscopy. *T. brucei* cultures in mid-log phase (5×10^6 to 5×10^7 cells/ml) were used for immunofluorescence imaging as described previously (39). Aliquots of 1 ml were washed twice in 1 ml of phosphate-buffered saline (PBS), resuspended in 1 ml of PBS–0.01% paraformaldehyde, and incubated on ice for 5 min. The cells were centrifuged and resuspended in 0.5 ml of PBS. Approximately 20 μl of the cell suspension was spread on a microscope slide, dried at room temperature (RT), and then fixed at −20°C in acetone for 5 min and at −20°C in methanol for 5 min. The slides were dried at RT, and cells were rehydrated with 1 ml of PBS for 15 min and then blocked for 1.5 h at RT with blocking solution (PBS, 5% normal goat serum, 5% BSA). Blocked cells were incubated for 1.5 h in a rabbit anti-protein A antibody (Sigma) at 1:3,000 in blocking solution, washed 3× with PBS-T (PBS plus 0.05% Tween 20), incubated in 1:3,000 anti-rabbit IgG Alexa 488 (Invitrogen), washed three times with PBS-T and once with PBS, mounted on slides with Vectashield (Vector Laboratories) containing 4′,6-diamidino-2-phenylindole (DAPI), and viewed by fluorescence microscopy.

Metabolic labeling assay. [^{35}S]methionine incorporation was determined as described previously (27). RNAi-induced and uninduced TbE6$^{+/PTP}$ RNAi mid-log-phase cultures were centrifuged at 3,000 rpm at RT, washed once in methionine-free SM medium, and resuspended to a concentration of 1×10^7 cells/ml in methionine-free SM medium supplemented with 50 μCi/ml L-[*methyl*-^{35}S]methionine. After 1 h of incubation at 28°C, 50-μl aliquots were lysed (5 μl of 10% SDS, 2.5 μl of 1 M NaOH) and 10-μl volumes of these lysates were spotted in triplicate onto Whatman filter papers and dried at RT. The filters were then incubated on ice in 10% trichloroacetic acid (TCA) for 15 min and then boiled in 5% TCA for 10 min. After one methanol wash and one acetone wash, the filters were dried at RT. The radiolabel incorporated into proteins was measured with a Beckman LS 6500 Scintillation Counter. Experiments were performed three times in triplicate. The standard error was calculated and plotted in Microsoft Excel. Significance *P* values were calculated by one-way analysis of variance (ANOVA) (GraphPad Prism 5).

Flagellar attachment physical stress assay. WT and TbE6$^{+/PTP}$ RNAi cells with and without Tet were grown to mid-log phase. One-milliliter aliquots of primary culture were transferred to a microcentrifuge tube and subjected to 3,000 rpm in a desktop microcentrifuge (Eppendorf model 5415R) for 5 min at RT. The cell pellets were resuspended and washed twice in 1 ml of PBS with two additional 5-min spins at 3,000 rpm and then resuspended in 1 ml of PBS–10 μl of paraformaldehyde. An aliquot was spread on poly-L-lysine-treated coverslips and allowed to air dry before being mounted with coverslips and Vectashield (Vector Laboratories). Flagellar integrity was assessed by light microscopy at ×100 magnification. A total of 100 cells were scored for each of the three conditions, and the results were plotted with standard errors. Significance *P* values were calculated by one-way ANOVA (GraphPad Prism 5). A cell was scored as "detached" if the flagellum was looped away from the cell body, separated from part or all of the cell body, or absent altogether.

Sedimentation assay. Motility in a liquid environment was quantified by spectrophotometry similar to what was described elsewhere (40). Cells with integrated RNAi constructions were incubated with or without Tet for 72 h and then resuspended at 5×10^6/ml in fresh medium with or without the drug. Six replicates (1 ml) were transferred to cuvettes and incubated without shaking under standard conditions. The optical density at 600 nm (OD_{600}) was measured in triplicate every 8 h, with three cuvettes left undisturbed to measure sedimentation and three cuvettes mixed prior to measurement. The ΔOD_{600} of each sample was calculated by dividing the OD_{600} of the resuspended samples by those of the undisturbed samples.

SoMo assays. SoMo assays on semisolid agarose plates were performed as described previously (41). Plates contained either methanol (diluent) or Tet (final concentration, 1 μg/ml) for the "minus-Tet" and "plus-Tet" conditions, respectively. The plates were inoculated with 5.5 μl of cells from suspension cultures at approximately 1.0×10^7 cells/ml. The plus-Tet cells were induced for 72 h prior to plating. Following inoculation, the plates were closed, left to sit for 20 min, sealed with Parafilm, and then incubated at 27°C with 5% CO_2. Plates were photographed at 120 h with a white light box and a velvet cloth to provide background contrast. Images were acquired with a Pentax Optio M30 camera and cropped in Adobe Photoshop.

Yeast-two hybrid assays. Yeast strain PJ69-4A was cultivated overnight at 30°C in YPD medium (42). Each transformation used 1 ml of a cell suspension washed and resuspended in 100 μl of Tris-EDTA (TE)–100 mM lithium acetate buffer and incubated at RT for 15 min. The cells were centrifuged and resuspended in 360 μl of transformation buffer (1× TE, 1 mM lithium acetate, 50% PEG 8000, 2 mg/ml boiled salmon sperm DNA), simultaneously transformed with GBK (Tryp$^+$) and GAD (Leu$^+$) plasmids expressing individual *T. brucei* 4E and 4G homologs, and incubated for 30 min at RT. Subsequently, the cells were incubated at 42°C for 20 min and then centrifuged. The pellet was resuspended in 2 ml of dropout medium (minimal medium minus tryptophan and leucine) and incubated overnight at 30°C. After dropout incubation, the OD_{600} was checked and all of the cultures were centrifuged, diluted to an OD_{600} of 0.5 in dropout medium (minimal medium minus tryptophan, leucine, and histidine), plated on solid dropout medium containing 3-amino-1,2,4-triazole (3AT) in serial dilutions, and incubated at 30°C for 5 days. The positive-control plates used plasmids pGADT7-T and pGBKT7-53 (Clontech Laboratories Inc.) for transformation.

Native gel electrophoresis. Blue native gel analysis was performed as described previously (43). Samples were prepared as follows: Mid-log-phase culture cells were washed twice in PBS, resuspended in 24 μl of extraction buffer (25 mM HEPES, 150 mM sucrose, 20 mM potassium glutamate, 3 mM $MgCl_2$, 0.5% NP-40, 150 mM KCl, 0.5 mM DTT, Sigma*FAST* EDTA-free protease inhibitor cocktail [Sigma-Aldrich]), incubated on ice for 20 min, and centrifuged at full speed for 10 min at 4°C. Eighteen microliters of the supernatant was added to 6.25 μl of 4× native PAGE buffer and 1 μl of G-250 Coomassie sample buffer. The samples were electrophoresed through precast 4 to 16% native PAGE Novex Bis-Tris gels in accordance with the manufacturer's specifications (Life Technologies). The NativeMark unstained protein standard (Life Technologies) was used to estimate complex sizes. Proteins were transferred to 0.2-μm Immun-Blot polyvinylidene difluoride membranes (Bio-Rad). Membranes were fixed in 8% acetic acid for 15 min, rinsed with water, and incubated with a primary or secondary antibody. The size marker lane was removed prior to antibody incubation, air dried, equilibrated with methanol, and stained with Coomassie dye for visualization.

Tandem affinity purification. Purification was performed with 500 ml of culture (5×10^6 cell/ml). For tandem affinity purification, the PTP tag was used and purification was performed as described previously (35). The total elution from the protein C column was either (i) resolved by SDS-PAGE and visualized by silver staining (Bio-Rad Silver Staining plus) or (ii) TCA precipitated and subjected to multidimensional protein identification technology (MudPIT) mass spectrometry.

MudPIT. The TCA-precipitated proteins were digested by trypsin and subjected to mass spectrometry as described previously (44). The proteomic data were analyzed by using the SEQUEST and DTASelect2 algorithms against the *T. brucei* genome database (1), filtering by a peptide-level false-positivity rate of 5%, and a minimum of two peptides per protein (45).

RESULTS

Two new members of the kinetoplastid eIF4E homolog family. The dearth of transcriptional control in trypanosomes means that the organism must rely on downstream control mechanisms to modulate levels of gene expression. Therefore, mRNA is an attractive target for regulation and we chose to search for cap-binding proteins that could mediate recognition of transcripts in general or perhaps of specific subgroups of messages. Reexamination of the GeneDB database with eIF4E family members from baker's yeast revealed a new protein, Tb927.10.5020, that we duly named TbEIF4E5 and refer to here as TbE5. A reciprocal BLAST search with the TbE5 sequence revealed a further related protein, Tb927.7.1670, that we designated TbEIF4E6 (TbE6). Here we present the functional characterization of TbE6.

Both TbE5 and TbE6 carry the hallmarks of the IF4E superfamily core domain, including motifs required for RNA cap binding and for eIF4G protein interaction (Fig. 1; see Table S2 in the supplemental material). Atypically, both cap-binding pi-pi sandwich residues showed a conservative replacement of tryptophan (W) with phenylalanine (F). Replacement of W73 with a nonconservative ring-containing histidine (H) was found in the eIF4G interaction domain. Both proteins have orthologs in all *Leishmania* species, as exemplified here by *L. tarentolae*, and in the distantly related parabodonid *B. saltans* (see Fig. S2A in the supplemental material). An additional conserved block spanning 7 of 13 amino

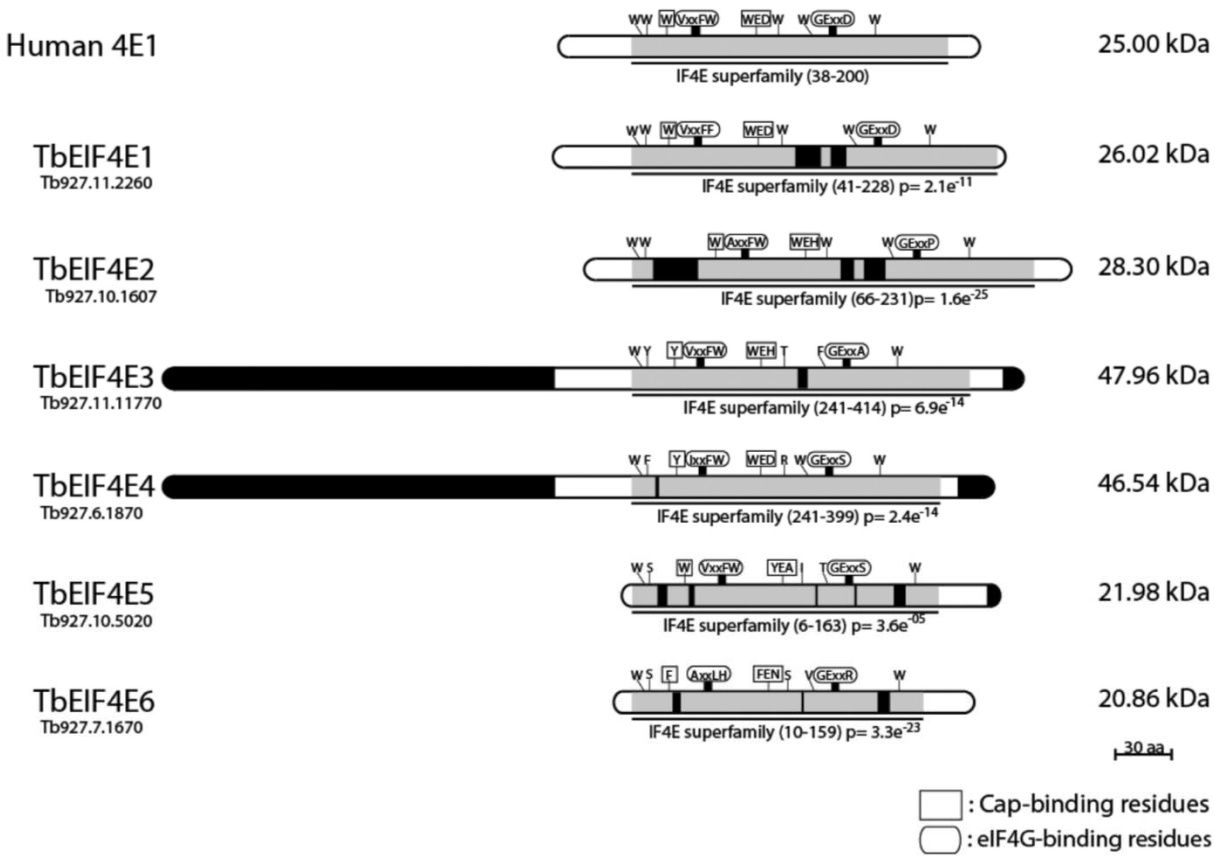

FIG 1 The key domains and motifs of the *T. brucei* and human eIF4E homologs are conserved. This comprehensive diagram aligns the IF4E superfamily domains of the six proteins and highlights nucleotides and motifs critical for RNA cap binding. Highlights include the conservation of the family domain (gray) with *P* values indicated, insertions (black), and the amino acids involved in cap binding (in squares) and eIF4G binding (in elongated circles).

acids (aa) was observed in the short NH-terminal domain. The conservation of TbE6 eIF4E-like homologs suggests a common role in kinetoplastid biology.

TbE6 binds cap analogs *in vitro*. To determine if TbE6 could bind mRNA cap structures, we measured the efficiency of recombinant TbE6 binding to four cap analogs *in vitro*. The hypermethylated SL RNA cap equivalent was represented by cap 4, while the standard cap 0 structure binding was tested with the m^7GTP and m^7GpppA substrates. GTP served as a control not expected to interact with a cap-binding protein. The fluorescence titrations carried out for the four analogs revealed poor binding of TbE6 to the m^7GpppA analog, with a K_{as} similar to that observed for LeishIFE-1, LeishIFE-2, and LeishIFe-3, and better binding to m^7GTP with a K_{as} of $0.16 \pm 0.1\ \mu M^{-1}$ and the cap 4 analog with a K_{as} of $0.16 \pm 0.2\ \mu M^{-1}$ (Fig. 2). Relative to *Leishmania* (26), TbE6 bound m^7GTP with an affinity identical to that of LeishIFE-1 and bound cap 4 with an affinity between those of LeishIFE-3 and LeishIFE-1.

The relatively low levels of cap recognition relative to the isolated mouse protein may reflect a requirement for other structural elements, such as eIF4G or an RNA chain, to facilitate RNA binding (46–49).

TbE6 is cytosolic. The four kinetoplastid eIF4E protein family

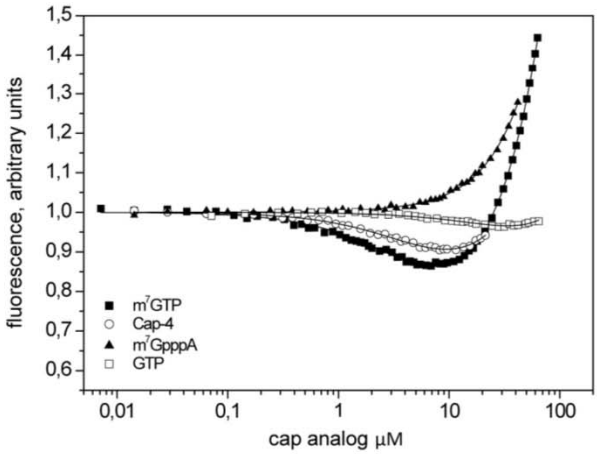

FIG 2 Cap-binding activity of recombinant TbE6. The fluorescence titration curves with four cap analogs were determined by TbE6 fluorescence quenching observed at 325 nm. Protein fluorescence was excited at 280 nm. The trypanosome WT mRNA cap is hypermethylated Cap-4, and the typical eukaryotic cap structure is represented by both the m^7GTP and m^7GpppA cap 0 analogs. Nonmethylated GTP is a negative control for cap 0-specific binding.

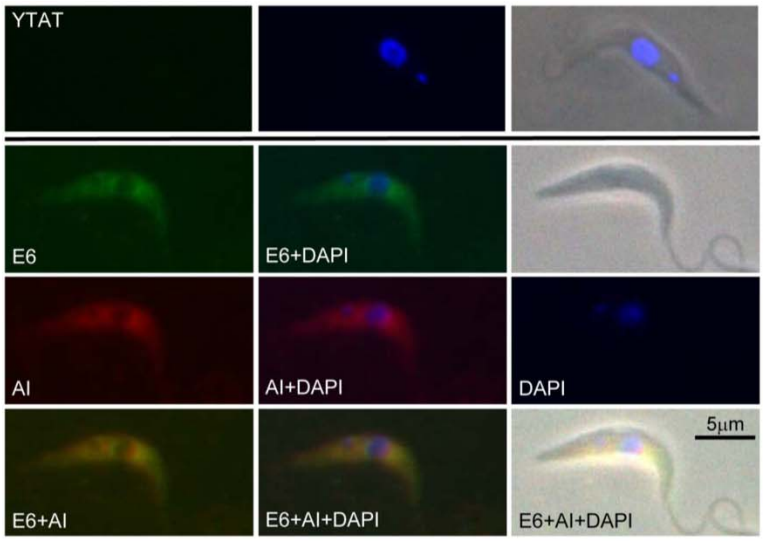

FIG 3 TbE6 is cytosolic. The subcellular localization of TbE6 in *T. brucei* procyclic cells was determined by IFA analysis with an anti-protein A antibody that recognized the TbE6-PTP fusion protein epitope tag (green). The positive control for cytosolic location was counterstaining with a rabbit antibody against the TbEIF4AI protein (red) (51). The outline of the cell is indicated in the phase-contrast image. The negative control was nontransfected control YTAT cells. Nuclear and kinetoplast DNAs were visualized by DAPI staining.

members either localize to the cytosol or are present in both the nucleus and the cytosol (27, 50). To assess function, the TbE6 protein was localized and assayed for its requirement in procyclic cell viability under normal culture conditions. The absence of strong antibodies to our target protein and the availability of excellent epitope-tagging systems prompted us to generate an epitope (PTP)-tagged gene line lacking the endogenous WT gene, TbE6$^{-/PTP}$ (see Fig. S1A in the supplemental material).

Immunolocalization of the TbE6$^{-/PTP}$ protein with the PTP tag revealed a diffuse cytosolic distribution and majority exclusion from the nucleus (Fig. 3), similar to TbE3 and TbE4 (27, 50). As a cytosolic localization control, the slide was counterstained with an antibody recognizing TbEIF4AI (51). The kinetoplast and nuclear DNAs were stained with DAPI.

To facilitate the monitoring of RNAi knockdown of the TbE6 protein, we used a TbE6$^{+/PTP}$ RNAi cell line (see Fig. S1B in the supplemental material) for our assays. RNAi against the TbE6 transcript resulted in the reduction of epitope-tagged TbE6 levels to approximately 12.5% of the uninduced levels by day 3 (see Fig. S3A). A minor difference in the growth rate compared to that of the WT was detected in our lines (Fig. 4A). This result suggests that TbE6 is not essential for WT cell division; however, the result is contrary to those obtained in the high-throughput RNAi analysis conducted by Alsford et al., which indicates that TbE6 is essential for normal growth (52). To provide ample time for the RNAi effect to be seen, we extended the analysis for 15 days and saw no relative change in culture growth despite continued knockdown of TbE6 protein levels (see Fig. S3B). The relative efficiency of the knockdown may explain the discrepancy, if an approximately 12.5% level of TbE6 is sufficient for viability.

To test TbE6 for a role in general translation, we quantitated the effect of RNAi knockdown on protein synthesis. RNAi cells at days 4 and 7 postinduction were metabolically labeled with [^{35}S]methionine (Fig. 4B). The isotope incorporation levels of

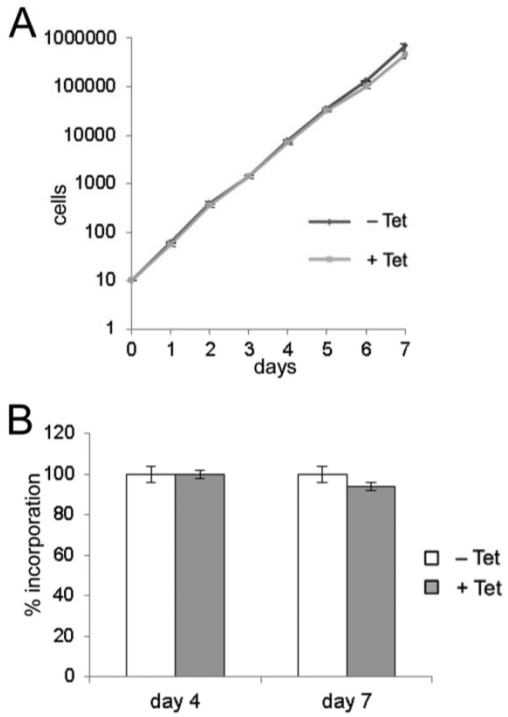

FIG 4 The TbE6 protein does not have a primary role in translation. (A) Growth curve for triplicate RNAi knockdowns of TbE6 in procyclic cells marked with standard errors. Induced TbE6$^{+/PTP}$ RNAi cultures (+ Tet) are compared to uninduced (− Tet) TbE6$^{+/PTP}$ RNAi cells. (B) [^{35}S]methionine metabolic labeling of cultures induced for TbE5 RNAi knockdown at 4 and 7 days postinduction compared to that of noninduced cultures.

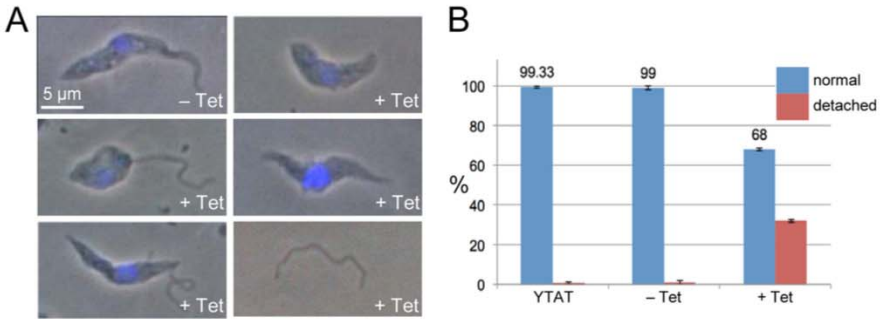

FIG 5 Knockdown of TbE6 results in flagellar detachment upon manipulation. (A) Phase-contrast microscopy of cells left uninduced or induced for RNAi against TbE6. DNA was visualized by counterstaining with DAPI. The cells were prepared for IFA analysis of TbE6-PTP. Flagella detached from the cell body are shown below the minus-Tet control panel; absent or free flagella are shown to the right. (B) Histogram showing the integrity of flagellar attachment along the length of the cell body as measured after benchtop centrifugation, including standard errors. WT (YTAT) and uninduced TbE6$^{+/PTP}$ RNAi cells were compared with induced TbE6$^{+/PTP}$ RNAi cells.

both uninduced and induced cultures were comparable on day 4; by day 7, the ^{35}S levels in the induced cultures were 6% lower than those in the uninduced lines. The nonsignificant reduction (P = 0.2375) of methionine incorporation in the presence of approximately 85% reduced TbE6 levels indicates that TbE6 does not have a primary role in general translation initiation. We cannot definitively rule out a scenario in which approximately 12.5% of the WT TbE6 level is sufficient for a normal level of translation.

Because of the survivorship of the cultures, we attempted to create a genetic TbE6 knockout line by eliminating both endogenous alleles. Three failed attempts to remove the second TbE6 allele (data not shown) suggested that the protein is indeed essential for the survival of procyclic cells. The behavior of our RNAi inductions relative to the study of Alsford et al. could be due to a variety of factors, including the relative efficacy of knockdown, the integration site, the vector choice, and/or the presence of the PTP tag on the protein. Alternative approaches using knockout lines in combination with inducible copies of the TbE6 gene (53, 54) or RNAi targeting of the PTP tag (55) are being explored to resolve the issue.

Knockdown of the TbE6 protein affects motility and the stability of flagellar attachment. The survivorship of our RNAi line provided an opportunity to examine the function of TbE6. While pursuing our analysis of TbE6 under RNAi induction conditions, we noted a difference in the morphology of induced cells.

On slides fixed for indirect immunofluorescence assay (IFA) analysis, cells grown in the presence of Tet had a high proportion of abnormal flagellar phenotypes. Specifically, their flagella were detached from the length of the cell body or in many cases completely absent and visible in isolation on a slide (Fig. 5A). Flagellar detachment was not evident in live cultures or cultures diluted for counting in a Neubauer chamber and appeared to be dependent on forces such as those experienced during centrifugation and resuspension. To follow up on this observation, we devised a physical-stress assay. Induced TbE6 RNAi cells were centrifuged for 5 min at 3,000 rpm, the standard conditions used to pellet *T. brucei* cells from culture. By counting a total of approximately 100 cells by light microscopy, we assessed the percentage of detached flagella. Over 30% of the induced cells showed various levels of flagellar detachment or loss after this treatment (Fig. 5B). In uninduced and WT cells, flagella were largely intact under all of the conditions tested. Thus, a decrease (P = <0.001) in flagellar attachment strength is manifest with the reduction of TbE6.

The potential for impaired motility due to this fragile condition was gauged via a sedimentation assay to assess the ability of induced cells to remain in suspension in liquid media. Induced and uninduced cultures were placed in pairs of spectrophotometer cuvettes, and OD_{600} was measured at various time points. A control cuvette was shaken prior to measurement and compared with its unshaken counterpart. Comparison of WT YTAT cells with uninduced and induced TbE6 RNAi cultures revealed no difference (P = 0.1612) in cell settling (Fig. 6A); thus, basic motility appeared normal. Next, the ability of TbE6-depleted cells to participate in SoMo behavior was examined by assessing the formation of projections along semisolid surfaces (41). This assay revealed a significant difference (P = 0.0032). Uninduced cells showed 100% SoMo (17/17) with a mean of 8.59 ± 1.06 projections per plate, while RNAi-induced cells showed 44.4% SoMo (8/18 plates) with a mean of 3 ± 1 projections per plate (Fig. 6B and C; see Fig. S4 in the supplemental material). While the RNAi-induced cells produced significantly fewer projections, the cells themselves were viable and continued to divide at the point of inoculation.

TbE6 binds the TbG5 homolog. Translation initiation is mediated by a three-component complex in which eIF4G acts as a scaffold for interactions with eIF4A and eIF4E (56). In trypanosomes, the six eIF4E proteins have a selection of five known eIF4G homologs to choose from and, in addition to Leish4E-IP (57), likely a cohort of as-yet-unknown partners. To determine which, if any, of the TbEIF4G homologs interact with TbE6, each potential pairing was tested individually in a heterologous system.

The yeast two-hybrid assay detects interactions between two proteins, termed "bait" and "prey," as indicated by the activation of a promoter in the yeast cells that permits growth. In this assay, yeast growth in the presence of 5.0 mM 3AT indicates a strong interaction. By placing our proteins of interest in "bait" and "prey" positions, we tested potential interactions for our five possible combinations (Fig. 7A). TbE6 paired exclusively with TbEIF4G5 (TbG5; 84.6 kDa; Tb927.8.4500), an essential protein in the procyclic stage, according to the Alsford RNAi study (52), and showed no interaction with any of the other TbEIF4G family members (see Fig. S5 in the supplemental material).

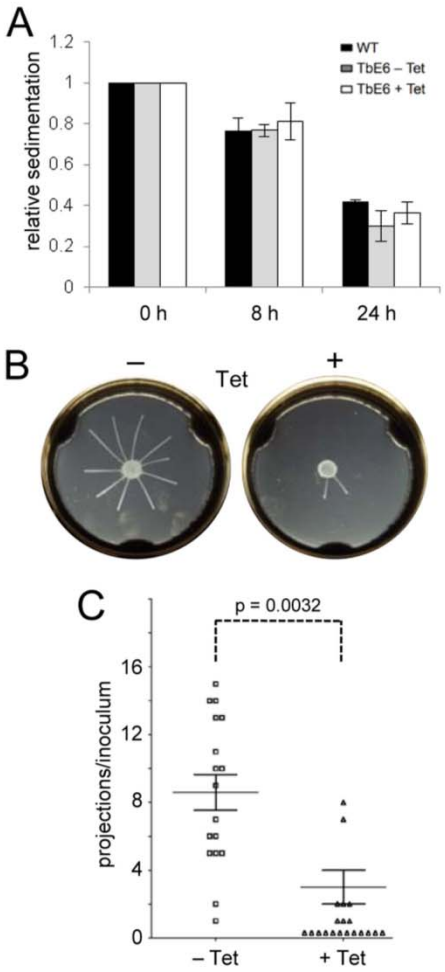

FIG 6 TbE6 depletion does not affect motility in liquid culture but results in reduced SoMo. (A) Turbidity assay measuring cell sedimentation in stationary cuvettes. Standard error bars were derived from experiments performed in triplicate for 0-, 8-, and 24-h samples. (B) SoMo assessment under TbE6 RNAi knockdown conditions. Representative semisoft agarose plate SoMo assays of uninduced or induced cells incubated for 5 days postinoculation are shown. Cell mass projections were scored as a measurement of SoMo, with 10 and 2 projections scored on the minus-Tet and plus-Tet sample plates, respectively. (C) Graphic summary of the TbE6 SoMo assay indicating means and standard errors for 17 control and 18 induction plates. Each point represents the number of radial projections from the site of inoculation. *P* values were determined by unpaired two-tailed *t* tests.

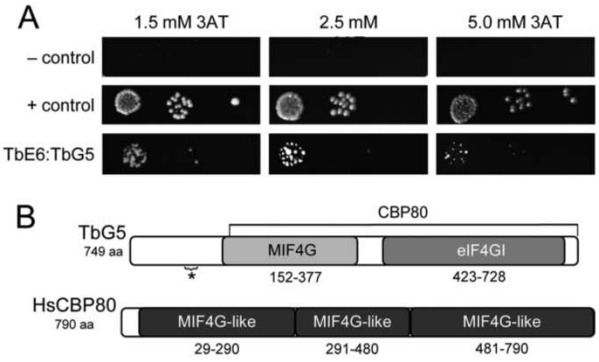

FIG 7 Direct interaction of TbE6 with TbG5. (A) Yeast-two-hybrid assay used to detect any interactions between TbE6 and the five Tb4G homologs in the presence of three concentrations of 3AT to vary the stringency of the interaction. For the full panel tested, see Fig. S5 in the supplemental material. The positive interaction is shown here with the controls. The positive control was a combination of pGADT7-T and pGBKT7-53; the negative control contained the empty vectors. Interaction strength is inferred by colony size as follows: ≥2 mm, strong; 1 to 2 mm, moderate; ≤1 mm, weak. (B) Structural domains protein identified by PHYRE^2 in the TbG5. In TbG5, the asterisk denotes a low-confidence HMG box (70), a possible nucleic acid binding site. MIF4G/DAP5, middle of 4G/death-associated protein (61); eIF4GI, human isoform I (71).

TbG5 carries three domains with potential nucleic acid interaction potential (Fig. 7B). Starting from the amino terminus, PHYRE^2 examination revealed an ~20-aa stretch with general similarity to DNA-binding α-helical structures (high-mobility group [HMG] box; 36 to 52% confidence), followed by a central midle-of-eIF4G (MIF4G) domain (100% confidence) and ending with an eIF4GI-like domain (98.4% confidence). Both of the high-confidence domains showed a match to human nuclear cap-binding complex subunit CBP80 (94.5% confidence) encompassing the C-terminal HEAT2 and HEAT3 domains (a repeat found in Huntingtin, elongation factor 3, protein phosphatase 2A, and TOR1 proteins) (58), an interesting hit since a CBP80 homolog was not found in the *T. brucei* nuclear cap-binding complex (59).

The exclusivity of the interaction of TbE6 with TbG5 is an indication that specific functions are associated with different family members. The TbG5 protein contains several suggestive domains, including a predicted HMG box for nucleic acid binding in the amino-terminal domain and a MIF4G domain similar to those found in the related proteins cwc22 and dap5, which are involved in exon junction complex assembly and internal ribosome entry site-mediated translation (60, 61). Thus, TbG5 may carry two regions with RNA selection potential. The incorporation of other proteins or RNAs into the equation may shed light on the function of the TbE6 complex.

TbE6 is a member of a protein complex. Our yeast two-hybrid interaction assays indicate that TbE6 associates with the TbG5 homolog, and validation of their binding in *T. brucei* with each other and with other proteins was examined by monitoring the sizes of complexes containing tagged proteins first by blue native gel electrophoresis and then by MudPIT mass spectroscopy analysis of individual components in tandem affinity-purified complexes.

To validate that TbE6 was in a high-molecular-mass complex and to estimate the size(s) of the protein complex(es), extracts of TbE6$^{-/PTP}$ were visualized by blue native gel analysis and Western blotting with anti-protein A antibody. The analysis of ~41-kDa PTP-tagged TbE6 revealed a major band migrating between the 242- and 480-kDa markers at ~300 kDa and a minor band between the 66- and 146-kDa markers migrating at ~90 kDa (Fig. 8). A high-molecular-mass complex at ~300 kDa containing ~104-kDa TbG5-PTP was detected in a TbG5$^{-/PTP}$ line (see Fig. S1 in the supplemental material). The ~90-kDa TbE6-containing band was not detected in the TbG5-PTP sample and may represent free TbE6-PTP or a subcomplex not containing TbG5.

The combined data from these experiments are consistent with

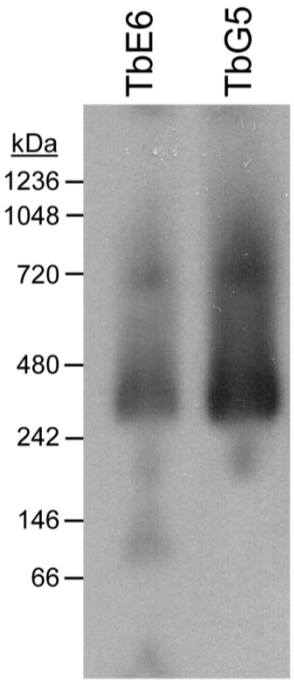

FIG 8 TbE6 migration supports interaction with a high-molecular-mass complex. Blue native gel electrophoresis of cell extracts from TbE6-PTP- and TbG5-PTP-transfected *T. brucei*. Lysates were transferred to nitrocellulose membranes and probed with an antibody directed against the protein A domain of the PTP tag of TbE6 and TbG5.

the formation of the predicted Tb4E/Tb4G complex *in vivo* and suggest the presence of additional components in the complexes formed by both proteins.

A protein with mRNA capping domains copurifies with TbE6. To isolate the specific complexes and identify their constituents, the TbE6$^{-/PTP}$ line was used for tandem affinity complex purification with subsequent protein identification by MudPIT. Purifications were performed a minimum of three times with various levels of elution stringency, and the products were subjected to tryptic digestion and analyzed by tandem mass spectrometry. Two peptide hits are required for the validated identification of a given protein. A limitation of this procedure is an inability to identify peptides that carry modifications that alter their mass, since the *in silico* values generated from GeneDB are based on pure amino acid weights.

Two proteins similar in peptide coverage consistently associated with TbE6 (Table 1). In agreement with the TbE6-TbG5 yeast two-hybrid result, TbG5 scored strongly in the TbE6-PTP purifications. The third hit was a protein of 70.3 kDa (Tb927.11.14590) annotated as "hypothetical" that was scored as essential for procyclics and the other three life stages assayed by RNAi (52) and is referred to here as TbG5-IP (TbG5-interacting protein). Both TbG5 and TbG5-IP are well conserved in kinetoplastid protozoa (see Fig. S2B and C in the supplemental material). Confirmation of the interaction of this trio and elimination of the purification-specific background were accomplished by performing PTP purifications from tagged TbG5 and TbG5-IP cell lines (see Fig. S1C and D). Consistent with the blue native gel migration, TbE6 copurified with TbG5-PTP; the TbG5-IP abundance score was >85% of that of TbG5-PTP itself, compared to ~33% relative abundance for TbE6 in this purification (Table 2). Likewise, TbG5-IP-PTP MudPIT analysis yielded itself, TbG5, and TbE6 in order of decreasing abundance, with the fourth hit present at 25% of the level of TbE6 (Table 3). Considering the top 20 proteins identified in each of the three purifications (11 to 20 are not shown), 2 additional proteins are common to all three analyses, a paraflagellar rod component protein (Tb927.10.11300) and a voltage-dependent anion-selective channel protein (Tb927.2.2510). Taken together, these data are indicative of a primary interaction between TbG5 and the TbG5-IP hypothetical protein, with a strong association of that pair and the TbE6 protein. This is reminiscent of eIF4G acting as a scaffold that brings accessory proteins to eIF4E once it has captured a capped RNA.

To determine the target of physical interaction of TbG5-IP within the TbE6 complex, a yeast two-hybrid assay was used to test the potential for direct binding with TbE6 or TbG5. The TbG5 protein bound to the 70.3-kDa TbG5-IP protein in both the bait and prey configurations, while both TbE6 trials were negative for yeast growth (Fig. 9A), indicating that TbG5 is the scaffold for both TbE6 and TbG5-IP. Localization of TbG5-IP-PTP was performed with the protein C antibody to visualize the target. The staining pattern indicated a cytosolic localization for this third complex member (Fig. 9B), mirroring the distribution seen for

TABLE 1 Proteins copurifying with TbE6-PTP in three different purifications identified by MudPIT

Gene product	GeneDB identifier[a]	Molecular mass (kDa)	AvUniPepts[b]	% Coverage	NSAF[c]
TbEIF4E6	Tb927.7.1670	20.90	19	54.30	45,527.06
TbEIF4G5	Tb927.8.4500	84.60	50	46.30	14,270.11
Hypothetical protein	Tb927.11.14590	70.30	20	29.60	2,606.34
Paraflagellar rod component	Tb927.10.11300	14.32	5	27.00	1,434.29
Hypothetical protein	Tb927.5.2260	12.40	3	23.90	1,204.16
Glycerol-3-phosphate dehydrogenase	Tb927.8.3530	37.80	8	23.20	911.62
Cytochrome oxidase V	Tb927.9.3170	22.23	2	9.70	790.32
Hypothetical protein	Tb927.4.2740	16.32	4	30.00	774.52
EF1b	Tb927.4.3590	24.30	4	22.60	544.04
Triosephosphate isomerase	Tb927.11.5520	26.81	5	25.20	516.34

[a] GeneDB identifiers are from *T. brucei* 927, version 6.0 (www.genedb.org and www.tritrypdb.org). Temporary GeneDB identifiers retrieved from peptide analysis based on *T. brucei* 927 version 2.2: Tb927.11.14590, Tb11.01.6200; Tb927.9.3170, Tb09.160.1820; Tb927.11.5520, Tb11.02.3210.
[b] AvUniPepts, number of peptides identified.
[c] NSAF, normalized spectral abundance factor.

TABLE 2 MudPIT identification of proteins copurifying with TbG5-PTP

Gene product	GeneDB identifier[a]	Molecular mass (kDa)	AvUniPepts[b]	% Coverage	NSAF[c]
TbEIF4G5	Tb927.8.4500	84.60	60	56.10	12,149.62
Hypothetical protein TbG5-IP	Tb927.11.14590	70.30	34	44.40	10,487.22
TbEIF4E6	Tb927.7.1670	20.90	8	22.00	3,979.55
Voltage-dependent anion channel	Tb927.2.2510	29.19	12	49.60	3,507.47
Histone H3	Tb927.1.2470	14.80	4	32.30	2,373.47
Histone H2A	Tb927.7.2900	14.20	2	14.20	1,056.03
UMSBP	Tb927.10.6070	14.60	6	37.90	544.26
UMSBP	Tb927.10.6060	21.83	7	27.70	408.84
ALBA3	Tb927.4.2040	20.80	5	33.20	343.75
Cyclophilin A	Tb927.11.880	18.71	3	14.10	307.49

[a] GeneDB identifiers are from *T. brucei* 927, version 6.0 (www.genedb.org and www.tritrypdb.org). Temporary GeneDB identifiers retrieved from peptide analysis based on *T. brucei* 927 version 2.2: Tb927.11.14590, Tb11.01.6200; Tb927.11.880, Tb11.03.0250.
[b] AvUniPepts, number of peptides identified.
[c] NSAF = normalized spectral abundance factor.

TbE6-PTP and the cytosolic control TbEIF4AI. Examination of the migration of TbG5-IP-PTP in the blue native gel system revealed a broad band whose front migrated faster than the 242-kDa marker and the TbE6 and TbG5 complexes but tailed into an overlap with the other bands (Fig. 9C).

Bioinformatic analysis of TbG5-IP by PHYRE^2 (62) revealed two provocative domains associated with mRNA 5′ cap formation (Fig. 10A). The amino half of TbG5-IP displayed similarity to nucleoside triphosphate (NTP) hydrolase secondary structure (99.1% confidence), a broad domain that includes the triphosphatase enzymes involved in the first step in cap 0 formation on primary transcripts. The carboxyl half of the protein consisted almost entirely of a guanylyltransferase domain (99.8% confidence). Adjacent to the gene for TbG5-IP (Tb927.11.14590) on chromosome 11 is a gene for a protein (Tb927.11.14580) identified previously on the basis of guanylyltransferase activity named capping enzyme 1 or TbCE1 (63). TbCE1 has the same domains as TbG5-IP, each with 100% confidence as ascribed by PHYRE^2, and differs primarily through the NH-terminal extension on TbG5-IP. The high level of sequence similarity indicates that these genetic neighbors arose through a duplication event in the genome. TbCE1 is not thought to perform the cap 0 addition on the SL RNA, as that task is ascribed to the triphosphatase TbCET1 (15) and the bifunctional guanylyltransferase TbCGM1 (16, 17).

The TbE6 complex contains three consistent members, each of which purifies the other two in PTP and MudPIT analyses, with TbG5 serving as a scaffold between TbE6 and TbG5-IP (Fig. 10B). The predicted size of this complex is 194.7 kDa when including a PTP tag, somewhat smaller than the ~300 kDa indicated by blue native gel analysis of TbE6 and TbG5 (Fig. 8) but more consistent with the analysis of TbG5-IP (Fig. 9C). The complex may be dynamic with respect to protein composition, causing the apparent anomalies in migration. Other variables that could affect migration through this nondenaturing gel system include proteins that may remain in association with the PTP-tagged complex in the blue native system but are lost upon affinity purification. In nondenaturing gels, the size of the complex is unlikely to reflect the additive molecular mass of its components because of the effects of quaternary structure.

The functional domains carried by TbG5-IP indicate that this complex has a role in the modulation of gene expression through the modification of mRNA 5′ ends. Coupled with the observation of compromised flagellar attachment upon TbE6 depletion and the general cytosolic distribution of the three proteins identified, this complex may represent a gateway for the expression of proteins involved in flagellar attachment to the cell body either directly or secondarily.

DISCUSSION

Posttranscriptional mechanisms of control in organisms such as trypanosomes that lack specific transcriptional modulation for the vast majority of their genes must play a key role in gene ex-

TABLE 3 MudPIT identification of proteins copurifying with TbG5-IP-PTP

Gene product	GeneDB identifier[a]	Molecular mass (kDa)	AvUniPepts[b]	% Coverage	NSAF[c]
Hypothetical protein TbG5-IP	Tb927.11.14590	70.30	33	51.70	1,627.54
TbEIF4G5	Tb927.8.4500	84.60	52	51.70	7,113.24
TbEIF4E6	Tb927.7.1670	20.90	9	41.40	2,163.60
UMSBP	Tb927.10.6070	14.60	6	37.90	499.91
RBP16	Tb927.11.7900	15.11	7	42.60	496.37
Glyceraldehyde 3-phosphate dehydrogenase	Tb927.6.4280	39.04	9	33.70	487.38
ALBA3	Tb927.4.2040	20.80	8	38.40	460.45
UMSBP	Tb927.10.6060	21.83	8	33.80	451.80
Cyclophilin A	Tb927.11.880	18.71	3	19.20	395.41
Hypothetical protein	Tb927.9.4960	7.60	2	31.20	364.52

[a] GeneDB identifiers are from *T. brucei* 927, version 6.0 (www.genedb.org and www.tritrypdb.org). Temporary GeneDB identifiers retrieved from peptide analysis based on *T. brucei* 927 version 2.2: Tb927.11.14590, Tb11.01.6200; Tb927.11.7900, Tb11.02.5770; Tb927.11.880, Tb11.03.0250; Tb927.9.4960, Tb09.160.3530.
[b] AvUniPepts, number of peptides identified.
[c] NSAF, normalized spectral abundance factor.

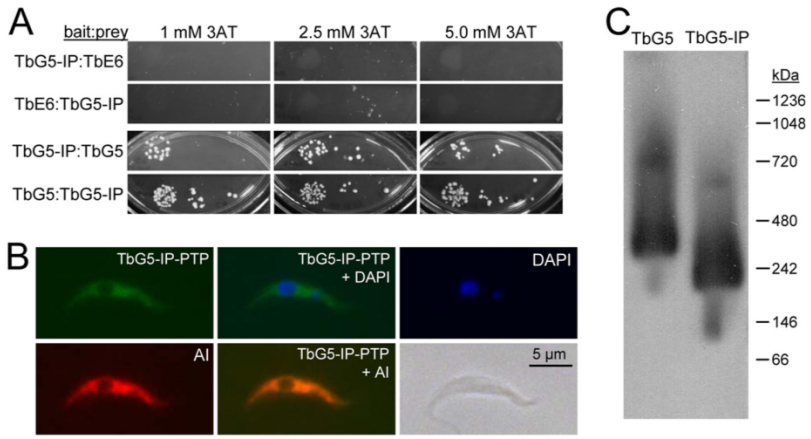

FIG 9 TbG5-IP interacts with the TbE6 complex through direct binding to TbG5 and localizes to the cytosol. A yeast two-hybrid assay tested the interaction potential between TbG5-IP and TbE6 or TbG5 in reciprocal bait and prey orientations. The conditions and interpretation are as noted in the legend to Fig. 6. (B) Localization of TbG5-IP with the TbG5-IP$^{-/PTP}$ cell line and anti-protein A antibody for detection (green). The positive control for cytosolic location was counterstaining with rabbit antibody against the TbEIF4AI protein (red) (51). The negative control is shown in Fig. 3. The outline of the cell is shown in the phase-contrast image. (C) Blue native gel analysis of the TbG5-IP-kDa protein. The TbG5 lane shown for comparison is the same as that shown in Fig. 8.

pression. The *T. brucei* eIF4E family of RNA cap-binding proteins now has two new members, one of which is characterized here and brings the total number of homologs to six. TbE6 is a cytosolic protein that binds RNA cap analogs *in vitro*, specifically, the cap 4 structure carried on the 5′ end of every nucleus-encoded mRNA and on the mature SL RNA *trans*-splicing substrate. The smallest member of the family, TbE6, interacts exclusively with the TbG5 member of the TbEIF4G family, a protein that, in turn, mediates the association of an interesting 70.3-kDa protein named TbG5-IP that shows similarity to two domains associated with RNA cap 0 formation. Knockdown of TbE6 revealed a phenotype consistent with a weakening of the flagellar attachment along the length of the cell body. These compromised cells remain in liquid suspension and appear intact when cultures are not physically manipulated. However, the disturbance associated with centrifugation and pipetting resulted in a high proportion of flagella separating from along the cell body or release altogether, and the ability of TbE6-depleted cells to participate in SoMo behavior on a semisolid surface was reduced. Translation levels were not reduced catastrophically upon TbE6 depletion; thus, the implication of this study is that a subset of proteins associated with maintaining the integrity of flagellar attachment are reduced or missing because of direct or secondary consequences of TbE6 manipulation, a model that we are exploring actively.

A genome-wide RNAi survey performed by Alsford et al. indicated that each of the three members of the TbE6 complex is essential for normal cell growth, with the behavior of TbG5 in differentiating bloodstream forms being the only exception (52). As the level of knockdown achieved in our TbE6 RNAi line allowed cell division approximating that of WT culture, we were afforded a chance to assess the effects of depletion of a key protein. The observed detachment of the flagellum from the length of the cell body resembles that reported following RNAi knockdown of calmodulin (64) and may represent an underlying fault in membrane integrity. Detachment could be elicited in induced cultures in the absence of the fixation step (data not shown) and was dependent on physical manipulation such as centrifugation or vigorous pipetting. The distinction between the maintenance of suspension in liquid media and SoMo behavior may reveal the limit of external stimuli that compromised TbE6-depleted cells can tolerate with respect to the normal integrity and function of their flagellum. If SoMo-level force is required for cell survival in the wild, loss of TbE6 could, like defects in integral flagellum components (65), result in a loss or decrease of parasite virulence.

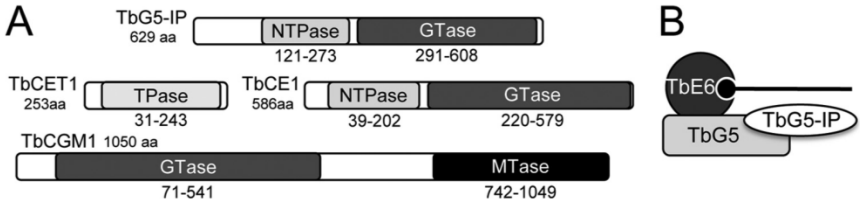

FIG 10 Composition of the TbE6 complex and domains predicted for the TbE6-associated proteins compared to related proteins. (A) Schematic locations of the conserved structural domains in TbG5 and the TbE6-associated mRNA capping enzyme homolog TbG5-IP as predicted by PHYRE^2. The TbCE1 gene lies adjacent to the TbG5-IP gene; TbCET1 and TbCGM1 carry the activities thought to be involved in cap 0 formation on the SL RNA. NTPase, NTP hydrolase; GTase, guanylyltransferase; TPase, triphosphatase; MTase, methyltransferase. (B) The components that copurified with TbE6 are shown, not scaled for size. The RNA (black line; the black circle represents 5′-end cap 4) is recognized by the cap-binding eIF4E component (gray circle). The scaffold protein TbG5 (light gray rectangle) interacts directly with both TbE6 and TbG5-IP.

Whether the defect directly affects a component involved in flagellum attachment, indirectly affects a control step in flagellum structure and maintenance, or represents a nonspecific event is under investigation.

The regulation of subsets of genes at the posttranscriptional level is known to occur in multiple systems but is not well understood mechanistically. Variables such as RNA stability, cytosolic partitioning, or sequestration can come into play, with the key signals carried on the mRNA itself, often in the untranslated region flanking the gene. The mRNA-binding specificity of the TbE6 complex and the catalytic possibilities of TbG5-IP are being examined currently and will provide the best indication of the function of the TbE6 complex. Given the heavy hints provided by the NTP hydrolase and guanylyltransferase domains, mRNA cap modifications are a reasonable assumption if active catalysis by TbG5-IP is involved. If acting on an intact cap 4 structure, removal of cap 0 could serve to destabilize target mRNAs, while previously decapped transcripts might begin their return path to active transcription by passing through this complex. As a precedent, a cytosolic capping activity has been identified in mammalian cells (66). Alternatively, the complex may serve as a selector of mRNAs, constituting a set of coordinated transcripts termed a regulon (67–69), by recognizing specific nucleic acid sequence motifs or structures, presumably through sequences other than the universal SL exon, or perhaps via an RNA-binding protein intermediary.

Our future studies will be directed at determining the enzymatic activity of TbG5-IP, focusing initially on *in vitro* activities on various mRNA cap structures. Concurrently, the identities of the mRNAs associated with the E6-PTP complex and the proteins impacted by E6 knockdown are being explored. We seek to determine what subpopulation of genes is controlled by the TbE6 complex, the molecular signal responsible for conferring specificity, and the specific mechanism that may be repressing the translation of a subset of genes involved in flagellar attachment and possibly other pathways.

ACKNOWLEDGMENTS

This work was supported by a UCLA Stein-Oppenheimer award to D.A.C., NIH awards AI056034 and AI073806 to D.A.C. and N.R.S. and TW009035 to D.A.C. and O.P.D.M.N., NIH award AI052348 to K.H., and NIH award GM089778 to J.A.W. Scholarships for A.M.M. and J.D.F.N. were provided by the Brazilian Funding Agencies FACEPE, CAPES, and CNPq. E.D. and J.Z. were supported by the National Science Center of Poland (UMO-2012/07/B/NZ1/00118 and UMO-2013/08/A/NZ1/00866).

We thank Bidyottam Mittra, Jun Urano, Laurie Read, and Fuyu Tamanoi for strains, reagents, and help with the Y2H assay and Arthur Günzl for the PTP immunofluorescence protocol.

REFERENCES

1. **Berriman M, Ghedin E, Hertz-Fowler C, Blandin G, Renauld H, Bartholomeu DC, Lennard NJ, Caler E, Hamlin NE, Haas B, Bohme U, Hannick L, Aslett MA, Shallom J, Marcello L, Hou L, Wickstead B, Alsmark UC, Arrowsmith C, Atkin RJ, Barron AJ, Bringaud F, Brooks K, Carrington M, Cherevach I, Chillingworth TJ, Churcher C, Clark LN, Corton CH, Cronin A, Davies RM, Doggett J, Djikeng A, Feldblyum T, Field MC, Fraser A, Goodhead I, Hance Z, Harper D, Harris BR, Hauser H, Hostetler J, Ivens A, Jagels K, Johnson D, Johnson J, Jones K, Kerhornou AX, Koo H, Larke N, et al.** 2005. The genome of the African trypanosome *Trypanosoma brucei*. Science **309:**416–422. http://dx.doi.org/10.1126/science.1112642.
2. **Kelly S, Kramer S, Schwede A, Maini PK, Gull K, Carrington M.** 2012. Genome organization is a major component of gene expression control in response to stress and during the cell division cycle in trypanosomes. Open Biol. **2:**120033. http://dx.doi.org/10.1098/rsob.120033.
3. **Clayton C.** 2002. Life without transcriptional control? From fly to man and back again. EMBO J. **21:**1881–1888. http://dx.doi.org/10.1093/emboj/21.8.1881.
4. **Kramer S.** 2012. Developmental regulation of gene expression in the absence of transcriptional control: the case of kinetoplastids. Mol. Biochem. Parasitol. **181:**61–72. http://dx.doi.org/10.1016/j.molbiopara.2011.10.002.
5. **Horn D, McCulloch R.** 2010. Molecular mechanisms underlying the control of antigenic variation in African trypanosomes. Curr. Opin. Microbiol. **13:**700–705. http://dx.doi.org/10.1016/j.mib.2010.08.009.
6. **Rudenko G.** 2010. Epigenetics and transcriptional control in African trypanosomes. Essays Biochem. **48:**201–219. http://dx.doi.org/10.1042/bse0480201.
7. **Liang X-H, Haritan A, Uliel S, Michaeli S.** 2003. *trans* and *cis* splicing in trypanosomatids: mechanisms, factors, and regulation. Eukaryot. Cell **2:**830–840. http://dx.doi.org/10.1128/EC.2.5.830-840.2003.
8. **Sturm NR, Zamudio JR, Campbell DA.** 2012. SL RNA biogenesis in kinetoplastids: a long and winding road, p 29–47. *In* Bindereif A (ed), RNA metabolism in trypanosomes. Springer, Berlin, Germany.
9. **Bangs JD, Crain PF, Hashizume T, McCloskey JA, Boothroyd JC.** 1992. Mass spectrometry of mRNA cap 4 from trypanosomatids reveals two novel nucleosides. J. Biol. Chem. **267:**9805–9815.
10. **Matthews KR, Tschudi C, Ullu E.** 1994. A common pyrimidine-rich motif governs trans-splicing and polyadenylation of tubulin polycistronic pre-mRNA in trypanosomes. Genes Dev. **8:**491–501. http://dx.doi.org/10.1101/gad.8.4.491.
11. **Nilsen TW.** 2001. Evolutionary origin of SL-addition *trans*-splicing: still an enigma. Trends Genet. **17:**678–680. http://dx.doi.org/10.1016/S0168-9525(01)02499-4.
12. **Lasda EL, Blumenthal T.** 2011. *Trans*-splicing. Wiley Interdiscip Rev. RNA **2:**417–434. http://dx.doi.org/10.1002/wrna.71.
13. **Bitar M, Boroni M, Macedo AM, Machado CR, Franco GR.** 2013. The spliced leader trans-splicing mechanism in different organisms: molecular details and possible biological roles. Front. Genet. **4:**199. http://dx.doi.org/10.3389/fgene.2013.00199.
14. **Ghosh A, Lima CD.** 2010. Enzymology of RNA cap synthesis. Wiley Interdiscip. Rev. RNA **1:**152–172. http://dx.doi.org/10.1002/wrna.
15. **Ho CK, Shuman S.** 2001. *Trypanosoma brucei* RNA triphosphatase. J. Biol. Chem. **276:**46182–46186. http://dx.doi.org/10.1074/jbc.M108706200.
16. **Takagi Y, Sindkar S, Ekonomidis D, Hall MP, Ho CK.** 2007. *Trypanosoma brucei* encodes a bifunctional capping enzyme essential for cap 4 formation on the spliced leader RNA. J. Biol. Chem. **282:**15995–16005. http://dx.doi.org/10.1074/jbc.M701569200.
17. **Ruan J-P, Shen S, Ullu E, Tschudi C.** 2007. Evidence for a capping enzyme with specificity for the trypanosome spliced leader RNA. Mol. Biochem. Parasitol. **156:**246–254. http://dx.doi.org/10.1016/j.molbiopara.2007.09.001.
18. **Zamudio JR, Mittra B, Campbell DA, Sturm NR.** 2009. Hypermethylated cap 4 maximizes *Trypanosoma brucei* translation. Mol. Microbiol. **72:**1100–1110. http://dx.doi.org/10.1111/j.1365-2958.2009.06696.x.
19. **Haile S, Papadopoulou B.** 2007. Developmental regulation of gene expression in trypanosomatid parasitic protozoa. Curr. Opin. Microbiol. **10:**569–577. http://dx.doi.org/10.1016/j.mib.2007.10.001.
20. **Richter JD, Sonenberg N.** 2005. Regulation of cap-dependent translation by eIF4E inhibitory proteins. Nature **433:**477–480. http://dx.doi.org/10.1038/nature03205.
21. **Gallie DR, Browning KS.** 2001. eIF4G functionally differs from eIFiso4G in promoting internal initiation, cap-independent translation, and translation of structured mRNAs. J. Biol. Chem. **276:**36951–36960. http://dx.doi.org/10.1074/jbc.M103869200.
22. **Clarkson BK, Gilbert WV, Doudna JA.** 2010. Functional overlap between eIF4G isoforms in *Saccharomyces cerevisiae*. PLoS One **5:**e9114. http://dx.doi.org/10.1371/journal.pone.0009114.
23. **Ptushkina M, Malys N, McCarthy JE.** 2004. eIF4E isoform 2 in *Schizosaccharomyces pombe* is a novel stress-response factor. EMBO Rep. **5:**311–316. http://dx.doi.org/10.1038/sj.embor.7400088.
24. **Keiper BD, Lamphear BJ, Deshpande AM, Jankowska-Anyszka M, Aamodt EJ, Blumenthal T, Rhoads RE.** 2000. Functional characterization of five eIF4E isoforms in *Caenorhabditis elegans*. J. Biol. Chem. **275:**10590–10596. http://dx.doi.org/10.1074/jbc.275.14.10590.
25. **Contreras V, Richardson MA, Hao E, Keiper BD.** 2008. Depletion of the

cap-associated isoform of translation factor eIF4G induces germline apoptosis in C. elegans. Cell Death Differ. **15:**1232–1242. http://dx.doi.org/10.1038/cdd.2008.46.

26. **Yoffe Y, Zuberek J, Lerer A, Lewdorowicz M, Stepinski J, Altmann M, Darzynkiewicz E, Shapira M.** 2006. Binding specificities and potential roles of isoforms of eukaryotic initiation factor eIF4E in *Leishmania*. Eukaryot. Cell **5:**1969–1979. http://dx.doi.org/10.1128/EC.00230-06.
27. **Freire ER, Dhalia R, Moura DM, da Costa Lima TD, Lima RP, Reis CR, Hughes K, Figueiredo RC, Standart N, Carrington M, de Melo Neto OP.** 2011. The four trypanosomatid eIF4E homologues fall into two separate groups, with distinct features in primary sequence and biological properties. Mol. Biochem. Parasitol. **176:**25–36. http://dx.doi.org/10.1016/j.molbiopara.2010.11.011.
28. **Yoffe Y, Léger M, Zinoviev A, Zuberek J, Darzynkiewicz E, Wagner G, Shapira M.** 2009. Evolutionary changes in the *Leishmania* eIF4F complex involve variations in the eIF4E-eIF4G interactions. Nucleic Acids Res. **10:**3243–3253. http://dx.doi.org/10.1093/nar/gkp190.
29. **Zinoviev A, Shapira M.** 2012. Evolutionary conservation and diversification of the translation initiation apparatus in trypanosomatids. Comp. Funct. Genomics **2012:**813718. http://dx.doi.org/10.1155/2012/813718.
30. **Vasquez JJ, Hon CC, Vanselow JT, Schlosser A, Siegel TN.** 2014. Comparative ribosome profiling reveals extensive translational complexity in different *Trypanosoma brucei* life cycle stages. Nucleic Acids Res. **42:**3623–3637. http://dx.doi.org/10.1093/nar/gkt1386.
31. **Hertz-Fowler C, Peacock CS, Wood V, Aslett M, Kerhornou A, Mooney P, Tivey A, Berriman M, Hall N, Rutherford K, Parkhill J, Ivens AC, Rajandream MA, Barrell B.** 2004. GeneDB: a resource for prokaryotic and eukaryotic organisms. Nucleic Acids Res. **32:**D339–D343. http://dx.doi.org/10.1093/nar/gkh007.
32. **Aslett M, Aurrecoechea C, Berriman M, Brestelli J, Brunk BP, Carrington M, Depledge DP, Fischer S, Gajria B, Gao X, Gardner MJ, Gingle A, Grant G, Harb OS, Heiges M, Hertz-Fowler C, Houston R, Innamorato F, Iodice J, Kissinger JC, Kraemer E, Li W, Logan FJ, Miller JA, Mitra S, Myler PJ, Nayak V, Pennington C, Phan I, Pinney DF, Ramasamy G, Rogers MB, Roos DS, Ross C, Sivam D, Smith DF, Srinivasamoorthy G, Stoeckert CJ, Jr, Subramanian S, Thibodeau R, Tivey A, Treatman C, Velarde G, Wang H.** 2010. TriTrypDB: a functional genomic resource for the Trypanosomatidae. Nucleic Acids Res. **38:**D457–D462. http://dx.doi.org/10.1093/nar/gkp851.
33. **Jackson AP, Quail MA, Berriman M.** 2008. Insights into the genome sequence of a free-living Kinetoplastid: *Bodo saltans* (Kinetoplastida: Euglenozoa). BMC Genomics **9:**594. http://dx.doi.org/10.1186/1471-2164-9-594.
34. **Wickstead B, Ersfeld K, Gull K.** 2002. Targeting of a tetracycline-inducible expression system to the transcriptionally silent minichromosomes of Trypanosoma brucei. Mol. Biochem. Parasitol. **125:**211–216. http://dx.doi.org/10.1016/S0166-6851(02)00238-4.
35. **Schimanski B, Nguyen TN, Günzl A.** 2005. Highly efficient tandem affinity purification of trypanosome protein complexes based on a novel epitope combination. Eukaryot. Cell **4:**1942–1950. http://dx.doi.org/10.1128/EC.4.11.1942-1950.2005.
36. **Niedzwiecka A, Marcotrigiano J, Stepinski J, Jankowska-Anyszka M, Wyslouch-Cieszynska A, Dadlez M, Gingras AC, Mak P, Darzynkiewicz E, Sonenberg N, Burley SK, Stolarski R.** 2002. Biophysical studies of eIF4E cap-binding protein: recognition of mRNA 5′ cap structure and synthetic fragments of eIF4G and 4E-BP1 proteins. J. Mol. Biol. **319:**615–635. http://dx.doi.org/10.1016/S0022-2836(02)00328-5.
37. **Cunningham I.** 1977. New culture medium for maintenance of tsetse tissues and growth of trypanosomatids. J. Protozool. **24:**325–329. http://dx.doi.org/10.1111/j.1550-7408.1977.tb00987.x.
38. **Hill KL, Hutchings NR, Russell DG, Donelson JE.** 1999. A novel protein targeting domain directs proteins to the anterior cytoplasmic face of the flagellar pocket in African trypanosomes. J. Cell Sci. **112:**3091–3101.
39. **Oberholzer M, Langousis G, Nguyen HT, Saada EA, Shimogawa MM, Jonsson ZO, Nguyen SM, Wohlschlegel JA, Hill KL.** 2011. Independent analysis of the flagellum surface and matrix proteomes provides insight into flagellum signaling in mammalian-infectious Trypanosoma brucei. Mol. Cell. Proteomics **10:**M111.010538. http://dx.doi.org/10.1074/mcp.M111.010538.
40. **Bastin P, Pullen TJ, Sherwin T, Gull K.** 1999. Protein transport and flagellum assembly dynamics revealed by analysis of the paralysed trypanosome mutant snl-1. J. Cell Sci. **112:**3769–3777.
41. **Oberholzer M, Lopez MA, McLelland BT, Hill KL.** 2010. Social motility in African trypanosomes. PLoS Pathog. **6:**e1000739. http://dx.doi.org/10.1371/journal.ppat.1000739.
42. **Ammerman ML, Downey KM, Hashimi H, Fisk JC, Tomasello DL, Faktorova D, Kafkova L, King T, Lukes J, Read LK.** 2012. Architecture of the trypanosome RNA editing accessory complex, MRB1. Nucleic Acids Res. **40:**5637–5650. http://dx.doi.org/10.1093/nar/gks211.
43. **Schägger H, von Jagow G.** 1991. Blue native electrophoresis for isolation of membrane protein complexes in enzymatically active form. Anal. Biochem. **199:**223–231. http://dx.doi.org/10.1016/0003-2697(91)90094-A.
44. **Zamudio JR, Mittra B, Chattopadhyay A, Wohlschlegel JA, Sturm NR, Campbell DA.** 2009. *Trypanosoma brucei* spliced leader RNA maturation by the cap 1 2′-*O*-ribose methyltransferase and SLA1 H/ACA snoRNA pseudouridine synthase complex. Mol. Cell. Biol. **29:**1202–1211. http://dx.doi.org/10.1128/MCB.01496-08.
45. **Peng J, Elias JE, Thoreen CC, Licklider LJ, Gygi SP.** 2002. Evaluation of multidimensional chromatography coupled with tandem mass spectrometry (LC/LC-MS/MS) for large-scale protein analysis: the yeast proteome. J. Proteome Res. **2:**43–50. http://dx.doi.org/10.1021/pr025556v.
46. **Haghighat A, Sonenberg N.** 1997. eIF4G dramatically enhances the binding of eIF4E to the mRNA 5′-cap structure. J. Biol. Chem. **272:**21677–21680. http://dx.doi.org/10.1074/jbc.272.35.21677.
47. **von Der Haar T, Ball PD, McCarthy JE.** 2000. Stabilization of eukaryotic initiation factor 4E binding to the mRNA 5′-Cap by domains of eIF4G. J. Biol. Chem. **275:**30551–30555. http://dx.doi.org/10.1074/jbc.M004565200.
48. **Kaye NM, Emmett KJ, Merrick WC, Jankowsky E.** 2009. Intrinsic RNA binding by the eukaryotic initiation factor 4F depends on a minimal RNA length but not on the m7G cap. J. Biol. Chem. **284:**17742–17750. http://dx.doi.org/10.1074/jbc.M109.009001.
49. **Yanagiya A, Svitkin YV, Shibata S, Mikami S, Imataka H, Sonenberg N.** 2009. Requirement of RNA binding of mammalian eukaryotic translation initiation factor 4GI (eIF4GI) for efficient interaction of eIF4E with the mRNA cap. Mol. Cell. Biol. **29:**1661–1669. http://dx.doi.org/10.1128/MCB.01187-08.
50. **Kramer S, Queiroz R, Ellis L, Webb H, Hoheisel JD, Clayton C, Carrington M.** 2008. Heat shock causes a decrease in polysomes and the appearance of stress granules in trypanosomes independently of eIF2α phosphorylation at Thr169. J. Cell Sci. **121:**3002–3014. http://dx.doi.org/10.1242/jcs.031823.
51. **Dhalia R, Marinsek N, Reis CR, Katz R, Muniz JR, Standart N, Carrington M, de Melo Neto OP.** 2006. The two eIF4A helicases in *Trypanosoma brucei* are functionally distinct. Nucleic Acids Res. **34:**2495–2507. http://dx.doi.org/10.1093/nar/gkl290.
52. **Alsford S, Turner DJ, Obado SO, Sanchez-Flores A, Glover L, Berriman M, Hertz-Fowler C, Horn D.** 2011. High-throughput phenotyping using parallel sequencing of RNA interference targets in the African trypanosome. Genome Res. **21:**915–924. http://dx.doi.org/10.1101/gr.115089.110.
53. **Kim HS, Li Z, Boothroyd C, Cross GA.** 2013. Strategies to construct null and conditional null *Trypanosoma brucei* mutants using Cre-recombinase and loxP. Mol. Biochem. Parasitol. **191:**16–19. http://dx.doi.org/10.1016/j.molbiopara.2013.08.001.
54. **Merritt C, Stuart K.** 2013. Identification of essential and non-essential protein kinases by a fusion PCR method for efficient production of transgenic *Trypanosoma brucei*. Mol. Biochem. Parasitol. **190:**44–49. http://dx.doi.org/10.1016/j.molbiopara.2013.05.002.
55. **Park SH, Nguyen BN, Kirkham JK, Nguyen TN, Gunzl A.** 11 April 2014. A new strategy of RNA interference that targets heterologous sequences reveals CITFA1 as an essential component of class I transcription factor A in *Trypanosoma brucei*. Eukaryot. Cell http://dx.doi.org/10.1128/EC.00014-14.
56. **Gingras AC, Raught B, Sonenberg N.** 1999. eIF4 initiation factors: effectors of mRNA recruitment to ribosomes and regulators of translation. Annu. Rev. Biochem. **68:**913–963. http://dx.doi.org/10.1146/annurev.biochem.68.1.913.
57. **Zinoviev A, Leger M, Wagner G, Shapira M.** 2011. A novel 4E-interacting protein in Leishmania is involved in stage-specific translation pathways. Nucleic Acids Res. **39:**8404–8415. http://dx.doi.org/10.1093/nar/gkr555.
58. **Marintchev A, Wagner G.** 2005. eIF4G and CBP80 share a common origin and similar domain organization: implications for the structure and function of eIF4G. Biochemistry **44:**12265–12272. http://dx.doi.org/10.1021/bi051271v.
59. **Li H, Tschudi C.** 2005. Novel and essential subunits in the 300-kilodalton

nuclear cap binding complex of *Trypanosoma brucei*. Mol. Cell. Biol. **25:** 2216–2226. http://dx.doi.org/10.1128/MCB.25.6.2216-2226.2005.

60. **Barbosa I, Haque N, Fiorini F, Barrandon C, Tomasetto C, Blanchette M, Le Hir H.** 2012. Human CWC22 escorts the helicase eIF4AIII to spliceosomes and promotes exon junction complex assembly. Nat. Struct. Mol. Biol. **19:**983–990. http://dx.doi.org/10.1038/nsmb.2380.
61. **Virgili G, Frank F, Feoktistova K, Sawicki M, Sonenberg N, Fraser CS, Nagar B.** 2013. Structural analysis of the DAP5 MIF4G domain and its interaction with eIF4A. Structure **21:**517–527. http://dx.doi.org/10.1016/j.str.2013.01.015.
62. **Kelley LA, Sternberg MJ.** 2009. Protein structure prediction on the Web: a case study using the Phyre server. Nat. Protoc. **4:**363–371. http://dx.doi.org/10.1038/nprot.2009.2.
63. **Silva E, Ullu E, Kobayashi R, Tschudi C.** 1998. Trypanosome capping enzymes display a novel two-domain structure. Mol. Cell. Biol. **18:**4612–4619.
64. **Ginger ML, Collingridge PW, Brown RW, Sproat R, Shaw MK, Gull K.** 2013. Calmodulin is required for paraflagellar rod assembly and flagellum-cell body attachment in trypanosomes. Protist **164:**528–540. http://dx.doi.org/10.1016/j.protis.2013.05.002.
65. **Kisalu NK, Langousis G, Bentolila LA, Ralston KS, Hill KL.** 2014. Mouse infection and pathogenesis by *Trypanosoma brucei* motility mutants. Cell Microbiol. **16:**912–924. http://dx.doi.org/10.1111/cmi.12244.
66. **Otsuka Y, Kedersha NL, Schoenberg DR.** 2009. Identification of a cytoplasmic complex that adds a cap onto 5′-monophosphate RNA. Mol. Cell. Biol. **29:**2155–2167. http://dx.doi.org/10.1128/MCB.01325-08.
67. **Culjkovic B, Topisirovic I, Skrabanek L, Ruiz-Gutierrez M, Borden KL.** 2006. eIF4E is a central node of an RNA regulon that governs cellular proliferation. J. Cell Biol. **175:**415–426. http://dx.doi.org/10.1083/jcb.200607020.
68. **Keene JD.** 2007. RNA regulons: coordination of post-transcriptional events. Nat. Rev. Genet. **8:**533–543. http://dx.doi.org/10.1038/nrg2111.
69. **Ouellette M, Papadopoulou B.** 2009. Coordinated gene expression by post-transcriptional regulons in African trypanosomes. J. Biol. **8:**100. http://dx.doi.org/10.1186/jbiol203.
70. **Landsman D, Bustin M.** 1993. A signature for the HMG-1 box DNA-binding proteins. Bioessays **15:**539–546. http://dx.doi.org/10.1002/bies.950150807.
71. **Marcotrigiano J, Lomakin IB, Sonenberg N, Pestova TV, Hellen CU, Burley SK.** 2001. A conserved HEAT domain within eIF4G directs assembly of the translation initiation machinery. Mol. Cell **7:**193–203. http://dx.doi.org/10.1016/S1097-2765(01)00167-8.

eIF4F-like complexes formed by cap-binding homolog TbEIF4E5 with TbEIF4G1 or TbEIF4G2 are implicated in post-transcriptional regulation in *Trypanosoma brucei*

EDEN R. FREIRE,[1] AJAY A. VASHISHT,[2] AMARANTA M. MALVEZZI,[1,3] JOANNA ZUBEREK,[4] GERASIMOS LANGOUSIS,[1] EDWIN A. SAADA,[1] JANAÍNA DE F. NASCIMENTO,[3] JANUSZ STEPINSKI,[4] EDWARD DARZYNKIEWICZ,[4,5] KENT HILL,[1] OSVALDO P. DE MELO NETO,[3] JAMES A. WOHLSCHLEGEL,[2] NANCY R. STURM,[1] and DAVID A. CAMPBELL[1]

[1]Department of Microbiology, Immunology and Molecular Genetics, David Geffen School of Medicine, University of California at Los Angeles, Los Angeles, California 90095, USA
[2]Department of Biological Chemistry, David Geffen School of Medicine, University of California at Los Angeles, Los Angeles, California 90095, USA
[3]Department of Microbiology, Centro de Pesquisas Aggeu Magalhães, Fundação Oswaldo Cruz, Recife, Pernambuco 50670-420, Brazil
[4]Division of Biophysics, Institute of Experimental Physics, Faculty of Physics, University of Warsaw, 02-089 Warsaw, Poland
[5]Centre of New Technologies, University of Warsaw, 02-089 Warsaw, Poland

ABSTRACT

Members of the eIF4E mRNA cap-binding family are involved in translation and the modulation of transcript availability in other systems as part of a three-component complex including eIF4G and eIF4A. The kinetoplastids possess four described eIF4E and five eIF4G homologs. We have identified two new eIF4E family proteins in *Trypanosoma brucei*, and define distinct complexes associated with the fifth member, TbEIF4E5. The cytosolic TbEIF4E5 protein binds cap 0 in vitro. TbEIF4E5 was found in association with two of the five TbEIF4Gs. TbIF4EG1 bound TbEIF4E5, a 47.5-kDa protein with two RNA-binding domains, and either the regulatory protein 14-3-3 II or a 117.5-kDa protein with guanylyltransferase and methyltransferase domains in a potentially dynamic interaction. The TbEIF4G2/TbEIF4E5 complex was associated with a 17.9-kDa hypothetical protein and both 14-3-3 variants I and II. Knockdown of TbEIF4E5 resulted in the loss of productive cell movement, as evidenced by the inability of the cells to remain in suspension in liquid culture and the loss of social motility on semisolid plating medium, as well as a minor reduction of translation. Cells appeared lethargic, as opposed to compromised in flagellar function per se. The minimal use of transcriptional control in kinetoplastids requires these organisms to implement downstream mechanisms to regulate gene expression, and the TbEIF4E5/TbEIF4G1/117.5-kDa complex in particular may be a key player in that process. We suggest that a pathway involved in cell motility is affected, directly or indirectly, by one of the TbEIF4E5 complexes.

Keywords: 14-3-3 protein; kinetoplastid; mRNA cap; social motility; translation initiation factor

INTRODUCTION

Trypanosoma brucei is a kinetoplastid protozoan belonging to the Excavata, a group that contains free-living and parasitic representatives (Adl et al. 2012). During the digenetic life-cycle, *T. brucei* is commonly found in the intestinal tract and salivary glands of tsetse flies and in the blood and cerebrospinal fluid of mammalian hosts, in which the parasite causes the tropical diseases human African trypanosomiasis and nagana in cattle. Transmission of the parasite occurs through the bite of the hematophagous tsetse fly vector, which harbors distinct intestinal and salivary forms. The kinetoplastid protozoa share unusual features of gene expression. Most protein-coding genes are arranged in directional gene clusters that are transcribed polycistronically (Alsford et al. 2012). Mature mRNAs possessing 5′ caps and 3′ poly(A) tails are generated by *trans*-splicing, which is linked mechanistically to polyadenylation (Liang et al. 2003; Preußer et al. 2012). Regulation of transcription initiation by RNA polymerase II is minimal (Martínez-Calvillo et al. 2010; Günzl 2012). The control of protein abundance and function during the parasite lifecycle is mediated predominantly through post-transcriptional mechanisms such as mRNA stability and availability, translational efficiency, post-translational modification, and protein stability (Clayton and Shapira 2007; Fernandez-Moya and Estevez 2010; Kramer 2012).

Corresponding author: nsturm.ucla@gmail.com
Article published online ahead of print. Article and publication date are at http://www.rnajournal.org/cgi/doi/10.1261/rna.045534.114.

A key step in post-transcriptional control is the regulation of translation initiation by the tripartite mRNA-binding complex eIF4F (Topisirovic et al. 2011). The core eIF4F complex consists of three proteins: eIF4E, an mRNA m^7G cap-binding protein; eIF4G, a large scaffold protein interacting directly with both eIF4E and the poly(A)-binding protein PABP; and eIF4A, a helicase linked to eIF4G that unwinds RNA secondary structure between the 5′ cap and the initiation codon (Gingras et al. 1999). Binding of eIF4F to the mRNA enables recruitment of multiple other translation initiation factors and the two ribosomal subunits to the initiation codon (Aitken and Lorsch 2012). eIF4E function represents a central control point in translational regulation (Jackson et al. 2010). The ability to bind eIF4G can be negated by 4E-binding proteins (Raught and Gingras 1999; Richter and Sonenberg 2005), and binding activity is implicated in the selective translation of RNA subgroups designated "regulons" (Culjkovic et al. 2007; Keene 2007). The existence of coordinated mRNA regulons is supported in the kinetoplastid protozoa (Ouellette and Papadopoulou 2009; Queiroz et al. 2009; Das et al. 2012; De Gaudenzi et al. 2013), however their mechanism of cap-mediated translation regulation remains a mystery.

The complexity of eIF4F components varies among organisms, including the protists (Joshi et al. 2005; Jagus et al. 2012). The yeast *Saccharomyces cerevisiae* possesses a single eIF4E and two eIF4Gs with distinct functions (Prévôt et al. 2003; Clarkson et al. 2010); humans have four eIF4E isoforms and two eIF4Gs (Prévôt et al. 2003; Joshi et al. 2004). The nematode *Caenorhabditis elegans*, in contrast, possesses five eIF4E variants (Keiper et al. 2000) that displays distinct preferences for m^7G and $m^{2,2,7}G$ cap structures (Jankowska-Anyszka et al. 1998), and a single eIF4G gene that gives rise to two isoforms (Contreras et al. 2008). Variants of eIF4E may show developmental regulation. *Drosophila melanogaster* has eight isoforms that show distinct patterns of expression during embryogenesis (Hernández et al. 2005). Distinct variant eIF4E–eIF4G interactions are thus expected and observed (Ptushkina et al. 2001). Not all homologs of eIF4E have a role in constitutive translation initiation (Rhoads 2009); they may function as competitive inhibitors of eIF4G recruitment and as scaffolds for interactions with other potential regulatory proteins (Groppo and Richter 2009; Blewett and Goldstrohm 2012; Gosselin et al. 2013). Some eIF4E-binding proteins like 4E-BP repress translation by inhibiting eIF4F formation, whereas other eIF4E-binding proteins, such as Cup and Maskin, use alternative 3′ UTR–protein interactions for selective repression of translation (Groppo and Richter 2009). Further, selective translation of mRNAs can occur via cap binding of an eIF4E homologous protein, 4E-HP (Cho et al. 2005) and discrete protein–3′ UTR interactions (Lasko et al. 2005).

The related pathogens *T. brucei* and *Leishmania spp*. have four eIF4E homologs (EIF4E) and five eIF4G homologs (EIF4G) (Dhalia et al. 2005; Freire et al. 2011; Zinoviev and Shapira 2012). In some cases, the respective interacting partners have been identified: EIF4E3 binds to EIF4G4, and EIF4E4 binds to EIF4G3 (Yoffe et al. 2009; Freire et al. 2011; Zinoviev et al. 2012), whereas EIF4E1 appears to lack an EIF4G partner (Zinoviev et al. 2011). The kinetoplastid mRNA cap, termed cap 4, is a complex 5-nt structure comprised of three base methylations and four ribose methylations (Bangs et al. 1992). The *Leishmania* EIF4E variants display differing affinities for synthetic cap analogs in vitro (Yoffe et al. 2006), suggesting differential roles in cap recognition. EIF4E4 is the best candidate for the workhorse translation initiation factor (Yoffe et al. 2009; Zinoviev et al. 2012).

The functions of the extended family of EIF4E proteins in kinetoplastids remain obscure. Here we extend the *T. brucei* EIF4E family with the identification of the fifth and sixth members, designated TbEIF4E5 and TbEIF4E6, and characterize the properties and macromolecular composition of TbEIF4E5 (or TbE5). We demonstrate that TbE5 binds to mRNA caps in vitro, is cytosolic, and associates with multiprotein complexes including either the TbEIF4G1 or TbEIF4G2 proteins (also called TbG1 or TbG2, respectively). The TbE5:TbG1 complex contains one protein with two RNA-binding domains and another with both guanylyltransferase and methyltransferase motifs, implicating the complex in cap modification of specific transcripts. The TbE5:TbG2 complex is distinguished by the presence of both 14-3-3 isoforms (Inoue et al. 2005; Benz et al. 2010), hetero- and homodimer forming proteins whose functions are determined by interactions with phosphorylated serine or threonine residues (Mackintosh 2004). The manifestation of a specific phenotype upon knockdown of the TbE5 protein is suggestive of a role for post-transcriptional gene regulation of at least one cellular pathway by a TbE5-containing complex.

RESULTS

Two new members of the kinetoplastid eIF4E-homolog family

In pursuit of our longstanding interest in SL RNA cap function in kinetoplastid gene expression, a search was conducted for potential cap-binding proteins using known entities from other model systems. The eIF4E protein that recognizes the cap 0 structure as a first step in mRNA translation fits this description, and searches using the yeast eIF4E sequence yielded a set of five potential eIF4E family members that are present in *T. brucei* (Tb4EIF4E), *T. cruzi*, and *Leishmania spp*. Of this set, four have been identified and studied to varying degrees by other groups (Yoffe et al. 2004, 2006, 2009; Dhalia et al. 2005; Freire et al. 2011). A sixth homolog was identified by reciprocal BLAST with the uncharacterized TbEIF4E sequence. Here we designate the additional two putative members as TbEIF4E5 (Tb927.10.5020) and TbEIF4E6 (Tb927.7.1670) and present the molecular characterization of TbEIF4E5, a.k.a. TbE5.

The TbE5 and TbEIF4E6 genes produce the two smallest members of the Tb4EIF4E family at estimated molecular weights of 21.9 and 20.8 kDa, respectively (Fig. 1A). Both proteins carry features conserved generally in eIF4Es, including the eIF4E "core" and amino acids suggestive of RNA cap 0 binding as indicated. Key tryptophan residues are conserved in the trypanosome proteins. The tryptophan at position 73, relative to the human eIF4E-1 numbering, that is key for eIF4G interaction is found in TbE5 and shows a substitution by histidine in TbEIF4E6. Tryptophans at positions 56 and 102 of the human protein act in cap binding through stacking interactions with m^7G of the cap structure. Position 56 is conserved in TbE5, while TbEIF4E6 carries a conservative substitution with phenylalanine. Both *T. brucei* homologs show conservative substitutions to either tyrosine or phenylalanine at position 102. Position 166, which in the human protein is implicated in m^7G recognition, shows absolute conservation in the kinetoplastid proteins, as does the tryptophan at position 43. Phylogenetic and BLAST analyses suggest that TbE5 and TbEIF4E6 are more closely related to each other than to other TbEIF4Es (data not shown) and may thus represent a distinct category within this RNA cap-binding protein family.

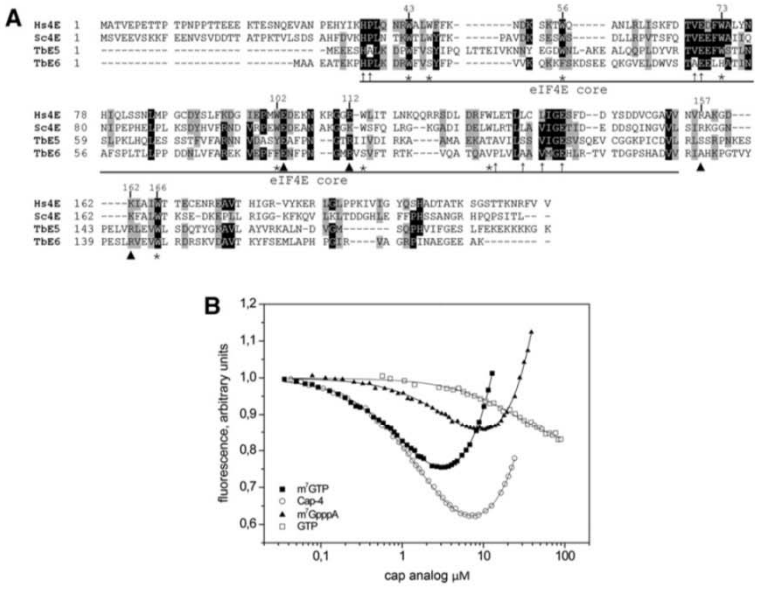

FIGURE 1. TbEIF4E5 and TbEIF4E6 are shorter than the eIF4E homologs from yeast and human. (*A*) Alignment of the sequences was performed using Clustal W. Identical amino acids are indicated by black shading. Amino acids defined as similar, by the BLOSUM 62 Matrix, in >60% of the sequences are shaded gray. Dashes represent spaces that were inserted to allow better alignment. Asterisks represent tryptophan residues conserved in the eIF4E protein family. Arrowheads indicate nontryptophan residues required for the interaction with the cap structure: E103 hydrogen bonded with guanine; and, basic residues at positions 112, 157, and 162 with the phosphate bridge (Marcotrigiano et al. 1997). Thin arrows indicate conserved nontryptophan residues shown to be involved in eIF4G binding (Marcotrigiano et al. 1999). GenBank Accession numbers: Hs (human) eIF4E-1, NP_001959; Sc (yeast) eIF4E, NP_014502. (*B*) In vitro cap-binding ability of recombinant TbE5. The fluorescence-titration curves with four cap analogs were determined by fluorescence-binding assays. The protein fluorescence was excited at 280 nm and observed at 340 nm. The WT mRNA cap in trypanosomes was represented by hypermethylated cap 4, while the typical eukaryotic cap structure was represented by both the m^7GTP and m^7GpppA cap 0 structures. The nonmethylated GTP served as a negative control for cap 0-specific binding.

TbEIF4E5 binds cap analogs in vitro

The conservation of aromatic amino acids corresponding to positions 56, 102, and 166 suggests that TbE5 should be capable of binding mRNA caps. Basic arginine residues at positions 112 and 162 could interact with the phosphate chain of the cap via hydrogen bonds. Recombinant TbE5 protein was tested in vitro for binding ability to various cap analogs using fluorescence assays (Fig. 1B). TbE5 bound better to the cap 4 analog corresponding to the structure found on all kinetoplastid nuclear mRNAs ($K_{as} = 0.55 \pm 0.01\ \mu M^{-1}$) and the m^7GTP analog ($K_{as} = 0.65 \pm 0.01\ \mu M^{-1}$) than to m^7GpppA ($K_{as} = 0.12 \pm 0.01\ \mu M^{-1}$) or GTP ($K_{as} = \sim 0.037\ \mu M^{-1}$). TbE5 bound the trypanosome-specific substrate 47-fold less than the mouse eIF4E (Yoffe et al. 2006). The association constant for TbE5 with cap 4 was within the range observed for *Leishmania major* EIF4Es (Yoffe et al. 2006), falling between LeishIF4E-2 and LeishIF4E-4. Generally, TbE5 and all *Leishmania* EIF4Es show a preference for cap analogs with an N7-methylated guanosine. The energetic gain from methylation of the guanine ring for TbE5 is similar by $\Delta\Delta G^O$ of about –1.6 kcal/mol. The presence of additional nucleotides that simulate an mRNA 5′ end showed decreased binding relative to the m^7GTP substrate. In all instances, including mouse, the cap 4 substrate was bound better than the cap 0 analog, probably due to the stabilization effect of the phosphate group in the oligonucleotide.

Due to the virtual absence of transcriptional control in kinetoplastids, downstream methods for the modulation of gene expression are of particular interest. The divergent TbE5 protein represents a potential player in the modulation of post-transcriptional control events in the parasite.

TbEIF4E5 interacts directly with two of the five TbEIF4Gs

A hallmark characteristic of the eIF4E proteins is their association with eIF4Gs. In *T. brucei* five EIF4G family members have been described, thus the potential for specific interactions among the EIF4E and EIF4G homologs could

yield a range of combinatorial arrangements leading to an array of biological consequences. To determine if any of these interactions are favored by TbE5 we performed an exhaustive interaction study between the prospective players.

The yeast two-hybrid assay detects interactions between two proteins, termed "bait" and "prey," as indicated by the activation of a promoter in the yeast cells that permits growth (Fig. 2). The reciprocal interactions were tested, with compatible results (data not shown). The assays revealed either large yeast colonies indicating that TbE5 associated strongly with TbEIF4G2 (Tb09.160.3980; TbG2) or smaller colonies indicating a weaker interaction with TbEIF4G1 (Tb927.5.1490; TbG1). In the yeast two-hybrid assay, binding between TbEIF4E and TbEIF4G proteins in the presence of 5.0 mM 3AT indicates a strong interaction, to the exclusion of other weaker TbEIF4E–TbEIF4G pairings.

The interaction of TbE5 with more than one TbEIF4G may be an indication of specific functions associated with either TbG1 or TbG2 pairings. With the exception of the site of EIF4E:EIF4G interaction in *Leishmania* (Yoffe et al. 2009), no functionality can be predicted for any of the five TbEIF4G sequences outside the core family-defining MIF4G domain (Dhalia et al. 2005). TbG1 and TbG2 have not been observed to interact with other trypanosomatid EIF4E homologs to date. They are the two largest members of the TbEIF4G family and may serve as a scaffold for binding of additional proteins, as observed in humans and yeast (Pestova and Hellen 2003; Jackson et al. 2010). These isolated interactions serve as a guide for the behaviors of proteins in *T. brucei*, however the incorporation of other proteins or RNAs into the equation may alter the actual complex components.

TbEIF4E5 is present in high molecular weight complexes

The typical eIF4F complex contains three components: eIF4E, eIF4G, and eIF4A (Gingras et al. 1999). Our yeast two-hybrid interaction assays indicate TbE5 associates with two specific TbEIF4G homologs, TbG1 and TbG2. The interaction of

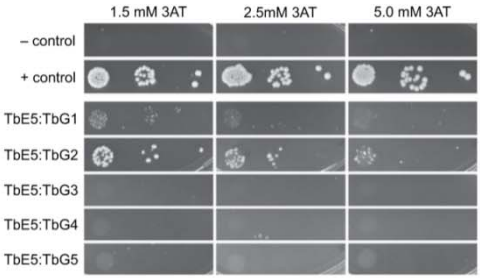

FIGURE 2. Direct interaction of TbEIF4E5 with two of the five *T. brucei* EIF4G homologs. Interactions between TbE5 and the five TbEIF4G homologs were challenged using the yeast two-hybrid assay in the presence of increasing amounts of 3AT, increasing the stringency of the assay. Positive controls were pGADT7-T and pGBKT7-53; the negative controls were the empty vectors. Interaction strength is inferred by colony size: ≥2 mm = strong; 1–2 mm = moderate; ≤1 mm = weak.

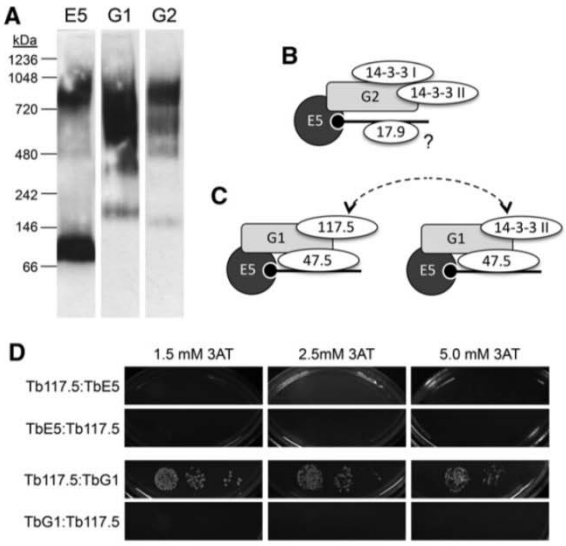

FIGURE 3. TbEIF4E5 is present in high molecular weight complexes. (*A*) Blue Native gel electrophoresis of cell extracts from transfected *T. brucei* containing PTP-tagged proteins. Lysates were run through Blue Native gels, transferred to nitrocellulose membranes and probed with antibody directed against the protein A domain of the PTP tag (TbE5, TbG1, TbG2 = E5, G1, G2, respectively). The migration of size standards is indicated in kDa. (*B*) The components that co-purified with TbEIF4E5 and TbEIF4G2. The RNA (black line; black circle represents 5′ end cap 4) is recognized by the cap-binding eIF4E component TbE5 (dark gray circle, E5). The eIF4G-like scaffold protein TbG2 (light gray rectangle, G2) interacts directly with TbE5, as indicated by overlap of the respective shapes. Other TbE5-associated proteins are shown as ovals. Overlap of the ovals with other shapes is speculative and based on the assumed scaffold function of TbG2, and shapes do not reflect protein size. The placement of Tb17.9 on the RNA is speculative, as indicated by the "?". (*C*) The TbEIF4E5/TbEIF4G1 dynamic complex model. The 117.5-kDa protein in association with the TbG1 scaffold may be regulated by the presence of the 14-3-3 II homodimer, the binding of which is dependent on TbG1 phosphorylation. The dotted arrows highlight the either/or aspect of the complexes. (*D*) Yeast two-hybrid analysis of Tb117.5 with TbE5 or TbG1 in both bait and prey orientations. Controls and interpretations are shown in Figure 2.

TbE5 and the two TbEIF4G subunits observed in yeast was examined in *T. brucei* first by visualizing the size of complexes containing PTP-tagged proteins by Blue Native gel electrophoresis, followed by MudPIT analysis of tandem-affinity purified complexes.

To validate that TbE5 was in a high molecular weight complex(es), extracts of $TbE5^{-/PTP}$ were resolved by Blue Native gel analysis and visualized by Western blotting using anti-protein A antibody. Two bands of ~100 kDa (migrating between the 66 and 146 kDa markers) and ~900 kDa (migrating between the 720 and 1048 kDa markers) were detected in the TbE5 extracts (Fig. 3A), indicating complexes of substantially greater size than predicted for free TbE5 (22 kDa + 19 kDa for the PTP tag), which was either undetectable or not running true to predicted size. The proteins implicated by yeast two-hybrid analysis, TbG1 and TbG2, were PTP-tagged as

well to allow reciprocal comparisons. For both TbG1$^{-/PTP}$ and TbG2$^{-/PTP}$ lines multiple discrete and smeared higher molecular weight bands were seen, suggestive of their involvement in multiple distinct complexes, some of which may contain TbE5. The predicted sizes of TbG1 and TbG2 are 122.1 kDa and 97.3 kDa, respectively; thus adding the contribution of the PTP tags, the bottom bands in each lane likely represent the migration of free proteins. The size markers may not represent true complex sizes, as the shape of the complex will play a major role in the migration of species through this nondenaturing gel system. Both of the TbEIF4G proteins show more complex patterns than TbE5.

The combined data from these experiments are consistent with the prediction that TbEIF4E/TbEIF4G form high MW complexes in vivo, and indicate the presence of additional components in the complexes formed by TbE5, TbG1, and TbG2 proteins.

TbEIF4E5 associates with two distinct sub-complexes

To isolate the specific complexes and identify their constituents, the TbE5$^{-/PTP}$ line was used for tandem-affinity complex purification with subsequent protein identification by MudPIT. The purification was performed four times under different salt conditions. The comparative results revealed 11 proteins that co-purified with TbE5 in all four preparations (Table 1). Based on low abundance, low numbers of peptides detected, and in some cases the identity of the protein, the bottom four proteins are considered to be contaminants.

In accordance with the yeast two-hybrid assay both TbG1 and TbG2 co-purified consistently with TbE5. Additional proteins that co-purified with TbE5 complex include both isoforms of the ~30 kDa phosphoserine/phosphothreonine-binding protein named Tb14-3-3 I and Tb14-3-3 II (Inoue et al. 2005), and proteins of 17.9, 47.5, and 117.5 kDa all designated as "hypothetical" in GeneDB.

Based on the yeast two-hybrid and TbE5$^{-/PTP}$ MudPIT results, extracts from the TbG1$^{-/PTP}$ and TbG2$^{-/PTP}$ cell lines were subjected to tandem-affinity chromatography and subsequent MudPIT analysis. These purifications partitioned the proteins co-purifying with TbE5 into two distinct subsets. The TbG1-PTP purifications identified 14 proteins that co-purified in two separate preparations (Table 2). Of these, five were present in all TbE5-PTP purifications, supporting the existence of a discrete complex comprised of five members: TbE5, TbG1, Tb14-3-3 II, and the 47.5-kDa and 117.5-kDa proteins. Notably, the first six proteins identified other than TbG1 itself were not present in the TbE5-PTP purification; thus although they may be legitimate associates of TbG1, at this point there is no evidence to include them in the TbE5/TbG1 complex. TbG1 may participate in multiple complexes, not all of which include TbE5, consistent with the wider range of complexes visible for TbG1 in the Blue Native gel analysis (see Fig. 3A). Three tandem-affinity preparations of TbG2-PTP yielded a set of 13 proteins, of which five were present in all TbE5-PTP purifications (Table 3). The second TbE5 complex was thus defined by the presence of TbG2 along with TbE5, Tb14-3-3 I, Tb14-3-3 II, and the 17.9-kDa hypothetical protein (Fig. 3B), yielding a predicted complex mass of 196.5 kDa. In the case of TbG2, the top five identifications in terms of NSAF score are found in the TbE5 purification, and several of the remaining proteins are common to the TbG1 purification, indicating that they may function in a chaperoning role or be contaminants of EIF4G

TABLE 1. Proteins that co-purify consistently with TbEIF4E5-PTP

Gene	GeneDB ID[a]	GeneDB ID[b]	NSAFe5[c]	kDa	# Peptides	RNAi[d]
TbEIF4E5	Tb927.10.5020	Tb11.02.4700	22387.585	21.9	21	1-1-0[e]-1
14-3-3 II	Tb927.11.6870		12514.799	29.1	14	0-0-1[f]-0
Hypothetical	Tb927.11.6010	Tb11.02.3830	8724.748	17.9	9	0-0-0-0
Hypothetical	Tb927.11.6720	Tb11.02.4550	6892.809	117.5	50	0-0-0-0
14-3-3 I	Tb927.11.9530	Tb11.01.1290	5795.657	30.3	11	0-0-0-0
TbEIF4G2	Tb927.9.5460	Tb09.160.3980	3824.758	97.3	30	1-0-1-0
TbEIF4G1	Tb927.5.1490		3160.416	122.1	40	1-0-1-1
Hypothetical	Tb927.11.350	Tb11.03.0790	1409.713	47.5	7	1-1-1-1
TEF1-α	Tb927.10.2090		1262.683	37.8	5	0-0-0-0
Dynein light chain LC8	Tb927.11.18680	Tb11.50.0007	1135.602	10.4	2	1-0-0-0
Mitochondrial carrier prot.	Tb927.9.10310	Tb09.211.1750	138.176	34.3	2	1-0-1-1
Hypothetical	Tb927.8.4560		46.685	137.9	2	1-1-0-1

Four different preparations were analyzed by MudPIT. Peptide recovery shown represents extracts that were treated with 150 mM KCl for 20 min before affinity chromatography.
[a]GeneDB identifier from *T. brucei* 927 version 6.0, www.genedb.org and www.tritrypdb.org.
[b]Temporary GeneDB identifier retrieved from peptide analysis based on *T. brucei* 927 version 2.2.
[c]NSAF, normalized spectral abundance factor.
[d]High-throughput RNAi data and abbreviations from Alsford et al. (2011). Reported as BF3-BF6-PC-diff: BF3, bloodstream form 3 d; BF6, bloodstream form 6 d; PC, procyclic forms; diff, differentiating bloodstream forms; 1 = Normal; 0 = Abnormal, significant loss of fitness.
[e]TbE5 procyclic forms showed normal growth curves after RNAi (this manuscript).
[f]RNAi showed abnormal growth curves of procyclic forms after 6 d (Inoue et al. 2005).

TABLE 2. Proteins co-purifying with TbEIF4G1-PTP in multiple purifications

Gene	GeneDB ID[a]	GeneDB ID[b]	NSAFe5[c]	kDa	# Peptides	E5-PTP[d]
TbEIF4G1	Tb927.5.1490	Tb09.160.3270	1264.422	122.1	49	yes
TbEIF4A1	Tb927.9.4680		1083.045	45.4	13	
Hypothetical	Tb927.9.1520	Tb09.160.0465	923.937	97.6	4	
TEF-1 β	Tb927.4.3590		730.755	24.3	8	
TEF-1 β	Tb927.10.5840		669.805	21.9	5	
ALBA3	Tb927.4.2040		472.389	20.8	5	
ALBA2	Tb927.11.4450	Tb11.02.2030	383.564	12.8	4	
Hypothetical "117.5"	Tb927.11.6720	Tb11.02.4550	297.198	117.5	17	yes
14-3-3 II	Tb927.11.6870	Tb11.02.4700	267.125	29.1	4	yes
TEF-1 α	Tb927.8.5880		260.912	19.4	4	
DHH1	Tb927.10.3990		221.069	46.5	6	
TbEIF4E5	Tb927.10.5020		172.604	21.9	3	yes
eIF2 β	Tb927.5.3120		143.377	35.0	4	
Hypothetical "47.5"	Tb927.11.350	Tb11.03.0790	128.957	47.5	4	yes

Two different preparations were analyzed by MudPIT. Peptide recovery shown is from extracts incubated in 150 mM KCl.
[a]GeneDB identifier, www.genedb.org and www.tritrypdb.org.
[b]Temporary GeneDB identifier retrieved from peptide analysis.
[c]NSAF, normalized spectral abundance factor.
[d]Protein present in MudPIT of PTP-tagged TbE5.

purifications. The TbEIF4A1 protein in particular is interesting, since it is a known homolog of the standard eIF4F translation initiation complex; however, the absence of this protein from the TbE5 purification essentially eliminates it from both the TbG1- and TbG2-containing complexes. Yeast two-hybrid analyses detected no interactions between Tb17.9 and either TbE5 or TbG2 (data not shown), and if this result reflects the behavior of the protein in *T. brucei*, at least two possibilities may remain: Tb17.9 (1) binds to the 14-3-3 I protein, or (2) interacts with an RNA recognized by the complex. Alternatively, this could be a case of the fusion proteins interfering with the assay. The presence of the PTP tag may interfere with binding of a particular protein, but in this case the TbEIF4A1 protein is predicted to interact directly with the TbEIF4G scaffold; because the PTP construction exists in the absence of the wild-type (WT) allele, PTP tag interference should have resulted in nonviable or impaired cells, and these lines behaved as WT.

These results validate the unusual association of two distinct TbEIF4G proteins with a single TbEIF4E cap-binding protein. While the reciprocal scenario of multiple eIF4E proteins binding a single eIF4G scaffold has been documented (Prévôt et al. 2003; Clarkson et al. 2010), the TbE5 situation is notable. Furthermore, the associates of each complex are distinct, implying that the two complexes could perform unique regulatory functions.

Dynamic associations within the TbEIF4E5/TbEIF4G1 complex implied

To get a better understanding of the TbE5/TbG1 complex, we performed a PTP purification using a third component. Analysis of a stringent purification using the 117.5-kDa protein tagged with PTP revealed the presence of the 47.5-kDa protein, TbG1, and TbE5 (Table 4), along with other proteins (data not shown). The 14-3-3 II protein was absent from the 117.5-kDa protein-based purification, thus 117.5-kDa protein binding may be modulated by 14-3-3 II interaction with TbG1 (Fig. 3C). Switching between a bound 14-3-3 II dimer and the 117.5-kDa protein could reflect a key dynamic within the TbE5–TbG1 complex. Alternatively, the PTP tag on the 117.5-kDa protein may impair 14-3-3 II binding to the complex. The aggregate molecular weights of these two alternatives are 309 kDa for the 117.5 kDa–protein complex and 249.7 kDa for the 14-3-3 complex, including the dimer form of 14-3-3 II. Examination of 14-3-3 II was considered; however, since the protein is known to interact in numerous cellular pathways

TABLE 3. Proteins co-purifying with TbEIF4G2-PTP in multiple purifications

Gene	GeneDB ID[a]	GeneDB ID[b]	NSAFe5[c]	kDa	# Peptides	E5-PTP[d]
14-3-3 II	Tb927.11.6870	Tb11.02.4700	6534.474	29.1	24	yes
Hypothetical "17.9"	Tb927.11.6010	Tb11.02.3830	5268.922	17.9	15	yes
TbEIF4G2	Tb927.9.5460	Tb09.160.3980	4883.723	97.3	51	yes
TbEIF4E5	Tb927.10.5020	Tb10.70.2180	3762.424	21.9	24	yes
14-3-3 I	Tb927.11.9530	Tb11.01.1290	3609.246	30.3	4	yes
ALBA 3	Tb927.4.2040		429.048	20.8	6	
TbEIF4A1	Tb927.9.4680	Tb09.160.3270	322.848	45.4	8	
Hypothetical	Tb927.10.8940		277.681	45.4	6	
TEF-1 β	Tb927.4.3590		249.867	24.3	3	
Hypothetical	Tb927.11.13180	Tb11.01.4740	160.941	61.2	2	
Hypothetical	Tb927.11.7780	Tb11.02.5660	155.645	46.2	4	
Hypothetical	Tb927.10.4880		145.57	26.0	2	

Three different preparations were analyzed by MudPIT. Peptide recovery shown for extracts treated with 150 mM KCl.
[a]GeneDB identifier, www.genedb.org and www.tritrypdb.org.
[b]Temporary GeneDB identifier retrieved from peptide analysis.
[c]NSAF, normalized spectral abundance factor.
[d]Protein present in MudPIT of PTP-tagged TbE5.

TABLE 4. Proteins co-purifying with PTP-tagged 117.5-kDa protein also present with TbEIF4E5-PTP and TbEIF4G1-PTP

Gene	GeneDB ID[a]	NSAFe5[b]	kDa	# Peptides
Hypothetical "117.5"	Tb927.11.6720	2107.168	117.5	53
Hypothetical "47.5"	Tb927.11.350	963.474	47.5	13
TbEIF4G1	Tb927.5.1490	728.330	122.1	11
TbEIF4E5	Tb927.10.5020	368.449	21.9	3

One preparation was analyzed by MudPIT. The extract was treated with 300 mM KCl.
[a]GeneDB identifier, www.genedb.org and www.tritrypdb.org.
[b]NSAF, normalized spectral abundance factor.

and would thus not guarantee a definitive result, we will pursue other experimental avenues to validate this interaction model. Yeast two-hybrid analysis was consistent with direct interaction between TbG1 and the 117.5-kDa protein, with one orientation substantially stronger than the other; results were negative for TbE5–Tb117.5 interaction (Fig. 3D).

The dynamic interactions within the TbE5/TbG1 complex led to the definition of three TbE5-containing complexes, each of which may have different roles in post-transcriptional gene regulation. Association of the phosphoprotein-binding 14-3-3 components may serve to inactivate the action of the Tb117.5 proteins (see below).

TbEIF4E5 is a cytosolic protein resistant to gene knockout

The four published kinetoplastid EIF4E protein family members are either cytosolic or present in both the nucleus and cytosol (Kramer et al. 2008; Freire et al. 2011). The family member involved in the lion's share of mRNA translation should be critical for cell survival. To assess function, the TbE5 protein was localized and assayed for its importance in cell viability under normal procyclic culture conditions. The absence of strong antibodies for our target proteins and the availability of excellent epitope tagging systems prompted us to generate a cell line designated TbE5$^{-/PTP}$, with one WT allele replaced by a PHLEO-resistance marker and the other allele tagged in situ by insertion of PTP epitope sequences (Schimanski et al. 2005). The robust behavior of the TbE5$^{-/PTP}$ line indicated that the PTP tag was not interfering with TbE5 protein function.

Immunolocalization of the TbE5 fusion protein in the TbE5$^{-/PTP}$ line via the PTP tag revealed a diffuse cytosolic distribution with numerous foci of greater intensity, and apparent exclusion from the nucleus (Fig. 4), similar to what was seen for homologs TbEIF4E3 and TbEIF4E4 (Kramer et al. 2008; Freire et al. 2011).

In our hands, inducible double-stranded RNA interference (RNAi) directed against the TbE5 transcript in both TbE5$^{+/+}$ and TbE5$^{+/PTP}$ RNAi procyclic cells showed no catastrophic effect on cell growth in standard growth medium (Fig. 5A). The level of epitope-tagged TbE5 was reduced to <12.5% of uninduced levels by day 2 (Fig. 5B). To provide the cells with ample time to display any effects, we extended our RNAi analysis to 15 d, well beyond our usual 7-d limit, at which point RNAi cell lines are prone to escape the RNAi constraints. The induced TbE5$^{+/PTP}$ RNAi cell lines continued to divide under TbE5 knockdown, albeit at a slightly reduced rate relative to the uninduced culture (data not shown). To quantitate the effect of protein knockdown on general translation, RNAi cells at day 4 and day 7 post-induction were labeled metabolically with ^{35}S-methionine (Fig. 5C). The level of isotope incorporation was similar for both uninduced and induced cultures on day 4. By day 7, isotope incorporation in induced TbE5 cells was reduced by 16%.

As a general rule, when an RNAi line shows no significant growth defect, the next experimental step is to create a knockout cell line so that the absence of the protein of interest can be assessed in a clean background. No third allele was detected in the construction of the TbE5$^{-/PTP}$ line, thus the diploid nature of these genes was confirmed. Double allele knockout of the TbE5 gene was attempted three times, and all attempts failed in the elimination of the second targeted allele. In both cases a WT allele persisted, despite integration of the second selective marker (data not shown). We interpret this to signify that the TbE5 protein is essential, and the lowered protein levels achieved by our RNAi inductions allowed evaluation at reduced levels of TbE5 function. Discordant results for individual genes and the Alsford study (Alsford et al. 2011) are not unknown (Badjatia et al. 2013). The inability to obtain a knockout TbE5 line may be technical rather than linked to the function of the gene, and alternative approaches (Kim et al. 2013; Merritt and Stuart 2013; Park et al. 2014) are in progress.

Knockdown of the TbEIF4E5 protein affects motility

During the course of the RNAi experiments, the culture phenotype of TbE5 RNAi-induced cells was altered. Initially, after 48 h of stationary incubation, we observed that cells accumulated on the bottom of the culture flasks while noninduced

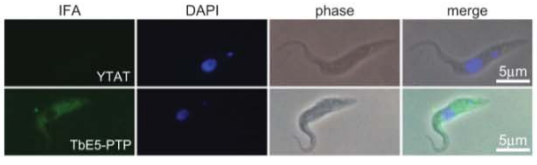

FIGURE 4. TbEIF4E5 is cytosolic in *T. brucei* procyclic cells. Subcellular localization was determined by indirect immunofluorescence using antibody against the protein A component of the PTP tag on the TbE5 fusion protein. Nontransfected control YTAT cells served as the negative control. Nuclear and kinetoplast DNA was visualized by counterstaining with DAPI.

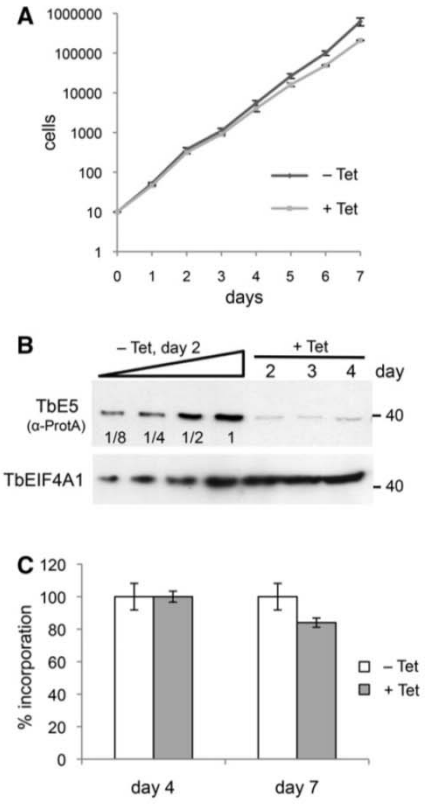

FIGURE 5. TbEIF4E5 does not have a primary role in translation. (*A*) Growth of TbE5 RNAi tetracycline (Tet) induced and uninduced cells measured over 7 d. (*B*) Assessment of protein knockdown by RNAi using the $TbE5^{PTP/+}$ background cell line. SDS-PAGE analysis of protein levels at days 2, 3, and 4 post-induction. TbE5-PTP was detected by anti-Protein A antibody (α-ProtA). Serial twofold dilutions of uninduced samples at day 2 are shown for comparison. Levels of TbEIF4A1 are included as protein loading controls. (*C*) Metabolic labeling of cultures induced for TbE5 RNAi knockdown as measured by ^{35}S-methionine incorporation at 4 and 7 d post-induction.

cells remained in suspension. This "settling" phenotype was reproducible, and was measured by OD_{600} changes over 24 h.

For each tetracycline (Tet) treatment, six equivalent cultures were established. At each time point, three cultures were shaken to resuspend the cells, accommodating for the effect of cell growth during the experimental period. The OD_{600} relative sedimentation measurements for each time period were determined by dividing the experimental unshaken cuvette reading by the shaken cuvette reading for the same culture condition. The sedimentation assays showed a significant reduction in OD_{600} at 8 h and 24 h for the TbE5 RNAi-induced culture relative to the uninduced culture (Fig. 6A). At the beginning of the experiment, all cultures showed a 1:1 ratio of suspended cells. After 8 h, WT and the uninduced TbE5 RNAi cultures were not different, but both showed signs of cell settling in the 20%–25% range. In contrast, the induced TbE5 RNAi line displayed a markedly higher level of settling, with about half of the cells settled. This trend continued in the 24-h sample, with the induced sample at ~50% the level of suspension relative to the WT and uninduced cultures. The settling phenotype is slower than observed for mutants with defects in proteins directly related to motility, e.g., flagellar proteins (Ralston and Hill 2006; Ralston et al. 2006).

The settling phenotype of TbE5 RNAi-induced cells prompted us to examine whether there was a comparable effect on Social Motility (SoMo) on semisolid agar plates (Oberholzer et al. 2010). SoMo is visualized by the formation of massed cell projections from a single inoculum point after 5 d. Under conditions of RNAi knockdown the TbE5 cell line showed a significant defect in SoMo as measured by counting

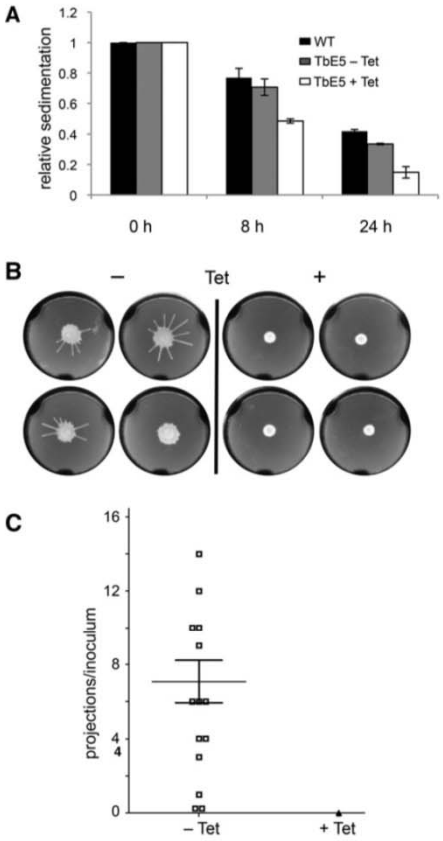

FIGURE 6. Reduction of TbEIF4E5 results in motility defects. (*A*) Culture turbidity was measured to assess cell settling in nonshaken cultures. Cells induced for RNAi against TbE5 (white column) were compared with noninduced culture (gray column) and WT cells (black column). Standard error was determined for experiments performed in triplicate. (*B*) Representative soft agarose plate Social Motility assays for TbE5 RNAi-uninduced (−Tet) or RNAi-induced cells (+Tet) 5 d post-plating. The − plate was scored as showing 10 radial projections, a typical manifestation of social motility in *T. brucei*. (*C*) Graphical summary of two sets of SoMo assays indicating means and standard errors. Symbols represent the number of radial projections from the site of inoculation: Open squares represent uninduced (−Tet); the single filled triangle represents all 14 induced samples (+Tet).

Sturm et al. 2012). The further impact on distinct aspects of cell motility following knockdown of the TbE5 suggests unidentified roles for the complexes in the regulation of protein expression and function in these parasites.

The Alsford genome-wide RNAi study indicates that TbE5 is an essential protein in the cultured insect stage; however, TbE5 is not required for viability in bloodstream forms and differentiating bloodform cells (Alsford et al. 2011). In our hands, procyclic RNAi lines targeting the TbE5 transcript are viable, with protein levels reduced but detectable. Several phenotypic oddities were noted in our TbE5 RNAi knockdowns. TbE5 cells did not remain in suspension in liquid culture and showed "lethargic" activity, and social motility behavior was abolished. The role of an RNA-cap-binding protein in eliciting downstream effects on motility could be direct or indirect depending on whether mRNAs are recognized with specificity or nonspecifically. The absence of a dramatic cell-death or growth-arrest phenotype in the TbE5 knockdown coupled with the lack of a catastrophic effect on ^{35}S-methionine incorporation indicates that TbE5 is not the primary EIF4E responsible for general translation in *T. brucei*. The lack of effect on translation for TbE5 knockdown on day 4 contrasts the 64% and 72% reduction in translation observed on day 4 RNAi knockdown of TbEIF4E3 and TbEIF4E4, respectively (Freire et al. 2011), the best candidates for a main role in translation initiation. The third component of the eIF4F complex, TbEIF4A, did not co-purify with PTP-tagged TbE5 or the PTP-tagged 117.5-kDa protein, however it was relatively abundant in the TbG1-PTP preparation and of low abundance in the TbG2 preparation. RNAi knockdown of flagellum components often are detrimental to the cell cycle and cell division (Branche et al. 2006; Broadhead et al. 2006; Ralston et al. 2006); no such defects were observed during TbE5 knockdown. The small decrease in translation hints at a minor role in translation or an indirect role in regulation, nevertheless an insufficient level of knockdown or secondary effects cannot be discounted.

TbE5 interacts with proteins associated with the TbEIF4F complex, specifically members of the anticipated TbEIF4G family. As with the TbEIF4E proteins, in kinetoplastids the TbEIF4G family is expanded relative to other eukaryotes, containing five identified members (Dhalia et al. 2006). The direct interaction between the TbE5 and the TbG1 and TbG2 homologs predicted by the initial yeast two-hybrid assay was confirmed in vivo. TbE5 was purified from *T. brucei* extracts in association with either TbG1 or TbG2 in distinct complexes. In mouse, the eIF4G interaction domain of eIF4E is defined as a pocket that contains three conserved acidic amino acids and four conserved nonpolar residues (Marcotrigiano et al. 1997), thus given the conservation of predicted tertiary structure for TbE5 the same region is expected to determine the specificity of a specific TbEIF4E and specific TbEIF4Gs.

A TbE5 complex containing TbG1 is associated with a predicted 117.5-kDa bifunctional capping enzyme, which contains guanylyltransferase and N7-methyltransferase domains, and is essential in multiple life stages of the parasite (Alsford et al. 2011). The associated 47.5-kDa protein likely possesses RNA-binding activity that may confer transcript selection specificity to the protein aggregate. An alternative complex that swaps the 117.5-kDa protein for a 14-3-3 II protein suggests that association of the 117.5-kDa protein may be modulated by phosphorylations recognized by a 14-3-3 II homodimer, most likely of the scaffold provided by TbG1. The third complex contains TbG2 along with three other proteins that are all essential in the Alsford RNAi analysis (Alsford et al. 2011). The additional members of the third TbE5 complex include a "hypothetical" protein and two related phosphoserine/phosphothreonine-binding proteins, Tb14-3-3 I and Tb14-3-3 II. Tb14-3-3 I/II likely function as homo- or heterodimeric regulators of activity (Mackintosh 2004) and may interact with one of the other protein components to block or facilitate complex formation or RNA binding.

The kinetoplastid 14-3-3 proteins can interact with multiple partners via different motifs (Inoue et al. 2010) so pleiotropic effects are expected in RNAi experiments. Indeed, defects in surface glycoprotein recycling (Benz et al. 2010), motility, cell cycle, and cytokinesis (Inoue et al. 2005) have been observed. The settling phenotype observed for TbE5 in our motility assay is similar to that seen for 14-3-3 knockdowns in procyclic cells (Inoue et al. 2005), suggesting that the phenotype may be the result of a common defect in the protein complex described here. Differential phosphorylation of TbE5 cannot be ruled out as the determinant; TbE5 is predicted to contain four phosphorylation sites (Palmeri et al. 2011), however no phosphorylation was detected in vivo on TbE5 in either procyclic or bloodstream stage (Urbaniak et al. 2013). In TbG1 five phosphorylated serines and one tyrosine have been detected (Urbaniak et al. 2013). TbG2, which has a human eIF4G counterpart with a scaffold function (Prévôt et al. 2003), has three phosphorylated serines and two phosphorylated threonines (Urbaniak et al. 2013), making it the best candidate for 14-3-3 binding.

The presence of a potential 5′-capping enzyme in a TbE5-containing complex raises a paradox, as the TbE5 recognizes m^{7}G-capped RNA 5′ ends, yet the guanylyltransferase acts on 5′ diphosphates, and the N7-methyltransferase requires an unmodified inverted guanosine. What therefore is the substrate for the capping enzyme? The TbE5 component is likely to form a stable interaction with the RNA, while proteins with cap-forming and cap-modifying activities may have a transient association with their substrate. The interplay of the two proteins, with their distinct activities and affinities, will dictate which is the driving force for complex functions. The potential roles of the TbE5 complexes in the manipulation and remodeling of RNA 5′ end structure could have major repercussions for the captured transcripts in terms of stability and translation, providing a vital junction of control

for translation initiation in a genetic system believed to be subject to constitutive transcription.

Our working model is that capped mRNAs are recognized and bound by TbE5, which serves a role of recruiting mRNAs, but does not perform any direct catalysis on the transcript. TbE5 is bound by a distinct EIF4G, either TbG1 or TbG2, which provides a scaffold for additional protein interactions. Candidate interactors include the 117.5-kDa protein, which has the potential to modify transcripts released from TbE5. TbE5 complex formation, or action upon a bound RNA, may be regulated by interaction of the Tb14-3-3 II proteins with any of the other associated components, the most direct possibility being the modulation of the 117.5-kDa protein activity upon mRNAs bound to the complex. The presence of a TbCGM1-like protein in an eIF4F-like structure opens a broad range of possibilities for the fate of mRNAs that we can assess. For example, mammalian eIF4E has been implicated in targeting mRNAs to P-bodies (Andrei et al. 2005; Ferraiuolo et al. 2005). The provocative possibility of cytosolic mRNA capping activities highlights the elusive identity of the kinetoplastid mRNA 5′-decapping enzyme (Clayton and Shapira 2007; Banerjee et al. 2009), a lynchpin in the control of translation initiation. Cytosolic 5′ decapping of mRNA is one of two major pathways for eukaryotic mRNA degradation (Coller and Parker 2004), however it is not necessarily the end of life for the mRNA (Topisirovic et al. 2011). Candidate activities, such as a cytosolic complex isolated from human cells, can add a cap structure onto RNA molecules with a 5′ monophosphate (Otsuka et al. 2009). A goal in future studies will be to identify the mRNAs or other capped RNA species associated with each TbE5 complex, and to determine if they change during the lifecycle or in response to select stresses. Other members of the kinetoplastid EIF4E family, TbEIF4E1 through TbEIF4E4, respond to stress by forming cytosolic granules (Kramer et al. 2008, 2012), and comparable behavior has been noted for TbE5 (data not shown). In a group of organisms that predominantly lack regulation of gene/protein expression at the level of transcription initiation (Martínez-Calvillo et al. 2010; Alsford et al. 2012; Kramer 2012), the presence of a putative cytosolic capping enzyme suggests a specific role for RNA processing and/or regulation by the TbE5 complexes. The link between cytosolic mRNA metabolism and the motility-defect phenotypes could lie in TbEIF4E-mediated control of RNA regulons associated with motility.

MATERIALS AND METHODS

Bioinformatics

The two newest *T. brucei* EIF4E homologs were identified in BLAST searches of the GeneDB database (Hertz-Fowler et al. 2004). TbEIF4E5 was identified using the yeast eIF4E (GenBank number P07260) as a query. Multiple sequence alignment and phylogenetic analysis was performed with Clustal W (http://www.ebi.ac.uk/Tools/msa/clustalw/). Secondary structure predictions were performed using Phyre[2] (Kelley and Sternberg 2009).

Plasmid construction

Recombinant TbE5 was expressed from the p2171 plasmid (Dhalia et al. 2006). For interaction assays, the TbE5 and TbEIF4G homolog ORFs were amplified by PCR, and cloned into the yeast two-hybrid vectors pGAD and pGBK. For conditional knockdown by RNAi, gene-internal fragments were PCR-amplified and cloned into the p2T7-177 vector (Wickstead et al. 2002). Gene-specific allele knockout constructions were made by insertion of the respective 5′ and 3′ flanking regions into the pKO vector (Lamb et al. 2001). The 3′ terminal gene fragments required for carboxy-terminal epitope tagging were amplified and the resulting fragments cloned into the pC-PTP-Neo plasmid (Schimanski et al. 2005).

In vitro cap-binding assay

His_6-tagged recombinant TbE5 protein was expressed in *Escherichia coli* Rosetta 2 (DE3) cells. Expression was induced with 0.5 mM IPTG for 3 h at 37°C. Cells were harvested, disrupted by sonication, and centrifuged. The pellet was washed two times in 20 mM HEPES/KOH (pH 7.2) 1 M guanidine hydrochloride, 2 mM DTT, 10% glycerol. Inclusion bodies were dissolved in 50 mM HEPES/KOH (pH 7.2), 6 M guanidine hydrochloride, 10% glycerol, 2 mM DTT. Cell debris was removed by centrifugation (43,000*g* for 30 min). The protein was diluted to <0.1 mg/mL and refolded by one-step dialysis against 50 mM HEPES/KOH (pH 7.2), 100 mM KCl, 0,5 mM EDTA, 2 mM DTT, and purified by ion exchange chromatography through a HiTrap SP column.

Time-synchronized fluorescence titrations were carried out on a PerkinElmer LS 55 Fluorescence Spectrometer at 20 ± 0.3°C (Niedzwiecka et al. 2002) in 50 mM HEPES/KOH (pH 7.2), 100 mM KCl, 0.5 mM EDTA, 2 mM DTT. During the time-course titration, aliquots of 1 µL cap analog solution (Yoffe et al. 2006) were added to 1400 µL protein solution (0.1 µM, 0.2 µM, or 0.3 µM protein concentration). Changes in fluorescence intensities were measured at 325 nm or 340 nm with excitation at 280 nm and corrected for sample dilution and inner-filter effects. Equilibrium association constants (K_{as}) were determined by fitting the theoretical curve of fluorescence intensity for total cap analog concentration to the experimental data points (Niedzwiecka et al. 2002). The final K_{as} was calculated as a weighted average of three to five independent titrations. The fitting procedure utilized nonlinear, least-squared regression analysis and was performed using ORIGIN 6.0 (Microcal Software). The Gibbs free energy of binding was calculated from the K_{as} value according to the standard equation $\Delta G^{\circ} = -RT\ln K_{as}$.

T. brucei cell culture and RNAi

YTAT procyclic *T. brucei* was grown at 27°C in SM medium (Cunningham 1977) supplemented with 10% fetal bovine serum, and was used for PTP-targeted integrations for MudPIT analyses. Procyclic forms of *T. brucei* Lister 427 strain 29-13 were used for RNAi. Transfection was performed as described (Hill et al. 1999). Selection was performed with G418 (15 µg/mL), puromycin (10 µg/mL), or phleomycin (2.5 µg/mL), and clonal lines of selected

cultures were obtained by limiting dilution in 96-well plates. To induce RNAi, 1 μg/mL tetracycline (Tet) was added to mid-log phase cultures and the growth measured daily. Single knockout/PTP-tagged lines in YTAT were constructed as described (Schimanski et al. 2005). The 29-13 cell line was transfected with the plasmid cPTP-puro-TbE5, selected with puromycin and checked for PTP-tagged protein expression, then transfected with the RNAi plasmid p2T7-177-TbE5 and selected with phleomycin, generating the $TbE5^{+/PTP}$RNAi cell line. PTP tagging of TbE5 to monitor knockdown in the 29-13 RNAi cell line affected one allele, leaving the second as WT.

Fluorescence microscopy

T. brucei cultures in mid-log phase ($5 \times 10^6 - 10^7$ cells/mL) were used for immunofluorescence imaging as described (Oberholzer et al. 2011). Aliquots of 1 mL were washed twice in 1 mL PBS, resuspended in 1 mL PBS/0.01% paraformaldehyde, and incubated on ice for 5 min. The cells were centrifuged and resuspended in 0.5 mL PBS. Approximately 20 μL of the cell suspension was spread on a microscope slide and dried at room temperature (RT), followed by fixation at −20°C in acetone for 5 min and −20°C in methanol for 5 min. The slides were dried at RT, the cells were rehydrated with 1 mL PBS for 15 min and blocked for 1.5 h at RT with blocking solution (PBS/5% Normal Goat Serum/5% BSA). Blocked cells were incubated for 1.5 h in a 1:3000 Anti-Protein A antibody produced in rabbit (Sigma) in blocking solution, washed three times with PBS-T (PBS/0.05% Tween 20), incubated in 1:3000 anti-rabbit IgG Alexa 488 (Invitrogen), washed three times with PBS-T, once with PBS and mounted on slides with Vectashield (Vector Laboratories) containing DAPI, and viewed by fluorescence microscopy.

Metabolic labeling assay

[^{35}S]-methionine incorporation was determined as described (Freire et al. 2011). RNAi-induced and uninduced $TbE5^{+/PTP}$RNAi mid-log phase cultures were centrifuged at 3000 RPM at RT, washed once in methionine-free SM medium, and resuspended to a concentration of 1×10^7 cells/mL in the methionine-free SM medium supplemented with 50 μCi/mL [^{35}S]-methionine. After 1-h incubation at 28°C, 50 μL aliquots were lysed (5 μL 10% SDS, 2.5 μL 1 M NaOH), 10 μL of these lysates were spotted in triplicate to Whatman filter papers, and dried at RT. The filters were then incubated on ice in 10% TCA for 15 min followed by boiling in 5% TCA for 10 min. After one methanol wash and one acetone wash the filters were dried at RT. The radiolabel incorporated into proteins was measured with a Beckman LS 6500 Scintillation Counter. Experiments were performed three times in triplicate. Standard error was calculated and plotted in Microsoft Excel.

Sedimentation assay

Motility in a liquid environment was quantified by spectrophotometry (Bastin et al. 1999). Cells with integrated RNAi constructions were incubated +/–Tet for 72 h, then resuspended at 5×10^6 cells/mL in fresh medium with or without drug. Six replicates (1 mL) were transferred to cuvettes and incubated without shaking under standard conditions. The optical density at 600 nm (OD_{600}) was measured in triplicate every 8 h, with three cuvettes left undisturbed to measure sedimentation and three cuvettes mixed prior to measurement. The ΔOD_{600} for each sample was calculated by dividing the OD_{600} of the resuspended samples by those of the undisturbed samples.

Motility assay

Social motility assays on semi-solid 0.4% agarose plates were performed as described (Oberholzer et al. 2010). Plates contained either methanol (diluent) or Tet (final 1 μg/mL) for "–Tet" and "+Tet" conditions. The plates were inoculated using 5.5 μL cells from suspension cultures at $\sim 1.0 \times 10^7$ cells/mL. The +Tet cells were induced for 72 h prior to plating. Following inoculation, the plates were closed, left to sit for 20 min, then sealed with Parafilm and incubated at 27°C with 5% CO_2. Plates were photographed at 120 h using a white light box and a velvet cloth to provide background contrast. Images were acquired using a Pentax Optio M30 camera, and cropped in Adobe Photoshop.

Yeast two-hybrid assays

Yeast strain PJ69-4A was cultivated overnight at 30°C in YPD medium (Ammerman et al. 2012). Each transformation used 1 mL cell suspension washed and resuspended in 100 μL TE/100 mM lithium acetate buffer and incubated at RT for 15 min. The cells were centrifuged and resuspended in 360 μL transformation buffer (1 × TE/1 mM LiOAc; 50% PEG 8000 and 2 mg/mL boiled salmon sperm DNA), simultaneously transformed with GBK (tryp+) and GAD (leu+) plasmids expressing TbE5 and individual *T. brucei* 4G homologs, and incubated for 30 min at RT. Subsequently, the cells were incubated at 42°C for 20 min, and then spun down. The pellet was resuspended in 2 mL dropout medium (minimal medium minus tryptophan and leucine) and incubated overnight at 30°C. After dropout incubation the OD_{600} was checked and all cultures centrifuged, diluted to OD_{600} 0.5 in dropout medium (minimal medium minus tryptophan, leucine, and histidine), applied on to 2% agar dropout medium plates containing 3-amino-1,2,4-triazole (3AT) in serial dilutions, and incubated at 30°C for 5 d. The positive control plates used plasmids pGADT7-T and pGBKT7-53 (CLONTECH Laboratories Inc.) for transformation.

Native gel electrophoresis for protein complex detection and sizing

Blue Native gel analysis was performed according to manufacturer instructions (Novex). Samples were prepared as follows: Mid-Log phase culture cells were washed twice in PBS, resuspended in 24 μL extraction buffer (25 mM HEPES, 150 mM sucrose, 20 mM potassium glutamate, 3 mM $MgCl_2$, 0.5% NP40, 150 mM KCl, 0.5 mM DTT, and SIGMA*FAST* Protease Inhibitor Cocktail, EDTA-free [Sigma-Aldrich]), incubated on ice for 20 min, and centrifuged at full speed for 10 min/4°C. Eighteen microliters of the supernatant was added to 6.25 μL of 4× Native PAGE buffer and 1 μL of G-250 Coomassie sample buffer. The samples were electrophoresed through precast 4%–16% NativePAGE Novex Bis-Tris gels following the manufacturer specifications (Life Technologies). The

NativeMark Unstained Protein standard (Life Technologies) was used to estimate complex sizes. Proteins were transferred to Immun-Blot PVDF 0.2 μm membranes (BioRad). Membranes were fixed in 8% acetic acid for 15 min, rinsed with water, and incubated with primary or secondary antibody. The size marker lane was removed prior to antibody incubation, air-dried, equilibrated with methanol, and stained with Coomassie dye for visualization.

Tandem-affinity purification

Purification was performed from 500 mL of culture (5×10^6 cell/mL). For tandem-affinity purification, the PTP tag was utilized and purification performed as described (Schimanski et al. 2005). Total elution from the protein C column was resolved either by SDS-PAGE and visualized by silver staining (BioRad Silver Staining plus), or TCA precipitation and subjected to tandem mass spectrometry (MudPIT).

MudPIT

The TCA precipitated proteins were digested by trypsin and subjected to mass spectrometry as described (Zamudio et al. 2009). The proteomic data were analyzed using the SEQUEST and DTASelect2 algorithms against the *T. brucei* genome database (Berriman et al. 2005), filtering by a peptide-level false-positive rate of 5%, and a minimum of two peptides per protein (Peng et al. 2002).

ACKNOWLEDGMENTS

We thank Bidyottam Mittra, Jun Urano, Laurie Read, and Fuyu Tamanoi for strains, reagents, and help with the Y2H assay; and Arthur Günzl for the PTP-immunofluorescence protocol. This work was supported by a UCLA Stein-Oppenheimer award; the National Institute of Allergy and Infectious Diseases, the National Institutes of Health, and the National Institute of General Medical Sciences (grant numbers AI056034, AI073806, TW009035 to D.A.C. and N.R.S., grant number GM089778 to J.A.W., and grant number AI052348 to K.H.); and the National Science Centre, Poland (grant numbers UMO-2012/07/B/NZ1/00118 and UMO-2013/08/A/NZ1/00866 to E.D. and J.Z.). Scholarship support for A.M.M. and J.F.N. was provided by Fundação de Amparo à Ciência e Tecnologia de Pernambuco; Coordenação de Aperfeiçoamento de Pessoal de Nível Superior; and Conselho Nacional de Desenvolvimento Científico e Tecnológico.

Received March 25, 2014; accepted May 12, 2014.

REFERENCES

Adl SM, Simpson AG, Lane CE, Lukes J, Bass D, Bowser SS, Brown MW, Burki F, Dunthorn M, Hampl V, et al. 2012. The revised classification of eukaryotes. *J Eukaryot Microbiol* **59:** 429–493.

Aitken CE, Lorsch JR. 2012. A mechanistic overview of translation initiation in eukaryotes. *Nat Struct Mol Biol* **19:** 568–576.

Alsford S, Turner DJ, Obado SO, Sanchez-Flores A, Glover L, Berriman M, Hertz-Fowler C, Horn D. 2011. High-throughput phenotyping using parallel sequencing of RNA interference targets in the African trypanosome. *Genome Res* **21:** 915–924.

Alsford S, duBois K, Horn D, Field MC. 2012. Epigenetic mechanisms, nuclear architecture and the control of gene expression in trypanosomes. *Expert Rev Mol Med* **14:** e13.

Ammerman ML, Downey KM, Hashimi H, Fisk JC, Tomasello DL, Faktorova D, Kafkova L, King T, Lukes J, Read LK. 2012. Architecture of the trypanosome RNA editing accessory complex, MRB1. *Nucleic Acids Res* **40:** 5637–5650.

Andrei MA, Ingelfinger D, Heintzmann R, Achsel T, Rivera-Pomar R, Luhrmann R. 2005. A role for eIF4E and eIF4E-transporter in targeting mRNPs to mammalian processing bodies. *RNA* **11:** 717–727.

Badjatia N, Ambrosio DL, Lee JH, Gunzl A. 2013. Trypanosome cdc2-related kinase 9 controls spliced leader RNA cap4 methylation and phosphorylation of RNA polymerase II subunit RPB1. *Mol Cell Biol* **33:** 1965–1975.

Banerjee H, Palenchar JB, Lukaszewicz M, Bojarska E, Stepinski J, Jemielity J, Guranowski A, Ng S, Wah DA, Darzynkiewicz E, et al. 2009. Identification of the HIT-45 protein from *Trypanosoma brucei* as an FHIT protein/dinucleoside triphosphatase: substrate specificity studies on the recombinant and endogenous proteins. *RNA* **15:** 1554–1564.

Bangs JD, Crain PF, Hashizume T, McCloskey JA, Boothroyd JC. 1992. Mass spectrometry of mRNA cap 4 from trypanosomatids reveals two novel nucleosides. *J Biol Chem* **267:** 9805–9815.

Bastin P, Pullen TJ, Sherwin T, Gull K. 1999. Protein transport and flagellum assembly dynamics revealed by analysis of the paralysed trypanosome mutant snl-1. *J Cell Sci* **112:** 3769–3777.

Benz C, Engstler M, Hillmer S, Clayton C. 2010. Depletion of 14-3-3 proteins in bloodstream-form *Trypanosoma brucei* inhibits variant surface glycoprotein recycling. *Int J Parasitol* **40:** 629–634.

Berriman M, Ghedin E, Hertz-Fowler C, Blandin G, Renauld H, Bartholomeu DC, Lennard NJ, Caler E, Hamlin NE, Haas B, et al. 2005. The genome of the African trypanosome *Trypanosoma brucei*. *Science* **309:** 416–422.

Blewett NH, Goldstrohm AC. 2012. A eukaryotic translation initiation factor 4E-binding protein promotes mRNA decapping and is required for PUF repression. *Mol Cell Biol* **32:** 4181–4194.

Branche C, Kohl L, Toutirais G, Buisson J, Cosson J, Bastin P. 2006. Conserved and specific functions of axoneme components in trypanosome motility. *J Cell Sci* **119:** 3443–3455.

Broadhead R, Dawe HR, Farr H, Griffiths S, Hart SR, Portman N, Shaw MK, Ginger ML, Gaskell SJ, McKean PG, et al. 2006. Flagellar motility is required for the viability of the bloodstream trypanosome. *Nature* **440:** 224–227.

Cho PF, Poulin F, Cho-Park YA, Cho-Park IB, Chicoine JD, Lasko P, Sonenberg N. 2005. A new paradigm for translational control: inhibition via 5′–3′ mRNA tethering by Bicoid and the eIF4E cognate 4EHP. *Cell* **121:** 411–423.

Clarkson BK, Gilbert WV, Doudna JA. 2010. Functional overlap between eIF4G isoforms in *Saccharomyces cerevisiae*. *PLoS One* **5:** e9114.

Clayton C, Shapira M. 2007. Post-transcriptional regulation of gene expression in trypanosomes and leishmanias. *Mol Biochem Parasitol* **156:** 93–101.

Coller J, Parker R. 2004. Eukaryotic mRNA decapping. *Ann Rev Biochem* **73:** 861–890.

Contreras V, Richardson MA, Hao E, Keiper BD. 2008. Depletion of the cap-associated isoform of translation factor eIF4G induces germline apoptosis in *C. elegans*. *Cell Death Differ* **15:** 1232–1242.

Culjkovic B, Topisirovic I, Skrabanek L, Ruiz-Gutierrez M, Borden KL. 2005. eIF4E promotes nuclear export of cyclin D1 mRNAs via an element in the 3′UTR. *J Cell Biol* **169:** 245–256.

Culjkovic B, Topisirovic I, Skrabanek L, Ruiz-Gutierrez M, Borden KL. 2006. eIF4E is a central node of an RNA regulon that governs cellular proliferation. *J Cell Biol* **175:** 415–426.

Culjkovic B, Topisirovic I, Borden KL. 2007. Controlling gene expression through RNA regulons: the role of the eukaryotic translation initiation factor eIF4E. *Cell Cycle* **6:** 65–69.

Cunningham I. 1977. New culture medium for maintenance of tsetse tissues and growth of trypanosomatids. *J Protozool* **24:** 325–329.

Das A, Morales R, Banday M, Garcia S, Hao L, Cross GA, Estevez AM, Bellofatto V. 2012. The essential polysome-associated RNA-binding protein RBP42 targets mRNAs involved in *Trypanosoma brucei* energy metabolism. *RNA* **18:** 1968–1983.

De Gaudenzi JG, Carmona SJ, Aguero F, Frasch AC. 2013. Genome-wide analysis of 3′-untranslated regions supports the existence of post-transcriptional regulons controlling gene expression in trypanosomes. *PeerJ* **1:** e118.

Dhalia R, Reis CR, Freire ER, Rocha PO, Katz R, Muniz JR, Standart N, de Melo Neto OP. 2005. Translation initiation in *Leishmania major*: characterisation of multiple eIF4F subunit homologues. *Mol Biochem Parasitol* **140:** 23–41.

Dhalia R, Marinsek N, Reis CR, Katz R, Muniz JR, Standart N, Carrington M, de Melo Neto OP. 2006. The two eIF4A helicases in *Trypanosoma brucei* are functionally distinct. *Nucleic Acids Res* **34:** 2495–2507.

Estévez AM. 2008. The RNA-binding protein TbDRBD3 regulates the stability of a specific subset of mRNAs in trypanosomes. *Nucleic Acids Res* **36:** 4573–4586.

Fernandez-Moya SM, Estevez AM. 2010. Posttranscriptional control and the role of RNA-binding proteins in gene regulation in trypanosomatid protozoan parasites. *Wiley Interdiscip Rev RNA* **1:** 34–46.

Fernandez-Moya SM, Garcia-Perez A, Kramer S, Carrington M, Estevez AM. 2012. Alterations in DRBD3 ribonucleoprotein complexes in response to stress in *Trypanosoma brucei*. *PLoS One* **7:** e48870.

Ferraiuolo MA, Basak S, Dostie J, Murray EL, Schoenberg DR, Sonenberg N. 2005. A role for the eIF4E-binding protein 4E-T in P-body formation and mRNA decay. *J Cell Biol* **170:** 913–924.

Freire ER, Dhalia R, Moura DM, da Costa Lima TD, Lima RP, Reis CR, Hughes K, Figueiredo RC, Standart N, Carrington M, et al. 2011. The four trypanosomatid eIF4E homologues fall into two separate groups, with distinct features in primary sequence and biological properties. *Mol Biochem Parasitol* **176:** 25–36.

Ghosh A, Lima CD. 2010. Enzymology of RNA cap synthesis. *Wiley Interdiscip Rev RNA* **1:** 152–172.

Gingras AC, Raught B, Sonenberg N. 1999. eIF4 initiation factors: effectors of mRNA recruitment to ribosomes and regulators of translation. *Annu Rev Biochem* **68:** 913–963.

Gosselin P, Martineau Y, Morales J, Czjzek M, Glippa V, Gauffeny I, Morin E, Le Corguille G, Pyronnet S, Cormier P, et al. 2013. Tracking a refined eIF4E-binding motif reveals Angel1 as a new partner of eIF4E. *Nucleic Acids Res* **41:** 7783–7792.

Groppo R, Richter JD. 2009. Translational control from head to tail. *Curr Opin Cell Biol* **21:** 444–451.

Günzl A. 2012. RNA polymerases and transcription factors of trypanosomes. In *RNA metabolism in trypanosomes* (ed. Bindereif A), Vol. 28, pp. 1–27. Springer, Berlin.

Hernández G, Altmann M, Sierra JM, Urlaub H, Diez del Corral R, Schwartz P, Rivera-Pomar R. 2005. Functional analysis of seven genes encoding eight translation initiation factor 4E (eIF4E) isoforms in *Drosophila*. *Mech Dev* **122:** 529–543.

Hertz-Fowler C, Peacock CS, Wood V, Aslett M, Kerhornou A, Mooney P, Tivey A, Berriman M, Hall N, Rutherford K, et al. 2004. GeneDB: a resource for prokaryotic and eukaryotic organisms. *Nucleic Acids Res* **32:** D339–D343.

Hill KL, Hutchings NR, Russell DG, Donelson JE. 1999. A novel protein targeting domain directs proteins to the anterior cytoplasmic face of the flagellar pocket in African trypanosomes. *J Cell Sci* **112:** 3091–3101.

Inoue M, Nakamura Y, Yasuda K, Yasaka N, Hara T, Schnaufer A, Stuart K, Fukuma T. 2005. The 14-3-3 proteins of *Trypanosoma brucei* function in motility, cytokinesis, and cell cycle. *J Biol Chem* **280:** 14085–14096.

Inoue M, Yasuda K, Uemura H, Yasaka N, Inoue H, Sei Y, Horikoshi N, Fukuma T. 2010. Phosphorylation-dependent protein interaction with *Trypanosoma brucei* 14-3-3 proteins that display atypical target recognition. *PLoS One* **5:** e15566.

Jackson RJ, Hellen CU, Pestova TV. 2010. The mechanism of eukaryotic translation initiation and principles of its regulation. *Nat Rev Mol Cell Biol* **11:** 113–127.

Jagus R, Bachvaroff TR, Joshi B, Place AR. 2012. Diversity of eukaryotic translational initiation factor eIF4E in protists. *Comp Funct Genomics* **2012:** 134839.

Jankowska-Anyszka M, Lamphear BJ, Aamodt EJ, Harrington T, Darzynkiewicz E, Stolarski R, Rhoads RE. 1998. Multiple isoforms of eukaryotic protein synthesis initiation factor 4E in *Caenorhabditis elegans* can distinguish between mono- and trimethylated cap structures. *J Biol Chem* **273:** 10538–10542.

Joshi B, Cameron A, Jagus R. 2004. Characterization of mammalian eIF4E-family members. *Eur J Biochem* **271:** 2189–2203.

Joshi B, Lee K, Maeder DL, Jagus R. 2005. Phylogenetic analysis of eIF4E-family members. *BMC Evol Biol* **5:** 48.

Keene JD. 2007. RNA regulons: coordination of post-transcriptional events. *Nat Rev Genet* **8:** 533–543.

Keiper BD, Lamphear BJ, Deshpande AM, Jankowska-Anyszka M, Aamodt EJ, Blumenthal T, Rhoads RE. 2000. Functional characterization of five eIF4E isoforms in *Caenorhabditis elegans*. *J Biol Chem* **275:** 10590–10596.

Kelley LA, Sternberg MJ. 2009. Protein structure prediction on the Web: a case study using the Phyre server. *Nat Protoc* **4:** 363–371.

Kim HS, Li Z, Boothroyd C, Cross GA. 2013. Strategies to construct null and conditional null *Trypanosoma brucei* mutants using Cre-recombinase and loxP. *Mol Biochem Parasitol* **191:** 16–19.

Kramer S. 2012. Developmental regulation of gene expression in the absence of transcriptional control: the case of kinetoplastids. *Mol Biochem Parasitol* **181:** 61–72.

Kramer S, Queiroz R, Ellis L, Webb H, Hoheisel JD, Clayton C, Carrington M. 2008. Heat shock causes a decrease in polysomes and the appearance of stress granules in trypanosomes independently of eIF2α phosphorylation at Thr169. *J Cell Sci* **121:** 3002–3014.

Kramer S, Marnef A, Standart N, Carrington M. 2012. Inhibition of mRNA maturation in trypanosomes causes the formation of novel foci at the nuclear periphery containing cytoplasmic regulators of mRNA fate. *J Cell Sci* **125:** 2896–2909.

Lamb JR, Fu V, Wirtz E, Bangs JD. 2001. Functional analysis of the trypanosomal AAA protein TbVCP with trans-dominant ATP hydrolysis mutants. *J Biol Chem* **276:** 21512–21520.

Lasko P, Cho P, Poulin F, Sonenberg N. 2005. Contrasting mechanisms of regulating translation of specific *Drosophila* germline mRNAs at the level of 5′-cap structure binding. *Biochem Soc Trans* **33:** 1544–1546.

Liang X-h, Haritan A, Uliel S, Michaeli S. 2003. *trans* and *cis* splicing in trypanosomatids: mechanisms, factors, and regulation. *Eukaryot Cell* **2:** 830–840.

Mackintosh C. 2004. Dynamic interactions between 14-3-3 proteins and phosphoproteins regulate diverse cellular processes. *Biochem J* **381:** 329–342.

Marcotrigiano J, Gingras AC, Sonenberg N, Burley SK. 1997. Cocrystal structure of the messenger RNA 5′ cap-binding protein (eIF4E) bound to 7-methyl-GDP. *Cell* **89:** 951–961.

Marcotrigiano J, Gingras AC, Sonenberg N, Burley SK. 1999. Cap-dependent translation initiation in eukaryotes is regulated by a molecular mimic of eIF4G. *Mol Cell* **3:** 707–716.

Martínez-Calvillo S, Vizuet-de-Rueda JC, Florencio-Martínez LE, Manning-Cela RG, Figueroa-Angulo EE. 2010. Gene expression in trypanosomatid parasites. *J Biomed Biotechnol* **2010:** 525241.

Merritt C, Stuart K. 2013. Identification of essential and non-essential protein kinases by a fusion PCR method for efficient production of transgenic *Trypanosoma brucei*. *Mol Biochem Parasitol* **190:** 44–49.

Mony BM, MacGregor P, Ivens A, Rojas F, Cowton A, Young J, Horn D, Matthews K. 2014. Genome-wide dissection of the quorum sensing signalling pathway in *Trypanosoma brucei*. *Nature* **505:** 681–685.

Niedzwiecka A, Marcotrigiano J, Stepinski J, Jankowska-Anyszka M, Wyslouch-Cieszynska A, Dadlez M, Gingras AC, Mak P, Darzynkiewicz E, Sonenberg N, et al. 2002. Biophysical studies of eIF4E cap-binding protein: recognition of mRNA 5′ cap structure and synthetic fragments of eIF4G and 4E-BP1 proteins. *J Mol Biol* **319:** 615–635.

Oberholzer M, Lopez MA, McLelland BT, Hill KL. 2010. Social motility in african trypanosomes. *PLoS Pathogens* **6:** e1000739.
Oberholzer M, Langousis G, Nguyen HT, Saada EA, Shimogawa MM, Jonsson ZO, Nguyen SM, Wohlschlegel JA, Hill KL. 2011. Independent analysis of the flagellum surface and matrix proteomes provides insight into flagellum signaling in mammalian-infectious *Trypanosoma brucei*. *Mol Cell Proteomics* **10:** M111.010538.
Otsuka Y, Kedersha NL, Schoenberg DR. 2009. Identification of a cytoplasmic complex that adds a cap onto 5′-monophosphate RNA. *Mol Cell Biol* **29:** 2155–2167.
Ouellette M, Papadopoulou B. 2009. Coordinated gene expression by post-transcriptional regulons in African trypanosomes. *J Biol* **8:** 100.
Palmeri A, Gherardini PF, Tsigankov P, Ausiello G, Spath GF, Zilberstein D, Helmer-Citterich M. 2011. PhosTryp: a phosphorylation site predictor specific for parasitic protozoa of the family trypanosomatidae. *BMC Genomics* **12:** 614.
Park SH, Nguyen BN, Kirkham JK, Nguyen TN, Gunzl A. 2014. A new strategy of RNA interference that targets heterologous sequences reveals CITFA1 as an essential component of class I transcription factor A in *Trypanosoma brucei*. *Eukaryot Cell* **13:** 785–795.
Parker R, Sheth U. 2007. P bodies and the control of mRNA translation and degradation. *Mol Cell* **25:** 635–646.
Peng J, Elias JE, Thoreen CC, Licklider LJ, Gygi SP. 2002. Evaluation of multidimensional chromatography coupled with tandem mass spectrometry (LC/LC-MS/MS) for large-scale protein analysis: the yeast proteome. *J Proteome Res* **2:** 43–50.
Pestova TV, Hellen CU. 2003. Coupled folding during translation initiation. *Cell* **115:** 650–652.
Preußer C, Jaé N, Günzl A, Bindereif A. 2012. Pre-mRNA splicing in *Trypanosoma brucei*: factors, mechanisms, and regulation. In *RNA metabolism in trypanosomes* (ed. Bindereif A), pp. 49–78. Springer, Berlin.
Prévôt D, Darlix JL, Ohlmann T. 2003. Conducting the initiation of protein synthesis: the role of eIF4G. *Biol Cell* **95:** 141–156.
Ptushkina M, Berthelot K, von der Haar T, Geffers L, Warwicker J, McCarthy JE. 2001. A second eIF4E protein in *Schizosaccharomyces pombe* has distinct eIF4G-binding properties. *Nucleic Acids Res* **29:** 4561–4569.
Queiroz R, Benz C, Fellenberg K, Hoheisel JD, Clayton C. 2009. Transcriptome analysis of differentiating trypanosomes reveals the existence of multiple post-transcriptional regulons. *BMC Genomics* **10:** 495.
Ralston KS, Hill KL. 2006. Trypanin, a component of the flagellar Dynein regulatory complex, is essential in bloodstream form African trypanosomes. *PLoS Pathogens* **2:** e101.
Ralston KS, Lerner AG, Diener DR, Hill KL. 2006. Flagellar motility contributes to cytokinesis in *Trypanosoma brucei* and is modulated by an evolutionarily conserved dynein regulatory system. *Eukaryot Cell* **5:** 696–711.
Raught B, Gingras AC. 1999. eIF4E activity is regulated at multiple levels. *Int J Biochem Cell Biol* **31:** 43–57.
Rhoads RE. 2009. eIF4E: new family members, new binding partners, new roles. *J Biol Chem* **284:** 16711–16715.
Richter JD, Sonenberg N. 2005. Regulation of cap-dependent translation by eIF4E inhibitory proteins. *Nature* **433:** 477–480.
Ruan J-p, Shen S, Ullu E, Tschudi C. 2007. Evidence for a capping enzyme with specificity for the trypanosome spliced leader RNA. *Mol Biochem Parasitol* **156:** 246–254.
Schimanski B, Nguyen TN, Günzl A. 2005. Highly efficient tandem affinity purification of trypanosome protein complexes based on a novel epitope combination. *Eukaryot Cell* **4:** 1942–1950.
Sturm NR, Zamudio JR, Campbell DA. 2012. SL RNA biogenesis in kinetoplastids: a long and winding road. In *RNA metabolism in trypanosomes* (ed. Bindereif A), pp. 29–47. Springer, Berlin.
Takagi Y, Sindkar S, Ekonomidis D, Hall MP, Ho CK. 2007. *Trypanosoma brucei* encodes a bifunctional capping enzyme essential for cap 4 formation on the spliced leader RNA. *J Biol Chem* **282:** 15995–16005.
Topisirovic I, Svitkin YV, Sonenberg N, Shatkin AJ. 2011. Cap and cap-binding proteins in the control of gene expression. *Wiley Interdiscip Rev RNA* **2:** 277–298.
Urbaniak MD, Martin DM, Ferguson MA. 2013. Global quantitative SILAC phosphoproteomics reveals differential phosphorylation is widespread between the procyclic and bloodstream form lifecycle stages of *Trypanosoma brucei*. *J Proteome Res* **12:** 2233–2244.
Wickstead B, Ersfeld K, Gull K. 2002. Targeting of a tetracycline-inducible expression system to the transcriptionally silent minichromosomes of *Trypanosoma brucei*. *Mol Biochem Parasitol* **125:** 211–216.
Yoffe Y, Zuberek J, Lewdorowicz M, Zeira Z, Keasar C, Orr-Dahan I, Jankowska-Anyszka M, Stepinski J, Darzynkiewicz E, Shapira M. 2004. Cap-binding activity of an eIF4E homolog from *Leishmania*. *RNA* **10:** 1764–1775.
Yoffe Y, Zuberek J, Lerer A, Lewdorowicz M, Stepinski J, Altmann M, Darzynkiewicz E, Shapira M. 2006. Binding specificities and potential roles of isoforms of eukaryotic initiation factor eIF4E in *Leishmania*. *Eukaryot Cell* **5:** 1969–1979.
Yoffe Y, Léger M, Zinoviev A, Zuberek J, Darzynkiewicz E, Wagner G, Shapira M. 2009. Evolutionary changes in the *Leishmania* eIF4F complex involve variations in the eIF4E-eIF4G interactions. *Nucleic Acids Res* **10:** 3243–3253.
Zamudio JR, Mittra B, Chattopadhyay A, Wohlschlegel JA, Sturm NR, Campbell DA. 2009. *Trypanosoma brucei* spliced leader RNA maturation by the cap 1 2′-*O*-ribose methyltransferase and SLA1 H/ACA snoRNA pseudouridine synthase complex. *Mol Cell Biol* **29:** 1202–1211.
Zhang X, Cui J, Nilsson D, Gunasekera K, Chanfon A, Song X, Wang H, Xu Y, Ochsenreiter T. 2010. The *Trypanosoma brucei* MitoCarta and its regulation and splicing pattern during development. *Nucleic Acids Res* **38:** 7378–7387.
Zick A, Onn I, Bezalel R, Margalit H, Shlomai J. 2005. Assigning functions to genes: identification of S-phase expressed genes in *Leishmania major* based on post-transcriptional control elements. *Nucleic Acids Res* **33:** 4235–4242.
Zinoviev A, Shapira M. 2012. Evolutionary conservation and diversification of the translation initiation apparatus in trypanosomatids. *Comp Funct Genomics* **2012:** 813718.
Zinoviev A, Leger M, Wagner G, Shapira M. 2011. A novel 4E-interacting protein in *Leishmania* is involved in stage-specific translation pathways. *Nucleic Acids Res* **39:** 8404–8415.
Zinoviev A, Manor S, Shapira M. 2012. Nutritional stress affects an atypical cap-binding protein in *Leishmania*. *RNA Biol* **9:** 1450–1460.